Solar Thermal Test Facilities

USERS ASSOCIATION

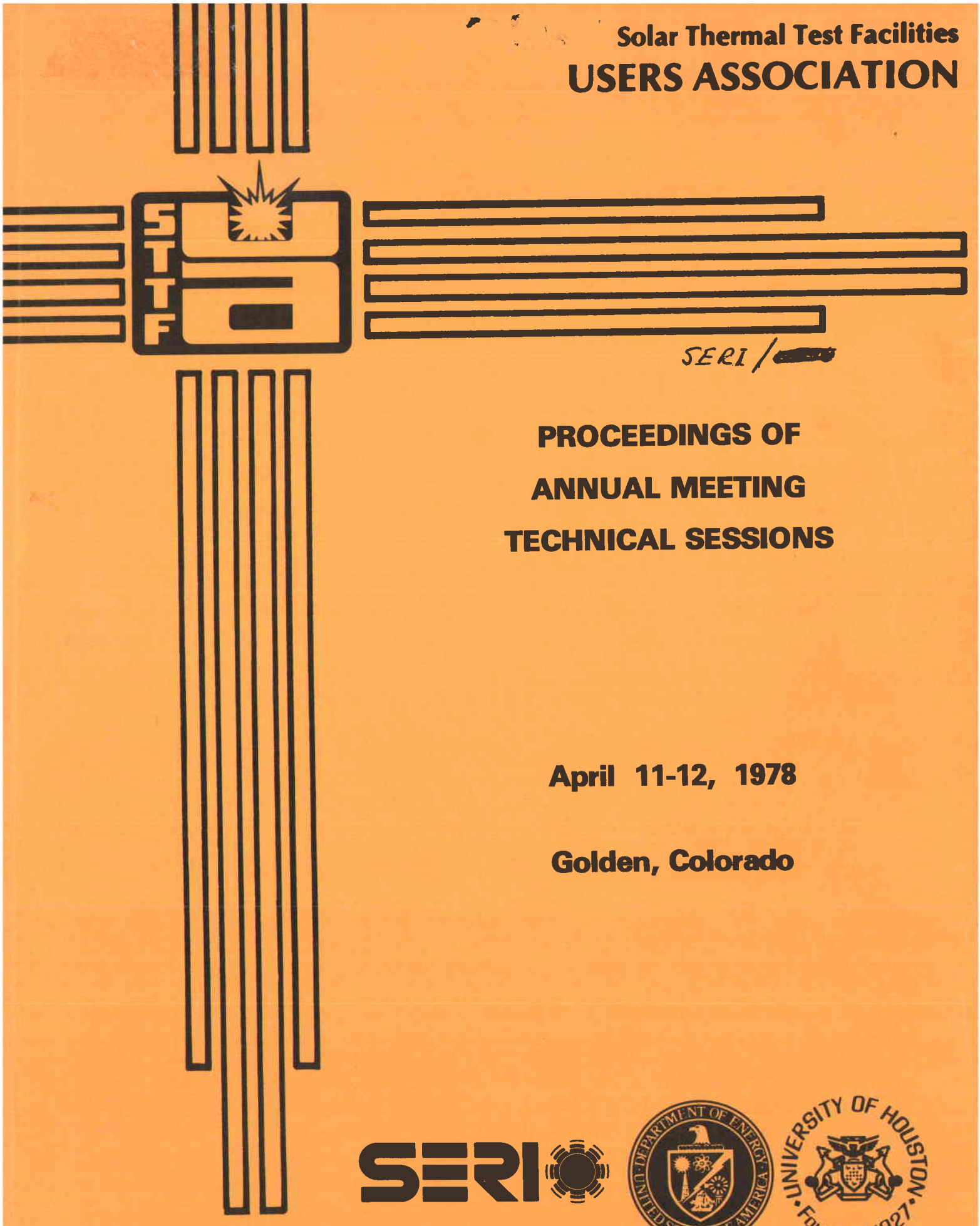

SERI /

PROCEEDINGS OF
ANNUAL MEETING
TECHNICAL SESSIONS

April 11-12, 1978

Golden, Colorado

SERI

DEPARTMENT OF ENERGY · UNITED STATES OF AMERICA

UNIVERSITY OF HOUSTON · Founded 1927

NOTICE

Printed in the United States of America

Available from:

National Technical Information Service
US Department of Commerce
5285 Port Royal Road
Springfield, VA 22161
Price: Printed Copy $11.00; Microfiche $5.50

PROCEEDINGS OF ANNUAL MEETING

April 11-12, 1978

Golden, Colorado

Solar Thermal Test Facilities Users Association

Table of Contents

I. FOREWORD

This is the proceedings of the technical sessions of the Solar Thermal Test Facilities Users Association annual meeting held April 11-12, 1978, in Golden, Colorado. The Association was organized in April 1977, at the request of DOE (then ERDA) to encourage and help coordinate experiments on high-temperature solar facilities in Albuquerque and Atlanta. The Association now also has cooperative experimental programs with the Army White Sands Solar Furnace at White Sands, NM, and the CNRS solar furnace at Odeillo, France.

Representatives of the Department of Energy and the Solar Energy Research Institute discussed their plans and programs. In addition, Professor Michel Rodot, Director of PIRDES, of the French CNRS talked "About The Uses of Highly Concentrated Solar Energy," and Professor Tetsuo Noguchi of the Government Industrial Research Institute in Japan discussed "Solar Energy R&D in Japan." Operators of the solar test facilities described their installations.

Other technical sessions included discussions of solar Optics and Systems, Materials, Energy Conversion and Storage, Industrial Chemical Processes, and Testing and Simulation.

II. SESSION I: OPENING REMARKS

Dr. A. F. Hildebrandt, Chairman

STTF Users Association
University of Houston

Chairman Hildebrandt - Good morning and welcome to the Second Annual STTF Users Association Meeting. I'm Alvin Hildebrandt, the Chairman of the Association.

We are very grateful to our SERI hosts, Charles Grosskreutz and Paul Rappaport; I believe you'll hear from Paul later. I wish to thank Chuck Bishop and Vicky Curry for excellent arrangements here and Marylee Adams for helping in those arrangements.

We are especially pleased to have Professor Michael Rodot, Herb Budd and Claude Royere from CNRS, and we'll have Dr. Noguchi from Japan tomorrow, I believe.

We truly now do have an international interest and I would like at this time to thank the Executive Committee and the other committees for diligent and valiant efforts in the last year to keep us going and, in particular, I would like to recognize the Program Committee and its Chairman, Terry Cole, for burning the midnight oil to get the conference together.

As you may know, The STTF is closely related to the Central Receiver Program and it appears that each year we have an in-depth

January review at higher levels of the agency, be it ERDA or DOE, and then we have the April or May Users Association Meeting. I'm sure you'll hear more about that later but the Central Receiver Program has passed the annual review twice. It's very gratifying to see the RFP's and 10-MW contracts moving, thanks to Marty Gutstein, who I see in the audience, Gerry Braun and Hank Marvin, who have been doing a superhuman effort in keeping the program moving. The 5 MW, first, is being followed by a 10 MW and other advanced concepts that were briefly mentioned by Al Skinrood at San Diego. There's a lot to do in the advanced receivers, materials, storage and transmission and the membership is growing and I hope we have a very productive meeting. Our number may be small but our potential for impact and growth is, I feel, very great.

I would like to apologize for the fact that we have a parallel program tomorrow morning. We weren't sure what the paper response would be and it was rather late in the program that suddenly we got a very strong response and, in fact, I think we got some papers that we were not able to include in the program, but I think it's a very interesting agenda.

Our first speaker will be Frank Smith, who is the Executive Director, and who will give an executive overview of the Users Association. Frank.

USERS ASSOCIATION: FIRST YEAR AND THE FUTURE

Frank B. Smith
Solar Thermal Test Facilities Users Association
Albuquerque, New Mexico

The genesis of the Solar Thermal Test Facilities Users Association (STTFUA) goes back to 1975 or 1976 when Bob Seamans, then Administrator of ERDA, was first considering the construction of a central tower-type solar facility by Sandia Laboratories in Albuquerque. One of Dr. Seamans' primary concerns was that the facility (representing a significant investment of federal funds) should be managed so that it could be made available, with the fewest obstacles possible, to experimenters from universities, commercial firms and other government R&D labs which might have creative ideas for rapid advancement of solar high-temperature research and technology, as well as to in-house ERDA experimenters and contractors. The consensus reached during those early discussions was that the construction and operation of large test facilities could probably best be done by an organization with experience and resources for handling such large enterprises (like Sandia) but that an independent Users Association could be more effective in providing liaison among experimenters and facility operators, and in facilitating the use of government-owned facilities by outside experimenters.

To assure objectivity in recommending federal funding of competitive proposals, it was also decided that Users Association membership should be open to persons from government, educational institutions, commercial organizations, and the public, and that its objectivity would be more assured if it were funded independently of the STTF operating organization. Not everyone fully understood or agreed with those concepts but the Users Association is established on that basis and I feel our experience is already proving the concept to be valid.

In 1976, a group organized by Alvin F. Hildebrandt drafted a charter and bylaws and the Users Association was officially organized in April of 1977, in Albuquerque. Hildebrandt was elected President and Chairman of the Executive Committee. Within hours following its election, the Executive Committee asked if I would serve as interim Executive Director and I agreed--initially for a period of six months, just to get the organization started. Within one week following that, we drafted a proposal to ERDA and after the usual two or three redrafts and trips to Washington, a grant was awarded to the University of Houston to fund the first six months operation of the STTFUA and to set up a permanent Association office in Albuquerque.

Much has occurred since award of that grant last June. As most of you know, the office is now established in Albuquerque, in Suite 1507 of the First National Bank Building East, about half way between the airport and the Sandia-Kirtland AFB gate. Many meetings and discussions have been held; and some fairly complex financial, procedural, and administrative issues have been resolved. As examples: the Users Association is now officially a part of the SERI, Golden operation; I have agreed to stay on as permanent Executive Director and have moved to Albuquerque; the Georgia Tech Solar Facility became a fully participating facility with the Users Association in addition to Sandia; we have an operating cooperative agreement with the White Sands Solar Furnace, and with the French Solar Furnace in Odeillo, although formal written agreements have not yet been drafted. Also, by the time this paper is published I believe we will have had some initial discussions with Japanese solar research leaders. Some details of those and other events follow.

Users Association Roles and Objectives

The Executive Committee held its second meeting in June 1977, with representatives of Sandia, Georgia Tech, and the DOE Albuquerque Operations Office, to begin working out statements of roles and objectives and to consider more detailed procedures for management, proposal handling, funding, experiment coordination, etc. A major milestone resulting from that meeting was adoption of the following statement of roles and objectives, which have subsequently been accepted by DOE Headquarters and have become the foundation of the Users Association's operations:

1. To act as the point of contact for Users of the STTFs and as primary access link between Users and STTFs.
2. To solicit and review proposals and make recommendations to DOE regarding utilization of the STTFs.
3. To disseminate STTF information on a regular basis.
4. To provide funding for STTF Users, subject to DOE program approval.

In July 1977, the Users Association leased office space in the First National Bank Building East in Albuquerque, as noted above. The Association also employed Marylee Adams, formerly with the Sandia Solar Energy Projects Department, as Project Administrator. The Association office also has a full-time secretary, Win Rohla.

Another milestone was a decision regarding handling of prospective STTF experimenters, which was made at a meeting at DOE Headquarters in Washington, on July 11, 1977.

Participants in this meeting included Henry Marvin and Gerry Braun of DOE, Jim Scott and Glen Brandvold of Sandia, myself and others. At this meeting two categories of experiments were defined, and the Users Association's responsibilities relative to them were clarified. The first category, large hardware development programs funded and managed directly by DOE Headquarters would continue to be the responsibility of DOE and national labs, with minimal direct participation by the Users Association. The Users Association, however, was given primary responsibility for the second category, generally defined as "all other experiments," including foreign experimenters who wish to utilize the Sandia or Georgia Tech STTFs. These decisions were important since, prior to that time, it had not been entirely clear whether the Users Association would function in an advisory capacity only or whether it would have a more responsible role as originally visualized. The decisions of the July meeting clearly established that the Association would serve as the primary access link through which non-DOE users would gain approval and funding for STTF experiments.

Subsequent to that time, the Users Association has also reviewed proposals submitted to DOE national laboratories and recommended DOE funding via DOE internal Form 189s. I believe this is an interesting and unique situation in which, perhaps for the first time, proposals from universities, commercial firms, and in-house government laboratories are being reviewed by the same reviewers using the same criteria. Only the funding mechanisms differ.

White Sands and Odeillo Participation

During the summer of 1977, the Association initiated discussions with officials of the US Army Solar Furnace at White Sands and the CNRS French Solar Furnace at Odeillo, France. Although we have not drafted elaborate written agreements (primarily because I am not convinced they were necessary or even helpful at the outset), we do have working understandings with both facilities by which the Users Association may fund some experimenters wishing to work on those two facilities. Conversely, prospective US military or foreign national experimenters wishing to use the DOE-funded STTFs in Albuquerque or Atlanta, may be referred to the Users Association. Each party assists the other without imposing restrictions on the normal day-to-day operation of the other party. We understand the funding and scheduling priority requirements of these facilities and, at some time, anticipate that questions will arise regarding publications or patent rights. Initially we expect to deal with those questions on a case-by-case basis as they occur.

The SERI Connection

During the time that the STTF Users Association was struggling through its first few months of existence and attempting to establish its position vis-a-vis DOE Washington, Sandia Laboratories, Albuquerque Operations Office, Oak Ridge Operations Office, Georgia Institute of Technology, University of Houston, the US Army, the French CNRS, and the US Internal Revenue Service, another new DOE solar energy offspring, the Solar Energy Research Institute (SERI), was going through similar experiences. In late summer or fall of 1977, a decision was made which I feel is beneficial to both organizations: The Users Association now reports administratively to SERI, and the Association's future funding will be from DOE Washington to SERI to the University of Houston to support the Users Association. For the past several months we have been working closely with Paul Rappaport, Charlie Grosskreutz and Chuck Bishop of SERI, and in my view our working relationships are excellent. We have a common goal to advance solar technology in the fastest way possible, efficiently and economically, but with as little administrative red tape as reasonably possible--just enough administrative and financial control, hopefully, to avoid serious errors in judgment and rip-offs.

Our new one-year subcontract from SERI is expected to run about $350,000, which will include about $75,000 for support of small experiments directly by the Users Association (actually through University of Houston subcontracts). We understand that an additional $150,000 to $200,000 has been allocated by DOE and SERI for support of more expensive experiments whose funding is recommended to SERI by the Users Association. These larger experiments will be funded via SERI subcontracts to the experimenters or, in the case of DOE national laboratories like Los Alamos or Oak Ridge, 189s signed off by DOE Washington Headquarters.

Experiments and Proposals

Last year about 2,500 bulletins announcing the existence of the STTF Users Association and the availability of funds for STTF experiments were distributed to university, industrial and government researchers, and proposals have been evaluated by the Users Association Experiments and Technical Committee as they were received.

The Committee has recommended funding of four experiments to the Executive Committee, which in turn has recommended funding to SERI and DOE. These four are Aden and Marjorie Meinel of the University of Arizona, George Mulholland of New Mexico State

University, Bob Skaggs of Los Alamos Scientific Laboratory, and J. M. Schreyer of Union Carbide Corporation. The Meinels will consider a reconcentrator for use with one of the heliostats at the Sandia STTF to provide a concentration ratio of about 1000X over a 5" x 7" test area. They will make comparative cost and performance analyses of a system proposed by themselves and other commercially available systems. Mulholland will use the White Sands Solar Furnace to study changes in the strength of concrete resulting from exposure to high levels of solar radiation.

Skaggs and Jean-Pierre Coutures of Odeillo, will run an experiment at Odeillo using solar heat to reduce molybdenum ore. Skaggs and Coutures, who have previously collaborated on such experiments, plan to build a small pilot plant at Odeillo this summer to process kilogram amounts of ore. This will be the Users Association's first experience with international cooperation: Part of the expense of running the experiment will be borne by Odeillo.

Schreyer plans to test a number of high-temperature coatings with favorable absorptivity/reflectivity properties. He also expects to use the White Sands Solar Furnace. Six other proposals are also currently under review by the Experiments Committee.

The Association office is now drafting a somewhat more formal announcement of the availability of funds for STTF experiments. This announcement will probably establish deadlines, perhaps quarterly, for the receipt and evaluation of proposals to allow more direct competition among proposals, better visibility of funds and expenditures, and more orderly scheduling of facility time.

STTFUA Workshops

The first major STTFUA workshop was held in Albuquerque in November 1977. The Association received some very valuable assistance from John Margrave, Vice President for Research of Rice University and Editor/Publisher of High Temperature Science. He identified about 15 or 20 high-temperature scientists who met with STTF operators and managers and other Users Association representatives to consider the current status and needs of high-temperature research and to define some of the types of experimental work which might be undertaken on solar high-temperature test facilities. Mr. Claude Royere and Dr. Jean-Pierre Coutures of the French CNRS Odeillo facility also attended the workshop and passed on much of the valuable knowledge they have gained through years of experience with the French high-temperature solar facilities. A number of

promising STTF experiments were suggested and discussed at the meeting and several STTF proposals have already been submitted as direct products of that workshop. Workshop Proceedings are available through the Users Association office.

A second workshop to explore further the possibilities of using STTF concepts for high-temperature high-energy-consuming industrial processes such as cement making, reduction of metallic ores such as iron or aluminum, carbon monoxide production, or hydrogen production is being planned. This workshop is now being discussed with DOE Washington, SERI, Jet Propulsion Laboratory, and other organizations which have similar interests.

The Sandia 5-MW_t STTF will soon be operational. The tower top and the 42.7-m levels are fairly heavily committed for the next year or two for large central receiver tests, but testing time will be available at the 36.6-m and 48.8-m levels.

At Georgia Tech the new tower in the center of the mirror field will soon be complete and testing of the Sanders Associates receiver will begin shortly thereafter. The facility's schedule does allow room for additional testing during the first several months of 1979.

Instrumentation and control systems of the White Sands Solar Furnace have been upgraded and operations have resumed. Two Users Association-funded experiments will be scheduled on the WSSF soon and additional facility time can probably be made available if needed. In addition, New Mexico State University is completing engineering design studies for conversion of a White Sands 84-ft radar dish to a solar concentrator. If the Army approves and funds the new facility, which will develop 300-325 kW_t on a 6-18" diameter target area, it too can be made available, perhaps next year, for Users Association experiments.

In conclusion, the Users Association during its first year has had some growing-pain problems but probably no more or no fewer than might have been expected, considering that the organization is a rather unique one whose purposes and activities to some extent had to be defined as we went along. At times we are really mysterious. I still give up sometimes in trying to explain to vendors that we are the Solar Thermal Test Facilities Users Association--a part of the University of Houston in Albuquerque--under a DOE contract, working with Sandia and Georgia Tech and White Sands and CNRS in Paris--but reporting to SERI in Colorado. What??

Actually, the timing is good. We should have funded experimenters with experiments ready to go about the time the STTFs are ready to accommodate them.

PROPOSAL EVALUATION AND FUNDING PROCEDURES

Dr. George Mulholland, New Mexico State University
Co-Chairman, UA Experiments Review Committee

Chairman Hildebrandt - Dr. George Mulholland, of the Experiments Review Committee, will talk on "Proposal Evaluation and Funding Procedures." I would like to add that John Gintz, George's co-chairman on that committee, is in Cologne and not able to be with us today. George.

Dr. Mulholland - As Al alluded, these guidelines were formulated by John Gintz with modifications by Frank Smith and myself and there were further modifications yesterday at our Technical Committee meeting. These are the topics we'd like to discuss.

Figure 1 - Discussion Topics

- UA Proposal Funding
- Types of Proposals
- Suggested Proposal Content and Submission Procedures
- Proposal Evaluation and Program Approval Process
- Function of Committee
- Organization of Committee
- Formation of Evaluation Teams

Figure 2 - Objectives

- Provide a Source of Easily Accessible Funding for Small Experiments
- Assist in Funding and Approval Process for Larger Experiments
- Assist SERI in Identifying and Implementing New Test Capabilities

Figure 3 - Funding Gates

- UA Can Approve Directly $5000 Experiments
  - Supplement Existing Funding for University Research
  - Promote Screening and Checkout of "Ideas"
  - Assist Small Users in Proof of Concept
- Can Fund Up To $25K with SERI Approval
- Experiments Over $25K Must Have DOE Concurrence

We have various funding gates, funding mechanisms. The $5000 number, I believe, is fairly loose. As Frank Smith mentioned, it could go up to $10,000, so there is a number somewhere in the neighborhood of $5000 from which the Users Association in Albuquerque can fund directly.

There's another limit which I believe is about $25,000 where SERI has to approve, and then above $25,000, it also has to be approved by the Department of Energy.

Figure 4 - Types of Proposals

- Experiments to Use Solar Thermal Test Facilities to Increase Scientific Knowledge or Engineering Data Base for Solar Applications Primarily
- Experiments to Improve Solar Testing Techniques or Facility Capabilities
- Engineering Studies to Define and Plan Experiments
- Basic Research Leading to Solar Tests
- Other Experiments Which Use Facilities but Are Not Direct Solar Applications (e.g., Astronomy)

Figure 4 outlines the types of proposals; the last two were added yesterday. It is interesting to note that the astronomy-type experiments could use the facilities at night.

Figure 5 was changed quite a bit yesterday. These are the suggested contents or general guidelines for submission of proposals. In other words, any proposal submitted should have these things in it. There is no minimum desirable or extra trimmings on this. All of these items are expected to be in each proposal.

Figure 5 - General Guidelines for Submission of Proposals

1. Technical Objectives - What You Plan to Accomplish and Resultant Data Output
2. Background Information on SOA in this Field of Research and How Proposed Experiment Relates
3. Concise Description of Test Set-up and Solar Test Requirements
4. Brief Statement of Work Experimenter Will Perform Under UA Sponsorship

Figure 5 - General Guidelines for Submission of Proposals (Cont.)

5. Cost Estimate Broken Down by Manhours, Material, Travel, etc.
6. Definition of Support Requirements from Facility--Instrumentation, etc.
7. Description of Total Program, Participants, Funding Level, Phases of Total Program, and Timetable
8. Brief Background and Experimence of Key Personnel (One Page Maximum for Each Investigator)
9. Discussion of Potential Follow-On Phases of Program
10. Rationale for Selection of Test Facility, Experiment Size, etc.
11. Anticipated Test Results

Item 7 was changed slightly--the phrase "Phases of Total Program" implies that some of these proposals are for initiation of research and asking for funding for an initial phase. What we'd like to see is how, in addition to what they want the fund-for, the follow-up research will proceed. We also changed Item 11 since it was pointed out that if the investigator already knew how the test was going to turn out, it would be ridiculous to do the test.

Figure 6 - Functions of Committee

- Evaluation of Proposals
  - Select Team(s) from Appropriate Regional Subcommittee
  - Recommend Action to Executive Committee
  - Establish Priority for Funding and Scheduling of Experiments
- Suggest Facility Capabilities
  - Assess Capabilities Versus Experimenters Needs
  - Recommend Facility Needs and/or New Facilities to Meet Needs

The functions of the committee, then, are to evaluate proposals and also to suggest facility capabilities. The original word "Evaluation" is, in that context, not a good choice since the Users Association is not going to evaluate each facility. I don't think that is within our charge but we probably will make suggestions.

Figure 7 - Committee Organization and Responsibilities

Technical Committee

- Membership
  - Entire Technical Committee, Including Chairman and Members of All Subcommittees
- Responsibility
  - A Review Team will be Selected from the Technical Committee to Review Large Proposals (Requiring DOE Approval); the Reviews will be Submitted to the Chairman, who will Report the Results to the Executive Committee
  - Recommend Facility Improvements at Annual Meeting

Regional Subcommittee

- Membership
  - Association Members Residing Within the Region Who Have a) Volunteered, b) Been Requested to Serve on Proposal Evaluation Teams
- Responsibility
  - Serve on Proposal Evaluation Teams to Evaluate Proposals which Require Only SERI Approval

Priority Review Committee

- Membership
  - All Regional Subcommittee Chairmen and Proposal Evaluation Team Chairmen
- Responsibility
  - Review Proposal Evaluation Reports and Rank Programs According to Priority

We have changed original "General Committee" to "Technical Committee." The membership of this Technical Committee, which is set up to look at large proposals, will include the Chairman and the members of all four Regional Subcommittees. Instead of evaluating all proposals over $25,000, a review team will be selected from the Technical Committee membership to review large proposals, which are defined as those which require DOE approval, and the reviews will be submitted to the Chairman of the Technical Committee, who will report the results to the Executive Committee. The Regional Subcommittee membership will include Association members residing within the region who have either volunteered or been requested to serve on evaluation teams.

Their responsibility will be to serve on proposal evaluation teams to evaluate proposals which require only SERI approval. We also have a Priority Review Committee. The membership includes subcommittee chairmen and proposal evaluation team chairmen and their responsibility is to review proposal evaluation reports and rank programs according to priority.

Figure 8 - Committee Organization

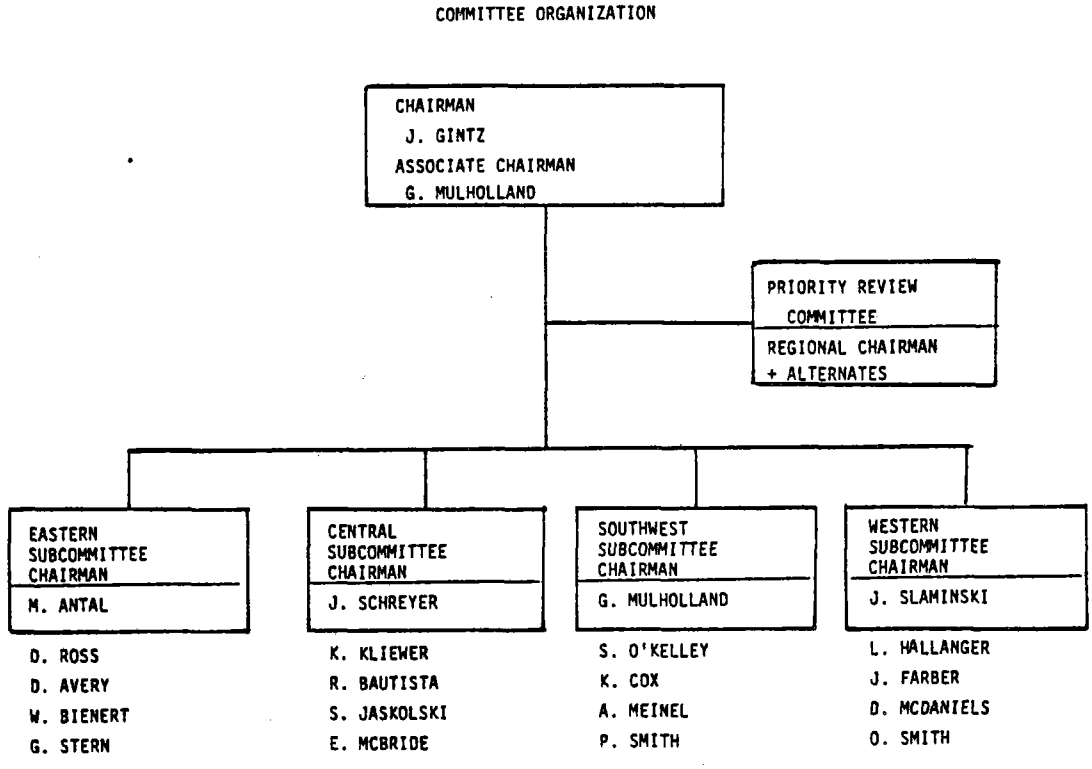

At the present time, this is the make-up of the Technical Committee.

Following is close to what will be the normal operating procedure for someone who submits a proposal. The proposal will be submitted to the Users Association Executive Director's office, which is Frank Smith's office in Albuquerque. The proposal will then be sent to one of the regional evaluation teams for review. After it is reviewed by one of these teams, a report will be formulated by the regional chairman, who will then report the results to the Technical Committee Chairman. He will in turn summarize the findings and submit a report to the Priority Committee, which will rank the various proposals. In turn, those recommendations will be sent to the Executive Committee, which will decide on either a positive or negative recommendation. The

arrows between the boxes signify that at any time in the process communication between these groups is allowed and even encouraged. Hopefully, this process can be achieved in a time frame of 13 to 17 weeks. It should be accomplished within that 3-4 month period because if it gets much longer than that, it's going to defeat the whole purpose, which is to provide accessible funds for small experiments.

Figure 9 - STTFUA Proposal Review Procedure

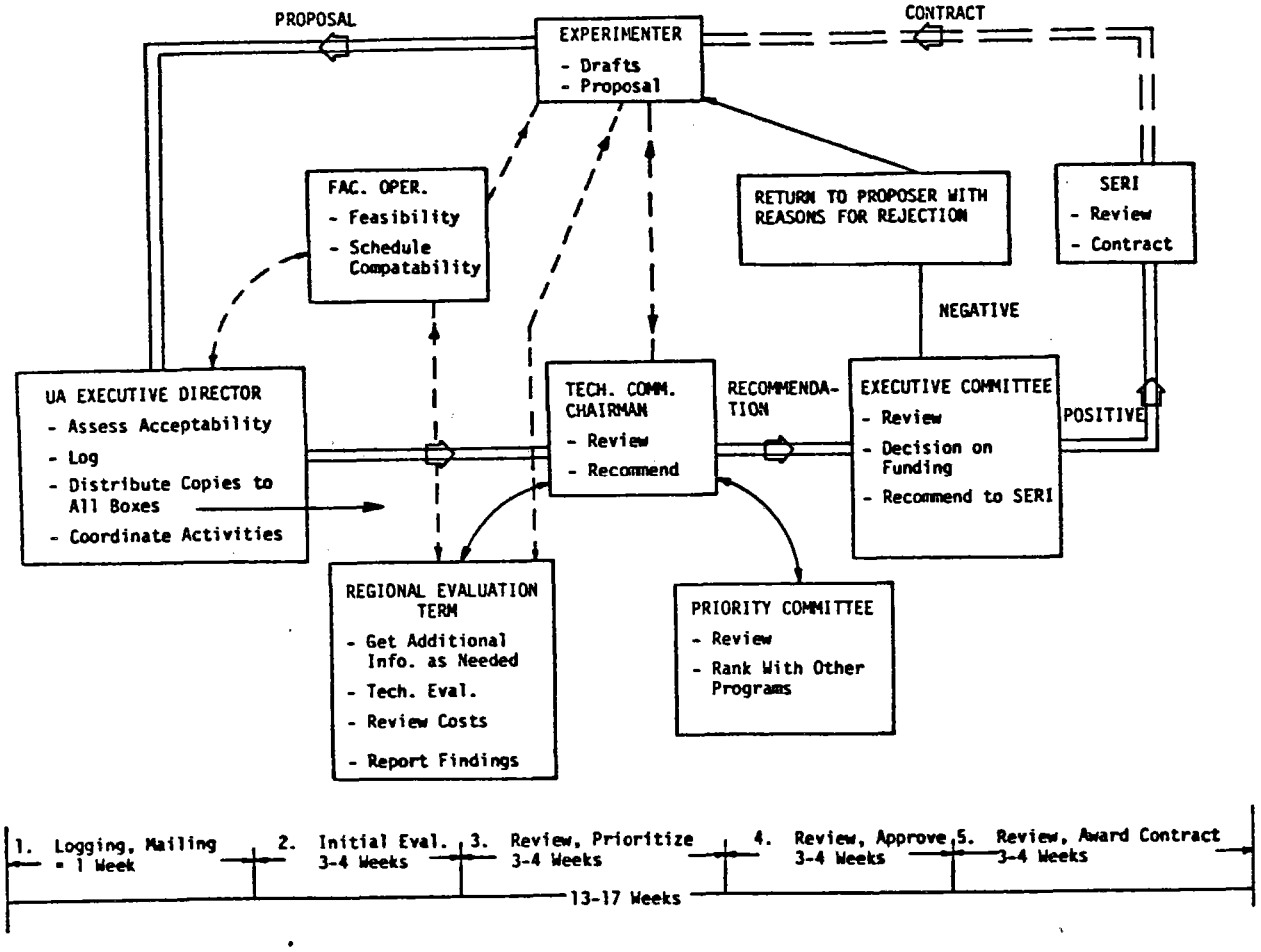

The following figure shows the four regions from which the regional subcommittees are formed.

Figure 10 - Map of Subcommittee Regions

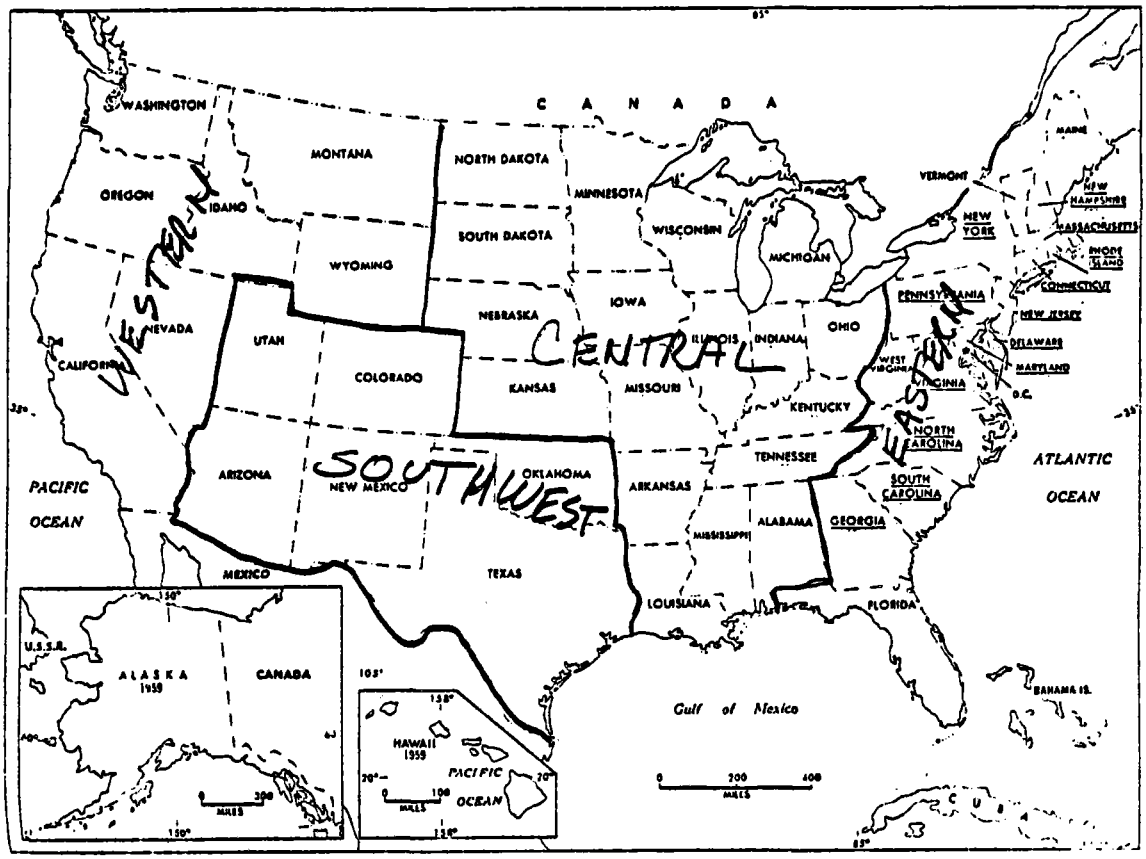

Are there any questions?

Dr. Skaggs - I'm Bob Skaggs of Los Alamos and I want to know what you have done to take into account the difference between the Form 189 and your proposal guidelines. I had to make out the 189 for DOE and it is very specific in its requirements and your guidelines are very specific also. Do you feel that a 189 will be sufficient to satisfy your requirements or do you want someone like myself who fills out a 189 to then fill out another proposal along your guidelines?

Dr. Mulholland - The 189, I guess, is a government form. We don't want ours to be as rigorous as an NSF or a full-scale DOE-type proposal. We'd like it simpler than that but a little more detailed than a 189. I think what we'd like to see in a proposal is minimum requirements which include the items on that list we put up earlier. We can see that in a number of cases those items could be explained with a few sentences or it could take many pages.

Dr. Skaggs - I have another proposal that has been funded so far and as I indicated, the 189 is very specific. There are many places where it overlaps your guidelines. Somebody came back to Frank Smith and he came to me and said, "Would you please expand the breakdown of your funding and the number of people that are going to work on the program," and I see several things on there which I didn't do. For instance, I didn't provide a curriculum vitae of my work experience. Something that's on the 189, though, that I didn't see on your list was what reports I have published that are pertinent to this kind of work. That was included in the 189. I just want to know how much overlap there is and how much of this stuff I have to do separately. In other words, do I have to make duplicates when I submit a second one?

Mr. Smith - Our problem here, as I think you begin to see already, is that what's required on the 189 is normally quite a bit less information than the Review Committee would require to evaluate a proposal competitively with other proposals coming from universities and R&D organizations from all over.

There is an interesting little side light on this, by the way. This has been a source of contention with the universities ever since the beginning of ERDA, that the universities have to put in a 100-page proposal whereas in-house laboratories looking for approval for the same amount of money can put in four or five sentences. I think there may be some exaggeration there. 189s might not be all that easy. In other words, if proposals are going to be reviewed by the same team, you must put down enough information so the reviewers really know what it is you want to do, why you want to do it, what you hope to learn--the usual stuff that goes in proposals--why you think it's justified, and then some detail as to what it's going to cost.

Then, regardless of where it comes from, the reviewers can say, "Yes, we think that's a good idea and worth the money," or whatever. So, Bob, I think the answer is, I don't know any way to avoid it; there undoubtedly will be some duplication. It might be that some of what is in your 189 can be included in the other proposal.

Dr. Skaggs - I'd like to make a suggestion, then, that the Review Committee look over the 189 requirements and their own guidelines and prepare a list of requirements that are necessary in addition to the 189 information for the new proposal.

Mr. Smith - That's possible, yes.

Dr. Cubicciotti - I'd like to criticize the geographical break-up of the committee. I would think it would be more important to have the committees broken down according to technical expertise and the fact that they can't meet together as easily might not be so important as the fact that they could compare notes on the same kind of scientific technology.

Chairman Hildebrandt - We did have a logistics problem originally; there is travel involved and we really tried to minimize the overall impact in our budgeting. There's a considerable component in that area and that was largely the reason we tried to pull regional committees together. But that's a point well taken.

Mr. Smith - Might I clarify one thing quickly? Did I hear Gerry Braun and Marty Gutstein say we're going to fund astronomy experiments? I got that impression anyway. I expect that was news to you. This question came up yesterday and I voiced an opinion which I hope you'll back me up on, that, yes, the facilities could be made available for a worthwhile scientific experiment. I did not imply that your budget would necessarily pay for it.

Chairman Hildebrandt - One comment I'd like to make concerning the Executive Committee meeting we had last night, and we will be discussing that further later on, is on this particular slide, Figure 9. It involves proposals going to the Executive Director, then to the Experiments Review Committee, and then going to the Executive Committee. In our discussion last night, we agreed that it is essential that there be some feedback as far as looking at the budget, the work statement and reworking things. That may be difficult for a Review Committee to do. That is, for the Review Committee to, shall we say, negotiate. I don't think it's the intent of the Review Committee to negotiate a particular operation, and yet something should come forward to the Executive Committee for a decision. That is, it also has to decide on technical merit and overall value, so the Executive Director will be assisting in getting the staff work and the material to the Technical Committee. He also will be virtually in a position to negotiate a posture of trying to clarify issues on the proposals themselves before they go to the Executive Committee. Therefore, the Executive Director should be an ex officio member of the Executive Committee but that wasn't called out here; maybe that's the easiest way to do that. Certainly before the Executive Committee receives the proposal, the Executive Director should have looked at it. We need that input because of the staff work requirement.

Question - Is that necessarily an overall project funding level or does that just refer to the use of the facility? In other words, you could have a DOE contract for, say, $50,000 or $100,000, and associated with that might be $10,000 worth of tests at the facility. Now, how do you distinguish between a large contract like that and a smaller contract?

Mr. Smith - I think the simplest answer to that is, what amount of money would you be asking for from the Users Association? If you have additional funding from some place else, that handles the majority of your experiment and you need, say, only $12,500 to run your test on the facility, then that would be what we're talking about. I might add to that, by the way, that in the case of Sandia and Georgia Tech, the daily operating cost of the facilities is provided already, so you do not need to budget for that. That is not true in the case of White Sands and probably is not true for Odeillo. This is one of the things we still have to negotiate with Odeillo. The costs at White Sands are about $500 a day, which you must pay. The cost at Odeillo sounded as though they are going to run about $300-400 an hour (they are going to tell us).

Chairman Hildebrandt - To clarify that a little bit further, if you had a $100,000 contract, you may have included the test money, but the actual operation of the facility would not be included in money received from the Users Association or the original $100,000. If you were asking about specialized instrumentation that you hadn't originally included in your program, then that would be considered, although I suspect that if you have a totally acceptable program of $100,000, you already had that instrumentation anyway. We're talking here about small experiments, relatively small experiments where you do the program development and the apparatus development and then you take it to the test facility.

Comment - We have already had a case of that where the experiment needed just about $5000; $40,000 or $50,000 behind already. We have already done it. We didn't need money except for that specific small piece, both for travel and so he asked us for that so we built it.

Chairman Hildebrandt - I don't think you want to get in the position that if you have a $100,000 program and then you just need $2000 extra, you have to go through the channels. It can well be made available but not necessarily totally if you already had a program.

Dr. Farber - I'm a little confused. Are you saying if someone gets a DOE contract which already has $10,000 in it for use at Sandia's facilities, that the Users Association is not involved?

Chairman Hildebrandt - If he already has $10,000--what kind of money is available?

Dr. Farber - DOE money funds. I thought the Users Association was supposed to determine the priorities and so forth for those various tasks to be done. Now, if we have a separate source funding these, that's what I want to get clarified now.

Chairman Hildebrandt - I think that there's a program effort, like the central receiver components, where those programs are actually handled separately. We're aware of them but we do not handle the large-scale testing at Sandia.

Mr. Smith - I think your question was, what if you already had a contract for $10,000 to do testing on an STTF? I don't think you're going to have such contracts because Marty and Gerry Braun are going to refer to the UA any proposal they get for that kind of use of the STTF.

Dr. Farber - That's what I'm trying to make sure of; is that true?

Mr. Smith - Well, is that true, Marty?

Mr. Gutstein - We are looking to the Users Association for nonprogrammatic experiments. Where we have a program that involves testing of various components (and they may be small dollars also), but if it's marching along a certain path to achieve particular objectives in a multiyear program, that will be funded separately from the Users Association. Users Association experimenters will use the facilities as well and there will have to be coordination between the Users Association and these programmatic needs and we'll have to do that internally. The programmatic type work will be funded outside of the Users Association. The rest is the Users Association.

Dr. Farber - Suppose you're funding a long-range development on boiler concepts but want to test a subelement which is not programmatic, such as a long-range heat transfer element. How would you handle that?

Mr. Gutstein - If it serves the need of the programmatic thrust, then it becomes a part of a Headquarters program.

Dr. Farber - All of these things are programmatic in the long run; it depends on your perspective.

Mr. Gutstein - Well, yes, but we're looking to the Users Association to get innovative ideas tested early, and perhaps the results of these tests will generate bigger programs in the future. But for now we're looking for the innovation. The facilities may also be used for nonsolar testing and that's another area that's clearly out of our program responsibility. Yet the facilities can be used for testing in other areas and we look to the Users Association to handle that.

Chairman Hildebrandt - Pilot testing, for instance, is programmed and, say, a basic research experiment: photo-optical degradation would be a Users task.

Mr. Gutstein - Right, or perhaps photovoltaics or something.

Question - You mentioned that you were going to set priorities on the various programs that you evaluate. Does that mean you set priorities on all the tests on one facility or do you just set the priorities for those proposals which you evaluate?

Chairman Hildebrandt - The latter. It's more also to evaluate quality than experience.

Question - It appears that the thrust of your program here is for discreet experiments, not incremental funding for other projects which have been funded by other governmental agencies. Is the purpose of the funding to cover the entire cost or just to fund those costs directly associated with the use of a facility so that, for example, if some graduate student at a university had a bright idea worth testing, could you fund their labor and costs back at the university or is that associated with the full expenditures at the facility?

Chairman Hildebrandt - The facility is already funded.

Same Questioner - Are you paying the whole thing?

Chairman Hildebrandt - The facility is funded.

Comment - So you're paying the cost of the project regardless of where it might be done. Another question then is, it appears there is a very large organization with perhaps not too large a budget to spend, and with this type of cycle you're going

through, there is an awful lot of committee meetings and travel. Is the budget for experiments support the same budget by which the whole organization is being run? It appears that you ought to have some percent limit on how much you're willing to spend on the process so that you have some left over to spend on the project.

(Laughter)

Chairman Hildebrandt - You are right. But we're not having any problem getting sufficient funding for the experiments and we're obviously trying to keep the travel component down. The Review Committee members and the Executive Committee members are all volunteer. We reimburse travel expenses only. There is not a huge budget.

I think we should go on now to our next speaker.

MAJOR SOLAR POWER PROJECTS

G. W. Braun
Department of Energy
Division of Solar Technology

Chairman Hildebrandt - Our next speaker, Gerry Braun, I'm sure you all know. I've known Gerry since 1973. He's been in the utility industry and he well understands the real problems that solar thermal experiences in developing. This morning he'll talk to us on "Major Solar Power Projects."

Gerry is in dynamic Washington. The last data was, he's Assistant Director for Thermal Power Systems. I'd be interested in hearing if there are any dynamic changes in the Washington scene, Gerry.

Mr. Braun - Thank you, Al. I would also be interested to know if there are any dynamic changes.

I missed my last opportunity to address this group, but I have been watching the progress of the Users Association very closely and with a great deal of interest.

I want to compliment Frank Smith and the SERI people who have organized this gathering. The turnout is very gratifying and certainly I see some people who are noted by their past contributions to the solar thermal area. I also see some faces that I don't recognize that tells me that the Users Association is really achieving its purpose of mixing people and new ideas with the people who understand where the program is right now.

I'd also like to add my welcome to those who have traveled here from abroad. This response is also very gratifying. I think we have much to learn from the work that is going on overseas, especially, in the case of the French effort that's been there ahead of us. I was pleased to have the opportunity to visit and tour the French experimental facilities earlier this year and was very much impressed by the quality of their effort. Indeed, there are some aspects of the experience there that directly bear on the Users Association and its objectives.

It's interesting to note that I have been on board with ERDA and DOE roughly one year and that really is also roughly the period of time that the Users Association has really been on its feet. I hope that all of you who have been a part of the Users Association have arrived at the same state of enthusiasm that I have about the solar

thermal power program and what we can accomplish both in the program and in the course of experiments that are not directly tied to it.

A question comes to mind that I faced recently when my wife was looking over my itinerary for this trip. She gave me a kind of strange look and said, "What is a Users Association?" I wonder how many of you have had to answer that question. I'd like to know what some of the answers were.

In return, what I'd like to do for you here today is to respond briefly to Al's allusion to what has transpired in the last year back in Washington. Then I'll use the topic of "major projects" as a way of giving you a brief overview of the solar thermal program. Finally, I'll come back to some of the challenges that I see for the Users Association. Certainly the indication from the discussion that has just transpired is that there are some very important issues ahead. And, certainly the Users Association, as all organizations having a role in solar programs, needs to be a very dynamic, very flexible and indeed very adaptable entity. I can see ahead an evolution of the use of the facilities and that certainly will stimulate an evolution in the structure and character of the Users Association, as the potential and progress in the various applications of high-temperature solar heat become apparent and R&D programs get underway.

Certainly the recent birth of DOE has brought with it a period of great excitement and, I think, a very beneficial period of ferment and of questioning. Of course, not all of the questions were welcome, but by and large I would say that the net effect has been very beneficial to the solar effort in general, and certainly to the solar thermal effort. If I had to characterize what I think has resulted from this transition to DOE, I would name two major things: First, we have, I think, had an opportunity to follow up on what I'm sure was the original and long-standing intent in the solar program leadership to really focus on the near-term potential. That hasn't necessarily been the way solar has been categorized in the minds of the management of the energy programs in the past, but with DOE coming into being, there has been encouragement and, indeed, an insistence on a near-term focus. That really has had quite a good effect in turning us toward some programs that were merely a gleam in our eye a year ago and to seeing how they fit into a strategy that brings the various solar technologies to the point of having an impact in the next decade. We are fitting these new thrusts into a logical sequence of development that leads to a major impact beyond this coming decade.

The DOE outlook toward solar is very much an opportunistic view, looking at the regional opportunities, the dispersed character of solar energy, tending away from the former thrust toward a single big fix in the national energy programs, i.e., some single thing that the country could spend billions of dollars on and that would solve all of our problems. I have to say personally that I think the opportunistic, near-term focus is very much a beneficial strategy from the point of view of solar.

In the solar thermal program, we are turning toward programs that tend to pull the technology out into the real world as soon as the technical homework has been done. As practiced in other programs, this "market pull" approach involves solicitations that invite industry and user participation on a cost-sharing basis in establishing multiple experiments. I think solar thermal technology is in many cases nearly ready for this.

Now let me turn to the major projects.

What I would like to do is give you a view of the solar thermal program. In dealing with the major projects, of course, I'm at liberty to define major projects any way I want, which then lets me talk about the program any way I want. I should point out that the major projects in the solar thermal conversion area that are already ongoing or that have been completed represent an investment on the order or in excess of 200 million dollars. These are the projects I will mention specifically today.

They fall largely in the two applications subprograms under solar thermal. The overall program is split into three subprograms. One program aims at the small-scale dispersed, or on-site applications. The other program relates directly to utility or large-scale applications. In each case, embedded within these programs is the technology that has been determined most promising for the scale of application. In the case of utility scale systems, the central receiver system can be scaled to the requisite large module sizes. The distributed receiver technology and related subsystem development is embedded within the dispersed program. Two major efforts are underway here, one dealing with linear focusing collectors and the other dealing with dish-type collectors, including both stationary and movable dishes.

The advanced thermal technology program is, as you know, the home for the Users Association, the advanced applications of solar thermal, those that in truth I hope will ultimately realize the full potential of having a clean, extremely high-temperature heat source. That, of course, is the research edge of the program where

we're looking beyond those technologies that can be incorporated into systems today and with which you can go out and build an experiment and operate it in connection with a clearly defined application.

I don't like to dwell on budgets, but I would like to give you a size and shape of the program and where the emphasis is, if indeed you can measure that in terms of budget. We are at a level in FY 78 of roughly 100 million which, with the President's request in '79, will remain at roughly that level.

The split in the technology development area represents a fair balance between programs aiming at dispersed applications, the total energy approach, small electric power applications, small community applications, and related technology and programs aiming at the large-scale central and utility applications based on the central receiver development.

In summary, you will find a split in R&D money of roughly forty, forty and twenty percent in the central, dispersed, and advanced technology areas, respectively, with a major separate item for the construction of the 10-MW pilot plant at Barstow.

One way of giving you a sense of where the program stands is to indicate what we expect to accomplish in 1979, leaving out the expected accomplishments in the advanced technology area. That is a relatively new program and Marty Gutstein will have an opportunity to review that with many of you at the upcoming semiannual review. I will focus on the major projects which tend to fall in the dispersed and central areas.

In the dispersed applications area, we have three major total energy projects underway at an individual scale of roughly 200 to 300 kilowatts electric, and a commensurate related amount of heat production. All of these are in the preliminary design stage and I will deal with each of them separately as we go along.

We have in operation an irrigation pumping experiment at Willard, New Mexico. The second irrigation experiment will be coming on line at Collidge, Arizona, in '79.

We'll also be selecting a site for a 1-MW small community experiment of a design to be determined as a result of a conceptual design effort that is now underway with three contractors working in support of the JPL-managed effort in that area.

In the central power area, a major turn toward the retrofit applications of water/steam central receivers is something that we hope to make and, in fact, are making, with the Barstow 10-MW project serving as essentially the technology underpinning for what has come to be known as repowering; repowering involves taking a central receiver and integrating it with an existing oil- or gas-fired power plant.

We would also expect to be in support of the small central receiver Brayton hybrid power plant that the Electric Power Research Institute has in their plan and likewise continue several other central receiver related efforts, covering storage-coupled and hybrid systems, as well as the basic development of low-cost heliostat and receiver designs for both advanced concepts and for water/steam central receivers.

And the Barstow project, last but certainly not least, is well underway now and has cleared some of the problems that came up recently. There appear to be no clouds on the horizon in terms of getting that critically important project fully underway.

I would like to briefly discuss some of the projects starting in the dispersed area and then going to the central area and finally to the major test facilities supporting all three areas.

The first major system experiment that we have in place is a 25-horsepower irrigation pumping experiment at Willard, New Mexico, which was completed in mid-'77. I should say that the pumping system covers an irrigation area of roughly 100 acres of potatoes--I say potatoes, because I've eaten some of them--but I can't remember what else; two or three other crops that are served by this shallow well pumping experiment. It is a parabolic trough concept which powers a small organic Rankine engine. It's being expanded to 50 horsepower to allow the system to power a center pivot system. I would like to say that this has provided the high point of the year, in that the collector cost experience related to this project has been very encouraging. We're at a point of around $20 a square foot on the trough-type collectors, based on the bids that have been received on the expansion of the facility. That is certainly gratifying, given that it is roughly two or two and a half times above our goals for this specific collector type. I hope that we can bring the heliostat cost experience to a similar point very quickly.

There is also a second-generation irrigation experiment that will be completed in FY 79 at Coolidge, Arizona. It is roughly a 200-horsepower system for a deep

well as opposed to the Willard system which powers a 75-foot head pump. Again, the parabolic trough approach is employed, with some improvements in all of the subsystems. It represents an opportunity for us to take the next step, having cut our teeth on the Willard experiment.

The next set of projects that I'm going to discuss briefly all have to do with the total energy program. This particular experiment is not a solar thermal total energy experiment but rather a photovoltaic total energy experiment that has found a home in our total energy program. It will be located at the Mississippi County Community College in Blytheville, Arkansas, with a net electric capability of roughly 250 kW. It will supply heating and cooling to the classrooms as well as the electric power requirements. This project is being funded as a grant to the college. I believe the grant amount is in the neighborhood of six million dollars and, in fact, this experiment has had the interesting aspect of causing us to question the schedule on the two solar thermal total energy experiments. In fact, we have pulled the schedule up tight on both of them by somewhere between six and ten months as a result of the simple indication that this experiment seemed to be able to be completed some time at the turn of '79 and '80.

There is also a planned total energy experiment at Shenandoah, Georgia, that is being funded as part of a cooperative agreement with the Georgia Power Company. This is a similar size experiment but with parabolic dish-type collectors driving a thermally activated total energy system. The application is also different in that it is a knitwear manufacturing plant.

The concentrator concept for the Blytheville photovoltaic experiment was a Fresnel reflector. So, we have in these experiments a combination of different applications for total energy, different technical approaches, but roughly the same scale.

The project that had the earliest start in the total energy area is a total energy experiment to power a part of the barracks complex at Fort Hood, Texas. In this case, a trough-type collector is applied to a system of similar scale roughly 200 kW electric output. We have reached a point where we have sized the collector field to roughly 125,000 square feet, which gives the optimum combination, at least at present costs, of electric and heat production.

Now, something that is easy to talk about and something that I'm sure many of you have followed closely as it has proceeded, the 10-MW central receiver pilot plant.

Let me try to bring you up to date, and for those of you who have not followed closely, I'll try to start at the beginning. In 1975 an effort was initiated to develop a conceptual design for a 10-MW water/steam central receiver pilot plant. Three parallel system design studies were initiated and, in addition, a fourth study to develop heliostats as a separate effort.

These efforts lasted two years and involved both the conceptual design development and proof experiments on all of the major subsystems, including tests of five different heliostat concepts, three receiver concepts, and two thermal storage concepts, all of which, I might add, were successful. Indeed, the whole effort on Phase One was very, very well done by the contractors involved and produced, I think, an excellent stepping off point for the central receiver program and certainly some confidence that has been the basis for the thrust toward repowering in the near term.

In this case, the system configuration selected was an external receiver configuration with a surrounding field of heliostats. Going back to some of the key dates, the site was selected in January of 1977, having been proposed by a consortium from the State of California involving two major utilities and the state energy office. The concept selection was reached in August 1977. We did have a period late in 1977 where we were asked to review the project in the context of the DOE mission. As you know, DOE came into being around October 1st and Secretary Schlesinger asked for an opportunity to review this project among several others. I'm happy to say that that review was favorable to the project and the project is now underway. We did, during that period, have an opportunity to review the schedule for the project and proposed a new schedule against what I think many had earlier felt was perhaps an unrealistic target, to get the plan on line in December of 1980. The review that took place in late '77 leaves us now with a firm 1981 operational date for the Barstow project.

I think that's a good lead-in to discuss the three major test facilities.

The type of receiver that was selected for the Barstow 10-MW project is simply a panel of closely spaced boiler tubes extending roughly 50 or 60 feet in the linear dimension and a little over 3 feet in width. This panel becomes the first test object in direct support of the central receiver development program that will make direct use of the central receiver test facility at Albuquerque.

One of the things that we are learning as we gain experience is to define a little better what we mean by our data. The initial commitment was to have the

Albuquerque central receiver test facility complete, whatever is meant by "complete," in December 1977. It would appear that the first test operation of that facility will be more like mid-July, with the period between December and that time needed to fully check out the facility and to set up the initial experiments.

Every photo that I have seen of the test facility, until the most recent one that I just saw, had a crane hanging over the top of the tower and I know with it gone that there's some sense of near completion on the construction, although I do understand that there are certain odds and ends being tied up.

You may not be familiar with another project, the solar total energy test facility for distributed receivers and arrays and midtemperature subsystems that is also at Albuquerque. The original parabolic troughs are still in place, as is the original storage area. There is also a new storage subsystem now in place. There is also a terminal building housing a small, organic Rankine cycle turbine and a 100-ton absorption cycle chiller. There are also additional arrays and collectors, a SLATS-type collector and a fixed mirror. The fixed mirror has a concrete substrate with the receiver being the moving element of the concentrator. This facility now becomes a working facility, having given us the experience with array operation and the system integration. It now becomes a place where we can do very essential work to improve the components and subsystems in the context of a working system. So this, then, becomes an opportunity, hopefully, in the true sense of a user facility, to incorporate the next and the next and the next generation of subsystems, of improved subsystems, of lower cost subsystems, of higher performance subsystems, and helps us obtain the operating data that is needed to identify what improvements are cost-effective and what are not.

The 400-kW_t Advanced Components Test Facility at Georgia Tech is the place where the advanced technology subprogram does its high-temperature receiver and subsystem development work. I might add that if you look at the three test facilities I have discussed, you'll notice that for each of the three major programs in the solar thermal area there is one test facility that by design serves the specific need of a place to do the technical homework of that particular program.

In the case of the Central Power Program, it is the central receiver test facility at Albuquerque. In the case of the Dispersed Applications Program, it is the midtemperature distributed receiver facility also at Albuquerque, and in the case of the Advanced Technology Program, it is the Georgia Tech Advanced Components Test Facility.

Of course, there will be additional test facility needs--JPL has a need for some capability to test individual modular dish-type configurations, and certainly SERI is actively exploring their needs for facilities in support of thermal research.

Let me turn now to a perspective on some of the things I have talked to you about. If you look at the major projects, they fall into two categories. Certainly the test facilities are one major category. Really, the test facilities are the leading edge of any technology development program such as this. They represent the place where there can be an interaction between the industry and the program, in a way that takes some of the risk out of the component development and provides the technology that feeds into the applications programs.

I think most of you are engineers and probably can relate very well to the need for the system experiments involved in the major projects that I have described. It's very difficult sometimes to say why you have to build a system. However, I think we can go back in the experience we've had in these projects, even to date, and point to the tremendous catalytic effect of forcing together the people who really know what they're doing. When you face someone with the prospect of having to build something, he's forced to go find the people who really know how to do it and to get them involved. That is one very important reason for these major projects, but also really as the step that is necessary to provide the confidence, the assurance that users and industry need to make any commitments to what we would categorize as the initial commercialization or the initial implementation of these technologies. Unless the concept exists as a working system that is representative of how that system would be applied, there will be no commitment of private capital to build such things. So, I think the major projects are very important to any program, particularly in the solar thermal area. We've had the benefit of having gotten started in this kind of activity very early and I think we're in a very good posture relative to some of the other solar programs as a result.

Let me finish by offering my own personal perspective on the Users Association. In terms of the test facilities that directly support the solar thermal program, there is certainly a tremendous investment of dollars; they represent very powerful tools. Certainly, as the capability of the DOE facilities is demonstrated, they should prove to be very powerful tools to accomplish things that can be accomplished in no other way. The striking thing, however, is that each facility, no matter what its origin or original purpose, has very unique capabilities. This certainly raises a challenge, I think, for the Users Association. There really is no real model for this

group. You can't just say there was a major facility, or we can look to the French experience, or there was a major weapons facility that is like these facilities. There are no direct analogues and I really think that poses a big challenge for this organization to deal with the facilities and their uniqueness.

In the case of the Albuquerque facility, that is one that was designed specifically to test subsystems of central receivers. However, to satisfy that design objective, there are really excess capabilities in that facility. How to use those excess capabilities is an issue. Those excess capabilities may not be exactly what you want for the expanded R&D in that facility, but we must search out the opportunities that are there in order to use that tool.

I would like to just also say that there has been some discussion here this morning in terms of what should be the strategy for the Users Association. I simply want you to keep in mind in these deliberations that from the point of view of the solar thermal program, whether or not the work that can be accomplished at these facilities is in direct support of the solar thermal program, we are fully committed to see these facilities used as broadly and as effectively as possible. We certainly have a full schedule of programmatic experiments lined up, but there's no ambivalence whatsoever about our desire to have the Users Association really catalyze the multiple use of these facilities. We certainly want to encourage, as Frank has mentioned, the experiments that might be coming from abroad. That, of course, is not an altruistic type of thing. We can certainly learn from the work that is brought here to use the unique capabilities of the facilities in the United States. Certainly from the point of view of the solar thermal program, it's very gratifying to see other countries actively in pursuit of this technology. Ultimately it has to get us all there sooner than we would get there if only one country were pursuing solar thermal conversion.

You may have some question about my raising the specter of a DOE mind set on near-term applications. Let me say this: I see no inconsistency whatsoever in the near-term focus in the applications programs, to pull the technology that is ready, out of the laboratory and onto the street, so to speak. You would hope that if we do that successfully and quickly, that the central receiver and the low-cost concentrators will be available, the heliostat costs will be where we think they can be, and the dish costs will be where we think they can be and so on. This, then, would suggest that what we, in anticipation of that success, ought to be doing now is developing the technology that takes advantage of that and broadens the application of that concentrator technology.

We ought to be really doing the homework that anticipates that indeed heliostats will come down to $10 a square foot and dishes will come down to $10 a square foot and look at how to prepare for a broader use of this technology beyond electric power plants and beyond small total energy systems and what have you. Certainly we all as engineers take it for granted that what we're doing is useful and worthwhile, but we do tend to have a communications problem in explaining to people why we're doing what we're doing. I would hope that the Users Association would be sort of a window on the world for us in getting the word out that there are opportunities, that there is a tremendously versatile capability here represented in a high-temperature solar heat source, and that we should be pursuing that. The Users Association can provide a focal point for the interest that is probably out there but which we as engineers in the past have perhaps neglected to stimulate.

There is no excuse for us not to fund good proposals. As you can see from the size of the budget that I disucssed, we would be very hard pressed to say that we can't afford to fund something that comes along that is really worthwhile.

I'd like you all to keep that in mind and I am certainly very happy to see this turnout and to have had the opportunity to talk to you this morning.

Chairman Hildebrandt - I'm sure we all appreciate those encouraging remarks. Would you answer a question or so?

Mr. Braun - If I can.

Question - What do you consider as the next major large-scale project? One would be the retrofit, the 100-MW, and then there's the super higher powered system. Have you established any forecasting projections at this point?

Mr. Braun - One thing that I didn't want to discuss as part of this presentation was the sense of new thrusts in the coming year because, of course, they are not well defined and there is also a budget cycle going on at this point. However, let me just say that in the central area, clearly the thrust would be on the retrofit applications, leading hopefully to projects that would repower existing power plants in late 1982 or 1983 at a scale of, say, 25-50 MW. Of course, there would be a necessity to develop the heliostat production capability in parallel, and that, of course, also could be looked at as a major project.

Following on directly, looking at repowering as something of an entry point for central receiver technology, there is a need to continue the development of storage-coupled systems and to explore the possibility of hybrids. I did mention the EPRI experiment related to hybrids. I would hope that in FY 79 we would begin to look at conceptual designs for full-scale modules, not necessarily full-scale power plants but full-scale modules of commercial power plants. In fact, we must identify the best approach, whether it's water/steam or not, and the intrinsic modularity of the different options. A sodium receiver-type system might have a different modularity than a Brayton cycle central receiver, and so forth.

In the dispersed area, the near-term thrust will be to assist the emerging industry, the parabolic trough industry, perhaps even to pull the central receiver down to the scale for dispersed applications. We hope to initiate at least one major experiment on the scale that I talked of in the dispersed program, to apply a central receiver to perhaps a total energy application and initiate that in the near term. I would say that the major thrust in the dispersed area would be to open the program to proposals from industry and users for specific applications, specific systems. We could essentially be driven by that interest as opposed to specifying a certain kind of system.

Chairman Hildebrandt - Thank you very much.

III. SESSION II-A: SOLAR FACILITIES

THE CNRS ODEILLO 1000-KW_{th} SOALR FURNACE UTILIZATION

C. Royere, Responsable du Service Traitements de Materiaux
Laboratoire D'Energetique Solaire
BP 5, Odeillo 66120, Font-Romeu, France

Background and Preliminary Remarks on the Meeting*

A previous international seminar,(1) sponsored by NSF and organized by New Mexico State University, was held in November 1974, near the White Sands Solar Facility. The main objective of this international seminar on large-scale solar energy test facilities was to share the experience and knowledge in conception, design construction and operation of this type of facility with representatives (designers and operators) of the existing facilities. This exchange was to help in the development of a 5-MW_{th} STTF of the central receiver concept for testing components of large electricity generating solar power plants.

All the facilities existing and operated at that time (but one: the Algiers, La Bouzareah solar furnace) were represented: the Montlouis 50-kW_{th} solar furnace (1952, CNRS, France); the Natick then White Sands 35-kW_{th} solar furnace (1958, 1973 US Army, USA); the Sant Illario central receiver-type 100-kW_{th} facility (1961, University of Genoa, Italy); the Sendai 40-kW_{th} solar furnace (1963, Tohoku University, Japan); the Odeillo 1000-kW_{th} solar furnace (1968, CNRS, France); and the Odeillo 42-kW_{th} solar furnace (1971, French Army LCA, France).

This time DOE sponsors two workshops organized in Albuquerque by the STTF Users Association through the University of Houston. Since 1974 two new US facilities have been completed and join the Club of the STTF: the Albuquerque 5-MW_{th} STTF (1977, ERDA/DOE, Sandia Laboratories) and the Atlanta 400-kW_{th} STTF (1977, ERDA/DOE, GIT), plus a Japanese STTF (Mitsubishi). Additionally, different projects of electric solar pilot plants are set across the world in the US, in France, in the EEC and among IEA. In some way the massive use of concentrated solar energy is started. This is very encouraging for the few who pioneered some approaches in this field--in some cases a long time ago.

*This paper was not ready in time to be published in the Proceedings of the November 1977 Facility Operators/High-Temperature Sciences Workshops held by the STTF Users Association.

(1) Large Scale Solar Energy Test Facilities Proceedings, edited by H. L. Connell, PSL, National Science Foundation International Seminar, New Mexico State University, November 18-19, 1974.

The meeting today is devoted to an operators workshop (to develop the exchange of experience in operating and characterizing of the existing facilities) and to a high-temperature workshop (to share the experience in the use of these facilities and promote further utilization through a comprehensive reciprocal exchange between the specialists in the two fields). To some extent this meeting could be considered as an extension of the 1976 Houston meeting[2] which was limited to US participants.

As far as participants are concerned, it is very important to notice that there is among them a very high level panel of high-temperature scientists. It is worth noticing because such specific meetings bringing together solar and high-temperature experts did not occur very often in the past. On the other side, unfortunately, we are missing representatives of some solar facilities--we are not yet so many that hopefully next time we should all be together.

Introduction

The purpose of this paper is to summarize and update for the reader the contribution of France in the utilization of large solar furnaces which are a category of STTF. I should rather say CNRS because although, in the short period of time allowed, I have devoted part of my presentation to some slides and explanations of the French Army LCA Odeillo facility (42-kW_{th} solar furnace) since their representative could not participate in this meeting, it would be beyond the scope of this paper to cover it adequately (a separate paper would be more appropriate).

French CNRS Solar Furnaces

F. Frombe and coworkers in France, with the support of Centre National de la Recherche Scientifique (CNRS), have pioneered and developed during the last 30 years thermal uses of focused solar radiation successively in Meudon, Montlouis and then Odeillo. The main milestones along this long venture have been the development of small laboratory scale solar furnaces in the power range of 1 to 2 kW_{th}, the construction in 1952 of the Montlouis 50-kW_{th} bench model solar furnace and in 1968 the completion of the 1000-kW_{th} Odeillo performance prototype solar furnace.

(2) Report on the Symposium and Workshop on the 5-MW_{th} Solar Thermal Test Facility, May 17-19, 1976, Houston, Texas, ALO/3701-76/1

Details of the history of this effort and the characteristics and performance of these facilities are presented elsewhere.(3),(4),(5),(6),(7)

First, we have to start with a review of the main characteristics of the point focused solar energy; then it is possible to look at the past and present uses of the Montlouis and Odeillo facilities, draw some conclusions and set some prospects.

Point Focused Solar Energy as a Process Heat Source

From a general point of view, point focused solar energy can be considered as a renewable source of heat in some range of temperatures. With this kind of very broad approach, it is possible to envision this energy as a source of process heat for widespread chemical processes and as a heat source for thermodynamic generation of mechanical and electrical energy through conversion cycles. In this case, the difficulties to overcome are very serious: capital cost for collection, discontinuity of this energy source, and, to some extent, a limited amount of power available from one unit facility. All of these factors contribute to the cost of the kwhr thermal and electrical which have to compete with conventional well implemented and used to energy sources. However some similar problems were already solved in Britain and other countries in the 16th and 17th centuries when coal slowly replaced wood and charcoal.(8)

Point Focused Solar Energy: Specific Characteristics

The second possible approach of point focused solar energy consists in being more specific and in trying to take the best advantage of the most peculiar features of this energy. It is well established and the fact is thoroughly documented that point

---

(3) Les Hautes Temperatures et leurs utilisations en Chimie, P. Lebeau, F. Trombe, Masson et Cie - Paris 1950

(4) Applications Thermiques de l'Energie Solaire dans le domaine de la recherche et de l'industrie, Montlouis 23-28 Juin 1958, Colloques internationaux du CNRS, CNRS Paris 1961

(5) Les Hautes Temperatures et leurs utilisations en physique et en chimie, G. Chaudron, F. Trombe, Masson et Cie Paris 1973

(6) Les Fours Solaires et les Fours a Images, Journees d'dtudes Odeillo Font-Romeu, 1-2 Octobre 1971, Revue Internationale des Hautes Temperatures et des Refractaires, 1973 t.10 n°4

(7) The French CNRS 1000KW Solar Furnace: description, performance characteristics, present utilizations and perspectives, F. Trombe, A. Le Phat Vinh and C. Royere, op.cit. (1)

(8) An Early Energy Crisis, Scientific American, November 1977

focused solar energy is a source of heat for medium and high temperatures, let us say in the range of 1000°C up to 2700°C and higher with the following specific characteristics coming from the fact that it is thermal radiant energy which allows to achieve:

- medium and high temperatures
- processing of material at these temperatures without any contamination of the processed material either by the source of heat itself (radiant heat) or by the support (self-contained technique, water-cooled supports), thus giving the possibility of elaborate very high purity materials, or with controlled impurities, without any pollution of the environment
- high reaction rates by increasing the temperature and using most of the time liquid phase
- processing under oxidizing atmosphere at any temperature and particularly under free air without concealing the possibility of controlled atmospheres; both capabilities are very useful for ceramics and metallurgy
- high efficiencies since it is a matter of thermal applications without thermodynamic conversion
- thermal cycles of a very wide variety (energy without inertia, being able to be pulsed in many different ways)
- physical measurements in the absence of intense magnetic fields (microwave transmission measurements)
- high spectral energy densities (photo chemistry and photovoltaic conversion).

All (or nearly all) of these advantages belong to generally so-called imaging techniques. The difference in the case of point focused solar energy is that it can be extended to high ranges of thermal power with good efficiencies and simultaneously provide impinging radiant energy on large areas (or volumes) with fairly uniform flux distribution, avoiding if necessary high thermal gradients.

Solar Furnace Utilization Demonstration: the 50-KW_{th} Montlouis Furnace

The Montlouis furnace (Figures 1 and 2) has been a simple and efficient model of a large furnace. It has been used extensively by Trombe and coworkers for about 15 years since 1952 after completion to explore the possible fields of applications of large solar furnaces. This task was performed in tight connection with basic studies using small solar furnaces (consisting of 1.5 or 2-m diameter fixed searchlights with single heliostats).

The utilization of this furnace has been developed in two ways: applied research or pilot scale experiments and processing on an industrial basis.

Batches up to 100 kg at a time could be processed and more than 10 tons of zirconium oxide have been sintered and stabilized at high temperature for the French industry of refractory ceramics in the late fifties.

The different fields of explored applications cover a large number of uses of solar furnaces:

- high-temperature oxides and ceramics: sintering, melting, synthesis, purification on an applied research or pilot scale experiments and industrial processing basis
- ore processing: decomposition, oxidation, roasting, reduction, volatilization
- metallurgical processes
- thermal shock resistance studies of materials, oxidation studies and ignition under high flux densities of thermal radiant energy.

All of the results and techniques developed in the course of these programs with the 50-kW_{th} Montlouis solar furnace are described in many specific articles and the reader may find a good background and much information in (4).

It is worth noting that in each case attempts have been made to evaluate the competitiveness of the studied solar processes versus processes based on nonrenewable energy sources.

At that time, in the fifties and early sixties, the situation in the field of energy was such that the only fields where competitiveness could be demonstrated were those of refractory ceramics, refractory alloys and thermal shock studies on materials for very specific uses: finally the range of applications in which the specific characteristics of point focused solar energy can be uniquely developed and applied.

These conclusions have been a basis and guideline for developing the utilization and application of the Odeillo 1000-kW_{th} solar furnace.

Solar Furnace Utilization Demonstration: The 1000-kW_{th} Odeillo Furnace

Montlouis 50-kW_{th} and Odeillo 1000-kW_{th} Solar Furnaces performance comparison: general overview --

The first evident difference between the two facilities is the power level--the step is from a bench model in Montlouis to an industrial scale facility. The Odeillo furnace has a power capability comparable to that of a high-frequency furnace in industry.

Due to a significant difference in optical aperture D/f, Montlouis (D/f = 10/6) was limited to 3000°C and practically to 2700°C and Odeillo (D/f > 54/18) (Figures 3 and 4) has the capability of 3800°C (1600 W/cm^2), practically more than 3200°C (thoria is melted at a rate of about 20 kg/hr). Another major difference is that Odeillo delivers high radiant heat fluxes on large areas (total power within a diameter in the focal plane of about 80 cm) allowing testing of large bodies of materials. In connection with this, the maximum of the flux density at the focus is rather flat along the focal axis (nearly constant irradiance despite thermal shocks, spalling, sintering, ablative effects), see Figure 5.

A final advantage of Odeillo versus Montlouis is that of a multiheliostat facility versus a simple one which provides the capability of adjusting the power level and the flux density distribution over shapes under test in the focal zone, Figures 6 through 11.

General considerations on the use of the Odeillo 1000-kW_{th} facility --

The Odeillo furnace is a multifaceted facility: 11,340 pieces of flat mirror 50 cm square on the 63 heliostats and a little over 9,000 mechanically bent tempered glass mirrors on the 54 x 40 meter parabola, Figures 12 and 13. All of these individual mirrors have to be aligned after installation to reach the nominal performances with the furnace. The auto collimation method using a theodolite has been used for the facets on the heliostats and a sun imaging technique to get the proper alignment and curvature on each facet of the parabola. It takes about 15 minutes for one operator to adjust one facet on the parabola and about 9 minutes for aligning one facet on the heliostat. That is to say, 6 man hours per square meter of heliostat and a little bit over 1 man hour per square meter of parabola. These figures can, interestingly, be compared with the present and projected costs of heliostats, Figures 14 through 19.

By chance, these adjustments are fairly stable over long periods of time providing one facet is not shifted to another place during coating maintenance operation (in the case of heliostats).

The general annual maintenance of the facility concerns hydraulics and mechanics (500 man hours per year), optics and electronics (100 man hours per year). All these tasks can be performed nearly without any interference with normal operation of the facility.

After 10 years of operation, on-site weathering effects are very noticeable on the coatings on the backs of the mirrors on the heliostats, Figure 20. In Montlouis the facet coatings are still in very good shape after 25 years. This lifetime is in direct connection with the quality of varnish and paint used to protect silver and copper coatings. The main origin of the degradation seems to be erosion (wind, dust particles, rain, snow). Hardness might be the most prominent property to check for characterizing coatings among all the other standard tests performed presently.

We are just in the process right now of recoating all the facets on the heliostats with new coatings which have been tested for more than 18 months in the laboratory and seem to be able to last over 25 years.

Recoating flat polished glass of the original mirrors is more interesting than buying new mirrors made out of float glass. Financially there is a factor of 2 on the cost and technically there is a factor of 4 to 5 on the dispersion of reflected beams.

The performances of the facility (power and flux density levels) have dropped down about 40 percent after 10 years with an increasing rate (12 percent a year in 1977), Figures 21 through 23.

It is worth noting that the loss of reflectivity on the mirrors is the major factor of the facility performance degradation and that the disalignment of the facets does not appear to have any noticeable effect. By next October, 1978, we should recover the nominal performance.

Another important practical consideration on this facility is the time per year available to operate it. As a mean average through many years we have 1200 hours per year of possible operation with direct sun radiation above 600 W/cm^2--50 percent of this time falls into holidays, weekends, lunchtime, starting time. Finally, with a very limited staff (5 people), we use the facility actually 600 hours per year.

On this basis (600 hours per year), the most recent estimates show the real cost to be 4 F/peak 1 kWhr th (including: initial capital investment amortized, personnel,

operating and maintenance expenses). It is possible to find an optimum of this cost below 3 F/kwhr th by using more people in the operating staff to operate the facility more than the present 600 hrs/year (capability of shifting).

Some remarks on characterizing techniques --

The basic measurements needed to characterize this kind of facility are: total power, flux density distribution and temperature measurements.

For the Odeillo furnace we have adapted and developed the use of laboratory scale techniques to perform these measurements:

- total power and power distribution over focal plane, using large integral water-cooled calorimeters with a coating checked for solar absorptance during the power measurement, Figure 24
- radiant heat flux distributions using:
  - integrating sphere
  - thin skin calorimeters
  - Gardon type water-cooled radiometers
  - magnesia coating pyrometric reflectance radiometer.

All of these devices are calibrated against a primary standard consisting of a small water-cooled calorimeter, Figures 25 through 28. For this standard, two configurations are currently used: either cavity type with small aperature or fingertip with external flat receiving area.

A wide variety of devices and mountings are desired to have the capability of being very flexible to solve any flux density measurement according to the specific problems of each program performed with the facility.

Temperature measurements in the high range necessitate the use of optical pyrometry which has its own problems (emissivity in situ measurement) plus a specific problem when used in solar (reflectance measurement). Although many methods and techniques have been designed and used for small solar furnaces, a few of them can be used for large facilities. For the Odeillo furnace, we currently use optical pyrometry in the visible for cavity type measurements and in IR for noncavity type measurements.

Among the characterizing techniques the field of temperature measurements is the one where efforts are still needed to develop practical and flexible measurement methods.

Odeillo 1000-kW_{th} solar furnace applications --

Processing oxides under oxidizing atmosphere:

This kind of operation is the easiest to perform and illustrates a specific capability of solar furnaces.

The technology for melting oxides developed for the Odeillo facility relies mainly on three types of furnaces:

- the flat plate, water-cooled furnace, Figure 29
- the fixed cavity piston type furnace, Figure 30
- the centrifugal (or rotary) cavity type furnace, Figures 31 and 32.

The main feature of these devices is that the thermal efficiency increases about 10 times from the first to the third one. However, besides its own efficiency each device has its own advantages or disadvantages: continuous or batch process, amount of material involved in one operation, possibility of using short or long periods of solar radiation. In fact, these three types of furnaces supplement themselves and are used according to the possibilities they offer to solve each process to be performed, Figures 33 through 40. Presently it is possible to say that the centrifugal (or rotary) furnace is the most adequate technique for processing large quantities of materials with the best efficiencies.

This is the reason why we are presently adding to the batch rotary furnace we used until now all the auxiliary equipment necessary to be able to perform continuous processes on solid or molten materials with this technique (continuous inlet material feeder, outlet material recuperator, gasses and fumes recuperator.

When melting refractory materials for applied research or industrial purposes, large pieces of solidified material are very often not desired because, for instance, for later applications in ceramics, crushing and grinding is an expensive process which contaminates the material. So, in the case of the Odeillo facility, we developed a technique using strong jets of fluid (gas or water) impinging on the molten material

and leading to the solidification into tiny particles (more or less spherical) with mean average diameters down to 200 μm, Figures 29 through 32 and 34.

This noncontaminating grinding process in the liquid phase is operational with the flat plate water-cooled furnace and the fixed cavity furnace. It is being adapted to the rotary furnace to process large quantities of materials for industry.

To illustrate this field of applications it is worth quoting a limited number of examples of processes typically developed with the Odeillo facility for industrial applied research or mass production:

- production of stabilized zirconia through melting the calcined precipitated monoclinic oxide mixed with different stabilizers (calcia, magnesia, yttria)
- production of high purity alumina from the precipitated oxide
- production of ceramic materials from bauxites and feldspath mixtures
- synthesis of β alumina
- synthesis of vitroceramics and special glasses (barium titanate vitroceramics, hexacelsiane glasses, chemcor type glasses, vanadium oxide glasses).

In addition to these processes, purification of materials is considered as a potentially very attractive application of this type of facility. In some cases, the added value is so important compared to the cost of crude material that competitiveness can be achieved.

For instance, we have demonstrated with the Odeillo facility the possibility of purifying:

- alumina from 99.5% purity to less than 200 ppm total impurities
- quartz (crystal rock) from 99.8% purity down to less than 100 ppm total impurities (a final process leading to silica).

These two processes are now studied to increase the hourly rates of production and the thermal efficiencies to develop industrial competitive applications.

Odeillo 1000-kW_{th} Solar Furnace applications: processing materials under inert protective gasses --

Some extractive metallurgical processes can be performed with solar furnaces without any special arrangement to protect the materials under inert gas blankets but only with the help of a cover made of a layer of molten oxides. For instance, the feasibility of

the extraction of chromium from chromium sesquioxide through the silicon reduction of the oxide has been demonstrated in an open air cavity type rotary furnace with the Montlouis facility.

On the opposite, other metallurgical processes need to be performed under the protection of very pure inert or reactive gasses (with low N_2, O_2, H_2O content). For instance, it is the case of:

- recovering chromium by reducing chromium sesquioxide with hydrogen
- melting and casting titanium alloys under argon for making massive pieces from sponge and flakes.

These two operations have been demonstrated with a 2-kW_{th} solar furnace where simple bell jars solve easily the problem of blanketing, but not with large solar furnaces.

However, in the course of another program the demonstration has been made that it is possible to operate under selected gasses with a large solar furnace. A leak proof rotary furnace, Figures 41 through 46, has been designed and built and used inside a vessel equipped with a large quartz window to let focused radiation enter the furnace and provided with a circulation of gas.

This equipment has been used successfully for melting and casting boron under pure argon.

In the same way melting and casting of borides, carbides, nitrides and high-temperature alloys could be processed with the same technology.

In fact, there is a need for new efforts to be devoted to the technical problem consisting in controlling the gasses surrounding the focal reaction zone of large solar focusing facilities for potential industrial applications of chemical processes in general.

Odeillo 1000-kW_{th} Solar Furnace applications: materials evaluation, thermal shock resistance, physical measurements --

This field corresponds to some specific characteristics of point focused solar radiation and in the case of the Odeillo facility to some typical features of the 1000-kW_{th} Solar Furnace.

Auxiliary equipment has been designed and built consisting of different kinds of shutters (size, time constant), Figure 47, providing the capability of pulsing the radiant heat at the focus on targets of various sizes submitted to thermal cycles covering a range of time length from a few seconds to some hours under radiant flux densities up to 1600 W/cm^2.

A large number of investigations have been performed with the Odeillo furnace on materials concerning space and defense applications (electromagnetic windows, ablative materials), Figures 47 through 51.

Such a program has been developed in the last two years for the evaluation of refractories for steel plants. The tests performed on these materials with the furnace have put in evidence more capabilities and flexibility than any other experimental procedure currently used in laboratory or industry.

Materials evaluation and physical measurements at medium and high temperatures under radiant heat for solar or nonsolar applications are a significant part of the utilization of this kind of STTF.

Odeillo 1000-kW_{th} Solar Furnace applications: components testing for central receiver power plants --

In the past few years, the Odeillo Solar Furnace has been proved to be a very useful tool for testing different kinds of bench model receivers for solar tower electricity generating plants. In 1976 a high-temperature, high-pressure superheated steam receiver was tested for ERDA, Figure 52. In 1976 and 1977 an organic heat transfer fluid receiver, Figures 53 through 55, was tested as part of the French PIRDES activities for thermodynamic conversion of solar energy. This receiver is connected to a small conversion facility including thermal storage, steam generator and turbo alternator for electricity production. The system was connected for the first time to the local French electricity network in November 1976.

These tests on bench model receivers were very useful to demonstrate the possibility of operating such receivers with point focused solar radiation and to evaluate their specific performances under solar conditions on a significant scale.

As a conclusion, and as far as prospects are concerned, it is possible to say that after reviewing particularly the utilization of the 1000-kW_{th} solar furnace, all the

existing STTFs have, obviously, a prominent role to play in exploring the possibilities of point focused solar energy as a source of renewable heat at medium and high temperatures.

The major present trend is to convert this heat to electric power through thermodynamic conversion. Pilot plants are under construction in different countries. These programs develop a better understanding of the capabilities of these facilities and many efforts to attempt to decrease the cost of the components for these facilities are under way in a search for competitiveness.

However and along with this, many efforts need to be devoted to establishing carefully the possibilities of future second generation point focusing pilot plants for process heat. Fuel synthesis, chemical storage, materials processing, and chemical processes are very attractive ways to use this medium- and high-temperature renewable heat. Many processes are feasible; many need to be demonstrated at the STTF scale. In each case, there is an optimum to find between the constraints of this thermal energy source, the capabilities of the facilities, the cost of these facilities, and the added value due to the process performed--a lot of activities for point focusing STTFs.

F. Trombe, L. Gion, C. Royere
Perfectionnement aux procédés et dispositifs de granulation et de sphéroidïsation de matières notamment de matières réfractaires.
demande de Brvet ANVAR N° 70-28-385 du 31 Julliet 1970
Brevet Anvar 2.098.951 du 14 Février 1972

F. Trombe, L. Gion, C. Royere, J. F. Robert
Traitement d'oxydes réfractaires au Four Solaire 1000kW du CNRS
C.R. Acad.Sc.Paris T 272 pages 1971-1973 - 14 Juin 1971

J. D. Walton, C. Royere
Evaluating the Thermal Shock Resistance of Ceramics in a Radiant Thermal Energy Environment
Science of Ceramics 1973

E. Bilgen, C. Royere
Transient Heat Transfer at the Focal Plane of Solar Furnaces, Fredericton 26-30 Mai 1975

F. Trombe, A. Le Phat Vinh, C. Royere
The French CNRS 1000kW Solar Furnace. Description Performance Characteristics. Present Utilization and Perspective
New Mexico - 18-19 Novembre 1974

C. Royere
Remarques sur les Chaudières Solaires
Reunion project THEM. 18 Fébrier 1976

D. Balageas, A. Sarremejean, C. Royere
High Temperature Electrical Evaluation of Slip-Cast. Fuzed Silica Radome Using Solar Energy
Office National d'Etudes et de Recherches Aérospatiales. 21-23 Septembre 1976

B. Courbet
Etude des pertes par rayonnement réfléchi à travers l'orifice d'une chaudière solaire à cavité.
Rapport de stage 1976

Tr. Tracey, F. A. Blake, C. Royere, T. Brown
$1MW_{th}$ Solar Cavity Steam Generator. Solar Test Program.
LSES Journal 30 Avril 1977

Martin Marietta - Engineering Experiment Station - Georgia Institute of Technology - CNRS
$1MW_{th}$ Bench Model Solar Cavity Receiver Steam Generator Build and Test.
Phase 3 Summary Report June 1977

Tr. Tracey, F. A. Blake, C. Royere, C. T. Brown
$1MW_{th}$ Solar Cavity Steam Generator. Solar Test Program.
Washington Aout 1977

B. Faydide
Etude théorique et expérimentale de l'évolution des températures d'un matériau soumis à un choc thermique.
Rapport de state 22 Mars-17 Juin 1977

O. Alcayaga
Contribution à l'étude de la répartition de la densité de flux énergétique dans l'espace focal d'un système concentrateur de thèse 14 Novembre 1977

C. Royere
1000kW$_{th}$ CNRS Solar Furnace Applications
STTF User's Association High Temperature and Operators Workshops
Albuquerque, New Mexico 27-29 Novembre 1977

C. Royere
Génie Chimique Solaire: réacteurs solaires et projects de recherches
Rapport interne 19-12-77

C. Royere
Programme de recherche et d'essais sur un récepteur solaire à cavité centrifuge.
Rapport interne 15-01-78

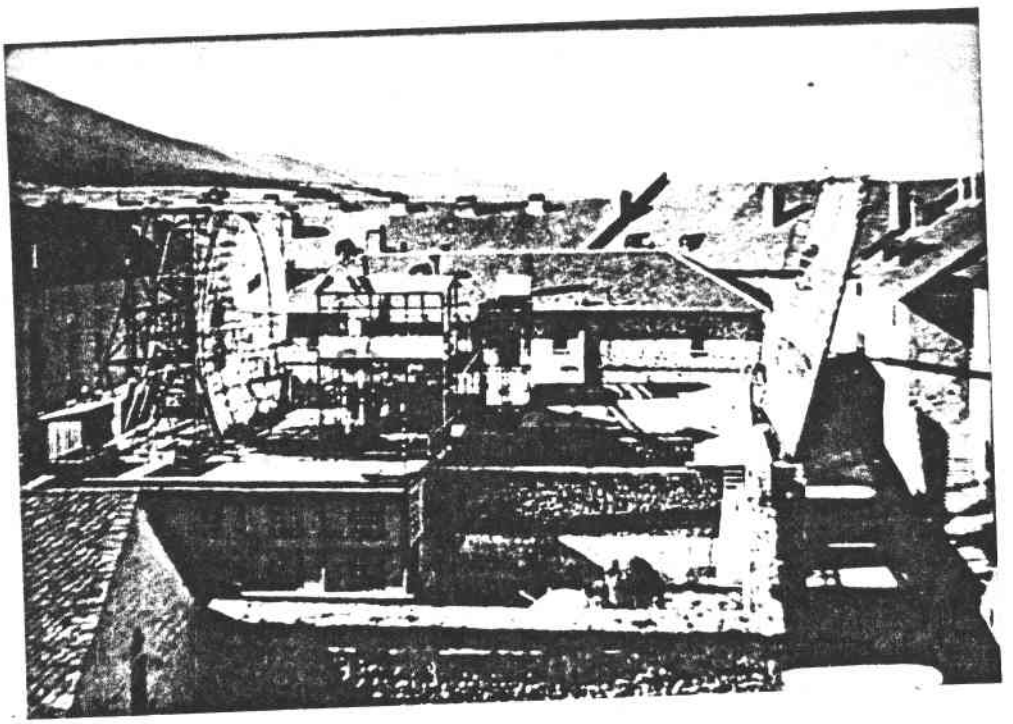

Figure 1

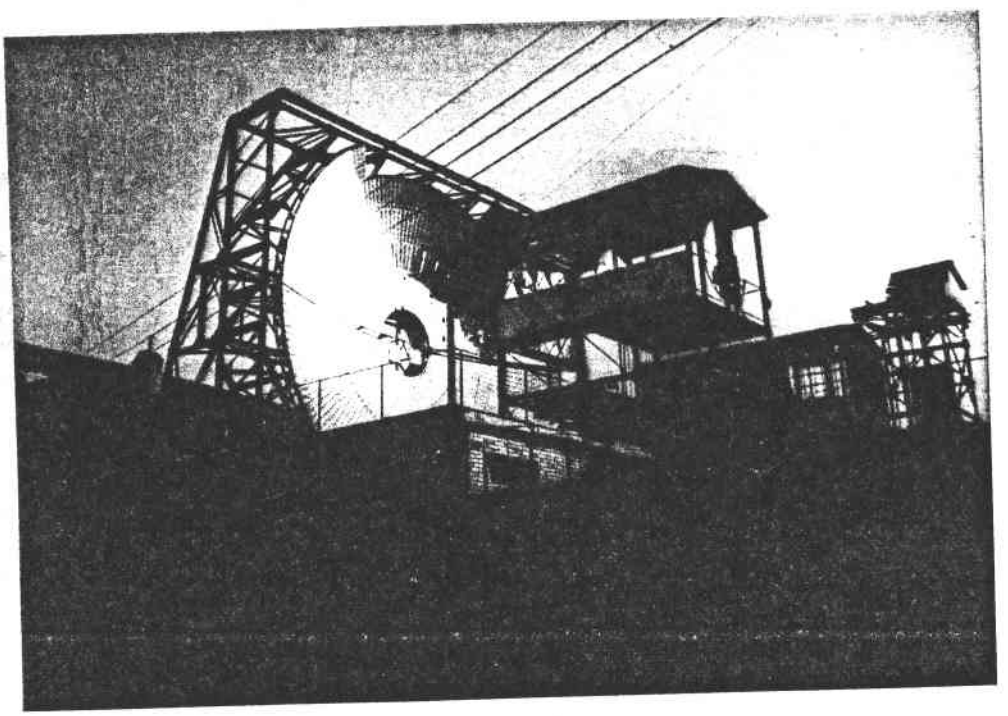

Figure 2

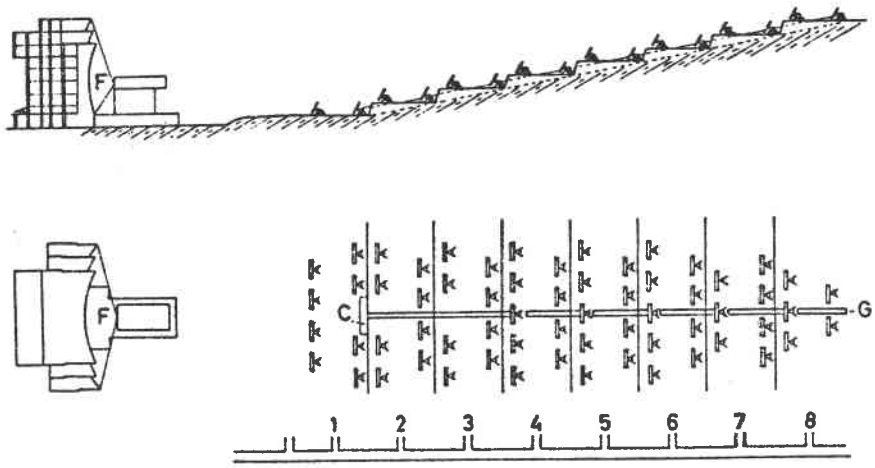

Figure 3

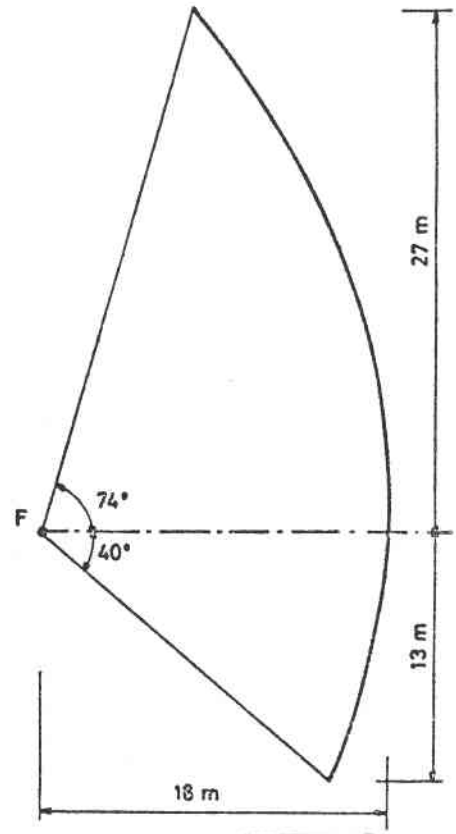

Figure 4

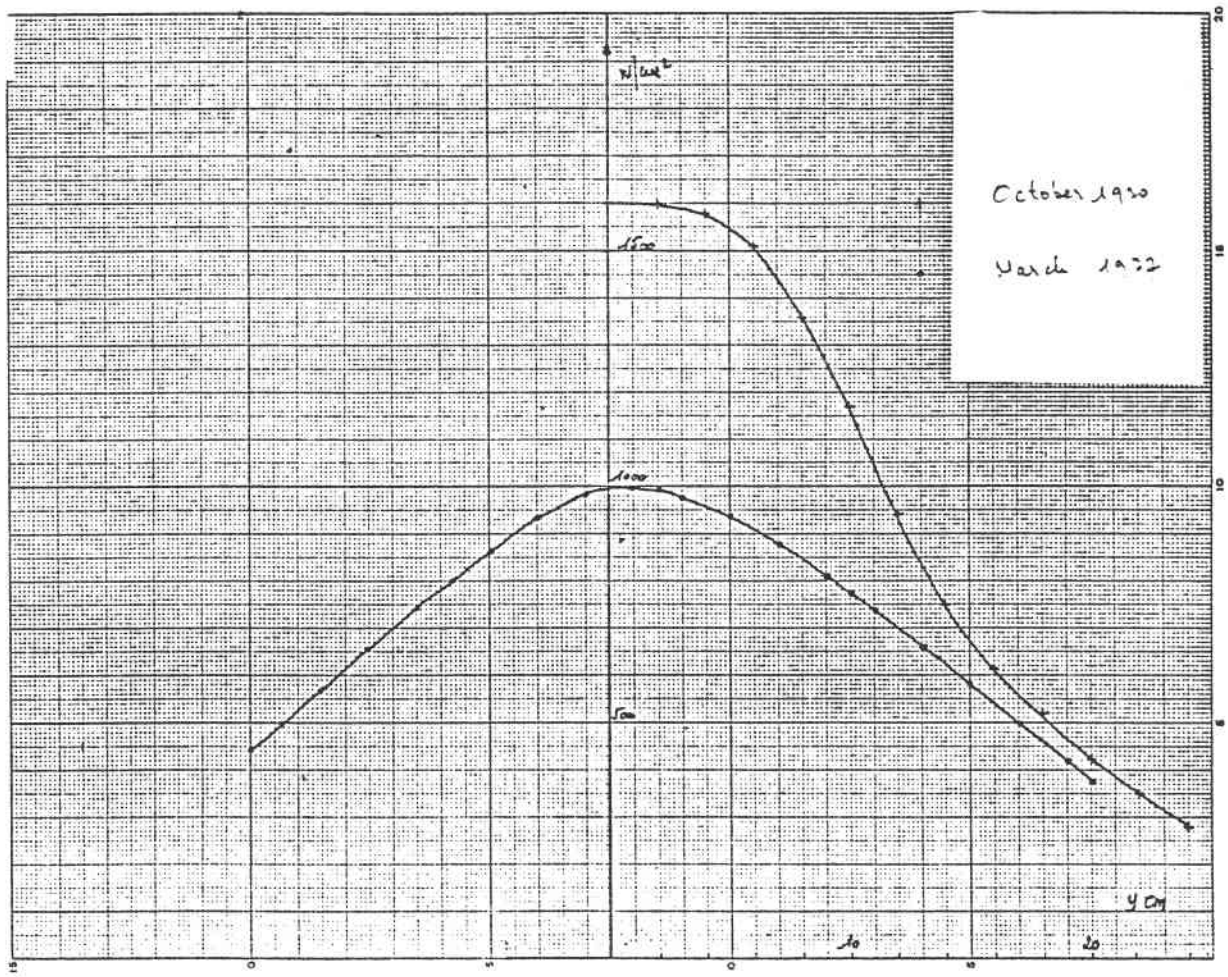

Figure 5

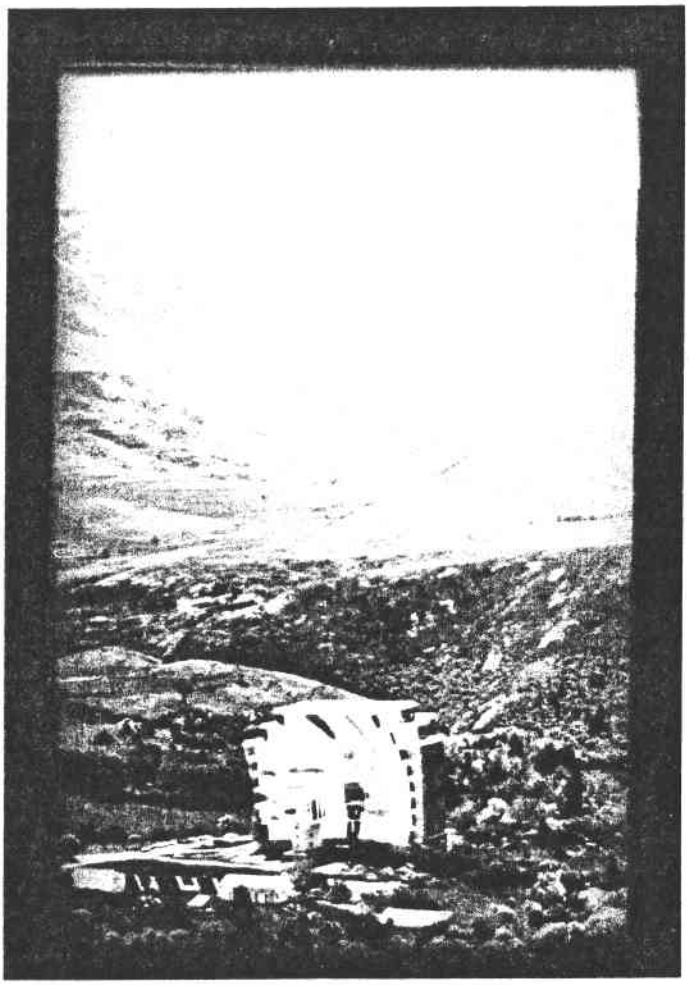

Figure 6.

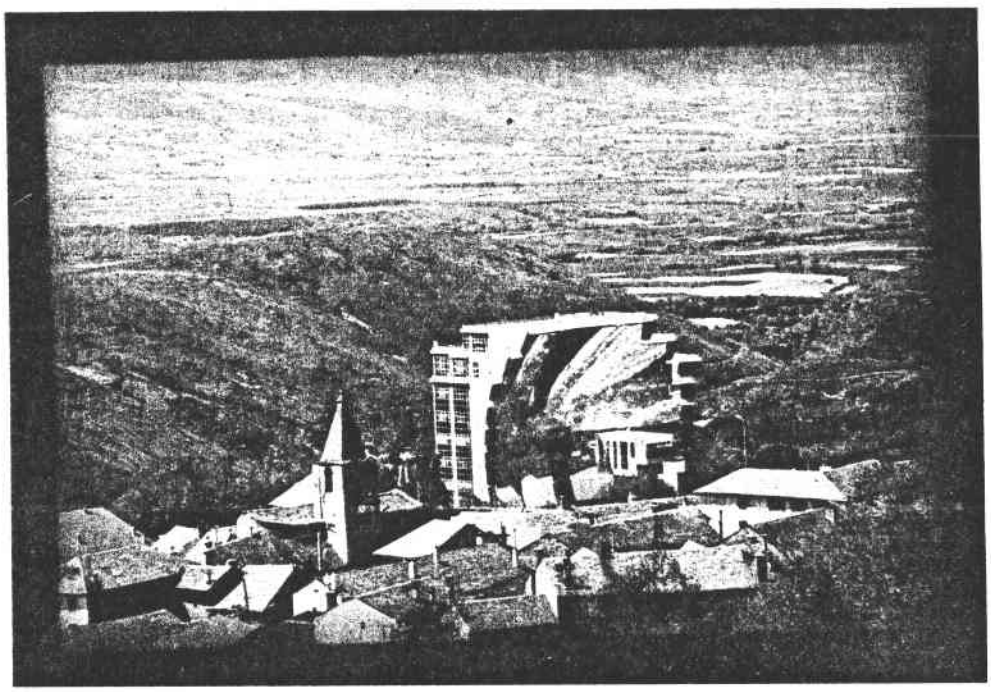

Figure 7

Figure 8

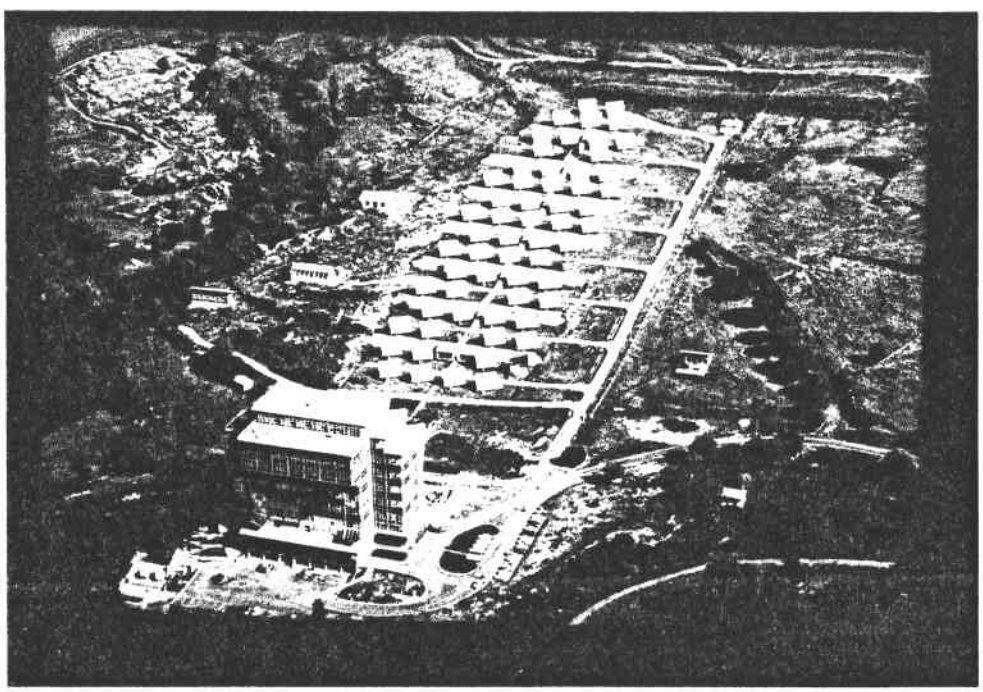

Figure 9

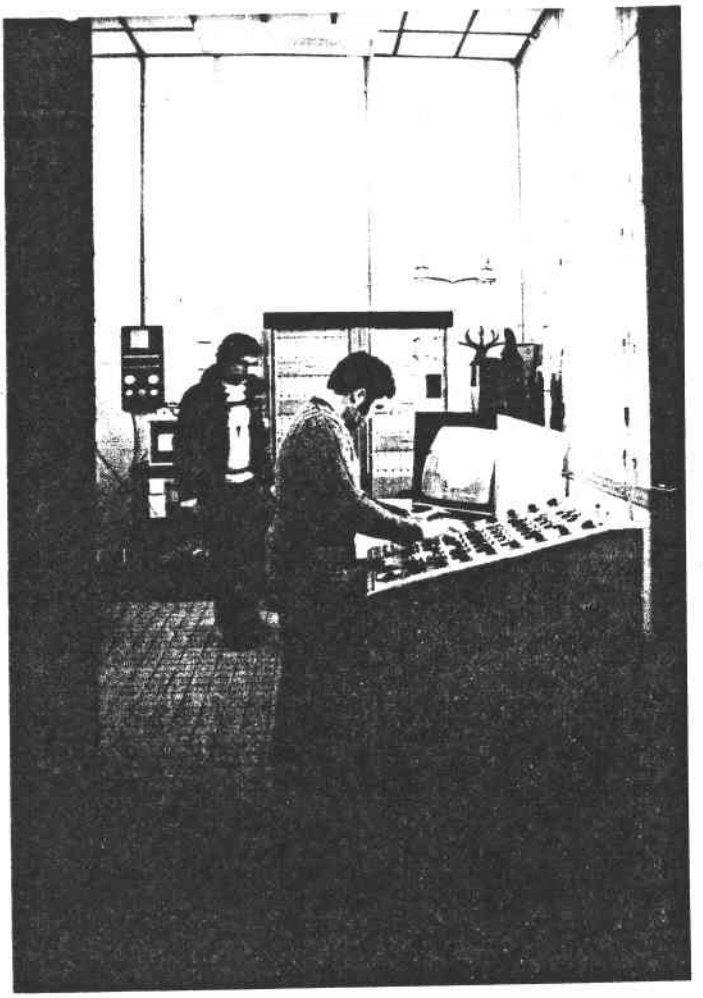

Figure 10

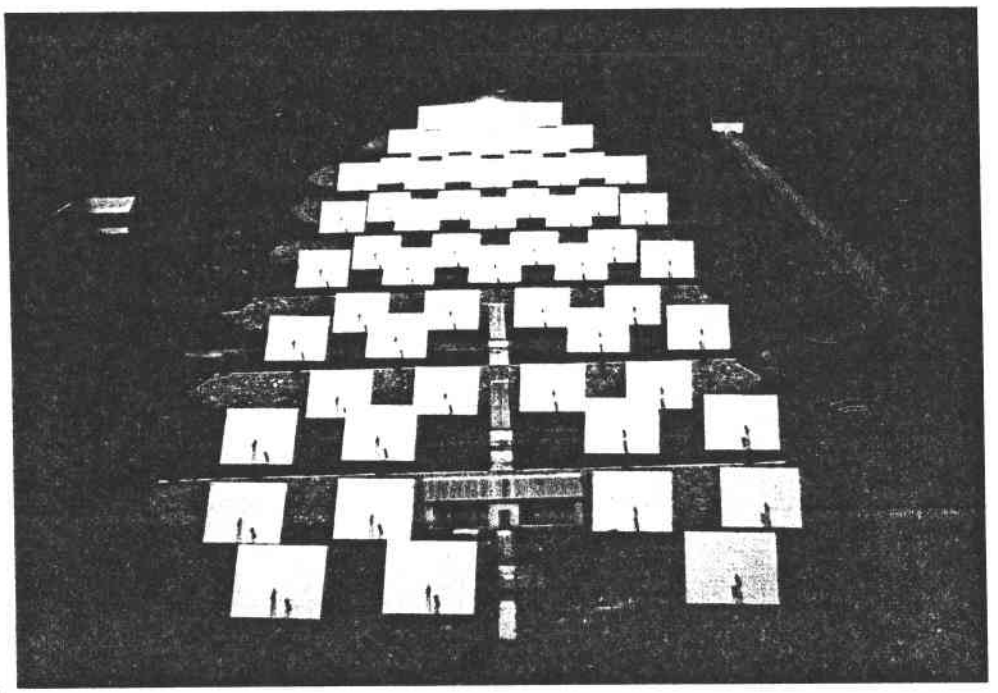

Figure 11

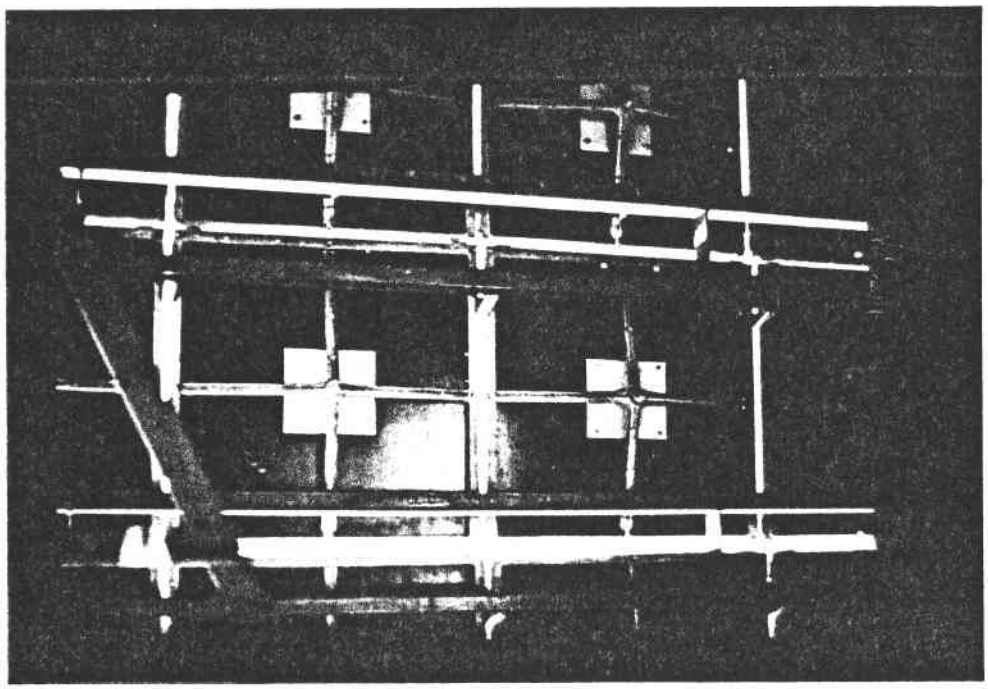

Figure 12

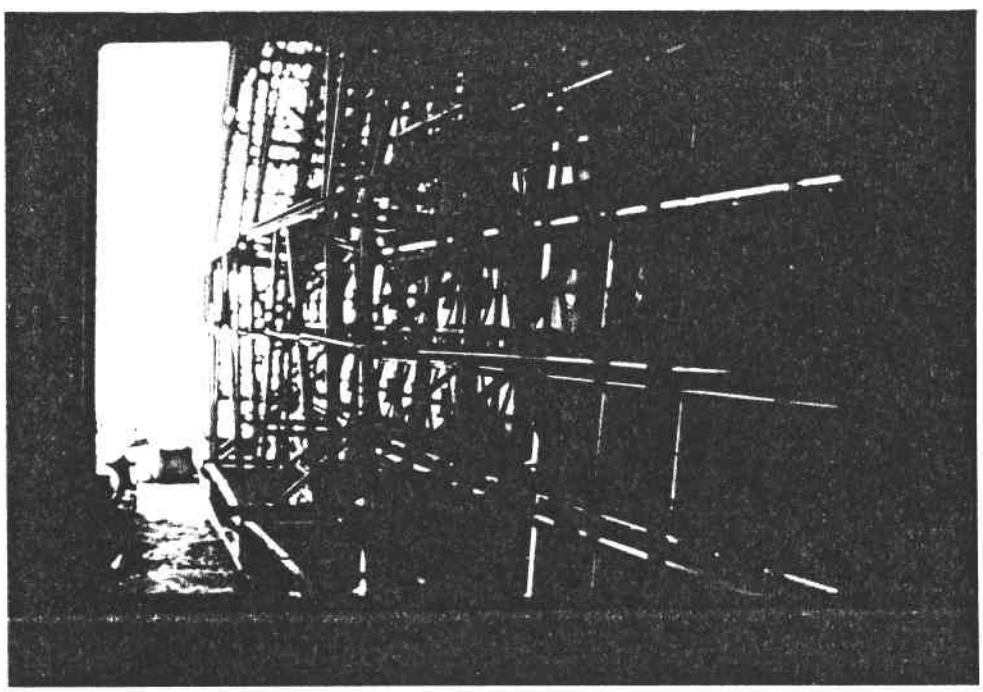

Figure 13

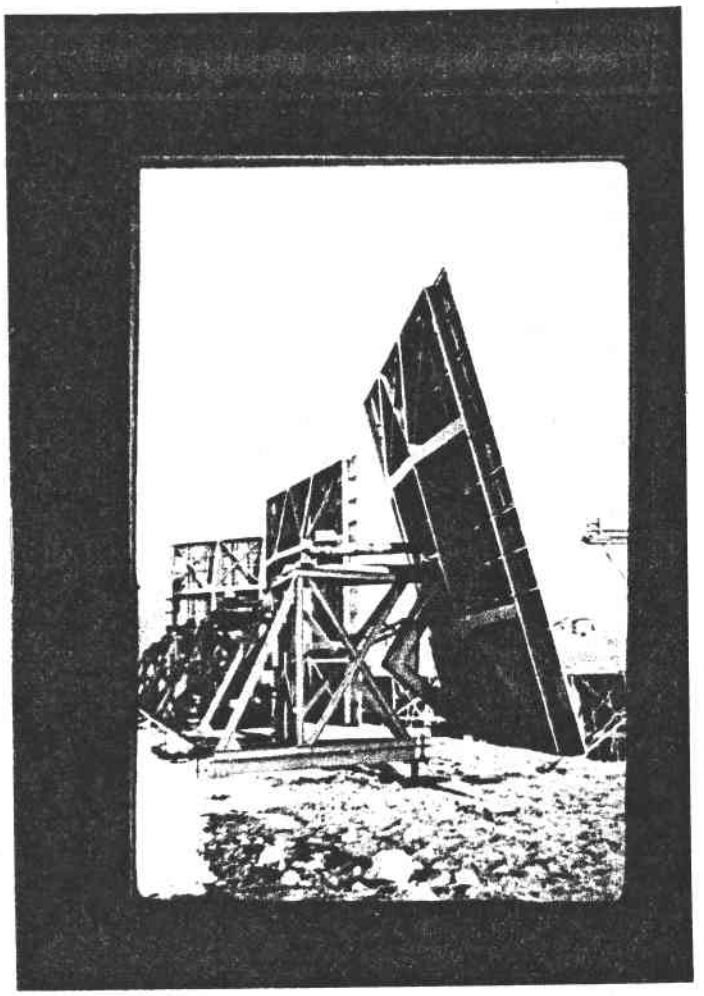

Figure 14

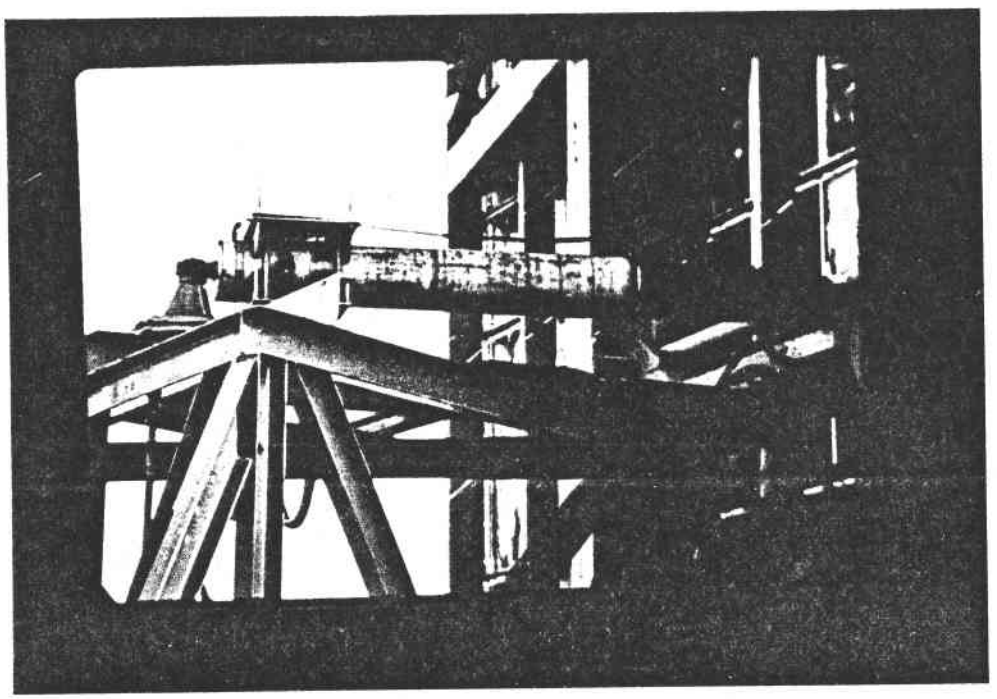

Figure 15

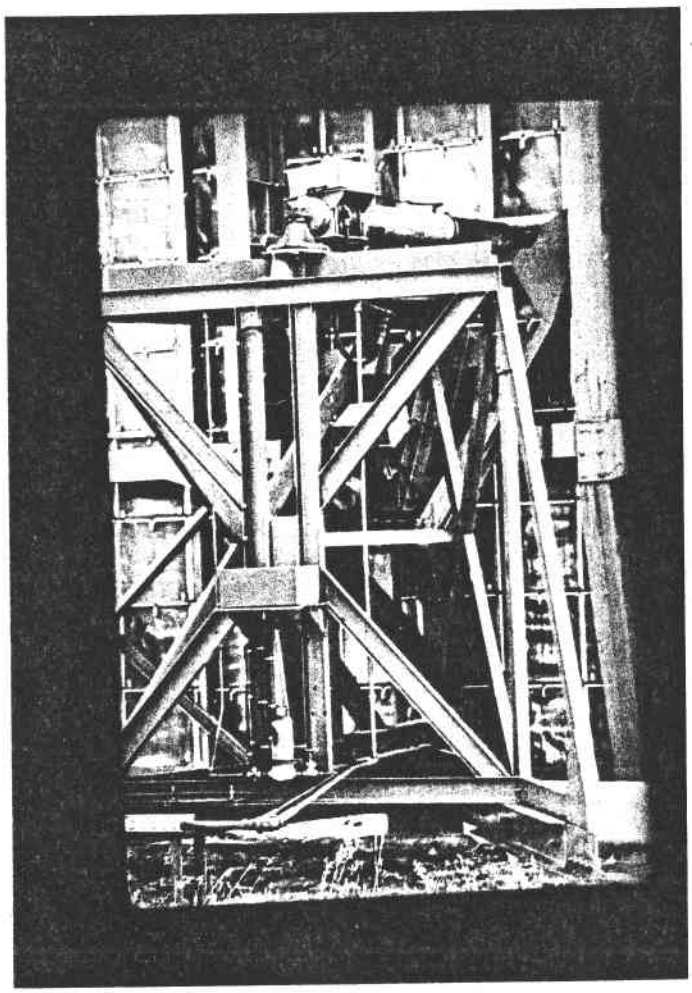

Figure 16

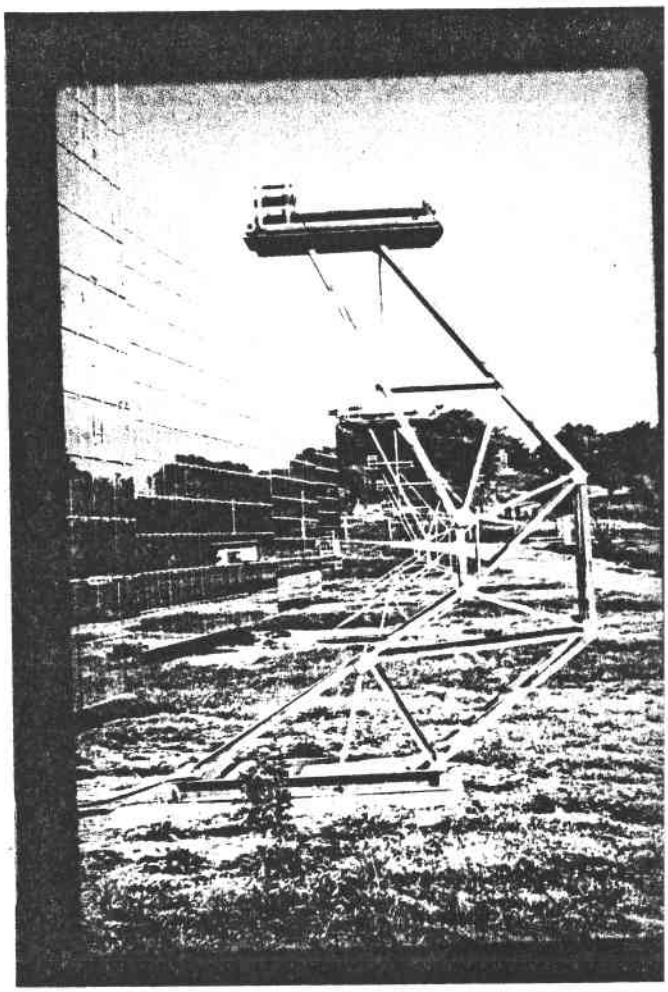

Figure 17

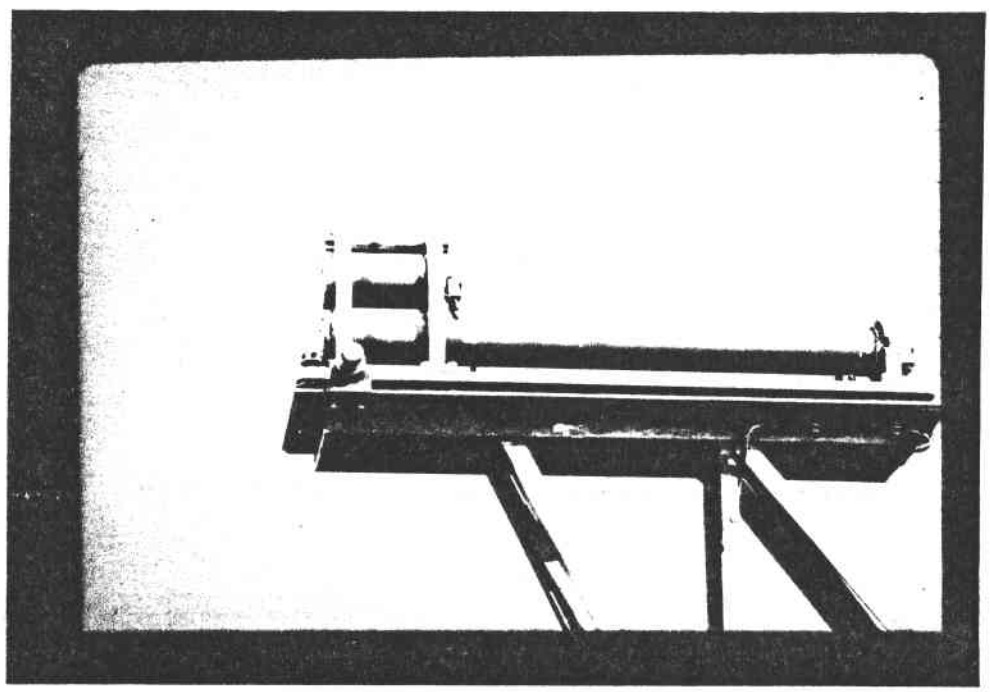

Figure 18

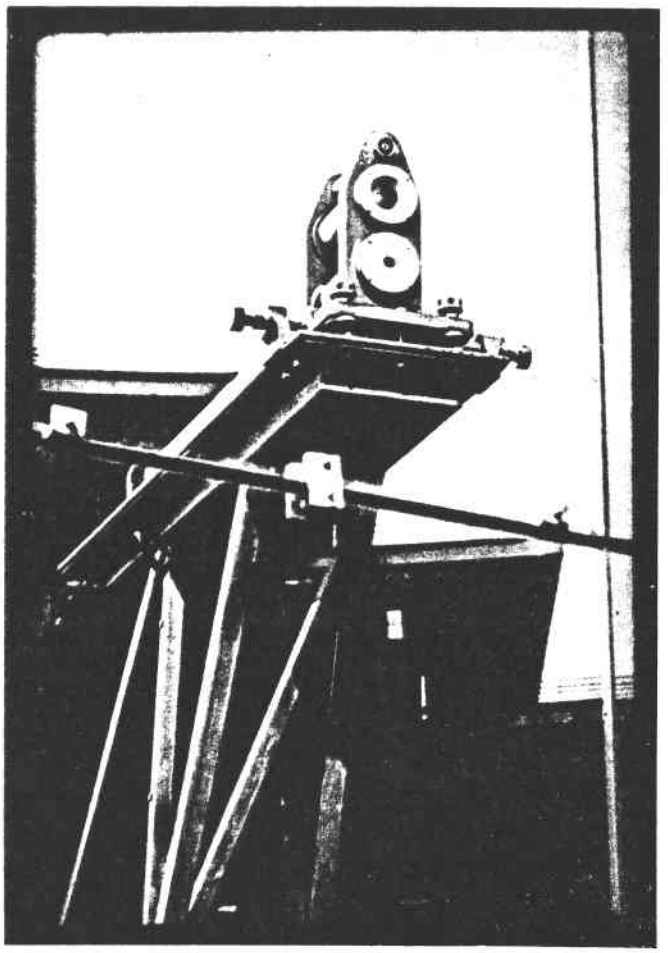

Figure 19

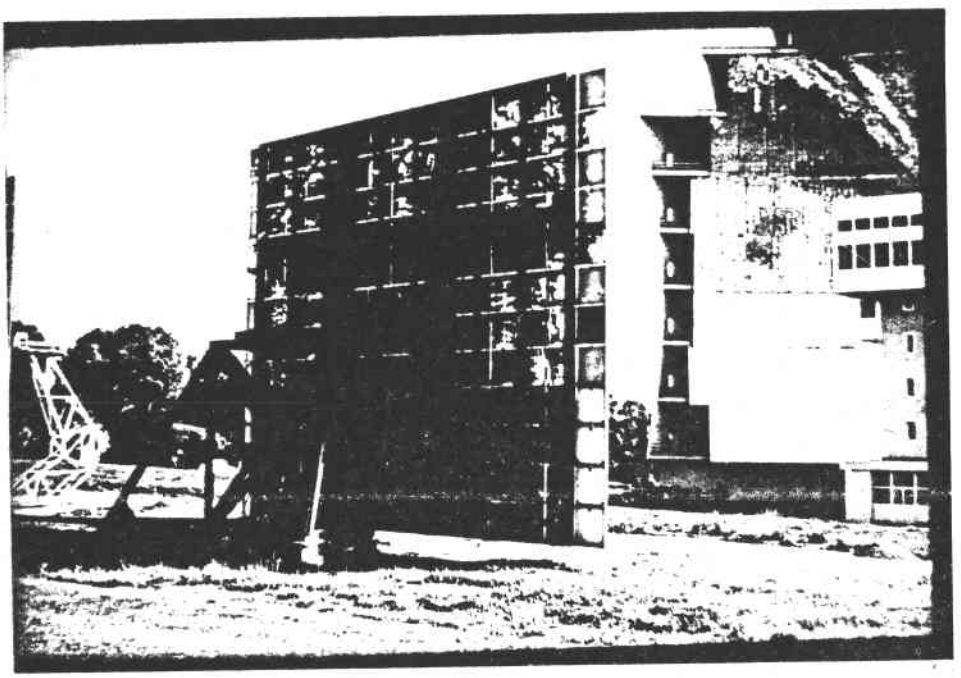

Figure 20

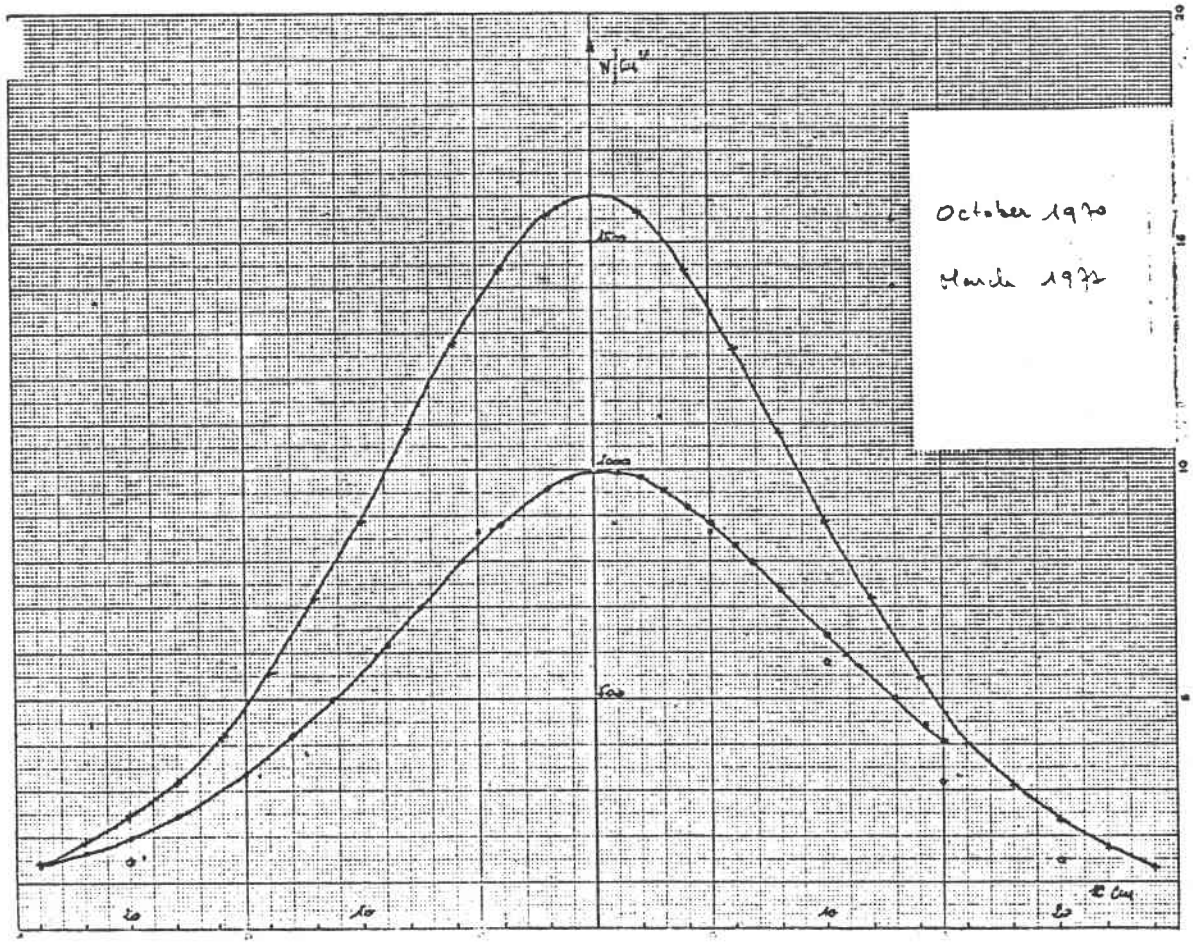

Figure 21

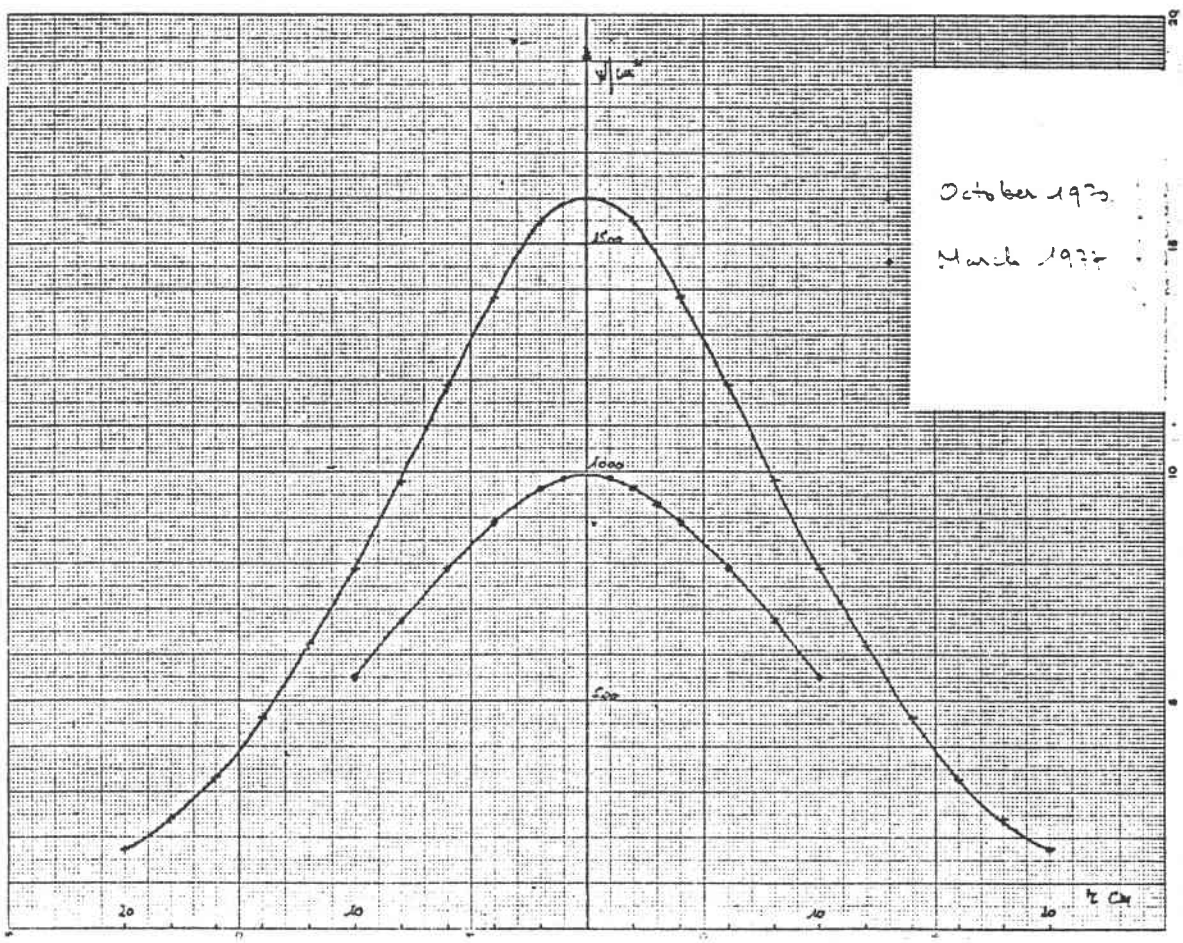

Figure 22

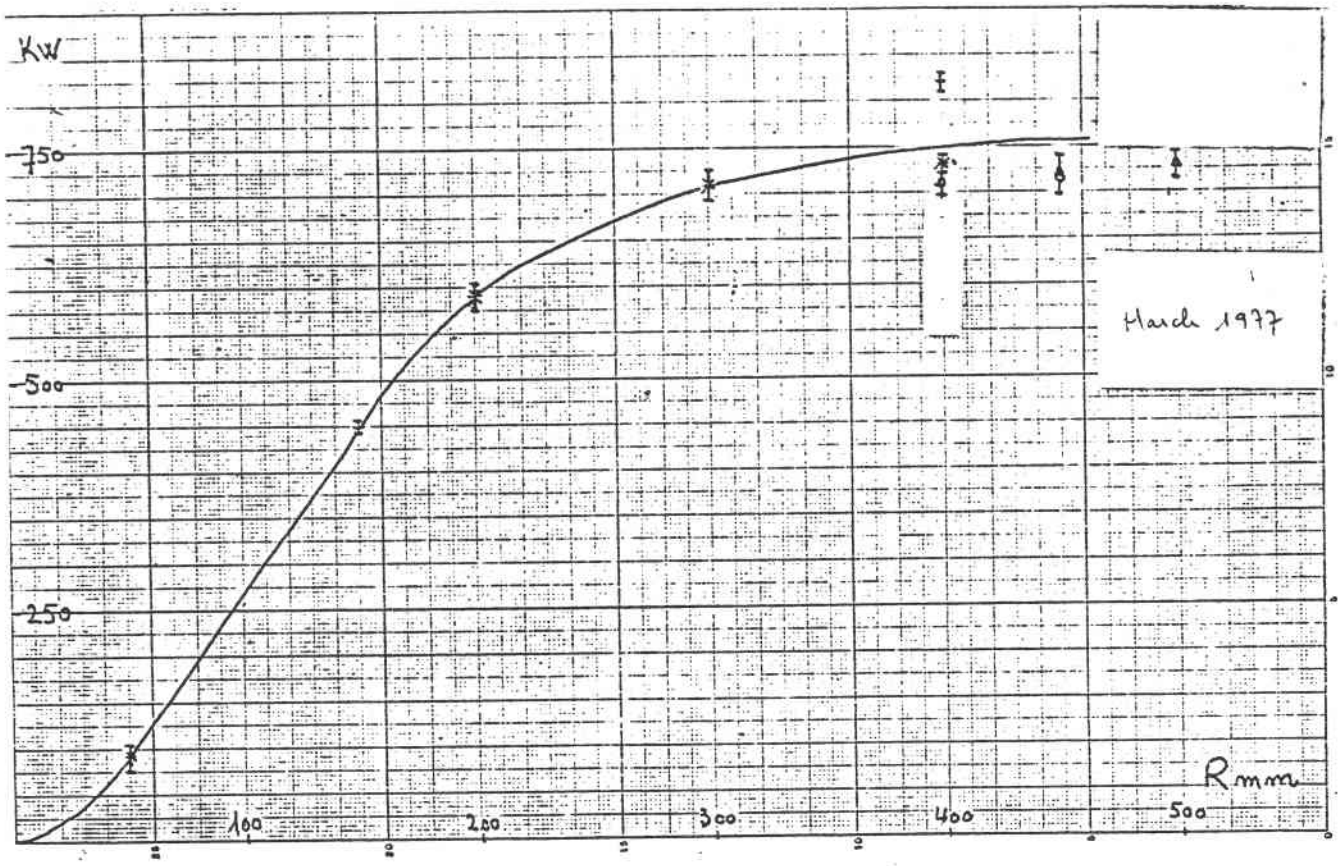

Figure 23

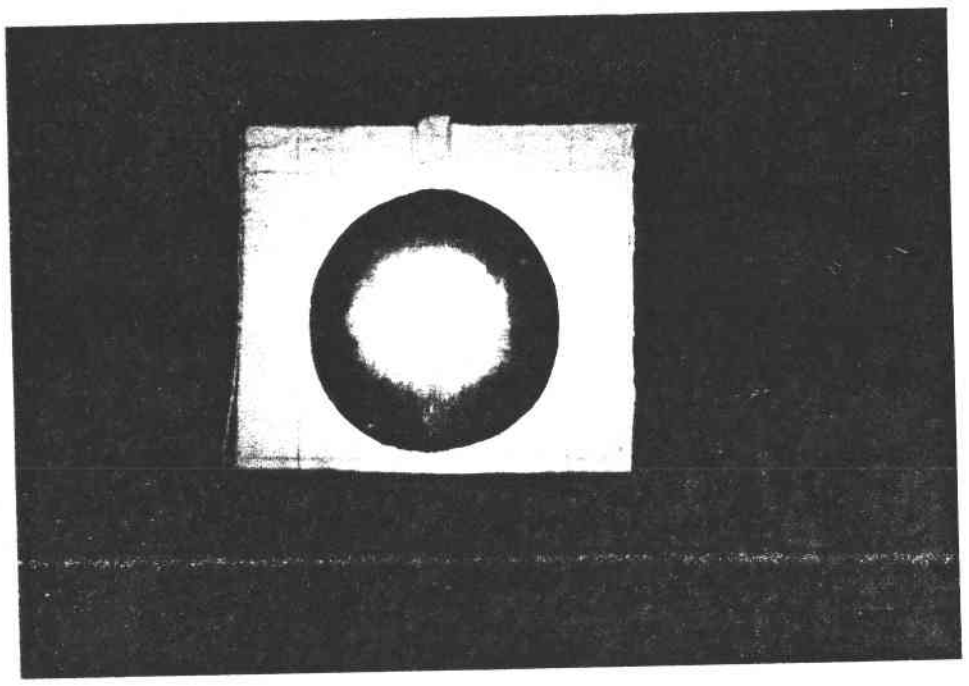

Figure 24

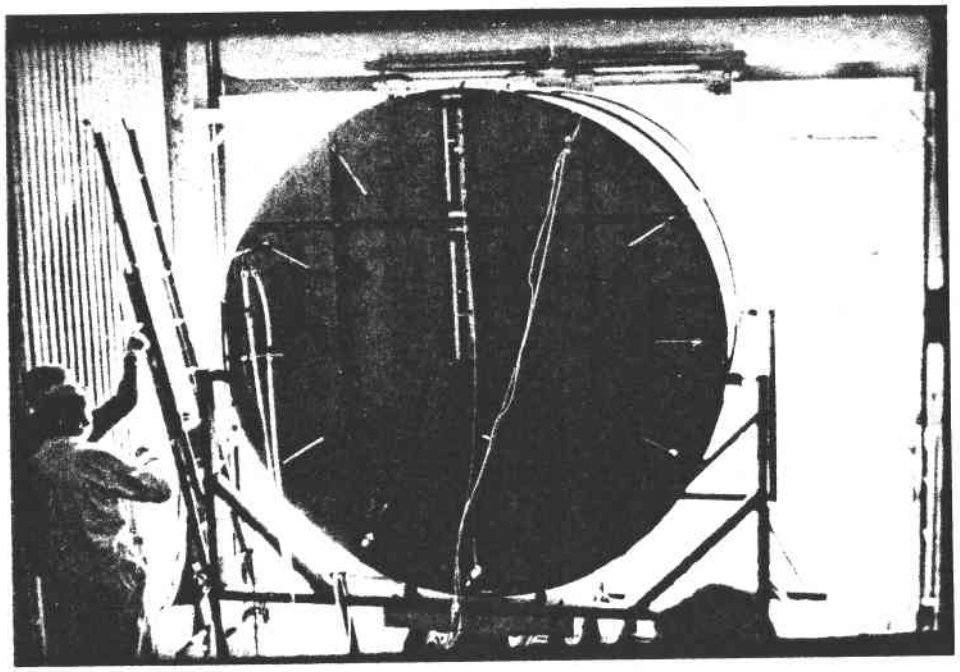

Figure 25

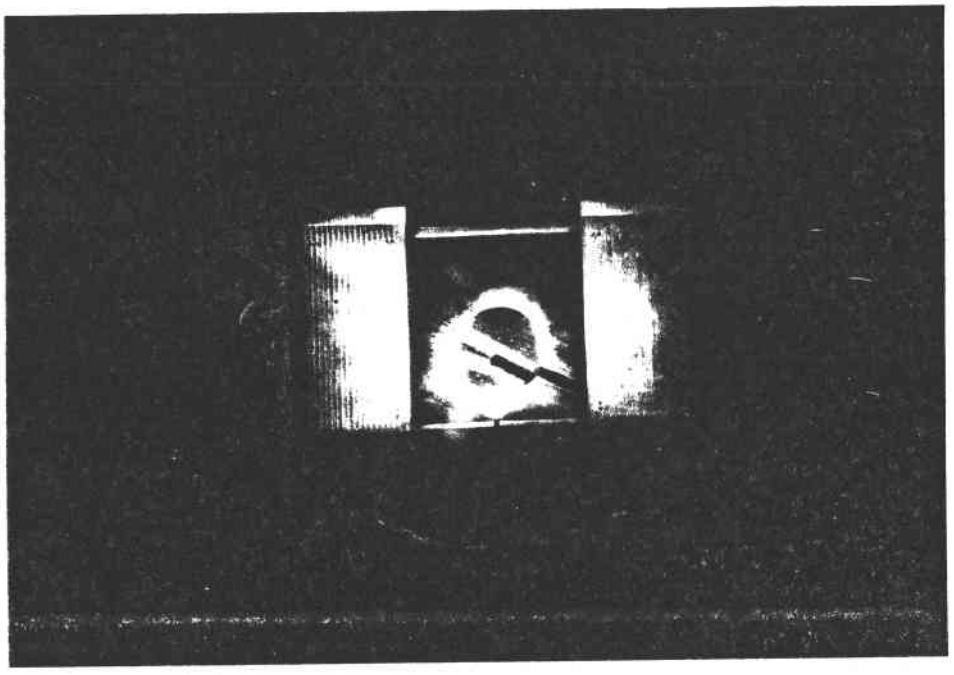

Figure 26

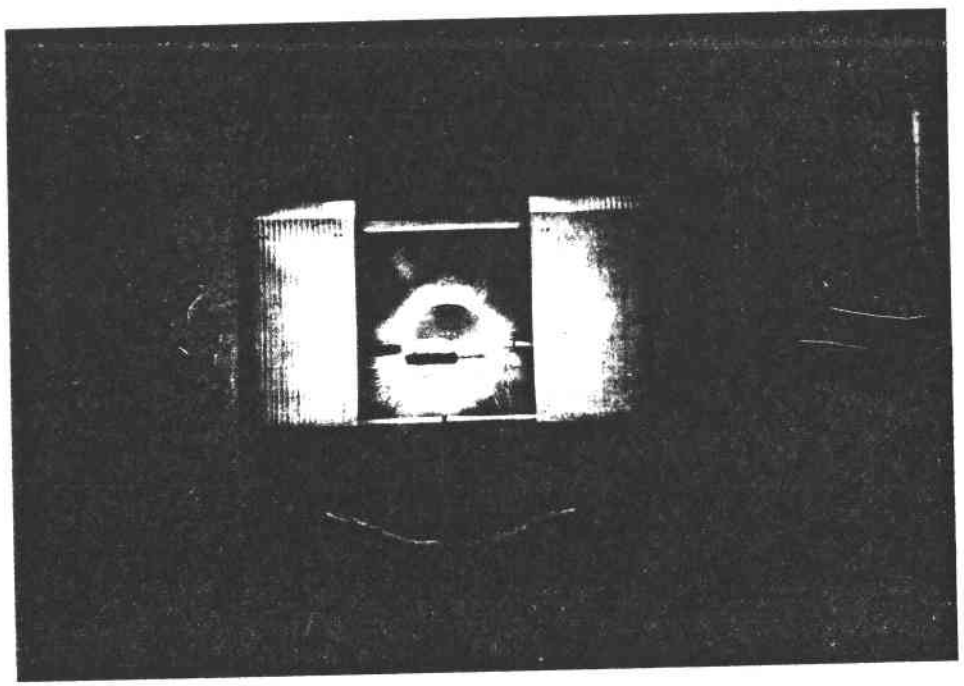

Figure 27

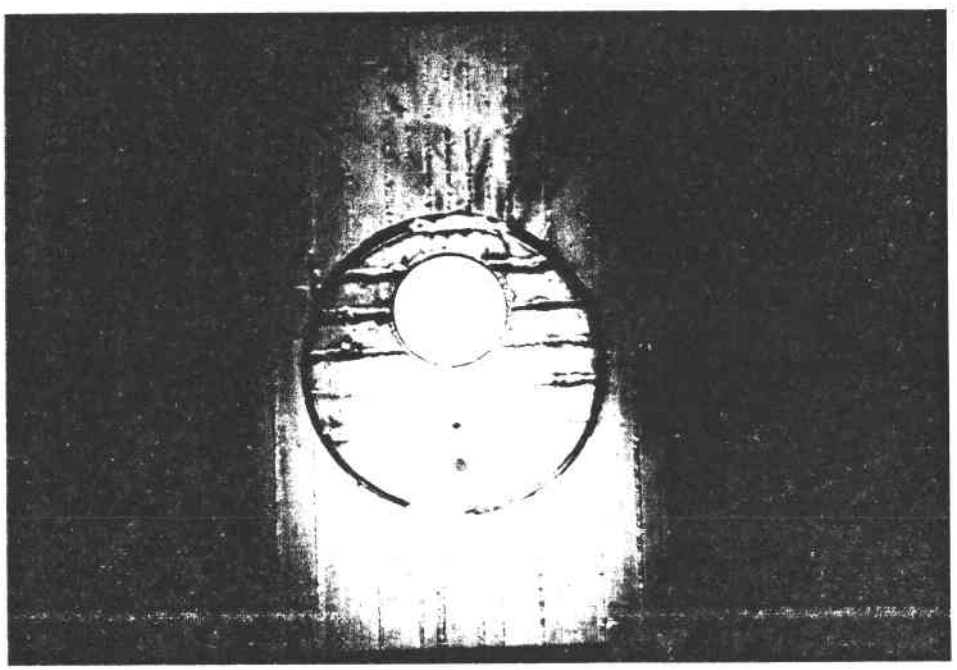

Figure 28

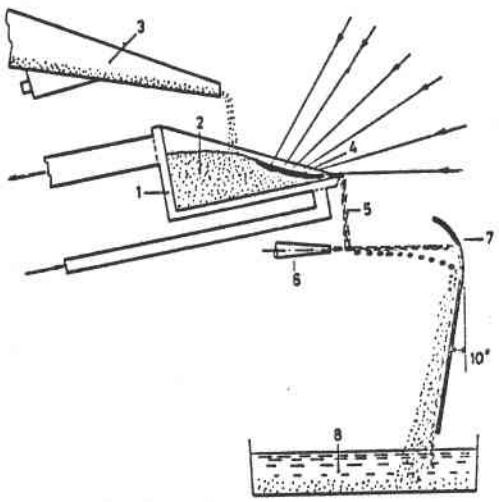

Figure 29

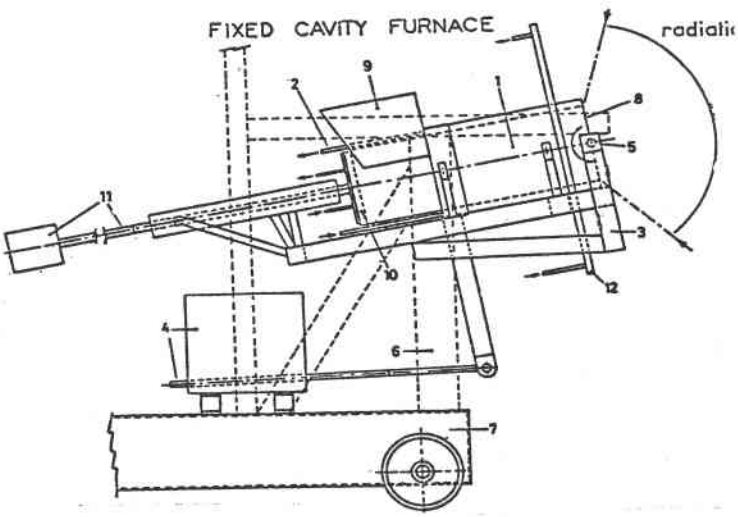

Figure 30

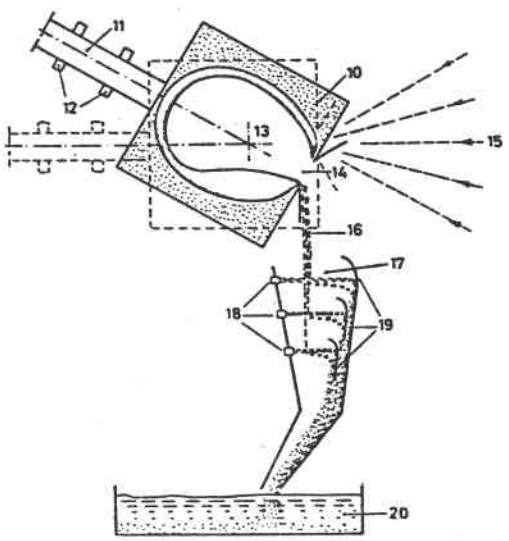

Figure 31

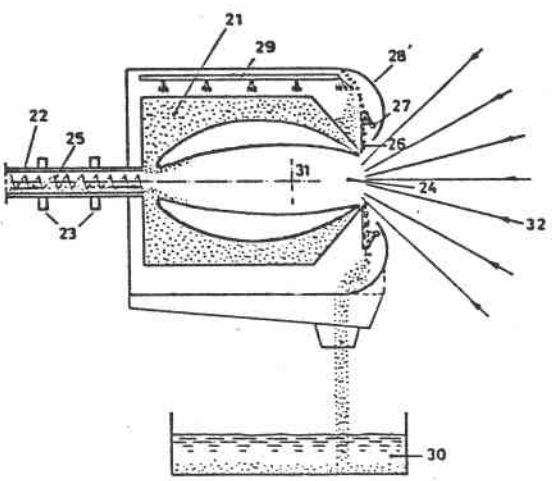

Figure 32

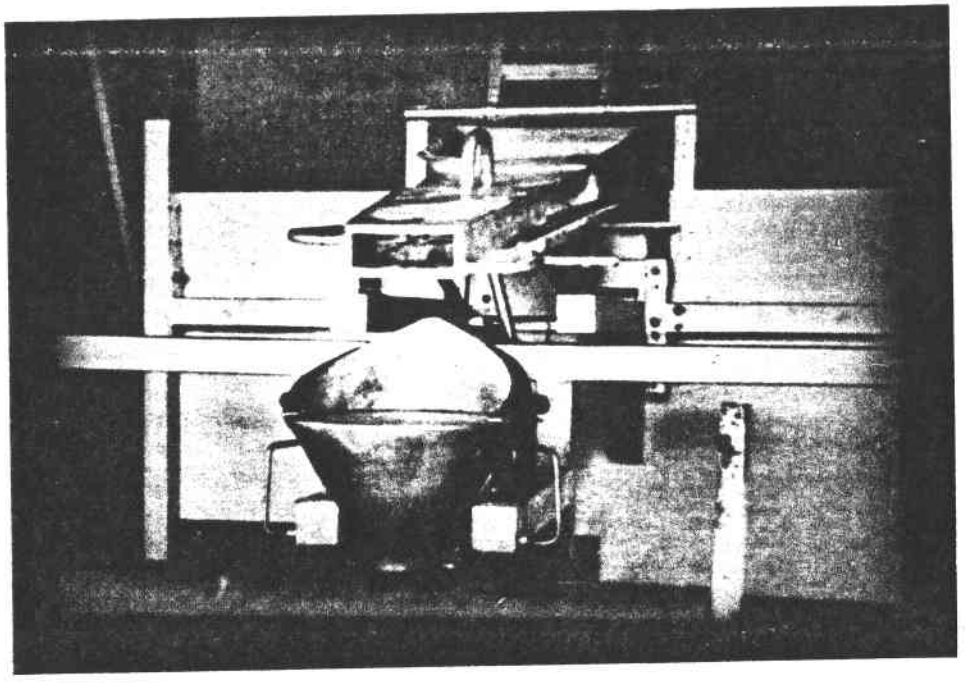

Figure 33

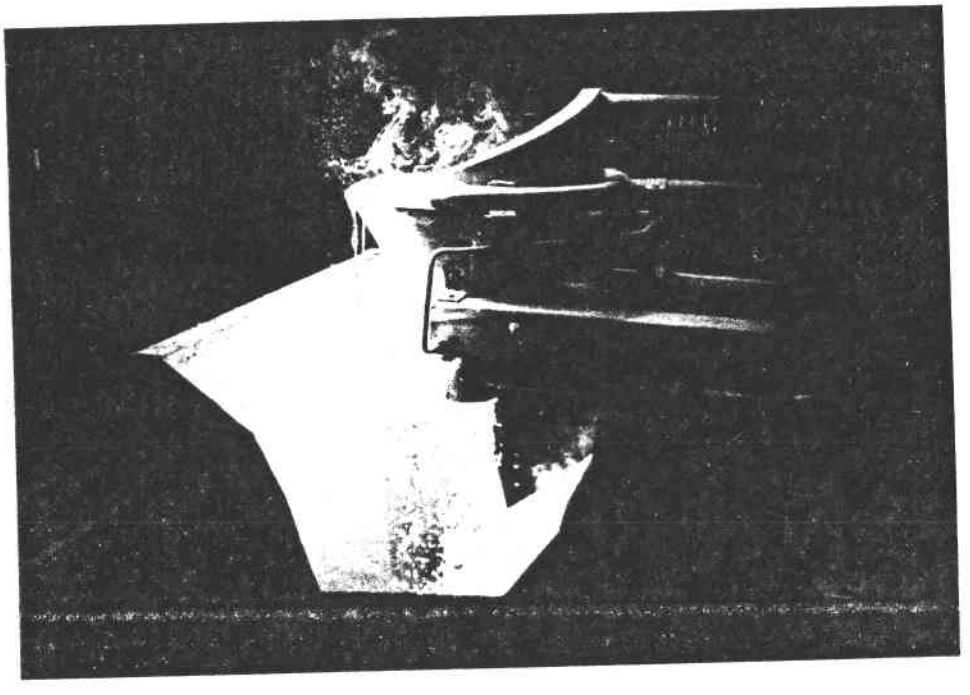

Figure 34

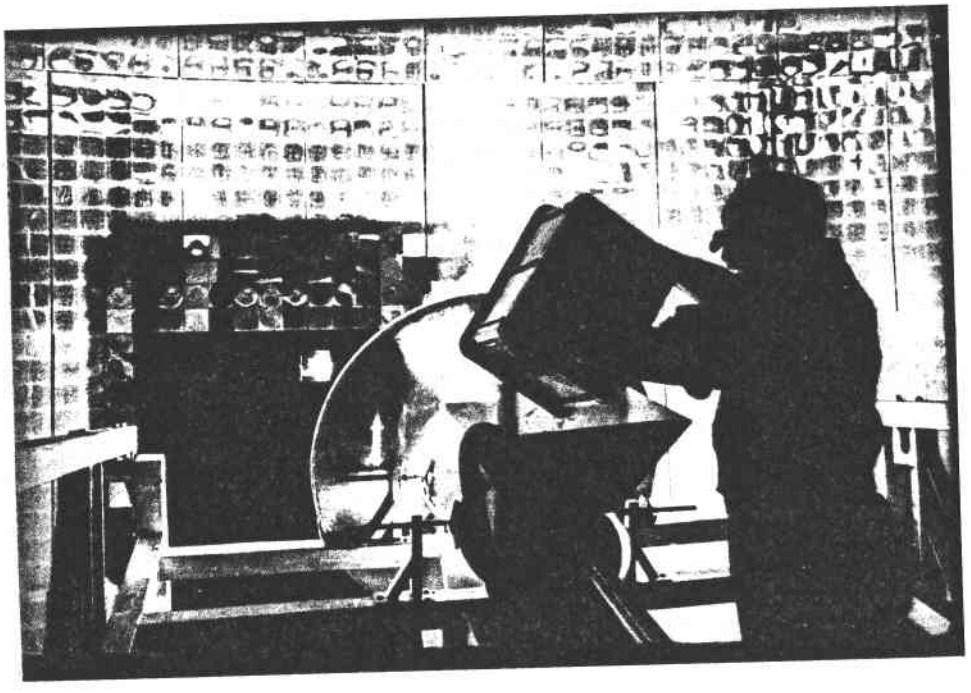

Figure 35

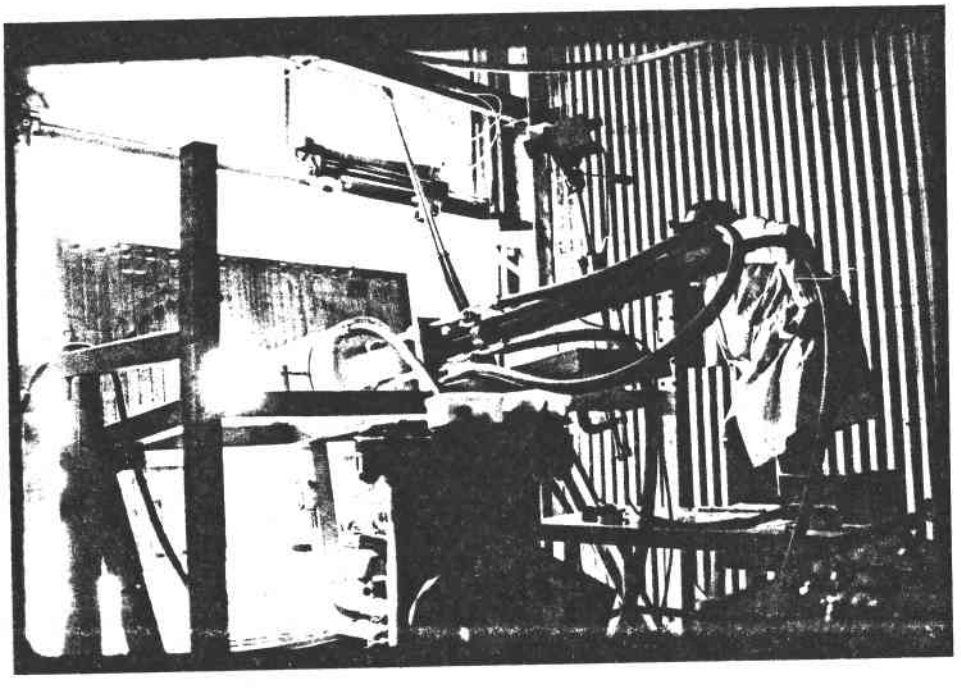

Figure 36

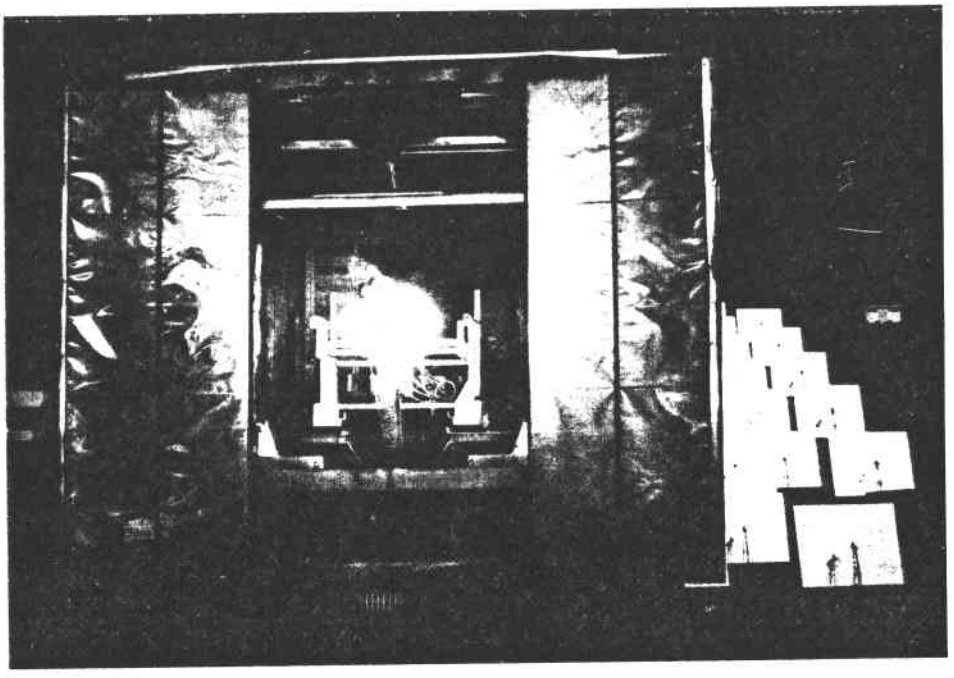

Figure 37

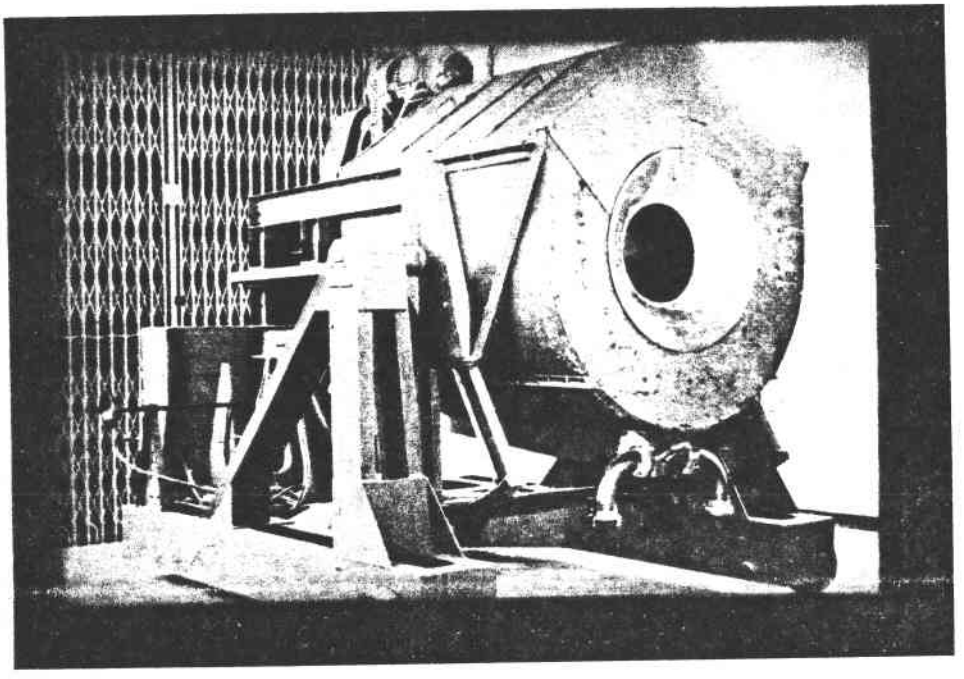

Figure 38

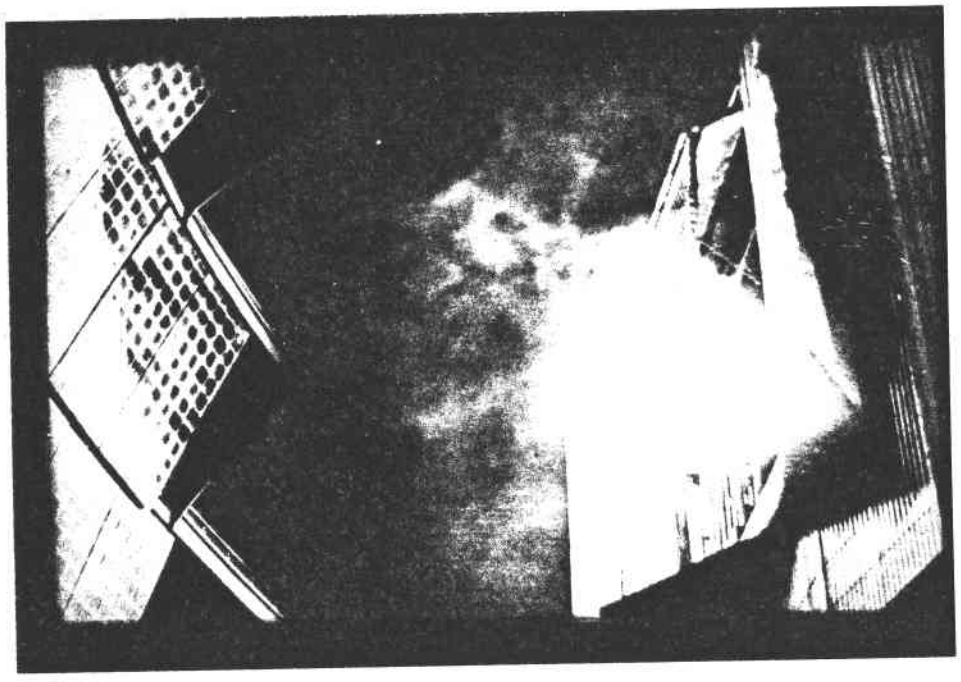

Figure 39

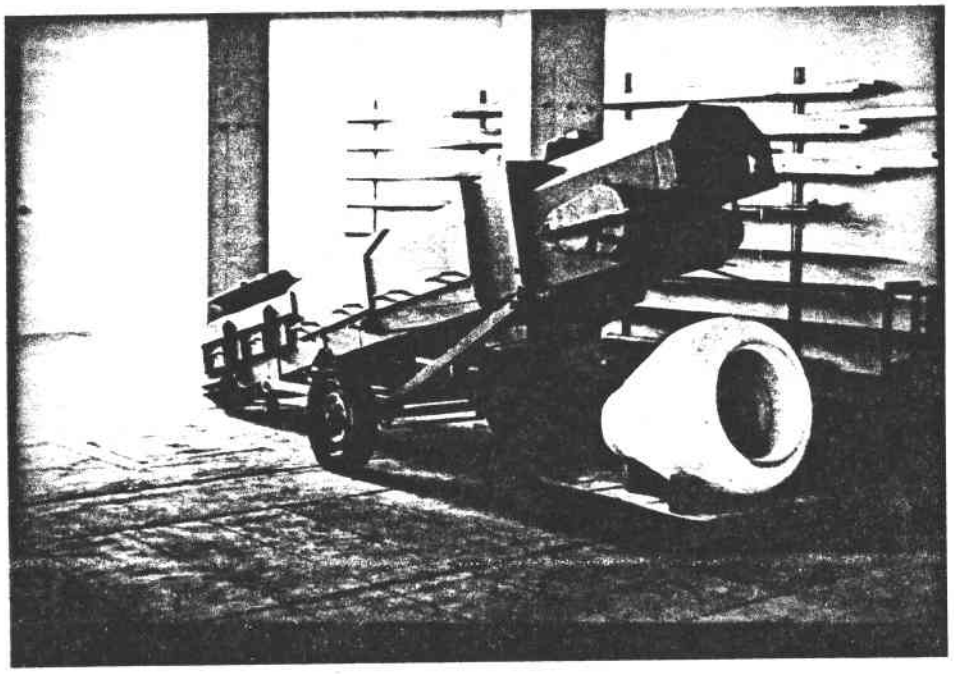

Figure 40

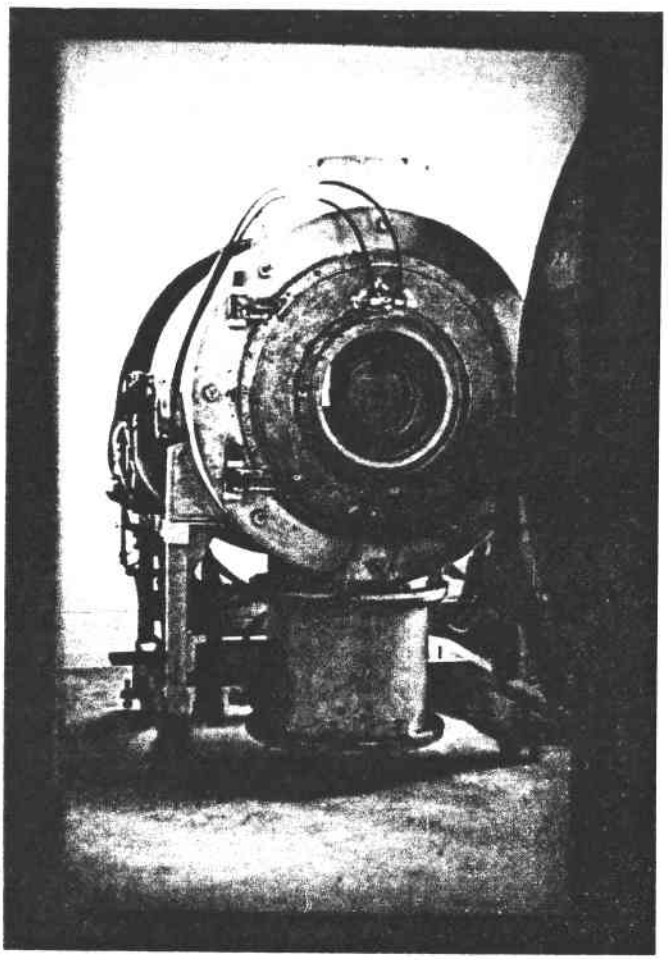

Figure 41

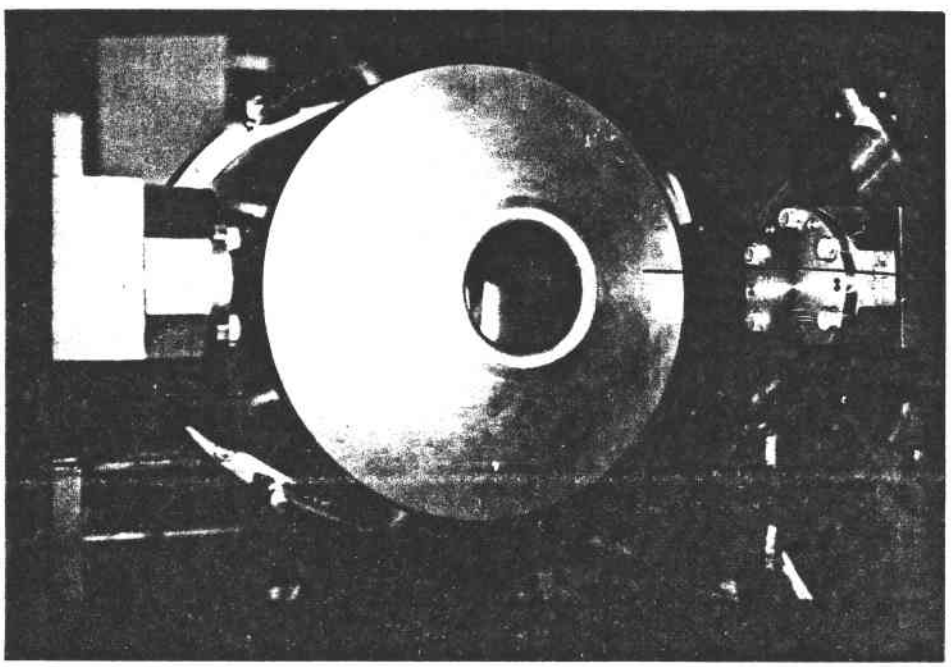

Figure 42

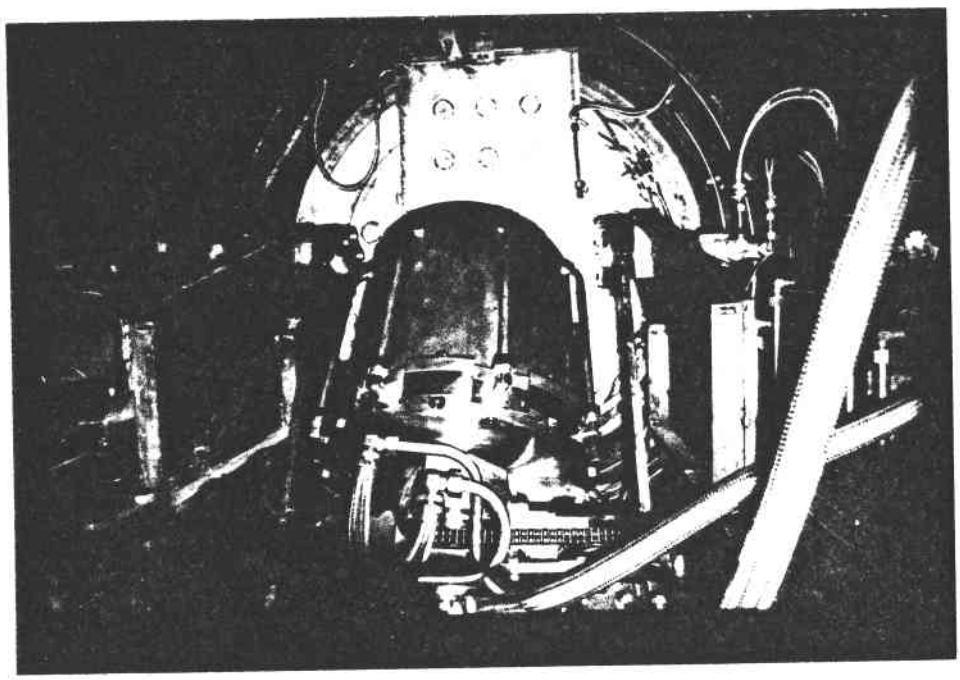

Figure 43

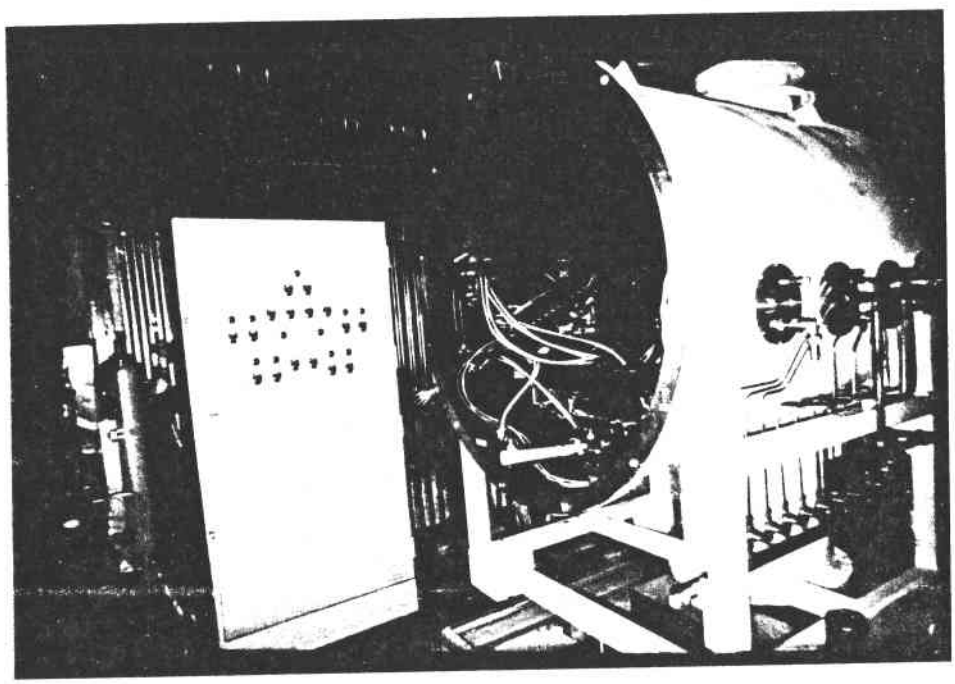

Figure 44

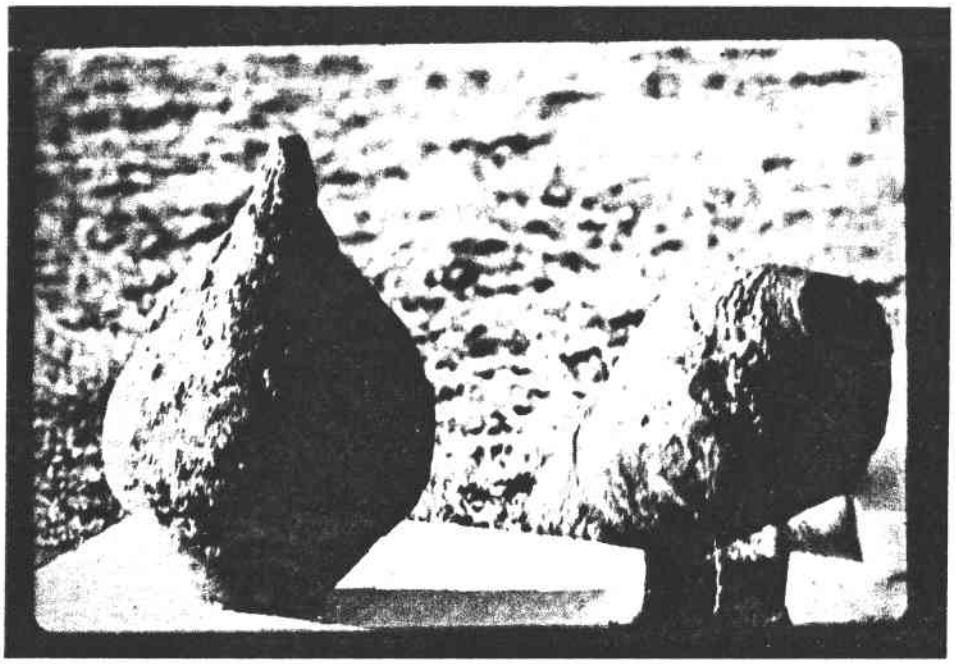

Figure 45

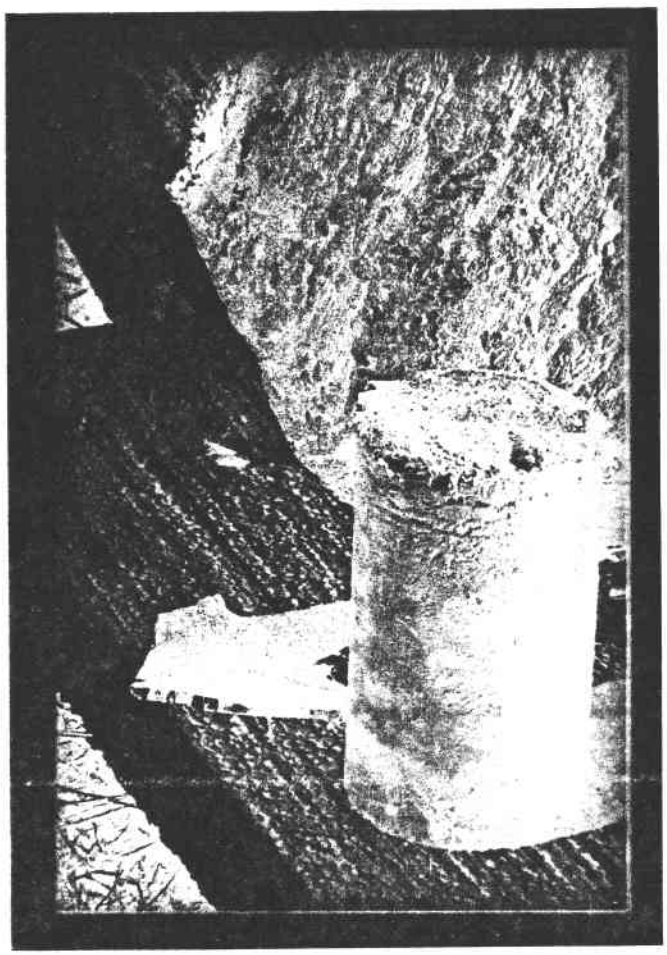

Figure 46

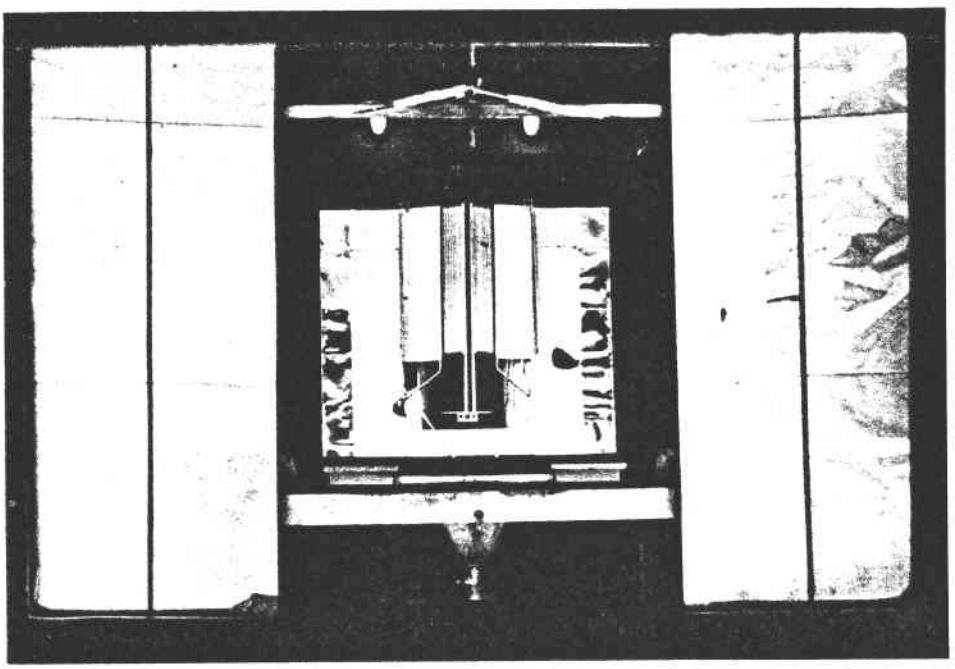

Figure 47

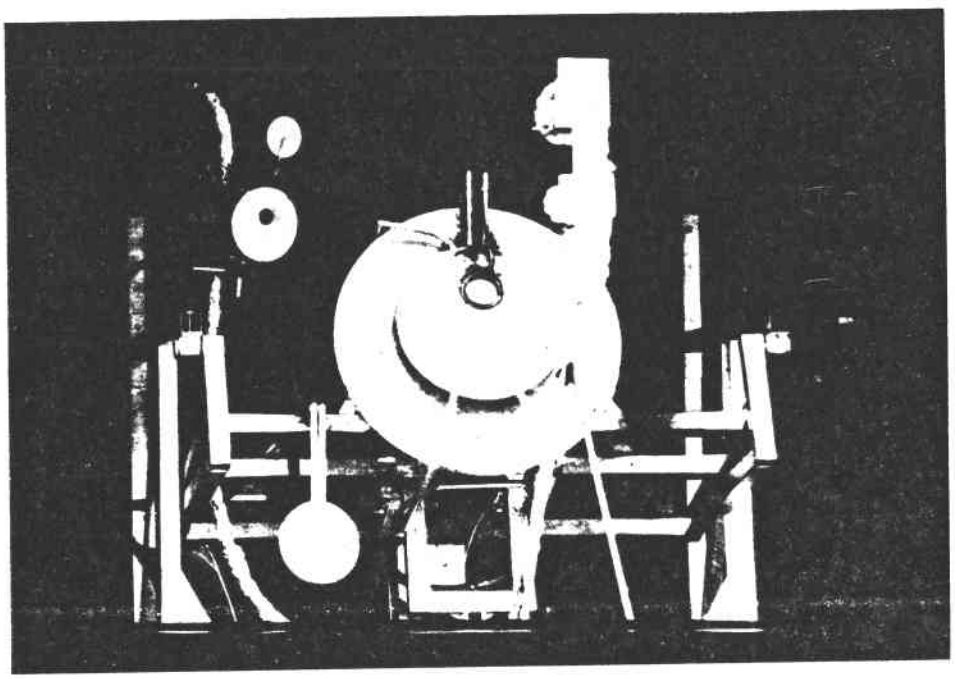

Figure 48

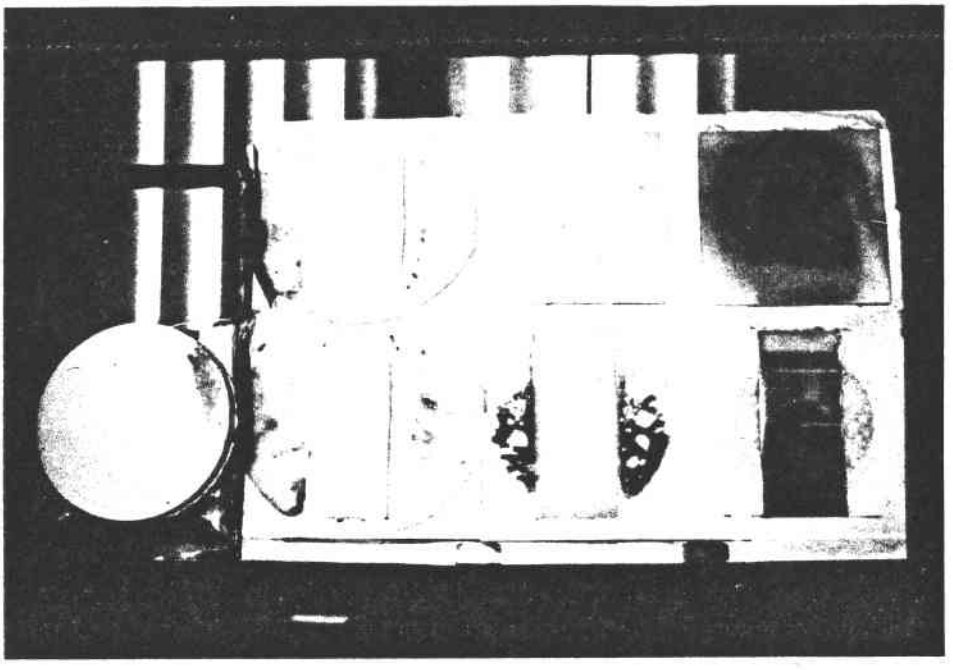

Figure 49

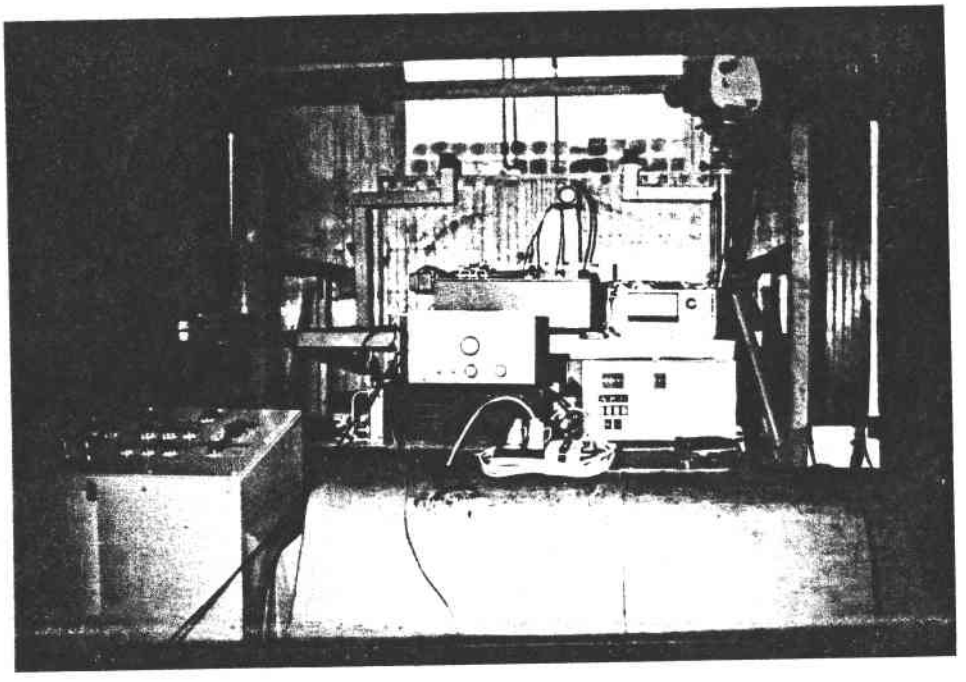

Figure 50

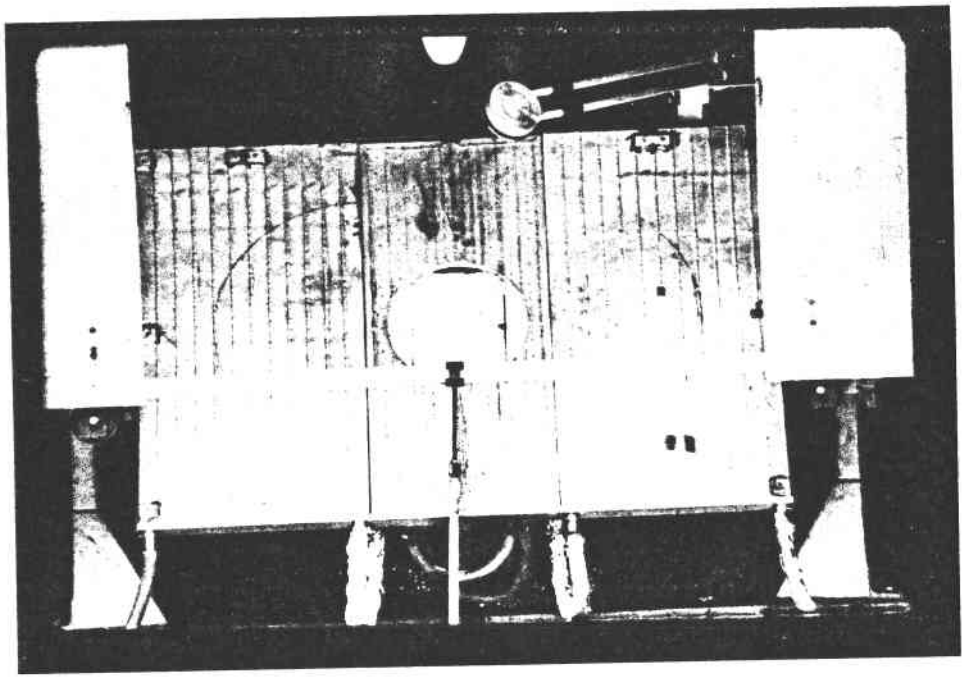

Figure 51

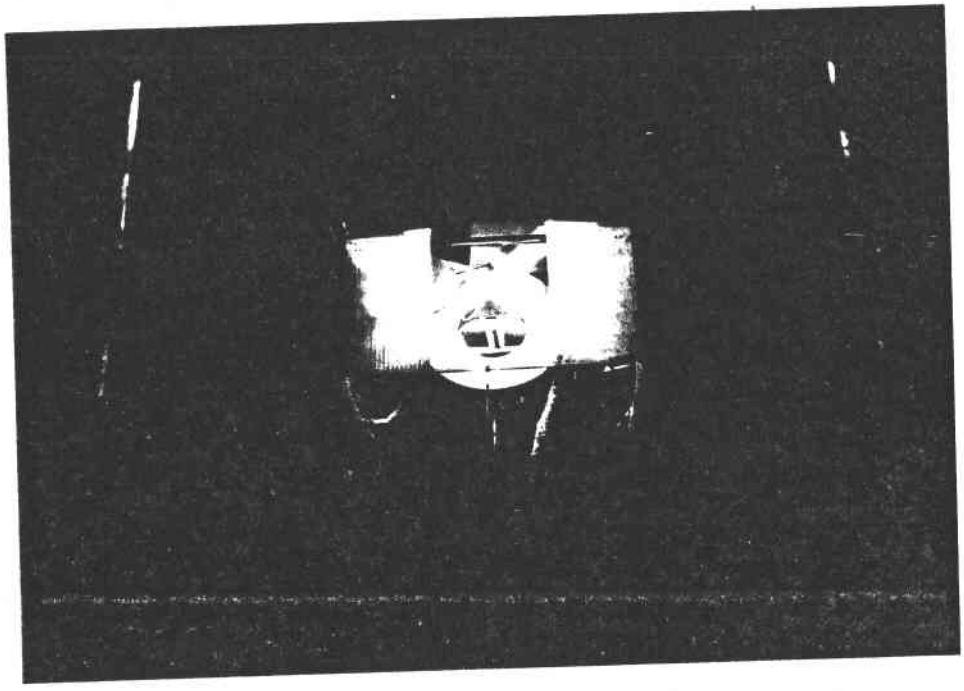

Figure 52

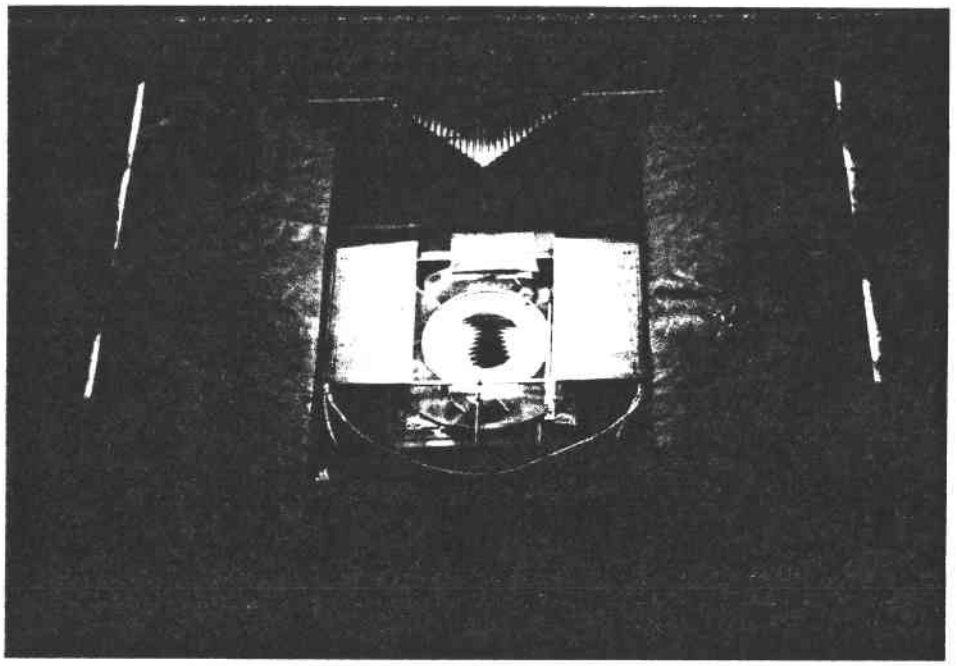

Figure 53

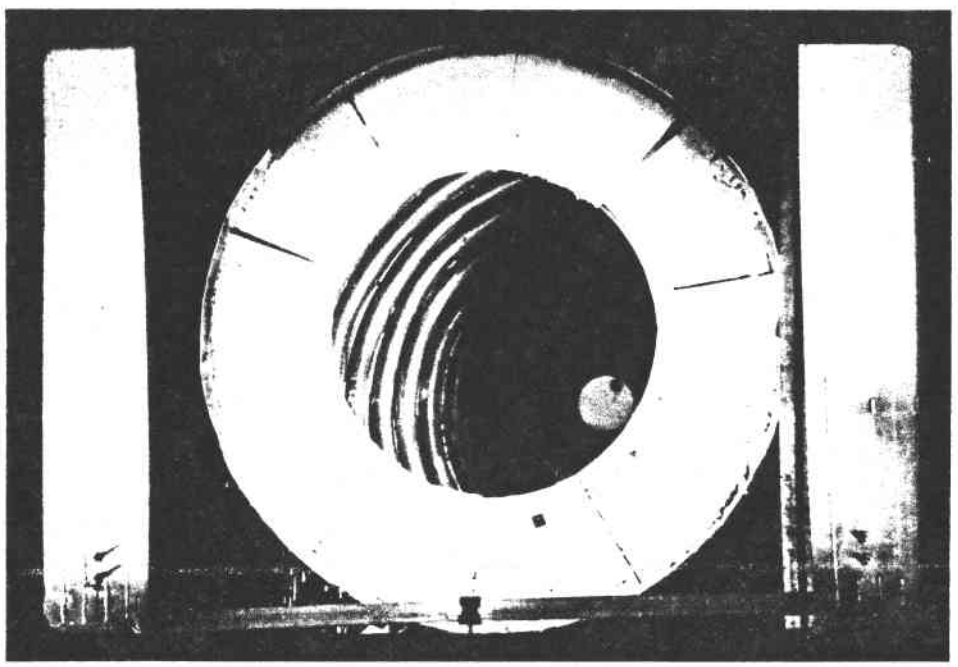

Figure 54

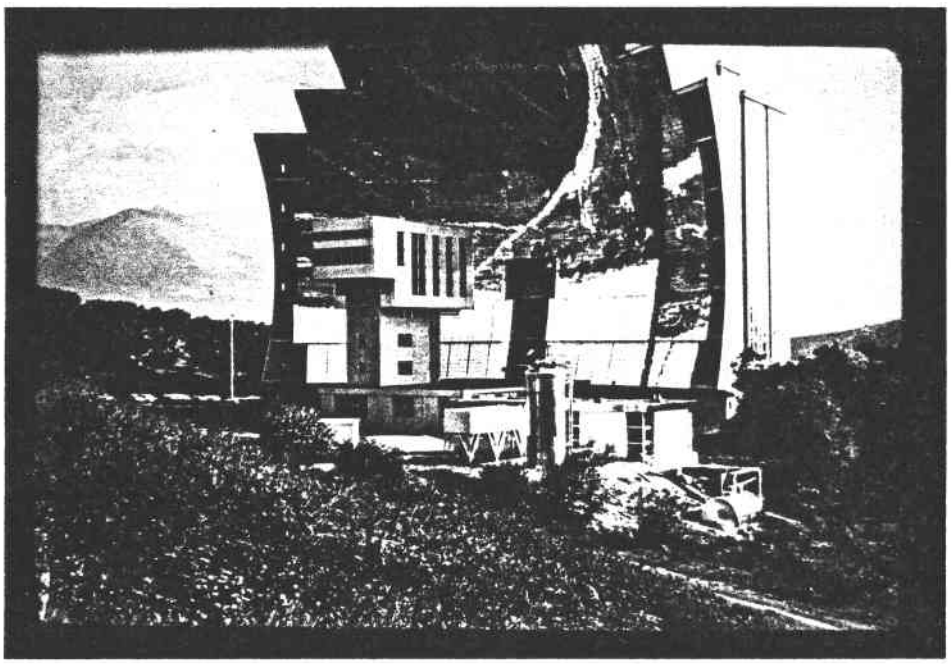

Figure 55

A short note on:

TEMPERATURE LIMITATIONS OF SOLAR ENERGY POINT FOCUSING FACILITIES: OPTIMIZATION OF CAVITY RECEIVERS

C. Royere, Responsable du Service Traitements de Materiaux
Laboratoire D'Energetique Solaire, BP 5, Odeillo 66120, Font-Romeu, France

From Figure 1 considering the following quantities:

Pu = thermal power available + receiver losses (convection and conduction)

$$Pu = \alpha o\ Pi - s\ \epsilon_0 \sigma\ (T^4 - To^4)$$

$$Pi = Po\ \frac{I}{Io}\ f(s) \qquad \begin{matrix} f(s,t) \text{ for solar tower} \\ f(s) \quad \text{for solar furnace} \end{matrix}$$

one can derive the expression of the actual radiative efficiency:

$$\frac{Pu}{Pox\frac{I}{Io}} = \alpha o\ f(s) \ - \frac{s\ \epsilon o\ \sigma\ (T^4 - To^4}{Po\ \frac{I}{Io}}$$

f(s): derived from measurements or calculations

αo(and ϵo): functions of α (and ϵ) and dimensions of cavity and flux distributions on walls derived from measurements or calculations*

* αo(and ϵo) are given by the well known relations:

$$Xo = \frac{x\left[1+(1-x)\ \left(\frac{s}{S} - \sin^2\theta\right)\right]}{x\left(1-\frac{s}{S}\right) + \frac{s}{S}}$$

$$\text{or } Xo = \frac{x\ \frac{S}{s}}{1+x\ \left(\frac{S}{s} - 1\right)}$$

where Xo is the apparent solar absorptance of the cavity (or emittance) and x the corresponding quantity characterizing the material of the cavity.

α has been taken equal to 0.6 and ϵ = 0.8 in the case of receivers for energy conversion. Otherwise in the case of thermal applications for processing materials with solar furnace type facilities, α has been taken equal to 0.3 and ϵ = 0.8. These assumptions are conservative and correspond to current actual values.

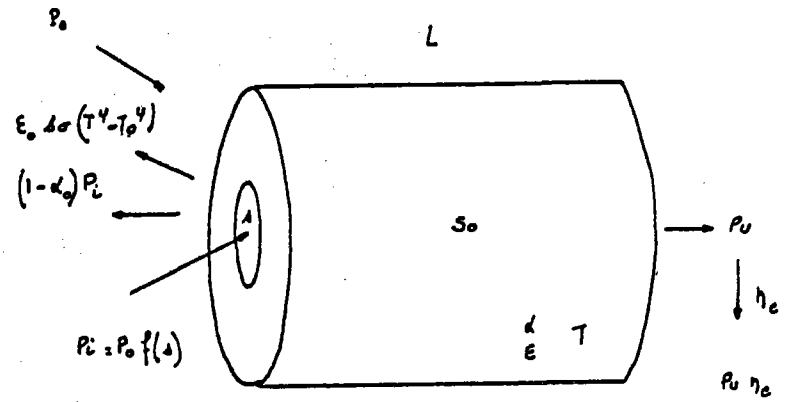

Figure 1. Radiative Heat Transfer in a Cavity Receiver

1°/ The cavity is characterized by the ratio

$\frac{Pu}{Pi}$ which is a function decreasing when temperature increases

The theoretical Carnot efficiency:

$\eta_C = 1 - \frac{To}{T}$ is a function increasing when temperature increases

The efficiency $\frac{Pu}{Pi} \times \eta_C$, which characterizes the use of Pi for thermodynamic conversion, shows a maximum versus temperature: this point is the optimum of operation for a given facility and a given cavity receiver.

But since Pi can be picked arbitrarily (Pi depends on the choice of s), this efficiency does not give any information on the best possible use of this facility which is characterized in fact by $\frac{Pu}{Po}$ or $\frac{Pu}{Po \times \frac{I}{Io}}$

2°/ $\frac{Pu}{Pi}$ is a function decreasing when s increases at a given temperature

$\frac{Pi}{Po}$ is a function increasing when s increases

The efficiency $\frac{Pu}{Po}$, which characterizes the use of the facility, shows a maximum versus s at a given temperature: this point gives the optimum size of s at that temperature and for this facility for an optimum thermal efficiency $\frac{Pu}{Po}$.

Figure 2 shows:

$\frac{Pu}{Po}$ function of $\lambda = \frac{s}{so}$

with $so = \frac{Po}{Eo}$ and $Eo = 3500\ kW/m^2$

$Po = 12\ MW_{th}$

in the case of a Gaussian type distribution of Pi over the focal plane

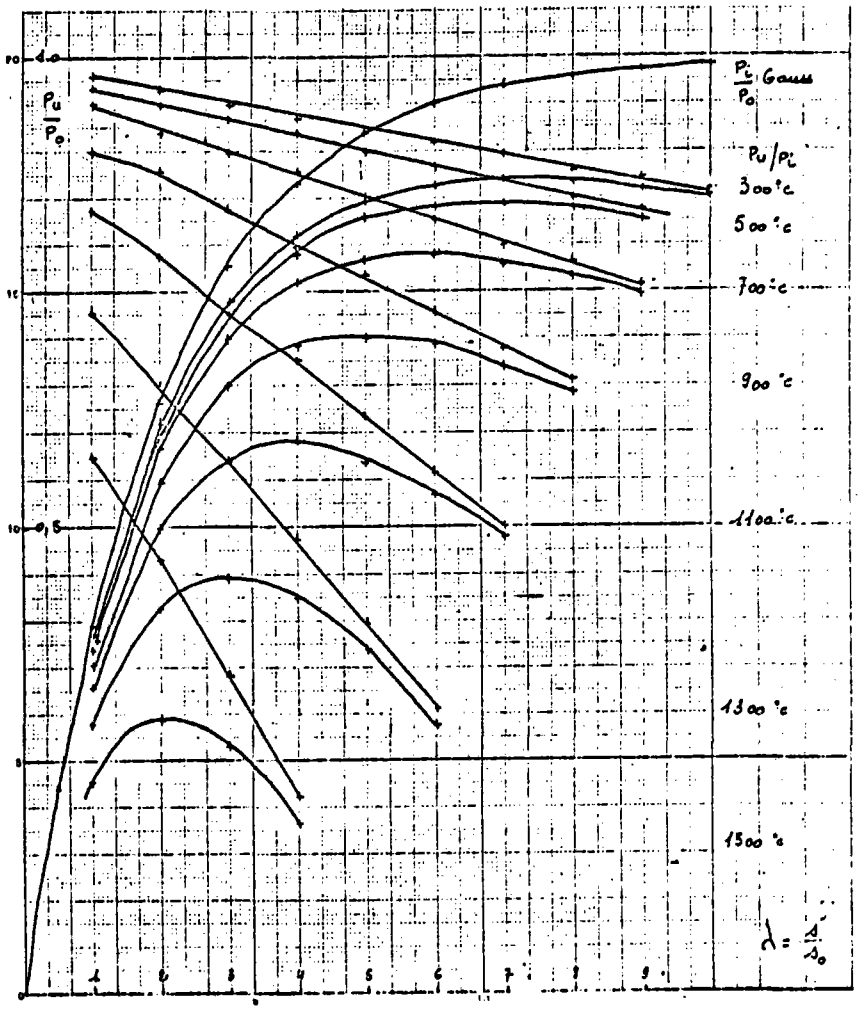

Figure 2

3°/ the optimum values of $\frac{Pu}{Po}$ and η_c versus temperature give the optimum global conversion efficiency of the facility and the optimum operating temperature.

Figure 3 shows:

$\frac{Pu}{Po}$ function of temperature

either optimized

or on the basis of $\frac{Pi}{Po} = 0,99$

and $\frac{Pu}{Po} \times \eta_c$ in both cases

Curves show the optimum temperatures

660°C versus 520°C

The same curves show that for this given facility at 1250°C the thermal efficiency is

48% for an optimized receiver

0 for the nonoptimized one

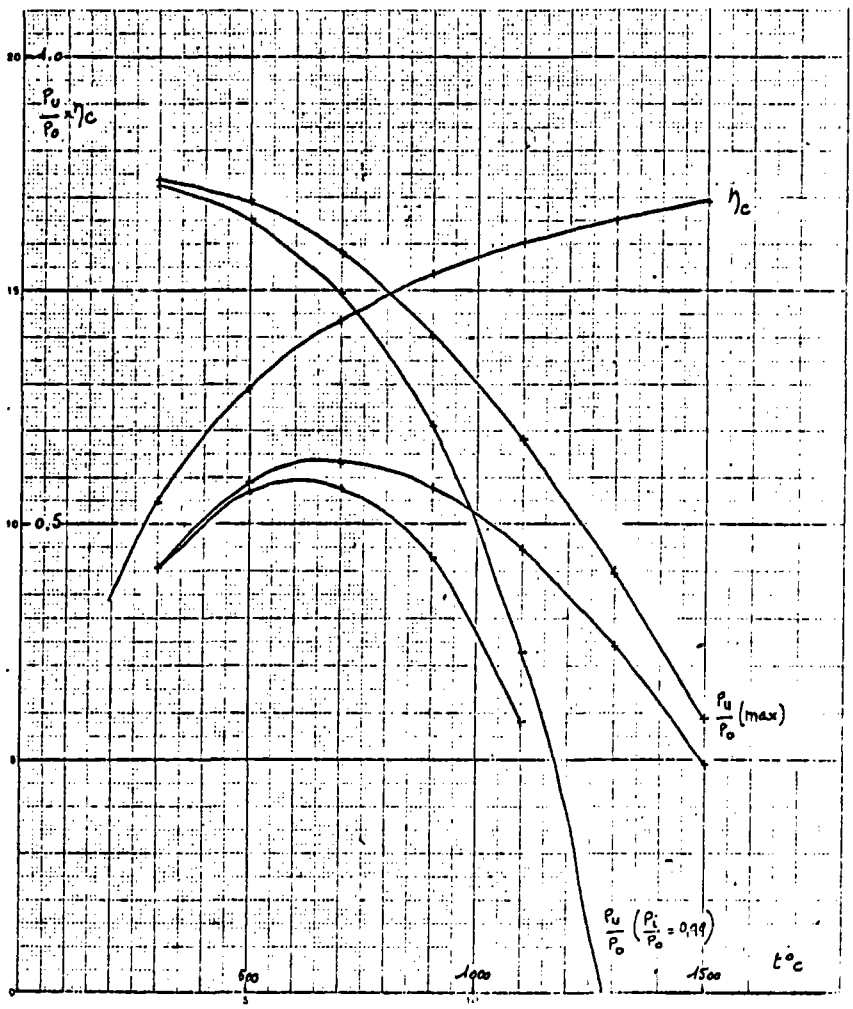

Figure 3

Figures 4 and 5 are the same as Figures 2 and 3 for a tower facility

$\frac{Pi}{Po}$ from calculations

Eo = 1700 kW/m^2

Po = 12 MW$_{th}$

δ = 4 x 10^{-3}rd

June 21 noon

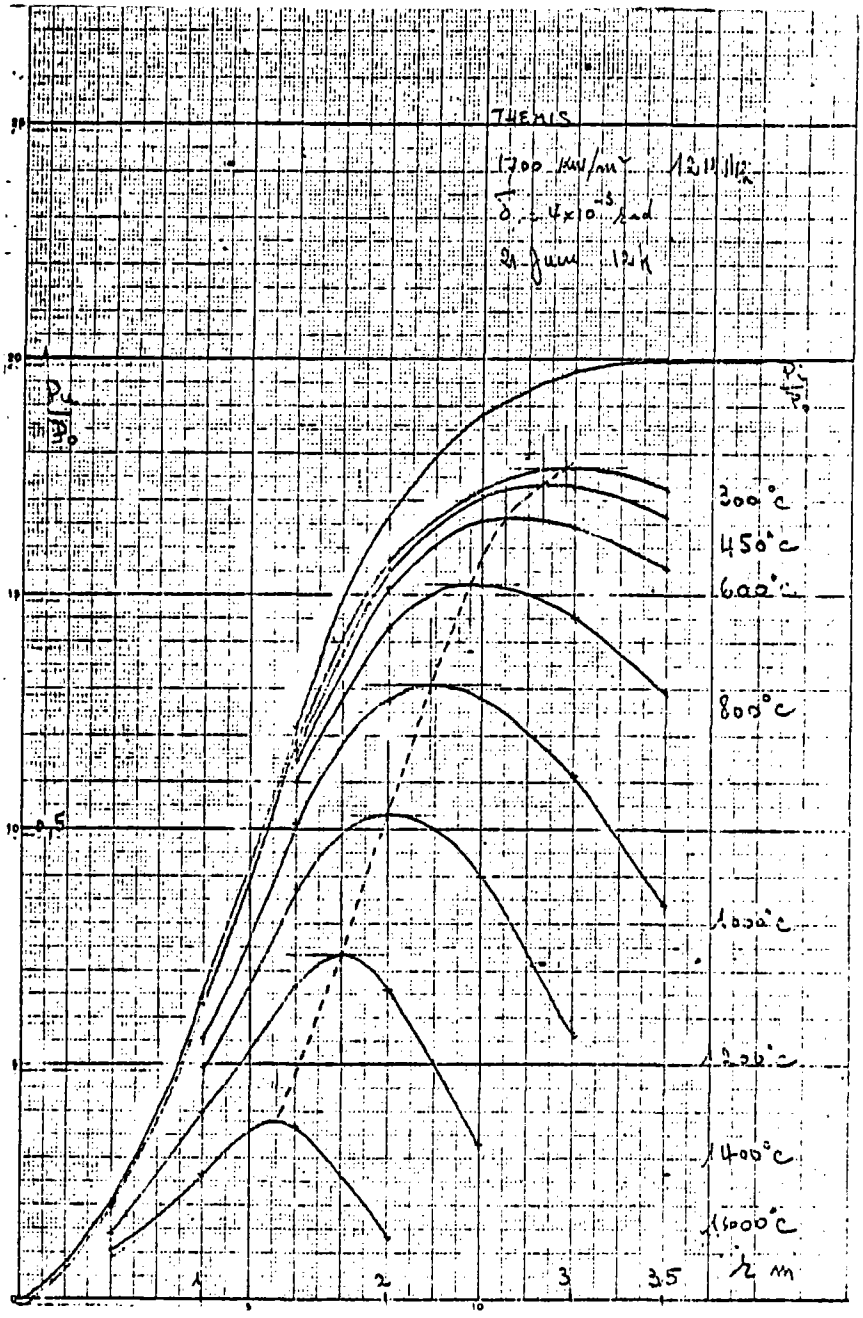

Figure 4

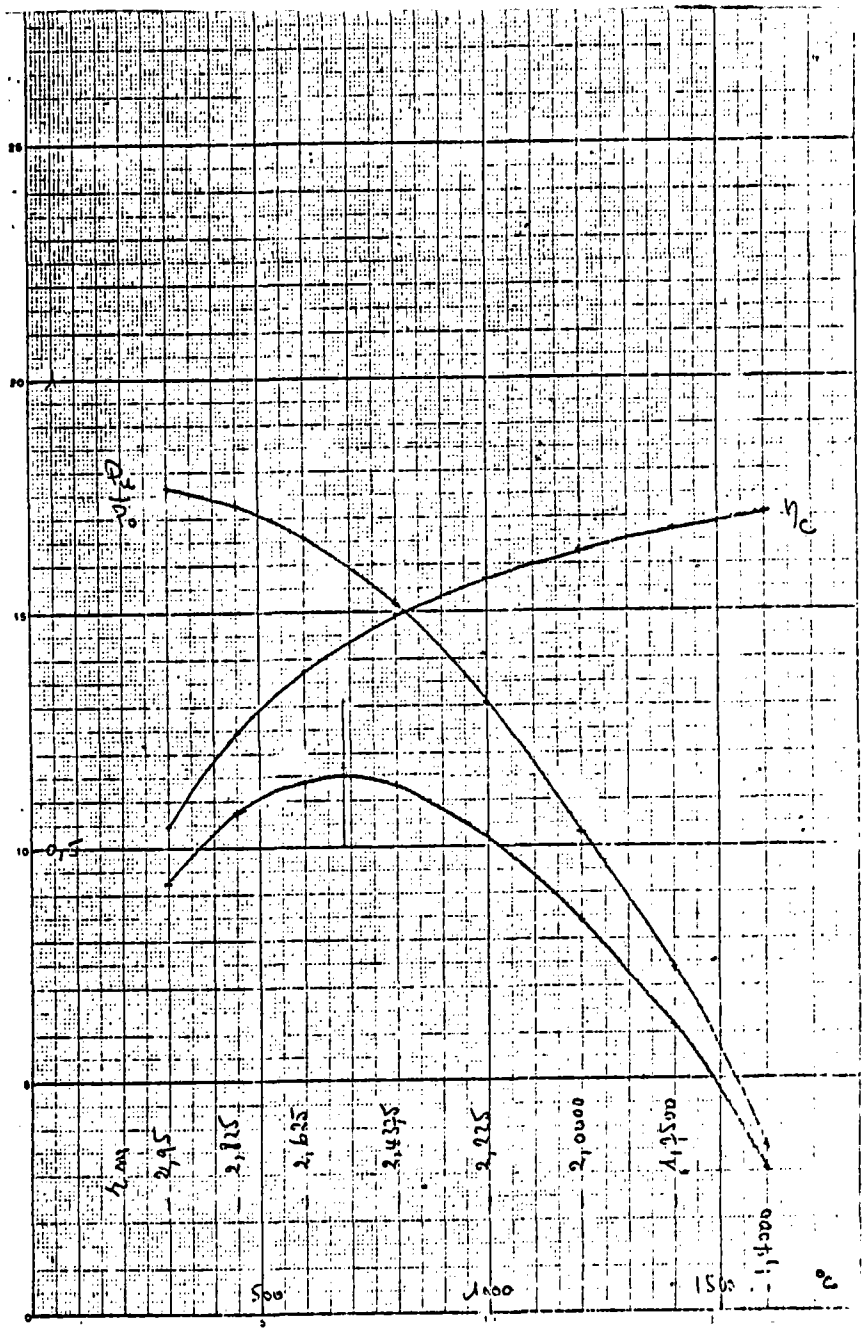

Figure 5

For comparison:

Figures 6 and 7 illustrate the possibilities of thermal applications in the case of a 1000 kW_{th} solar furnace with a Gaussian distribution $\frac{Pi}{Po}$ and Eo = 1200 kW/m^2.

Figure 4 gives the characteristics $\frac{Pu}{Po}$ for a receiver not optimized below 1800°C.

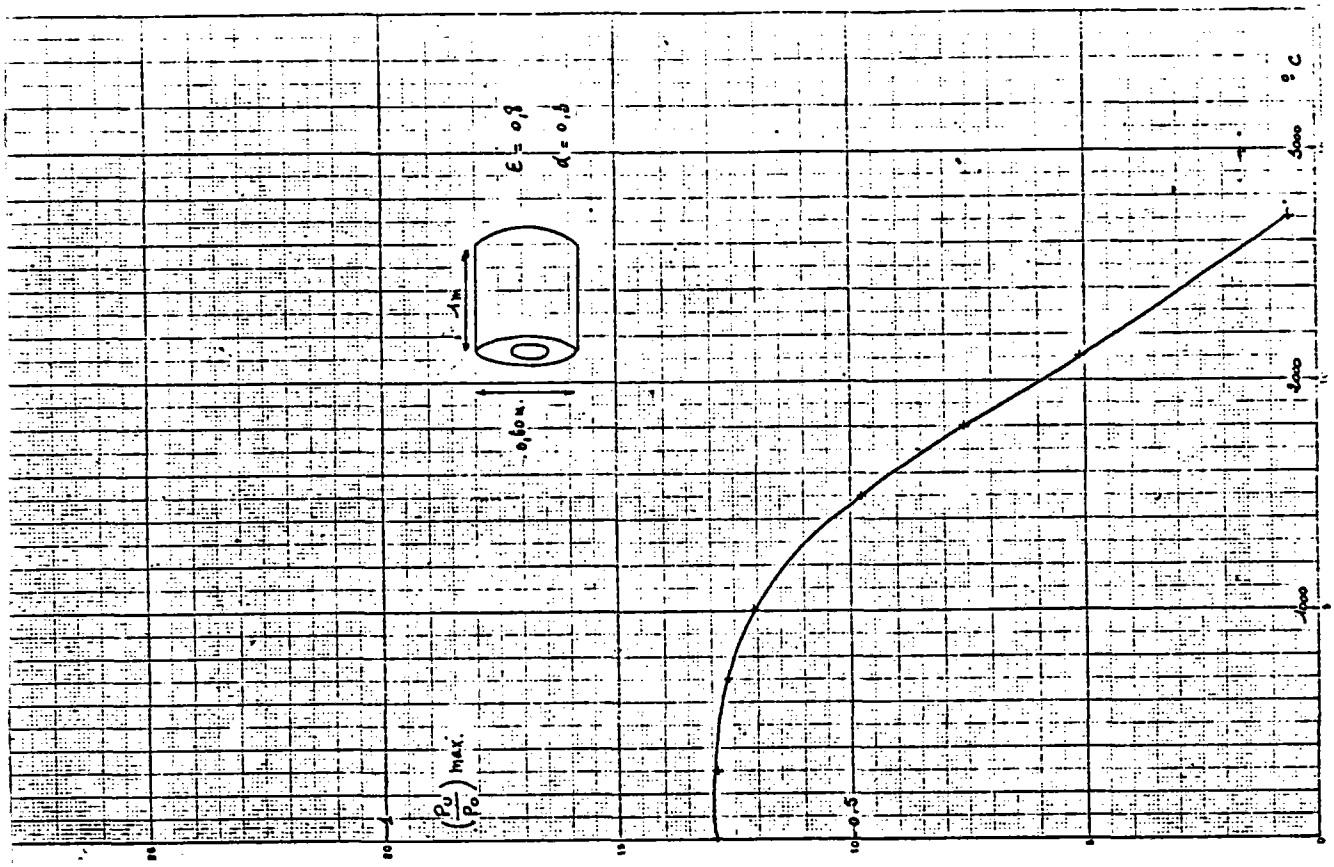

Figure 7

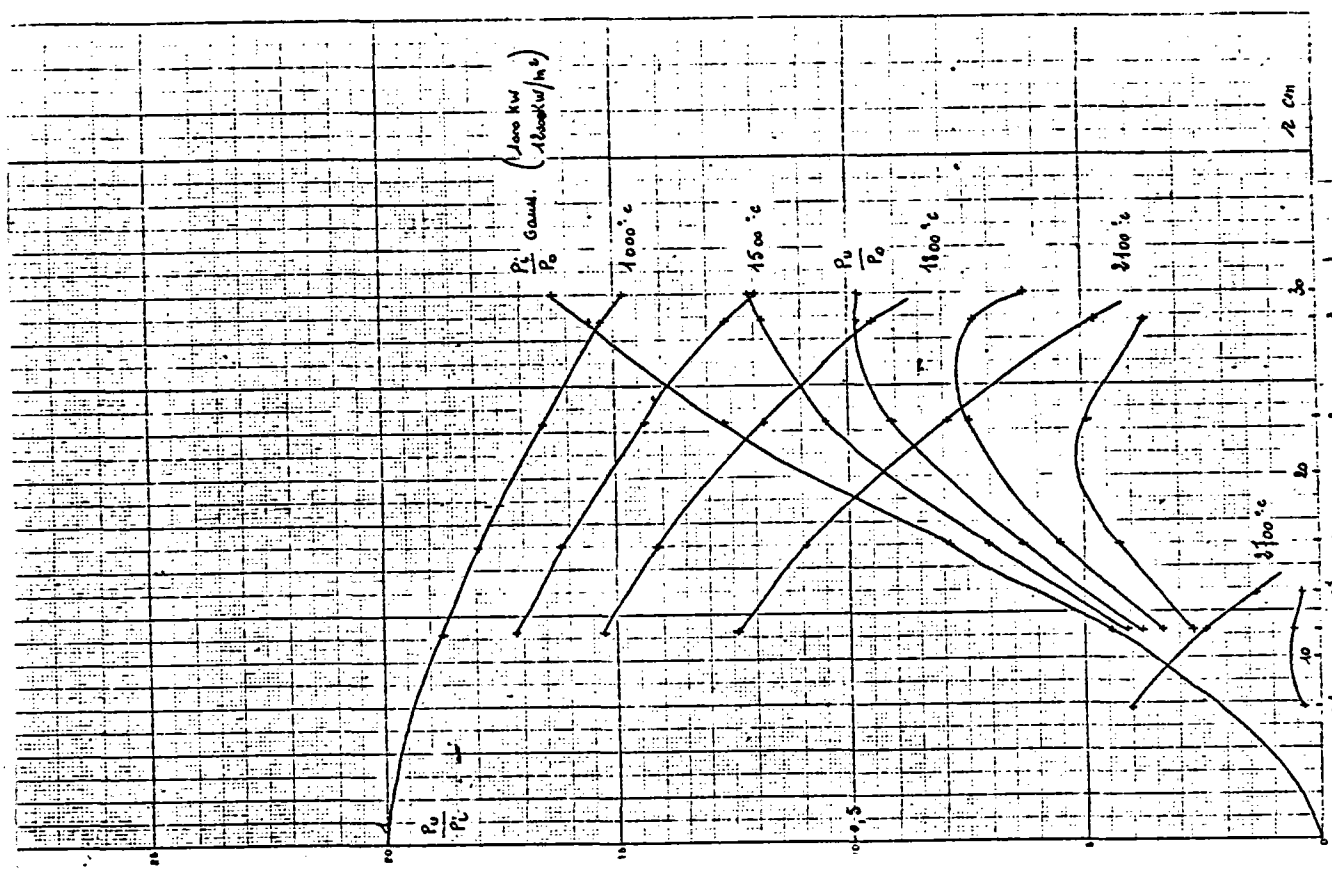

Figure 6

Figures 8 and 9 show the same results in the case of the Odeillo 1000-kW_{th} solar furnace with the nominal 1970 characteristics as measured Po = 1000 kW Eo = 16000 kW/m^2.

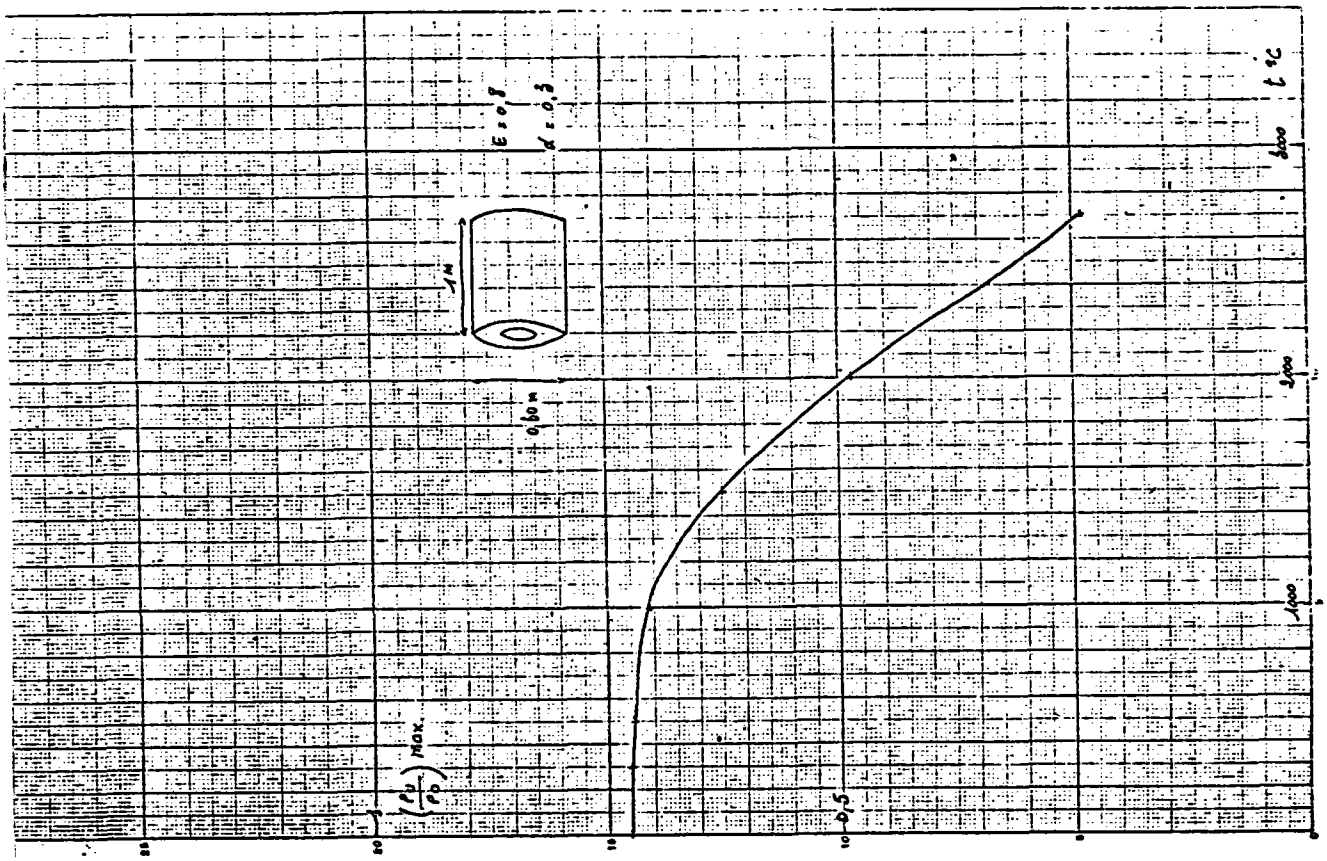

Figure 9

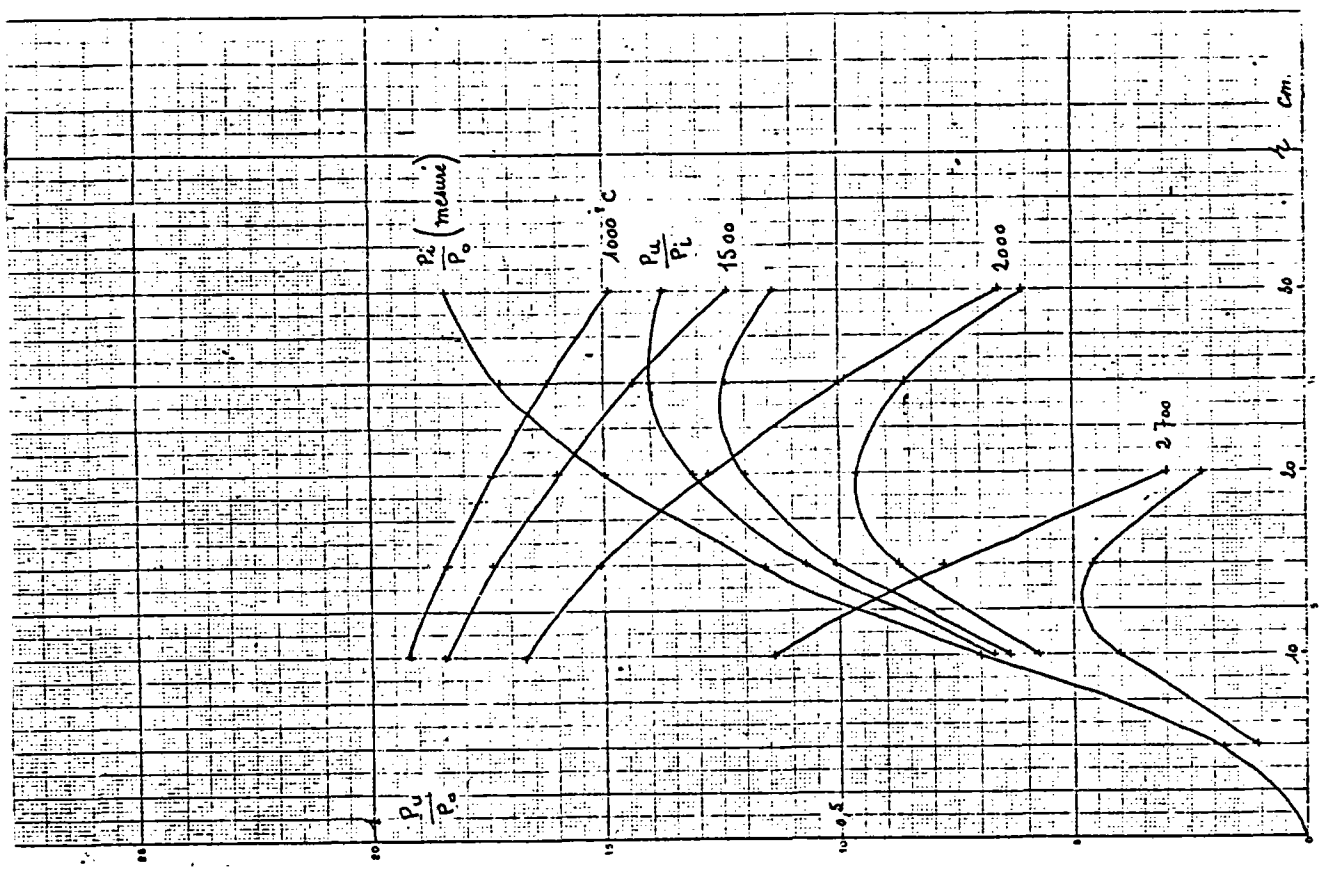

Figure 8

Figures 10 and 11 illustrate: The case of the Odeillo 1000-kW_{th} solar furnace with the characteristics as measured in March 1977. One can see the effect of the degradation of the facility.

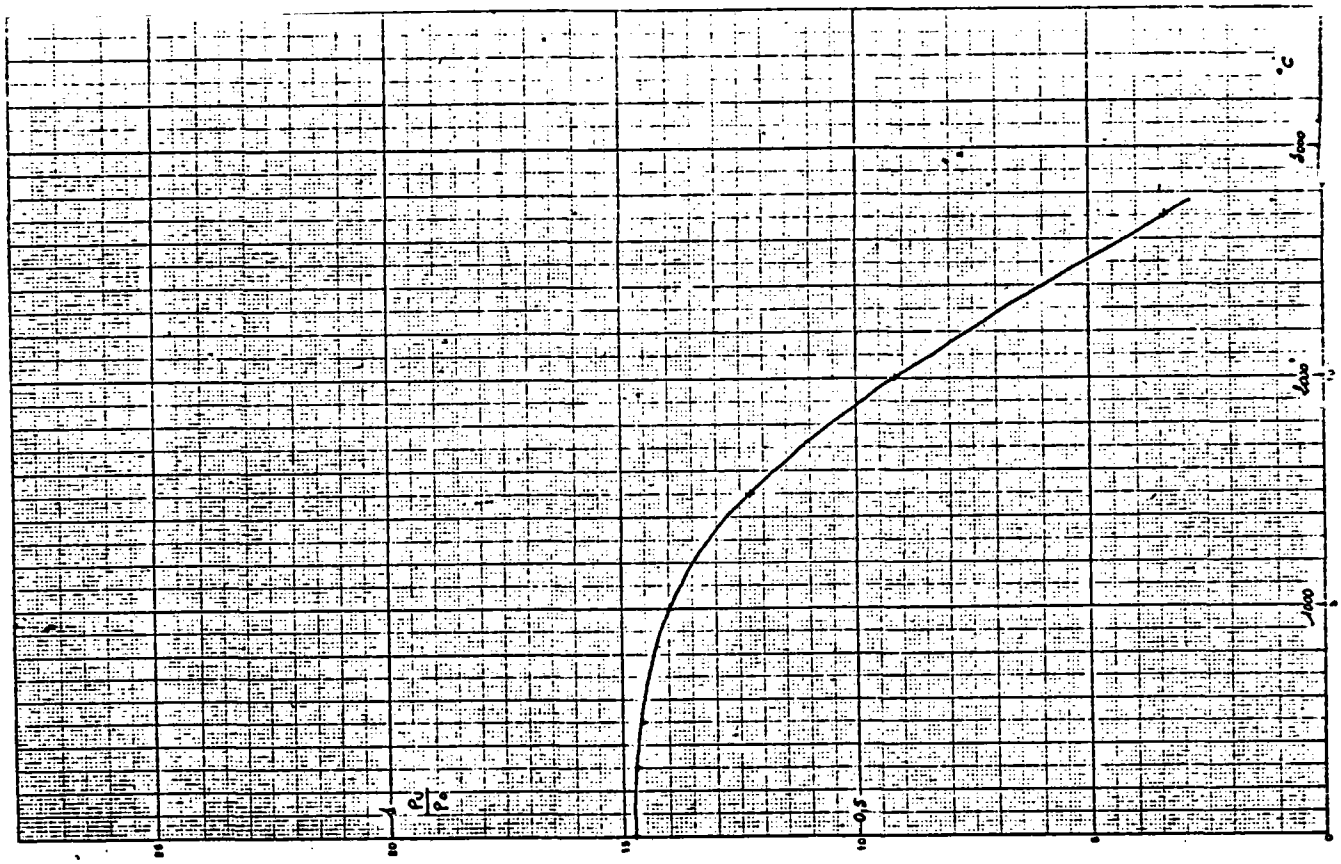

Figure 11

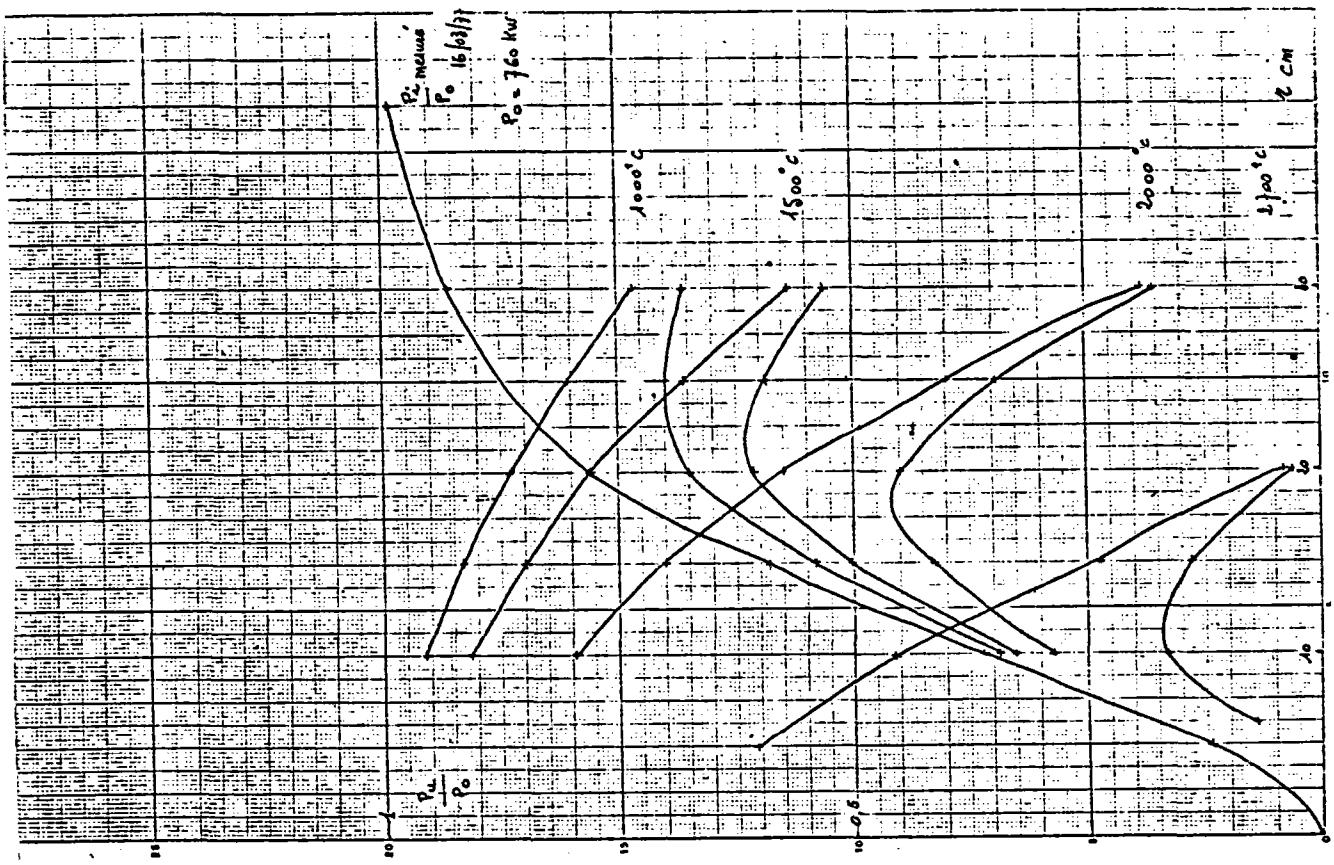

Figure 10

Figure 12 puts in evidence: The influence of α on $\frac{Pu}{Po}$ for an optimized (α = 0,3) receiver at different temperatures; this influence decreases when temperature increases.

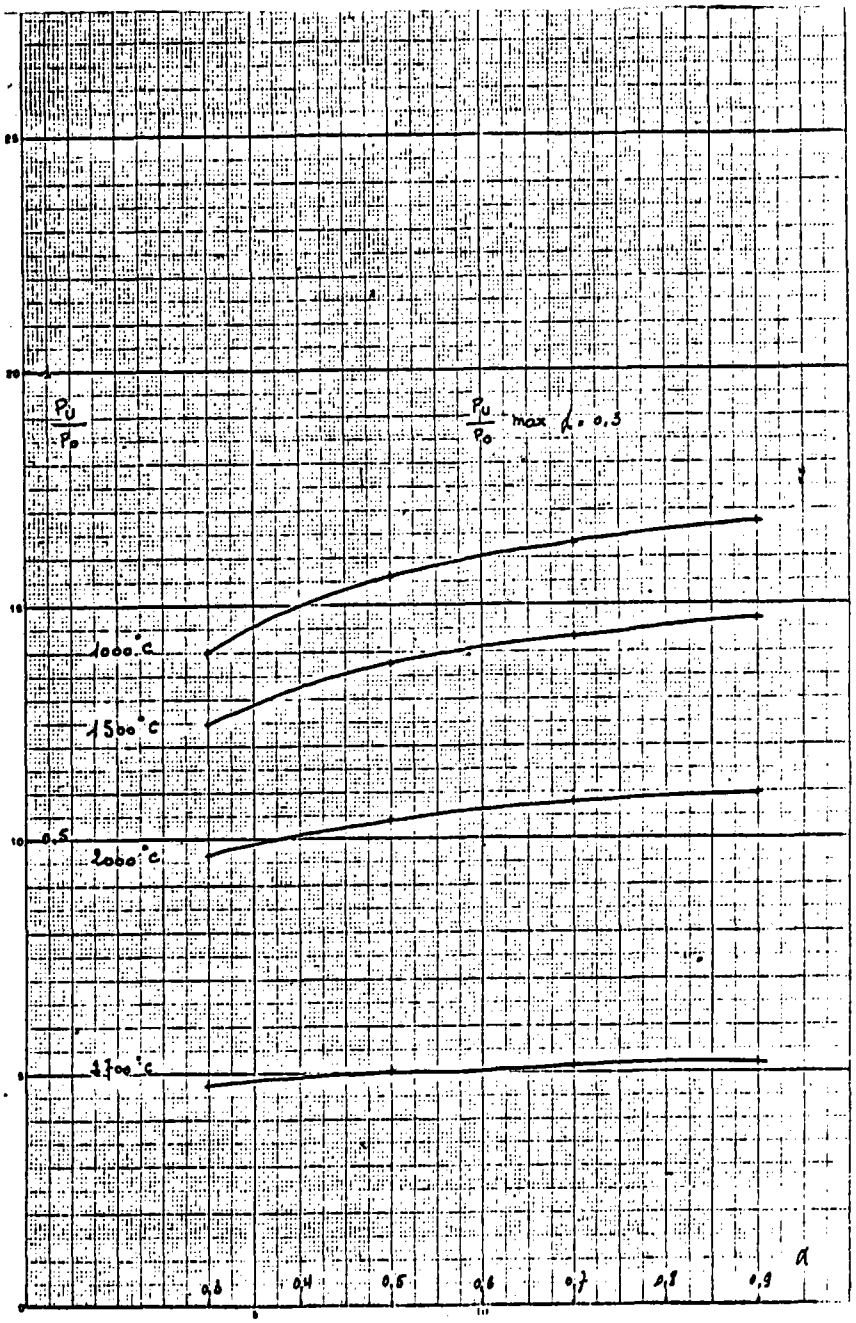

Figure 12

Figure 13 illustrates: The influence of $\frac{I}{Io}$ on $\frac{Pu}{Po}$ at different temperatures for an optimized receiver ($\frac{I}{Io} = 1$); this influence increases strongly when temperature increases.

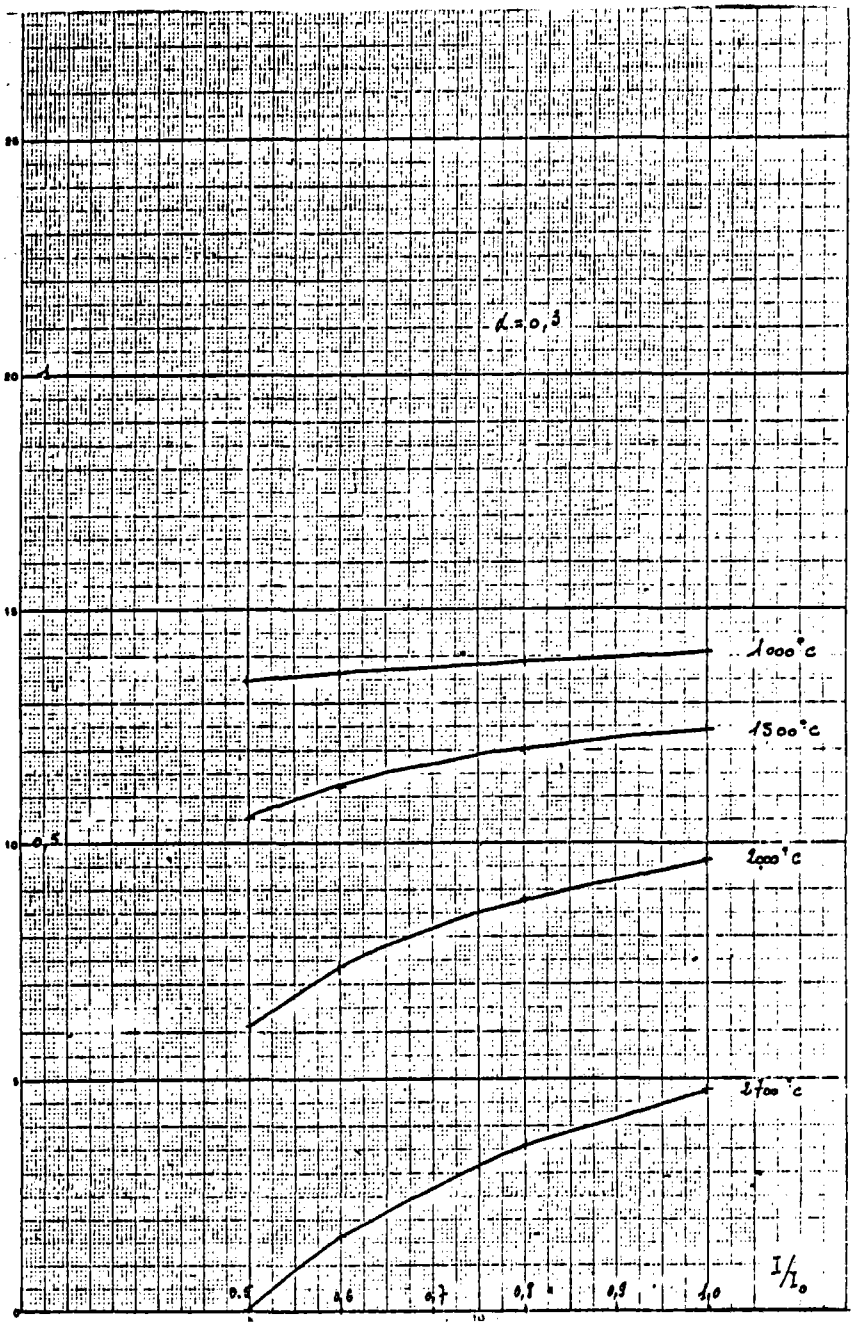

Figure 13

Conclusions

Each solar energy point focusing facility has its own typical characteristics: optimized thermal efficiency and conversion cycle temperature.

The main factor is the distribution characteristic $\frac{Pi}{Po}$ over the focal plane.

The economics of a chemical process at a given temperature with point focused solar energy necessitates knowing with accuracy the cost of $\frac{Pi}{Po}$ with increasing sharpness: at each temperature there is an optimum facility adapted to the process envisioned and so an optimum of cost per kWhr thermal efficient.

This means clearly that in the range of 1000°C to 1300°C there is a temperature limit above which, at least presently, solar towers cannot compete with double reflection type solar furnaces.

Sandia Laboratories
Solar Energy

SOLAR THERMAL TEST FACILITY

THE 5MW SOLAR THERMAL TEST FACILITY

John T. Holmes
Sandia Laboratories
Division 5713
Albuquerque, NM 87185

Abstract

The world's largest high intensity solar experimental facility will be fully operational in 1978. The Solar Thermal Test Facility is capable of delivering 5 million watts of thermal power to experimental equipment. The primary STTF testing programs will involve prototype components for central receiver solar electric power plants. The STTF also provides unique capabilities for other high solar flux and high temperature research and development work. Two hundred twenty-two mirror assemblies (called heliostats) are used to concentrate the sun's energy to an experiment located on the 61 metre tall concrete tower. Operation at partial power of about 1.8MW_t was achieved in May of 1977.

Presented at: STTF Users Association 1978 Annual Meeting, Golden, Colorado, April 11, 1978

THE 5MW SOLAR THERMAL TEST FACILITY

John T. Holmes

INTRODUCTION

The 5MW Solar Thermal Test Facility (STTF) is being constructed to provide for the testing of prototype components for central receiver solar electric power plants and to provide a high solar flux, high temperature test bed for other research and development work. The STTF is being built by the USA Department of Energy and will be operated by the Sandia Laboratories.

The STTF conceptual design was begun in the fall of 1975. Construction started in the summer of 1976 and will be completed about 24 months later in mid-1978. At that time, the facility will consist of a centrally located, 61m tall, experiment tower, 222 computer controlled heliostats capable of directing about 5MW$_t$ to an experiment on the tower, a computer and control building and offices for the experimenters and the operating staff. The total design and construction cost for this versatile, high intensity solar test facility is 21.25 million dollars.

EXPERIMENT CAPABILITIES

Tower

The primary purpose of the centrally located tower is to provide locations with support utilities where experiments may be placed in view of the facility heliostats. The tower rises 61m (200 ft) above ground level and extends 15.2m (50 ft) below ground. Four primary experiment locations have been designed into the tower. Large experiments are located atop the tower which will probably prove to be the most heavily used experiment location. Three test bays for smaller experiments are located on platforms at the 36.6m, 42.7m, and 48.8m (120, 140 and 160 ft) levels as shown in Figure 1. The two lower test bays are configured as rooms and the upper test bay is an outside shelf.

Elevators and Hoists

The tower interior contains an elevating module that can be positioned with its experiment platform (roof) anywhere between ground level and the 61m (200 ft) level. Ground level access to the roof is by a 9.8m (32 ft) wide by 16.8 (55 ft) high door on the north side of the tower. The elevating module will lift 90,700 kg (200,000 pounds). The elevating module contains support equipment for the experimenter including instrumentation terminal panels, computer control and data acquisition hardware and a light machine shop.

Equipment and material can also be lifted into position up the outside or inside of the tower with a number of 4536 kg (10,000 pound) jib cranes. The test bays at the 36.6m and 42.7m (120 and 140 ft) levels are serviced by 4536 kg (10,000 pound) hand-geared bridge cranes.

Heat Rejection System (HRS)

Most of the STTF heat rejection equipment is housed in the tower. The heat rejection system is capable of handling water or air as the coolant fluid.

Figure 2 shows the water/steam heat rejection system. This system is composed of dry cooling towers, a condenser, pumps, heat exchangers, and other necessary equipment.

The HRS can supply demineralized water at a maximum rate of 3.2 l/s (50 gpm) and a maximum temperature and pressure of 288°C (550°F) and 15.5 MPa (2240 psi), respectively. 9000 Kg/hr (20,000 lbm/hr) of 518°C (965°F) steam at 13.8MPa (2000 psi) can be accommodated by the HRS.

To assure the experimenter of high quality demineralized water, a water quality monitoring system is used. This system measures temperatures, specific conductance, cation conductance, and pH. Hydrazine and a deaerator are used to control the water pH and oxygen content.

A closed-loop dry cooling tower system provides coolant to dissipate the excess energy in the feedwater/steam loop. A 25.2 l/s (400 gpm) pump also brings coolant from the cooling tower and pumps it through a tower manifold to provide low temperature cooling capabilities throughout the tower.

The air heat rejection system supplies 2.7 kg/s (6 lbm/s) air at a maximum temperature and pressure of 121°C (250°F) and 1.0 MPa (150 psia), respectively. Refer to Figure 3.

Four rotary type diesel driven compressors provide the air supply. Two hydrocarbon analyzers are used to monitor the hydrocarbon content of the compressed air. One is used to monitor and display hydrocarbon content for the experimenter and the other is used to stop the input to the system if the air becomes contaminated.

As is true for the water heat rejection system, the air system can be used at any tower location.

Master Control System

Coordinated control of all STTF operating and data systems is provided by a Master Control System (MCS). The MCS is an overall command, control, and data system performing control management and supervision as well as data collection, analysis, and presentation.

The MCS uses three digital minicomputers in a modular, function-oriented network as shown in Figure 4.

1. MCS-Control is the interface for the facility operator's and experimenter's consoles through which the entire STTF can be controlled.

2. MCS-Data is used to control and acquire data from the heat rejection system, four meteorological stations, and from the MCS-Tower minicomputer.

3. The MCS-Tower minicomputer acquires data from experiments in the tower and generates control signals.

Up to 500 channels of analog data can be connected to the MCS measurement equipment multiplexers at any tower elevation. Control signals are either digital, for on-off control, or analog, such as proportional voltage or current to adjust set-points for analog proportional controllers.

The facility operator will be able to display any of three color coded data or status pictures stored in his console's refresh memory. One display is the heliostat field status and other current information such as time and weather data; another is the Heat Rejection System schematic. A third picture will be tailored for experimental data, such as a color image depicting temperature or stress regions within the

boiler. The facility operator's keyboard is used to enter real time, on-line commands which are analyzed and tested for validity, then passed to the HAC's for immediate execution or to the MCS-Data mini-computer to change the data acquisition configuration or to the heat rejection system controller set points.

The experimenter sits at a console identical to the facility operator's and may look at the same three data or status pictures, but cannot change the contents of any but the experiment data picture.

Off-line post-test programs allow (1) reformatting the data for subsequent processing, (2) replaying the test data with time-scale changes for analysis, (3) analyzing and presenting data for more channels or with more time consuming analysis than possible in real time, and (4) archiving data.

Heliostat Array Subsystem

The STTF energy collection field consists of 222 heliostats, see Figure 5. Provisions for the addition of heliostats to an originally-planned total of 312 has been made in the construction. The total heliostat field is capable of concentrating in excess of 5 million thermal watts of power and produce a peak intensity of 2.5×10^6 watts/m^2 under favorable sun, heliostat, and target conditions. This is equal to a maximum black body absorber temperature of about 2570^0K.

For test flexibility, heliostats can be located on either of two general foundation arrays which form a northern or circular distribution with respect to the central tower (Figure 6).

The reflector surface of the heliostat is made up of 25 back-silvered glass mirror facets that total 37.2m^2 in area. The 25 facets are assembled into a mirror module. The mirror module is moved about by an azimuth and elevation mount and drive system. Each axis gimbal is driven by a dual motor system which provide angular rates of either 5.6 milliradians/sec or 0.3 milliradians/sec. The high gimbal rates are primarily used to move the mirror module rapidly for emergency, start-up and shut-down operations. The low rate is used for sun tracking operations. The position of each gimbal is known by a digital-output optical encoder.

The facets of each heliostat can be focused by mechanically warping the mirror. This is done in the production process.

Each reflected beam is aligned with each of the other beams so as to produce 25 coinciding facet beams. This focusing and aligning process produces concentrations of 10 to 50 depending on the focal length.

The alignment is accomplished using a collimated laser light beam the size of a facet which is directed to the facet of interest and the reflection is returned to a target. The control system positions the heliostat properly to create the required facet-to-facet orientation. The operator adjusts each facet support until the reflected beam returns to the target center. The geometry created by alignment is optimized for any solar day and hour, heliostat field location, and target location on the tower. Considerable beam spreading occurs when the overall geometry is much different than the chosen alignment condition. About eight man hours are required to align each heliostat.

A secondary concentrator is being designed that is a paraboloid of revolution in shape. It will produce a beam concentrated by about four to five times and about 0.3m in diameter. Achieving a flux density of about 10,000 kW/m^2 will give a maximum theoretical temperature of 3634°K using the secondary concentrator. A scale model concentrator will be built to verify the design.

Heliostat Control System

The overall heliostat control system is shown as it interfaces with the Master Control System in Figure 4. The heliostat pointing commands from the preprogrammed test sequence or from the facility operator are analyzed by Master Control System (MCS) and distributed to the heliostats for execution. Heliostat Array Controllers (HAC) communicate with up to 128 heliostats in their jurisdiction. The HAC's send MCS-generated commands, and HAC-generated azimuth and elevation pointing information to its four associated Heliostat Interface Modules (HIM) to be transmitted to the appropriate heliostats. Each heliostat receives these pointing vector updates once every second and responds with its own status. The HAC's also process alarm messages such as tracking or communication errors.

The commands and data transmitted to the individual heliostats are received and executed by the Heliostat Control Electronics (HCE's). The HCE provides the proper drive motor power until the gimbal axis encoders indicate that the appropriate heliostat attitude has been attained. The HCE and heliostat motors then await the next command.

Beam Characterization

The heliostat characterization system is used to evaluate individual facet and total heliostat performance. This device is a water-cooled 4.9m (16 ft) aluminum bar that is populated in 7.6 cm (3 in) increments along its length with thermal sensors (radiometers). The thermal sensors are interchangeable and range in capability from 1 sun to 100 suns.

In operation, either the instrumented bar is moved across the image to be measured or the bar is kept stationary while the image is moved across. Sensor readings are taken at computer controlled intervals and the accumulated data is stored for later analysis.

The data are available as contour plots as shown in Figure 7. The contour lines are drawn for 10%, 30%, 50%, 70%, and 90% of the maximum measured flux. The plus in the center of the plot indicates the centroid of the calculated flux pattern while the dashed circle indicates a 0.012 radian circle with respect to the centroid. The 0.012 radian circle is the design objective for 90% of the reflected power.

The data are also used to calculate the total integrated power with respect to the flux centroid as shown in Figure 8. The plus sign indicates the value of the power within a 0.012 radian circle with its center on the flux centroid.

The Real Time Aperture Flux System (RTAF) system is a multi-heliostat diagnostic tool. This system uses 0 to 3400 W/m^2 heat flux gages (calorimeter type) that exhibit a linear response over the entire spectral and thermal range. Their response time constant is about 100 milliseconds. Photon sensors are also used on the RTAF to achieve faster response times of a few microseconds. These photon sensors have a dynamic range of 40-4000 suns. Both types of detectors are mounted in 7.6 cm to 10.2 cm (3 to 4 in), spacings on a water cooled bar which will scan the receiver or experiment aperture. The STTF operator will use the data to fine-tune the heliostat beam and provide input flux information for the experimenter.

Heliostat Reflectivity

Environmental conditions influence reflector surface properties and cause average solar reflectance of these surfaces to vary with changing conditions. Preliminary results indicate that average solar reflectance can drop as much as 15% (from about 80% to about 65% in a month period). Preliminary results of using high pressure water and detergent spray system indicate that 80 to 90% of the reflectance losses can be recovered. Natural rains also improve the reflectivity significantly.

STTF TESTING PROGRAMS

US Department of Energy (DOE) Receiver Experiments

The US DOE commitment to a $10MW_e$ central receiver pilot plant has produced solar receiver hardware to be tested at the STTF. The pilot plant concept uses a Rankine cycle with water/steam cooled receiver.

The first of these receivers to be tested at the STTF is a prototype module of the once-through external absorbing receiver designed by a McDonnell Douglas/Rocketdyne team. This receiver module is .89m (35 in) wide by 12.5m (41 ft) high and requires $3MW_t$ of incident solar power to operate at the maximum nominal design conditions. The STTF will supply 288°C (550°F) feedwater and the receiver will output 516°C (960°F) steam at 10.4 MPa (1515 psia) pressure. The solar testing will begin in the fall of 1978 and last about four months.

The second of these prototype receivers to be tested at the STTF is an approximately 5MW thermal capacity scale model of a cavity type receiver using separate boiler, steam drum, and superheater sections. This receiver is a product of the Martin Marietta/Foster Wheeler team. The receiver including its support structure measures approximately 9.1m (30 ft) wide by 5.8m (19 ft) deep by 14.3m (47 ft) high and will weigh 77,300kg (170,000 pounds). The STTF will supply 205°C (400°F) feedwater to the receiver and the receiver will output 516°C (960°F) steam at 9.1 MPa (1325 psia) pressure. This test is tentatively scheduled for summer 1979.

$1MW_t$ Gas Cooled Receivers

The Electric Power Research Institute (EPRI) has initiated a program with Black & Veatch Consulting Engineers and Boeing Engineering and Construction Company to develop gas cooled receivers for Brayton cycle power plants.

The Boeing concept involves a closed helium cycle that will operate at a temperature of 816°C (1500°F). The Boeing 1MW thermal capacity prototype receiver will be tested at the STTF in the summer of 1978. The receiver will use air as the coolant during the STTF tests.

The Black & Veatch solar receiver will be used in an open cycle with a conventional combustor in parallel for added plant reliability. This system will operate at 1038°C (1900°F) using a ceramic receiving surface. A 1MW thermal capacity Black & Veatch prototype receiver will be tested at the STTF towards the end of 1979.

Heliostat Evaluation Capability

The STTF will evaluate heliostat performance including accuracy, beam quality and long term maintenance requirements. Testing will include evaluation of the 222 working STTF heliostats, 10MW pilot plant prototype heliostats, and heliostats developed during future programs. Evaluation techniques currently available or being developed include beam power and flux mapping, tracking accuracy and repeatability, structural stability, environmental integrity and reflectivity.

STTF Testing Schedule

Figure 9 gives the overall STTF test schedule. The STTF tower top test location is committed to DOE solar receiver testing for the next two years, the test bays are only partially committed and additional experiments are being sought. A DOE-sponsored high intensity photovoltaic array is anticipated for testing in 1979. In the conceptual stage are experiments on:

- Liquid metal, molten salt, oil, or gas cooled receivers or storage systems.
- High intensity photovoltaic or thermionic array evaluations.
- High temperature material performance studies and material process development.
- High intensity photochemical, photoelectrochemical and high temperature chemistry process development.

POTENTIAL EXPERIMENTERS

An active Users Association including government contractors, research institutes, universities, private companies, and foreign interests has been founded to assist experimenters and to encourage utilization of the STTF. Prospective experimenters are invited to contact the STTF Users Association, Suite 1507, First National Bank Building, East, Albuquerque, NM 87108. Detailed technical questions will be answered by direct contacts to the STTF Experiment Coordination Office. A publication, "Solar Thermal Test Facility Experiment Manual," SAND1173, October 1977, defines the services provided by the STTF and the requirements that experimenters must fulfill in order to implement an experiment at the STTF.

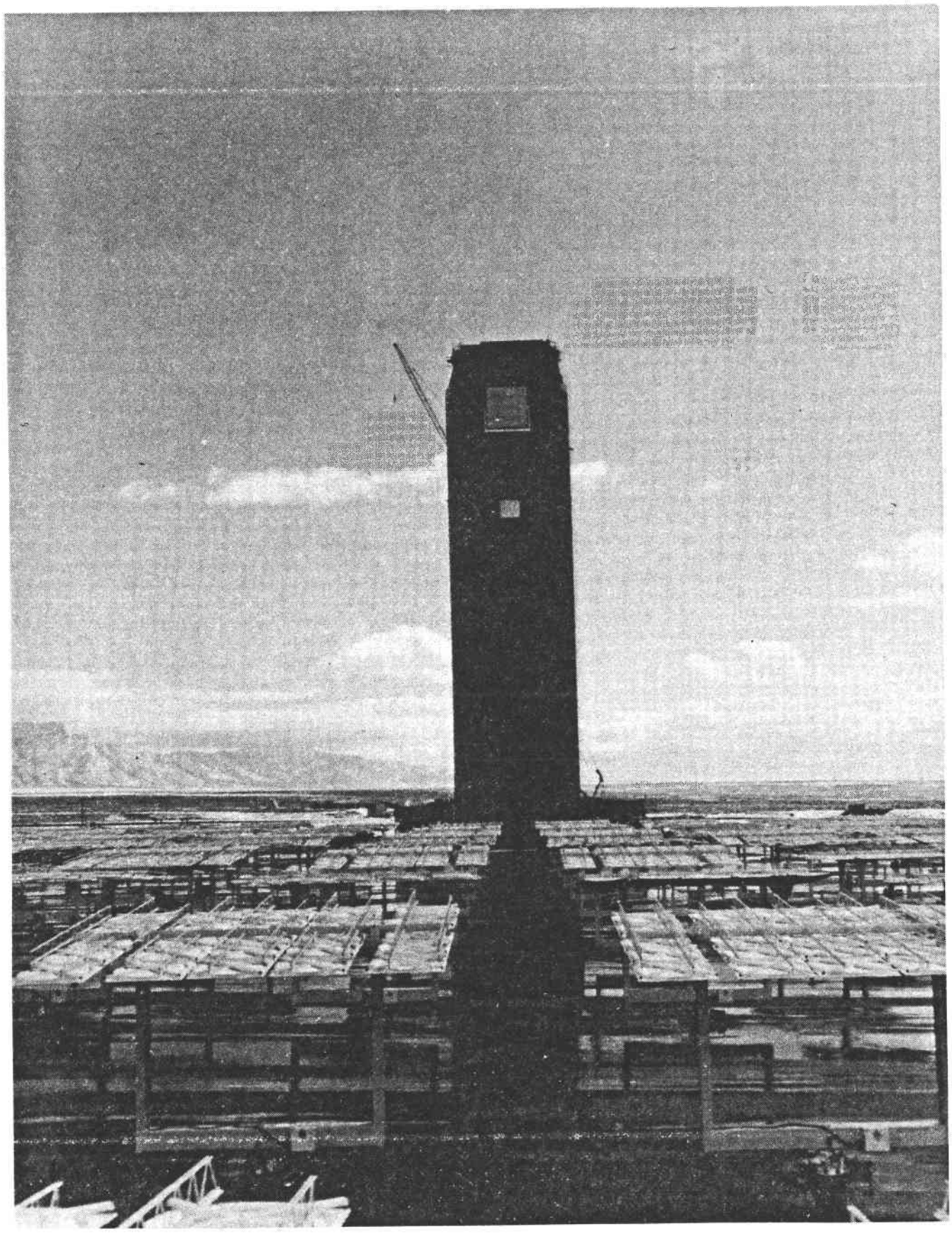

Figure 1
Solar Thermal Test Facility

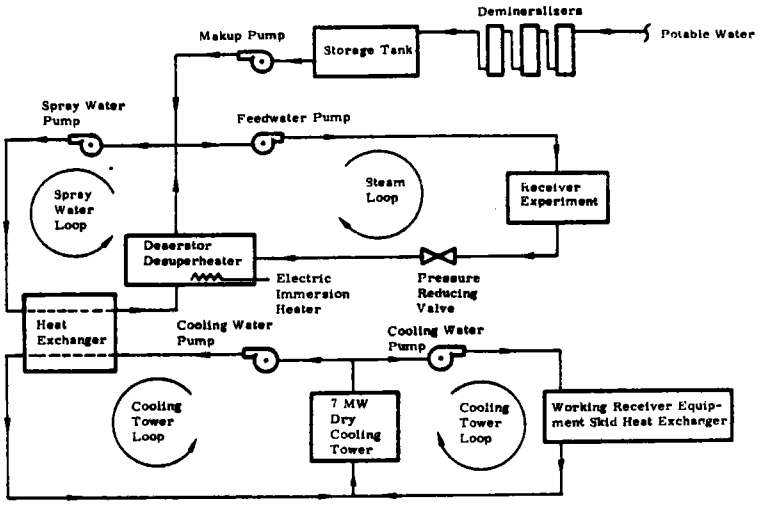

Figure 2
STTF Water/Steam Heat Rejection System

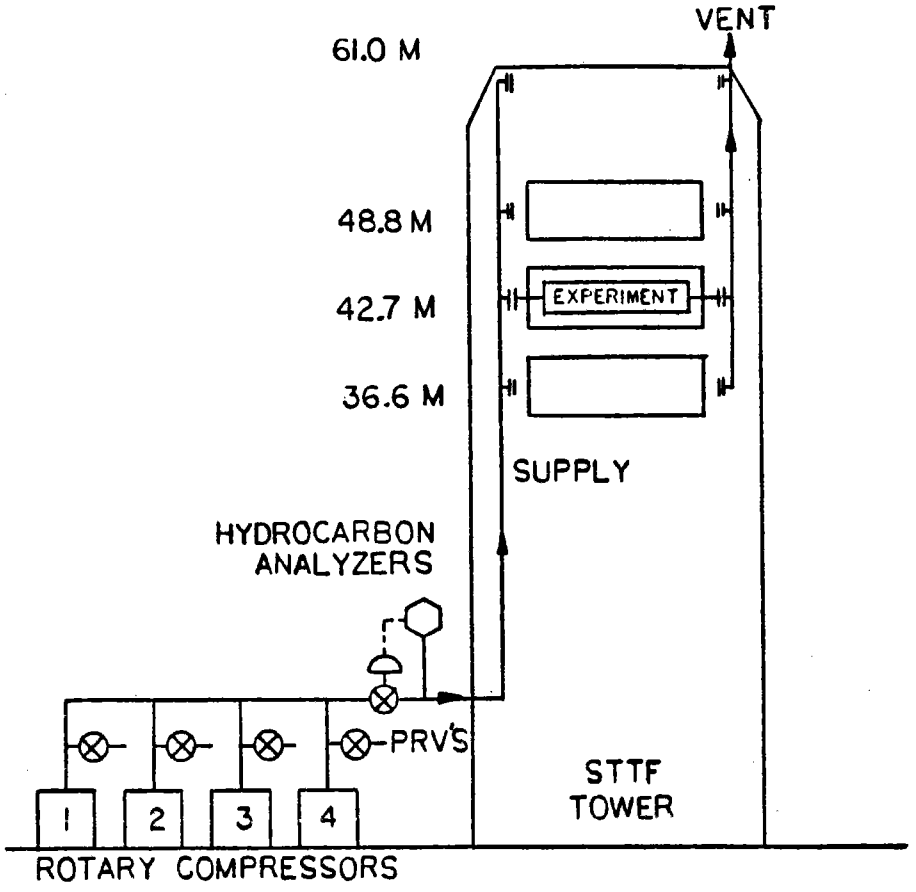

Figure 3
STTF Air Heat Rejection System

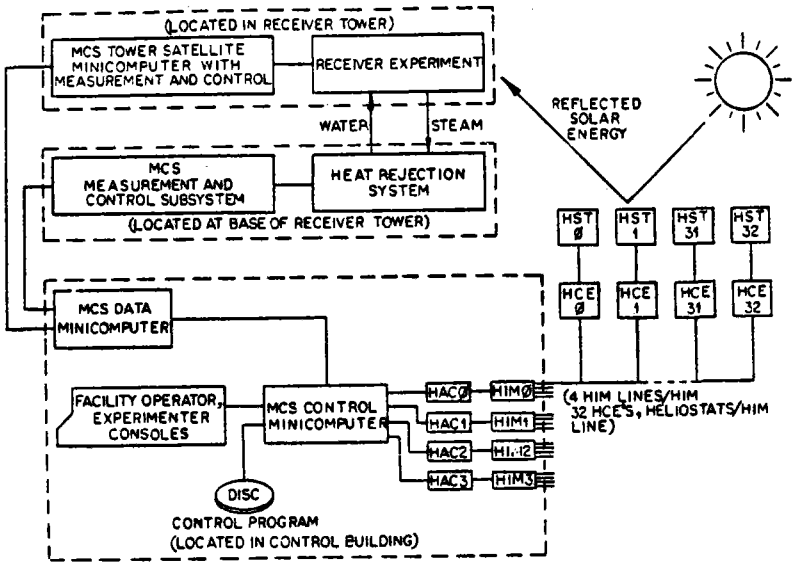

Figure 4
STTF Control and Data System

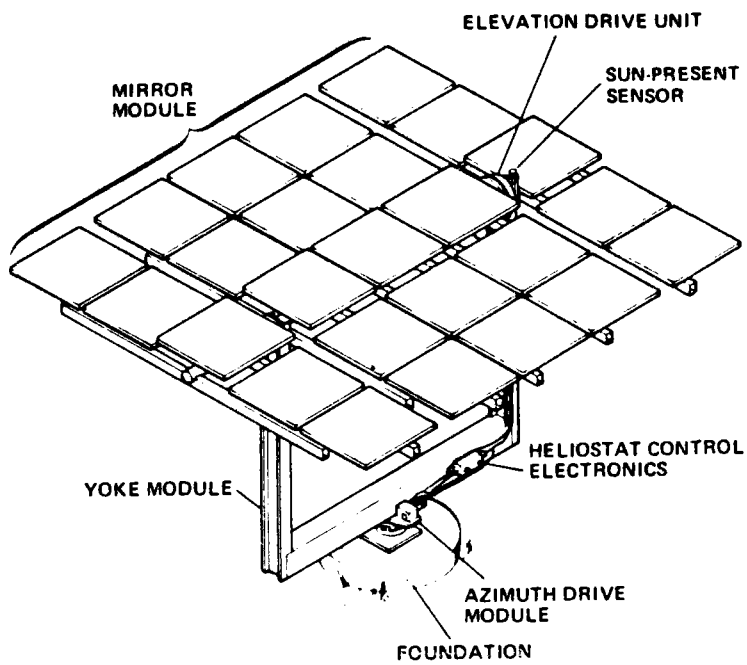

Figure 5
STTF Heliostat

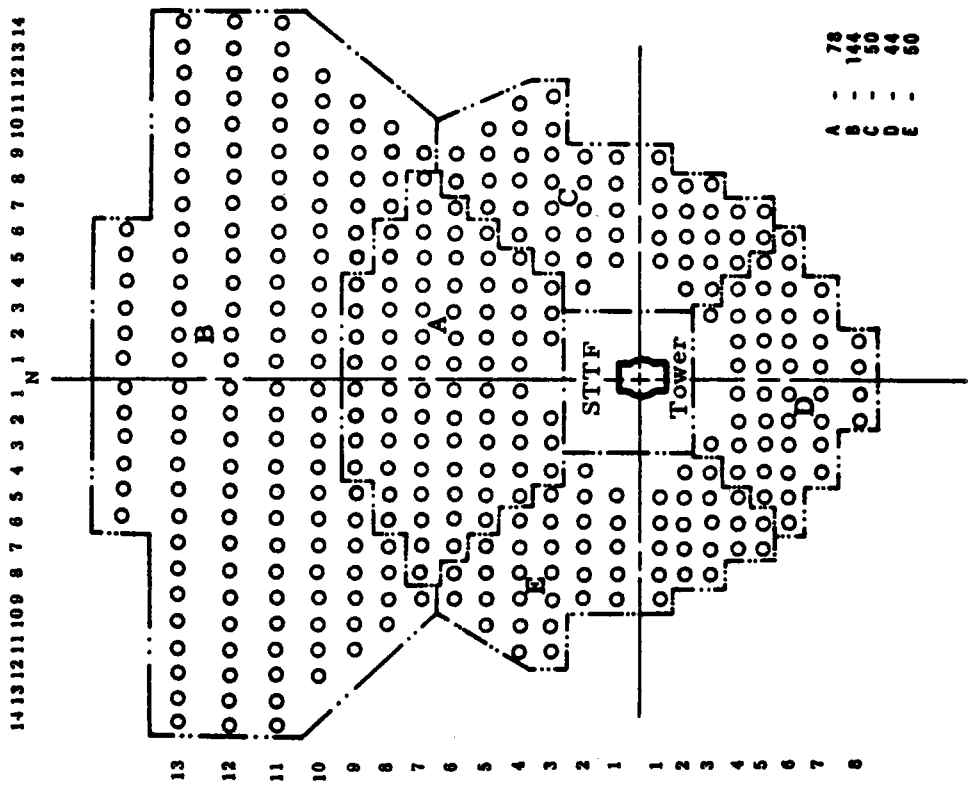

Figure 6
Heliostat Field Layout

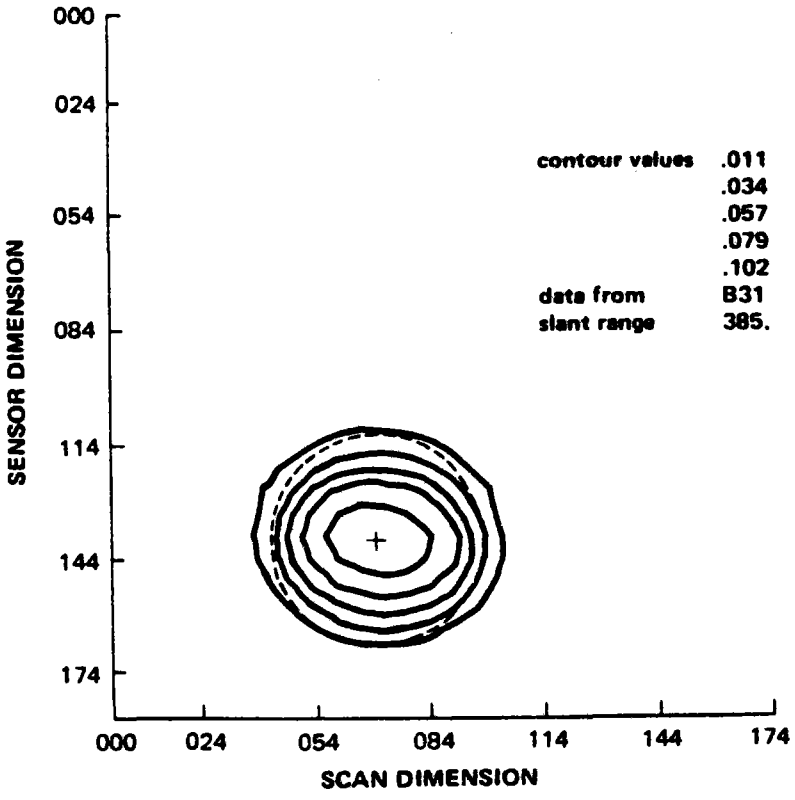

Figure 7
Heliostat Beam Flux Map

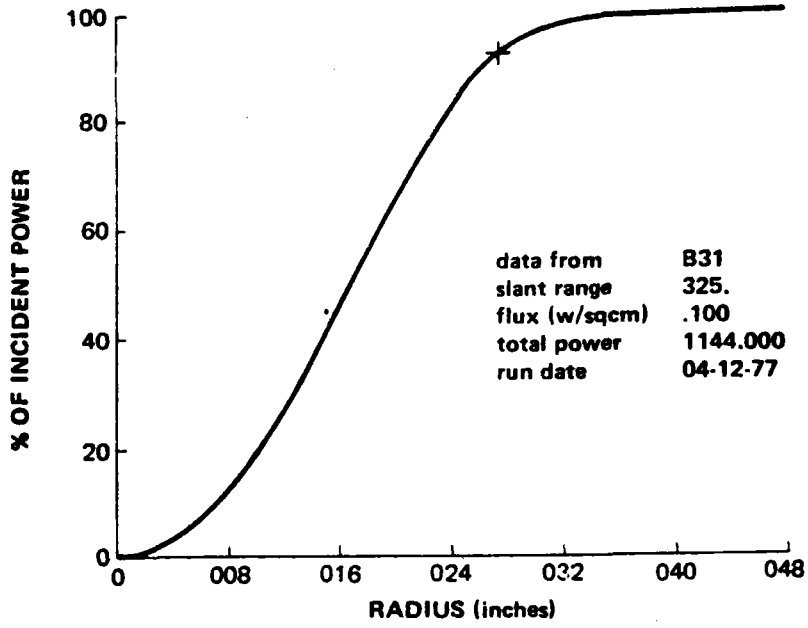

Figure 8
Heliostat Beam Power Curve

Sandia Laboratories

FIGURE 9

TENTATIVE STTF TESTING SCHEDULE (4/78)

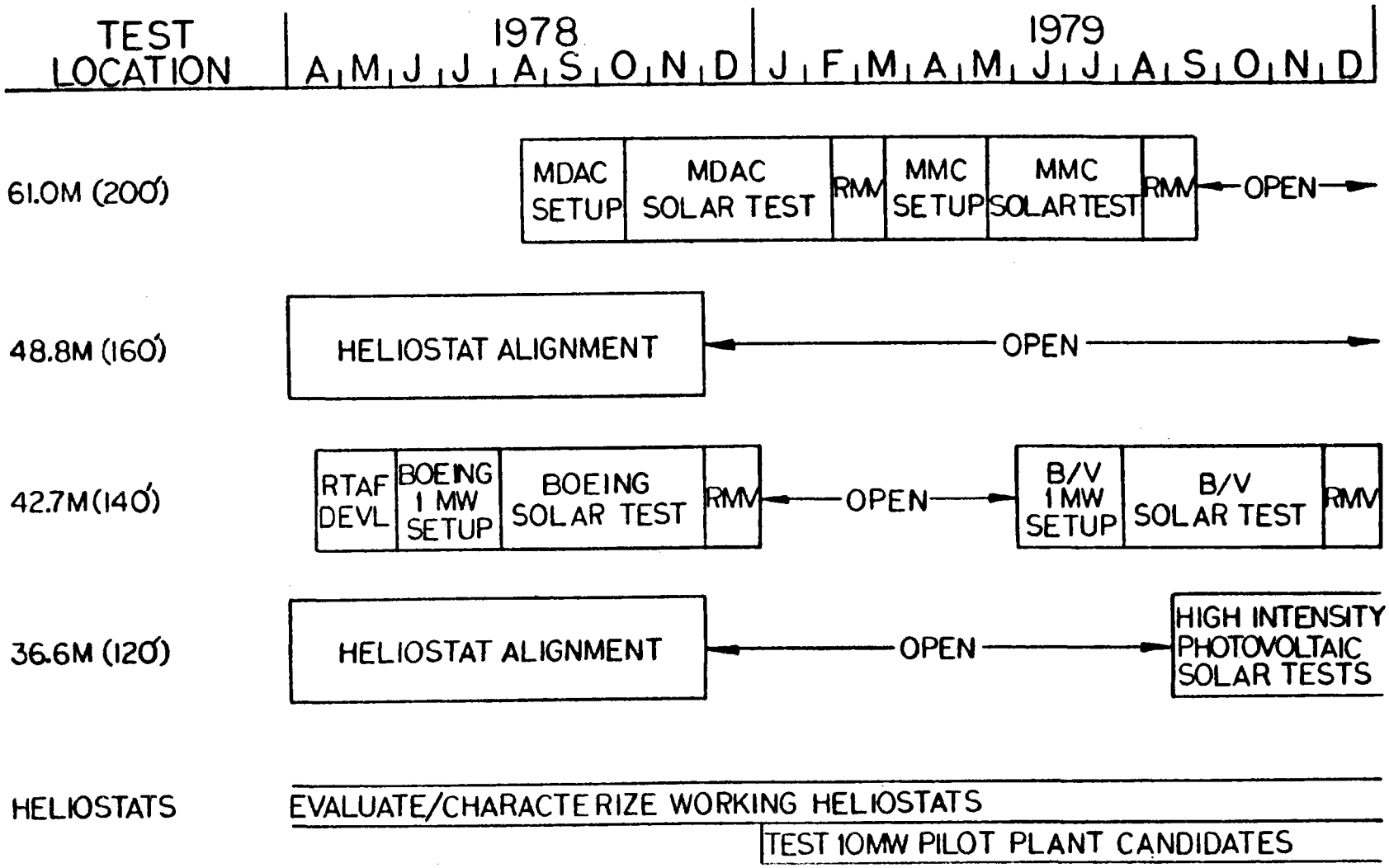

IV. ABOUT THE USES OF HIGHLY CONCENTRATED SOLAR ENERGY

Professor Michel Rodot
Centre National de la Recherche Scientific
Paris, France

Chairman Hildebrandt - Professor Michel Rodot is from the National Center for Scientific Research (CNRS) in France. He was previously a specialist in semiconductor materials, and was Director of the laboratory in Bellvue until 1976. Through that experience obviously he knew Paul Rappaport very well.

Professor Rodot is now the Director of a special interdisciplinary program created within CNRS to promote solar energy research and applications and under this program more than 150 staff scientists are working on various topics, like the central receiver thermal plans, dispersed thermal dynamic systems, photovoltaics, photosynthesis, and a variety of other subjects.

We are very fortunate indeed to have Professor Rodot with us today and he is going to talk about the initial applications of highly concentrated solar energy. Professor Rodot.

Dr. Rodot - Thank you sir. Let us examine why and how the use of high concentration can help arrive at a rational utilization of solar energy. There are at least three different cases:

- Chemical applications, when temperatures higher than 500°C or even 1000°C are required, as in the case of many interesting chemical reactions.
- Thermodynamic conversion, when a global efficiency of at least 10 to 20% is wanted.
- Solar photocells, in order to build cheap enough generators in spite of the high present costs of semiconductors.

We shall not consider the latter topic, which is outside the scope of this meeting.

Since antiquity, when Archimedes burned the enemy ships in Sicily by concentrating solar energy on them, military applications of solar energy disappeared. Maybe it is a pity that this technique fell asleep because wars have continued even under bad weather conditions.

How did this topic awake again? After some older episodes, like the Mouchot solar printing plant in 1878 and the Egyptian 30-kW plant at the beginning of this century, the true start of our present work is due to several individuals, initially to Felix Trombe.

I shall not go into details about the work of Trombe, whose pioneering action is well known. In his contribution to this meeting, Royere described the numerous research programs which are going on at Odeillo, at the 1000-kW CNRS solar furnace. The fact that Trombe succeeded in convincing the numerous agencies involved to build the Odeillo furnace, at a time when our gross national product was half the present one, implies by itself a first-order achievement. This opinion comes from a man involved in the THEMIS solar plant project, of similar magnitude, at a time when solar energy is much more fashionable than it was at the time of the solar furnace and, as such, well aware of the difficulty of this kind of project.

Let us pause for a moment and recall an episode which is less known: the work of Perrot at Algiers and Marseilles and his collaboration with Francia at Genova. Perrot worked with a photochemist who needed high-intensity, ultraviolet radiation on his reactors. He decided to use, not a double reflection on glass as at Montlouis (and later at Odeillo), but a single reflection on aluminum--in order to get a high efficiency for UV radiation. This led to the 8-meter diameter Algerian "heliodyne," built by Touchais, made of double-curved aluminum sections, which permanently tracked the sun through a high-accuracy equatorial mount. The result was a concentration ratio higher than 10,000. The first measurements took place in 1958, but the Algerian war interrupted this work for more than ten years. Now this apparatus is again being used by the Algerian scientists for a different but very interesting application, the production of a thermofluid at 300°C. The Algerian heliodyne was the forefather of what is now the Raytheon program in the USA and the CNRS THEK program in France.

Transferred to Marseilles, Perrot became interested in the energy applications and with Francia built a linear concentration boiler. As a result of this experiment, they chose to continue in a way which was advocated by Peri, who had built a mock-up, reduced 20 times, of a point-concentration plant composed of 78 focusing heliostats. This project, enriched by the very original ideas of Francia, was jointly presented by Perrot and Francia for NATO funding. It was accepted and was built in Genova, not Marseilles, because at that time (1965) France left the military organization of NATO. This was the beginning of the Francia technique, which was highly successful and was recently adopted by Walton, giving rise to the Georgia Tech solar thermal test facility in Atlanta.

The very concept of a tower-type power plant producing electricity was elaborated by Hildebrandt and Vant-Hull at the University of Houston. This concept

gave birth to the Sandia Albuquerque STTF through the ERDA program, and to projects of operational power plants which have been worked out and are now in progress in at least six countries.

Trombe's motivation was chemical. He wished to purify rare earth metals and to perform chemical and thermophysical experiments in a clean environment at very high temperatures. The energy motivation appeared later. Both of them led to similar instruments that now exist in slightly different versions at Odeillo, Atlanta and Albuquerque. And now, what will be the uses of these facilities?

First comes the work on energy, and with it an initial difficulty, which is to convince governments to get interested in thermohelioelectric plants. Oil specialists (who need large budgets for prospecting) and financial experts (who, at least in France, are not easily dazzled by concentrated solar energy) no longer say these plants are uninteresting; rather, they say these plants are simple things which only require assembling known components and need no new discoveries. We therefore know how to build them if necessary but don't need them now.

Well, we have to say clearly that we don't yet know how to build these plants efficiently. Large uncertainties exist concerning the cost of heliostats, atmospheric absorption between heliostats and receiver, receiver reliability, convection losses of receivers (topic of a meeting next week in Paris), plant management and global costs. Further, before us lies the huge problem of higher temperature plants using thermofluids like sodium, gases or molten salts at 800°C or perhaps 1000°C, which are largely unexplored today. So this is really a very broad research field.

Coming back now to the chemical studies, the possibility clearly exists of developing fundamental research programs which need the use of solar furnaces. Sometimes this work can also be performed with imaging furnaces or plasma furnaces, so that we shall have to choose among the possible projects those which explicitly apply to STTFs. But there is also another direction of research, which is neither high-temperature thermochemistry nor photochemistry, but energy-oriented thermochemistry at medium temperatures.

In France, in 1975, 12% of the energy used (i.e., 17 million oil equivalent tons) was consumed in the form of heat at temperatures between 600° and 1600°C, and as much was also consumed as specific electricity (i.e., electricity not transformed into heat). Large possibilities of energy savings exist there. It is true that injecting solar energy into side energy would be a little tricky and unrealistic, but

some fields where solar energy might substitute for fossil energies can be illustrated by the following cases:

- Cements. Cement must be baked at more than 1400°C in the Portland method. There exist so-called "pouzzolanic cements," prepared from very common ores, which may be baked at only 700°C. These are slow-hardening cements, but this is not a serious disadvantage. These materials might very well be prepared in simplified solar furnaces, leading to interesting fuel savings for the subtropical countries.
- Fuels from biomass. Various techniques of pyrolysis are conceivable for converting biomass (wood or vegetal wastes) into gaseous fuels or methanol. Such systems would use solar energy twice: first for biomass production and second for its conversion to fuels using solar furnaces.
- Hydrogen. Of course, the dream of thermolyzing water using various thermochemical cycles has met serious difficulties, but there still exists at least the possibility of mixed thermoelectrochemical cycles. An example of such a system might involve a water electrolysis cell containing at the anode an oxygen-avid material like SO_2 (which largely lowers the electrolysis voltage), a solar furnace in which the oxidized form (e.g., SO_3) is decomposed to give back the oxygen-poor form, and eventually some auxiliary installation. This system includes chemical storage elements under the forms of intermediate products and of hydrogen itself.

These various possibilities might lead to solar chemical plants which, like the solar electric plants, may contribute to easing the problem of energy resources in the next century. To these we may add the combination of both processes in which the receiver, placed at the focus of a tower plant, is a chemical reactor producing an energy material, the latter being then transported without thermal losses to a steam generator. Such a chemical heat pipe, replacing the usual thermofluids, also simplifies the storage problem associated with solar electric plants and might be of major interest for building large plants.

By developing all these systems, we may hopefully contribute to the design of competitive energy sources for tropical regions and to approach the time when competitive energy sources will be available in the less sunny climates like the Mediterranean. These "large" solar plants would, of course, be complemented by smaller ones working at lower temperatures to produce mainly heat and electricity.

For numerous reasons, in our world of today, close international links would be favorable for such a program--not so much because of the size of the installations to be built, which remains modest, but in order to save time, to insure complementary interface of equipment of different countries, and to obtain faster penetration of solar energy in the developing countries. Just like the US Department of Energy, just like Sandia Laboratories and Georgia Tech, CNRS is conscious of this necessity in the field of solar thermal test facilities and solar furnaces. It thus favors the proposed coupling of different Users' Associations and wishes a successful development of international relations through the present meeting and those to come in the future.

V. SESSION II-B: SOLAR FACILITIES

WHITE SANDS MISSILE RANGE SOLAR FURNACE TEST FACILITY

Richard Hays

Abstract

A description of the 30,000-watt thermal White Sands Solar Furnace Test Facility located at the Nuclear Weapon Effects Laboratory, White Sands Missile Range, New Mexico. The White Sands Solar Furnace (WSSF) is primarily used for nuclear weapon thermal effects testing, but is also used for solar energy research. The WSSF is capable of providing a maximum solar flux in excess of 80 cal/cm^2 sec over an exposure area of approximately 5 cm in diameter. The solar flux of the WSSF can be modulated to provide thermal pulse shaping, such as rectangular and nuclear, or operated in a steady-state exposure mode.

Introduction

The WSSF was originally constructed in 1958 and operated by the Quartermaster Research and Engineering Center at Natick, Massachusetts. In 1973 the WSSF was relocated at the White Sands Missile Range, New Mexico. The WSSF is available for use by the Department of Defense and its contractors, or other Government agencies and private industry.

The facility is operated by the Army's Nuclear Weapon Effects Laboratory primarily for nuclear weapon thermal effects testing but is also used for solar energy research by numerous Government agencies and universities.

Description of the WSSF

The WSSF is comprised of four main parts: the Heliostat, Attenuator, Concentrator and Test and Control Chamber, see Figure 1.

The Heliostat consists of 356 flat plate mirrors, each 0.635 cm in thickness and 62 x 62 cm square, mounted on a steel framework 1.2 meters wide and 11 meters high. The heliostat moves in azimuth ± 60 degrees and about 180 degrees north-south orientation and 0 to 90 degrees in elevation. The heliostat is an elevation over azimuth mounting with the drive systems located in the vertical and horizontal turret sections. The heliostat mirrors are front-surfaced standard

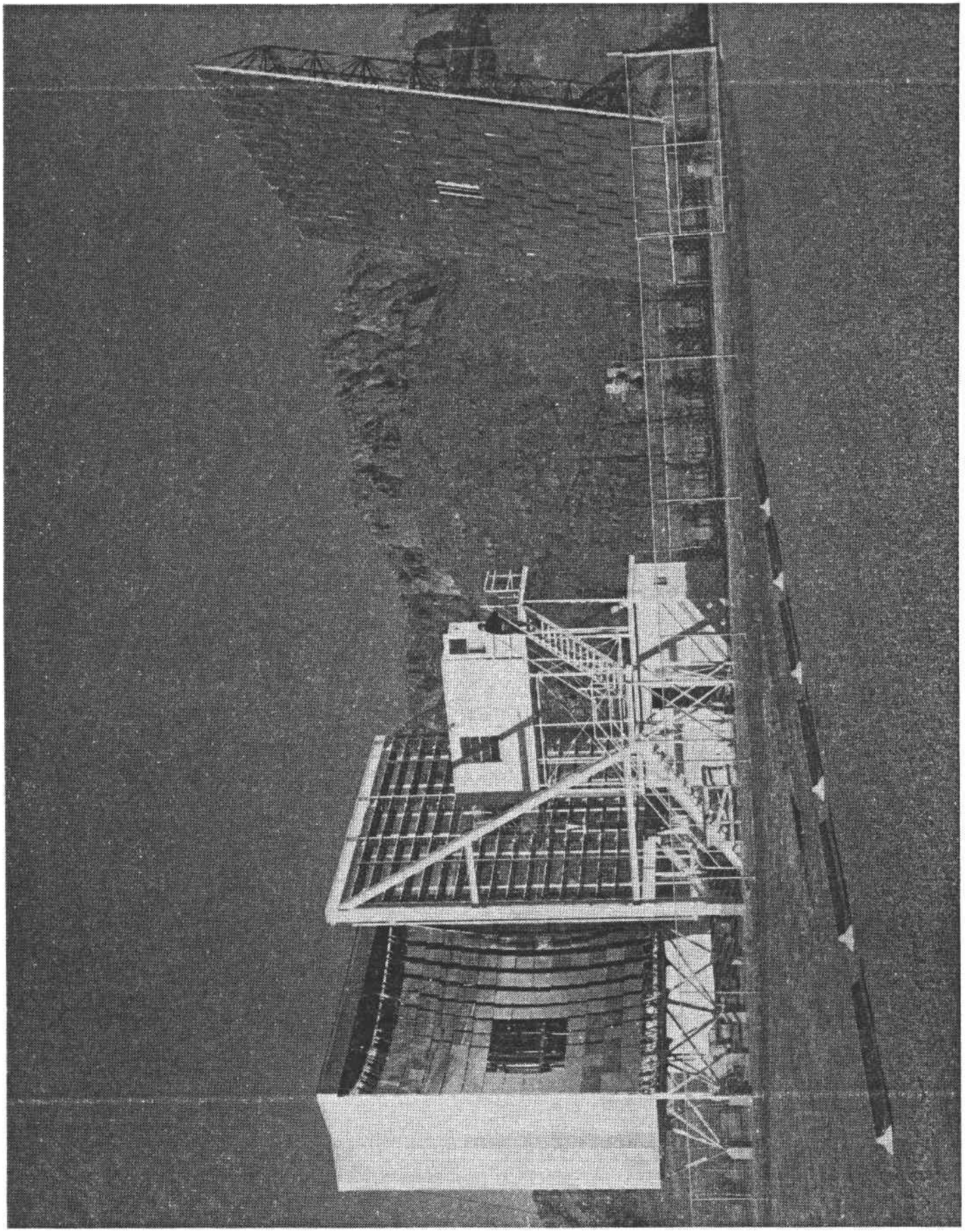

Figure 1

V. SESSION II-B: SOLAR FACILITIES

WHITE SANDS MISSILE RANGE SOLAR FURNACE TEST FACILITY

Richard Hays

Abstract

A description of the 30,000-watt thermal White Sands Solar Furnace Test Facility located at the Nuclear Weapon Effects Laboratory, White Sands Missile Range, New Mexico. The White Sands Solar Furnace (WSSF) is primarily used for nuclear weapon thermal effects testing, but is also used for solar energy research. The WSSF is capable of providing a maximum solar flux in excess of 80 cal/cm^2 sec over an exposure area of approximately 5 cm in diameter. The solar flux of the WSSF can be modulated to provide thermal pulse shaping, such as rectangular and nuclear, or operated in a steady-state exposure mode.

Introduction

The WSSF was originally constructed in 1958 and operated by the Quartermaster Research and Engineering Center at Natick, Massachusetts. In 1973 the WSSF was relocated at the White Sands Missile Range, New Mexico. The WSSF is available for use by the Department of Defense and its contractors, or other Government agencies and private industry.

The facility is operated by the Army's Nuclear Weapon Effects Laboratory primarily for nuclear weapon thermal effects testing but is also used for solar energy research by numerous Government agencies and universities.

Description of the WSSF

The WSSF is comprised of four main parts: the Heliostat, Attenuator, Concentrator and Test and Control Chamber, see Figure 1.

The Heliostat consists of 356 flat plate mirrors, each 0.635 cm in thickness and 62 x 62 cm square, mounted on a steel framework 1.2 meters wide and 11 meters high. The heliostat moves in azimuth ± 60 degrees and about 180 degrees north-south orientation and 0 to 90 degrees in elevation. The heliostat is an elevation over azimuth mounting with the drive systems located in the vertical and horizontal turret sections. The heliostat mirrors are front-surfaced standard

flat plate glass. The reflective surface consists of vacuum-deposited aluminum with an overcoating of silicon monoxide. Each mirror is mounted on three compression springs with stainless steel bolts through the mirror and spring and attached to the heliostat framework.

There are three modes of movement of the heliostat: slew, manual track and auto track. In the slew mode, two 1/2-hp AC motors (one AZ., one EL.), operating at 1725 rpm, are used to move the heliostat at rates of 7.2 degrees per minute in azimuth and 6.5 degrees per minute in elevation. The slew mode is used to bring the heliostat from the stow position to sun acquisition. In the manual mode, the same mechanical drive systems are used as in the slew mode. The difference between the slew and manual track modes being a further gear reduction and a variable-speed, 1/15-hp, 0-1725-rpm, DC motor coupled to the drive system through an electro-mechanical clutch. In the manual track mode, the heliostat is moved in azimuth at a maximum rate of 11.6 degrees per hour and in elevation at a maximum rate of 7.8 degrees per hour. The third mode of movement is auto track, which is the same as the manual track mode with the exception that the motor speed is controlled by position feedback from a photo detector. In this mode the heliostat automatically tracks the sun, keeping the heliostat positioned within 30 seconds of arc. The auto track system keeps the solar image at the focal plane positioned within 0.25 cm. Gusty winds above 15 knots and clouds passing between the sun and the heliostat can cause tracking instabilities with up to 1.25 cm of movement of the solar image or loss of track. If required, moon tracking can be accomplished with the same auto track system. By using the moon as a source, precise alignment of optical experiments can be performed without the intense concentrated solar heat and light associated with the sun.

The Concentrator consists of 180 spherical mirrors mounted on aluminum rings 59.7 cm in diameter, which are attached to the 9.1-meter square concentrator framework so that a solar image is positioned at the WSSF focal plane 10.7 meters away. All the concentrator mirrors are front-surfaced with vacuum-deposited aluminum and overcoated with silicon monoxide.

The Attenuator controls the useable thermal power of the WSSF, varying the power from zero to maximum within two minutes. The attenuator consists of 17 rows of rotatable horizontal blades. The blade angle is controlled by the solar furnace operator and varies from 45 to 90 degrees from vertical for complete to minimum

attenuation of the solar energy. If a hazardous condition occurs during testing, automatic safety circuits are coordinated with the attenuator drive circuits so that the attenuator may be closed within 0.5 second. The attenuator can operate in an auto control mode, compensating for changing atmospheric conditions, and thus keeping a constant flux level at the focal plane during long steady-state exposures. See Figure 2 for attenuator transmission characteristic. The test and control chamber is 2.4 by 2.4 meters in cross section presented to the solar energy reflected from the heliostat and 4.8 meters in the direction of the optical axis and houses the experimental area, the control console and the fast shutter system. Cooling water and high-pressure air supplies are available in the test and control chamber.

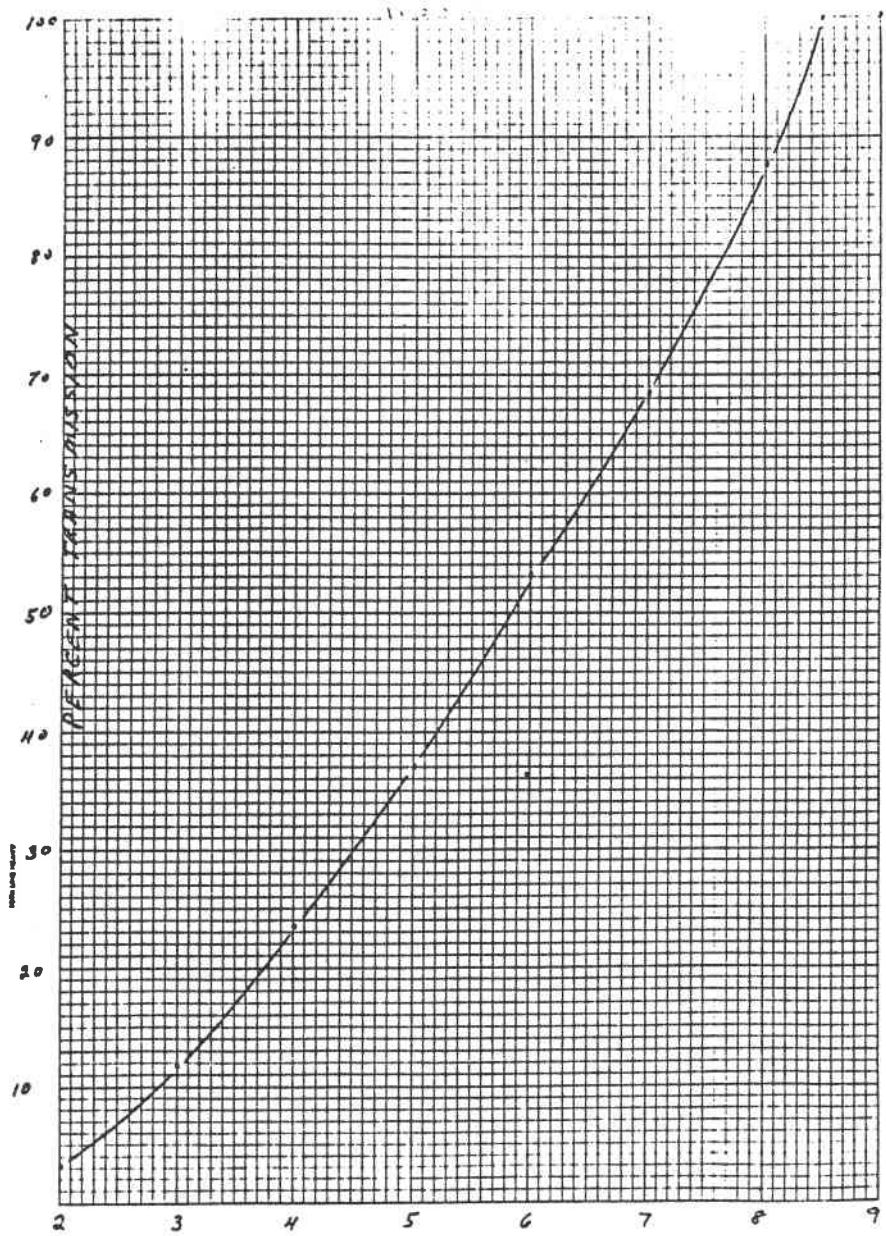

Figure 2

The Fast Shutter System consists of a water-cooled shutter, exposure shutter, and a limit shutter. The water-cooled aluminum shutter is 45.7 cm in diameter and protects the fast shutters and experiment from the 30,000 watts of thermal energy during nonexposure. The exposure and limit shutters have rise and fall times of 25 milliseconds and are mounted 5.1 cm in front of the focal plane. These two shutters produce a rectangular pulse duration as short as 100 milliseconds. The thermal pulse shaper for nuclear weapon simulation is mounted behind the fast shutters and can be for steady-state operation. Also, a wind tunnel which will accommodate 7.6 by 10-cm test specimens can be used in conjunction with the WSSF to provide air flow with velocities up to a maximum of 40,000 feet per minute.

Exposure Characteristics

The thermal exposure area is approximately 16 cm in diameter at the focal plane located 81.25 cm from the south wall of the test chamber and 1.06 meters above the test chamber floor. Larger exposure areas can be obtained by moving out of the focal plane but with reduced flux levels. The maximum available flux at the focal plane to date is 100 cal/cm^2 sec (90 cal/cm^2 sec readily obtainable), with a total available power of 30,000 watts thermal. Maximum flux levels with a 10% uniformity are obtained over an exposure diameter of 5 cm. The thermal flux profile at the focal plane has the 50% flux points occurring at a 5-cm radius from the center of the solar image as shown in Figure 3. Table I gives some of the important exposure characteristics of the WSSF.

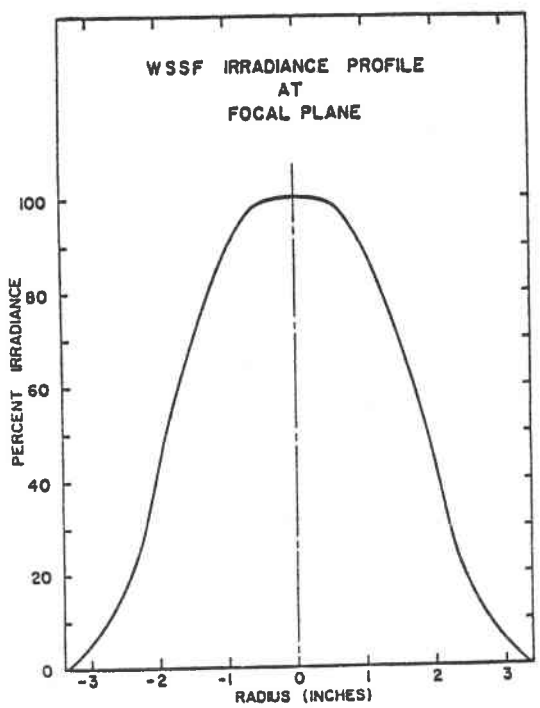

Figure 3

Table I

Diameter (in.)	1	2	3	4	5	6	6.5
Percent Total Power	6.5	24.6	49.5	74.5	91.5	99.1	100.0
Power, kilowatts	1.89	7.21	14.56	21.91	26.97	29.17	29.47
Min. Flux, cal/cm^2 sec	88.2	79.2	59.4	39.7	14.4	4.5	0
Mean Flux, cal/cm^2 sec	89.1	83.7	69.3	49.1	26.6	9.4	2.2

Operational Characteristics

Since the WSSF is dependent upon weather conditions for operations, the following weather data is used to help schedule experiments to be conducted at the WSSF. Wind and cloud cover data taken over a period of 22 years, by the Atmospheric Sciences Laboratory, indicates WSMR is a good location for the WSSF in regard to availability of usable operational hours. Information on wind and cloud cover by month and hour indicates an average of 1200 hours of operation time per year is available at the WSSF. This is based on a 2080-hour work year, 5-day work week, and an 0800 to 1600-hour work day, see Tables II and III. It must be remembered that the WSSF has two operational constraints, cloud cover and wind, when planning thermal tests.

Table II

Category	Cloud Cover	Winds	Available Hours
I	Clear	< 5 knots	395
II	Clear	< 14 knots	666
III	< 50%	< 5 knots	666
IV	< 50%	< 14 knots	1200

Table III lists the month of the year according to percent operational time available for that month in Category IV of Table II.

Table III

Month	% Operational Time
September	71
October	70
June	70
May	61
November	60
August	59
July	57
December	53
April	51
January	50
February	50
March	48

DOE ADVANCED COMPONENTS TEST FACILITY

C. T. Brown
Georgia Institute of Technology
Engineering Experiment Station
Atlanta, Georgia 30332

The DOE Advanced Components Test Facility is a 400-kW high-temperature solar thermal test facility operated by Georgia Tech for the US Department of Energy. This facility has as its mission the advancement of high-temperature solar thermal technology through the testing and evaluation of materials, components, subsystems and bench models of solar thermal devices whose development is sponsored by the US Department of Energy, by private industry or by other government agencies.

The facility is presently in the process of being converted from a Francia-type solar steam plant to a general-purpose test facility. The basic 400-kW solar steam plant was designed by Professor Giovanni Francia, engineered and fabricated by the Italian firm of Ansaldo, SpA, and was installed by Georgia Tech. The plant became operational in September 1977 as a high-temperature, high-pressure solar steam plant. The conversion of the facility to a general-purpose test facility started in December 1977.

The program was initiated in January 1976, with the following objectives:

a. Perform a technology transfer of the Francia-type solar thermal technology that has been developed in Italy over the past 15 years by importing, installing, operating and characterizing a 400-kW Francia solar steam plant, and

b. Following the characterization task, convert the solar steam plant to a general-purpose test facility to support the US solar thermal R&D effort.

The basic solar steam plant (see Figure 1) consisted of a mirror field containing 550 tracking heliostats called kinematic motions. These devices are, in many ways, similar to the equatorial mounts used on telescopes. Each kinematic motion supports and manipulates a 111-cm diameter circular, second surface, low iron glass mirror. Each mirror can be operated either flat or focused. The 550 kinematic motion devices are mechanically interconnected by torque tubes, and the entire field is driven by one 1-1/2 horsepower electric motor.

The focal plane of the test facility is located at the geometrical center of the field at an elevation of 21.46 meters above the mirror plane. This height, combined with the extent of the field, gives a nominal rim angle for the field of 45 degrees.

Conversion of the Francia steam plant to a general-purpose test facility started in December 1977, with the design of a new central tower to replace the articulating tower supplied as part of the Francia solar steam plant. An artist's concept of the new tower appears in Figure 2. The primary advantages of the new tower are its increased load capability and the ease of access to the experimental area provided by the support platform at the focal plane. The old tower had a capacity of approximately 1500 lbs. The new tower has a capacity of 20,000 lbs. The focal point for the facility is centered on the tower legs and at the floor level of the experiment platform. Access to the top of the platform is by ladder or man/material work hoist; access to the underneath side of the platform is by scissors lift platform. The scissors lift can be withdrawn to the 50-ft level during a test so as to minimize the blocking of radiation incident on the focal plane. The cantilevered part of the platform will house an instrument building.

Support equipment at the DOE/ACTF includes a computerized data acquisition system, a scanning flux calorimeter, pyrheliometers, a pyrometer, and a solar SERI blind infrared TV camera system. The computerized data acquisition system (see Figure 3) consists of two minicomputers, one located atop the tower which controls a 120-channel multiplexed A-to-D system and a second computer located in the control room. The control room processor manages the tower-top computer and also manipulates, stores and displays data according to the needs of tbe experimenter. Data output from the system includes strip chart recorder displays on a video terminal, line printer listings of selected channels, mag tape copies of both raw and processed data, and diskette copies of raw and/or processed data. Data input to the computerized data acquisition system can be from virtually any type of analog output transducer device. The A-to-D converter is front-ended by a programmable gain amplifier, allowing full-scale inputs from ± 10 millivolts to ± 10 volts in 8 different ranges.

The scanning flux calorimeter is a real-time device that allows an experimenter to scan the aperture of his experiment, thereby measuring the flux distribution incident on his experiment. This device is basically a water-cooled bar housing 37 Gardon gage-type calorimeters on 2-inch centers. This water-cooled bar is part of a water-cooled

support structure that can be mounted to the tower or to the experiment. The device operates under computer control in such a manner that a 2-inch by 2-inch grid of the incident flux distribution can be produced during an experiment in an elapsed time of approximately 3 minutes.

The Sandia Laboratories' central receiver computer model HELIOS has been adapted to the Georgia Tech computer and used to model the 400-kW facility. Experimental tracking data taken with single mirror images have been folded into this program and used to model the thermal profile of the concentrated beam. The extent of the beam at the focal plane is expected to be approximately 30 inches in diameter; the peak flux is expected to be approximately 250 watts/cm^2.

Use of the test facility by outside organizations is encouraged. A copy of our present test schedule appears as Figure 4.

The installation of the new tower is progressing rather rapidly. Groundbreaking for the tower occurred March 10, 1978; by March 24 the tower was at full height, all guy wires had been installed and tensioned, the basic facility had been completed and the installation of mechanical and electrical utilities was well underway. At the present time, it is predicted the tower installation will be completed by May 15. Activities to occur between May 15 and July 15 are those related to the characterization of the flux distribution of the facility. Photographs of the facility as it presently exists are shown in Figures 5 and 6. Other planned activities for the conversion of the solar steam plant to a general-purpose test facility include the design and construction of an assembly/shop building, the design and construction of a permanent control room adjacent to the mirror field, and the improvement of access ways and roads within the facility.

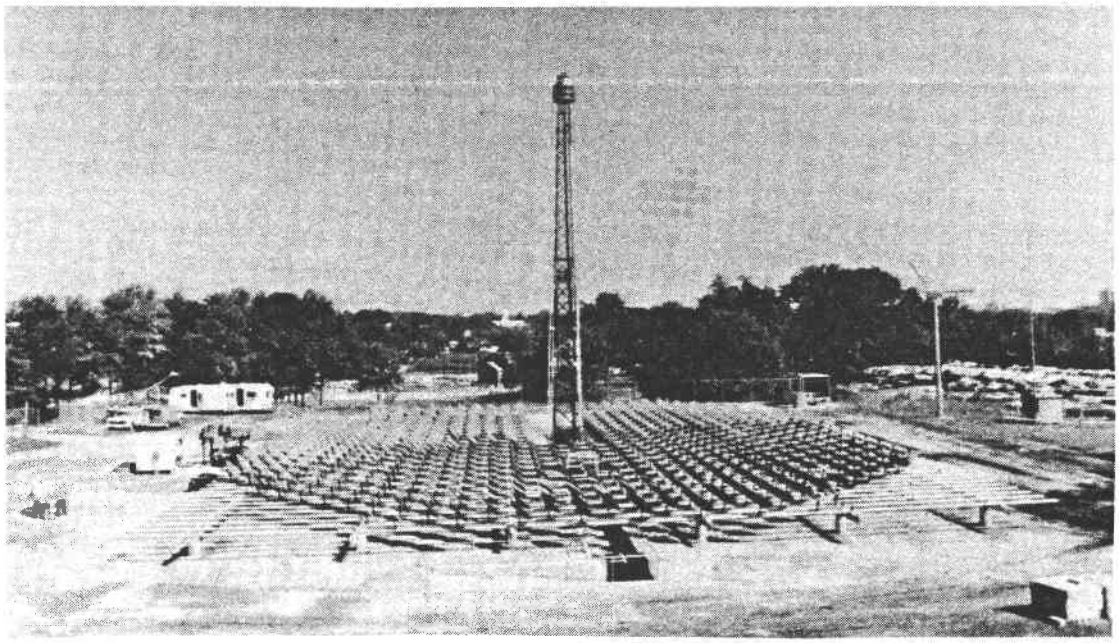

Figure 1. Basic Francia Type Solar Steam Plant as Installed on Georgia Tech Campus, September 1977

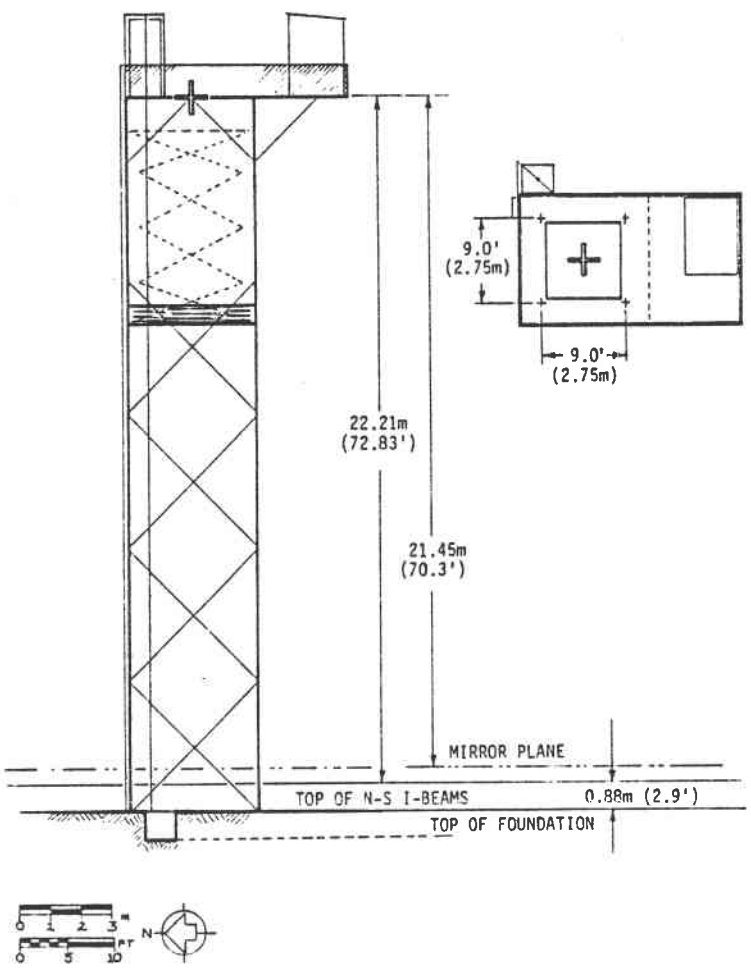

Figure 2. Concept Drawing of New Central Tower Showing Details of Working Level

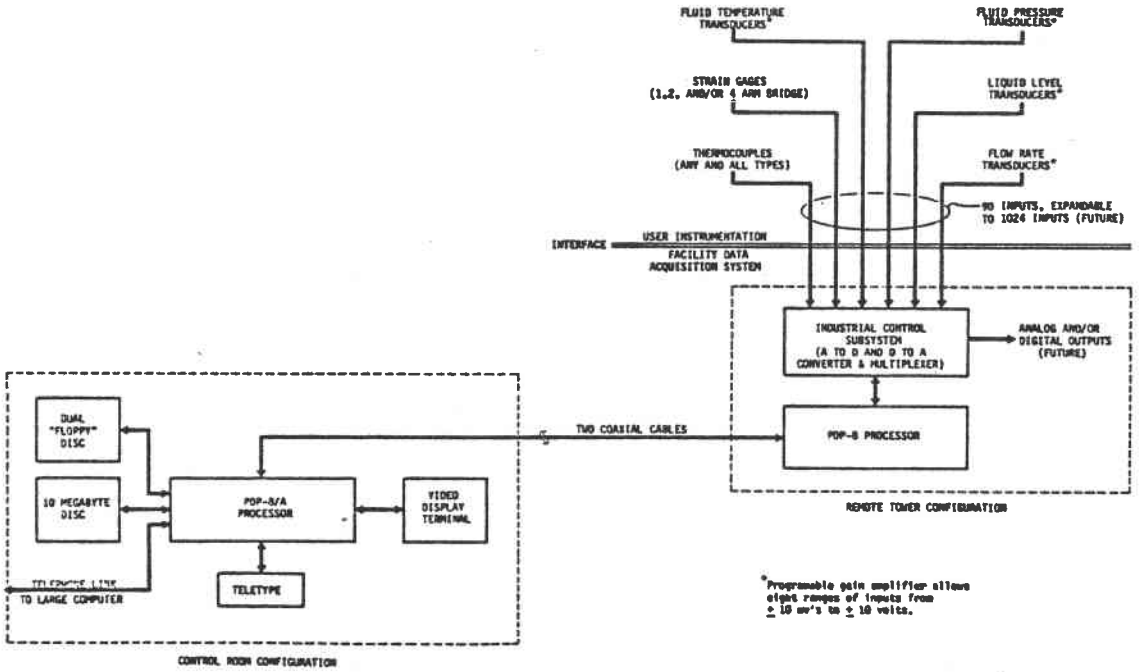

Figure 3. Schematic of ACTF Computerized Data Acquisition System

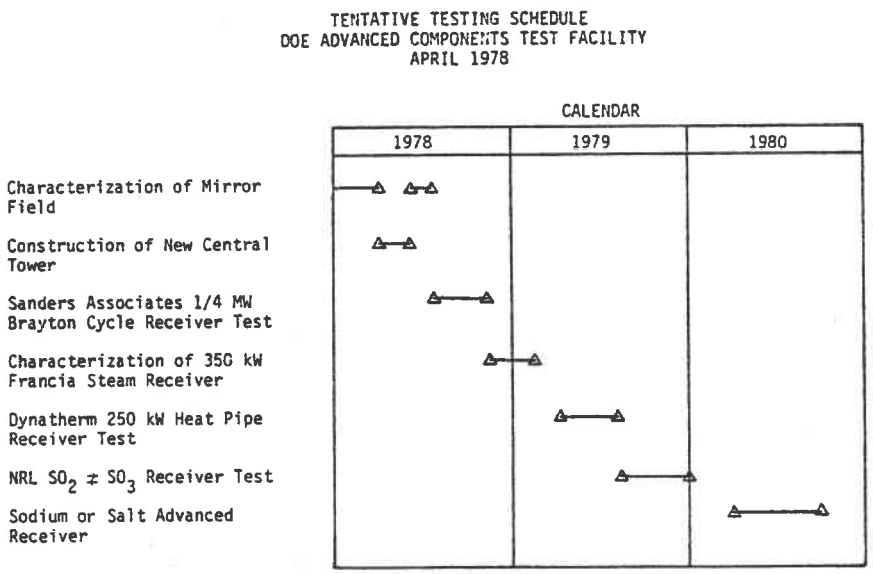

Figure 4. Preliminary Test Schedule for Advanced Components Test Facility

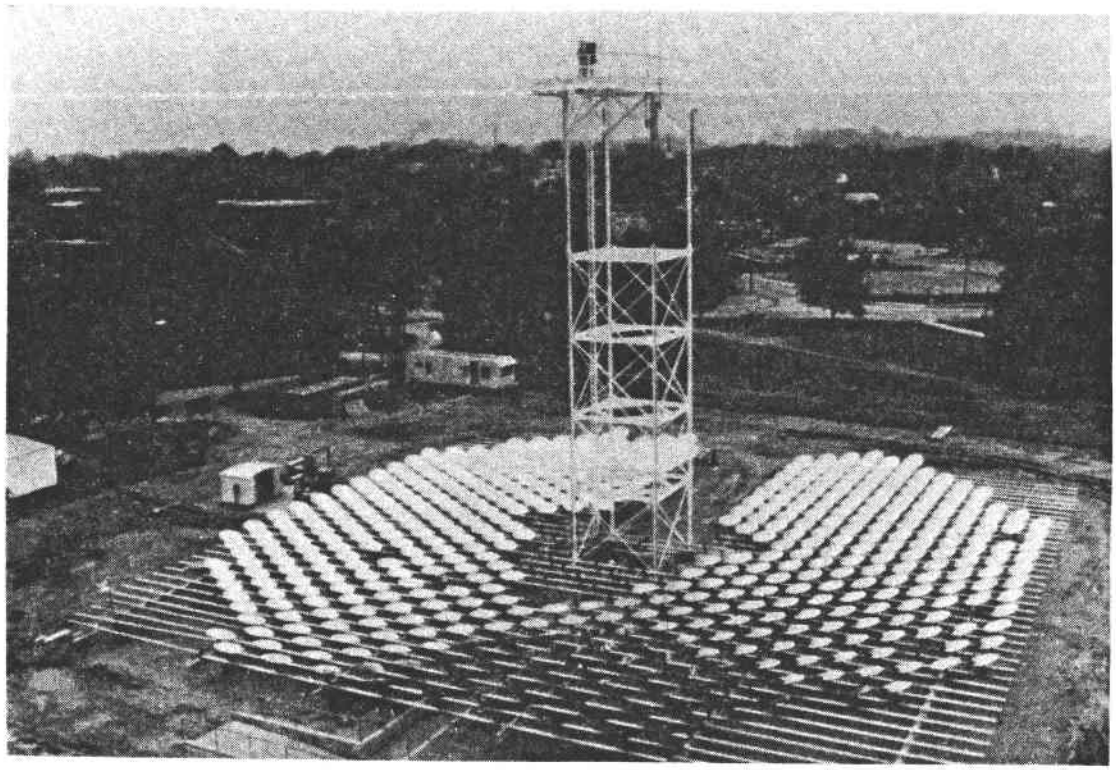

Figure 5. North Facing View of ACTS as Seen from "Cherry Picker"

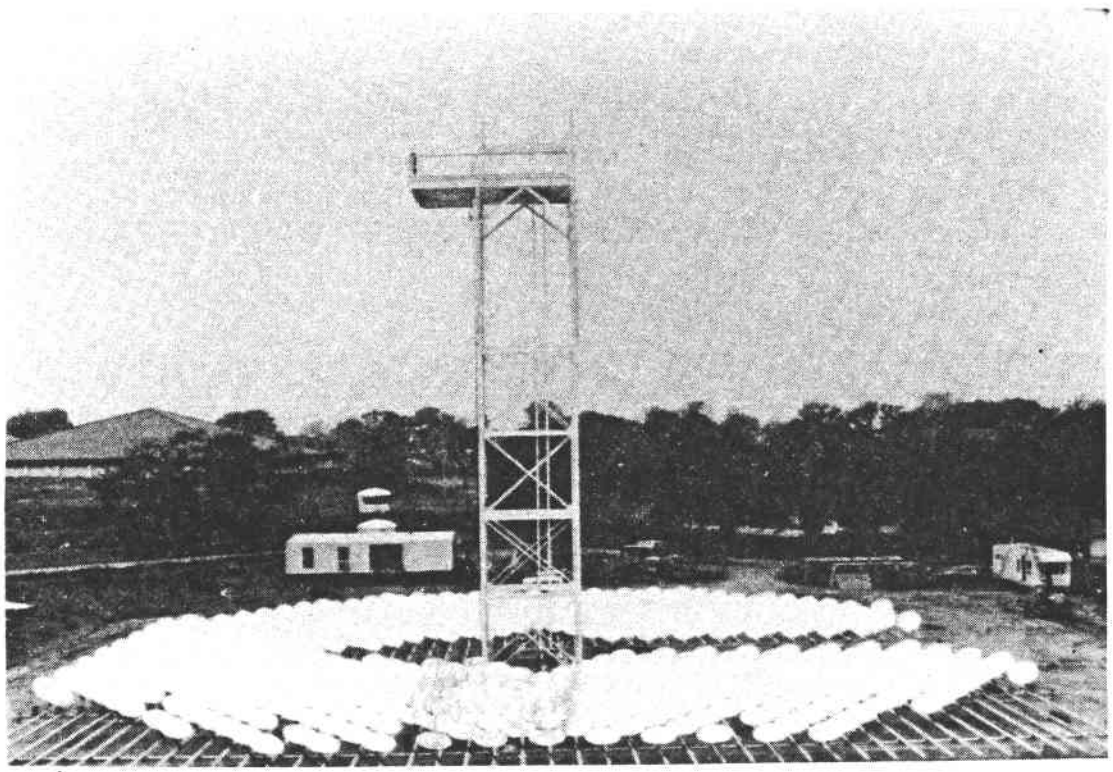

Figure 6. West Facing View of ACTF as Seen from "Cherry Picker"

VI. SESSION III: OPTICS AND SYSTEMS

A RECONCENTRATOR FACILITY FOR MATERIALS TESTING AT THE STTF

Aden B. Meinel & Marjorie P. Meinel

Optical Sciences Center
University of Arizona
Tucson, Arizona 85721

The STTF 5-MW_t facility is located at a point of easy access to researchers in the western United States. This facility will be used heavily in support of solar thermal system component development and testing. Access to the tower is therefore apt to be limited for many potential users. Many materials science studies will need many hours of exposure when lifetime studies are to be done. In general these studies cannot be accelerated by large time-scale factors because of the inadequacy of theory relating temperature/time dependencies. On the other hand such studies do not require the large spot size of the full STTF facility.

We have considered the possibility of using a single heliostat of the STTF plus a reconcentrator to produce the flux concentrations and temperatures necessary to the tests at hand. The advantage of a reconcentrator is that a single heliostat could be dedicated to this auxiliary facility. In fact there may be several heliostats placed at the STTF facility that are not part of the STTF and which could serve to feed a number of reconcentrators if the demand develops to require additional units. One could also consider separate parabolic tracking concentrators to provide this service independent of the STTF.

The advantage of locating this auxiliary facility at the STTF location whether or not it uses an STTF heliostat is the excellent support staff and facilities necessary to carry out the test programs. Some materials programs we have under consideration are the type that would not require the experimenters to be present and which require daily exposure of the samples for months of time. The personnel necessary to operate these long programs could be regularly part of the STTF staff, provided for this purpose.

Other facilities exist for thermal testing of materials, such as at Atlanta and at White Sands. Past experience indicates logistical difficulties and run duration limitations at White Sands. The Atlanta facilities are far from the western region, but otherwise would be quite suitable for many experiments that would be appropriate to the STTF reconcentrator.

The STTF facility appears attractive from the standpoint of logistical convenience and the prospect of contributing to the full use of the STTF capabilities represented by the range of competence of the personnel, the completeness of supporting-data handling and control capabilities, and the ready access to a wide range of auxiliary instrumentation available from the Sandia Laboratories. This proposed reconcentrator facility could easily be saturated, for example, by surface-degradation or diffusion experiments which require several thousand hours of irradiation and tens of thousands of cycles. Accelerated testing is always an option, but the extrapolation of a few hours actual test to 20 years of projected use is subject to many uncertainties. Even the substitution of ageing in a laboratory furnace is inadequate because of the fundamental differences between the heat from an IR thermal background and heat from the more energetic solar photons. We therefore feel that all available time will soon be scheduled on the reconcentrator, and the need for additional ones will become apparent. This first reconcentrator unit would then become the prototype for others, others that could be located at the site of users having a particularly heavy and continuing demand.

At the present time we have only started the examination of different forms for the reconcentrator. This study will be extended under support by the STTF Users Association to consider independent parabolic concentrators as well as heliostat-reconcentrators. We also wish to examine use modes to see how they operationally fit into potential demand and how they compliment other existing facilities.

Reconcentrator Geometry

The three basic options for providing a materials testing facility at the STTF are shown in Figure 1. Two of these options involve the use of a small short

focal length reconcentrating mirror. Position A is shown on one of the secondary test platforms of the STTF tower. These platforms were envisaged being located where smaller tests could be accommodated to aid in providing a full schedule of experiments for the STTF. Position B is shown on the ground adjacent to the STTF tower. Position A is preferred for minimizing the changes in the image size of the sun during the day, as formed by the Martin-Marietta focused heliostats. Position B is preferred for simplifying the apparatus and procedures so that materials tests could be performed independently of tests of the full heliostat array on one of the major programs for the STTF. Positions A and B both use a small diameter reconcentrating mirror. Position C shows an option completely independent of the STTF facility: the use of a tracking paraboloid to provide solar flux for materials testing. The study ahead will evaluate those possibilities and examine relative cost and operational advantages of each. We have no specific recommendation to make at this point.

The image properties of a reconcentrating mirror with focused heliostat and without are shown in Figure 2. In the case of no heliostat, or of a plane heliostat simply reflecting sunlight in a new direction, the solar image size is set by the angular size of the sun at 1/115 th the focal length of the concentrating mirror. In the case of a focused heliostat the entire heliostat appears to be filled with sunlight, so the solar image size is now set by the angular size of the heliostat as viewed from the reconcentrating mirror. Thus a small focal length reconcentrating mirror can provide a focus of considerable size.

The details of the image region are shown in Figure 3. The reconcentrator mirror is shown as oversize to collect rays that spill out of the optimum image formed by the heliostat, as for instance, when the sun is a considerable angle off the central meridian and the image is affected by uncompensated astigmatism. There will be a region of maximum concentration, the focus of the heliostat formed by the reconcentrator mirror. Note that this image will not have sharp edges because of the coma of a parabolic mirror, but the solar flux brightness will be reasonably uniform over the central 80% of this image. Note also that regions of lower than maximum concentration will be available by placing the

specimens under test either inside or outside this optimum focus. The study to be done will evaluate the uniformity of solar flux in several of these positions for the Martin-Marietta focused heliostat.

We have made a preliminary investigation of the type of mirror that could be used for the reconcentrator. The focal length of this mirror determines the effective maximum concentration. If a 60-inch diameter searchlight mirror is used the focal length is only 30 inches and the maximum concentration several thousand. A less curved mirror or longer focal length can yield 1000X concentration and have a large and convenient working area. Searchlight mirrors can be easily obtained, but result in cramped working space. A mirror made specifically for the reconcentrator will be much more expensive, and the tradeoff is not clear at this point.

At one point we explored the manufacture of a special mirror through the use of the Diamond Turning Facility at ORNL-Y-12. The substrate casting is not expensive but the forming of the mirror reflective surface adds considerable expense, perhaps not justified by the proposed use at the STTF. Diamond turned mirrors are an important DOE program, and the use of one here would add practical experience with these mirrors, and be of itself a materials evaluation. Recoating of the reflective surface after years of use poses questions that are not present with a rear-surfaced searchlight mirror.

If a separate paraboloid is preferred for materials testing then its location at the STTF may not be especially relevant. Some existing large paraboloids may already be available for this purpose, shortening the time and expense of getting the facility in operation. One existing unit is the 10-meter paraboloid Gamma Ray Telescope atop Mount Hopkins, south of Tucson, where materials tests by programs at the Optical Sciences Center would have readier access than at Albuquerque. Commercial paraboloids are becoming available, and a specific unit at locations where materials research is being done has attractive points.

The current study is scheduled for completion in August and it is hoped that the recommendations, if positive, would enable this materials testing capability for the western states to be in operation six months later.

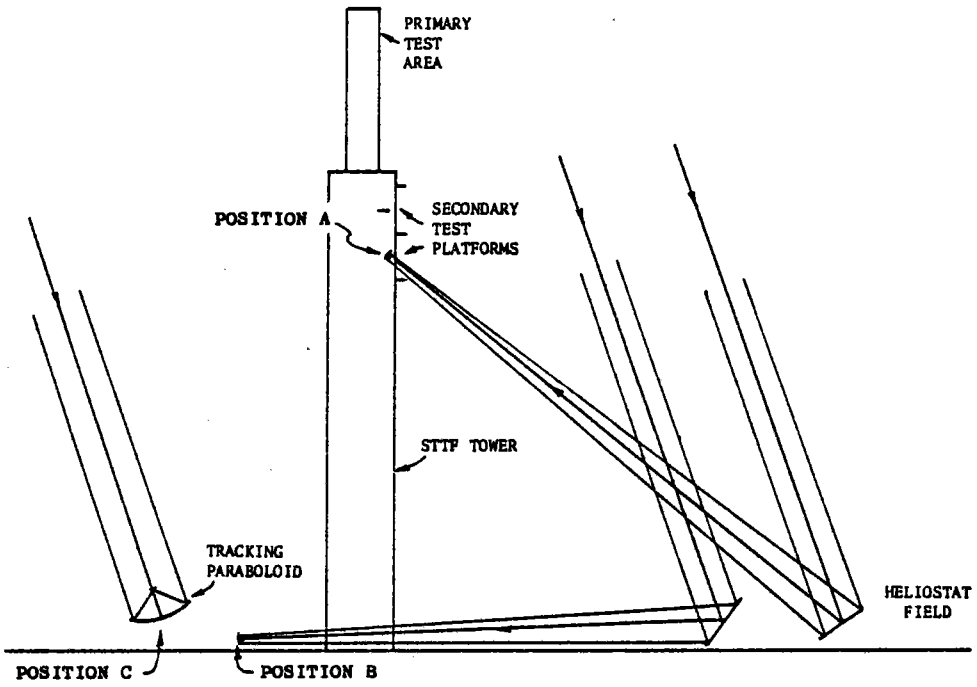

Figure 1. Possible Locations for a Reconcentrator Materials Testing Facility with Respect to the STTF Tower

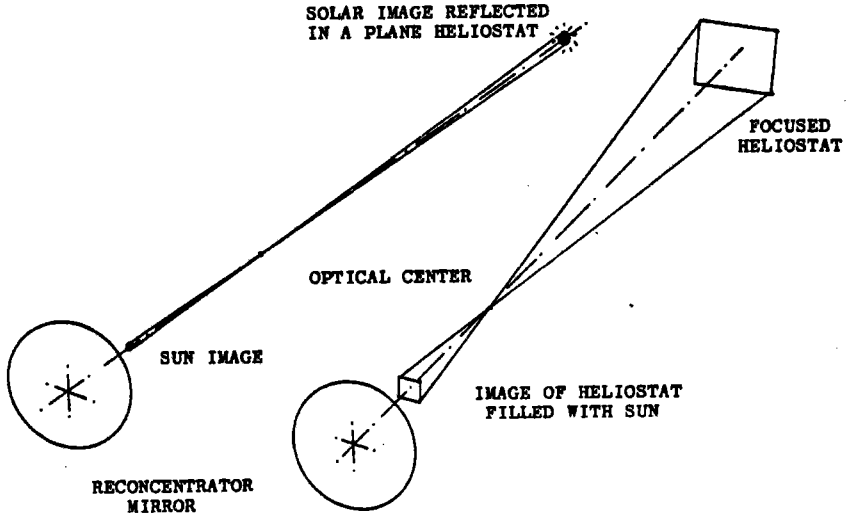

Figure 2. Basic Geometry of a Flux Reconcentrator with Focusing Heliostat Relative to One with a Plane Heliostat or a Tracking Paraboloid

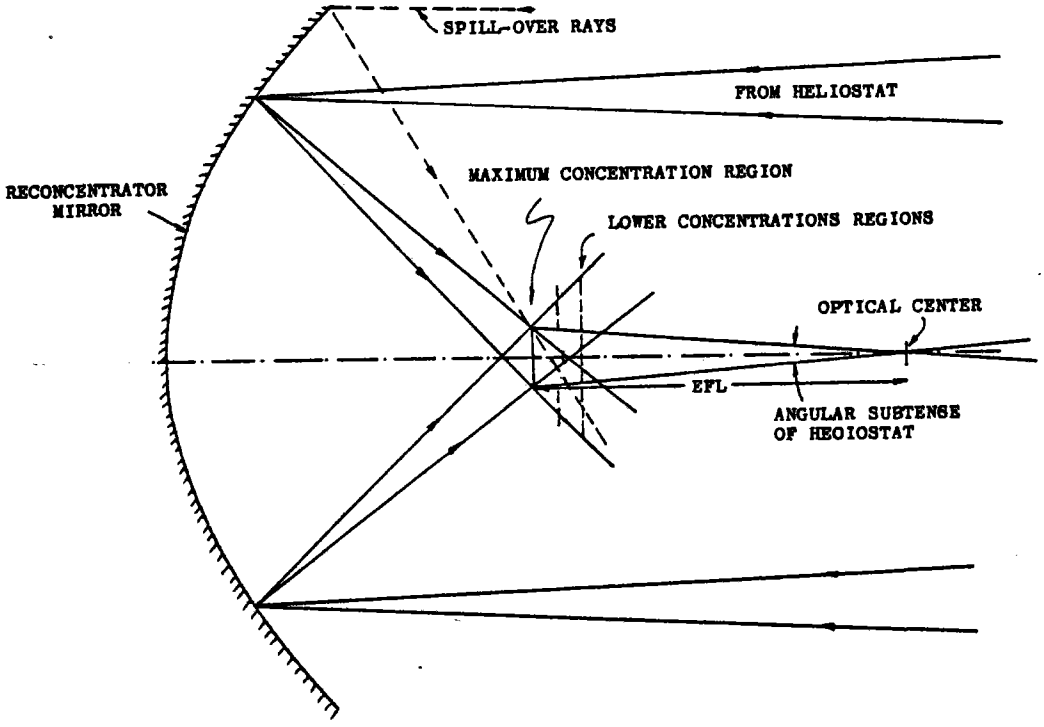

Figure 3. Geometry of the Reconcentrated Test Region Showing the Possibility for Changing Concentrations Without Requiring a Shutter or Diaphragm

PRELIMINARY OPTICAL TESTING OF A SECONDARY CONCENTRATOR FOR THE SANDIA STTF

G. P. Mulholland
Department of Mechanical Engineering
New Mexico State University
Las Cruces, NM 88003

L. K. Matthews
Testing Engineer
Division 5713
Sandia Laboratories
Albuquerque, NM 87185

Introduction

Nonimaging solar concentrators have been receiving much attention in the last few years. These efforts are due to the renewed interest in solar energy and the necessity of concentrating the incoming solar energy for high-temperature flat plate collectors and solar cell applications.

The purpose of this study was to design a nonimaging concentrator for the power tower at the Sandia Solar Thermal Test Facility. The work reported here is a preliminary study and certain refinements will be made on the design as the study progresses. At the time this report was written, the computer programs were still being debugged so no numerical results are presented.

Problem Formulation

The assumptions inherent in this formulation are the following:

1. Wavelength of the radiation is very small relative to any characteristic dimension.
2. The radiation travels in rays and propagates rectilinearly in an isotropic medium.
3. Diffraction and interference are neglected.
4. All surfaces are perfectly reflective.

The above are just the usual assumptions used in geometrical optics.

The ray trace expressions require that the angle between an incident ray and the surface normal be equal to the angle between the surface normal and the reflected ray

$$-\frac{\vec{V}_i}{|\vec{V}_i|} \cdot \hat{N} = \frac{\vec{V}_R}{|\vec{V}_R|} \cdot \hat{N} \tag{1}$$

and the incident ray, the reflected ray and the surface normal be coplanar

$$\left[\vec{V}_i \times \vec{V}_R\right] \cdot \hat{N} = 0 \tag{2}$$

For axisymmetric configurations, Eq. (2) is automatically satisfied.

The surface normal is obtained by using the fact that the gradient of a surface function is a normal vector to the surface

$$\vec{N} = -\nabla S_n \tag{3}$$

Substitution of Eq. (3) into Eqs. (1) and (2) gives

$$\left[\frac{\vec{V}_i}{|\vec{V}_i|} + \frac{\vec{V}_R}{|\vec{V}_R|}\right] \cdot (-\nabla S_n) = 0 \tag{4}$$

and

$$\left[\vec{V}_i \times \vec{V}_R\right] \cdot (-\nabla S_n) = 0 \tag{5}$$

Eqs. (4) and (5) are partial differential equations in terms of the surface function S_n.

For this discussion, axisymmetric concentrators will be considered. Eq. (5) will be automatically satisfied and Eq. (4) becomes a first-order differential equation. An energy balance is also used which, when substituted into the differential of Eq. (4) results in a second-order nonlinear differential equation. The solution of this equation gives the surface of the concentrator.

The coordinates (R_2, Z_2) are for the concentrator while (R_4, Z_4) are for the receiver, Figure 1. A normalized incident beam is given by

$$\frac{\vec{V}_i}{|\vec{V}_i|} = \sin(\theta)\,\hat{j} + \cos(\theta)\,\hat{k} \tag{6}$$

while the reflected beam is

$$\frac{\vec{V}_R}{|\vec{V}_R|} = \frac{\hat{j}\,(R_4 - R_2) + \hat{k}\,(\ell - Z_2)}{\sqrt{(R_4 - R_2)^2 + (\ell - Z_2)^2}} \tag{7}$$

where a flat receiver is assumed ($Z_4 = 0$).

In addition, the concentrator surface can be written as

$$R_2 = f(Z_2) \tag{8}$$

or

$$S(R_2,Z_2) = R_2 - f(Z_2) = 0 \tag{9}$$

A vector normal to the surface S is

$$\bar{N}_2 = -\nabla S_2 = -\hat{j} + f'\,\hat{k} \tag{10}$$

Eqs. (6), (7) and (10) satisfy Eq. (5) exactly. Substitution into Eq. (4) yields

$$f'\cos(\theta) - \sin(\theta) + \frac{f'(\ell - Z_2) - (R_4 - f)}{\sqrt{(R_4 - f)^2 + (\ell - Z_2)^2}} = 0 \tag{11}$$

Eq. (11) can be rewritten as

$$\left[f'\cos(\theta) - \sin(\theta)\right]\sqrt{(R_4 - f)^2} + (\ell - Z_2)^2 = (R_4 - f) - f'(\ell - Z_2) \tag{12}$$

Squaring both sides of Eq. (12) and rearranging, we obtain a simpler form of the ray-trace equation

$$\left[A - 1\right]\left[R_4 - f\right]^2 + 2f'(\ell - Z_2)(R_4 - f) + (A - f'^2)(\ell - Z_2)^2 = 0 \tag{13}$$

where

$$A = f'^2\cos^2(\theta) + \sin^2(\theta) - 2f'\cos(\theta)\sin(\theta) \tag{14}$$

The differential equation, Eq. (13), relates the reflector (f, Z_2) and receiver (R_4, Z_4) coordinates for any ray entering the concentrator.

Another equation relating the receiver and reflector coordinates is obtained by differentiating the ray-trace equation. The result is

$$f''\Big[(R_4 - f)^2\left(f'\cos^2(\theta) - \sin(\theta)\cos(\theta)\right) + (R_4 - f)(\ell - Z_2) + (\ell - Z_2)^2(f'\sin^2(\theta) + \sin(\theta)\cos(\theta)\Big] =$$

$$(\ell - Z_2)(A - f'^2) + f'(R_4 - f) - \left[\frac{dR_4}{dZ_2} - f'\right]\left[f'(\ell - Z_2) + (A - 1)(R_4 - f)\right] \tag{15}$$

Eq. (15) is a second-order nonlinear differential equation with f as the dependent variable and Z_2 as the independent variable. The quantities R_4 and $\frac{dR_4}{dZ_2}$ can be obtained as functions of f, f' and Z_2 from the ray-trace equation and an energy balance between the entrance and exit apertures, respectively.

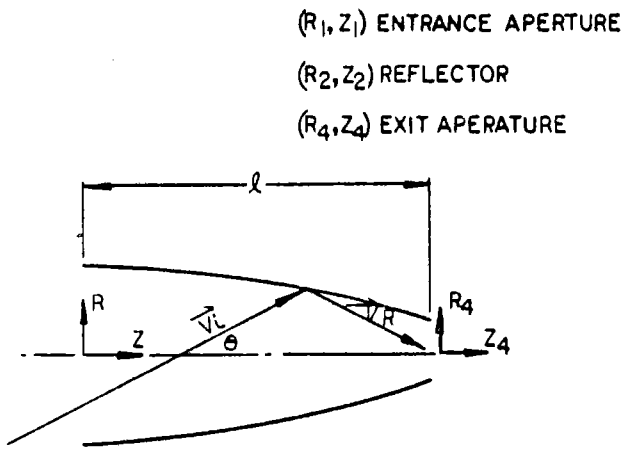

Figure 1. Geometry for Axisymmetric Concentrator

An energy balance between a differential ring at the entrance aperture and a differential ring on the receiver yields

$$2\pi R_1 dR_1 Q_1(R_1) = 2\pi R_4 dR_4 Q_4(R_4) \tag{16}$$

where Q_4 = flux density on receiver due to reflected energy. Since $R_1 = R_2 - Z_2 \tan\theta$, the Eq. (16) reduces to

$$\frac{dR_4}{dZ_2} = \frac{f - Z_2 \text{ Tan } (\theta)}{R_4}\left(f' - \text{Tan } (\theta)\right) \frac{Q_1(R_1)}{Q_4(R_4)} \tag{17}$$

From the ray-trace equation, Eq. (13), we have

$$R_4 - f = \frac{f' (\ell - Z_2)}{A - 1} - 1 \pm \sqrt{1 - \frac{(A - f'^2)(A - 1)}{f'^2}} \tag{18}$$

In Eq. (18), the proper root is chosen to insure that $R_4 - f < 0$.

When Eqs. (17) and (18) are used in Eq. (15), we have an equation which can be solved numerically for the reflector profile f as a function of the optic axis Z_2.

Boundary Conditions

The two boundary conditions associated with Eq. (15) are

$$f(0) = J_2 \tag{19}$$

$$f'(0) = 0 \tag{20}$$

Eq. (14) is obvious from Figure 1. Eq. (20) can be deduced from the ray-trace equation, Eq. (13), and from the conservation phase-space volume [1,2] which implies

$$J_4 \geq J_2 \sin(\theta) \tag{21}$$

$$\ell = (J_2 + J_4)\cot(\theta) \tag{22}$$

Also, for Z = 0

$$f = J_2,\ R_4 = -J_4,\ A = f'(0)^2 \cos^2(\theta) + \sin^2(\theta) - 2f'(0)\cos(\theta)\sin(\theta) \tag{23}$$

Substitution of Eqs. (21)-(23) into Eq. (13) gives

$$f'^2(0)\left[(J_2 + J_4)^2\cos^2(\theta) - \ell^2\sin^2(\theta)\right] + \ell^2\sin^2(\theta) - (J_2 + J_4)^2\cos^2(\theta) - 2f'(0)\left[\ell^2 + (J_2 + J_4)^2\sin(\theta)\cos(\theta) + \ell(J_2 + J_4)\right] = 0 \tag{24}$$

Since $\ell = (J_2 + J_4)\cot(\theta)$

$$\ell^2\sin^2(\theta) - (J_2 + J_4)^2\cos^2(\theta) = 0 \tag{25}$$

and Eq. (24) reduces to

$$f'(0)\left[\ell^2\left(1 + \frac{\sin(\theta)}{\cos(\theta)} + \frac{\sin^3(\theta)}{\cos(\theta)}\right)\right] = 0 \tag{26}$$

Thus f' (0) must equal zero to satisfy the ray-trace equation and Eqs. (21) and (22).

Summary

The problem to be solved is the differential equation given by Eq. (15)

$$f'' = \frac{(\ell - Z)(A - f'^2) + f'(R_4 - f) - \left[\frac{dR_4}{dZ} - f'\right]\left[f'(\ell - Z) + (A - 1)(R_4 - f)\right]}{(R_4 - f)^2\left(f'\cos^2\theta - \sin(\theta)\cos(\theta)\right) + (R_4 - f)(\ell - Z) - (\ell - Z)^2\left(f'\sin^2(\theta) + \sin(\theta)\cos(\theta)\right)}$$

and subject to the initial conditions

$$f(0) = J_2 \tag{19}$$

$$f'(0) = 0 \tag{20}$$

Also, in Eq. (15)

$$A = f'^2 \cos^2(\theta) + \sin^2(\theta) - 2f' \cos(\theta) \sin(\theta) \tag{14}$$

$$R_4 = f + \frac{f'(\ell - Z)}{A - 1}\left[-1 \quad \sqrt{1 - \frac{(A - f'^2)(A - 1)}{f'^2}}\right] \tag{18}$$

$$\frac{dR_4}{dZ} = \frac{f - Z \tan(\theta)}{R_4} \quad f' - \tan(\theta) \quad \frac{Q_1}{Q_4} \tag{17}$$

The above system of equations is being solved numerically and the results will be used to design the concentrator. Comparisons will be made between this design and the Winston three-dimensional concentrator by ray-tracing to determine which design is optional. A small model (6-inch diameter entrance aperture and 3-inch diameter exit aperture) will be built and tested at the White Sands Solar Furnace. The results from this test will determine if the cooling capabilities of the concentrator are adequate and what refinements are needed for the preliminary design. When this phase is completed, the design for the full-scale concentrator will begin.

References

1. Winston, R., "Light Collection Within the Framework of Geometrical Optics," Journal of the Optical Society of America, Vol. 60, No. 2, pp. 245-247, (1970)

2. Rabl, A., and Winston, R., "Ideal Concentrators for Finite Sources and Restricted Exit Angles," Applied Optics, Vol. 15, pp. 2880-2883, (1976)

THE WHITE SANDS MISSILE RANGE 400KW SOLAR FURNACE - PROJECT REVIEW

by

W. C. Hull
Associate Professor Mechanical Engineering
New Mexico State University

Abstract

New Mexico State University is currently funded by White Sands Missile Range to conduct a design study for conversion of a large radar tower to a 400 kilowatt solar furnace. A group of specialists have been assembled to analyze and evaluate the various design concepts important to the ultimate operation and performance of the solar furnace. Results to date indicate that desired flux levels of 250 cal/cm^2-sec with corresponding concentrations of 10,000 suns are achievable. Plans include establishment of a reflective surface over the existing 84 ft. parabolic dish, and the use of a Cassegrain reflector at the primary focus.

A test chamber similar to the test chamber at the existing 30 kilowatt White Sands Solar Furnace will be developed to provide for a variety of test modes at the anticipated extreme flux levels, including thermal nuclear shaped pulse, square wave pulses, and steady state exposures. Alternate test stations are being considered including a position at the bottom of the tower. Important research and development areas under study include: high temperature shutters and reflectors, optical ray tracing, heat transfer, wind loading, static and dynamic structural integrity, instrumentation, and digital control for tracking and test operations. A review of progress to date is presented.

INTRODUCTION

In October 1977 New Mexico State University received a one year contract from White Sands Missile Range to conduct a design study for the conversion of an existing radar facility into a solar furnace for the creation of extreme solar flux levels for weapon effects testing. A group of university specialists have been assembled to analyze and evaluate the surplus radar facility for its suitability for use as a solar furnace, and to provide the required design functions necessary to develope the new solar furnace. Figure 1 is an organizational chart of project participants. Members of four Engineering Departments and the New Mexico State University Physical Science Laboratory are included, along with graduate and undergraduate student assistants, technicians and technical consultants.

These individuals are currently involved with the details of the design phase of the project, and will later direct the actual fabrication and construction of the facility during phase two of the project. Phase two is scheduled to begin in October 1978. The construction phase will make heavy use of the fabrication shops, skilled craftsmen, and technicians of the Physical Science Laboratory with the possibility of some subcontractoral work.

EXISTING FACILITY

The radar facility as shown in Fig. 2 consists of an 84 ft. diameter elevation over azimuth tracking parabola having an f ratio of 0.3 which is mounted on a 60 ft. tower. The radar tracking accuracy is rated at 30 arc seconds pointing, with slew speeds of 12^{o} per second. The facility was built in 1961 by the Air Force

and operated until 1972, when it was decommissioned.

Adjacent to the radar tower there is an 8000 ft.^{2} ancilliary building which houses the existing tracking control console and backup electronics, as well as pumps, chillers, and air compressors which previously were used for cooling equipment used in operation of the radar, but will now be employed to cool shutters, relay mirrors, flux guides, and water cooled stops. Ample space will be available in the ancilliary building for the main furnace control station, contractor instrumentation room, office spaces, maintenance shops, equipment preparation space, and storage. Plans call for all test operations in the furnace to be controlled from the control console in the ancilliary building through use of remote TV cameras and digital controller.

The radar tower and ancilliary building are surrounded by a 100 ft. high radar back-scatter fence. The original purpose of the fence was to shield the radar dish from ground radiation reflections; however in the future it will serve mainly to attenuate pervailing winds. Initial estimates indicate that the fence will reduce wind speeds at the tower by as much as 37%. This is a definite advantage since the present open mesh dish will be changed to an essentially closed configuration to provide for the primary mirror surface and for the furnace attenuator shutter system. Static and dynamic dead weight and wind loading effects will be carefully evaluated as the design study continues.

FURNACE PERFORMANCE REQUIREMENTS

Design requirements for the new solar furnace are based on providing flux levels of 250 cal/cm^2-sec or concentrations to 10,000

suns. Optical analysis to date indicate that this flux level is achievable with the proposed Cassegrain optical configuration and use of tertiary reconcentrations.

Classical ray tracing techniques are being used to develop computer programs to project focal plane image sizes and concentration levels for the various furnace configurations under study. In addition, a variety of experimental optical apparatus will be fabricated and tested, to verify analytical predictions. This will involve tests using direct sun light, a laser as a light source, as well as tests using concentrated solar flux available at the existing White Sands 30 kilowatt Solar Furnace. Some of this work has been completed and preliminary analytical results verified.

A further requirement for the new furnace is that it be capable of providing controlled flux pulses including square wave pulses and pulses which simulate radiation from a nuclear detonation. A shutter system similar to that at the the White Sands 30 Kilowatt Solar Furnace is proposed for this purpose. This system consists of a water cooled shutter, two fast shutters, and a nuclear pulse shaper.

SOLAR FURNACE CONFIGURATIONS

Figure 3 illustrates the proposed general overall furnace configuration including the locations of the Cassegrain secondary mirror and attenuator. A variety of test stations are under study including the following:

(a) A station inside the parabolic dish between the primary and secondary mirrors.

(b) A station attached to the under side of the radar dish, adjacent to the torque tube.

(c) A station on the upper tower platform.

(d) A station at an upper level inside the tower.

(e) A station inside the tower at ground level.

Each of the listed configurations will be evaluated with respect to technological feasibility, functional characteristics, cost, and construction lead time. As a consequence of needing to redirect the concentrated solar flux through various optical paths to achieve the desired test station locations it will be necessary to develop articulated water cooled relay mirrors, flux guides, and reconcentrators. Prototype units will be designed and tested for this purpose.

A considerable effort has gone into identifying candidate materials for use in creating a reflective surface over the skin of the radar dish, and into candidates for the Cassegrain secondary. Design goals for these include: light weight, high specularity, small deviation from true optical figure, service longivity, resistance to wind loading effects, and relatively low cost. Several candidates have been identified and many will soon be tested to verify their suitability.

RESEARCH AND DEVELOPMENT AREAS UNDER STUDY

Several major areas of research and analysis are under study which relate to the design of the solar furnace, and to assuring the functional adequacy of the completed furnace. These include the following:

(a) mirrors and reflective materials

(b) high temperature shutters and reflectors

(c) optical design

(d) heat transfer

(e) wind loading

(f) static and dynamic structural integrity

(g) instrumentation

(h) digital control for tracking and test operations

Each of these areas will receive careful attention during phase one of the project.

SUMMARY

A decommissioned radar facility may soon become a 400 kilowatt solar furnace. Engineers and technicians at New Mexico State University are currently studying this possibility under contract to White Sands Missile Range. Objective flux levels for the new furnace are 250 cal/cm^2-sec or 10,000 sun concentrations. Early results indicate that these levels are attainable. The Construction phase of the project is projected to start in October 1978.

White Sands Missile Range
400 KW Solar Furnace Project

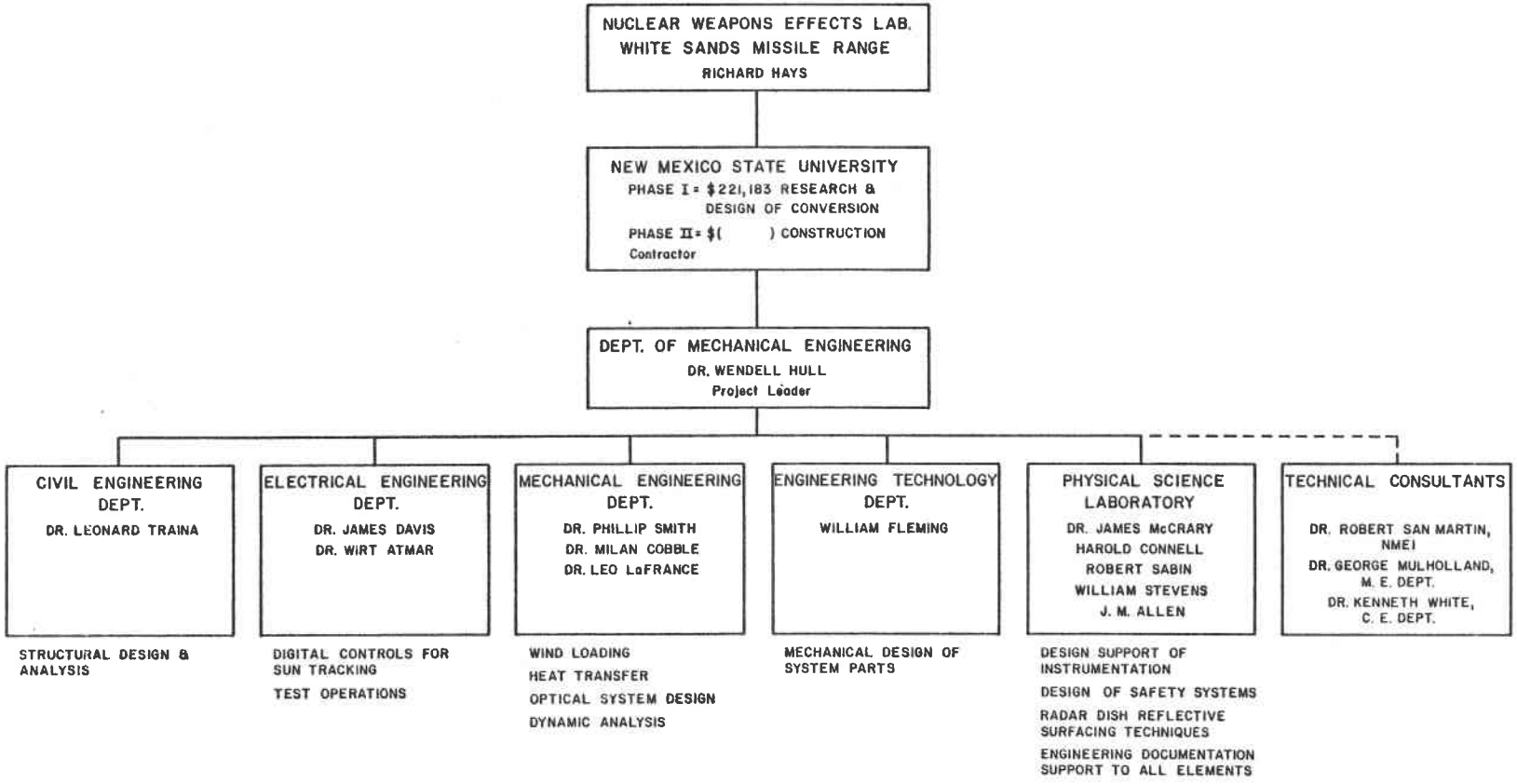

FIG. 1 Organization Chart of Program Participants

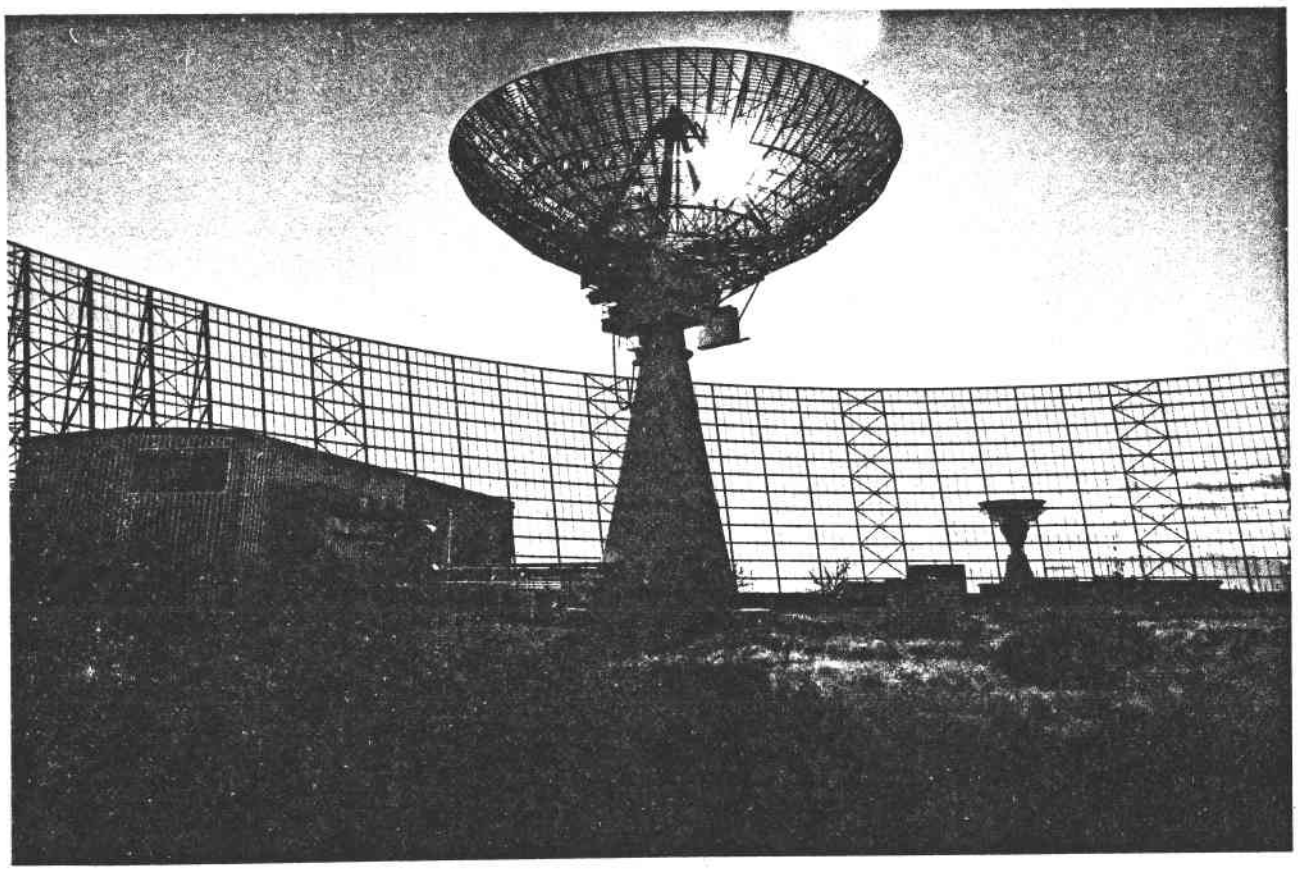

FIG. 2 Existing Radar Facility

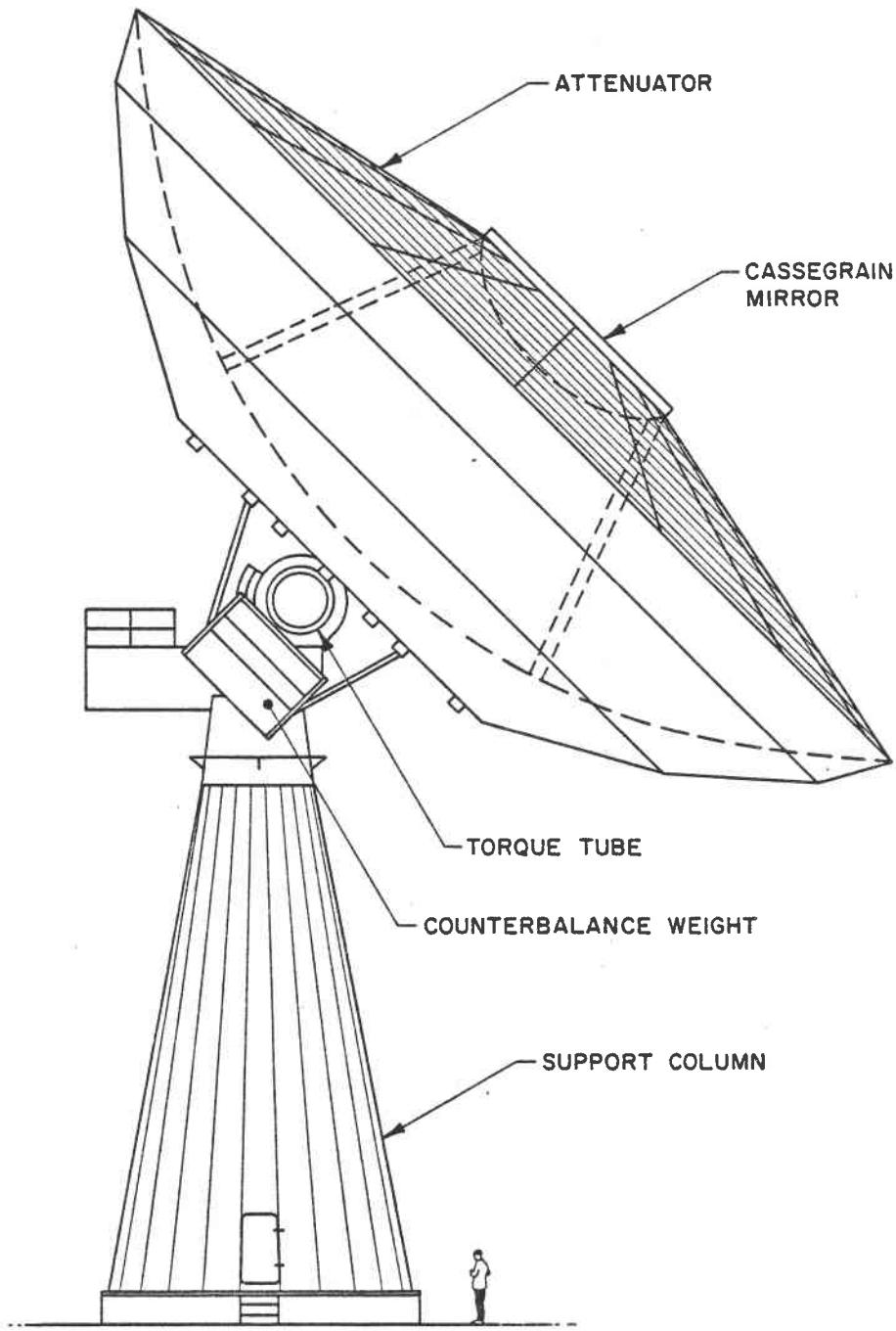

FIG. 3 Proposed General Furnace Configuration

HIGH PERFORMANCE SOLAR TRACKING IMAGING CONCENTRATOR

Samuel P. Lazzara, Senior Vice President
Stanley H. Zelinger, President

OMNIUM-G
Anaheim, California

Since 1965 Mr. Lazzara has been engaged in the advanced design, analysis, and application of high energy laser systems. His experience in high precision and high resolution laser beam formation, projection, and tracking has paved the way for his patented breakthrough in coherent optical adaptive systems for laser beam phase error compensation. Mr. Lazzara is currently Director of all technical activities at OMNIUM-G and is responsible for the techniques developed in supplying commercial solar powered total energy systems.

Mr. Zelinger has spent fourteen years in the design, fabrication, marketing, and sales of radar and computer systems. Aside from the responsibilities of the administrative activities of the company, Mr. Zelinger contributes in the design and fabrication of the electronic tracking and servo controls of the company's products.

The OMNIUM-G goal in providing a self-contained solar powered total energy system for remote decentralized applications has led to the development of a high concentration ratio solar imaging collector. This collector has now found use as a valuable tool in areas where high flux density research requires modest power as well.

Until now, the researcher had but few facilities available that provided both a significant amount of total power combined with flux densities in excess of 1000 watts/cm^2. Presented here is not only a description of the OMNIUM-G HELIODYNE HTC-25 tracking concentrator and its matched heliostat but a brief treatise on high concentration ratios—their utility in solar energy and why the collectors can be economically fabricated.

Figure 1 is the complete tracking concentrator shown with OMNIUM-G's receiver and prime mover for electrical power generation. Figures 2 and 3 show the flux density and contained power within a specified radius, respectively.

OMNIUM-G's HELIODYNE TRACKING CONCENTRATOR, Model HTC-25, is a two-dimensional solar imaging parabolic reflector. The unit, created by OMNIUM-G, focuses the sun's rays from a 6-meter diameter reflector with a concentration ratio of greater than 10,000:1. The low cost unit provides up to 25 kW for use by experimenters as an attractive long-life, low-maintenance source of energy for high-temperature research. Its uses include research on refractories, solar thermal conversion, coal gasification, direct laser pumping, hydrogen separation, and photovoltaic cell pumping.

The reflector is mounted on servo motor-controlled elevation-over-azimuth gimbals, and is pointed by both sun-seeking and open-loop data control.

The mirror construction techniques developed and employed by OMNIUM-G have resulted in a hundred-fold cost reduction in the fabrication of large, figured optical reflectors with precision adequate for solar energy. These reflectors are lightweight, strong, dimensionally stable, and designed to withstand harsh environmental conditions. The reflector and tracking mechanism can operate in winds up to 80 km/hr and can withstand 128-km/hr winds in the stow position. The system mounting base is a walk-in enclosure providing a suitable weather-proof housing for instrumentation and other experimental equipment. The HTC-25 has the versatility of handling experiment packages ranging up to 500 pounds maximum when placed on the elevation gimbal and an additional 750 pounds on the azimuth gimbal. Detailed specifications include:

FOCAL LENGTH: 4 meters

CENTRAL OBSTRUCTION DIAMETER: 1 meter

REFLECTIVITY: 83% minimum measured at a wavelength of 0.55 micrometers (typically 94% as measured over the solar spectrum).

REFLECTIVITY LIFE: Gradual degradation to 90% of installed condition after 5 years. Degradation limited to ordinary effects of weather. Wind-driven sand, dust, hail, and corrosive deposits from nearby effluent sources must be considered separately.

Figure 1 - OMNIUM-G's HELIODYNE^{tm} TRACKING CONCENTRATOR (HTC-25) 25 kWth, 1100 watts/cm^2

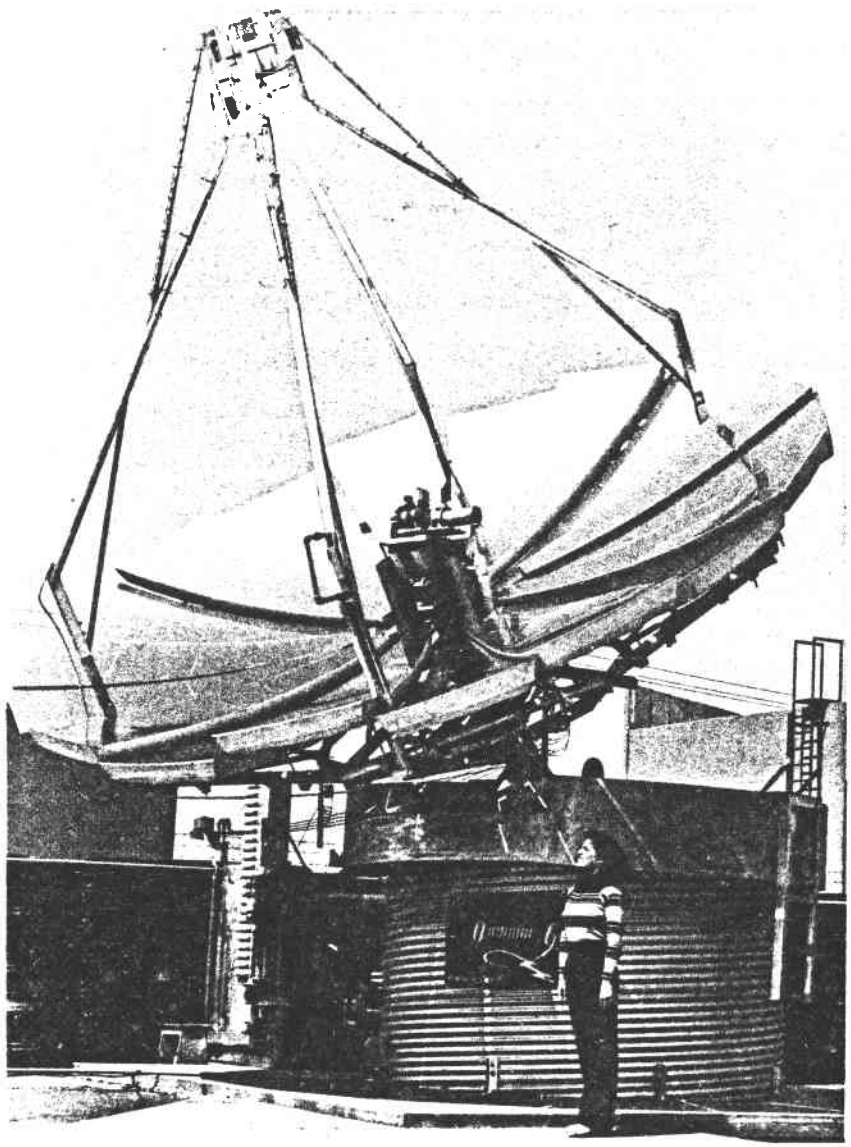

FIGURE 2

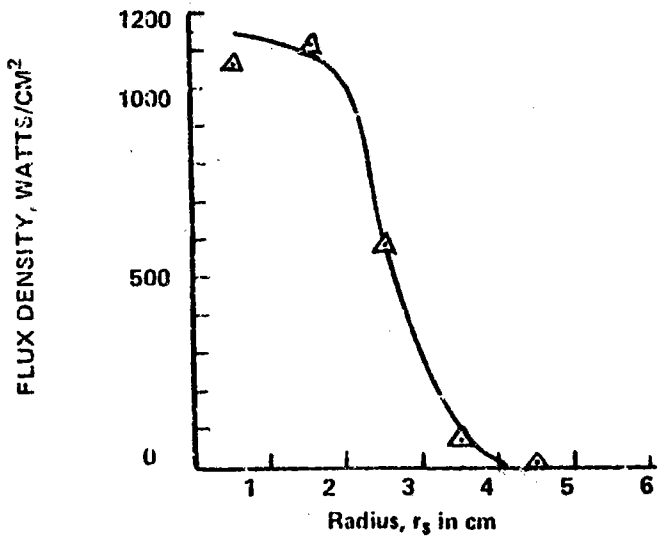

FOCAL PLANE FLUX DENSITY FOR 24.7 KW NET POWER AT FOCAL PLANE AND 979 WATTS/M² SOLAR FLUX

FIGURE 3

TYPICAL FOCAL PLANE SPOT CHARACTERISTICS AS MEASURED FROM BURN-PATTERNS ON OMNIUM-G'S HELIODYNE MODEL HTC-25 INSTALLED IN ANAHEIM, CALIFORNIA

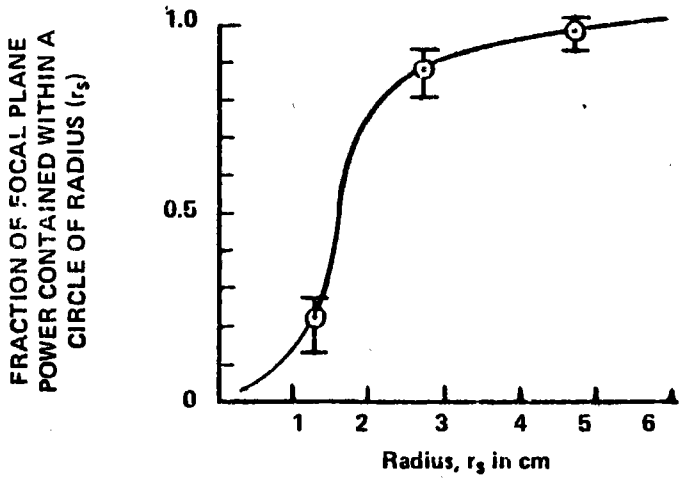

FOCAL PLANE SPOT POWER DISTRIBUTION

CONFIGURATION: 18 parabolic sections (petals) 3-point adjustable attachment to a common stiff-back structure.

FOCAL PLANE CONCENTRATION: Guaranteed performance specification—15-cm diameter containing all specular power; 6-cm containing at least 85% of specular power. Typical as measured in Anaheim, CA, is 9.4 cm and 5.4 cm, respectively.

POINTING: Servo motor-controlled elevation-over-azimuth gimbals.

TRACKING: Closed loop--0.36^{o} automatic reacquisition of up to 30 days of no sun.

COVERAGE: $\pm 180^{o}$ azimuthal to 90^{o} elevation horizon to zenith.

POWER CONSUMPTION: 0.3 kWH/Day

WEIGHT: 3,900 pounds

The HTC-25, by nature, must keep in fine track with the sun's trajectory. This requirement has placed finite restrictions as to weight, size, and orientation limitations on the equipment located at the focal plane. For this reason, OMNIUM-G has designed and is fabricating a matched heliostat to the HTC-25. The heliostat is shown in Figure 4. The heliostat may be configured for vertical or horizontal orientation. Figure 5 shows the horizontal. In these configurations, the experiment can be permanently affixed at the focal plane thus placing the burden of fine trajectory tracking on the heliostat controls. The heliostat has a total reflecting surface area of 600 square feet via 25 24-square foot flat mirror segments. Through a gimballing arrangement that produces foreshortening in only one axis, the heliostat will always present at least 400 square feet of net reflecting area to the concentrator. This uniqueness minimizes the area normally required of heliostats using conventional gimballing techniques. The gimbal arrangement is, in effect, a polar orientation where the concentrator is the pole. The mirrors are fabricated using the identical process as used for the HTC-25 figured mirrors. Other specifications are the same as for the concentrator. Figure 6 shows other views of the heliostat.

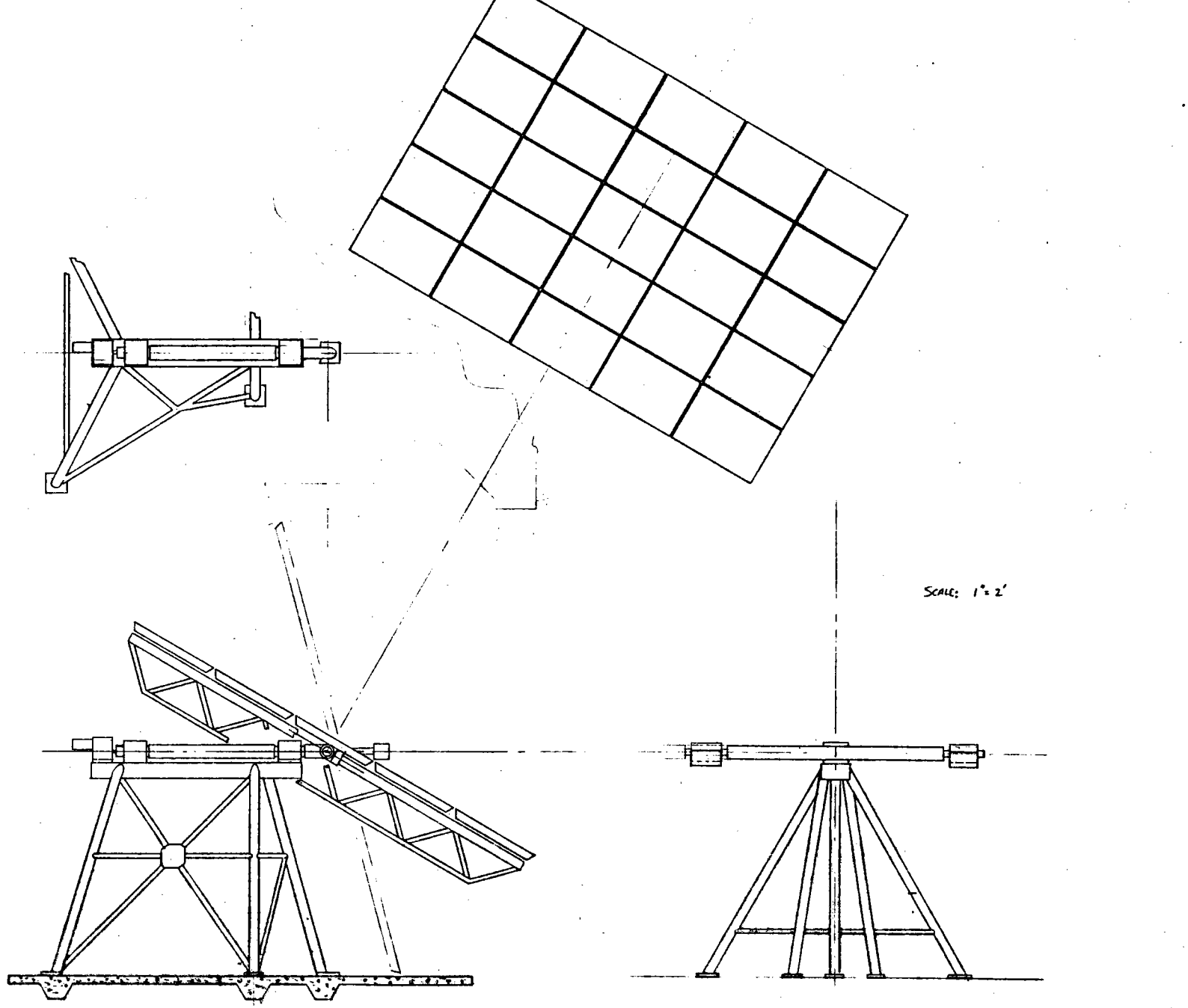

SCALE: 1" = 2'

SCALE 1" = 2'

HELIOSTAT OVERALL LAYOUT

HELIOSTAT

FIGURE 4

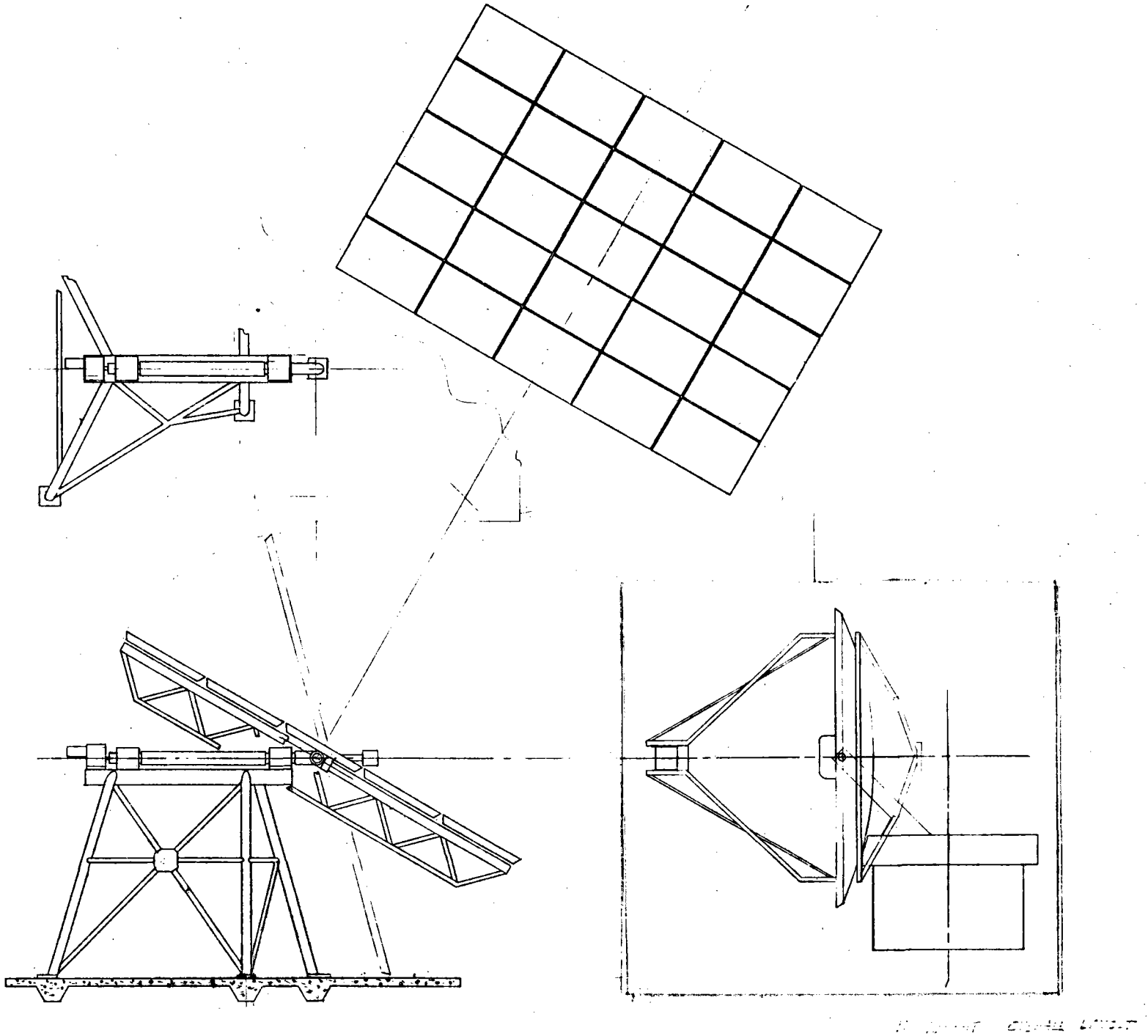

SCALE 1" = 2'

HELIOSTAT – CONCENTRATOR COMBINATION

FIGURE 5

OMNIUM - G

THE UTILITY OF HIGH CONCENTRATION RATIO

In designing a total energy system for remote decentralized operation, overall conversion efficiency is of primary importance. In dealing with temperatures in excess of 1200^{o}F, radiation and convection cooling losses are significant. In order to reduce these losses, it becomes clear that the energy must be channeled into as small an aperture as possible, entrapped within a protective cavity, then expended to manageable means for conversion and heat exchanging. Keeping within commercial goals of reduced costs and long life, materials must be standard whenever possible. The curve of Figure 7 shows the losses of a cavity with various wind conditions as a function of concentration ratio.

At a glance at Figure 7, it is immediately clear that concentration ratios less than 3000 to 1 have losses which climb dramatically with increasing wind velocity. Transparent windows have been considered for reducing these losses, but unfortunately add losses of their own via first surface reflection and internal heating due to absorption.

The trend toward building high concentration ratio collectors has not been as fast as one would expect from the results depicted in Figure 7 because of several reasons. First, there was an attempt to convert standard microwave surfaces using segment arrays of flats. These found limitations because of such low concentration ratios, figure maintenance, and reflective efficiency. Secondly, conventional optical techniques would produce mirrors so heavy that very costly gimballing arrangements would be required. Thus, little attention was given to techniques for building inexpensive high concentration ratio collectors.

Convinced that the only solution for efficient solar energy conversion was in having a collector concentration ratio in excess of 10,000:1, OMNIUM-G sought means of fabricating high precision figured mirrors that would be light enough in weight to allow gimballing that would not be extrordinarily sophisticated, heavy, or costly.

Electropolished anodized aluminum was chosen as the reflective surface because of its availability, durability and overall specular reflectivity. Its degradation due to dust and normal environmental conditions is so graceful, that

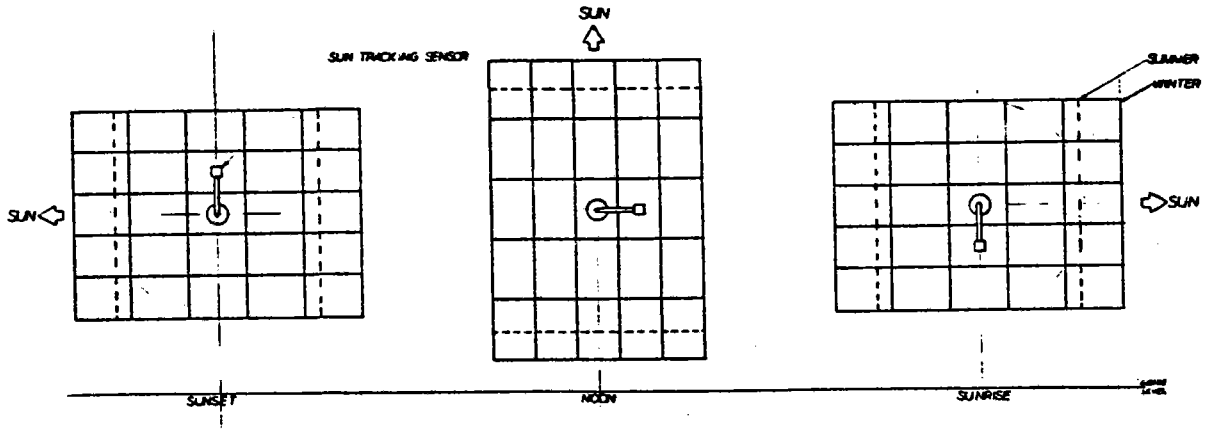

FIGURE 6
HELIOSTAT AS VIEWED FROM THE HTC-25

OMNIUM-G

FIGURE 7 - THERMAL LOSSES VS. CONCENTRATION RATIO

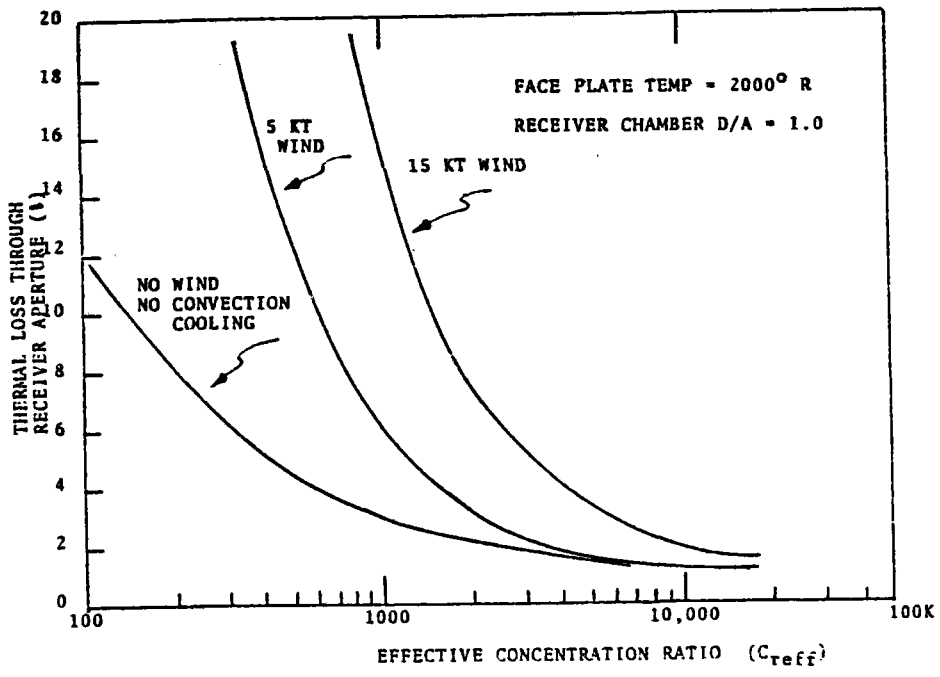

several weeks may elapse between cleanings, and its hardened surface is also quite resistive to wind-driven particles. Glass could not be a candidate because of its inability to form to our shape, nor was it considered because of its absorption and expense. The reflectivity of the ALZAK process electropolished aluminum has been measured repeatedly by measuring melt-through time of a sample of 0.032" ALZAK at the focal plane. Figure 8 shows that the probable reflectivity ranges from a minimum of 0.90 to a maximum of over 0.94. The uncertainty in incident solar flux level and exposure time to melt-through accounts for the span. The method of measurement is self-correcting because the same material is used for both the concentrator and the focal plane sample.

The process of forming the aluminum on a supporting structure had to be both precise and rigid for figure maintenance, and durable for long life in harsh environmental areas.

Polyurethane foam was chosen for its density-to-strength ratio and durability. The process developed by OMNIUM-G totally solved the problem of the foam's virtually uncontrollable physical behavior.

The process developed by OMNIUM-G allowed the casting of the aluminum to the polyurethane foam with a slope error of less than 1.0 mr. RMS. Our life cycle measurements on our mirrors show to date no measurable deviation in figure from the initial day of fabrication.

Figure 9 shows a burn pattern made on our system in Anaheim, California.

Having broken through the process of replicating high precision figured mirrors that are durable and extremely lightweight, it was a relatively straightforward task to build an elevation-over-azimuth gimbal structure that maintained the pointing accuracies necessary.

In conclusion, OMNIUM-G has developed a process whereby high concentration ratio collectors are inexpensively fabricated. Whether the use be for solar thermal electrical conversion or for use by researchers, more effective developments can be realized for costs far less than have previously been projected.

FIGURE 8

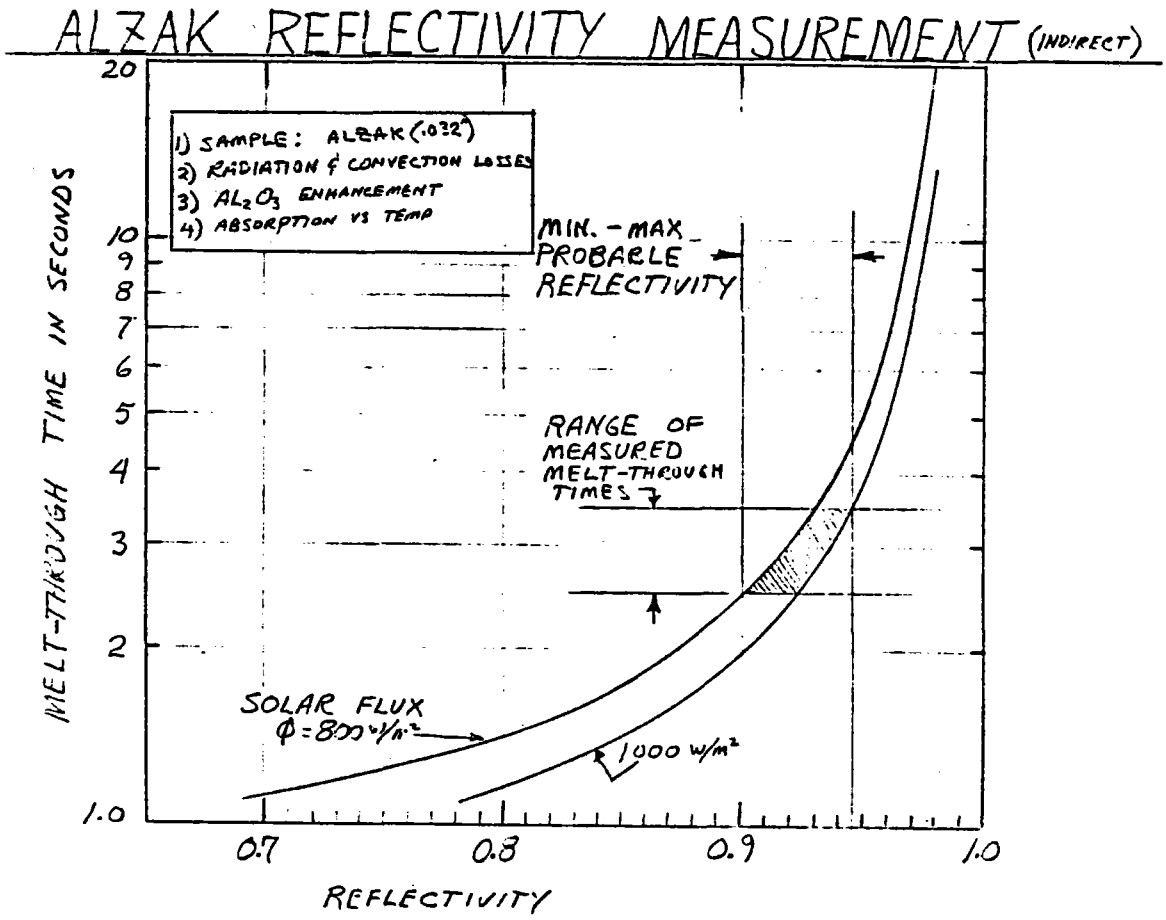

FIGURE 9 - BURN PATTERN TAKEN ON THE HTC-25 TRACKING CONCENTRATOR AT THE OMNIUM-G FACILITY

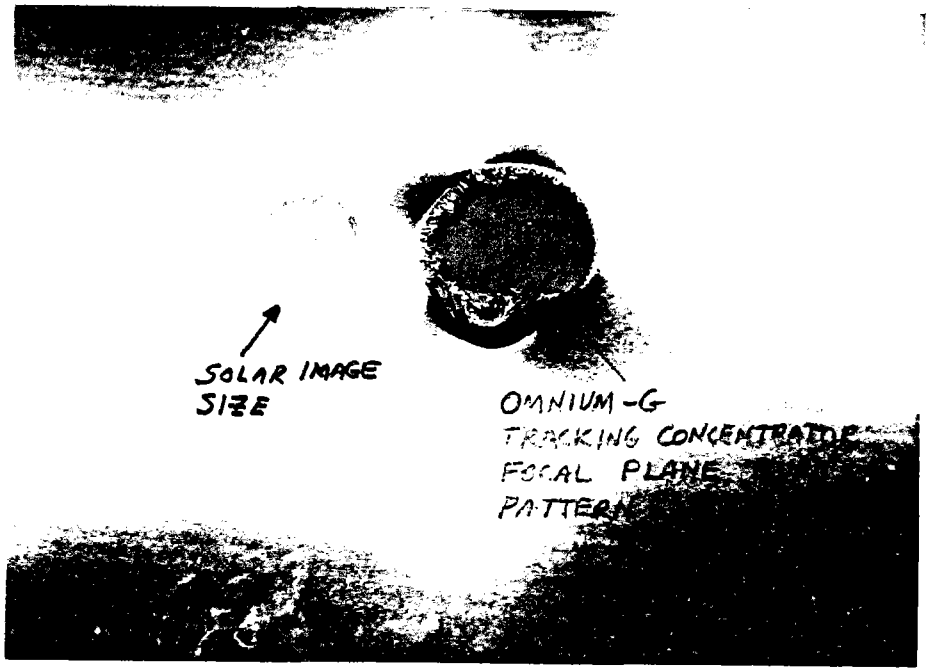

VII. DR. H. H. MARVIN

Department of Energy
Division of Solar Technology

Chairman Hildebrandt - It is my very great pleasure to introduce our evening speaker. I'm sure all of you know Dr. Henry Marvin. I would like to say that in the last year he has done an outstanding job in moving solar forward in every aspect and has truly been a supporter of the solar thermal program. He has also been a driving force behind the STTF Users Association. It gives me very great pleasure to introduce Hank tonight.

Dr. Marvin - Thank you, Al. I want to welcome our French guests; you honor us with your presence and you do double duty by continuing to pay attention to the field of solar energy. I think the thing that's hardest for us to stay with in this country is the international aspect of solar and particularly from France. We feel the welcome there and the repetitive presence here makes it easy to sell continued international activities in Washington.

I asked Al, since there wasn't a title for my talk, what he thought you might like to hear but he didn't really comment as I thought he would. What you'd like to hear about, of course, is money. Generally, the thing that elicits the most interest wherever I go and the thing you are most interested in here tonight is the question of money and the 1979 budget for DOE. I'll come to that but perhaps the thing to do is to come to it with an analogy, "The Perils of Pauline." I hadn't really landed on this until I heard the last paper this afternoon with regard to the perils of trying to bring on a product while working at another job and doing it nights and weekends, and it struck me that perhaps that is the right approach for putting the country's solar program in the right context.

I thought to work myself through the tenth chapter, which is the part in which you are interested, and just walk you who aren't aware of the vicissitudes gently through the first nine chapters until we get to the tenth, which is where my message lies.

I thought about this and it occurred to me that one first has to introduce the cast of characters and that really happened in 1956 with the Paley report. As in any play, this one went through the cast of characters and introduced them one at a time. All that got from the United States was a big yawn and the yawn went on for quite a while--something more than a decade. Only a few hands were paying attention to solar energy.

It was picked up again with the scene set in 1969/1970 when the RANN project was established, and the folks that went into that project beginning to put a handle on the things that some of the folks who had continued to work in solar had pointed up.

That rumbled along for a couple of years and then came a sudden change in pace with the oil nation blockade. Just as in "The Perils of Pauline," if you think about how that goes, the first segment doesn't have much that happens, but in the second segment there is a little more. By the time you get to the third segment, it has to begin to grab you a little or you won't be back for the fourth segment. In this case, what happened was that the Research, Development and Demonstration Act for Solar Heating and Cooling was passed by Congress in 1974 and at the same time ERDA was established. The most significant of those acts, I would say (being something of the house skeptic), was the R&D Act, which began to move things. That fairly well got Pauline a three-to-five-year reprieve, and for that period of time she wasn't going to be tied to the railroad tracks anyway.

By 1975, with all the noise from the band, the villain came on the scene, and this was the first budget we were putting together for ERDA. It turned out to be about forty million dollars. At that time I appeared on the scene and about three days after I got to Washington I had to report to the ERDA Budget Review Committee and defend the STTF, whatever that was. I had never had anything to do with solar at all, and I had not the least notion what I was talking about, but I had a little bit of the salesman in me and somehow or other the STTF stuck that year.

By the next year they were waiting for me but fortunately there was a hero in the back room. The hero then in 1976 was the FY 77 budget and I would say that the worst part was having to defend it, especially the Barstow project. In this case, there wasn't a dry eye in the house, I'll tell you.

There was no one but me who was interested in that project one whit, and yet nobody at ERDA had figured out how to say no. We got through alright, but Pauline would have been tied to the railroad tracks right then if it hadn't been for the arrival of a number of congressmen who had decided that it was time to move with solar energy. So the hero arrived and at that point the budget (as you'll recall if you were involved) went in from the President at 160 million dollars and came out of Congress at 290 million dollars, having wandered past 350 million dollars on the way. That got the hero on the scene and the cast was all put together.

Then there was a slight intermission as we went through the FY 78 budget preparation with no particular noise. But DOE was coming aboard and there was a new President aboard. His recommendation went through very much as it stood and came out with a split, DOE having divided the solar activities. Solar Technology came out at 282 million dollars, just below the earlier 290 million dollars for the whole shebang. This was about a hundred-million-dollar addition for the Solar Technology Division.

That's not such a bad story. You wouldn't think that was terrible from Pauline's point of view but then came the organization of DOE and from then on Pauline really has been tied to the tracks, I'll tell you.

The first serious action was, of course, the formation of SERI and this has to go with the Perils of Pauline version with tears, exclamation points, and applause from the audience. I'm very pleased to say that SERI appears at this point to have found itself. Any new organization takes time to sort out what its mission is, who its people are, and how it's going to function in the rather complex situation in which SERI found itself. I hadn't said this to anybody before, Charlie, but today was a great pleasure from my point of view. I was out for a relatively minor review but it's the kind of thing which, to a seasoned manager, says, "Aha, it's going!" So, if you're getting your first look at SERI, I assure you that you're seeing an organization that is up on its feet and going and has full support from Washington, now that the question of SERI and the little SERIs has been resolved.

I think you all know that tale. If you don't, I'll fill you in. The second aspect, then, of this serious action is the part where Pauline gets tied to the tracks and we dim the lights. The first thing that happened was that the C&SA Division was formed and you now have two solar energy operations instead of one, and I must say that we haven't yet figured out how to work. Neither one of us has to this point had an assistant secretary and both organizations in Washington are having trouble finding how to move on. Only the fact that we all knew each other has held things together to keep trouble from getting worse than it has. But the time is wearing on and it has been a long drag. If you find the folks you deal with in Washington a little more difficult to deal with than before, even, give them a little rope. This will straighten up. It has been a very difficult six months.

Then, finally, in this cliff hanger, we come to the point where Pauline really is tied to the tracks and we have the FY 79 budget. At this point, I'll

simply give you as best I can a reading as to where it stands. This is the same as the President's budget for 1978, all the lines within just a few million dollars of what they were the year before.

As you know, Congress' reaction to that was fairly violent and at this point everybody is back examining what to do next. I kind of suspect that the President's speech tomorrow night may have something to do with that. It was given publicity as having to do with inflation, energy, and something else I can't remember. There was also an announcement today that he will be at SERI for Sun Day. The great activity within the Department of Energy has to do with possible initiatives in 1979. All this says to me that somebody in Washington has recognized that it's time for the President to take some action with regard to solar and certainly the visit to SERI on Sun Day is a major step in that direction.

There are activities having to do with modifications of the '79 budget within DOE. They are called initiatives and there have been more initiatives than Heinz has pickles, at least, and it hasn't settled down yet, at least it hadn't when I left this morning. So, all I can tell you is that there is great activity at DOE.

Secondly, there was great activity on the part of the Authorization Committees in the House and Senate and you all know the results. The dollar levels were raised, but that's just the Authorization Committee and that's play money. It doesn't reach anybody. The Appropriations Committees, of course, have to deal with this, so I wouldn't be all that optimistic about how it might go.

One other activity has to do with a request for a Domestic Policy Council review. It's really quite unusual for a subject like solar to wind up on the Domestic Policy Council agenda. Dr. Schlesinger has not yet signed the request. It came jointly from the Council of Environmental Quality in the White House and from DOE. Once it is signed by Dr. Schlesinger, and I and everybody else presume it will be, then a look at solar by that Policy Council will take place and it is scheduled to be completed in August.

So, it may very well be that Pauline is going to stay right there tied to the tracks with the train whistling until August. "Don't hold your breath," is the message I guess I would give you, but it only has one way to go and that's up. The budget won't go down from what the present request is.

The other thing that goes with this cliff hanger that leaves us all somewhat confused is the instruction by DOE, by Dr. Schlesinger in particular, to pay attention to 1985. This is one of those arbitrary decisions that gets made, but 1985 is a nice round number so it was picked as the target year for decreasing the importation of oil. As you look at the target date, it says that the first duty of DOE is to work at the ways in which we can substitute domestic oil for imported oil and get the level of import down to what he had agreed to in Europe.

That says, then, that there was a sudden switch from the position we were in. You may have noticed this as you tried to deal with people in Washington. There was a sudden switch in the summer of last year from the situation where we were pretty much told by OMB, I guess told specifically by OMB, that it was not appropriate for ERDA, as it was then, to work on projects that would produce before 1985, as that was the role of industry.

That has changed completely, 180 degrees; it is now the role of DOE to work on things that will produce before 1985, because that's the target. So, suddenly there's a switch from long-term to near-term. This is very healthy. You ought to change every now and again. Once you look at these things as opportunities, they aren't problems.

We were having great troubles, as Al hinted, with the Barstow project. You may have heard about a few of them. I gather you have a cartoon that reflects something of that but the thing that sold it was that we sneaked something called "repowering" down the side road and the 1985 initiative was just coming along and that made the opposition puzzled, at least long enough so we could pull ourselves together. At this point, the charge to us, would you believe, from OMB is to modify the Barstow project to aim it at repowering, and that's a radical turn. So we turned clear around in each of the areas. In photovoltaics we have laid on a near-term program, a very strong near-term program, which is getting all kinds of attention in Washington this week. OMB couldn't stomach it and yet the thing is already published and out, so it's a little difficult not to go ahead with it. In solar thermal, as I say, repowering is the mode of the day.

There are now two small OTECs located on islands, Hawaii and Puerto Rico being the two that are mentioned, but not restricted to them. That allows one to move OTEC into a near-term version. We believe we can have those operating in early

1982, which is about ten years before we had ever said anything about OTEC. One of the initiatives, I'm sure, will have to do with wind because people feel that wind is simple. Of course, it isn't, but that's all right.

The one we couldn't move forward was the solar power satellite so we transferred that to the Office of Research so we don't have to worry about it.

That's where we are now and it leads me to my very short message to you--since you have sessions this evening that make you not want to listen to anybody very long. I had thought to bring along, and then didn't, pieces from Chemical and Engineering News, one of the journals I see with regularity, having to do with the Chemical Society's meeting in Anaheim about a month ago. There was a page on solar which talked about the great acceleration in solar research and what it had to do with a series of developments by government laboratories. I think it is correct to say there wasn't a single thing that wasn't out of a government laboratory, or something just like it, where the thrust was not all from industry. I went through the magazine and found a whole series of developments, an amazing array of things in research, which are opening doors that you and I who work in research knew would open but which we forget about in the hue and cry as we go about our daily chores. It struck me as I looked at that and then looked at your agenda that I see the same kind of thing. I would simply cheer you on, as I have cheered on a number of groups that were pretty heavily on the research side. What we have done to this point is attempt to build--it's always difficult to see what you're trying to do, but for hindsight, you understand--a solar program by building hardware in the field. There's nothing like getting something out so the people can say, "There is something," and then to fund the next display. If you simply conduct research, they say, "More studies." So we've gone the route of putting in place hardware but have been using present knowledge, basically. However, we all know that the real leverage lies in what research will turn up, so as you look at the aspects of your subject matter here, I would urge you to pay attention to research.

We now have SERI in place, one of the four regional solar energy centers in place, and the other three working and all will be in place, I think, by the end of this fiscal year. That's a real lift on the research side of solar. I think what you'll see over the next couple of years, certainly if I go out that far I'm safe, will be the toning down of the hardware part of solar in the sense that we will be

bumping our heads against the economics with no way to really break that in many of the options. The way the economics problem can be broken will be by attention to research. You all know that in Washington we are shifting the proportion of funding fairly sharply in the research direction. We'll carry on the hardware simply because that's how you find what research will make things go but certainly there is a strong recognition that you won't get there without the research results. So I give you an indication of a change in direction in Washington, a shift to the near term in hardware coupled with a heavy emphasis on research as such.

With that I'll close. I'll be glad to take questions. Thank you very much.

Question - From what you say, can we interpret that to mean there's likely to be more research money available for universities, for instance?

Dr. Marvin - We're doing university research in particular, and I don't have to tell you who are connected with universities that we've had some trouble handling unsolicited proposals. We know that, so what we're doing is working with SERI to put the responsibility with them in a fashion which will be organized so it can run. Yes, I expect that the proportion of research money would increase quite sharply.

Question - Hank, can you say anything about the international aspect of solar energy? We obviously have cooperation with France, but can you say anything about how DOE views the international market for solar energy for American industries, things of this nature?

Dr. Marvin - I don't think DOE is of one mind on this subject. What we have done ourselves is attempt to kick this open by making the international matter a line item on the budget. That calls it out for attention. There are several things happening. There is, for example, the Nuclear Non-Proliferation Act, which calls its direct attention to solar in the dispersed mode in developing countries, not totally undeveloped but the developing countries. The first two countries that are being worked on from that point of view are Egypt and Turkey. Teams are in Egypt and Turkey now. They studied for a while here, got people from there and brought them up to date, and they are back now beginning to work. Certainly the cooperation with

the IEA will continue very strongly. Bilateral agreements continue to get attention. I guess the one thing we haven't been able to sort out ourselves is the lesser developed countries, the LDCs.

Question - What's going to be the role of the Office of Energy Research in the support of research projects for solar?

Dr. Marvin - The Office of Research has taken a position that it will, in the main, be a monitor of research conducted within DOE because that research is already on-going. On the other hand, there's no reservation about taking on things such as the solar power satellite. It's something that's just beginning, so this is a good place to have it located. I think in that sense I wouldn't expect to see very rapid change there, but I think you will see those folks having an impact by the way of watching over our shoulders and either cheering or criticizing. I hope some mix. Probably not supporting very much research directly.

Question - This is in regard to your comment about repowering and also aggregate types of hybrid devices. What interface is there in DOE between the fossil energy division and the solar division if you start getting into these applications where you're going to have a combination of both fuel sources?

Dr. Marvin - In the case of repowering, as we use the term, of course, it's a retrofit, so there isn't that cross over. The company that's putting the thing in provides that. The place I see the cross over is in biomass where the desire to make gaseous fuels or liquid fuels from biomass sources uses technology that's either the same or very close to that used in coal. In that case, what we have done is bring one program manager of the three out of the fossil program and into the biomass program. At this point, he still sees both. When his memory runs out, we'll have to do something else.

Chairman Hildebrandt - You indicated a tendency toward research in conservation and solar applications or the heating and cooling area that's going to applications. Will the record also have research in it?

Dr. Marvin - I will have to quote something anybody from industry will appreciate. This was a remark that was made to me by Dale Myers, who oversees both of these operations. He said, "It's always the same. You guys come in wanting to do all kinds of heavy projects in the field and the conservation and solar applications

people come in wanting to do all the research." I think that's always so, you always get that cross over. Their function is very much to take things from the point where you can see what the product is going to be in the field, what it's going to sell. We say when it's twice the cost, that is has to be to be really economically viable, and therefore it is accessible to incentives. As soon as it turns to incentives, it's their role to pick it up. I think you'll find they won't be doing very much research, as such, except in the solar heating and cooling area where we had arbitrarily moved the R&D with it. I personally feel that if you separated those two it would do neither one any good; that is, separating the R&D from the actual solar heating and cooling applications, so those two will continue to go side by side. I think that's the exception.

Question - There was a recent General Advisory Committee report on the operation of the Division of Solar Energy that criticized some of the emphases. Are you going to go along with the recommendations of that report or how do you feel the report will influence your future actions?

Dr. Marvin - There have been a sea of reports.

Same Questioner - I'm talking about this latest one.

Dr. Marvin - Yes, I know which one you're talking about; I was going to come to that. First, I was trying to see whether Paul Rappaport was here. You said you did put him on a plane? Then I can speak freely.

The report that is the best and the strongest and has the most impact is the report to Congress by their own committee, the GAC report. Of all the reports, that is the swinger. The CEQ (Council on Environmental Quality) report is relatively shallow. It expressed a brand new point of view as far as government circles were concerned. Therefore, it has caught attention, although it doesn't have to do with individual program details. The GAC report is an ERDA report and I have not heard anybody mention it. ERDA is dead and everybody is glad.

Chairman Hildebrandt - Thank you very much, Hank.

VIII. SESSION IV: MATERIALS

MAXIMAL OPERATING TEMPERATURES FOR METALLIC FILMS SUBJECT TO DETERIORATION BY AGGLOMERATION: A FIRST PRINCIPLES CALCULATION

Richard Zito
Department of Physics, University of Arizona
Tucson, AZ 85721

Abstract

Metallic films in selective surfaces are subject to sustained elevated temperatures resulting in their ultimate deterioration by agglomeration. Using the basic techniques of statistical mechanics, one can establish formulas for the maximal operating temperature, above which deterioration of a metallic film is quite rapid. These formulas are expressed in terms of "fundamental" quantities.

Introduction

The deterioration of metallic films by agglomeration is well known. At sufficiently high temperatures (but below the melting point) a silver film 1000Å thick is observed to break up into hemispherical beads approximately 1 μm in diameter.[1] This means that material was taken from an area (called the catchment area[2]) whose rectangular dimensions would be about 1.5 μm on an edge. The verticies of the polygon shaped catchment area are marked by holes (bare spots) left behind by the inhomogeneous placement of material during deposition.[3] In this paper all the films dealt with are 1000Å thick. It will also be assumed that the size of the "beads," and thus the catchment areas, are the same regardless of the material from which the film is made. Since this paper is primarily concerned with determining the temperature for which the useful lifetime of a film is short (about 1 hour), we will use a model involving a catastrophic failure. That is, the film will be considered stable, with an infinite lifetime, until a temperature is reached such that the average kinetic energy of atoms along the catchment perimeter exceeds a value E. At that temperature, and all higher temperatures, the lifetime of the film will be considered to be zero. When this critical temperature is reached a large number of bonds along the catchment perimeter will be weakened, thus allowing interior material to move with respect to exterior material and "bead up" via Landau surface tension effects in crystalline materials.[4] Crystal planes of the catchment material with small Miller indicies will grow at the expense of crystal planes with large indicies. In practice this means that the equilibrium shape of the catchment material will consist of a small number of plane areas joined by rounded regions instead of intersecting at sharp angles.[5] The result is the usual hemispherical "bead."

Calculations

Consider an atom on the perimeter of some catchment area. Let the number of nearest neighbors be CN, and the number of bonds that this atom extends to nearest neighbors on the interior of the catchment perimeter be BN. If the film material we are considering has a heat of fusion H_f (in joules per mole), then, in general, an atom on the catchment perimeter must have a kinetic energy of at least $E = H_f(BN)/(CN)N_o$ (where N_o is Avogadros number) in order to weaken the BN bonds connecting it to material inside the catchment area. Next, suppose that a certain critical fraction, K, of the N bonds along the perimeter of the catchment area must be weakened before agglomeration takes place. Hence, we must find a temperature, T, such that

$$K = \langle n \rangle / N = (4/\sqrt{\pi}) \int_X^\infty X^2 \exp(-X^2)\, d_X = (2/\sqrt{\pi}) X \exp(-X^2) + \operatorname{erfc}(X)$$

where $X = \sqrt{(E/kT)}$, k is Boltzmann's constant, and $\langle n \rangle$ is the average number of weakened bonds at temperature T. For a given value of K there will be a unique value of T. When a film is subject to this high temperature, damage will begin along lines of weakness connecting deposition defects.

In this calculation we have treated the bonds of atoms as discrete "stick-like" entities confined between an atom and its nearest neighbors. This kind of "tinker toy" approach is justified whenever the tight binding approximatibn (LCAO) adequately describes the finding of atoms in the lattice of the film. The transition metals derive a substantial amount of their cohesive energy from the coupling of unpaired d electrons between atoms.[6] The bonds created this way are quite strong and account for the high melting points of these materials. This is especially true of the refractory metals.[7] The coupling of d electrons is quite adequately described by the LCAO.[8] The elements Cu, Ag, and Au have filled d shells, but electrons may be easily promoted to a close lying sp orbital (for example from 3d to the 4sp orbital in Cu).[9] Hence coupling of unpaired d electrons still comprises an important part of the cohesive energy (just as in the other transition elements). Aluminum has no unpaired d electrons, but band structure calculations based on the tight binding approximation are in qualitative accord with the observed structure.[10] Hence, the underlying use of the LCAO approximation is justified for the materials considered in this report.

Results

Meinel has collected data on the maximum usable operating temperatures of films 1000Å thick and of various composition.[11] At the upper limit of the bar graphs on page 9,

the lifetime of the film was about one hour in vacuum. One piece of the data may be used to establish the value of K. Use the heat of fusion and agglomeration temperature of a reasonably stable material like rhodium. Rhodium is stable in the sense that the lifetime of the film is not drastically reduced by heating in air. Indeed Rh has the lowest oxidation rate of any of the refractory metals.[12] Thus oxygen impurities in the vacuum chamber during deposition will minimally affect the measured agglomeration temperature. Rh also makes a good standard for calculating K because of its highly refractory nature. Thus, the tight binding approximation is quite valid for this material. Rh films 1000Å thick are the standard for face centered cubic (fcc) materials in this work. The resulting value of K is 0.7783. We may now use this value of K for all other fcc materials. For body centered cubic (bcc) materials, molybdenum will be our standard, with K = 0.5732. Mo has quite a high oxidation rate, but the experimental data for this metal was more reliable than for the other bcc materials. Hence, Mo was chosen as a standard. Perhaps, in the future, when more and better data are available, another standard will prove more satisfactory for the bcc system. The fact that K is lower for the bcc materials is probably an indication of structural weakness due to lower coordination number. The predicted values of the temperatures that give a 1 hour lifetime with the above formulas are marked with an "x" in the graph (p. 9). The experimental values of the temperature for 1 hour lifetime are approximate and should be taken with an error of ±20% of the kelvin agglomeration temperatures.[13] The data for aluminum and chromium are particularly rough but should lie within the error bars of the true value.[14]

Discussion and Conclusion

In this paper a "strength of materials" approach has been adopted. This seems plausible when we consider that the forging temperature for the bulk material of the elements considered is roughly the agglomeration temperature (for 0.1 films in vacuum).[15,16,17,18] During forging a meter undergoes plastic deformation. This is especially true during extrusion where the deformation is so plastic that the process may be described by the laws of hydrodynamics.[19] This kind of flow is not unlike the surface tension driven flow we might see during agglomeration in a thin film. The temperature at which forging proceeds easily is usually sufficient to excite a large number of atoms into vibrating with an amplitude on the order of the interatomic distance. Such excited vibrational states lie about 0.05 ev above the ground state, which is of the order of magnitude of the value of E used in the calculations presented in this paper. These considerations lend confidence to our procedure for computing E and to the "strength of materials"

approach as a whole. At this point one should realize that little has been said about the nature of the substrate on which the film was deposited. Our film was operating at temperatures that were so high that the film was essentially plastic and expanded with the substrate. Hence, thermal mismatch and its concomitant effects were not a concern.

Meinel has pointed out that the temperature at which rapid agglomeration occurs roughly follows the melting point of a material.[20] This trend, however, is not absolute. For example, Mo agglomerates quickly at temperatures below those for rapid agglomeration of Rh films, in spite of the fact that Mo has a higher melting point than Rh. This reversal of trend can also be seen with Pt and Cr. Recall that the agglomeration temperature depended on the value of K, and that each lattice type had its own specific K. If we group elements according to their value of K (i.e., according to lattice type), then within each group we find that Meinel's melting point rule is strictly obeyed. Furthermore, within each group an increase in melting point is invariably accompanied by an increase in the heat of fusion, which, as our formulas show, results in an increased temperature of rapid agglomeration. Hence, the nature of the melting point rule is explained.

The data and computations associated with Ni and W deserve special attention. These materials show agglomeration temperatures far below the predicted values, with discrepancies of 35% and 27% (of the experimentally measured kelvin temperature of agglomeration), respectively. The similarity in the magniture of these errors may imply that similar effects are involved. It is well known that bcc α-Ni makes a transition to fcc β-Ni at 625°K.[21] Perhaps, during this transition a sufficient amount of material is moved around in the film to result in the beginning of agglomeration damage. Tungsten exhibits a related phenomenon. At 21°C, tungsten exists as a mixture of 99.9% bcc α-W coexisting with the unstable simple cubic β-W structure.[22,23] As the temperature increases the relative proportions of the α and β phases may change. The net result is a transport of material with possible agglomeration damage. It should be noted that Cr also undergoes a crystalline phase transition, but this occurs at a temperature above the predicted agglomeration temperature,[24] and thus does not appear to affect the fit to experimental data. If these ideas are correct, perhaps the introduction of some impurity into films of Ni and W might "pin down" the crystal structure and allow these materials to reach their full thermal potential.

Finally, it is important to note that a film may agglomerate more quickly when exposed to sunlight than when heated in an oven. Recall that a certain threshold amount of energy, $H_f/N_o(CN)$, has to be supplied to each bond on the catchment perimeter during agglomeration. This energy was supplied vibrationally. But, when an optical photon pre-excited a bond (by being absorbed by an electron) less vibrational energy is needed to reach the threshold. Hence, failure is premature. Truly accurate data on film lifetimes can probably only be obtained by actual exposure of films at the Solar Thermal Test Facility.

Appendix

A crude, but useful, theory of maximal operating temperatures may be constructed which has no adjustable parameters. The starting point for such a theory is the Kosterlitz-Thouless-Feynman (KTF) theory of two-dimensional melting.[25] This theory was constructed to describe the melting of a rigid monolayer of adsorbed atoms ("ad-atoms") on a surface. Presland, Price and Trimm[26] (PPT) suggest that failure by agglomeration takes place along grain boundaries roughly aligned with the catchment perimeter. A grain boundary may be considered an adsorbed two-dimentional lattice forming a kind of monolayer over the surface of a well crystalized grain. This is because grain boundaries are often 1 or 2 atoms thick.[27] Furthermore, atoms on the grain boundary show some amount of crystalline disorganization with respect to atoms within a single grain, thus making the boundary somewhat distinct and allowing it to be described as an "adsorbed layer." More fundamentally, atoms along the boundary have a higher energy than those within the grain, thus making them energetically, as well as organizationally, distinct. Hence, we might try to predict agglomeration temperatures of films by applying the theory of two-dimensional melting to grain boundaries. The KTF theory predicts the 2-D melting temperature, $T_{M(2D)}$, as[28]

$$T_{M(2D)} = \frac{1}{(2\pi)^2} \frac{mkr^2 \theta^2}{8 \hbar^2}$$

where "k" is Boltzmann's constant, "m" is the mass of atoms in the film, "r" is the atomic radius as computed from the average volume per atom on the boundary, θ is the Debye temperature,[29] and $\hbar$ has its usual quantum mechanical meaning. This formula is in qualitative accord with the experimental maximal agglomeration temperature in the bar graph. Hence, the idea of PPT that agglomeration damage occurs along grain boundaries seems to have theoretical support. If damage does indeed progress along

grain boundaries, then more durable selective surfaces might be constructed from metal films with a larger grain structure. The reduction in the amount of grain boundary material may then result in a decreased probability of initiation and propagation of boundary damage.

Meinel has pointed out that the ratio of the agglomeration temperature to the melting point is about 1/2.[30] This becomes quite clear when one considers the Lindemann melting formula.[31] This formula gives the melting temperature of bulk material as

$$T_{M(3D)} = X^2 \frac{mkr^2 \theta^2}{9 \hbar^2}$$

where X is a number which seems to range between 0.2 and 0.25 for most materials. Putting X = 0.25 in the last formula shows that $T_{M(2D)}/T_{M(3D)} \approx 1/2$. Hence, Meinel's second rule is explained.

Acknowledgement

The author would like to thank Dr. Aden B. Meinel of the Department of Optical Sciences, University of Arizona, and Dr. Richard Young of the Department of Physics, University of Arizona, for their valuable discussions during the work.

References

1) A. E. B. Presland, G. L. Price and D. L. Trimm, Surface Science, 29, 435 (1972).
2) Ibid.
3) Ibid.
4) L. D. Landau and E. M. Lifshitz, Statistical Physics, (Addison-Wesley, Reading, MA, 1969), pp. 458-460.
5) Ibid.
6) I. Campbell and E. Sherwood, High Temperature Materials and Technology, (John Wiley, New York, 1967), pp. 152-154.
7) Ibid.
8) C. Kittel, Introduction to Solid State Physics, 5th ed., (John Wiley, New York, 1967), p. 262.
9) L. D. Landau and E. M. Lifshitz, Quantum Mechanics, (Pergamon Press, New York, 1965), p. 291.
10) Z. Matyas, Phil. Mag., 39, 429 (1948).
11) A. B. Meinel and M. P. Meinel, Applied Solar Energy, (Addison Wesley, Reading, MA, 1977), p. 270. Also see reference 1 and Presland, Price, Trimm, Surface Science, 29, 424 (1972). Additional information can be found in a paper by E. N. C. Andrade, The Structure of Metallic Coatings, Trans. Faraday Soc., 31, 1137 (1935). In short, agglomeration will be severe whenever the atomic mobility, of atoms in the metal film, is high.
12) See reference 6, p. 159.
13) Private communications, A. B. Meinel.
14) Aluminum films are known to be stable in air up to about 250°C. If the improvement in performance when heated in vacuum follows the trend set by other elements, we can expect Al films to be stable up to 675°K (see reference 11, p. 268 and 270). The data for chromium is inferred from the performance of "Black Chrome" selective surfaces (see reference 11, p. 313 of Applied Solar Energy).
15) Clauser, Fabian, Peckner, Riley, The Encyclopedia of Engineering Materials and Processes, (Reinhold Pub. Corp., New York, 1967), pp. 285-288.
16) Campbell and Sherwood, High Temperature Materials and Technology, (John Wiley, New York, 1967), pp. 166-167.
17) Baumeister and Marks, Standard Handbook for Mechanical Engineers, 7th ed., (McGraw Hill, New York, 1967), p. 6-80.
18) Taylor Lyman, Metals Handbook, (American Society for Metals, Philadelphia, 1964).

19) See reference 17, p. 13-31.
20) See reference 11.
21) Weast, Handbook of Chemistry and Physics, (Chemical Rubber Co., Cleveland, 1967), p. D-33.
22) A. Taylor, An Introduction to X-Ray Metallography, (John Wiley, New York, 1949), p. 386.
23) A. Taylor, X-Ray Metallography, (John Wiley, New York, 1961), p. 973.
24) Ibid, p. 964.
25) J. G. Dash, Films on Solid Surfaces, (Academic Press, New York, 1975), pp. 180-183.
26) See reference 1.
27) L. H. Van Vlack, Elements of Materials Science, second ed. (Addison-Wesley, Reading, MA, 1964), p. 95.
28) This is a correct statement of the KTF formula which appears incorrectly in several plates in the literature by a factor of "r".
29) When θ is the 3-D Debye temperature, then "r" is a radius, as we have said. However, if θ is the 2-D Debye temperature (as in the original work of KTF), then "r" becomes the inter-atomic distance.
30) See reference 11.
31) J. M. Ziman, Principles of The Theory of Solids, (Cambridge University Press, London, 1964), p. 63.

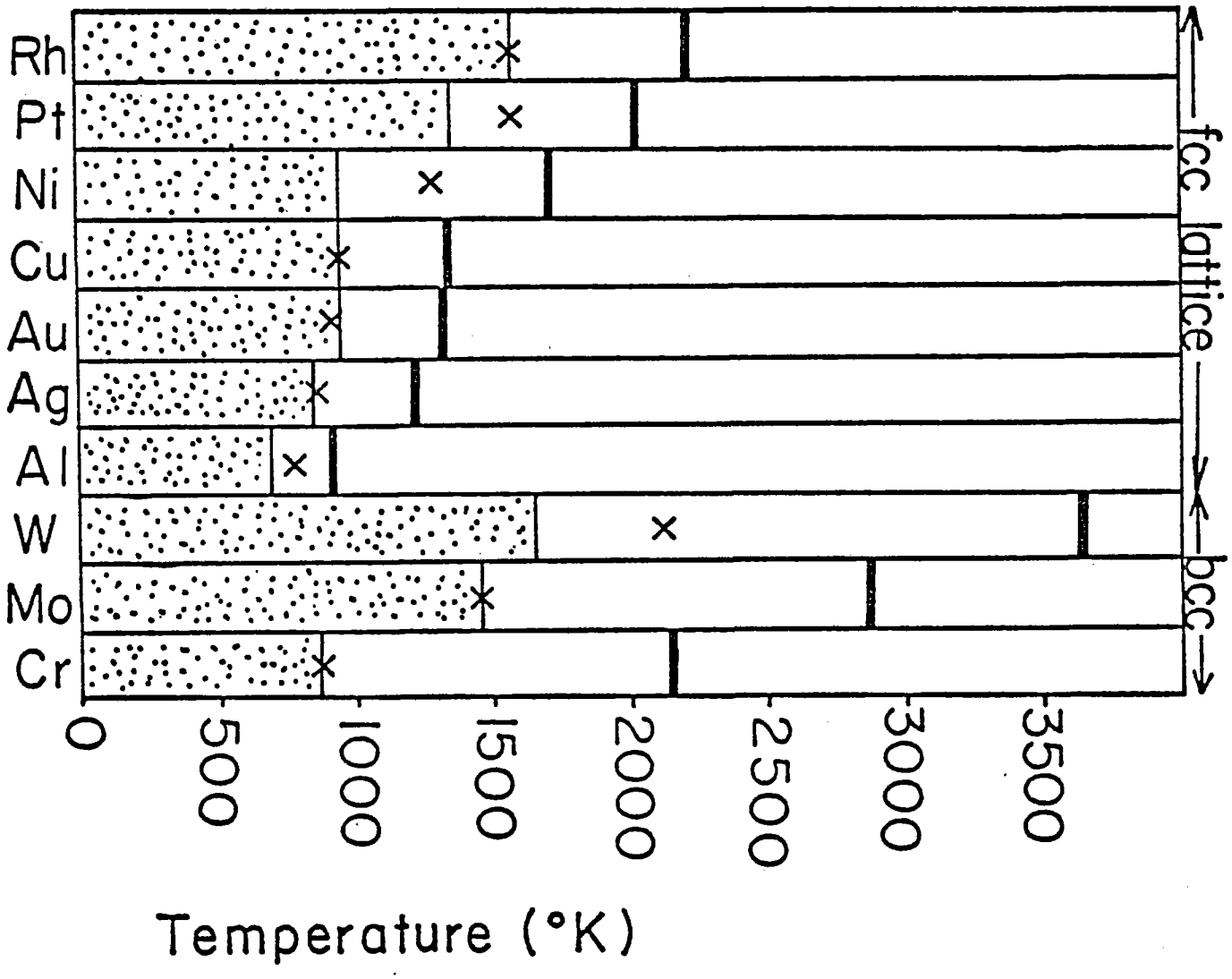

The top of the bars show the experimental temperature of one hour lifetime for films (1000Å thick) subject to deterioration by agglomeration. The crosses mark the theoretically predicted values. Both the theoretical and experimental values apply to laboratory vacuum conditions. The heavy lines indicate melting points.

ABSORBER COATINGS FOR SOLAR APPLICATIONS

Dr. Patrick Call

Solar Energy Research Institute
Golden, Colorado

Abstract

High solar absorptance is an essential property of receivers for viable solar systems at all temperatures. In addition, many applications benefit from the suppression of thermal emittance at the receiver and consequently selective absorbing surfaces have been the subject of research and development activities for 25 years. Recent analysis by the Jet Propulsion Laboratory which quantifies the value of selectivity in a number of applications will be reported and the candidate optical materials for these applications will be summarized.

The combination of high photon flux, high temperatures and environmental conditions that absorbing surfaces of concentrating systems are exposed to raises questions concerning the stability of the surface optical properties. Opportunities for important research in photochemistry and associated photon degradation mechanisms will be presented.

NOTE: This paper was not available for inclusion in the Proceedings; therefore, we are reprinting the abstract.

HIGH-TEMPERATURE MATERIAL TESTING

L. K. Matthews
Sandia Laboratories
Albuquerque, NM 87185

G. P. Mulholland
New Mexico State University
Las Cruces, NM 88003

Abstract

Six lightweight high-temperature insulating materials and three refractory firebricks were tested at the White Sands Solar Furnace to determine their ability to withstand high-intensity solar flux densities. The insulating materials were subjected to a 10-cm diameter beam.

The materials were tested at flux densities up to 2.75 MW/m^2 or until failure. Most materials failed before this limit occurred; the exceptions were a zirconia board and an alumina firebrick. The board withstood a 2.75 MW/m^2 flux density for three minutes without failure while the firebrick was adequate to 2.6 MW/m^2.

Nomenclature

k	thermal conductivity, cal/sec-cm°K
MW	megawatt
m	meter
q	heat flux, MW/m^2
ε	emissivity, dimensionless
ΔT	temperature difference between front and back surface

Introduction

The 5-MW_t Solar Thermal Test Facility (STTF), operated by Sandia Laboratories in Albuquerque, New Mexico, for the Department of Energy, is a high-solar-power-per-unit area concentrator utilizing the power tower concept.

During operation of this facility, several problems could arise from concentrated solar energy impinging on materials in and on the 60.96-m tall concrete tower. It became necessary to evaluate several high-temperature materials in severe solar environments to

determine their usability at the STTF. These materials have little available data on use with the solar spectrum. At high concentrations of solar energy, essentially no data has been taken.

The purpose of this study was to evaluate performance characteristics of several high-temperature insulating materials and different types of refractory firebrick. Testing was done at the White Sands Missile Range, New Mexico. The materials were tested at flux density levels up to 2.75 MW/m^2 or until failure. Most materials failed well before this limit; the exceptions were a zirconia board and an alumina firebrick. The zirconia board withstood a 2.75 MW/m^2 flux density for three minutes without failure while firebrick was adequate up to 2.5 MW/m^2. At large flux densities, some of the insulating materials exhibited characteristics similar to those observed in hot glass [1,2,3]. That is, the heat flux through the medium appeared to be greater than would occur by conduction. Surface temperature measurements were made on the front (hot) and back surfaces and surface emissivity values were approximated by means of an optical pyrometer.

The information gathered from this study is being used to design thermal protection for personnel and equipment positioned in the STTF tower plus protection for the tower itself.

Experimental Facility

The White Sands Solar Facility (WSSF) is a focusing-type solar facility consisting of a heliostat, attenuator, concentrator and control chamber [4]. This facility was originally constructed in 1958 and operated by the Quartermaster Research and Engineering Center at Natick, Massachusetts [5]. The facility was moved to White Sands Missile Range in 1973, Figure 1.

The heliostat consists of 356 flat plate mirrors, 0.6 meter by 0.6 meter mounted on a steel frame 12.2 meters wide and 11 meters high. By automatically tracking the sun, the concentrated focal image can be located in a fixed position for testing.

The concentrator has 180 spherical mirrors, 0.6 meter by 0.6 meter, mounted on a steel frame 9.1 meters by 9.1 meters. This component is located 29.3 meters south of the heliostat. Each mirror is individually positioned to concentrate the energy at the focal plane, 11 meters away.

The attenuator is a louvered structure whose blades can be positioned to regulate the amount of energy reaching the concentrator. The test and control chamber is 2.4 meters

in cross section presented to the reflected beam and is 4.8 meters long. This chamber contains the experimental test area and controls for both facility operation and the shutter systems which modulate the energy.

The maximum available flux level at the focal plane is 90 cal/cm^2-sec (3.77 MW/m^2) with a total useable power of 30 KW - thermal [1]. Flux levels approaching 107 cal/cm-sec (4.5 MW/m^2) have been obtained during certain times of the year under ideal conditions; these levels are unusual, so the 90 cal/cm-sec value is quoted since it can be attained during most of the year. Maximum flux levels with a uniformity of 10% are obtained over an exposure diameter of 5 cm, Figure 2. The basic flux is a skewed Gaussian distribution with the 50% flux density points occurring at a 5-cm radius from the center of the solar image.

A more complete description of this facility is given by Davies and Cotton [5] and Bliss [6]. These papers discuss the design [5] of the original facility and the expected performance [6] for this type of facility.

Material Testing

Six lightweight, high-temperature insulating materials and three refractory firebricks were tested in the White Sands Solar Furnace to determine their ability to withstand high-intensity solar flux densities. The insulating materials were subjected to a beam approximately 2.5 cm in diameter; this beam size was obtained by placing a 5-cm thick water-cooled aluminum plate with a 5-cm diameter hole approximately 5 cm in front of the focal plane, Figure 2. Based on visual observations of test specimens which melted, the flux density levels at the focal plane appeared to be similar to Figure 3, with the maximum flux density occurring over an exposure diameter of 2.5 cm. The firebricks were placed in the focal plane of the furnace and were subjected to a beam similar to that described in the previous section.

Intensity levels were obtained by placing a calorimeter in the focal plane and then opening the attenuator until the desired level was reached. The maximum levels obtained during the tests (July and August) were approximately 3 MW/m^2, although levels approaching 4.5 MW/m^2 have been obtained at this facility during certain times of the year under ideal conditions.

The materials tested along with a brief description are listed in Table 1. To facilitate the discussion an abbreviation will be used for each material.

TABLE 1

Description of Material Tested

Abbreviation	Melting Temperature (°C)	Description
MA1		A common alumina-silica board with a recommended use limit of 1260°C
MA2	1871	A 75% alumina-19% silica board with a recommended use limit 1650°C
MA3	>1871	An 85% alumina-15% silica board with a recommended use limit of 1500°C
MA4	>1871	A board with an alumina content in excess of 90%. The use limit is unknown
MZ1	2204	A yttria stablized board consisting of 87% zirconia
MZ2	2593	A yttria stabilized board composed of 100% zirconia
B1	1843	An insulating firebrick composed of 76% alumina and 21% silica
B2	1916	A refractory firebrick composed of 90% alumina and 10% silica
B3	2016	A refractory firebrick composed of 99.7% alumina

Material MA1 had two chromel-alumel thermocouples, one shielded and the other bare, inserted into the material approximately equidistant between the front and back surfaces. The material was subjected to a flux density of 0.25 MW/m^2 until steady-state was reached, Figure 4. A 34% difference was observed between the two thermocouples which illustrates that energy in this particular wavelength band (solar spectrum) is transported through these materials by both conduction and radiation even at these low levels. This large difference indicated that shielded thermocouples should be used for all temperature measurements.

A 1.9-cm thick and a 3.8-cm thick piece of MA2 were subjected to flux levels of 0.5 and 1.0 MW/m^2. This material performed very well at the lower flux density but at the higher flux density both pieces lasted less than one minute. At 40 seconds the beam melted a hole approximately halfway through the 1.9-cm specimen and at 55 seconds for the 3.8-cm

specimen. The tests were terminated at these points for safety reasons. Figures 5 and 6 show the back-surface temperatures during the tests. The thin piece had a steady-state temperature of 198°C while the thick piece read 130°C at the lower flux density.

The point of failure indicates the time at which the tests were terminated. The excellent insulating characteristics of this material are apparent when one observes that the back-surface temperature for both thicknesses is less than 100°C with the front surface melting at 1871°C, see Table 1. A 1.9-cm thick piece of this material was subjected to 0.3 MW/m^2 for two hours and to 0.6 MW/m^2 for one hour, Figure 7. The back surface temperature was 40°C for the lower density and 56°C for the higher flux density. A slight discoloration occurred on the front surface but the material performed very well at these levels.

The back-surface temperature of MA4 is shown in Figure 8. This material is a high alumina content board with a melting temperature in excess of 1871°C. It performed well up to 1.5 MW/m^2. At that level, the front surface started to sublime and formed a hole approximately halfway through the material; the test at this level was terminated after 90 seconds. For similar flux levels, the back-surface temperature of this material was comparable with MA2; this indicates both materials have similar protection capabilities.

Figures 9 and 10 show the back-surface temperatures of MZ1 and MZ2. The first material performed well up to 1.5 MW/m^2. At 2.0 MW/m^2, a portion of the front surface which had cracked during the previous run fell and the beam started to pass through the material. The test was terminated at this time, which was 20 seconds after initiation.

Material MZ2, which is almost 100% zirconium, performed well up to 2.5 MW/m^2. This run is not shown in Figure 7 because the thermocouple became detached from the surface and gave erroneous readings. The material withstood the 2.5 MW/m^2 level for four minutes and lasted approximately 15 seconds at 2.75 MW/m^2. The run had to be terminated at this point because the beam had almost penetrated the material.

A comparison of the back-surface temperatures for various materials at three different flux levels is given in Table 2. All the materials exhibit comparable insulating characteristics. The decision as to which material to use should be based primarily on the flux density level the material will see and, secondly, on cost. Material MA 2 is the

least expensive and can be safely used for flux density levels up to 0.6 MW/m^2*; MZ2 is the most expensive, but a 1.3-cm thick piece will offer protection for at least 150 seconds at 2.75 MW/m^2. These limits are based solely on our tests and further testing will undoubtedly enable us to refine them.

TABLE 2

Comparison of Back Surface

Flux Level MW/m^2	Material (Thickness) (cm)	Back-Surface Temperature (°C)
0.5	MA2 (1.9)	197
	MA4 (1.3)	242
	MZ1 (1.3)	216
	MZ2 (1.3)	
0.75	MA4 (1.3)	302
	MZ1 (1.3)	
	MZ2 (1.3)	331
1.0	MA4 (1.3)	
	MZ1 (1.3)	400
	MZ2 (1.3)	366

The three standard size firebricks were tested at levels of 0.5 MW/m^2, 1 MW/m^2, etc., until the sample failed. The purpose of these tests was to obtain a qualitative estimate of the protection these bricks could offer under high-flux density conditions. No attempt was made to obtain temperature profiles.

Brick B1 is a lightweight insulating firebrick (ρ = 6.4 gm/cm^3) with good insulating properties ($k \approx 1$ W/m-c). Significant melting occurred at 1.5 MW/m^2. A 2.5-cm depression existed after two minutes of exposure at this level. No spallation of the front surface was observed during the test and the back surface was cool enough to hold one's hand within 15 cm of the back surface immediately after the test was concluded.

Bricks B2 and B3 are heavy-duty firebrick with densities approximately 2.5 times and thermal conductivities approximately 3.5 times that of B1. B2 was able to withstand 2 MW/m^2 for five minutes. The brick began melting after 2.5 minutes and a 1.3-cm

*This level could be higher. We have no data between 0.6 and 1 MW/m^2.

depression was observed after the test was concluded. The back surface was cool enough to touch and a hand could be comfortably held within 20 cm of the front surface immediately after the test was concluded.

Brick B3 did not start melting until 3.5 minutes of exposure at 2.5 MW/m^2. The material did not crack and retained surface integrity throughout the test. Immediately after the test was concluded, a hand could be held comfortably within 2 cm of the back surface and within 15 cm of the front surface.

Surface Properties

An approximate value of the surface emissivity of MA3 was obtained by mounting a shielded thermocouple on the front surface and comparing its reading with that of an optical pyrometer. Values for the other materials were obtained by taking optical pyrometer readings just before the surface started melting and using the manufacturer's recommendations for melting temperature. The reader should be cautioned that values for emissivity obtained in this manner are rough approximations and should be treated as such. Further tests are being planned which will give much better results than those reported here, Table 3. A system similar to the one used by Noguchi and Kozuka [7, 8] will probably be utilized.

TABLE 3

Approximate Valves of Surface Emissivity

Material	Temperature (°C)	Emissivity
MA3	620	0.3
	980	0.2
	1315	0.1
MA2	1650	0.1
MZ1	2200	0.4
MZ2	2600	0.3

Conclusions

Based on the results of these tests at the White Sands Solar Furnace, the following conclusions were reached:

1. Thermocouples should be shielded when they are used to measure temperatures of lightweight, high-temperature insulating materials subjected to concentrated solar radiation.

2. For flux levels less than 0.6 MW/m^2, a material such as MA2 can be safely used. This material can probably withstand flux densities greater than 0.6 MW/m^2 but less than 1 MW/m^2. Additional testing will be done in the near future to better define the limitations of this material.

3. For flux density levels greater than 1 MW/m^2, materials like MA4, MZ1 or MZ2 should be used. MA4 can be safely used up to 1.5 MW/m^2 but less than 2 MW/m^2. MZ2 withstood a flux density of 2.75 MW/m^2 for 150 seconds. MA4 is about three times more expensive than MA2 while MZ1 and MZ2 are about 8.5 times more expensive than MA2.

4. Firebricks are very good protection materials. The lightweight brick (B1) can be safely used for flux densities up to 1.5 MW/m^2 as long as the exposure time is less than two minutes. For larger flux densities the heavy-duty firebrick should be used. Brick B3 can be safely used for flux densities up to 2.5 MW/m^2 providing the exposure time is less than 3.5 minutes. These bricks performed very well and should be given serious consideration as a protection material for large solar flux applications.

Further tests are contemplated in the WSSF to try and gain a better understanding of the conduction-radiation transfer mechanism which occurs in these materials, to obtain realistic surface property measurements and to determine better upper limits for the less expensive materials such as MA1 and MA2.

Acknowledgements

The authors would like to thank Carborundum Corporation, Babcock and Wilcox, and Zircar Products for providing the test materials. Also Sandia Laboratories and the Department of Energy who provided financial support for this project.

References

1. Kellett, B. S. "Transmission of Radiation Through Glass in Tank Furnaces," Journal of the Society of Glass Technology, Vol. 36, pp. 115-123 (1952).

2. Gordon, R., "The Emissivity of Transparent Materials," Journal of the American Ceramic Society, Vol. 39, No. 8, pp. 278-287 (1956).

3. Condon, E. V., "Radiative Transport in Hot Glass," J. Quant. Spectrosc. Radiat. Transfer, Vol. 8, pp. 369-385 (1968).

4. Experimenters Guide, - White Sands Solar Facility, Nuclear Weapon Effects Branch, Army Material Test and Evaluation, White Sands Missile Range, New Mexico (1977).

5. Davies, J. M. and Cotton, E. S., "Design of the Quartermaster Solar Furnace," Solar Energy, Vol. 1, Nos. 2, 3, April-July 1957.

6. Bliss, R. W., "Notes on Performance Design of Parabolic Solar Furnaces," Solar Energy, Vol. 1, No. 1, January 1957.

7. Noguchi, T. and Kozuka, T., "Temperature and Emissivity Measurement at 0.65μ with a Solar Furnace," Solar Energy, Vol. 10, No. 3, pp. 125-131 (1966).

8. Yamada, T. and Noguchi, T., "Digital Pyrometry in a Solar Furnace," Solar Energy, Vol. 18, pp. 533-539 (1976).

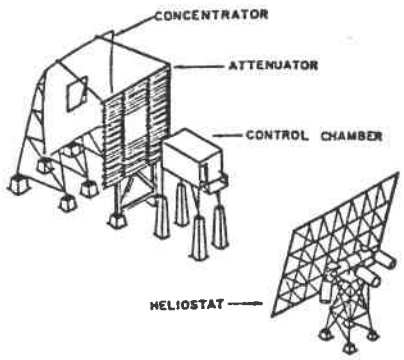

FIG. 1 SCHEMATIC OF WSSF

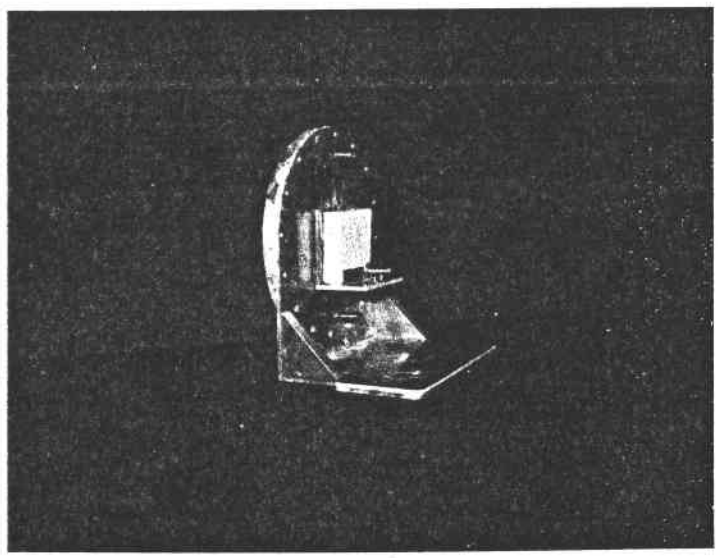

FIG. 2 WATER COOLED STOP WITH TEST MATERIAL IN PLACE

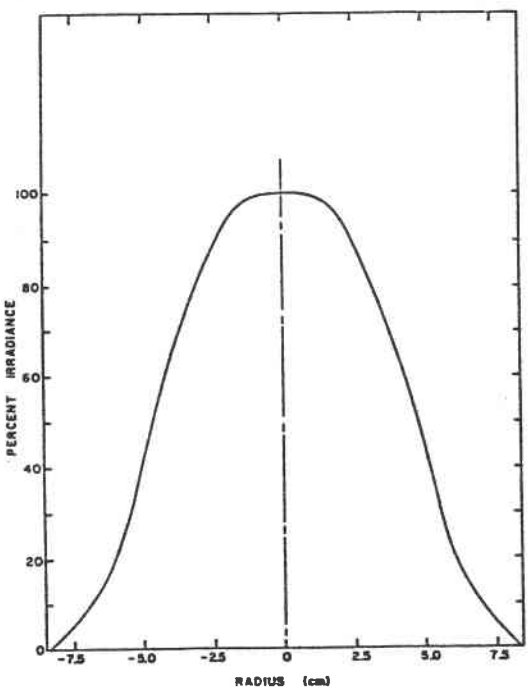

FIG. 3 IRRADIANCE PROFILE AT FOCAL PLANE

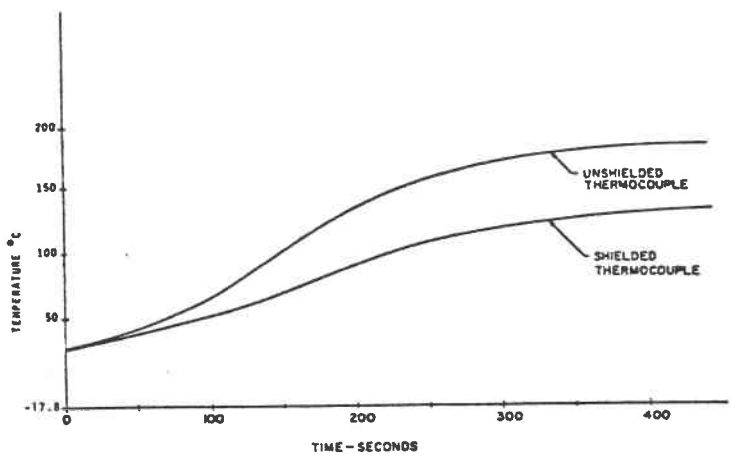

FIG. 4 DIFFERENCE BETWEEN SHIELDED AND UNSHIELDED THERMOCOUPLE READING
FLUX LEVEL WAS 0.25 MW/M^2

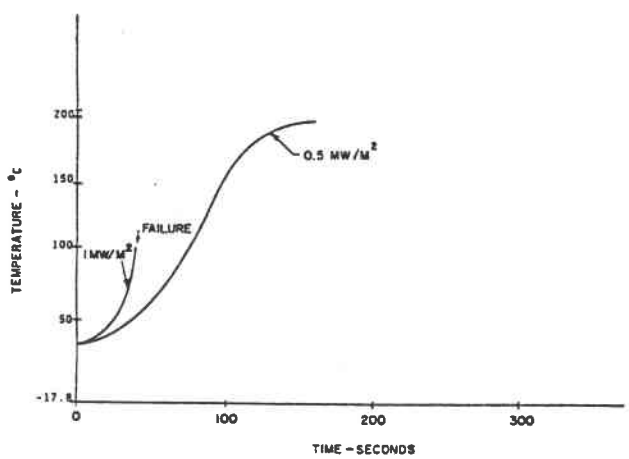

FIG. 5 BACK SURFACE TEMPERATURE OF MA2 - 0.75 INCHES THICK

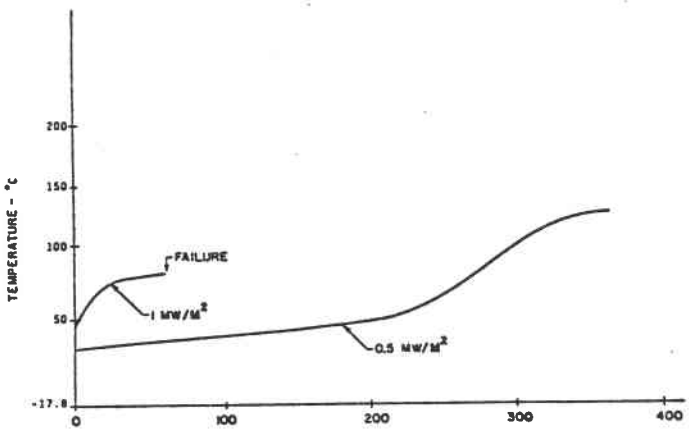

FIG. 6 BACK SURFACE TEMPERATURE OF MA2 - 1.5 INCHES THICK

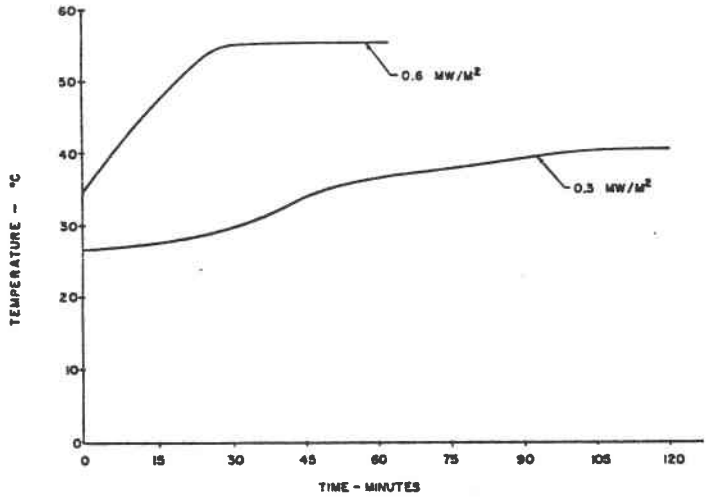

FIG. 7 BACK SURFACE TEMPERATURE OF MA-2 - 0.75 INCHES THICK

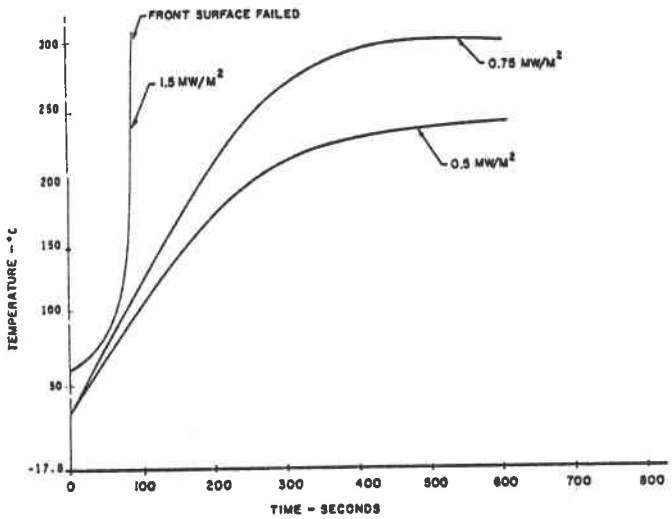

FIG. 8 BACK SURFACE TEMPERATURE OF MA-4 - 0.5 INCH THICK

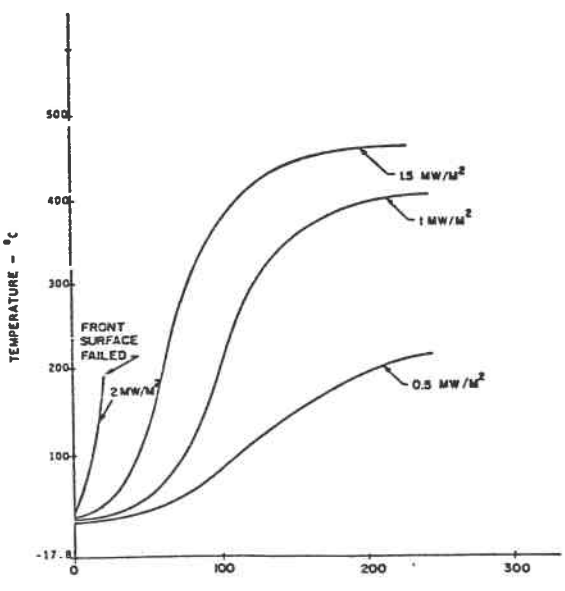

FIG. 9 BACK SURFACE TEMPERATURE OF MZI-0.5 INCH THICK

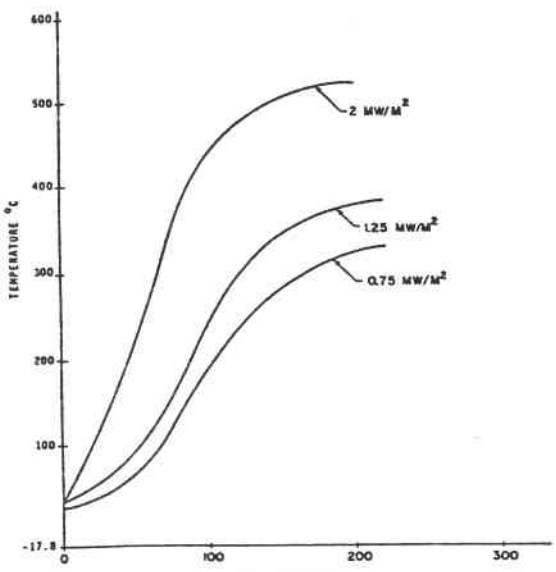

FIG. 10 BACK SURFACE TEMPERATURE OF MZ2 -0.5 INCH THICK

HIGH TEMPERATURE SOLID-SOLID REACTIONS: CEMENT

Dr. George P. Mulholland
Dr. Donald B. Wilson

New Mexico State University

Abstract

Cement is a major mineral in the world economy. As of September 1976 it is estimated that each US citizen requires 640 pounds of cement per year. By the year 2000 this value will be 1600 pounds per year. Cement production, however, is very energy-intensive, requiring 3800 Btu's per pound for manufacture (dry process). Currently 53% of the energy for all wet processing operations and 40% for all dry processing operations is supplied by natural gas or refined hydrocarbons. (In addition, both processes use 16% purchased electricity.) The remainder is supplied by coal. Coal will be the single energy source to meet the increased demand to the year 2000. Research needs exist for both the use of coal-fired kiln and the reduction of total energy consumption. The basic research requirement is for the kinetics of the cement production reactions. The Solar Thermal Test Facility furnace at White Sands provides the unique experiment system for significantly investigating the kinetics of reactions for cement manufacturing. The primary reaction occurs as a solid-solid reaction enhanced by sintering of appropriate additives. Cement properties are critically affected by the extent of this solid-solid reaction and the composition of the feed. Particle size is an important variable. The Solar Thermal Test Facility solar furnace provides a controlled temperature environment (ranges of 1200-2000^{o}C) and gas environment (oxidizing or reducing) corresponding to the actual industrial kiln. The specified Tracor TN-1710 DARASS System provides the necessary instrumentation for in-situ analysis of the cement reactions in the solar furnace facility.

NOTE: This paper was not available for inclusion in the Proceedings; therefore, we are reprinting the abstract.

DEGRADATION OF CONCRETE CAUSED BY CONCENTRATED SOLAR RADIATION

Dr. George P. Mulholland

New Mexico State University

Abstract

This investigation proposes to study the change of the compressive strength of concrete resulting from exposure to high levels of solar flux for various periods of time. The test specimens will be small concrete cylinders which will be exposed to solar flux in a circular surface band by rotating the specimen while a stationary solar beam impinges on the surface. After exposure, the specimens will be tested in compression. Flux density and exposure time are the controlled variables.

NOTE: This paper was not available for inclusion in the Proceedings; therefore, we are reprinting the abstract.

Y/DA-7748

Preprint

STABLE HIGH-TEMPERATURE SOLAR ABSORBING COATINGS

J. M. Schreyer

This Preprint was Prepared for Submission to

To be presented at Solar Thermal Test Facility Users Association Meeting, April 11-12, 1978, at Solar Energy Research Institute, Golden, Colorado

prepared for the U.S. DEPARTMENT OF ENERGY
under U.S. GOVERNMENT Contract W.7405 eng 26

March 6, 1978

STABLE HIGH-TEMPERATURE SOLAR ABSORBING COATINGS

INTRODUCTION

The development of cost-effective and efficient high-temperature coatings is basic to the application of solar energy to the solution of the national energy problem. Much of the work toward this goal has been concentrated on coatings utilizing silicates and special silicone vehicles which exhibit good ultraviolet radiation damage resistance at moderate temperatures, but few data are available at high temperatures. Performance of other inorganic coatings such as zinc oxide and stannic oxide have been extensively studied for stability against thermal shock, ultraviolet exposure, abrasions, and fatigue, but there is again little data available on the influence of high temperatures on the coating's optical properties.

High solar intensity can have a detrimental effect on the optical properties of coatings. Particle structural changes from sintering and crystal growth can be a significant factor which can result in erosion of the optical properties through changes in the surface morphology.

Plasma spray coatings of oxides, borides, carbides, beryllides, and metals can be expected to retain their integrity at high temperatures. These coatings are applied with a very high temperature arc and there is essentially no limit to the melting point of the materials which may be applied to the metal surface.

Since these materials have already been exposed to a high temperature arc at their melting points, changes in the surface morphology should not occur at high solar fluxes.

PRELIMINARY INVESTIGATION

Comparative solar absorption tests were carried out by exposing four-inch square, plasma-spray coated samples directly to the sun. The back sides of the plates were insulated and temperature measurements were obtained with thermistors and a digital recorder. A photograph of the experimental setup is shown in Slide 1.

The data on the plate temperatures on August 25, 1977, are shown in Slide 2. The average temperature differential for the plasma spray coatings was 90% of the temperature differential of the standard black-chrome coatings. It should

be pointed out that no quantitative control or investigation was made of the plasma coating parameters such as coating thickness, particle size, or uniformity. The temperatures at which these coatings were applied ranged from 1565°F (∿850°C) to 3880°F (∿2140°C). Data collected on other days during August 1977 gave comparable results.

Slide 3 shows a scanning electron micrograph (SEM) electroplated chrome-black standard used in this study.

Slide 4 shows an SEM of a plasma spray coating of hafnium diboride-titanium dioxide, and Slide 5 shows an SEM of a plasma spray coating of aluminum-carbon-silicate. These coatings demonstrate the versatility of the plasma-spray technology. Multilayer coatings with controlled microstructure can be applied to the metal surface to combine the best properties of the absorbing materials.

The very many variations which are possible with plasma sprayed coatings appear to justify more effort in this area.

SUGGESTED RESEARCH

The following program of study is needed to establish goals for future research.

1. Preparation of selected plasma-spray coatings on aluminum, copper, and steel.
2. Characterization of selected coatings physically and optically.
3. Exposure at selected solar flux in Solar Thermal Test Facility.
4. Characterization after Solar Tower test to establish changes in coating properties.

It is hoped that this preliminary program will create interest in a more detailed study in future years.

LONG RANGE RESEARCH

Based on the results of the preliminary study, the following research program is suggested.

1. Optimization of coating parameters in order to obtain the best optical properties.
2. Measurements of solar absorptance and infrared emittance to aid in the property optimization.

3. Cycling high temperature studies to establish changes in morphology.
4. Characterization of the final selected coatings.
5. Exposure to solar fluxes in Solar Thermal Test Facility.
6. Characterization of STTF tested specimens to establish any changes in coating properties.

It is expected that these proposed development programs will result in a series of improved-stable high temperature coatings which can be reduced quickly to commercial practice.

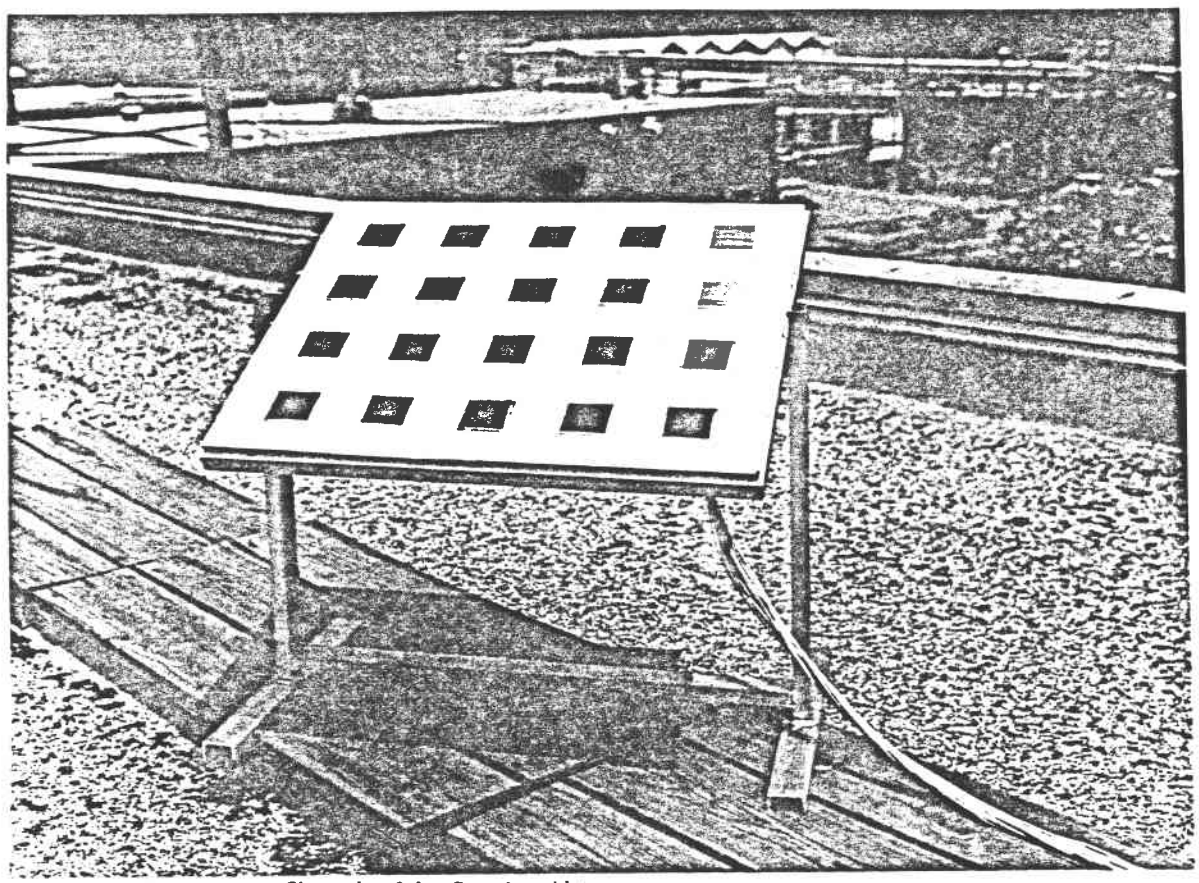

Figure 1. Solar Test Assembly

TEST PLATE TEMPERATURES
(AUGUST 25, 1977)

COATING COMPOSITION	PLASMA TEMPERATURE (°F)	AMBIENT TEMPERATURE (°F)	PLATE TEMPERATURE (°F)	COATING DENSITY (g/cm^2)
CHROME-BLACK	–	90	171	–
BLACK VELVET PAINT	–	90	152	–
$Ta + Cr_2O_3$	2996	90	162	0.007
V	1710	90	163	0.04
Fe_2O_3	1565	90	163	–
TaC	3880	90	163	0.03
Cr_2O_3	1990	90	161	0.008
TiB_2	2980	90	162	0.002
WC	2870	90	165	0.002

UNION CARBIDE

Y78-16

Figure 2

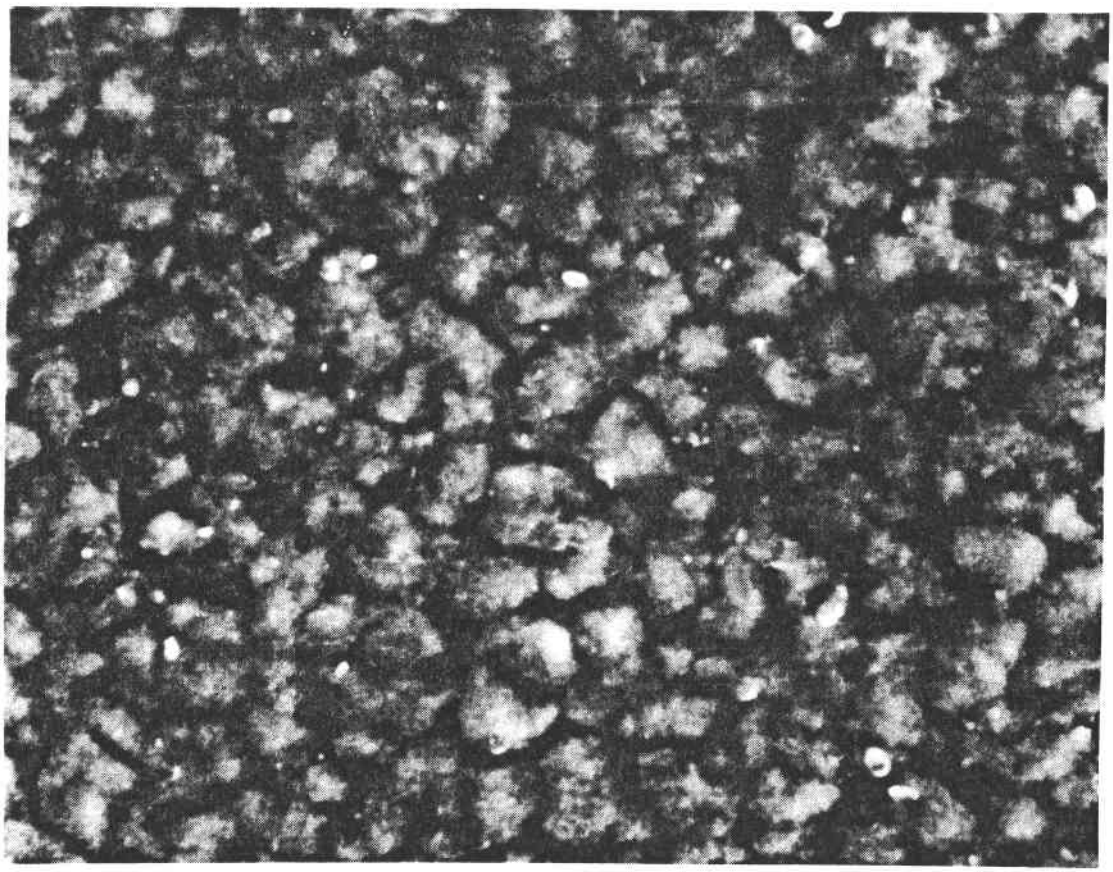

Figure 3. Electroplated Chrome-Black (Original 3000X)

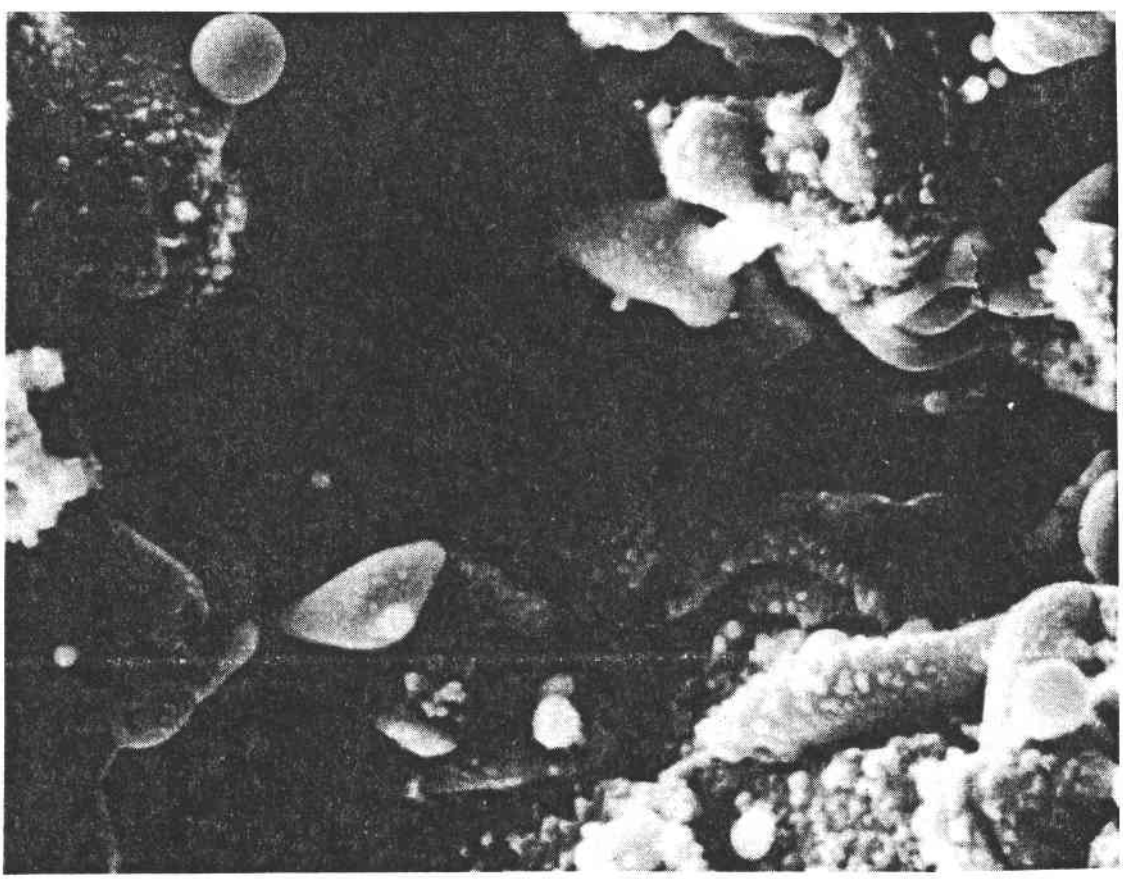

Figure 4. Plasma Sprayed Hafnium Diboride-Titanium Dioxide (Original 3000X)

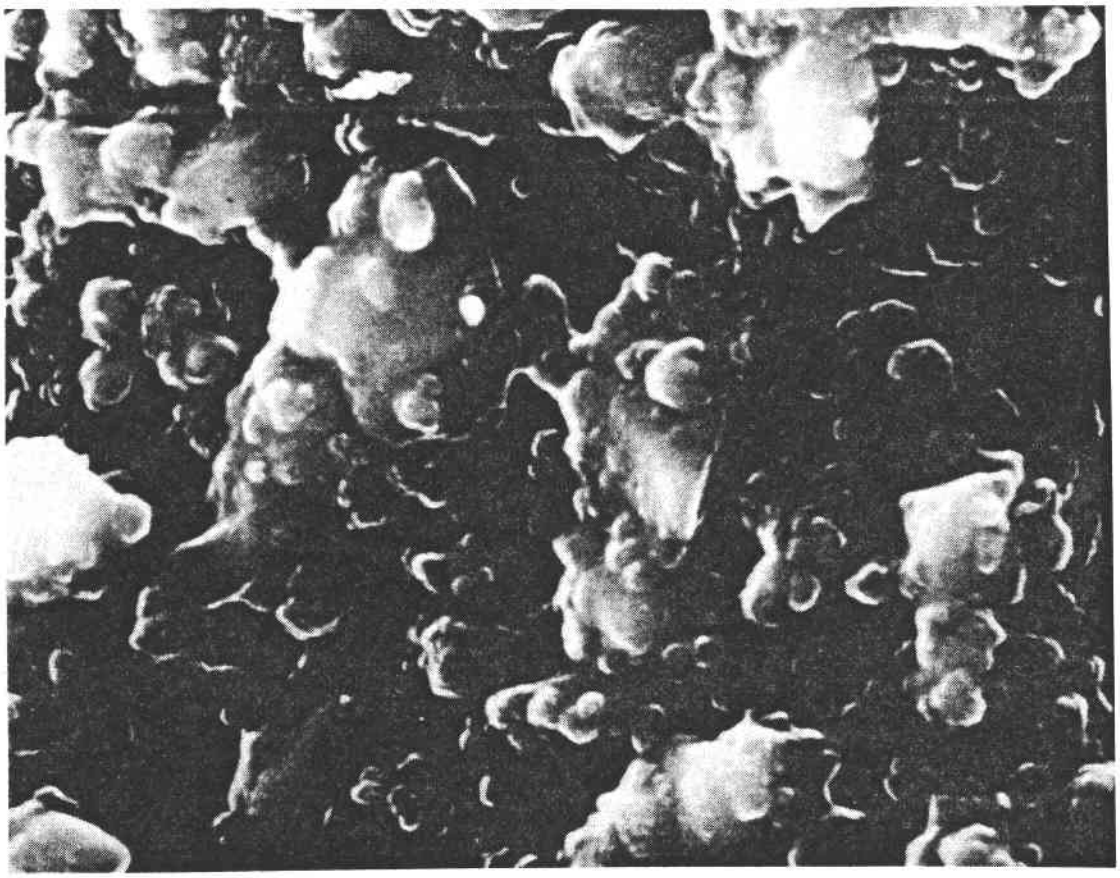

Figure 5. Plasma Sprayed Aluminum-Carbon-Silicate (Original 3000X)

IX. SESSION V: ENERGY CONVERSION AND STORAGE

PROPOSAL FOR ENGINEERING DESIGN STUDY OF CONVERSION OF SOLAR ENERGY TO CHEMICAL ENERGY THROUGH AMMONIA DISSOCIATION

Dr. Terry G. Lenz
Colorado State University
Ft. Collins, Colorado 80523

Abstract

It is proposed that an experiment be designed to investigate key components of a system for collection of solar energy utilizing reversible chemical reactions in a closed cycle gaseous working fluid. Concentrated solar energy would thermally dissociate ammonia in the presence of a catalyst into nitrogen and hydrogen. The gases are recombined at a central plant to yield ammonia plus high quality heat. Countercurrent heat exchangers at each chemical reactor allow the collection lines to operate near ambient temperature to minimize transport losses. The key component to be investigated is the solar absorber-chemical reactor-heat exchanger. The project has broad applicability to general energy transport and energy storage solutions as well as solar applications.

Introduction

Solar power plant concepts which have received considerable attention include flat plate absorbers and concentrating collectors utilizing thermal transport of the collected energy by means of a hot circulating fluid to a central station. Energy losses resulting from the collection and transport of the high temperature heat for such systems have limited their consideration to fairly small plants (<150 MW) and/or low temperature operations ($<200°$ to $300°C$).[1,2] Higher temperature operation at a larger scale is offered by a tower heliostat system in which the energy corradiation is performed optically between the collectors (heliostats) and a central absorber.

Recently, an alternate scheme for collection of solar energy using a distributed collector system has been proposed.[3,4] The energy transport system between the individual collectors and the central power plant utilizes reversible chemical reactions in a closed-cycle gaseous working fluid. The studies have indicated that by transporting the chemical energy in low temperature lines, the production of electrical energy at efficiencies of

25-30% (electrical output ÷ solar input) are achievable. Too, the system may lend itself to desirable energy storage techniques, either as chemical storage or intermediate temperature thermal storage.

The specific system which we propose to experimentally investigate utilizes ammonia as the working fluid. Carden[4] describes such a system which is shown schematically in Figure 1. Solar energy is collected at the focus of a paraboloidal mirror in a thermal absorber-chemical reactor. The thermal energy is used to dissociate ammonia at high temperatures in the presence of a catalyst. The hot dissociated gas mixture is cooled by the incoming ammonia in a countercurrent heat exchanger. The mixture is then piped to a common generating plant which accepts the feed of many identical solar collector units. The gas is reheated in another heat exchanger utilizing heat from the outflowing gases. In the power plant the nitrogen and hydrogen is recombined in a synthesis unit to yield ammonia plus heat. The heat is extracted to produce power, and the ammonia (and unreacted nitrogen and hydrogen) is cooled in the heat exchanger mentioned above, and returned to the solar collector units for another cycle through the system. Carden also includes a separator as shown in the figure, to recycle the unreacted H_2 and N_2 back to the synthesis reactor and feed pure NH_3 back to the collectors.

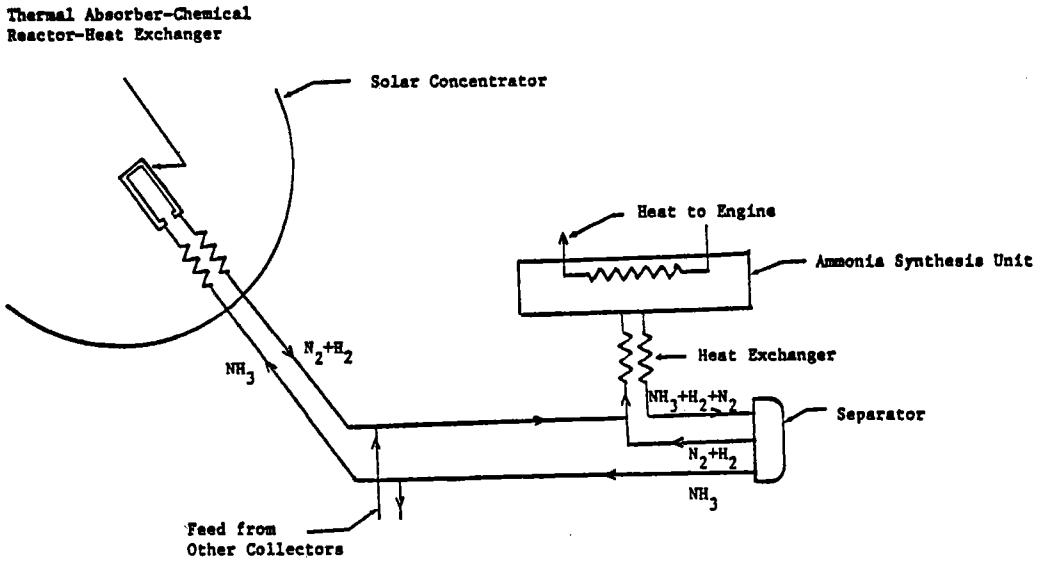

Figure 1. Schematic Diagram of Chemical Solar Power Plant

Characteristics of the Ammonia Cycle

The reversible chemical reaction to be investigated is:

$$2NH_3 + \Delta H \rightleftharpoons N_2 + 3H_2$$

where ΔH is the enthalpy of ammonia gas formation. Figure 2 shows some values for the ΔH of the synthesis reaction. The values are for 100% conversion into NH_3, whereas in industrial practice conversion is rarely greater than 20%. The corrected values, obtained by taking into account the heat of mixing of $NH_3(g)$ with $N_2 + H_2$ are appreciably different only for pressures above 300 atm.[6]

The total heat absorbed by 2 mol of dissociating ammonia is given as 31.5 kcal. This value is independent of the temperature at which the actual dissociation reaction occurs.[4]

The reversible ammonia reaction always tends toward an equilibrium condition, characterized by the percentage of ammonia in the mixture, which is a function of temperature and pressure. As can be seen from the data in Table 1,[7] high pressures and low temperatures favor large ammonia yields (high equilibrium yields of ammonia are desirable in the synthesis reactor) whereas low pressures and high temperatures favor large percentage yields of N_2 and H_2 (desirable in the dissociation reactor). However, before choosing a temperature and pressure at which to operate the system, the reaction rate must also be examined.

Reaction rate of a chemical system is dependent upon three factors: how close the mixture is to equilibrium for the mixture's temperature and pressure, the temperature, and the presence of a catalyst. Large departures from equilibrium, high temperatures, and the presence of a catalyst tend to favor high reaction rates.

TABLE 1. Equilibrium yields (in %) of NH_3 at different pressures and temperatures (as determined after expansion up to ambient pressure)

Temperature (°C)	Pressures (atm)				
	10	100	300	600	1000
200	50.66	81.54	89.94	95.37	98.29
300	14.73	52.04	70.96	84.21	92.55
400	3.85	25.37	48.18	66.17	79.82
450	2.11	16.40	35.87	54.00	69.69
500	1.21	10.51	25.80	42.32	57.47
550	0.76	6.82	18.23	32.18	41.16
600	0.49	4.53	12.84	24.04	31.43
700	0.23	2.18	7.28	12.60	12.87

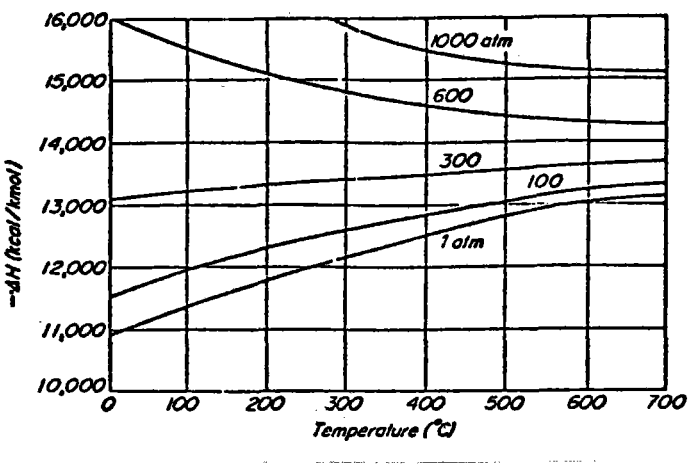

Figure 2. Enthalpy of ammonia gas formation at various pressures and temperatures (not taking into account the mixing heat of NH_3 and $N_2 + 3H_2$).[4]

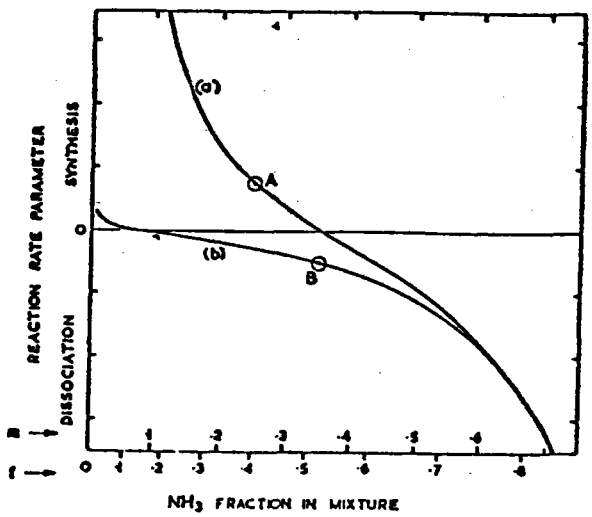

Figure 3. Reaction rate parameter vs. ammonia fraction. The parameter excludes temperature effects. The ammonia fraction scale is given both as mole fraction m and fraction by weight f. (a) Curve based on equilibrium point appropriate for 450°C and 300 atm. (b) Curve based on equilibrium point appropriate for 700°C and 300 atm. A, End point for typical synthesis process. B, End point for a typical dissociation process.[4]

Carden[4] has summarized the reaction kinetics considerations as follows. The Temkin-Pyzhev reaction rate equation[8]

$$W = K_2\left[K_P P_{N_2}\left(\frac{P_{H_2}^3}{P_{NH_3}^2}\right)^{\alpha} - \left(\frac{P_{NH_3}^2}{P_{H_2}^3}\right)^{1-\alpha}\right] ,$$

where K_p is the equilibrium constant, yields the synthesis reaction rate based on the generally accepted assumption that nitrogen chemisorption is the rate limiting step of the reaction. Vancini[8] gives evidence that this equation is also applicable to the decomposition of ammonia (more precisely fugacities should replace the partial pressures employed above). Taking $\alpha = 0.5$ and known values of K_p, Carden has evaluated the expression in square brackets in the equation. His results are plotted in Figure 3 vs m, the ammonia mole fraction. The two curves shown are for 700° and 450°C, and in each case the total pressure is 300 atm.

The parameter K_2 varies with temperature T (Bridger and Snowdon)[9] according to

$$K_2 = K_{2(0)} \exp\{-\left[\frac{\Delta E}{R}\left(\frac{1}{T} - \frac{1}{T_o}\right)\right]\}$$

and ΔE, the activation energy is 38 kcal/mole.

K_2 at 700°C is thus 854 times $K_{2(0)}$ at 450°C.

Point A on curve (a), Figure 3, corresponds to common commercial synthesis practice whereas point B represents the dissociation of ammonia to approximately 50% by mass. The ratio of the two reaction rates when the effect of temperature is included is Rate B/Rate A = 569.

It follows that approximately 569 times less catalyst should be required for conditions of point B compared to those of point A. Carden points out that since commercial synthesis plants employ about 4 tonnes/$MW_{thermal}$ we might therefore expect approximately 7g/KW of similar catalyst to be required in the dissociation chamber.[4]

Phase I - Design Feasibility

In an attempt to evaluate the feasibility of proceeding with the Phase I Engineering Study and Design, several initial design calculations have been performed. While some of the design assumptions and details noted below are subject to substantial revision and refinement, they are included to provide a feel for the size and operating characteristics of the system now envisioned.

Scale

One of the first issues which must be addressed is the choice of a power level at which to operate the system. From the chemical reactor-absorber standpoint, 25 KW would seem to be a reasonable choice. Very preliminary calculations indicate that sufficient heat transfer area, catalyst volume, and reactant flow could be provided in a simple cylindrical cavity reactor of about 1 ft diameter and 1 ft height with an 8 inch aperture. The interior walls of the cavity may possibly have to be of a folded fin design to provide sufficient wall area for convective transfer of heat from the reactor wall to the dissociating gas. Not only does this size reactor appear to be a convenient size with which to work, but it is a size which should provide operating data which could be applied to the design of a commercial sized component with a relatively low level of uncertainty. In addition, the choice of this size reactor will allow testing the system operation at a meaningful scale using a combined ammonia-nitrogen-hydrogen feed to the reactor to simulate a system which does not include an ammonia separator following the synthesis unit in the loop.

The more difficult part of designing a 25-KW reactor test is providing radiant power to such a system. A paraboloidal mirror capable of providing a 25-KW beam would have to be about 20 ft in diameter assuming typical reflector performances. Construction of such a system or its equivalent (perhaps a heliostat directing partially concentrated sunlight into a final, smaller concentrator) at Colorado State University is a possibility and will be examined during the Phase I activities.

Alternatively, testing of the reactor could be done using a portion of the 5-MW beam available at the Sandia Thermal Test Facility or at the White Sands Solar Test Furnace. This approach would maximize the use of existing facilities which are specifically designed for solar testing, as well as enabling us to make use of established solar testing expertise at Sandia or White Sands.

A third approach is to use a radiant heater lamp placed inside the absorber cavity. Advantages of this approach are that local testing could be performed to check out the system operability and the actual power input to the reactor would be easily measured. Follow-up testing at one of the above facilities for solar performance verification would be desirable. A private firm[10] which builds solar simulator lamp arrays indicated that construction of such a device was possible and estimated a total cost of $25-50,000. Sandia has also supplied similar information.

In summary, construction of a 25-KW reactor appears very feasible. While testing considerations might result in the choice of a smaller reactor, means of testing the 25-KW size are available.

Loop Pressure and Temperature

Choice of the pressure and temperature at which the components will be operated will influence the equilibrium mixtures to be formed in the synthesis and dissociation reactors as shown in Table 1. Higher temperatures are desirable from the standpoint that they encourage faster reaction rates and yield higher quality heat for the heat engine. Of course, higher temperatures at the absorber result in lower collection efficiencies due to greater radiation and convective losses. Higher pressures result in higher heat transfer rates and correspondingly more compact, albeit heavier, equipment. It is proposed to use the values given by Carden,[4] i.e., 300 atm pressure, 700°C in the dissociation reactor, and for modeling purposes, 450°C at the synthesis chamber. These values can be varied for different experimental runs, but the design point will be based upon the above temperatures and pressure. If the experiment can be designed for greater pressures (say up to 600 atm) without incurring too great a cost penalty, we would expect to do so.

REFERENCES

1. Honeywell (Minneapolis-Honeywell Co.) Dynamic Conversion of Solar Generated Heat to Electricity. NASA Contract No. NAS 3-18014. Progress Narrative No. 6, pp. 2-64 (1974).

2. Colorado State University and Westinghouse Electric Corp., Solar Thermal Electric Power Systems, Report NSF/RANN/SE-GI-37815/FR/74/3, Vol. 1, pp. 22-32 (1974).

3. T. A. Chubb, Analysis of Gas Dissociation Solar Thermal Power System, Solar Energy, Vol. 17, pp. 129-136, Pergamon Press (1975).

4. P. O. Carden, Energy Corradiation Using the Reversible Ammonia Reaction, Solar Energy, Vol. 19, pp. 365-378, Pergamon Press (1977).

5. T. A. Chubb, A Chemical Approach to Solar Energy, Chemtech, pp. 654-657, October (1976).

6. C. A. Vancini, Synthesis of Ammonia, (English Translation by L. Pirt), p. 24 MacMillan, London (1971).

7. C. A. Vancini, ibid., p. 27.

8. M. I. Temkin and V. Pyzhev, Acta. Physicochium (URSS) 12, 327 (also Vancini, ibid., p. 64).

9. G. W. Bridger and C. B. Snowdon, Catalyst Handbook, ICI, Chap. 7, p. 141 (1970).

10. Earl Niemela, Research, Inc., Minneapolis, MN, Private communication (1978).

TABLE 1

REACTION	ΔH KCAL/MOLE	KCAL/G
$SO_3 \rightleftharpoons SO_2 + \frac{1}{2}O_2$	+24*	0.29
$\frac{1}{2}H_2O + \frac{1}{2}CH_4 \rightleftharpoons \frac{1}{2}CO + 3/2H_2$	+24.5**	1.44
$COCl_2 \rightleftharpoons CO + Cl_2$	+26	0.26
$2NF_3 \rightleftharpoons N_2 + 3F_2$	+31	0.43
$CH_4 + CO_2 \rightleftharpoons 2CO + 2H_2$	+59	0.98
$CH_3OH \rightleftharpoons 2H_2 + CO$	+25	0.78
$2NH_3 \rightleftharpoons N_2 + 3H_2$	+25	0.79

* From Chubb

** From Hildebrandt

TABLE II

Catalyzed Reactions	ΔH°(kcal)[a] / mole	ΔS° ($\frac{cal}{deg}$)[a]	$T^* = \frac{\Delta H^\circ}{\Delta S^\circ}$	$\frac{\Delta H^\circ}{V}$ ($\frac{kcal}{\ell}$)	Comments and Conditions
$NH_3 \rightleftharpoons 1/2N_2 + 3/2H_2$	12.5	23.4	534	50	Stored at 100°C, 300 atm
$CH_{4(g)} + H_2O_{(g)} \rightleftharpoons CO_{(g)} + 3H_{2(g)}$ [b]	49.	51.	960	50	Gas storage at 100 atm and 25°C
$CH_{4(g)} + CO_{2(g)} \rightleftharpoons 2CO_{(g)} + 2H_{2(g)}$ [b]	59.	61.5	960	60	Gas storage at 100 atm and 25°C
$SO_{3(g)} \rightleftharpoons SO_{2(g)} + 1/2O_{2(g)}$ [b]	23.5	22.7	1,040	110	SO_2 as liquid $1/2O_2$ as gas at 100 atm and 25°C
$CH_3OH_{(g)} \rightleftharpoons 2H_{2(g)} + CO_{(g)}$ [b]	22.	53.	420	42	Back reaction at 300 atm and 327°C to $CH_3OH_{(\ell)}$
H_2 Storage $H_2O_{(g)} \rightleftharpoons H_{2(g)} + 1/2O_{2(g)}$ [b]	57.8	10.6	5,450	240	Storage of $H_{2(g)}$ only at 100 atm and 25°C

[a] Data taken from "Handbook of Chemistry and Physics," 51st Edition, 1970-1971, p. D-61;

[b] from Wentworth and Chen

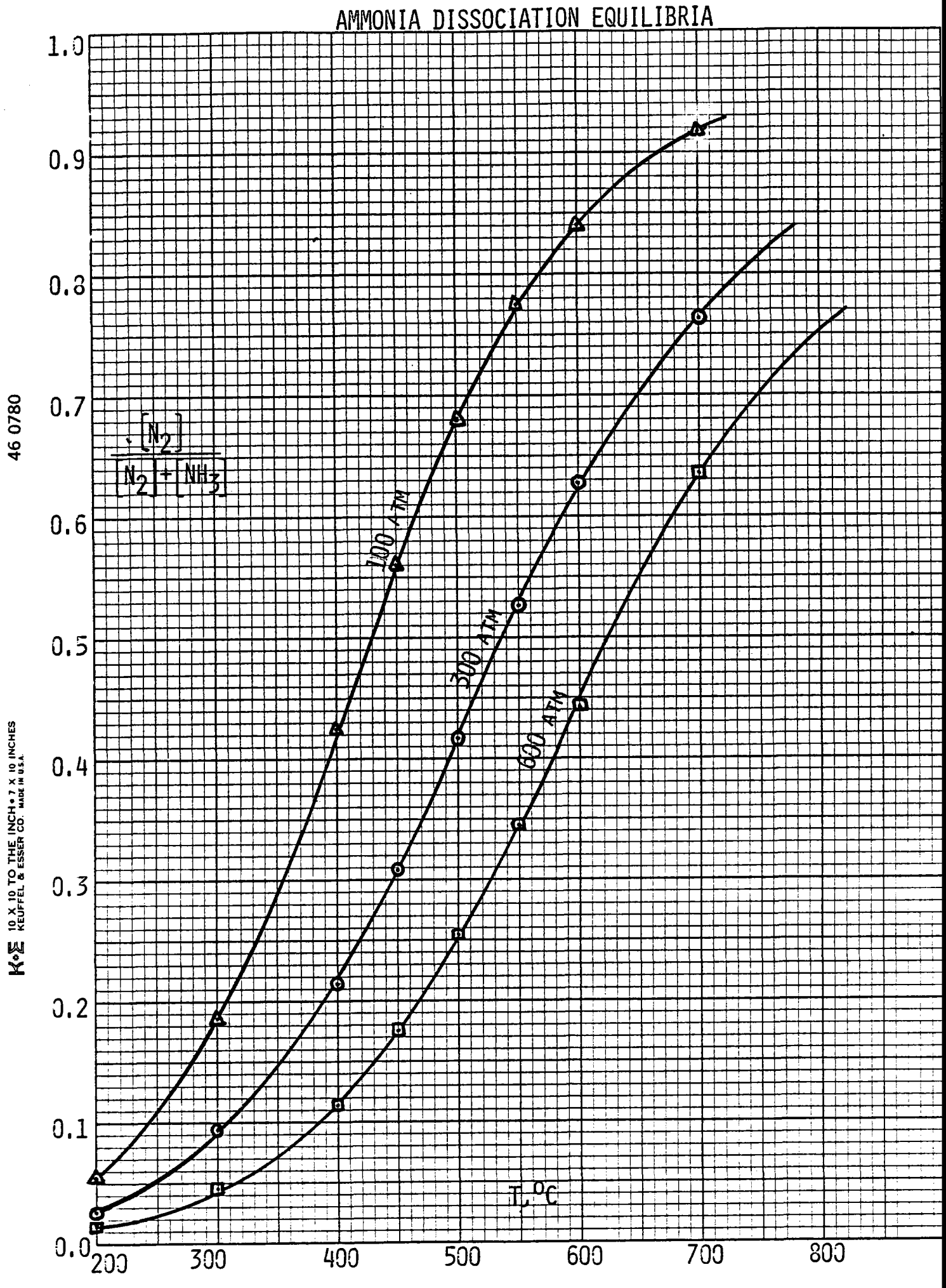
AMMONIA DISSOCIATION EQUILIBRIA
1.0
0.9
0.8
0.7
0.6
0.5
0.4
0.3
0.2
0.1
0.0
$\frac{[N_2]}{[N_2]+[NH_3]}$
100 ATM
300 ATM
600 ATM
T, °C
200
300
400
500
600
700
800
46 0780
K&E 10 X 10 TO THE INCH • 7 X 10 INCHES
KEUFFEL & ESSER CO. MADE IN U.S.A.

FIRST ESTIMATES FOR NH_3 DISSOCIATION REACTOR DESIGN PARAMETERS

REACTOR SIZE	6.25 KW	12.5 KW	25 KW
MIRROR SIZE (100% η)	9.25 FT DIA 2.8M	13.1' 4M	18.5' 5.64M
APERTURE SIZE	4" DIA	5.66" DIA	8" DIA
MASS FLOW (70% CONV.)	13.0 LB/HR 5900 G/HR	26 LB/HR 11,800 G/HR	52 LB/HR 23,600 G/HR
VOLUME FLOW (@ 700°C AND 300 ATM)	129 IN^3/MIN 2114 CC/MIN	258 IN^3/MIN 4228 CC/MIN	516 IN^3/MIN 8457 CC/MIN
CATALYST VOLUME (BASED ON SPACE VELOCITY = $\frac{1500}{HR}$)	5.16 IN^3	10.32 IN^3	20.64 IN^3

AMMONIA SYSTEM CHARACTERISTICS

TEMP'S. : 700°C → 450°C

PRESS. : 100 → 600 ATM

EFFICIENCY : 20-25% SOLAR → POWER

NH_3 CIRC. RATE : 4 TONS/H - MW_E

ENERGY DENSITY : 5600 BTU/FT^3

SYNTHESIS INV. : \$150/KW_E (THUS 86% OF \$1150/KW_E FOR COLLECTORS, STORAGE, ETC.)

ADVANTAGEOUS POINTS :
A. WELL-KNOWN LARGE SCALE TECHNOLOGY
B. NON-CORROSIVE & LESS TOXIC THAN MANY SYSTEMS
C. GOOD HEAT TRANSFER AT HIGHER PRESSURES & REDUCED EQUIPMENT SIZE

DISADVANTAGES :
A. SLIGHTLY POORER THERMODYNAMICS AND OVERALL EFFICIENCY

PERFORMANCE OF A 5 MWt SOLAR STEAM GENERATOR

W. J. Oberjohn and W. T. Southards

The Babcock & Wilcox Company

ABSTRACT

A radiant heat test was conducted to verify the functional performance of a 5 MWt solar steam generator. The steam generator modeled the essential features of a conceptual design proposed by the Honeywell team for the DOE 10 MWe Solar Pilot Plant.

This paper describes the experimental steam generator and its instrumetation. Selected test results and analyses are presented which demonstrate that steam generator performance was predictable, controllable, and responsive. From this, it is concluded that fossil boiler technology can form the basis for a successful solar steam generator design.

INTRODUCTION

Supplies of conventional fuels are being rapidly depleted. Solar energy provides an alternate to fossil and nuclear energy. One of the goals of the national energy program is to demonstrate the technical and economic feasibility of a central receiver solar power plant. On July 1, 1975 The Energy Research and Development Administration (ERDA) awarded one of several two-year contracts to the Honeywell team to carry out Phase I of this program. The Honeywell team* consisted of Honeywell, Inc. (HI), The Babcock and Wilcox Company, Northern States Power Company, Research, Inc., and Black and Veatch.

During Phase I, a preliminary design for a 10 MWe proof-of-concept solar pilot plant was developed and subsystem research experiments (SRE's) were conducted to support the design. The overall objectives of the receiver SRE were to demonstrate the adequacy of the steam generator design methods, to validate techniques for measuring incident and absorbed heat flux, and to demonstrate that a steam generator, scaled from the pilot plant design, would be reliable, controllable, and responsive. This paper briefly describes the steam generator and presents the overall results of the test program.

*Acknowledgement. The work reported in this paper was funded by ERDA Contract No. E(04-3)-1109. Honeywell, Inc. was the prime contractor and provided overall program management; The Babcock and Wilcox Company designed, fabricated and erected the steam generator and the steam generator instrumentation, and analyzed the test results; the Northern States Power Company provided test facilities and test support at the Riverside Plant in Minneapolis; Honeywell provided the steam generator controls and the computer controlled real time data acquisition system; Research, Inc. supplied the solar simulator; and Black and Veatch designed the mechanical and electrical interfaces between the steam generator and the test facilities. The testing and data reduction were carried out by Honeywell.

STEAM GENERATOR DESCRIPTION

To meet the schedule established for Phase I of the Central Receiver Program, the steam generator was designed using existing technology. Emphasis was placed on achieving a reliable design, on schedule, by using state-of-the-art fossil boiler technology.

The SRE steam generator was designed for a thermal output of 4.2 MW for steam conditions of 955°F and 1575 psia. It is a pump-assisted recirculating drum boiler with two superheaters and a spray attemperator for controlling steam temperature (Figure 1). The steam generator heat transfer surfaces approximate a vertical cylinder and form the interior walls of the receiver cavity. This geometry traps reflected and reradiated solar energy to increase cavity effective absorptance. The absorptance of the heat transfer surface is about 0.9 and is achieved by allowing natural oxidation to occur. Reradiation is minimized by locating the cooler heat transfer surfaces near the bottom of the cavity and the higher temperature surfaces at the top. The inside diameter of the cavity is 3.48 m (11.4 feet) and the height is 3.87 m (12.7 feet).

The steam generator is thoroughly insulated to minimize conduction losses and, in the absence of wind, the bottom opening cavity does not allow the buoyant hot air to escape, minimizing natural convection losses. For the SRE tests, a solar simulator was inserted into the lower half of the cavity which was closed by a bottom reflector. A flow schematic of the SRE steam generator is shown in Figure 2.

Feedwater is piped into the steam generator drum and mixed with saturated water. This slightly subcooled mixture flows from the drum, through a downcomer, and is pumped through the boiler supply line to the boiler section.

The water is distributed to the boiler section where steam generation takes place. A saturated steam-water mixture at an average quality of 10% (at maximum conditions) exits the boiler section and flows through the risers to the steam drum where the water and steam are separated by cyclone separators and scrubbers.

Moisture free steam from the drum flows through the saturated steam lines to the primary (first stage) superheater where it is heated to about 475°C (887°F).

The steam exiting the primary (first stage) superheater passes through the spray attemperator where additional feedwater is injected as required to control exit steam temperature.

The attemperated steam enters the secondary (second stage) superheater at about 410°C (770°F) where it is heated to 513°C (955°F).

The choice of the pump-assisted circulation concept for the solar steam generator as opposed to a natural circulation drum boiler or a once-through subcritical boiler is based on extensive fossil boiler experience which indicates that:

- Drum boilers are easier to start up and control during cyclic operation than once-through boilers because a bypass system and the associated heat recovery equipment are not required. Accordingly, fossil boilers currently designed for daily cycling are drum boilers.

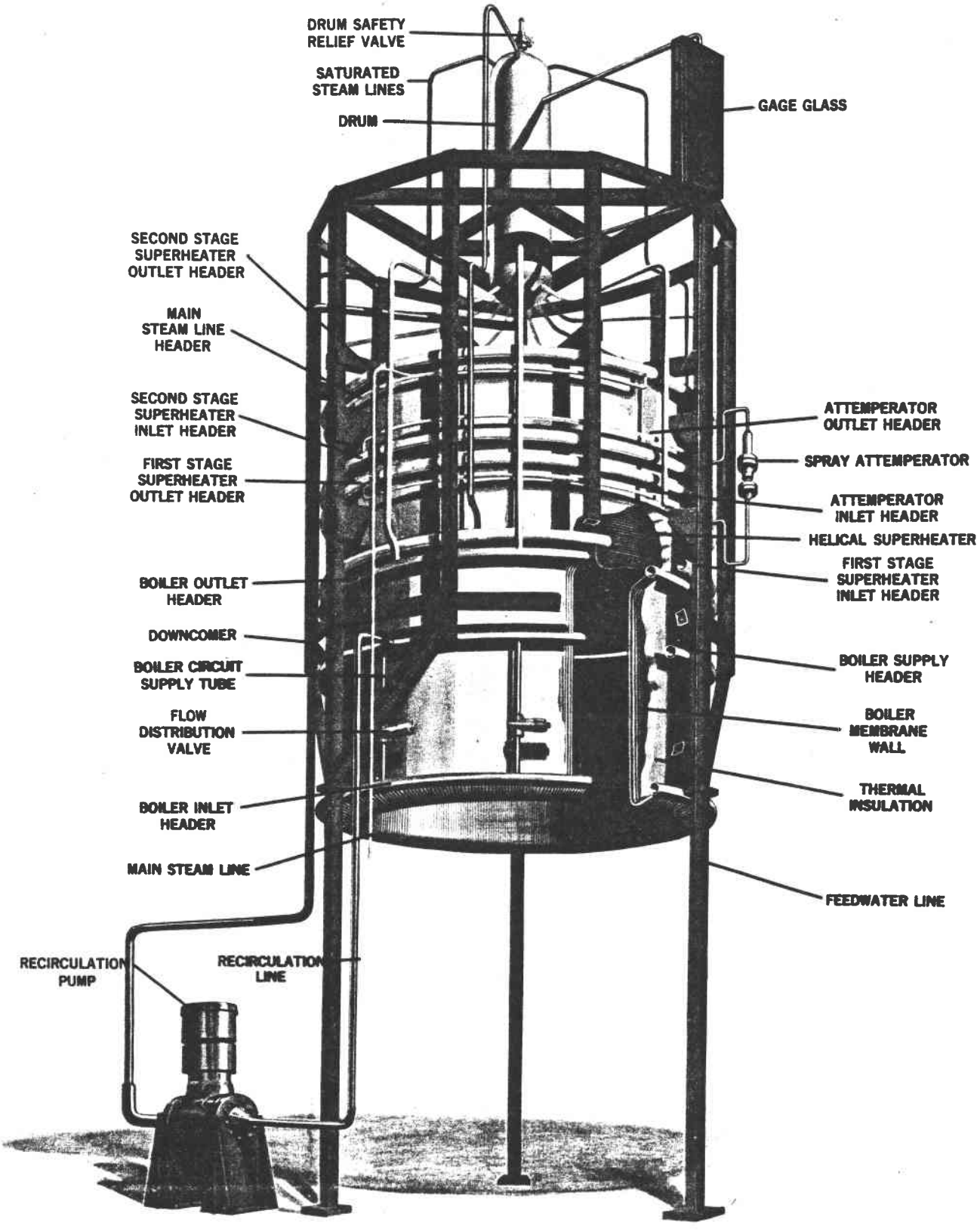

FIGURE 1 SUBSYSTEM RESEARCH EXPERIMENT (SRE) SOLAR STEAM GENERATOR

- Pump-assisted circulation boilers permit the use of increased pressure drop to assure adequate flow to each boiler tube independent of heat flux distribution. Pump-assisted circulation fossil boilers are used when the characteristics of the fuel being burned result in the possibility of large local variations in absorption that could result in the loss of natural circulation pumping head. For the solar steam generator this could occur when cloud shadowing reduced heat absorption to zero at some locations while the maximum absorption was maintained at other locations.

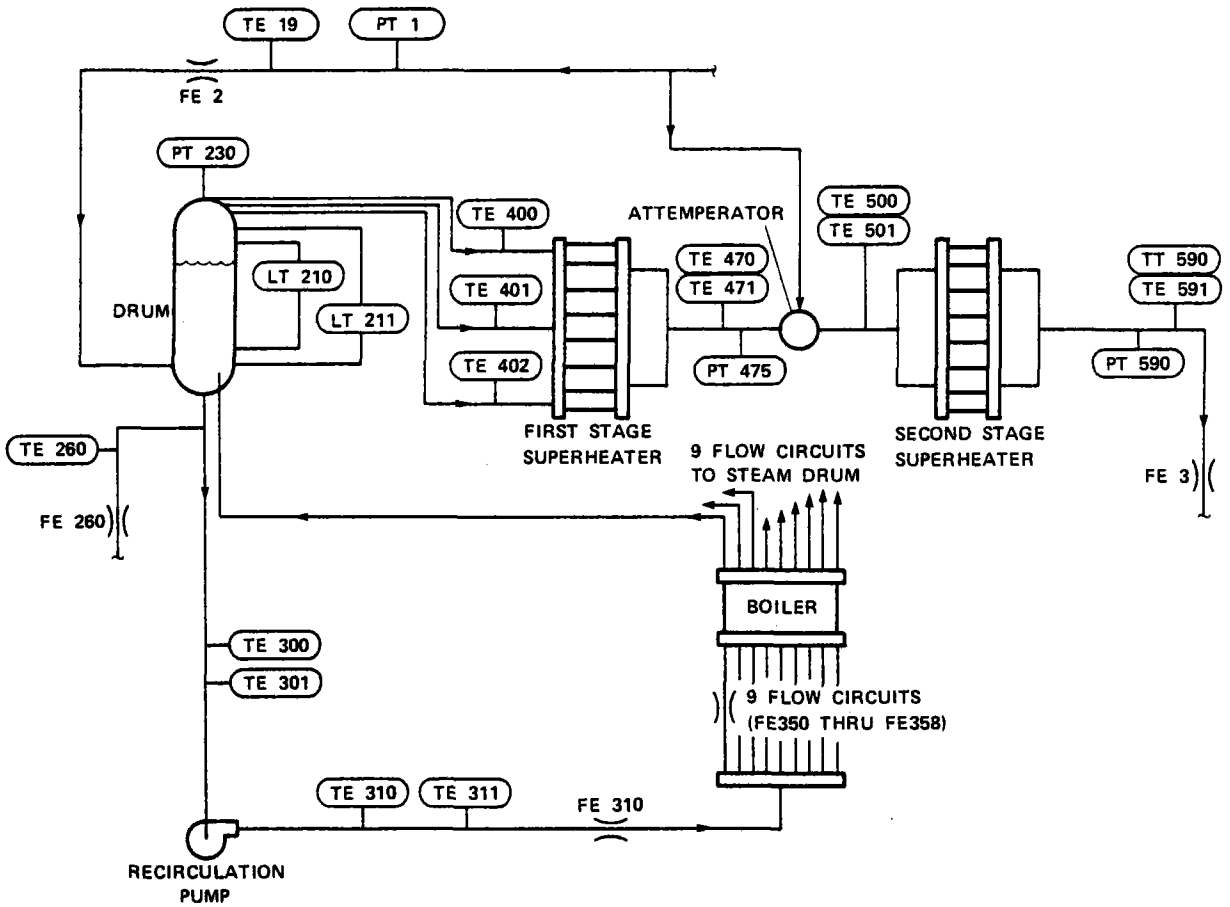

FIGURE 2 FLUID INSTRUMENTATION FLOW SCHEMATIC

The heat flux distribution on the cavity interior walls is determined primarily by the geometry of the heliostat field, tower height, aperture area and the geometry of the cavity itself. The solar simulator was designed to match predicted heat flux patterns for the 10 MWe Pilot Plant. Essentially, energy from the outermost heliostats is incident on the lower part of the cavity while the innermost heliostats provide the energy for the upper part of the cavity. Since there are more heliostats in the outer portion of the field, incident energy peaks in the lower part of the cavity and tapers off toward the top.

To take advantage of this characteristic, the boiler section, which can be designed to operate at high heat fluxes because it is effectively cooled by a sat-

urated steam-water mixture, is located in the lower half of the cavity. The first stage, or primary superheater, which receives saturated steam from the drum, is located in the middle portion of the cavity where heat flux and steam temperatures are moderate. The second stage, or secondary superheater, which receives higher temperature steam from the spray attemperator, is located in the upper portion of the cavity where heat flux is low. As a result of this arrangement of boiler and superheater surfaces, the maximum metal temperatures in the superheater are lowest where thermal stress is high and highest where thermal stress is low.

The cavity ceiling is insulated and most of the incident energy is either reflected or reradiated to the superheater or boiler.

The boiler and superheater heat transfer surface areas are determined by the requirements of the steam cycle and by the absorbed heat flux distribution within the cavity. The ratio of the energy required to produce saturated steam from the feedwater to the energy required to superheat the steam is about 72% at design conditions. Actually, the boiler surface has been sized to absorb only 65% of the total energy. The extra energy absorbed by the superheater is used to vaporize feedwater injected into the superheater circuit at the spray attemperator. At design conditions, the spray attemperator flow is 10% of the design steam flow.

As the sun changes position or as clouds partially shadow the heliostat field, the vertical distribution of energy changes within the cavity. Steam temperature at the exit of the second stage superheater can then be controlled by increasing or decreasing feedwater flow to the spray attemperator.

The boiler section heat transfer surface is a 1.79 m (5.88 feet) high 18-sided polygon fabricated from membrane panels. The boiler tubes are 2.223 cm (0.875 inch) outside diameter carbon steel with a minimum wall thickness of 0.376 cm (0.148 inch). Carbon steel membrane bars 0.635 cm (0.25 inch) thick are machine-welded between adjacent tubes. The tube spacing is 3.81 cm (1.5 inches).

Both the primary (first stage) and secondary (second stage) superheaters are identical and consist of an inlet header, 12 helically-coiled tubes each making 3-1/2 turns, and an outlet header. The tubes are 2.54 cm (1.0 inch) outside diameter, Croloy 2-1/4 (SA 213 T22), with a 0.419 cm (0.165 inch) minimum wall thickness. Each superheater coil is 1.04 m (41 inches) high and has a coil diameter of 3.46 m (136 inches).

The vertical steam drum is 2.49 m (98 inches) high and has an outside diameter of 0.71 m (28 inches). It contains a single cyclone primary separator and secondary scrubber plates to effectively remove moisture from the saturated steam.

A three-legged box beam structure supports the steam generator. The boiler and superheater are hung from the structure permitting free radial and axial thermal expansion. All headers and interconnecting piping are located between the heat transfer surface and the box beam frame. The downcomer, recirculation line, blowdown line, feedwater line, attemperator spray flow line, and main steam line are located along side the support legs. The boiler recirculation pump is located on the test floor adjacent to the support structure.

STEAM GENERATOR INSTRUMENTATION

The instrumentation provided the capability to determine fluid pressure, temperature, and flow throughout the steam generator, to monitor pertinent metal temperatures, and to alert operating personnel to potentially hazardous conditions. Table 1 provides a listing of all steam generator instrumentation.

Evaluation of steady-state and transient performance requires accurate heat and mass balances. Thus, net mass and energy inputs to the steam generator or its components must be determined. Fluid measurements necessary to satisfy this requirement are temperatures, pressures and flows for all connections to and from the steam generator and its components, and the mass accumulation within the generator system (drum level). Beyond the requirements for performance evaluation, other fluid measurements are necessary for control, flow balancing, and measurement cross-checking. The Fluid Instrumentation Flow Schematic (Figure 2) identifies the location of pertinent fluid instruments.

In addition to fluid instrumentation, metal or surface-mounted thermocouples installed on the steam generator indicated metal temperatures, absorbed heat flux, or fluid temperatures. At selected boiler membrane web locations, surface metal temperature measurements were used to calculate absorbed heat flux from the results of a two-dimensional conduction analysis (Figures 3 and 4). The increase in the bulk fluid temperature along the superheater tube length (determined using surface thermocouples on the backside of the superheater) was used to calculate superheater absorbed heat flux (Figure 5 and 6). Other surface thermocouples monitored metal temperatures in the cavity interior, on headers, on the drum, and on various supports and snubbers. Also surface thermocouples measuring superheater outlet tube temperatures detected possible tube-to-tube flow variations. All surface thermocouples were Cr-Al with 1/16-inch outside diameter 316 stainless steel, or Inconel 600 sheaths and grounded junctions.

Analog, digital, and manual monitoring of operating parameters and comparison with alarm values was necessary to alert operating personnel of potentially hazardous conditions throughout the test program.

TEST RESULTS AND ANALYSIS

Steady-state and transient functional performance test objectives were defined to satisfy the overall objectives stated previously. Steady-state performance test objectives were to verify design methods (using axisymmetric heat flux input), validate heat flux measurement techniques, and to determine performance effects of asymmetric heat flux input. Transient performance test objectives were to validate the steam generator transient model, evaluate steam generator controls, and to ascertain performance characteristics during equipment trips.

STEADY-STATE PERFORMANCE

After initial adjustment of the solar simulator and the control system, the steam generator was operated for about 70 hours at various steady-state power levels from mid-March to the end of April, 1977. Approximately 8 full sets of steady-state data were recorded. The following paragraphs present test results and data analyses for one of these runs.

TABLE 1 SRE INSTRUMENTATION

INSTRUMENT	IDENTIFICATION NO.	QUANTITY	CONTROL	FUNCTION		DATA ACQUISITION
				INDICATE	ALARM	
Pressure:						
Feedwater	Customer					
Drum (Transmitter)	PT 230	1			D/A	1
Drum (Gage)	PI 230	1		A		
Recir. Pump Outlet (Gage)	PI 300	1		A		
Attemperator Inlet - Steam	PT 475	1				1
Main Steam - Exit of SRE	PT 590	1		B		1
Main Steam - Control Valve	Customer					
Flow:						
Feedwater	Customer					
Blowdown	FE 260	1				
	FT 260	1		C		1
Boiler Inlet (Total)	FE 310	1				
	FT 310	1		C	D/A	1
	FS 310	1			I	
Boiler Inlet (9 Circuits)	FE 350-358	9				
	FT 350-352	3		C		3
Attemperator Spray Water	FE 480	1				
	FT 480	1		B		1
Main Steam	Customer					
Pump Cooling	FE 305	1				
	FS 305				I	
Level:						
Level Transmitter	LT 210	1	1	C	C	1
Level Transmitter	LT 211	1		B	D/A	1
Level Gage	GG 220	1		A		
Fluid Temperatures:						
Feedwater	Customer					
Attemperator Spray Water	TE 480	1				1
Blowdown	TE 260	1				1
Downcomer - Pump Inlet	TE 300	1			D/A	1
Downcomer - Pump Inlet	TE 301	1				1
Boiler Inlet - Pump Outlet	TE 310	1				1
Boiler Inlet - Pump Outlet	TE 311	1				1
Saturated Steam #1	TE 400	1				1
Saturated Steam #2	TE 401	1				1
Saturated Steam #3	TE 402	1				1
Steam into Attemperator	TE 475	1		B	D/A	1
Steam into Attemperator	TE 476	1				1
Attemperator Outlet	TE 500	1		B	D/A	1
Attemperator Outlet	TE 501	1				1
Main Steam - SRE Outlet	TT 590	1		C	C	1
Main Steam - SRE Outlet	TE 591	1		B	D/A	1
Main Steam - Control Valve	Customer					
Pump Cooling - Outlet	TT 306	1				1
Metal Temperatures:						
Drum Shell	TE 210-217	8				8
Boiler - Membrane (Heat Flux)	TE 330-389	60				60
1st Stage SH Inlet	TE 405-409	5			D/A	5
1st Stage SH (Heat Flux)	TE 420-440	21				21
1st Stage SH Outlet	TE 450-454	5			D/A	5
1st Stage SH Outlet Legs	TE 455-466	12				12
1st Stage SH Outlet Header	TE 470-471	2				2
2nd Stage SH Inlet	TE 505-509	5			D/A	5
2nd Stage SH (Heat Flux)	TE 520-540	21				21
2nd Stage SH Outlet	TE 550-554	5			D/A	5
2nd Stage SH Outlet Legs	TE 555-566	12				12
2nd Stage SH Outlet Header	TE 570-571	2				2
Boiler Outlet Support Lug	TE 600-602	3				3
1st Stage SH Outlet Support Lug	TE 603-605	3				3
2nd Stage SH Outlet Snubber Plate	TE 606-608	3				3
2nd Stage SH Outlet Tube Snubber Bracket	TE 609-611	3				3
Pump Seal Flush	TE 612	1				1

Definitions

Indicate
A - Visual Reading, i.e., gage
B - Chart Recorder
C - Indicator on Controller

Alarm
D/A - Alarm is activated by the data acquisition system
C - Alarm is activated by the controller
I - Alarm is an independent circuit

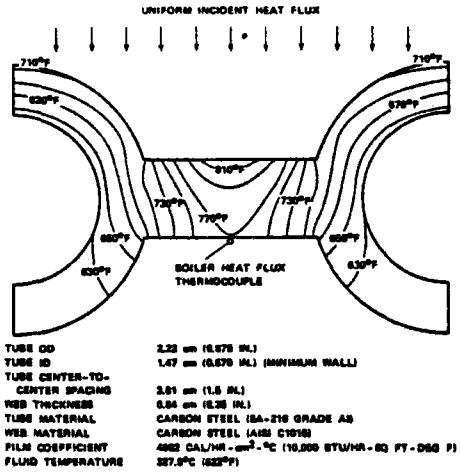

FIGURE 3 BOILER ABSORBED HEAT FLUX THERMOCOUPLE LOCATION IN RELATION TO ISOTHERMS

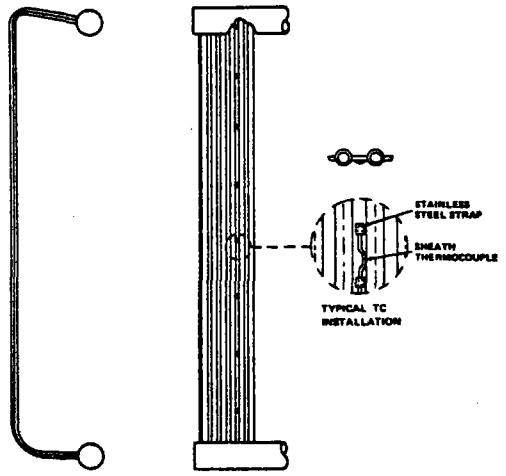

FIGURE 4 TYPICAL BOILER PANEL WITH THERMOCOUPLE LOCATIONS

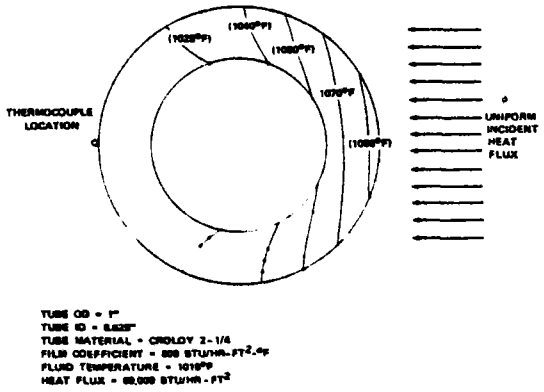

FIGURE 5 SUPERHEATER ABSORBED HEAT FLUX THERMOCOUPLE LOCATION IN RELATION TO ISOTHERMS

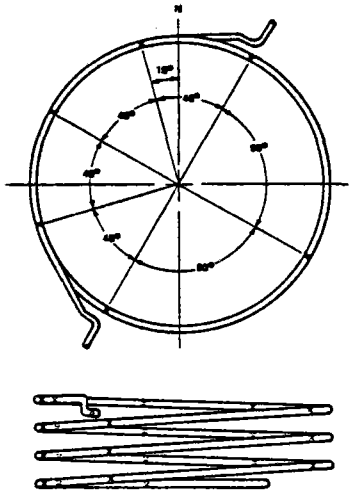

FIGURE 6 TYPICAL HELICALLY-COILED SUPERHEATER TUBE WITH THERMOCOUPLE LOCATIONS

Energy inputs, energy loss, measured flow parameters, and predicted pressures for this steady-state point are summarized in Table 2. The measured flow parameters were obtained from an on-line Performance Summary provided by the data acquisition system. The total energy absorbed and the energy absorbed by each component (boiler, primary superheater, and secondary superheater) was calculated by means of a heat balance on the total steam generator or the component of interest. The incident energy into the steam generator is the net radiant array power (power input to the array less cooling water losses). Pressure predictions shown were obtained by correcting predicted full power pressure losses to the test flow rates and test average specific volumes. Energy losses were calculated from cooldown rates for the various components.

TABLE 2 SRE STEADY-STATE DATA – APRIL 13, 1977 11:37 AM

INCIDENT ENERGY	3.2 MW
ENERGY LOSS	0.18 MW
ABSORBED ENERGY	3.0 MW
BOILER	2.1 MW
PRIMARY SUPERHEATER	0.67 MW
SECONDARY SUPERHEATER	0.22 MW

	MEASURED			PREDICTED
LOCATION	FLOW (LBM/HR)	TEMPERATURE (°F)	PRESSURE (PSIA)	PRESSURE (PSIA)
FEEDWATER	9924	469	1915	–
BOILER INLET	86900	603	–	–
BOILER OUTLET	86900	610	–	–
DRUM	10136	610	1670	1670
PRIMARY SH OUT	10136	843	1641	1642
SECONDARY SH OUT	10136	958	1601	1594

The differentials between peak metal and steam temperatures are displayed (Figure 7) for three points in the superheaters. The measured peak metal temperatures shown are at the primary superheater inlet, primary superheater outlet (also secondary superheater inlet) and secondary superheater outlet. Predicted values shown are based on a one-dimensional model using test fluid flow data as an input. Agreement between experimental results and predictions supports the validity of the design methods.

A design tolerance of 60°F was used for variation in superheater tube outlet steam temperatures. Measured bulk tube outlet fluid temperatures (Figure 8) exhibit temperature variations well within design limits, thus, supporting the design criteria. The small variations in temperatures between tubes infer good flow distribution, thus demonstrating effective header design methods.

The superheater fluid temperature profile (Figure 9) was obtained using backside surface temperature measurements described previously. The differential change in bulk fluid temperature with tube length was used to calculate the superheater absorbed heat flux (Figure 10).

Temperatures at selected points on the backside of the boiler membrane web were used with a two dimensional conduction analysis to determine the boiler absorbed heat flux. Summation of the resulting values of heat flux over the appropriate areas was compared to the boiler absorbed heat input obtained from a heat balance. The comparison resulted in an adjustment factor of 1.073 to make the summation of absorbed heat flux equal to the heat balance result. The adjusted boiler heat flux is plotted on Figure 10.

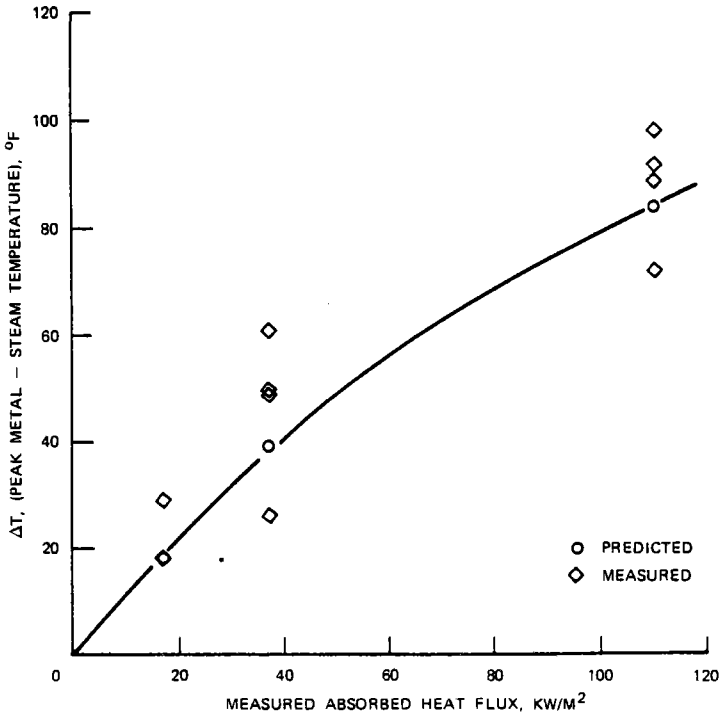

FIGURE 7 SUPERHEATER HEAT TRANSFER

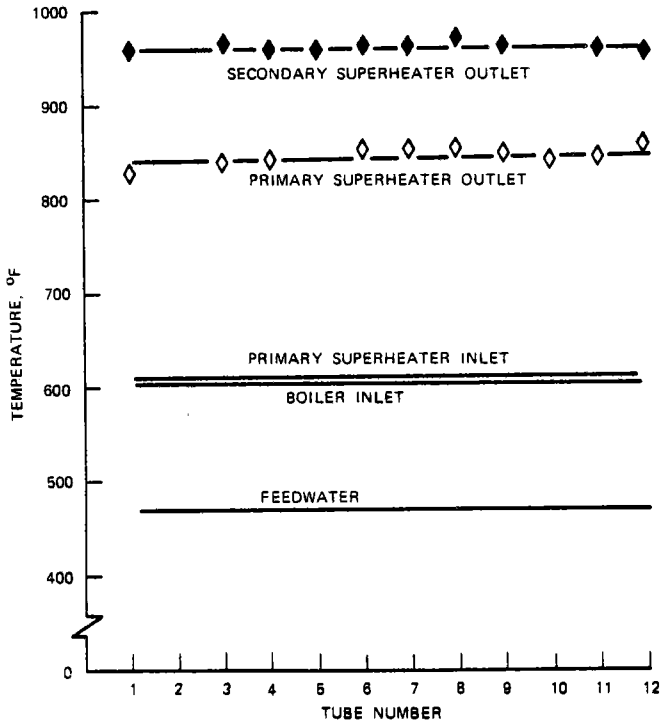

FIGURE 8 STEAM GENERATOR TEMPERATURE

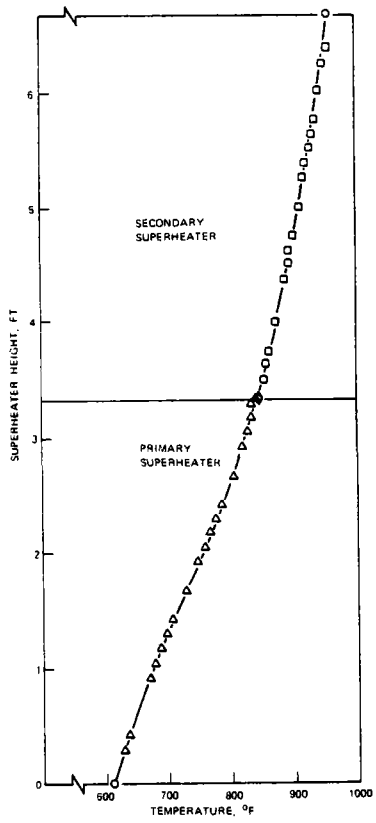

FIGURE 9 SUPERHEATER FLUID TEMPERATURE PROFILE

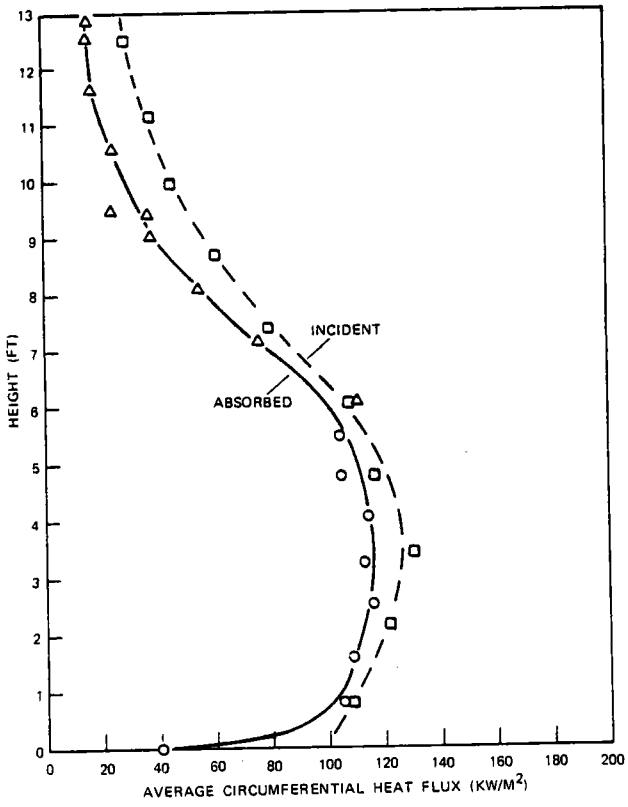

FIGURE 10 HEAT FLUX PROFILES

Adjusted circumferential average incident heat flux is plotted (Figure 10) along with the absorbed heat flux as determined above. The incident heat flux was obtained from raw data measured by the HI supplied flux boom. These data were averaged circumferentially for each flux sensor and adjusted by a constant of 0.780 so that the area summation of the incident flux would equal the net thermal output of the radiant array.

The agreement of the independently obtained incident and absorbed flux data supports the reliability of the measurement techniques.

TRANSIENT PERFORMANCE

Transient performance of the steam generator was evaluated by three types of tests: open loop, closed loop, and trip simulation. Open loop tests (controls are switched to manual, in steady-state, just prior to starting the transient) are used to determine the accuracy of the modeling of physical parameters defined by component masses, volumes, and interactions. Closed loop tests (automatic control throughout the transient) are used to evaluate the modeling of steam generator controls and determine the transient response of the steam generator system (complete with automatic controls). Trip simulations are used to verify expected behavior of the steam generator if critical plant or steam generator equipment trips or fails.

Open loop tests completed during the test sequence included a steam flow step, attemperator flow step, and an incident heat flux step. Of these three tests, the steam flow step was reviewed in detail and compared to pre-test predictions. The pre-test transient predictions were completed using a mathematical model developed to simulate the SRE steam generator.

Initial conditions of predicted and actual transients are compared in Table 3. Responses of the main steam flow, main steam pressure, primary superheater outlet temperature, and main steam temperature to the step change in steam flow are compared graphically in Figures 11 to 14* for the model predictions and actual tests. Predicted responses were normalized to the test initial conditions to make this comparison meaningful.

TABLE 3 MAIN STEAM TEMPERATURE (STEAM CONTROL VALVE STEP CHANGE)

INITIAL CONDITIONS

VARIABLE	PREDICTIONS	ACTUAL TESTS
FEEDWATER TEMPERATURE	400°F	475°F
POWER LEVEL (ABSORBED)	4.2 MW (100%)	3.02 MW (72%)
FLUX DISTRIBUTION	70% – BOILER 24.3% – FSH 5.7% – SSH	69.8% – BOILER 22.8% – FSH 7.4% – SSH
ATTEMPERATION FLOW	400. LBM/HR	0 LBM/HR

*The percentage change in steam flow indicated for each curve is the percentage of full load (4.2 MWt) steam flow.

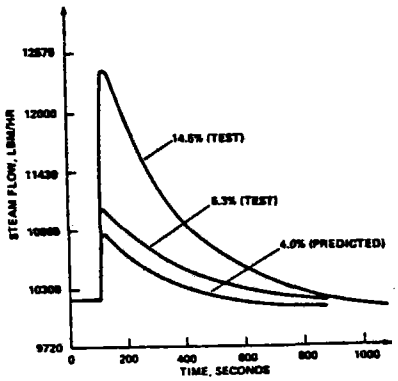

FIGURE 11 MAIN STEAM FLOW (STEAM CONTROL VALVE STEP CHANGE)

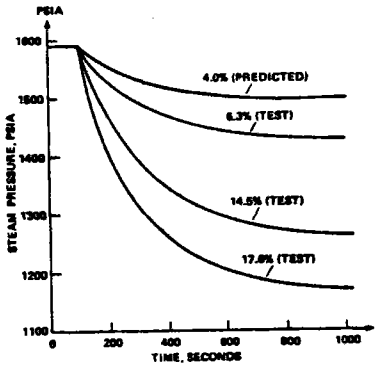

FIGURE 12 MAIN STEAM PRESSURE (STEAM CONTROL VALVE STEP CHANGE)

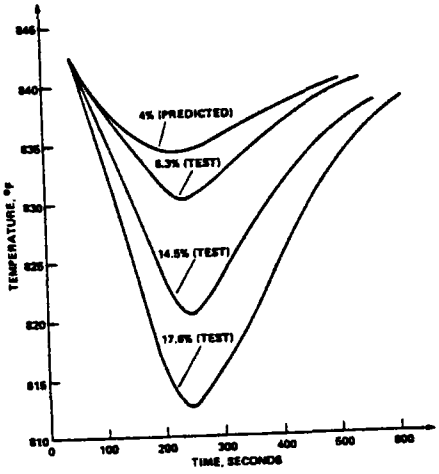

FIGURE 13 PRIMARY SUPERHEATER OUTLET TEMPERATURE (STEAM CONTROL VALVE STEP CHANGE)

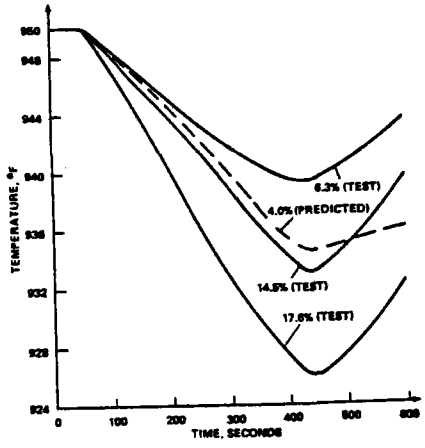

FIGURE 14 MAIN STEAM TEMPERATURE (STEAM CONTROL VALVE STEP CHANGE)

Differences in initial conditions for the predicted and test transients resulted in only slight discrepancies in the magnitude of reponses. The initial transient predictions made prior to testing were observed to have lower time constants or faster response than the actual tests. This was anticipated since the total boiler metal mass was not included in the model, resulting in insufficient boiler energy storage in the model. The model was then adjusted by adding the boiler metal mass producing the good agreement between data and predictions shown in Figures 11 to 14.

It is apparent that the transient model is a useful design tool. This type of modeling provides insight into the response of process variables and effective evaluation of operating control strategies.

Other transient performance tests completed during the program were a series of closed loop tests and trip simulation tests. Closed loop tests included a 9%/minute power ramp, boiler incident heat flux step, and total incident heat flux step. The steam generator was easily controlled during these tests. Trip simulation tests included a simulated heliostat trip, recirculation pump trip, and feedwater pump trip.

A cloud disturbance test involving a reduction from a high test power to zero and a subsequent restart after approximately 100 minutes was also completed. This test is also called a heliostat trip since it has the same effect as defocusing all heliostats (for protection from high winds, for example) but will not be referred to in that context for this discussion. The transient excursion is similar to what would occur if the entire heliostat field were cloud shadowed for a sustained period of time. During this time, the heliostats would remain in the focused position but no heat would reach the steam generator. When the cloud covering moved away, a very rapid restart would occur (since the field remained focused). The incident and absorbed power input over time for this test is shown in Figure 15. Responses of flow rates, drum level, pressures, fluid temperatures, and metal temperatures are displayed graphically (Figures 16 to 20). These graphs were plotted by the data acquisition system X-Y plotter. After the plots were made, the feedwater and steam flowmeter calibrations were corrected requiring that correction factors be applied to the absorbed power, feedwater flow, and steam flow curves shown in Figures 15 and 16.

The smooth, controlled shutdown and rapid but controllable restart of the steam generator demonstrates that it is responsive and controllable.

CONCLUSIONS

Testing of the SRE steam generator indicates its performance is reliable, predictable, controllable, and responsive. This conclusion is supported by the data presented above. The success of the SRE steam generator supports the premise that fossil boiler technology forms a basis for a successful solar steam generator design.

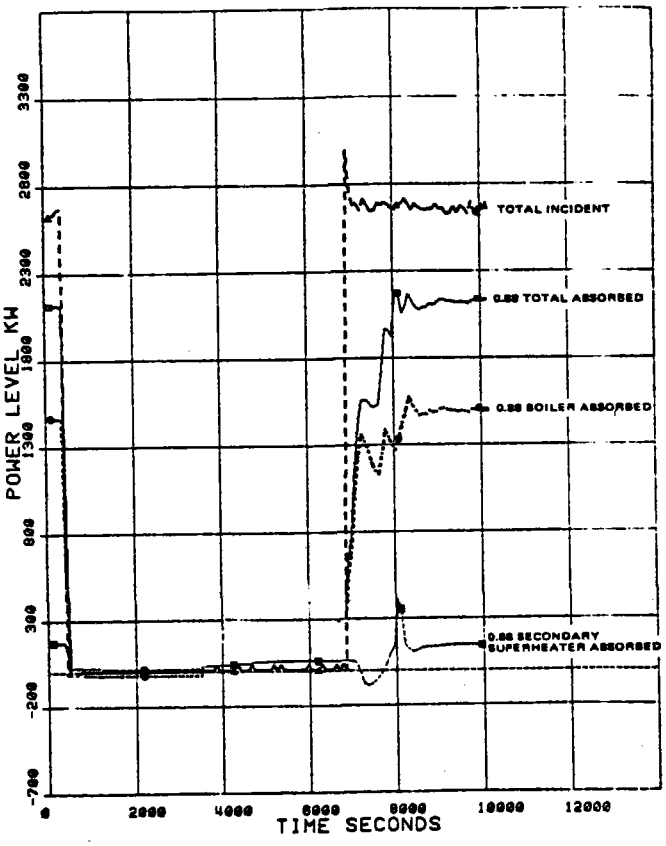

FIGURE 15 CLOUD TRANSIENT POWER INPUT

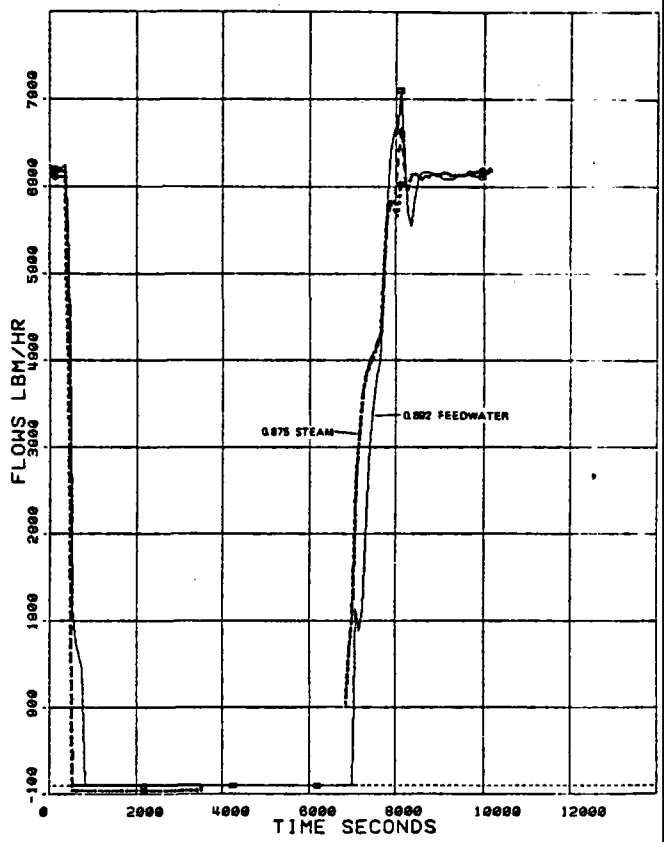

FIGURE 16 CLOUD TRANSIENT FLOW RESPONSE

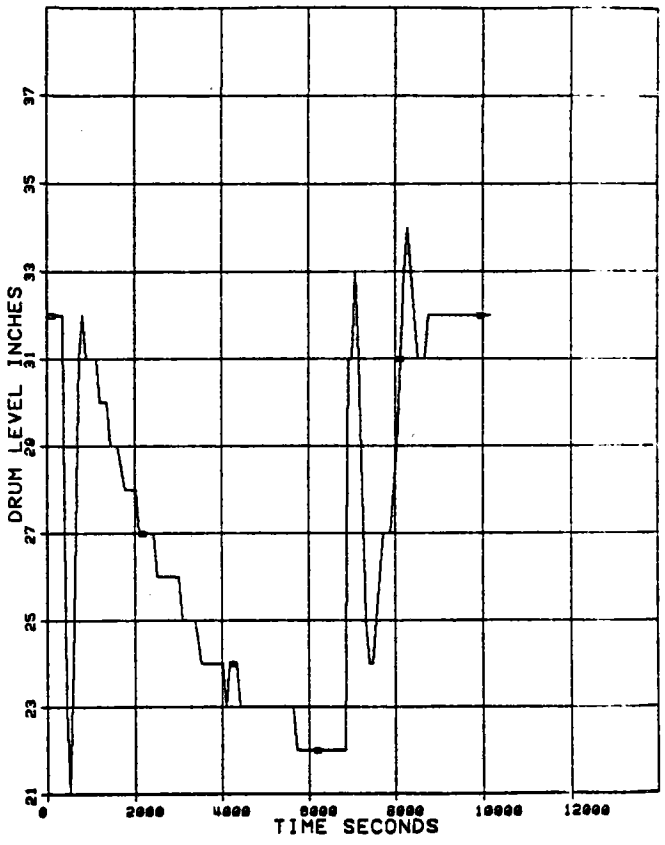

FIGURE 17 CLOUD TRANSIENT DRUM LEVEL RESPONSE

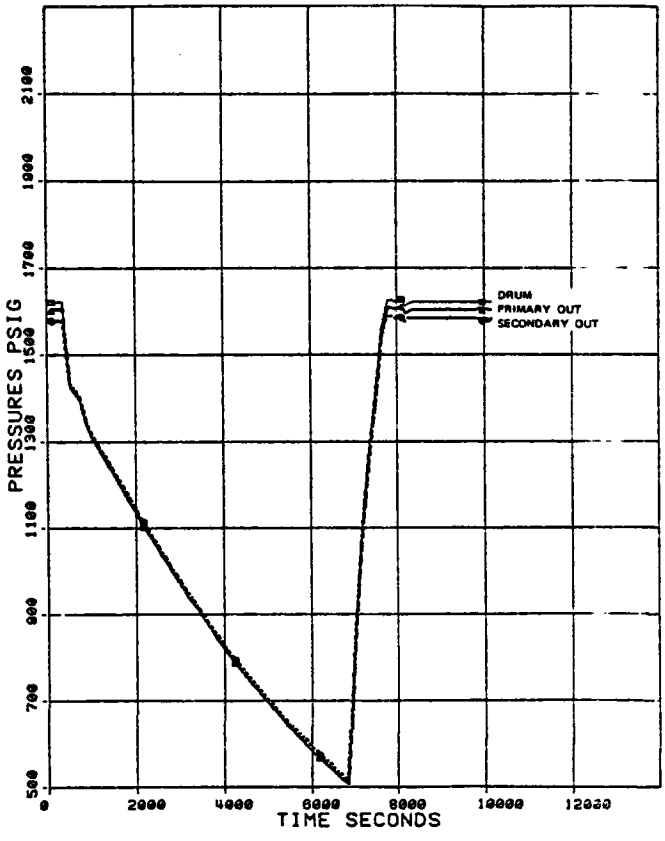

FIGURE 18 CLOUD TRANSIENT PRESSURE RESPONSE

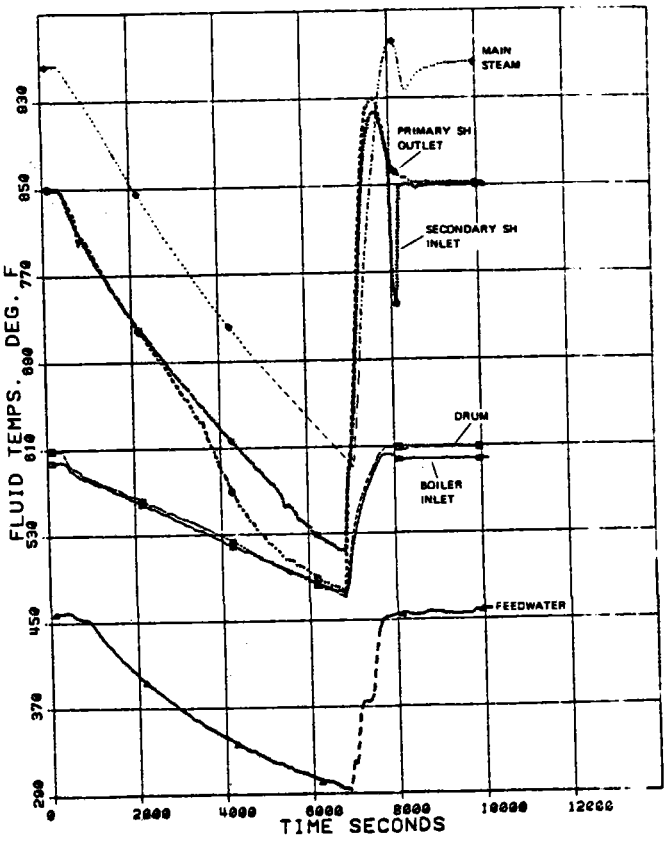

FIGURE 19 CLOUD TRANSIENT FLUID TEMPERATURE RESPONSE

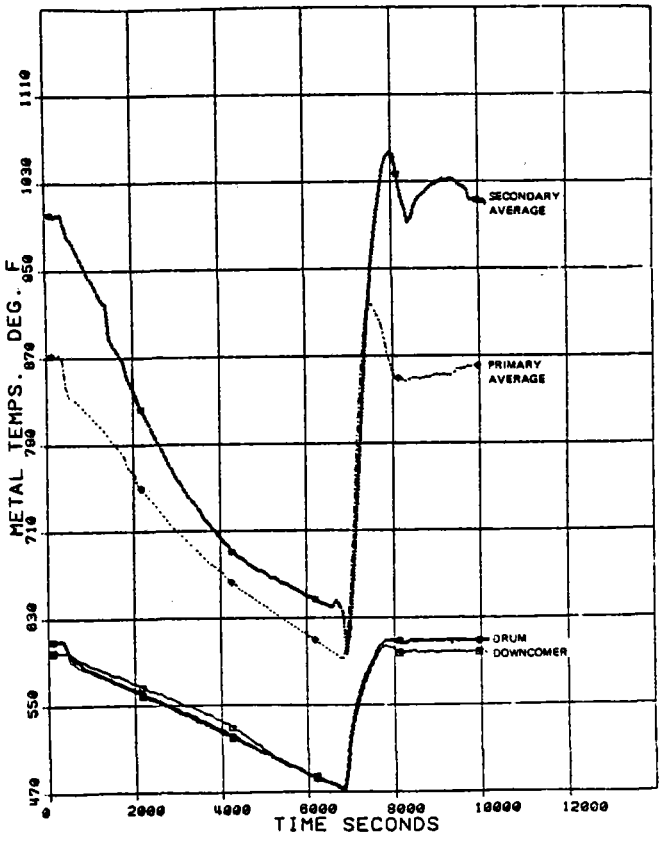

FIGURE 20 CLOUD TRANSIENT METAL TEMPERATURE RESPONSE

LA-UR - 78-606

TITLE: NIGHT STORAGE AND BACKUP GENERATION WITH ELECTROCHEMICAL ENGINES

AUTHOR(S): Guy R. B. Elliott
N. E. Vanderborgh

SUBMITTED TO: Talk and paper to be given at the Solar Thermal Test Facilities Users Association Annual Meeting, April 11, & 12, 1978.

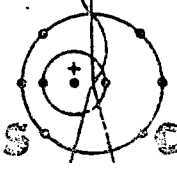

los alamos
scientific laboratory
of the University of California
LOS ALAMOS, NEW MEXICO 87545

DEVELOPMENT ADMINISTRATION
CONTRACT W-7405-ENG. 36

NIGHT STORAGE AND BACKUP GENERATION WITH ELECTROCHEMICAL ENGINES*

by

Guy R. B. Elliott

N. E. Vanderborgh

Los Alamos Scientific Laboratory
Los Alamos, NM 87545

ABSTRACT

Li/I_2 electrochemical engines both store and generate electric power. These dual capabilities complement solar photovoltaic generation in critical areas: Photovoltaics need backup storage at least for nights and, if possible, for two or three days' needs. Such storage must be relatively cheap and compact--aqueous batteries would have trouble filling these requirements. Likewise, photovoltaics need backup generation based on combustion of fossil fuels for periods of bad weather -- solar residences or communities will probably have to supply their own backup generation because central generating stations cannot be expected to keep large amounts of equipment on standby for solar users.

This paper describes Li/I_2 engine designs which could be developed to fill these needs of solar users, i.e., storing electricity generated by photovoltaics and generating additional electricity from fossil fuels as needed. Calculations based on laboratory performance indicate that the devices could be simple to manufacture, economically competitive, and efficient both in storage and generation.

These engines also could directly use solar energy from focused and tracking solar collectors, or they could indirectly use solar energy through the combustion of biomass materials.

*This work was supported by the U. S. Department of Energy.

Night Storage and Backup Generation with Electrochemical Engines

Guy R. B. Elliott
and
N. E. Vanderborgh

INTRODUCTION

Practical photovoltaic conversion systems will have to be used in association with devices which generate power during periods of low solar flux and which store power for nighttime use. No satisfactory devices of either type are now available for solar homes or for solar communities.

The lithium/iodine electrochemical engines of this presentation do offer both functions in a single, simple device. These electrochemical engines can efficiently generate power over a temperature gradient of roughly 350°C (625K) to ambient, and they can operate with less efficiency from 200°C (475K) to ambient. These same engines can (by simple and rapid switching operations) be converted into efficient molten-salt batteries which operate in the temperature range above. As such they have large storage capacities and can be charged by external electric power sources.

For generator operations during periods of bad weather or when power usage is especially heavy and extra power is needed, electrochemical engines would typically burn fossil fuels (gas, butane, fuel oil, etc.) to maintain the temperature gradient necessary to convert heat to electrical power.

The electrochemical engines offer two other approaches to the generation of electrical power based on solar energy--they could be heated by focused direct solar energy, or they could be heated by combustion of biomass materials which come from sunlight.

ORGANIZATION OF THIS PAPER

We first describe briefly how electrochemical engines act to convert heat energy to electrical energy. Next we discuss laboratory performance of electrochemical engines based on the Li/I_2 chemical system. Finally we calculate expected performance of particular Li/I_2 electrochemical engines used for storage and for each solar-to-electric conversion path mentioned above.

THE CONCEPT OF ELECTROCHEMICAL ENGINES

The driving force of electrochemical engines is the pressure dependence of gas-phase reactions. This dependence is described closely by mass action relationships. Thus for a general Reaction 1A in which liquid A reacts with gas B to form a liquid C, or its reverse Reaction 1B,

$$A_{(1)} + B_{(g)} = C_{(1)} \tag{1A}$$

$$C_{(1)} = A_{(1)} + B_{(g)} \tag{1B}$$

a high pressure of $B_{(g)}$ will favor Reaction 1A while a low pressure of $B_{(g)}$ will favor Reaction 1B.

Electrochemical engines use such reactions as the net electrochemical steps in cells of high temperature batteries. The cells are discharged by Reaction 1A at a high pressure of $B_{(g)}$, and they are charged by Reaction 1B at low pressure of $B_{(g)}$. The pressure of $B_{(g)}$ is controlled by the temperature of an independently heated condenser in which $B_{(g)}$ can be removed from or supplied to the cell region.

Lithium/Iodine Electrochemical System

If the reaction

$$2Li_{(1)} + I_{2(g)} = 2LiI_{(1)} \tag{2}$$

takes place in an electrochemical cell, the Gibbs free energy, ΔG, of the process can be extracted as maximum electrochemical work. At a temperature where I_2 is volatile, the free energy and the voltage ε will be given by

$$\Delta G = -nF\varepsilon = \Delta G^\circ - RT \ln (f_{I_2}/f^\circ_{I_2})$$

$$= \Delta G^\circ - RT \ln P_{I_2} \tag{3}$$

where the gas fugacity, f, is assumed equal to pressure, P, and where the reference fugacities are for 1 atm of iodine and for the condensed phases of the other reactants and products.

Figure 1 shows a schematic drawing of a cell which could be used to carry out the lithium/iodine reaction. Such prototype cells are in laboratory studies.

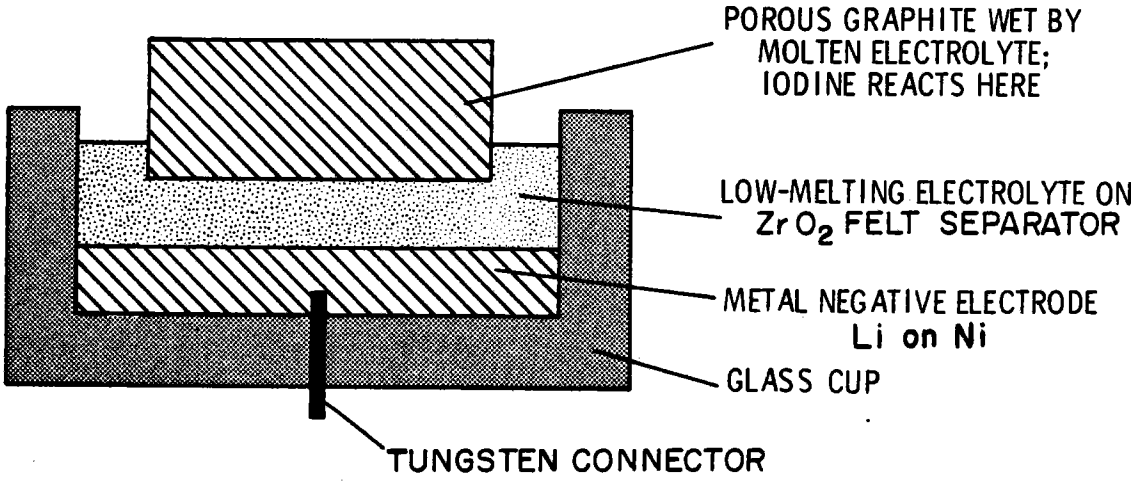

Fig. 1: Laboratory cell of lithium/iodine electrochemical engine.

In the figure a Pyrex cup with tungsten electrical connector holds three layers of material. The top layer is a porous-graphite disk on which the iodine reacts. The middle layer is a porous insulator of zirconia felt; this felt supports the graphite disk and rests on a bottom layer of porous nickel felt wet with molten lithium. A molten electrolyte containing LiI (plus other salts to lower its melting point) wets into void spaces in all three layers -- the lower layers are filled with electrolyte, and electrolyte partially fills the porous graphite by capillary action.

Electric power can be supplied by the cell by connections to the lithium-nickel felt-tungsten rod (negative electrode) and to the iodine-porous graphite electrode (positive electrode). The open circuit (no-drain) voltage of such a cell is calculable from thermodynamic data as in Eq. 3. Values for ΔG° at elevated temperatures are available from the JANAF Tables.

For a pressure of 1 atm of I_2 and a cell temperature of 625 K

$$-46{,}122\ \varepsilon_{(1\ atm)} = -121{,}800 - 4.575\ (625)\ \log 1$$

$$\varepsilon_{(1\ atm)} = 2.64\ \text{volts} \qquad (4)$$

For 20 atm (v.p. of I_2 at 625 K)

$$\varepsilon_{(20\ atm)} = 2.72\ \text{volts} \qquad (5)$$

and for 0.000405 atm (v.p. of I_2 at room temperature)

$$\varepsilon_{(0.000405\ atm)} = 2.43\ \text{volts} \qquad (6)$$

Laboratory Li/I_2 Electrochemical Engines

If cells are stacked and sealed into two evacuated, Pyrex, cell-stack units as shown in Fig. 2, then an electrochemical engine is formed. Here two identical cell-stack units are placed in electrical opposition by joining the positive junction of one unit to the positive junction of the other unit. Power can be drawn from the two negative leads if one condenser is cooled.

If the temperature in both condensers is the same, no net voltage is developed across the negative electrodes and no current flows. The individual (and opposing) voltages are given above. For T_1 = 625K the opposing emfs are 2.72 volts (Eq. 5) per cell or 16.32 volts per cell-stack unit for these conditions.

If one condenser is cooled to T_2 = 298 K, the pressure of iodine vapor in that unit will drop to 4.05×10^{-4} atm, and the emf will be 2.43 volts (Eq. 6) per cell or 14.58 volts from the cell-stack unit.

At this point the two units act as an electrochemical heat engine. As current flows, one unit is discharged and the other is charged. The net reaction per two Faradays of electricity generated is

$I_2(P_1,T_1,$ hi T condenser$) \rightarrow I_2(P_2,T_2,$ lo T condenser$)$

Li(side of hi T condenser) $\rightarrow$ Li(side of lo T condenser)

LiI(side of lo T condenser) $\rightarrow$ LiI(side of hi T condenser)

where Li and LiI remain at T_1 at all times and at essentially constant activity.

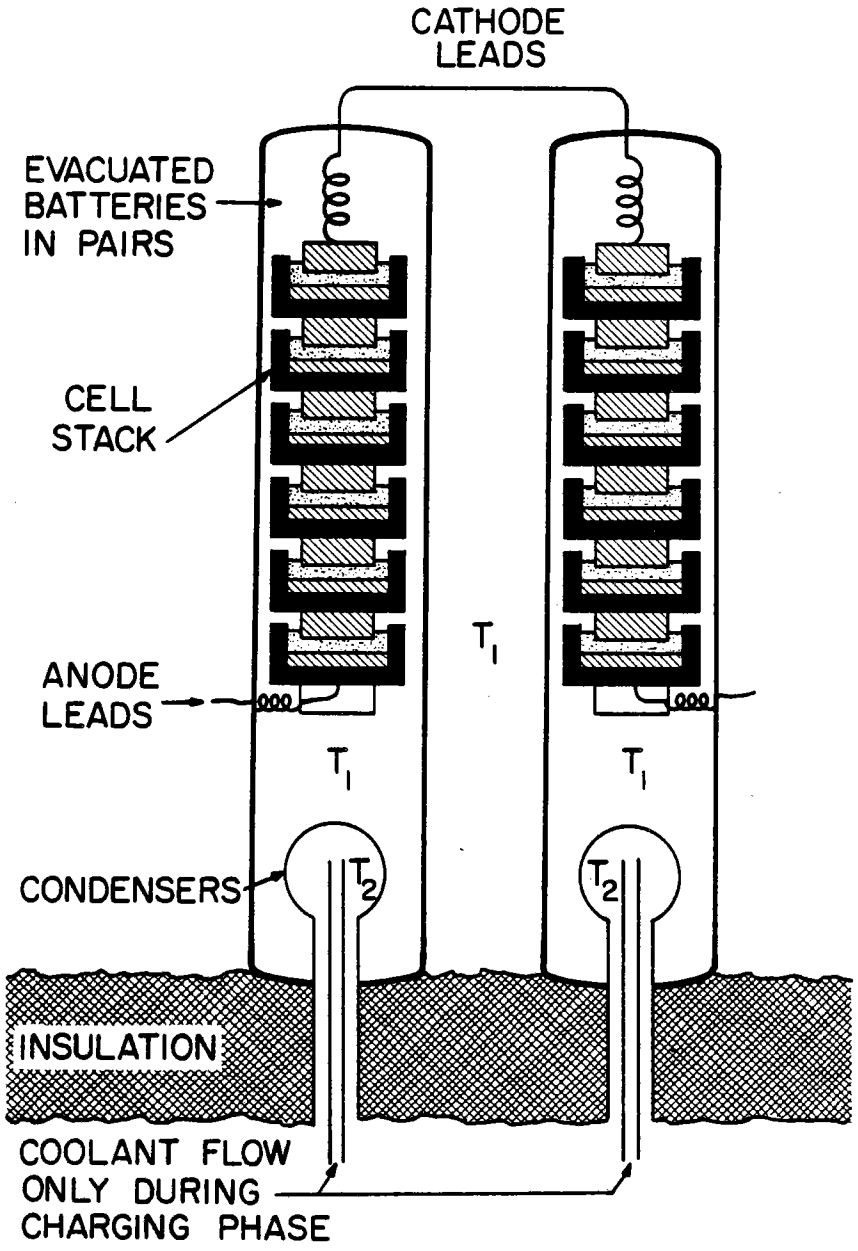

Fig. 2. Laboratory electrochemical engine with two cell-stack units of six cells each.

At very low drain the net emf will be 2.72-2.43 = 0.29 volts per cell pair or 16.32-14.58 = 1.74 volts from the two units which make up one electrochemical engine.

The electrochemical engine cycle starts with one fully charged cell-stack unit with (condenser) T_2 = 625 K and one fully discharged unit with T_2 = 298 K. Then, when the high voltage side has completely discharged, the low voltage side is completely charged. At this point the cold condenser is heated, the hot condenser is cooled, and current flows in the opposite direction (requiring an external switching to maintain the proper current direction). At the end of two such half cycles, the engine will be in its initial state, but net conversions of heat to electrical energy will have been accomplished.

(This behavior is consistent with Carnot limitations--the ΔH of vaporization of I_2 is supplied at the high temperature and the ΔH of condensation is discharged at low temperature, and this limits the efficiency of conversion.)

In addition to generating electric power, these cell-stack units can (by breaking the electrical connection between the two-cell stack units) each be used separately as an energy storage device. The voltage required to charge such a storage device is greater than 2.72 volts times the number of cells in a stack.

Experimental Behavior of Li/I_2 Electrochemical Cells and Engines

The experimental behavior of prototype cells using lithium and iodine with a molten electrolyte containing LiI is consistent with the theory mentioned earlier. Voltages in Eqs. 4 and 6 are found experimentally.

Experimental Li/I_2 cells have shown very small internal resistances, as low as 0.8 ohm/cm^2. Internal resistances are constant over wide current densities from 0.25 amps/cm^2 drain to 0.80 amps/cm^2 of charge. Such remarkable behavior could only be found in fused salt solutions.

On the basis of thermodynamics and the experimental performance, one can calculate the expected performance from commercially scaled models of these Li/I_2 electrochemical engines. Such estimates conclude this paper.

A POSTULATED COMMERCIAL Li/I_2 ELECTROCHEMICAL ENGINE

The Cell Design

Fig. 3 is a promising cell design suitable for mass production. Five different types of solid parts of the cell are shown. Electrolyte will be added after assembly into cell-stack units; the liquid and gaseous cell reactants will be formed at the generating station by electrolysis. Consequently handling of potentially hazardous chemicals (lithium metal and molecular iodine) will be eliminated.

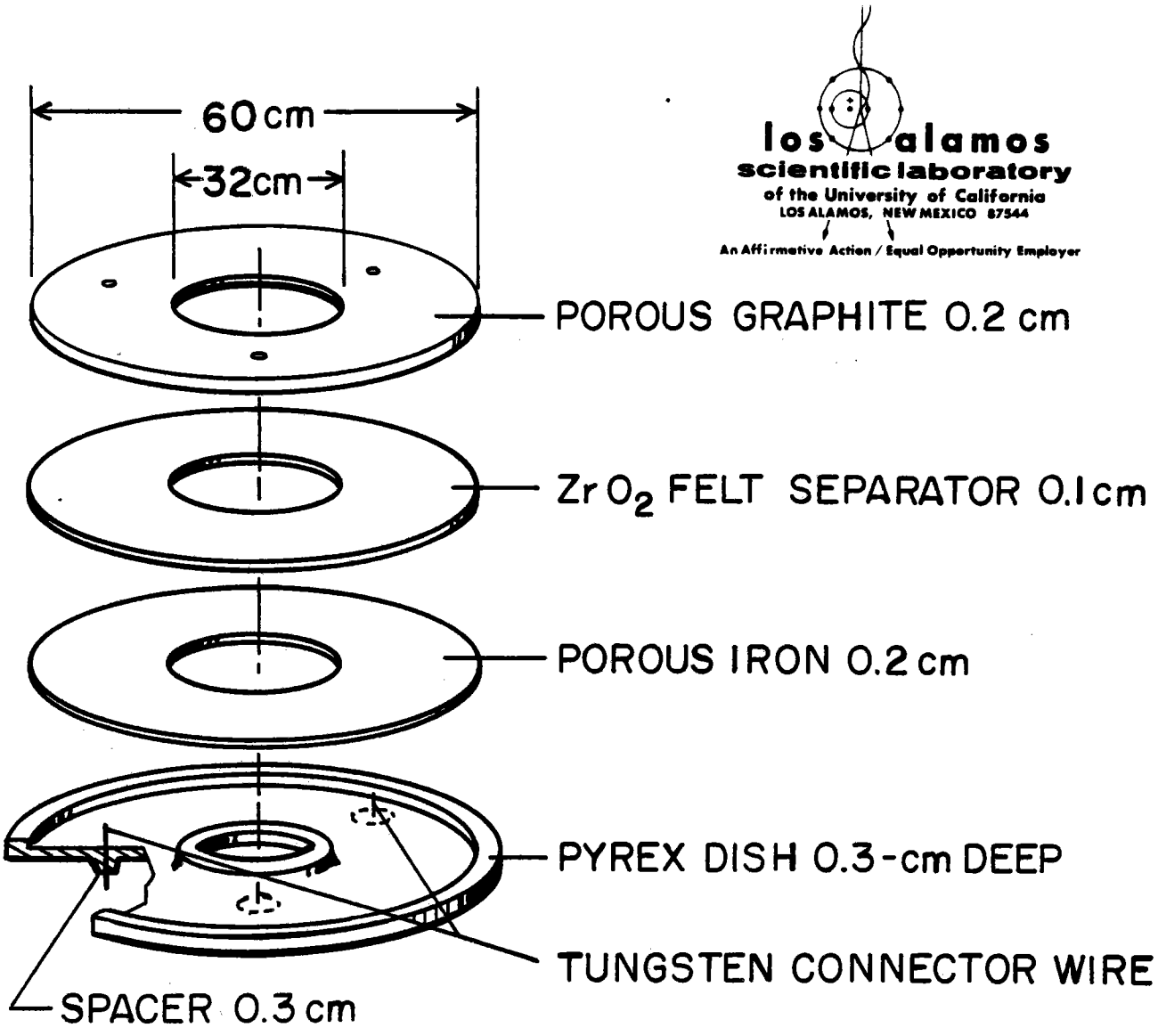

Fig. 3: Postulated commercial design of Li/I_2 electrochemical engine cells.

The top thin disk of porous graphite serves as the positive electrode. It has large electrode surface area, and it is thin to provide rapid iodine transport. This porous graphite has two sharply different pore-size ranges, thereby allowing capillary action to wet the electrode like a half-filled sponge. Because of the partial filling and different pore sizes, the same region of the cell has continuous paths for vapor movement, for electrolyte conduction, and for electronic conduction (graphite).

Next is the separator. ZrO_2 felt is indicated, but other materials may do as well. We find ZrO_2 is not significantly attacked by metallic lithium.

Below the separator is the negative current collector. This porous metal disk transports electrons. At present the current collector is made from sintered iron. Perhaps nickel coating to improve the wetting characteristics by the lithium will be necessary.

At the bottom are additional solid parts, a Pyrex cup and tungsten connector wires. The Pyrex cup holds the cell components and acts as a liquid electrolyte reservoir. The tungsten connector wires (tungsten is not corroded by iodine vapor) serve two purposes: First, they connect the negative electrode of one cell to the positive electrode of the next cell below in the stack. Second, they act as spacers to maintain unrestricted vapor transport.

These cells have an area of 2000 cm^2, an OD of 60 cm, an ID of 32 cm, and a thickness of 1.5 cm, including the spacers. The hole is included for heat-transfer purposes.

One hundred cells are stacked in a double cylindrical container made from protected steel. The cells touch the outer cylinder, but the inside cylinder (25-cm OD) is smaller than the holes in the cells. This construction allows heat to be supplied to the outside region while the inside region is cooled by air flow and serves as a condenser, and the space between the cells and the condenser presents unrestricted vapor paths. An open region below the cells serves as the I_2 reservoir.

When the construction of the cell-stack unit is essentially complete, the unit is dipped into a bath of molten electrolyte, then drained, thereby filling the cells with electrolyte. Finally, the cell-stack units are evacuated and sealed.

Once sealed, a cell-stack unit is not opened again.

The Cell-Stack Unit

Fig. 4 shows a cell-stack unit design.

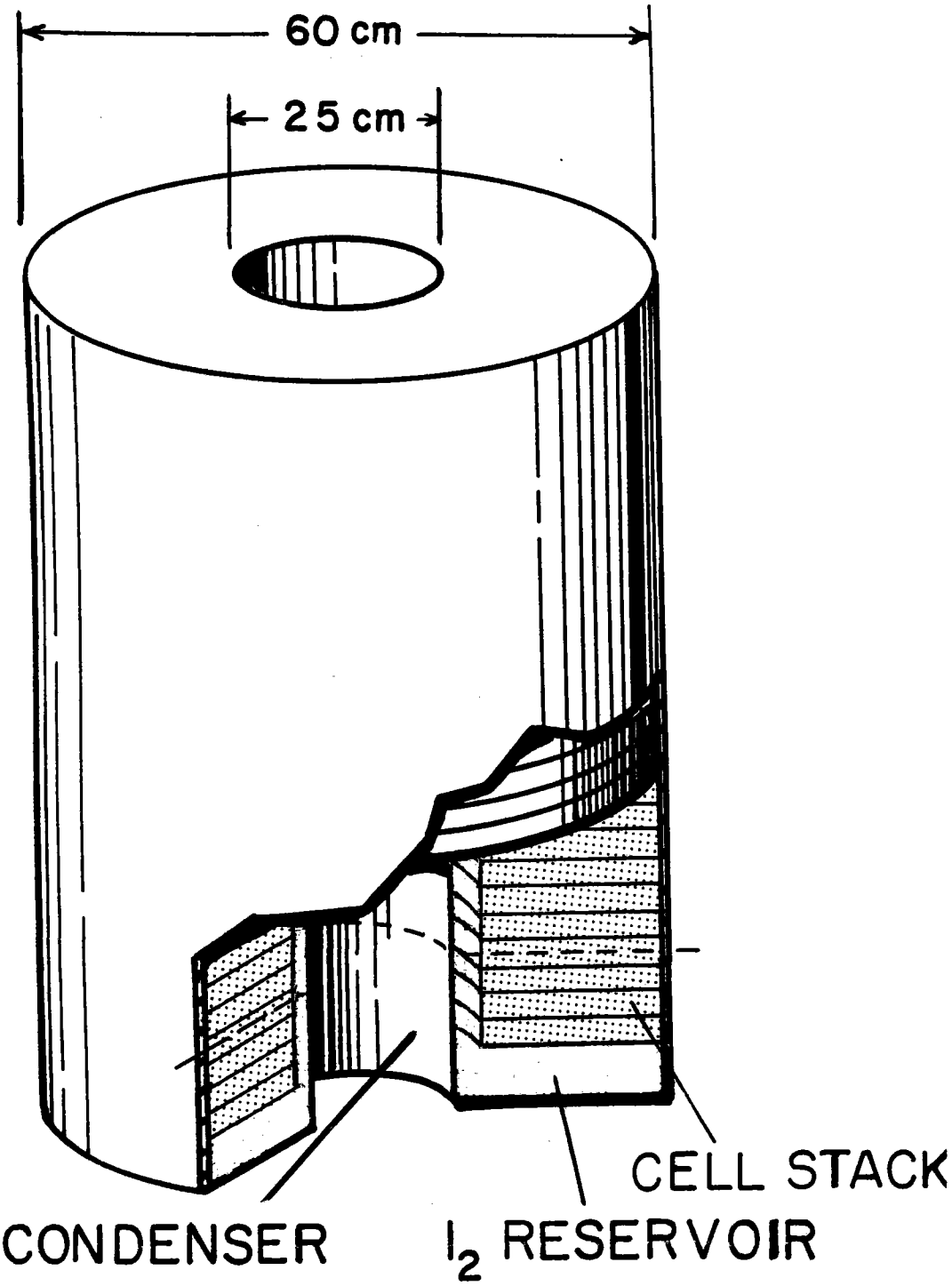

Fig. 4: A cell-stack unit of the postulated electrochemical engine design. (The dashed line indicates that the lower section of a cell stack could be electrically separated to act solely as a storage battery if that were desired.)

The Li/I_2 Electrochemical Engine Design

Fig. 5 shows our concept for the electrochemical engine design which will be useful with solar power. The device shown is one cell-stack unit installed in its insulating cover with provision for the heating and cooling necessary for operation. Two such units are needed for one electrochemical engine, see above.

Storage

For electrical storage, both fans are off, both vent doors are closed,and heat is supplied to maintain the operating temperature. We assume a temperature of 625K for the storage operation.

The calculated storage efficiency is high. For a 100-cell unit which drained 40 amps through 2000-cm^2 cells at 272 volts open circuit with a specific resistance of 0.8 ohm-cm^2, the internal voltage drop would be 100(40/2000)(0.8) = 1.6 volts. Even if we allow for concentration polarization during both charging and discharging and for limited self-discharge, the actual storage efficiency should still be over 95%.

The unit can store 40 KWH of electrical energy with a change of less than 1 mm in the depth of the electrolyte in the cells.

Generation

For generator operation one unit is maintained at 625K throughout by externally supplied heat. This is the discharge unit. The second unit will be heated more strongly to maintain the temperature while the unit does electrochemical work as charging occurs. Here the fan will circulate cooling air (cooled by a water wick in summer) through the condenser with the vent door open.

At small drains the discharging unit will generate 100(2.72) = 272 volts, and the charging unit will require 100(2.43) = 243 volts. A net gain of 272-243 = 29 volts is available to do external work.

Allowing for the specific internal resistance of 0.8 ohm-cm^2, and draining 50 amps through 2000 cm^2 in each of 200 cells will reduce the 29 volts by 0.8(50/2000) = 0.02 volts per cell or 4 volts overall. In addition there will be some concentration polarization over what we measured in our experiments (which were for short terms) as the cells are charging or discharging. Our present experimental data do not allow us to calculate this effect accurately, but it is probably adequate to estimate this loss as 4 volts overall.

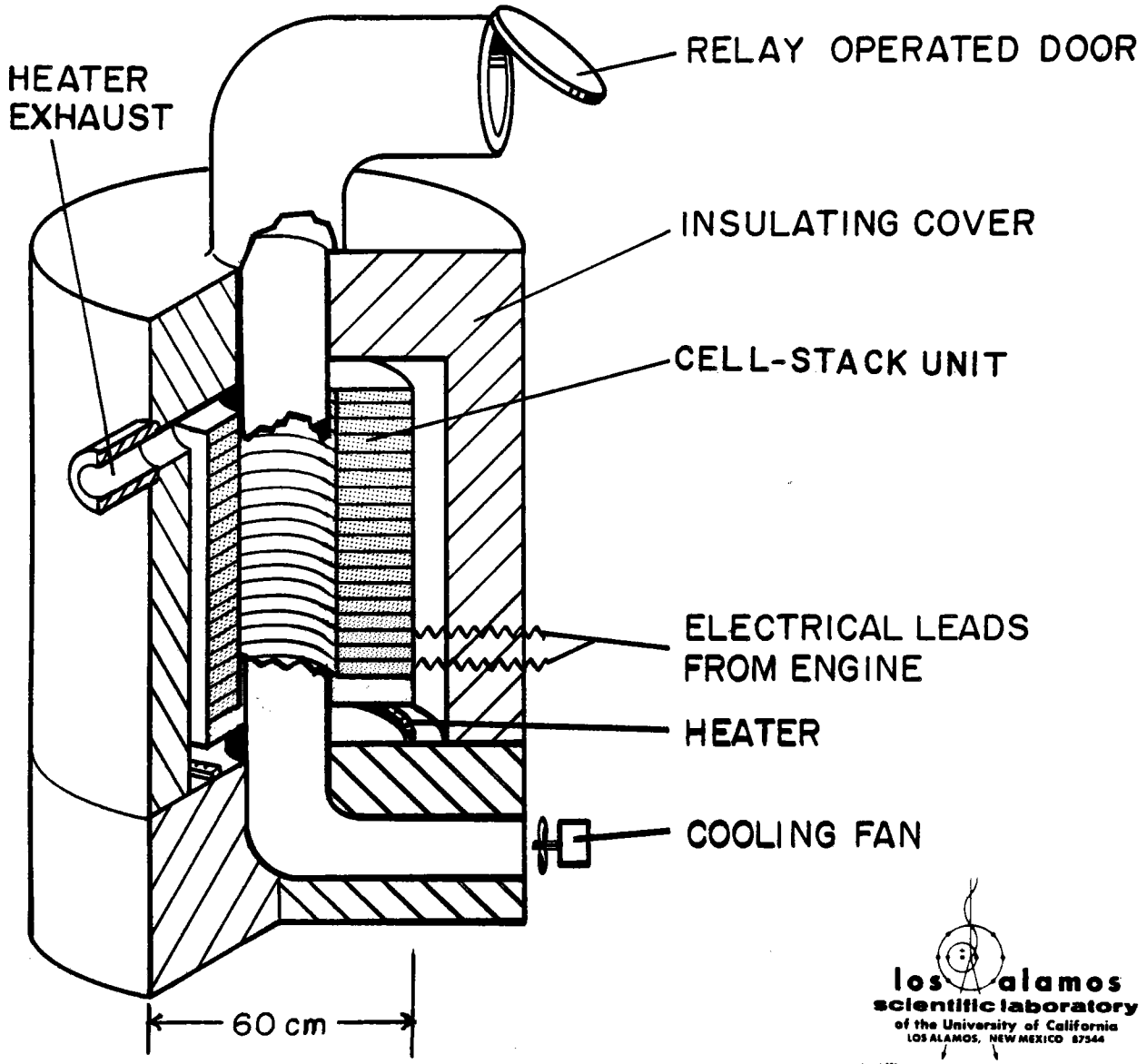

Fig. 5: Li/I_2 Electrochemical Engine Unit. (At least two are used together.)

This method of operation would produce 50(29-4-4) = 1.1 KW or 25 KWH per day. Considering the Carnot efficiency (625-300)/625 = 52%, the internal resistance and concentration effects (29-4-4)/29 = 72%, and the portion of the heat of air combustion of natural gas which can be delivered at 625K, i.e., 85%, leads to a very respectable energy conversion figure of 32% for gas heat of combustion to electric power at the busbar.

If more rapid power generation were required, the unit could put out 1.3 KW at a lowered efficiency of around 26%.

With more than two-days' worth of energy generation stored in one cell-stack unit, the charging-discharging roles of the two cell-stack units need switching only after about two days. To supply power during switching periods, and to level the home power usage load, an additional battery would undoubtedly be installed parallel to the home usage load. The load-leveling batteries could be incorporated as sections of the electrochemical engine's cell stacks and are not discussed additionally.

THE USE OF ELECTROCHEMICAL ENGINES WITH PHOTOVOLTAICS

Perhaps the most ideal combination for solar-powered electricity generation is photovoltaics and electrochemical engines. Here the photovoltaics operate in diffuse or direct sunlight, and the electrochemical engines supply the needed storage and backup generation.

The present electrochemical engine design allows storage of 80 KWH total in the two cell-stack units. This 80 KWH is four-days' supply for a home using 600 KWH per month. If one were sure that good weather was on the way, all this stored energy could be used, but usually one would not discharge more than one cell-stack unit (40 KWH) because the charge in the other unit would be needed to start backup generation if the bad weather continued.

In the longer periods of bad weather, the electrochemical engine would be used in the fossil-fueled generation mode to supply 1.1 KW or 25 KWH per day.

We estimate the cost of this electrochemical engine (two cell-stack units) to be well under $1000 with mass production, not including those chemicals which can be recovered. Both lithium and iodine could eventually be transferred into a new engine. Neither is consumed during extended periods of use.

Significant improvements in service could be effected if one hundred electrochemical engines of this design were operated jointly to serve a solar community.

FOCUSING SOLAR COLLECTORS WITH ELECTROCHEMICAL ENGINES

If solar photovoltaics must turn to major focusing and solar tracking, then the possibility of operation in diffuse sunlight is lost. In that case focusing solar energy onto a heat pipe which supplies an electrochemical engine is clearly superior. Here a single device has three functions: solar electric generation, storage, and backup fossil-fueled generation.

The 625K used in the preceding calculations could be supplied by tracking Fresnel lenses. Tracking trough collectors such as the Winston collector would also be possible for use with Li/I_2 electrochemical engines.

COMBUSTION OF BIOMASS TO HEAT ELECTROCHEMICAL ENGINES

When Li/I_2 electrochemical engines burn fuel, they are external combustion engines which do not require high-grade heat. In the present design they can operate by burning liquid or gaseous fuels, and even solid fuels can be used if a furnace is attached.

The calculation of electrochemical engine efficiencies with combustion of methane fuel was given two sections earlier in this paper. The generation efficiency with lower-grade fuels often would be slightly lower, e.g., perhaps 25% in converting heat available to electric power. For example, the conversion efficiency with combustion of dry cellulose would be about 26% where methane gave 32%.

SUMMARY

Li/I_2 electrochemical engines look promising for solar-to-electric conversion applications both in connection with photovoltaics and alone with focused solar collection and with combustion of biomass materials.

THERMOELECTRIC ENERGY CONVERSION WITH THE SODIUM HEAT ENGINE

Terry Cole, Neill Weber and T. K. Hunt
Research Staff
Ford Motor Company

The Sodium Heat Engine (SHE) is a new device for direct thermoelectric energy conversion. It uses the ionically conducting ceramic, β"-alumina to form a high-temperature concentration cell for elemental sodium. The vapor pressure (activity) gradient across the cell is maintained by a high-temperature heat source on one side of a β"-alumina membrane and a low-temperature condenser on the other side. The high-temperature (T_2) region operates in the range of 600-1000^{o}C with the low-temperature (T_1) region at 100-200^{o}C.

Theoretical analysis of the SHE shows that under quasi-reversible conditions the efficiency should be more than 90% of Carnot efficiency. For typical operating conditions of T_2 = 800^{o}C, T_1 = 100^{o}C, a specific power output of 0.7 watt/cm^2 has been achieved in test electrodes. If certain design criteria involving parasitic heat losses can be met, the SHE should achieve overall thermal efficiency in the range of 20-40% at a power output of 1 watt/cm^2. The efficiency of the SHE is virtually independent of its size. The device will accept heat from any source including solar collectors, has no moving parts, and is made from readily available materials.

Introduction

The Sodium Heat Engine (SHE) is a novel device capable of the direct conversion of heat into electrical energy. The SHE operates continuously as a concentration cell with the required concentration gradient maintained by the input heat source and output heat sink. In operation, sodium is expanded nearly isothermally through a beta-alumina solic electrolyte with electrical energy being extracted during the process. Theoretical analyses, combined with the measured parameters of operating sodium heat engines, predict an overall thermal-electrical conversion efficiency of 25-30% at 800^{o}C for single cells. These calculations use component performance levels already achieved and do not assume additional bottoming cycles. The operating characteristics of the SHE, especially its high efficiency in small sizes, make it well suited for the local generation of electric power from chemical fuels or from concentrated solar energy, in a total energy system. Preliminary calculations of the overall efficiency of a central power station utilizing a SHE as a topping cycle show that for presently available design parameters a SHE conversion efficiency of 15-20% should be possible with the SHE operating between an upper temperature of 900^{o}C and a lower temperature of 500^{o}C.

The fundamental operating principles of the SHE have been described in detail in previous papers.[1,2] A brief summary of these principles is presented here. Figure 1 shows a schematic diagram of the SHE. A closed container is partially filled with liquid sodium working fluid and is physically divided into high- and low-pressure regions by a pump and a tubular membrane of solid electrolyte which bears a porous metal electrode. The inner section of the device is maintained at a temperature T_2 by a heat source while the outer section is maintained at temperature T_1 ($T_2 > T_1$) by a heat sink. The temperature differential between the two regions gives rise to a sodium vapor pressure differential across the solid electrolyte membrane.

During operation sodium travels a closed cycle through the device. Starting in the high-temperature (high-pressure) region, the heat source raises the incoming liquid sodium to temperature T_2. Since β"-alumina has high conductivity for sodium ions and negligible electronic conductivity, a mole of electrons must exit the high-temperature zone for each mole of sodium ions entering the β"-alumina. Sodium ions then migrate through the β"-alumina membrane in response to the pressure differential (gradient of Gibbs free energy). After passing through the external load, the electrons are recombined with sodium ions at the porous electrode-solid electrolyte interface. Neutral sodium then evaporates from the porous electrode at pressure P_1 and temperature T_2 passing through the vapor space to the condenser at temperature T_1. The condensed liquid sodium is then returned to the high-temperature zone by an electromagnetic pump completing the cycle.

The processes occurring in the solid electrolyte and at its interface are very nearly equivalent to an isothermal expansion of sodium from pressure $P_v(T_2)$ to $P_v(T_1)$ at temperature T_2. Thus, the SHE is in effect a continuous concentration cell for sodium.

Analysis of SHE Operation

A thermodynamic analysis of an idealized device in which extraneous heat leaks from hot to cold reservoir have been ignored shows that

the open circuit (zero-load) efficiency exceeds 90% of the Carnot efficiency. The efficiency of the SHE is the quotient of the net work output divided by the heat input. The output, under quasi-equilibrium conditions, consists of the work (W_1) done by isothermal expansion of the sodium from $P_v(T_2)$ to $P_v(T_1)$, less the work necessary to recirculate the liquid sodium W_2. The heat input per mole of sodium circulated includes the isothermal expansion work W_1, the heat of vaporization of sodium (L) and the enthalpy of sodium $\Delta H \cong C_p(T_2 - T_1)$. Thus the efficiency

$$\eta = \frac{W_1 - W_2}{W_1 + L + \Delta H} \tag{1}$$

The following simplifying assumptions are made

(a) $$W_1 \gg W_2 \tag{2}$$

(b) Sodium behaves as a perfect gas, so the expansion work is given by

$$W_1 = RT_2 \, \ell n \left[P_v(T_2)/P_v(T_1)\right] \tag{3}$$

where $P_v(T_2)$ and $P_v(T_1)$ are the vapor pressures in the high- and low-pressure regions and R is the gas constant.

(c) The Clausius-Clapeyron equation describes the temperature dependence of Na vapor pressure

$$\ell n \left[P_v(T_2)/P_v(T_1)\right] = \frac{L}{R}\left[(T_2 - T_1)/T_1T_2\right] \tag{4}$$

Using (2), (3) and (4) the efficiency may be expressed in terms of the Carnot efficiency $\eta_c = (T_2 - T_1)/T_2$,

$$\eta = \frac{\eta_c}{1 + (\eta_c T_1 C_p/L)} \tag{5}$$

Eq. (5) gives a SHE efficiency of 46% for T_2 = 1000K and T_1 = 500K for which the Carnot efficiency would be 50%. Eq. (5) also shows that for this class of device, good efficiency is obtained by choosing a working fluid with a small value of C_p/L. For sodium $C_p/L = 3.4 \times 10^{-4}\ K^{-1}$.

The open circuit voltage is derived directly from Eq. (3) and is

$$V_{oc} = \frac{RT_2}{F} \ell n \left[P_v(T_2)/P_v(T_1)\right] \qquad (6)$$

where F is the Faraday. This is the Nernst equation for a concentration cell, with pressure in place of activity or concentration.

A small correction to Eq. (6) is appropriate in the present case for which $P_v(T_1)$ is sufficiently small that atoms leaving the porous electrode and bound for the condenser and vice-versa make on the average no equilibrating collisions in the intervening space. For this case, which is of general application for the SHE, the Langmuir assumption (that the effective pressure at a surface is that pressure which would give a condensation rate from the saturated vapor equal to the evaporation rate at the surface) can be applied to both the condenser and the porous electrode which directly faces it. At open circuit the number of Na atoms leaving the porous electrode per unit area at T_2 is

$$\dot{n} = P_{eff}(T_2)/\left[2\pi MRT_2\right]^{\frac{1}{2}} \qquad (7)$$

and since there is no net current this must be equal to the number leaving the condenser, $\dot{n} = P_v(T_2)/(2\pi MRT)^{\frac{1}{2}}$

The effective pressure $P_{eff}(T_2)$ at the porous electrode is then properly substituted for $P_v(T_1)$ in (6) above, yielding for the open circuit voltage

$$V_{oc} = \frac{RT_2}{F} \ell n \left[\frac{P_v(T_2)}{(T_2/T_1)^{\frac{1}{2}} P_v(T_1)}\right] \qquad (8)$$

The very small electronic conductivity of the solid electrolyte has been neglected. The correction Eq. (8) makes to Eq. (6) is small--amounting to about 50 mV for typical operating conditions.

When current is drawn from the SHE, an internal voltage drop occurs due to the resistance of the electrolyte-porous electrode system. In

addition, the Na concentration level at the porous electrode-electrolyte interface must increase above the level corresponding to the open circuit equilibrium in order that there be net evaporation from that interface sufficient to account for the current being drawn. Thus, under loaded conditions, the voltage is more accurately described by

$$V = \frac{RT_2}{F} \ell n\left[P_v(T_2)/\left\{(T_2/T_1)^{\frac{1}{2}}P_v(T_1) + \beta T_2^{\frac{1}{2}}I\right\}\right] - IR_o \qquad (9)$$

where the second term in the denominator represents a current-generated pressure.[2] An additional small correction results from the fact that at high pressures there is an increased tendency for the Na vapor to dimerize and thus to depart from the "ideal gas" situation which leads to Eq. (9). This correction reduces the output voltage at a given current by about 0.8 to 1.7% in the range from 500°C to 1100°C. It should be noted that for low values of T_1—below about 300°C and for values of the current density, $I > 0.1$ A/cm^2, the pressure term in the denominator of the logarithm is relatively small and the voltage-current relation is then given very closely by

$$V = A - B\ell n - IR_o, \quad B = RT_2/F \qquad (10)$$

The quality of the agreement of Eq. (10) with experiment can be seen in Fig. 8 and will be discussed further in the experimental section.

The efficiency of the SHE when parasitic heat losses are considered is given by the relation

$$\eta = \frac{W_1}{W_1 + L + \Delta H + Q_{loss}} \qquad (11)$$

If we are to make Eq. (11) explicit, we must itemize carefully and include the effects of the necessary electrical leads from hot device to cool load. These output leads must be optimized between two conflicting requirements in that they should present a low electrical resistance to the device to minimize I^2R losses in the leads and thus maximize the power delivered to the load but should present a high thermal resistance so as to minimize parasitic thermal conduction heat losses.

Since the ratio of thermal to electrical conductivity of metals, as given by the Wiedemann-Franz law[3] depends primarily on temperature and not on the choice of material, it will be seen that an optimum choice for the lead electrical resistance can be made. A more complete expression for the efficiency of the SHE including the effect of lead resistance R_ℓ is given by

$$\eta = \frac{I(V - ISR_\ell)}{I(V - \tfrac{1}{2}ISR_\ell + L/F) + IC_p(T_2 - T_1)/F + \tfrac{1}{2}\not{L}(T_2^2 - T_1^2)/R_1S + \sigma(T_2^4 - T_1^4)} \quad (12$$

Here the ΔT^4 term in the denominator represents the radiation transfer from the hot porous electrode to the cool condenser of reflectivity $(\frac{Z-1}{Z})$ in the near infrared and σ is the Stefan-Boltzmann constant. The ΔT^2 term is the parasitic thermal conduction loss term expressed via the Wiedemann-Franz ratio ($K_\rho = \pm T$) in terms of the lead resistance R_ℓ and the Lorenz number $\pm \approx 2.45 \times 10^{-8}$ watt/ohm deg^2. S is the active surface area of the device.

Figure 2 shows a family of power versus efficiency curves at different temperatures T_2 with T_1 fixed at 200°C, with Z = 20, and for a fixed value of the specific internal resistance $R_0 = 0.18\ \Omega\cdot cm^2$. In these curves the choice of R_ℓ in Eq. (12) has been optimized for maximum efficiency at each point on the curves. In comparison to fixed leads, this optimization procedure substantially extends the high efficiency operating region to both lower and higher powers. Figure 3 shows the variation of R_ℓ called for by this procedure both for the absolute maximum efficiency point and for leads optimized for efficiency at the maximum power point. It may be seen that maximum efficiency leads need only vary by a factor of 2 in the length to cross-sectional area ratio from 500°C to 1000°C, thus allowing for relatively simple design for a variable lead system, if desired. Figure 4 displays the maximum efficiency and the efficiency at maximum power as a function of temperature for the same device parameters used for Figure 2. At low T_2, it will be necessary to use substantially thinner electrolytes if the assumed $R_0 = 0.18\ \Omega\cdot cm^2$ is to be maintained. β"-alumina membranes have now been produced at tube wall thicknesses of 100 microns.[4] These membranes would have R_0, exclusive of polarization, from 0.017 $\Omega\cdot cm^2$ at 800°C to 0.03 $\Omega\cdot cm^2$ at 300°C.

To consider the SHE as a topping cycle, we calculate the effect of T_1 on the power-efficiency relation. Figure 5 shows a family of power-efficiency curves as a function of T_1 with T_2 fixed at 900°C and R_o = 0.18 $\Omega \cdot cm^2$ as before. These curves were calculated for optimized leads. The monatonic increase in efficiency with decreasing T_1 is reversed between 200°C and 100°C due to the increased radiation loss and enthalpy terms in a temperature range where no useful improvement in $P_v(T_1)$ is possible.

Because it is, in principle, possible to series connect SHE cells at high temperature before bringing the output leads to room temperature, it is possible to drastically reduce the lead losses and improve the overall efficiency of the system to 30-35% at high power levels.

Experimental

At present, the major thrust of our efforts is directed toward understanding and improving the performance of the porous electrode system on β"-alumina. This work is most conveniently performed on demountable test cells (DTC) in which electrode systems can be readily interchanged and instrumentation easily introduced. In these cells provision for Na recirculation is not generally provided and a fully accounted overall efficiency cannot, therefore, be determined. Before discussing this work, we summarize the status of our work with fully recirculating test cells (RTC).

We have demonstrated efficiencies of 10% at 10 watts with porous electrodes capable of a maximum specific power of 0.16 watt/cm^2. Despite very poor wetting of the condenser surfaces by the condensing liquid sodium in those early experiments, values of $Z \approx 10$ were achieved. A considerable variety of means are available to promote this wetting so as to provide a high reflectance specular surface and hence higher Z. We have shown that copper plating the condenser surface promotes good wetting, but we have not yet had an opportunity to measure Z in such a cell. The electromagnetic pump for recirculating the Na is easily self-powered by passing the output current through it and this has been shown experimentally to require less 0.5% of the output power. A completely sealed SHE system has operated for more than two weeks

with no indication of need for a permanent vacuum system attachment. The porous molybdenum electrode is physically stable in the SHE environment at temperatures above 800°C for periods of over 1000 hours. We have also shown that these electrodes can collect current at 15 amperes per cm^2 without damage.

In order to more easily build and investigate the electrode properties of electrode-electrolyte systems, single-pass non-recirculating SHEs have been built. These are generally built in a geometry inverted with respect to our RTCs. A schematic of this arrangement is shown in Figure 6. A typical DTC header with an electrolyte-electrode system in place is shown in Figure 7. In this system, similar to the schematic of Figure 6, the β"-alumina tube is partially filled with sodium metal, a heater well-thermocouple well system inserted and sealed in place with an inert cover gas such as helium or argon. The cover gas reduces the heat leak to the upper end of the system, thus reducing the required heater power while protecting the elastomer seal at the open end of the β"-alumina tube from excessive temperatures. Without the cover gas, the evaporation and condensation of the sodium (heat pipe effect) would cause a very large heat leak. In the DTC system the pump is not included and because the supply of sodium per experimental run is limited, small electrodes, generally about 1 cm^2, are used so that high specific current densities may be drawn without depleting the Na supply too rapidly. As a practical matter, a SHE current of 1 ampere calls for a sodium throughout of about 1 cm^3/hour. With these small electrodes, it is also possible to produce and test a number of electrodes during each experimental run. The system shown in Figure 7 was used for three such electrodes. The copper shield surrounding the central β" tube was used to reduce radiative heat losses from regions of the tube not under test. We continue to find that thin molybdenum electrodes deposited on the β"-alumina by chemical vapor deposition[5] have excellent properties. Films formed by thermal decomposition of Mo $(CO)_6$ have high in-plane electrical conductivity, good Na vapor permeability normal to the plane, good adhesion to the electrolyte surface and good high-temperature stability. These moly films have a columnar structure with the

grains perpendicular to the film plane, accounting for the useful porosity observed while the in-plane electrical conductivity appears to be within a factor of 2 of that expected for bulk molybdenum.

The electrical contacts are made to the porous electrode using a harness of molybdenum wire wrapped with Cu wire and cinched in place with a small bolt. The Cu bonds to the molybdenum surface when the electrode reaches operating temperatures. For the purposes of the present work, copper wires are strapped under, and voltage probes spot-welded to the molybdenum harness. The DTC also contains a window through which the cell may be observed visually and the surface temperature monitored with an optical pyrometer.

In Figure 8 we show a family of experimental current-voltage curves for a single electrode as a function of temperature. This electrode was deposited on a 15-mm diameter β"-alumina tube supplied by the University of Utah.[6] The wall thickness under this electrode averaged 0.073 cm. The condenser temperature for this system is about 50°C since no recirculation is attempted. The solid lines through the data points are plots of Eq. (9) with the coefficients A and R_o determined by a least squares fitting procedure. The fit is excellent over virtually the entire range as would be expected for a SHE having a very low T_1. This fitting procedure allows a rather precise determination of R_o and of the A term in Eq. (10). The latter term is associated with the open circuit voltage parameters and with any resistance to neutral Na flow through the porous electrode. The dashed lines are plots of Eq. (8) using as the only experimental input the value of R_o determined from the data fit discussed above. Thus, these curves display, with respect to the actual data, what is probably the net effect of Na flow impedance in the porous electrode. In this regard then, at 900°C the porous electrode in this test had a maximum power output within 10% of the ideal value for the experimental R_o. In Figure 9, we have plotted the values of A and R_o as a function of temperature for this same electrode. We also show the dependence of these coefficients on temperature for the case of an ideal electrode. The discrepancy in R_o between ideal and actual electrode performance is one measure of the"polarization" the major fraction of which is the

interfacial impedance between electrolyte and porous electrode. It is this polarization which ultimately limits the improvement in specific power and efficiency to be gained by operating with thinner electrolyte membranes for which the bulk resistivity contribution is reduced.

We have also conducted experiments on a series of similar electrodes deposited on electrolytes of varying thickness produced by grinding a single ceramic tube to different diameters. The i-V curves produced in this way were analyzed for A and R_o, and R_o then plotted as a function of the wall thickness δ. Such data are shown in Figure 10 for a temperature of 850°C. From the extrapolated zero thickness value of R_o, one may infer the polarization. The bulk resistivity of the electrolyte may be deduced from the slope of the line. The values of resistivity for the β"-alumina deduced in this way are in agreement to within 20% with those obtained by more direct means using a 4-terminal d-c approach.

The power-efficiency temperature curves in Figures 2 and 5 were calculated using for R_o the value obtained, at 900°C, for the experimental cell whose i-V characteristics are shown in Figure 8. This value, $R_o = 0.18\ \Omega \cdot cm^2$ was achieved for a wall thickness of 0.073 cm. Tube walls of this thickness are easily fabricated of β"-alumina even by the batch process in principal use today. Green-forming of β"-alumina tubes by extrusion has already shown the capability for producing dense high quality ceramic at wall thicknesses of 0.01 cm. With no further reduction in polarization beyond that presently achieved. Figure 10 shows that a wall thickness of 0.01 cm would yield $R_o = 0.05\ \Omega \cdot cm^2$ with specific power and efficiency substantially higher than those shown in Figures 2 and 5.

Recirculating Test Cell Design

The small electrodes and batch filling scheme so useful for repeated experiments on the electrode-electrolyte subsystem are not suitable for the experimental determination of efficiency. For this, a complete recirculating system with electrode on all of the heated electrolyte area is required so that proper accounting of all the heat

losses can be made and compared with the output power of the SHE. A photograph of an RTC with a nominal rating of 75 watts is shown in Figure 11.

Conclusions

In our experiments, the Sodium Heat Engine has demonstrated the elements of operation needed to deliver electric power at a conversion efficiency near 25%, and with thinner electrolyte and series connection at the high temperature, the SHE overall efficiency should reach 35-40% with no further breakthroughs in electrode performance required. Because the efficiency of the SHE does not depend on its size, it should be considered a prime candidate for distributed electric generation in residences, industrial and remote sites, especially in situations where the use of heat at the heat sink temperature is also called for. Little serious consideration has been given thus far to use of the SHE as a topping cycle with a steam turbine system for central station power generation, but the analysis of SHE operation suggests strongly that efficiencies of 15% can be achieved when the SHE exhaust temperature is as high as 500^{o}C.

References

1. N. Weber, Energy Conversion 14, 1 (1974).

2. T. K. Hunt, N. Weber, T. Cole, Proceedings of 10th Intersociety Energy Conversion Engineering Conference, Part Two, p. 231 (1975).

3. See for example, C. Kittel, Introduction to Solid State Physics, 2nd Ed., p. 241, J. Wiley & Son, New York, 1956.

4. G. J. Tennenhouse and R. A. Pett, Fabrication of Thin Layer Beta Alumina, Contract Report NASA-CR-135-308.

5. J. J. Lander and L. H. Germer, Metals Technology 14, 42 (No. 6), Tech. Publ. 2259 (1947).

6. Univ. of Utah, Department of Materials Science and Engineering -- Professor Ronald S. Gordon. The Production of β"-alumina tubes has now been transferred to Ceramatec, Inc., 580 Arapeen Drive, Suite 200, Salt Lake City, Utah 84108.

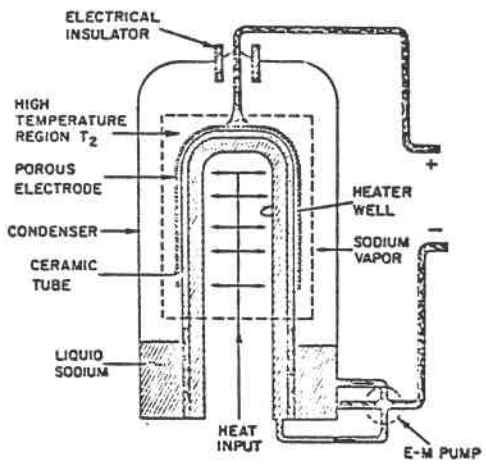

Fig. 1 - Schematic Diagram of Sodium Heat Engine

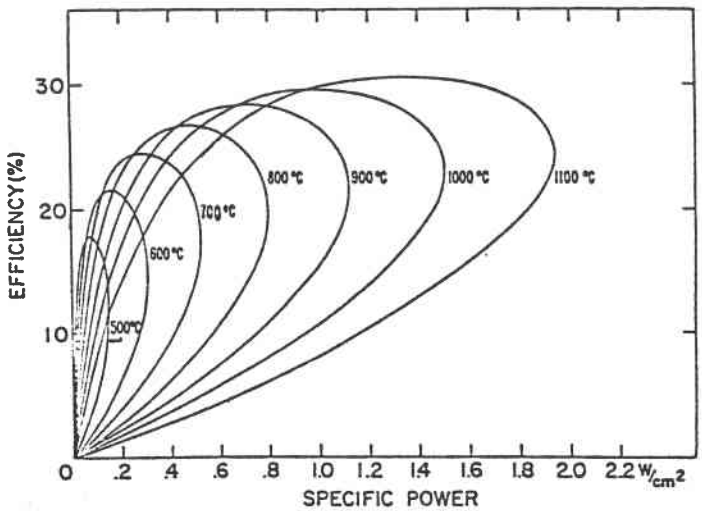

Fig. 2 - Calculated Power-Efficiency Performance of SHE vs T_2.
R_o = 0.18 cm^2, T_1 = 200°C, Z = 20.

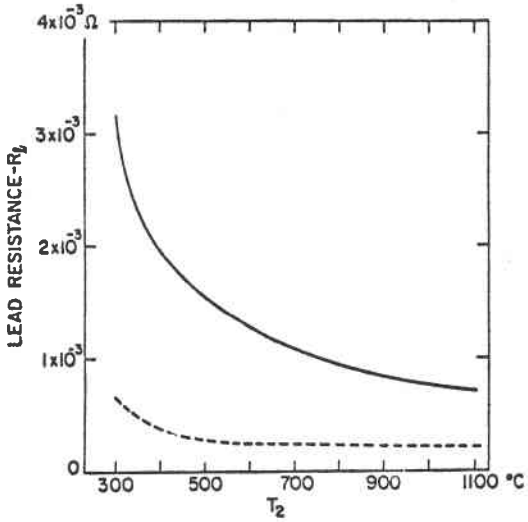

Fig. 3 - Optimum Lead Resistance: Solid Line--for Maximum Efficiency; Dashed Line--for Best Efficiency at Maximum Power Point.
R_o = 0.18 cm^2, T_1 = 200°C, Z = 20, S = 100 cm^2.

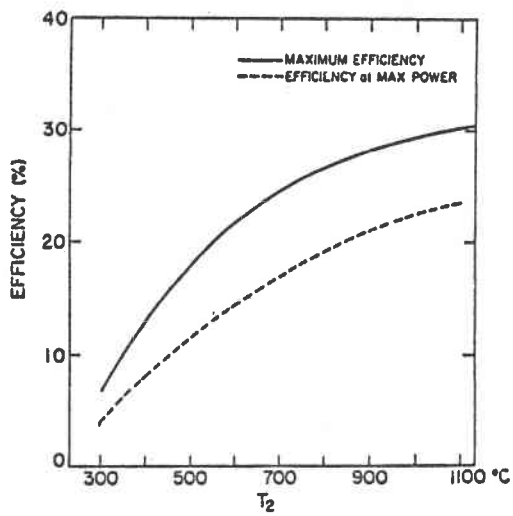

Fig. 4 - Efficiency vs T_2, Optimized Leads.
R_o = 0.18 cm^2, T_1 = 200°C, Z = 20.

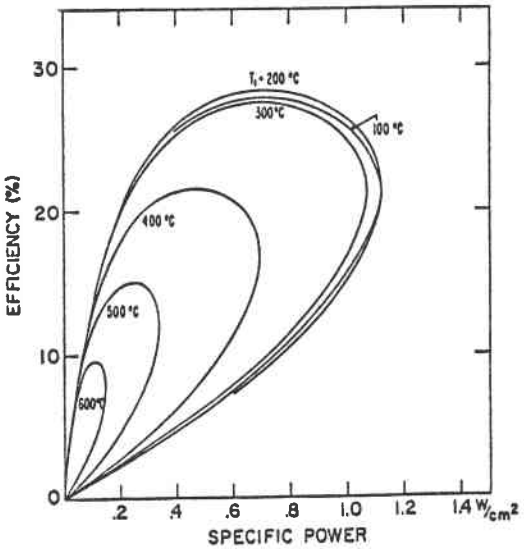

Fig. 5 - Calculated Power-Efficiency Performance of SHE vs T_1.
R_o = 0.18 cm^2, T_2 = 900°C, Z = 20.

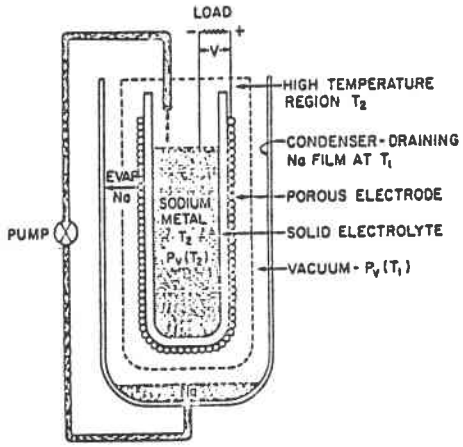

Fig. 6 - Schematic Diagram of SHE Showing Inverted Geometry Used in Demountable Test System

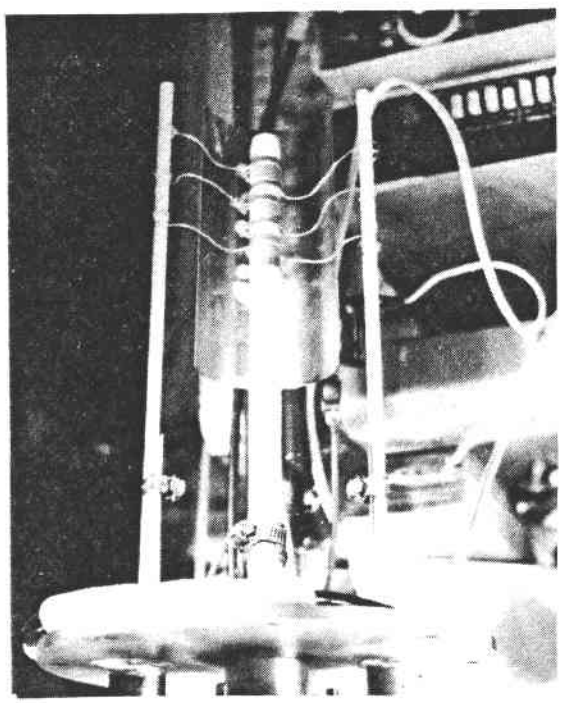

Fig. 7 - DTC With Assembled SHE cell.

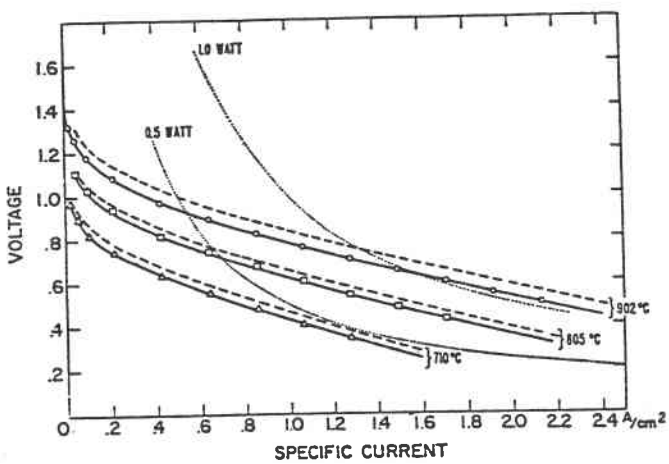

Fig. 8 - Experimental Voltage - Current Curv as a Function of Temperature T_2.

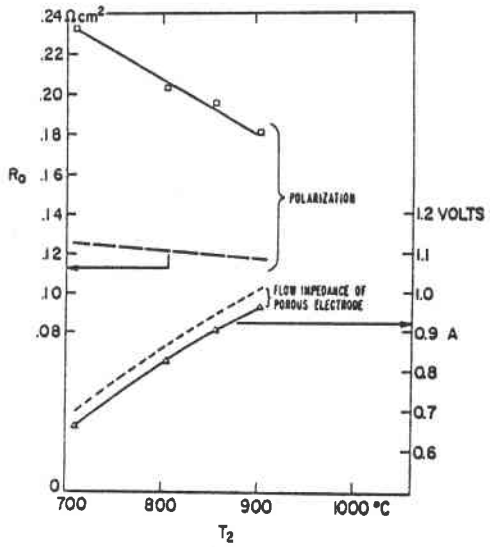

Fig. 9 - Coefficients of Voltage - Current Relation for Real (Solid Line) and Ideal (Dashed Line) Electrodes

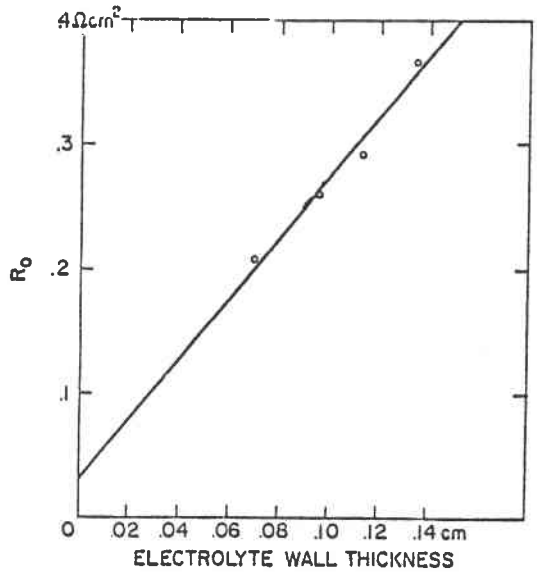

Fig. 10 - Specific Resistance of SHE vs Electrolyte Wall Thickness. T_2 = 850°C.

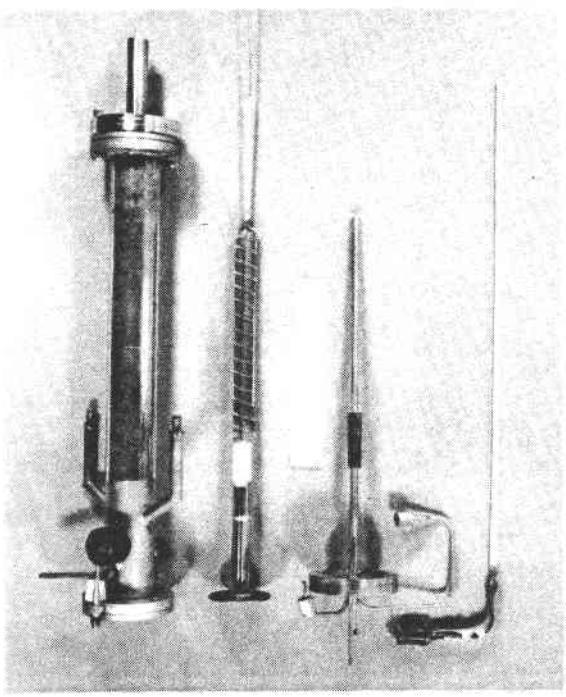

Fig. 11 - Experimental Recirculating SHE - Nominal 75-watt Design.

THERMIONIC ENERGY CONVERSION FOR SOLAR APPLICATIONS

BY

G. O. FITZPATRICK & E. J. BRITT

RASOR ASSOCIATES, INC.
253 HUMBOLDT COURT
SUNNYVALE, CALIFORNIA 94086

D. L. JACOBSEN

ARIZONA STATE UNIVERSITY, TEMPE, ARIZONA 85281

PRESENTED AT

SOLAR THERMAL TEST FACILITIES
USERS ASSOCIATION MEETING

APRIL 11 & 12, 1978

GOLDEN, COLORADO

THERMIONIC ENERGY CONVERSION FOR SOLAR APPLICATIONS

G. O. Fitzpatrick & E. J. Britt
Rasor Associates, Inc., Sunnyvale, California 94096

D. L. Jacobsen
Arizona State University, Tempe, Arizona 85281

Abstract

Thermionic energy conversion is a demonstrated and practical method of converting heat directly to electricity. It is well suited for use with the high temperatures and heat fluxes available from large solar concentrators. Typical converters operate in the temperature range of 1500°K to 2000°K and above, with heat fluxes between 10 and 100 w/cm^2. Long lifetimes with stable performance can be achieved at these temperatures since no moving parts or high pressures are required. Heat is rejected from thermionic converters at a sufficiently high temperature (800°K to 1000°K) to generate steam for turbogenerators in a combined cycle power plant or to provide high quality process heat for industrial applications.

As an example of a specific application, this paper describes a perturbation analysis of a combined thermionic-steam solar central receiver power plant which is based on the Sandia/McDonnell-Douglas (MDAC) design. The analysis indicates that the use of thermionics can increase the efficiency of the overall power plant using currently available converter performance from the reference level of 36% to as much as 45%. Reductions in the size of the heliostat field are possible with the more efficient combined cycle thermionic-steam system. This permits significant reductions in the plant cost-of-electricity. For a first commercial plant with a MDAC receiver, cost savings as large as 60 mills/kW-hr are calculated.

ADVANCED SOLAR THERMAL SYSTEMS

The thermal energy supplied to a solar thermal central receiver is one of the most expensive forms of heat available for energy conversion. The

collector system is very capital intensive with projected costs running as high as \$300/kW_t (>\$5/million BTU). Thus, there is a strong incentive to achieve the highest possible conversion efficiencies in order to minimize the collector cost.

To obtain high conversion efficiency it is necessary to operate with the largest possible temperature interval and to achieve the largest possible fraction of the Carnot efficiency available from that temperature interval. Extending the temperature interval by reducing the heat rejection temperature is very difficult, particularly in desert locations where dry cooling towers may be required. The only alternative is to increase the peak cycle temperature. Since high temperatures can be produced with concentrated solar flux, advanced conversion systems which extend the peak cycle temperatures should be attractive for solar energy conversion.

While the use of advanced conversion systems at high temperatures extends the available temperature interval it also introduces new losses which tend to reduce overall system efficiencies. The most important of these is thermal reradiation from the receiver cavity which increases with increasing temperature. Thus the efficiency of the receiver goes down while the Carnot efficiency of the energy conversion system increases and there is an optimum temperature for operation. These two efficiencies can be expressed as:

$$\eta_{Carnot} = \frac{T_H - T_C}{T_C}, \tag{1}$$

and

$$\eta_{cavity} = \frac{Q_{in} - \sigma T_H^4}{Q_{in}} \tag{2}$$

where T_H = peak temperature (°K)

T_C = heat rejection temperature (°K)

Q_{in} = input solar heat flux at the cavity aperture (watts/cm^2)

σ = Stephan Boltman constant (5.6×10^{-12} watts/cm^2-°K).

The ideal overall efficiency is the product of these two, viz:

$$\eta = \left(\frac{T_H - T_C}{T_C}\right)\left(\frac{Q_{in} - \sigma T_H^4}{Q_{in}}\right) \tag{3}$$

The peak temperature is optimum when the fraction of reradiated heat is:

$$\frac{\sigma T_H^4}{Q_{in}} = \frac{1}{4(T_H/T_C)^{-3}} \tag{4}$$

Eq(4) can be used to find the optimum temperature for the solar thermal facilities available to the STTF Users Association. If the ratio of the high to low temperatures in the conversion cycle is assumed to be $T_H/T_C = 4$, the optimum temperature as a function of heat flux shown in Fig. 1 is obtained. The heat fluxes available from the four solar thermal test facilities in the SSTFUA are indicated with arrows on the horizontal axis of the graph.

It can be seen that normal steam cycle peak temperatures are well below the curve of optimum temperatures and the use of an advanced system should be advantageous. As shown, the peak temperatures at which thermionic converters operate are well matched to the optimum. However, thermionic converters also reject their waste heat at high temperatures. In order to make full use of the complete temperature interval it is necessary to combine the thermionic system with a conventional steam cycle. A system of this type is shown diagrammatically in Fig. 2. The thermionic cycle removes a portion of the available heat at the optimum peak temperature of the system and generates an increment of electric power. The heat which passes from the thermionic unit into the steam cycle is used to produce high quality steam for running the turbogenerators. The combined thermionic-steam power plant significantly increases the overall efficiency of the system and, as will be shown, reduces the cost-of-electricity.

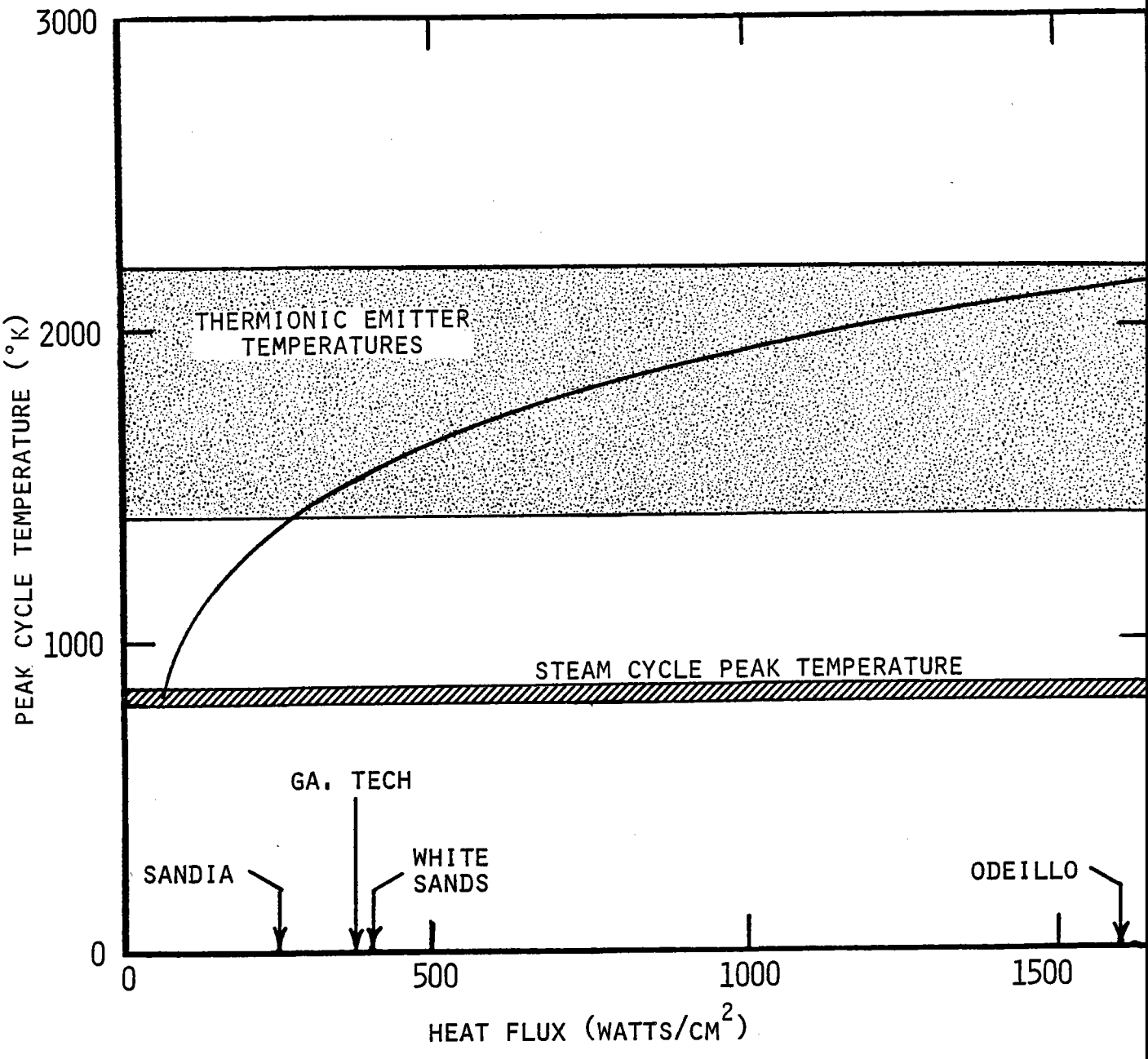

FIG. 1 - Optimum Peak Cycle Temperature for Solar Energy Conversion

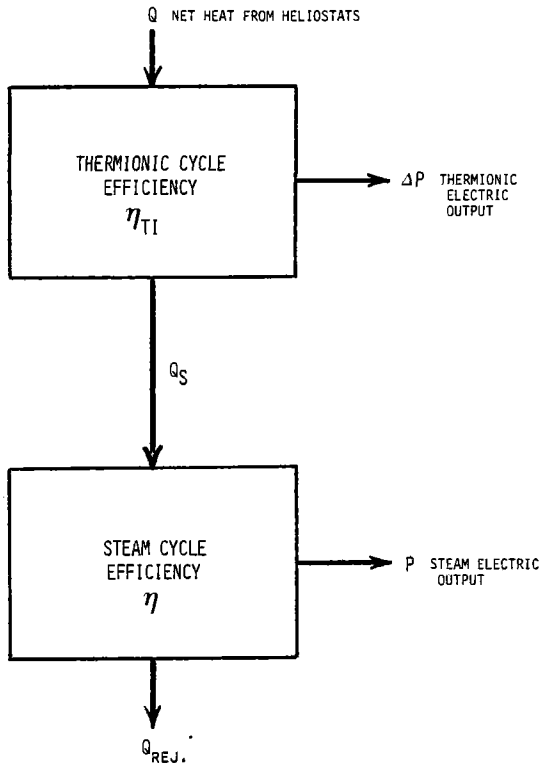

Fig. 2 - Combined Thermionic-Steam Cycle

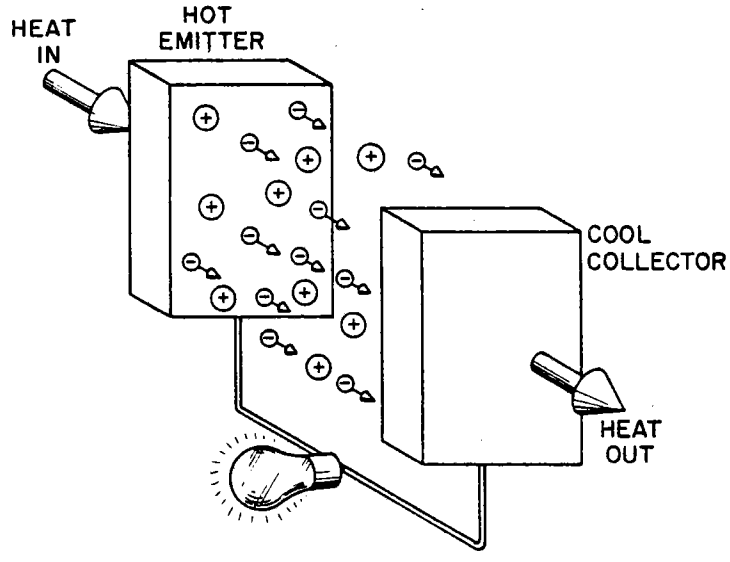

Fig. 3 - Idealized Thermionic Converter

THERMIONIC ENERGY CONVERSION

Converter Characteristics

Thermionic energy conversion is a method of converting heat directly to electricity. One electrode, the emitter, is heated sufficiently to emit electrons, as shown in Fig. 3. The electrons cross a narrow inter-electrode gap and are collected by another electrode, the collector. The flow of electrons constitute an electric current which delivers power to the load. The cycle has many similarities to a Rankine cycle which uses electrons as a working fluid. Unlike the normal Rankine cycle, however, the working fluids "heat of evaporation," approximately the emitter work function, and its "heat of condensation," approximately the collector work function, can be varied in the thermionic converter. This feature provides the converter with great flexibility in matching the operating constraints of any particular system.

Thermionic converters are attractive for the solar receiver system because they can accept heat at the highest available temperature at high heat fluxes. Some typical converter input power densities are shown in Fig. 4 as a function of emitter temperature with the current density of the device as a parameter. Operation at 5 to 20 amps/cm^2 is typical of most converters. Operation above 50 amps/cm^2 is difficult because of the necessity for large bus bars to conduct the high currents.

Converter efficiency versus current density for two levels of converter performance as shown in Fig. 5. Second generation performance is the 1982 goal of the DOE central station thermionic technology program, and third generation performance is the 1987 goal of the program. As can be seen, the efficiency of a thermionic converter is relatively insensitive to current density. As a result, the performance of the converter remains near the design level under part load conditions. The output power density of a converter, like the required input power density, is almost directly proportional to current density. Thus the current density is a parameter which may be adjusted to optimally match the thermionic system to the heat flux available from the solar receiver.

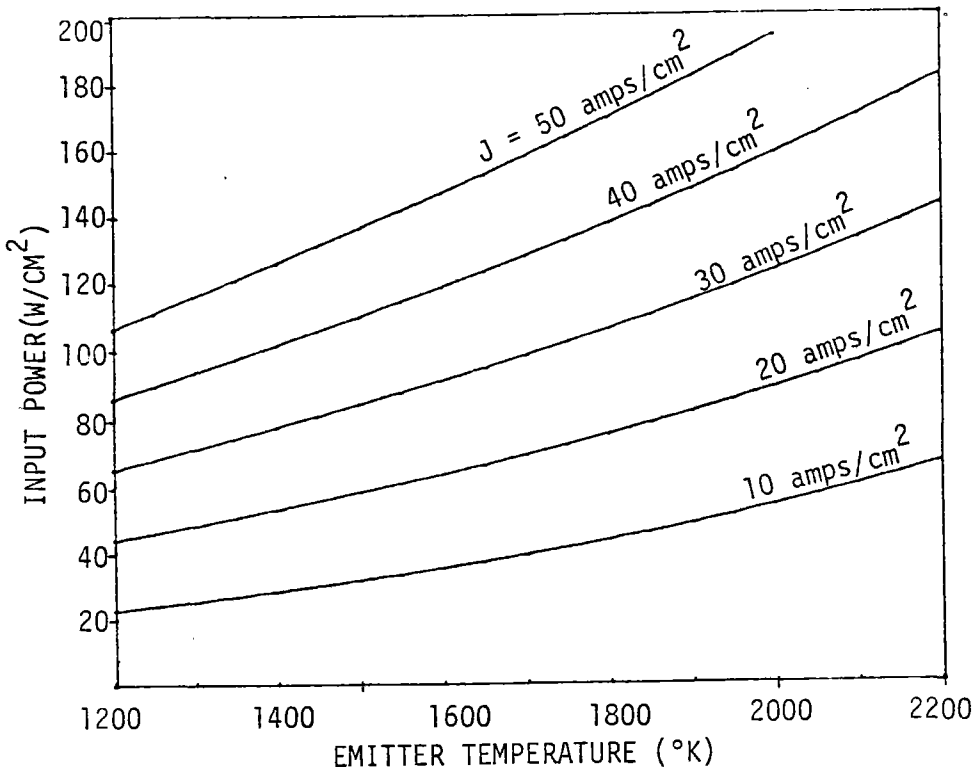

Fig. 4 - Converter Input Power Requirements

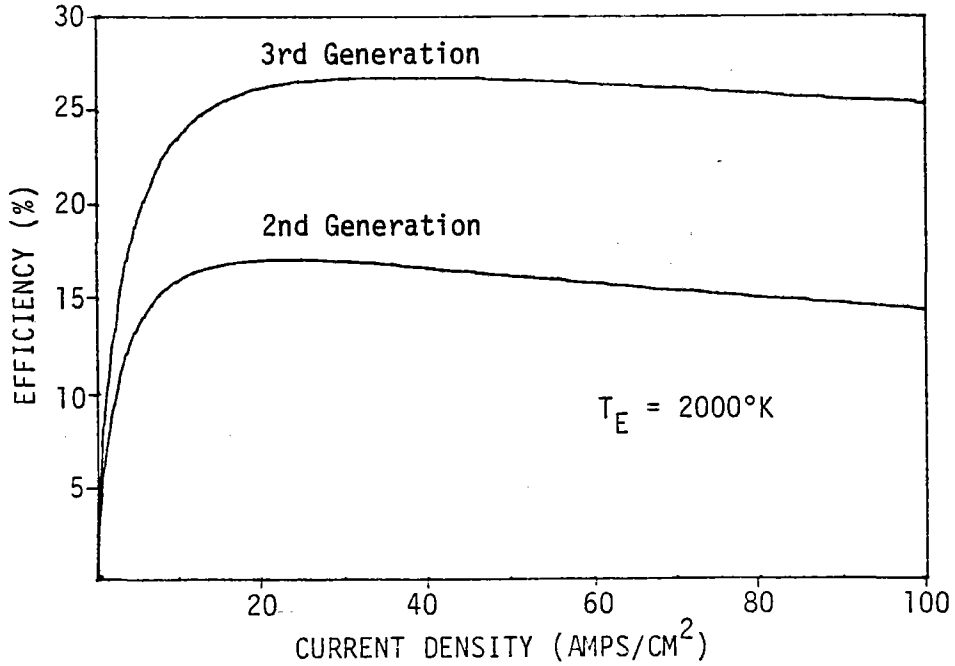

Fig. 5 - Converter Efficiency as a Function of Current Density and Barrier Index

These characteristics also permit the high efficiency of the thermionic system to be maintained with a variable heat source. The converter response to varying heat flux can be very rapid, since input power changes can be accommodated as fast as the current density can be changed (approximately 10^{-2} seconds). Furthermore, such changes can be accomplished with almost no variation in the emitter temperature. This is a significant advantage in a solar system, where the passage of an occasional cloud over part of the heliostat field would cause an abrupt transient in the solar heat flux.

Converter Hardware Experience

Thermionic converters have been developed for a variety of applications using solar, nuclear, and fossil fueled heat sources. Perhaps the largest effort has concentrated on developing converters for use with nuclear reactor heat sources in space. Currently a large effort is also directed at terrestrial applications, particularly coal-fired central station power plants.

The record holder for converter life is LC-9, a thermionic converter built for NASA by General Atomic as part of the in-core nuclear space reactor program. LC-9 operated with perfectly stable performance for over five years at an emitter temperature of 1970°K. As shown in Fig. 6 (ref. 1), LC-9 had an electrode efficiency of 17%, and generated 8 W/cm^2 of output power. The converter was still performing stably when tests were terminated for programmatic reasons. This test illustrates well the long life capability of the thermionic converter process. The tungsten/cesium high temperature emitter combination forms an equilibrium system with no known degradation mechanisms except emitter evaporation. At 2000°K this amounts to less than 10^{-2} mil per year in vacuum. In cesium the loss rate is significantly lower.

Solar heated converters developed for use in space have demonstrated the ability to operate at high current densities and power densities. The IV characteristics of four converters built in 1961 as part of the Solar Energy Thermionic (SET) program at the Jet Propulsion Laboratory, shown in Fig. 7 (ref. 2), illustrate this well. As can be seen, a current density of 30 A/cm^2 or higher can be obtained with an emitter temperature of 2000°K.

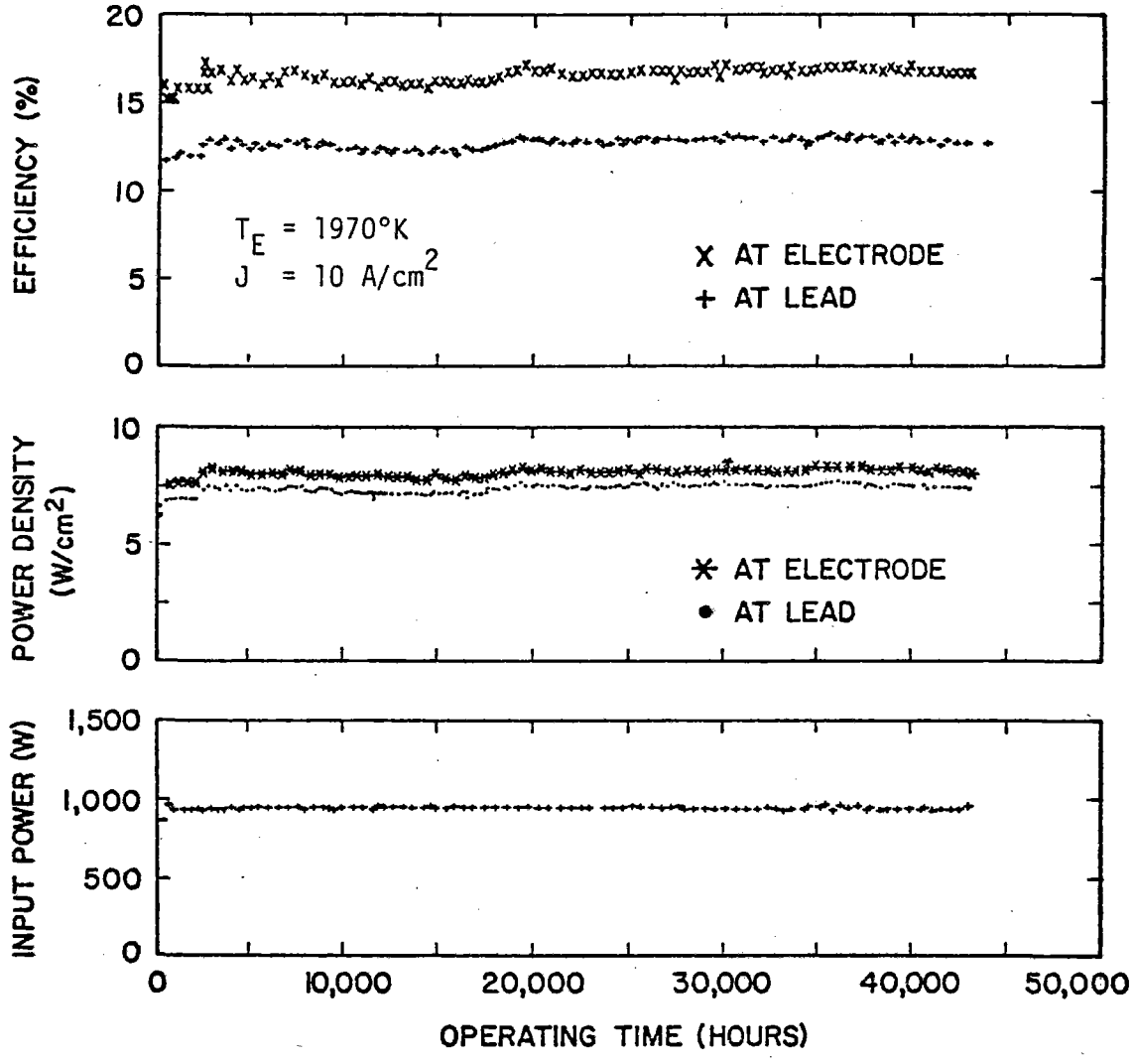

Fig. 6 - Operating History Converter LC-9. Five years of completely stable performance with no maintenance or failures.

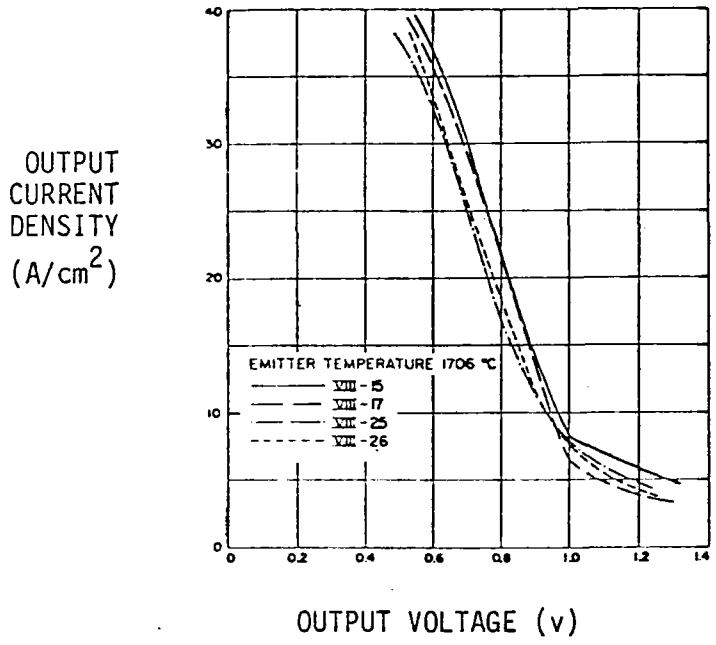

Fig. 7 - The Observed IV Characteristics of Converters Designed for Use in Space (ref. 4)

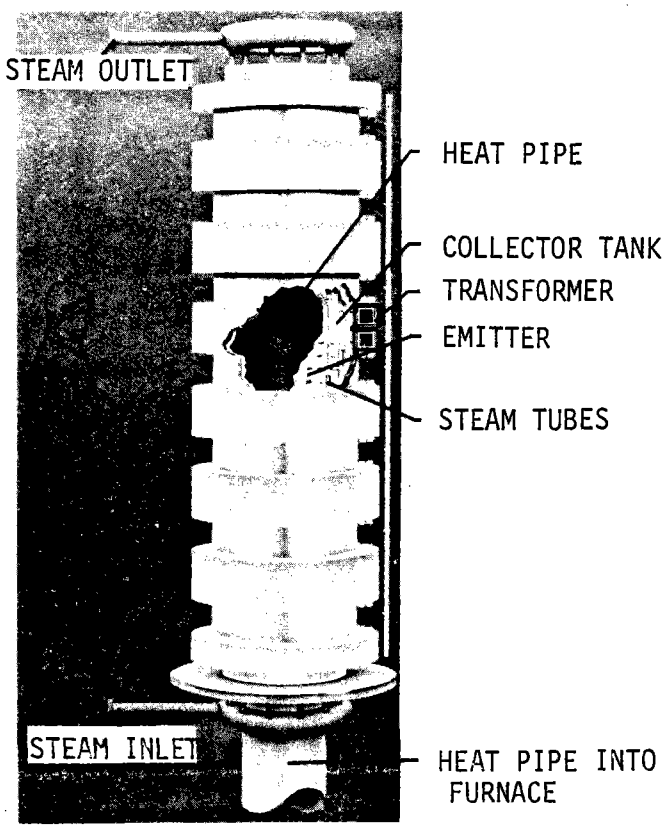

Fig. 8 - A 1/2 MWe THX Power Module Design Concept for Central Station Power Plants

While many of the converters designed previously for use in space were relatively small (~100 W_e), present DOE designs for terrestrial central station power plants include Thermionic Heat Exchanger (THX) modules, such as that shown in Fig. 8 (ref. 3), which will each provide 1/2 MWe or more.

Impact on System Design

The use of thermionic converters permits new innovations in system design. Some of the most interesting possibilities are associated with the solar plants requirement for energy storage. For example, the electric output of thermionic converters is typically a low voltage, high current DC form of power. One possibility for utilizing the electric output from the thermionic part of the system is to produce hydrogen by electrolysis. This would permit formation of a storable energy product which can be either used as fuel or recombined in a fuel cell to provide electric output during times when no solar flux is available. It is important to realize that hydrogen could be generated in this manner while the steam part of the system continues to operate normally.

The use of normal energy storage techniques at steam temperatures is still possible in the thermionic/steam power plant. It may also be possible to obtain the operational advantage of storing energy at the emitter temperature. Storage at emitter temperature would permit the stored energy to be converted to electricity with the efficiency of the combined thermionic/steam cycle, rather than that of the steam cycle alone. This would reduce the amount of heat storage required by the power plant. A variety of thermal energy storage materials appropriate for use with thermionic emitters have been identified. A few of these materials are listed along with their energy densities and melting points in Table 1. Except for lithium-hydride, higher energy densities occur with higher temperature materials. Thus emitter temperature energy storage could be accomplished with a smaller quantity of energy storage material than storage at steam temperatures.

TABLE 1

MATERIAL	ENERGY DENSITY (WATT-HRS/LB)	MELTING POINT (°K)
Li_2O-B_2O	148	923
LiF-MgF_2-NaF	106	957
LiH	359	982
LiF-MgF_2-KF	99	986
LiF-MgF_2	108	1015
LiF	132	1122
AlaF	100	1269
MgF_2	118	1536
Si	227	1686
LiO	247	2116
BeO-MgO	260	2145

Because of their modular nature, thermionic converters are particularly well suited to retrofit improvement of existing steam systems. Retrofiting an existing steam plant with a thermionic topping cycle involves replacement of the boiler with an array of thermionic heat exchangers or thermionic modules. The rest of the system, including the turbogenerator and condensors, is left unchanged. The thermionic part of the cycle can be tailored to reject the proper amount of heat required by the steam cycle. This retrofit potential has been studied for fossil fuel power plants and is one of the attractive features of the thermionic topping cycle. A similar potential exists in repowering an existing power plant with solar thermal heat sources.

THERMIONIC CENTRAL RECEIVER SYSTEM

An Example Reference Design

In order to assess the economic potential for solar thermionic topping systems, a perturbation analysis was made using a current central receiver design with the addition of thermionic topping. The costs and performance data for the thermionic part of the system were based on previous DOE studies of fossil-fired thermionic topping systems (ref. 3). The costs of other features of the solar central receiver system and its associated steam power plant were taken from the Sandia Livermore Laboratory/McDonnell-Douglas Astronautics Company central receiver system (ref. 4).

The solar thermionic-steam topping system studied is shown schematically in Fig. 9. Radiant flux from the collector is absorbed directly in tower-mounted thermionic converters in the cavity receiver. The thermionic units generate DC electric power at this point and reject the heat into a steam boiler, which is similar to the boiler systems currently envisioned for central receiver power plants. The steam then flows through the turbo-generators. The power produced by the steam system is not affected by adding the topping cycle, so the thermionic output adds an additional increment of power.

The cost distribution for the reference system is shown in Fig. 10. As can be seen, the major cost of the power plant is the collector system, while the electric power generation system (labeled EPGS on the diagram) comprises only a minor part of the capital investment. Addition of a thermionic topping system has the potential for reducing the cost of the collector by increasing the conversion efficiency, but at the expense of an increase in the cost of the electric power generation system. However the leverage acquired because of the large fraction of the cost attributed to the heliostats provides the potential for savings in the overall cost of electric energy.

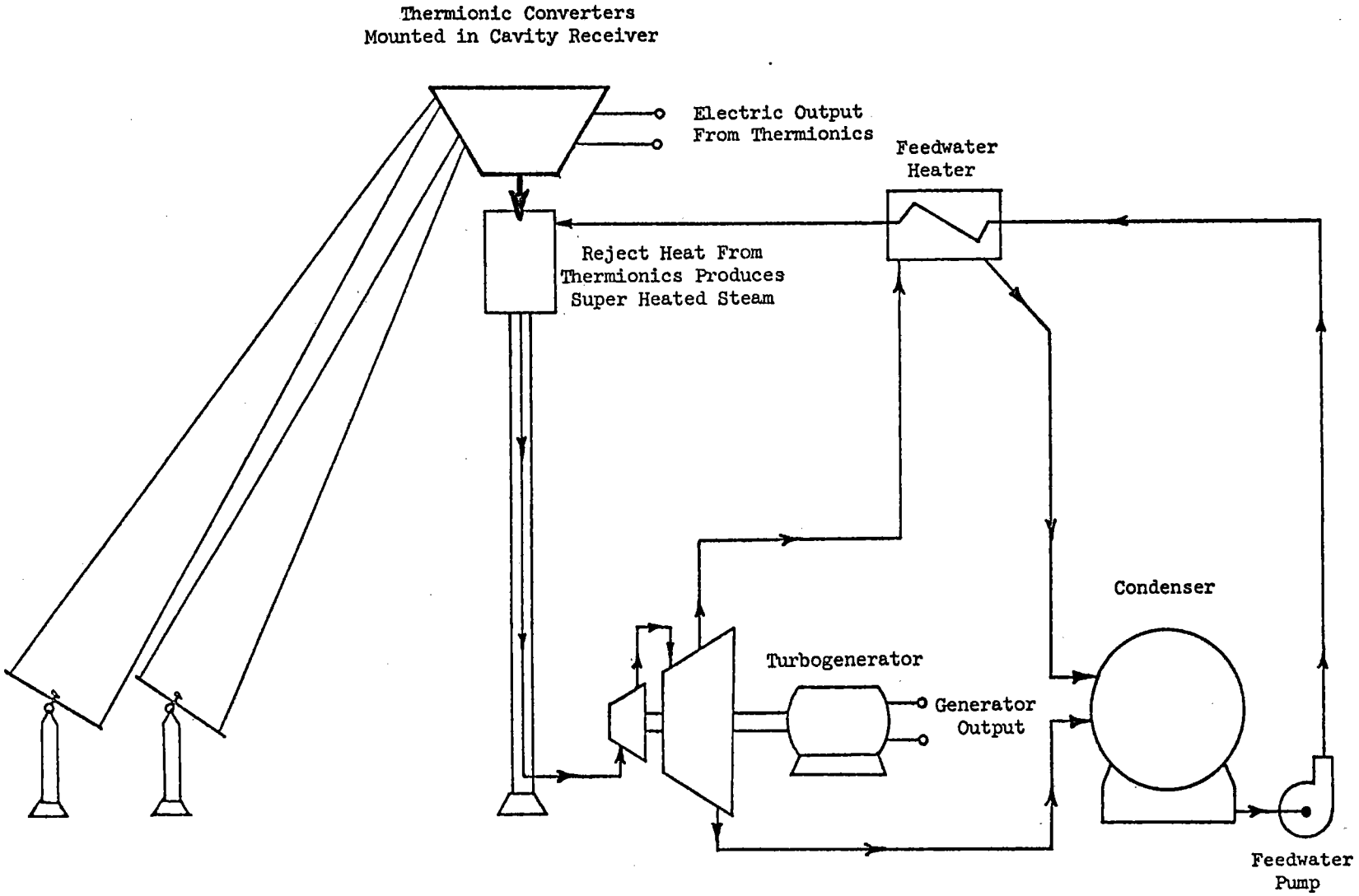

Fig. 9 - Thermionic Topped Solar Thermal Central Receiver Power Plant

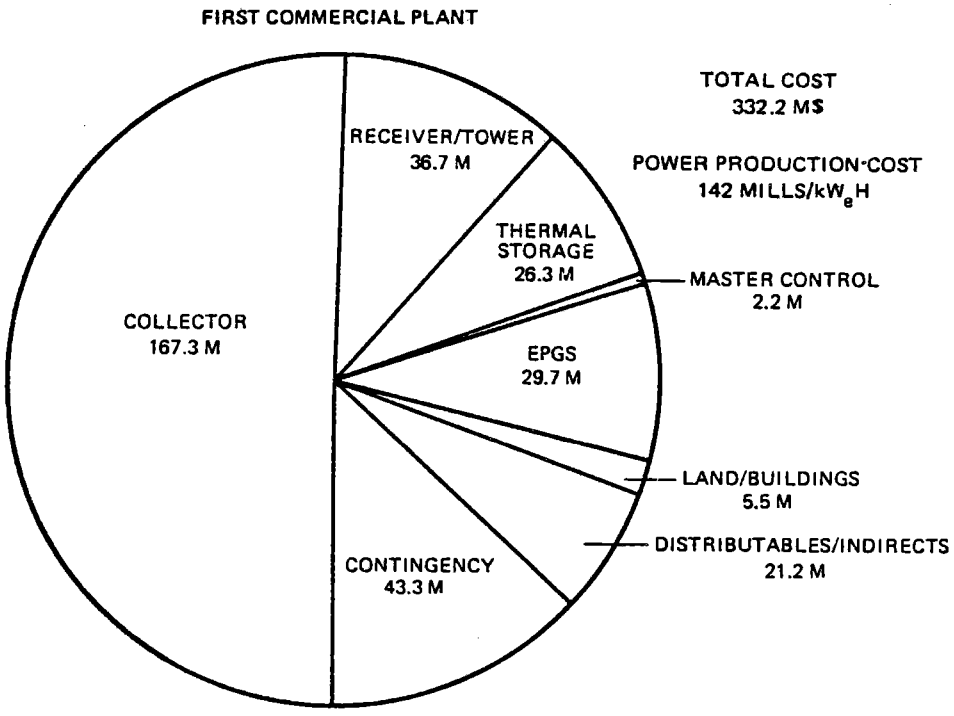

Fig. 10 - Cavity Receiver/Tower Cost Implications. Sandia revised cost estimates. McDonnell-Douglas heliostat and storage. Solar multiple of 2; storage capacity of 7 hours at 70 MW_e.

Cost Analysis - The cost perturbation analysis is based on the combined cycle system shown in Fig. 2. Using the symbols on Fig. 2; the overall combined cycle efficiency is expressed as $\eta^* = (P + \Delta P)/Q$.

It can be shown that:

$$\frac{\Delta P}{P + \Delta P} = \frac{\eta_{TI}}{\eta_{TI} + \eta(1 - \eta_{TI})} \tag{5}$$

and

$$\frac{\eta}{\eta^*} = \frac{\eta}{\eta_{TI} + \eta(1 - \eta_{TI})} \tag{6}$$

The capital cost of the untopped solar thermal steam cycle consists of two parts:

C_H = cost of heliostats ($/kWe)

C_S = cost of the remainder of the system ($/kWe)

The bus bar energy cost is then given by:

$$BBEC = \gamma(C_H + C_S) + OM + IT \tag{7}$$

where BBEC = energy cost (mills/kWhr)

γ = an amortizing multiplier that includes the capacity factor, depreciation, property taxes, interest, and escalation,

OM = operating and maintenance cost (mills/kWhr),

IT = income taxes (mills/kWhr).

The direct capital costs of the combined cycle plant are modified as shown below:

$$C_H^* = C_H \left(\frac{\eta}{\eta^*}\right) \tag{8}$$

$$C_S^* = C_S \left(\frac{P}{P + \Delta P}\right) \tag{9}$$

$$C_{TI}^* = C_{TI} \left(\frac{\Delta P}{P + \Delta P}\right) \tag{10}$$

where: C_H^* = modified heliostat cost in the combined cycle plant ($/kWe)

C_S^* = modified cost of the solar thermal steam cycle ($/kWe)

C_{TI} = cost of the thermionic cycle ($/thermionic-kWe)

C_{TI}^* = modified cost of the thermionic cycle ($/kWe)

The modified energy cost in the combined cycle plant is then

$$BBEC^* = \gamma \; C_H \left[\left(\frac{\eta}{\eta^*}\right) + C_S \left(\frac{P}{P + \Delta P}\right) + C_{TI} \left(\frac{\Delta P}{P + \Delta P}\right)\right] + OM + IT \tag{11}$$

The change in energy cost is obtained by taking the difference between the expression for BBEC as defined in Eq(7) and $BBEC^*$ in Eq(11). Anticipating a savings we define the difference as follows:

$$Sav = BBEC - BBEC^* \tag{12}$$

Substitutions are then made in Eq(12) from Eq(11) and Eq(7). Solving Eq(7) for γ allows the factor to be eliminated from the result. Additional simplification is possible by eliminating ΔP, P, and η^* using Eqs(5) and (6).

$$Sav = \frac{\eta_{TI} \; (BBEC - OM - IT)}{\eta_{TI} + \eta(1 - \eta_{TI})} \left[\frac{C_H(1 - \eta) + C_S - C_{TI}}{C_H + C_S}\right] \tag{13}$$

Equation (13) can be used to calculate the change in electric energy costs when a thermionic topping cycle is added to a solar thermal central receiver power plant. An important feature of Eq(13) is that the cost coefficients in the large square brackets are shown only as ratios; thus the effects of escalation or inflation cancel out.

Cost Results

The changes in total bus bar energy costs for the power plant were calculated as a function of thermionic efficiency. It was necessary to consider the variation of thermionic efficiency since the operating temperature of the system is not defined in this preliminary assessment. This also permits any desired degree of optimism regarding the performance of the thermionic converters. The results of the calculations are shown in Fig. 11.

The calculated bus bar energy cost for the untopped power plant is 142 mills/kW-hr (ref. 4). All the lines on the graph start from this point on the vertical axis of the left side. This value is then perturbed using Eq(13) to calculate the savings (or loss) as a function of the thermionic efficiency. The efficiency of the overall combined system is also shown on the ordinate.

Another important parameter in the cost saving equation is the cost of the thermionic system, C_{TI}. (Strictly speaking this represents the total cost differential incurred by adding the thermionic topping cycle, including any modification to the boiler or any other parts of the system.) This parameter can be varied to form a family of cost savings lines where each line represents a specific thermionic system cost expressed as dollars/kW of thermionic power. Inspection of Fig. 11 shows there is a loss whenever the thermionic system cost is more than $2600/kW. However when the thermionic system cost is less than $2600/kW there is a savings in energy cost that grows as thermionic efficiency (and the combined cycle efficiency) is increased.

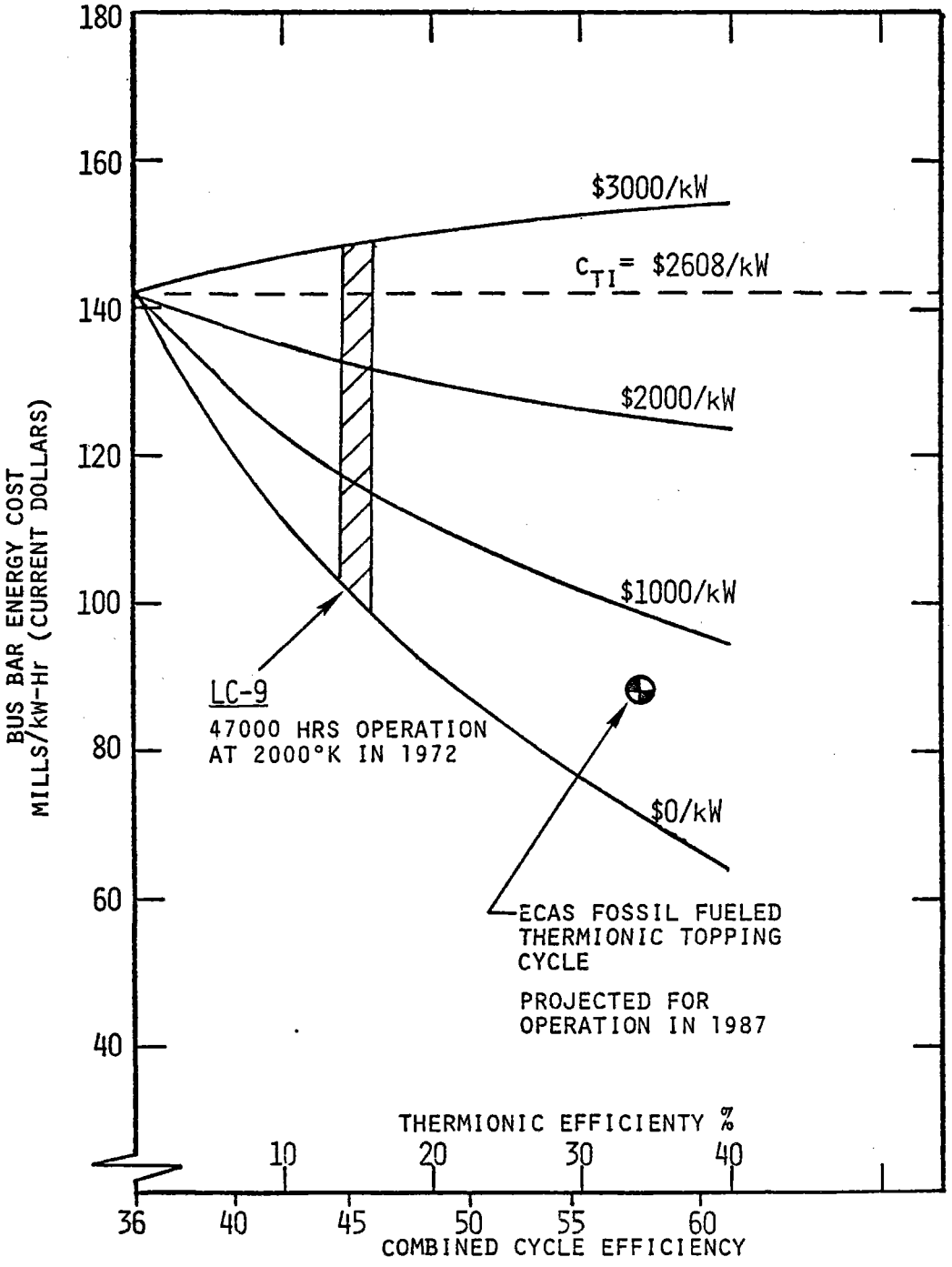

Fig. 11 - Energy Costs with Thermionic Topping Based on McDonnell-Douglas Design for First Commercial Solar Central Receiver Plant

Although the actual cost of the thermionic topping cycle for solar power plants cannot be calculated without a detailed system study, some estimate of expected cost can be obtained by comparison with results from previous studies of fossil fuel power plants. The efficiency and thermionic cost determined by the DOE study of fossil-fueled thermionic topping system is shown on the graph as a reference point. In a solar application this would give an expected savings of about 50 mills/kW-hr over the untopped system. In addition to the DOE study point, there is also a shaded area which shows the efficiency at which LC-9 (the longest life converter described earlier) operated. The cost for the thermionic topped solar thermal plant with converter performance equal to that of LC-9 has not been calculated; however, it is expected that such a system could be built with a cost differential of approximately $1000/kW. This would result in an electricity cost saving of approximately 25 mills/kW-hr.

Two factors which will strongly effect BBEC have not been treated in this perturbation analysis. First, the cost of a solar thermal central receiver with thermionic units has not been calculated specifically. Rather cost estimates representative of fossil fueled systems were used. Second, reradiation losses from the cavity receiver were not included in the cost analysis. Because of its higher operating temperature the thermionic topping cycle is likely to increase these reradiation heat losses unless substantial improvements are made in the receiver design. A more detailed study of a system designed specifically to utilize the characteristics of thermionic converters should be performed to determine if the potential BBEC savings projected in the study are optimistic or pessimistic.

CONCLUSION

The high temperature, high power density characteristics of thermionic converters make them an excellent match to the optimum operating temperature of a solar receiver. The fact that thermionic converters operate at low pressures, have no moving parts, and are modular make them particularly adaptable to solar application. The use of thermionic converters permits

new approaches to energy storage for the solar system either with emitter temperature storage or by the production of hydrogen. A first order perturbation analysis of the first commercial solar central station power plant design with a MDAC receiver indicates that the use of thermionics can potentially provide significant savings in the cost-of-electricity.

REFERENCES

1. "Thermionic Converter and Fuel Element Testing Summaries at Gulf General Atomic Company," GULF-GA-C12345.

2. "Thermionic Converter and Generator Tests," Peter Rouklove, Thermionic Conversion Specialist Conference, Palo Alto, California, Oct. 1967.

3. "Performance and Cost Evaluation for a Thermionic Topping Power Plant," G. Carnasciali, G. O. Fitzpatrick, and E. J. Britt, presented at the ASME Winter Meeting, Atlanta, Georgia, 77-Wa/ENER-7, 1977.

4. "Recommendations for the Conceptual Design of the Barstow, California, Solar Central Receiver Pilot Plant-Executive Summary" SAND77-8035, UC-62, Solar Project Division 8132, Sandia Laboratories, October 1977.

LA-UR

TITLE: Thermionic Topping of a Solar Power Plant Using Converters Containing Lanthanum Hexaboride Electrodes.*

AUTHOR(S): Edmund Storms

SUBMITTED TO: To be presented at the Solar Tower Test Facility (STTF) Users Association Annual Meeting, 11-12 April 1978, in Golden, CO. (uncl.) and to be published in the proceedings.

*Work completed under the auspices of the Department of Energy.

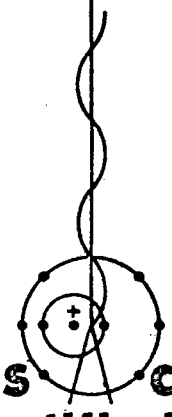

Form No. 836
St. No. 2629
1/75

UNITED STATES
ENERGY RESEARCH AND
DEVELOPMENT ADMINISTRATION
CONTRACT W-7405-ENG. 36

Introduction

The efficiency of thermionic conversion, as described in the previous paper, has increased as the processes occurring at the electrode surfaces have been better understood. The discovery that surface oxygen improves the behavior of a tungsten electrode made an important contribution and now the W-O-Cs electrode is the standard against which further progress is measured. Unfortunately, there are only a limited number of variables which can be manipulated to improve the performance of such electrodes. Consequently, efforts are being made to find other electrode materials having a sufficiently low vaporization rate for atoms while retaining a high emission rate for electrons in the presence of Cs, a fairly unusual combination of properties. Finding such materials is expensive and the low level of funding has not given much urgency to progress in this area. Recently, however, some success has resulted from using a thermionic emitter which has found application in other areas.

Several workers have demonstrated that a significant increase in converter efficiency is possible using lanthanum hexaboride electrodes. Russian experience, which leads the U.S. in this area, has added confidence to this approach. While LaB_6 appears to be superior to W-O-Cs, further development requires understanding a behavior which is not present when elemental electrodes are used. This paper will discuss some of the important variables associated with LaB_6 and, indeed, with compounds in general.

Discussion

The most important variable which determines the behavior of lanthanum hexaboride is its stoichiometry. This compound can exist over a composition range at high temperature as shown in the partial phase diagram in Fig. 1.[1] All of the properties change as the composition is changed across this rather narrow range. Because very little attention has been given to this variable in the past, most early work can only be used as a guide and must be repeated before the actual behavior is known.

For a thermionic application, where atom and electron vaporization rates are important, it is the surface composition which must be considered. When lanthanum hexaboride vaporizes in vacuum, the surface quickly acquires a composition which is different from the interior, unless the interior has the congruently vaporizing composition (CVC). Most samples used in either research or application will not be at this special composition and will, therefore, show an inconsistent behavior. Furthermore, this surface composition will change by reaction with ambient gases, when hot surfaces are nearby or when the temperature is changed. Failure to consider this behavior has lead to the impression that LaB_6 was approximately 100 times more volatile than is actually the case. Naturally, this error gave little encouragement to the use of LaB_6 in an application needing a lifetime of many years.

Regardless of the interior composition, the surface will tend to approach a value near $LaB_{6.05}$. However, the surface will be on the boron rich side of this composition if the interior is on the boron rich side and the reverse is true if the interior is on the boron poor side. Figure 2 shows how the surface composition is related to the interior composition at 1700 K. As the temperature

is increased, the surface composition becomes less influenced by the interior composition, as can be seen in Fig. 3 for 2100 K. From these figures we can conclude that the surface composition will change with temperature and this effect is strongest for interior compositions which are boron poor compared to $LaB_{6.0}$.

How does this behavior apply to the use of LaB_6 in a thermionic converter? The answer to this question involves three properties: the vaporization rate of atoms, which determines the life; the work function, which determines the efficiency; and the effect of Cs on these two properties. Other gases besides Cs may be useful with LaB_6, but this will not be discussed here.

Attrition caused by atom vaporization in vacuum at 1700 K is changed when the interior composition is changed, as shown in Fig. 4. This behavior will be modified if the samples are impure or if oxygen containing molecules are in the ambient gas. Oxygen causes the volatility of lanthanum hexaboride to increase through the formation of $LaO_{(g)}$ and various gaseous oxides of boron. The data presented are typical of slightly impure LaB_6 of commercial quality. When the temperature is changed, the change in attrition rate also depends on the interior composition. Figure 5 shows this change for samples consisting of LaB_4 + LaB_6 and LaB_6 + LaB_9. Again the presence of oxygen will change this behavior.

Work done in Russia [2] has shown that the vacuum work function is a strong function of composition. This explains in part why the various reported values are in such disagreement. Since the work function is sensitive to the surface composition and the surface composition will change if

the temperature or interior composition is changed, the measurement of a meaningful value for the work function is no easy task. If the value is based on the slope of a Log I/T^2 vs $1/T$ plot, the changing composition will produce an error. On the other hand, if the effective work function is calculated using the Richardson-Dushman equation with a value of 120 A/cm^2T^2 for the constant, the result may be in error because the constant may not apply to such compounds. In any case, the work function value will change when the temperature is changed because the surface composition changes. Consequently, when the electron emission current at one temperature is calculated from a reported work function value obtained at a different temperature, the result may be seriously in error. I mention this problem to show some of the difficulties in making decisions about the usefulness of such materials. Although the effect of composition makes accurate measurements difficult, it does give an additional variable which can be adjusted to improve the performance of a device.

The cesiated work function is expensive to measure and little information is available. Unpublished information suggests the compound behaves differently compared to the elements. The reactivity of Cs with lanthanum hexaboride will once again, be sensitive to the stoichiometry of the surface.

In spite of these sources of ignorance, the actual use of LaB_6 electrodes in a cesium diode has produced encouraging results. Shortly before the program was cancelled, Jim Morris and co-workers, at NASA Lewis, obtained the results shown in Figure 6.[3] Nearly stoichiometric LaB_6 was used as the emitter and slightly boron rich material was used as the collector. Without making any attempt to optimize the Cs pressure or temperature, they

obtained results which are a significant improvement compared to the W-O-Cs electrode.

I have attempted to summarize, in a brief and informal way, what is known about LaB_6. I have not discussed the increasing amount of information about the behavior of single crystals or the effects produced by impurities, such as carbon. Much work needs to be done, and, under the present approach, an application must be found to provide the financial support. While the use of this method in solar conversion is not the only, nor necessarily, the best application at this time, your appreciation of the potential of this technique can encourage the necessary support, and hopefully, lead to a diode which will be useful in the future.

References

1. Storms, E. and Mueller, B., J Phys. Chem. 82, 51 (1978).

2. Kudintesva, G. A., Kurnetsova, G. M., Mamedov, F. G., Meerson, G. A., Tsarev, B. M., Izv. Akad. Nauk. SSSR., Neorg. Mater. 4, 49 (1968).

3. Morris, J., Private Communication (1978).

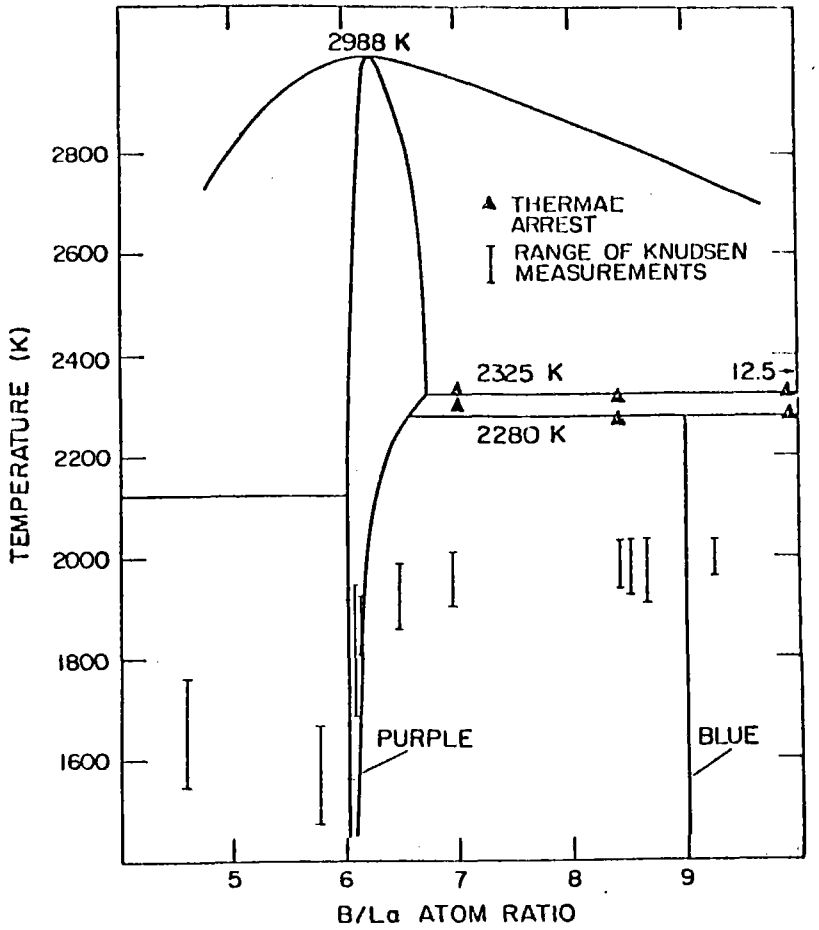

Figure 1. Partial Phase Diagram of the La-B System.

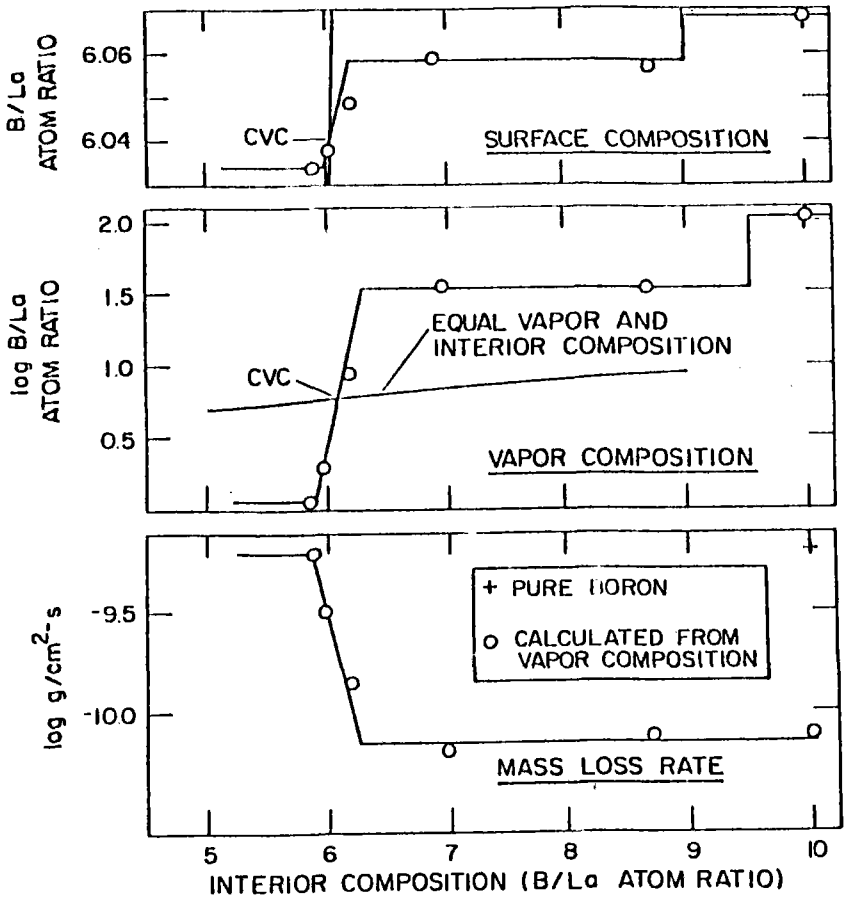

Figure 2. Relationship Between Surface Composition, Vapor Composition, and Mass Loss Rate as a Function of Interior Composition at 1700K for Freely Vaporizing Material.

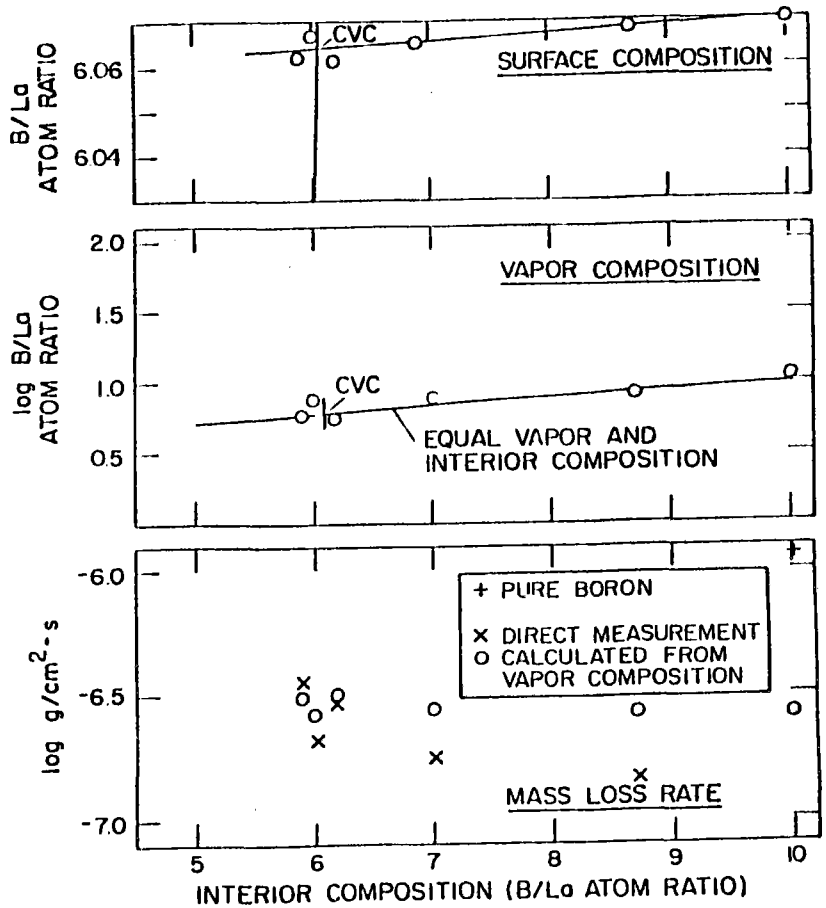

Figure 3. Relationship Between Surface Composition, Vapor Composition, and Mass Loss Rate as a Function of Interior Composition at 2100K for Freely Vaporizing Material.

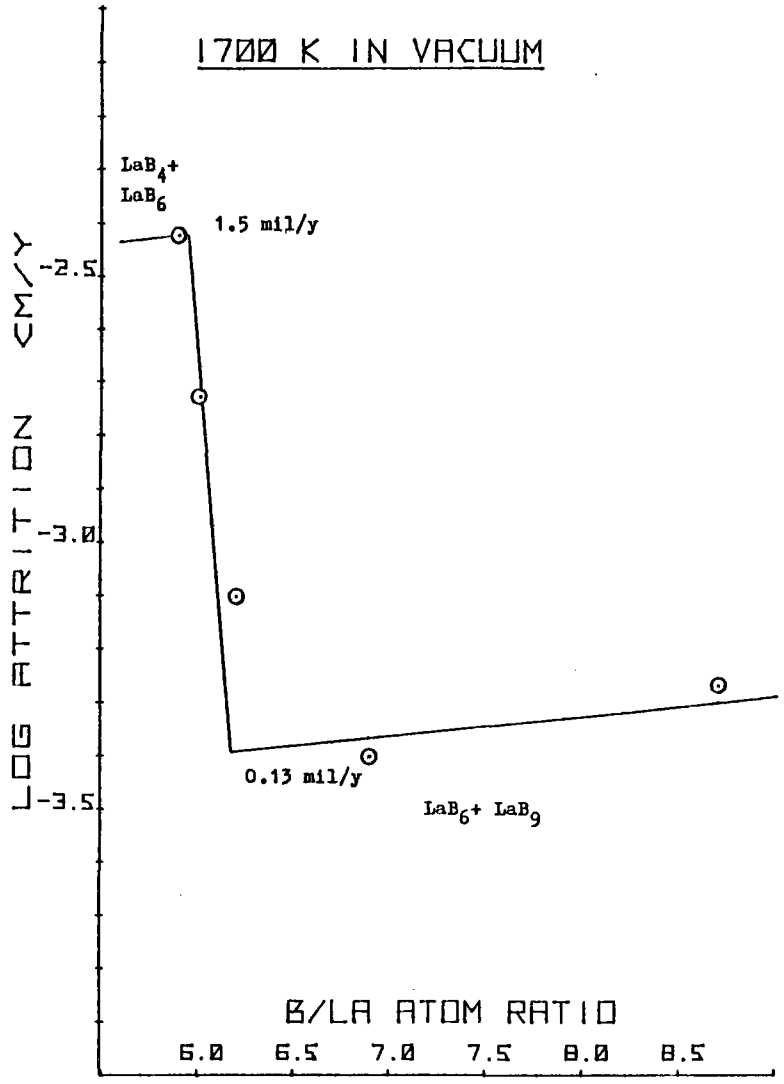

Figure 4. Attrition Rate for Various Compositions of Lanthanum Hexaboride at 1700K in Vacuum.

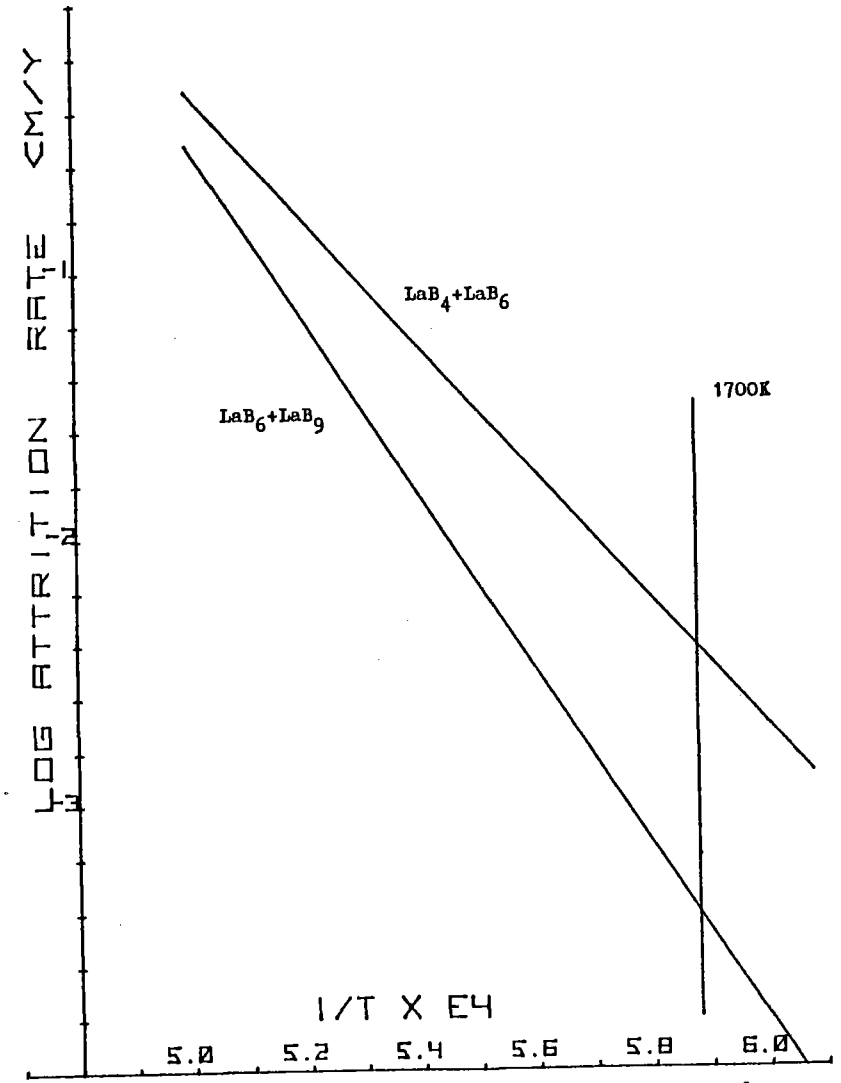

Figure 5. Attrition Rates for the Composition Extremes of Lanthanum Hexaboride vs 1/T.

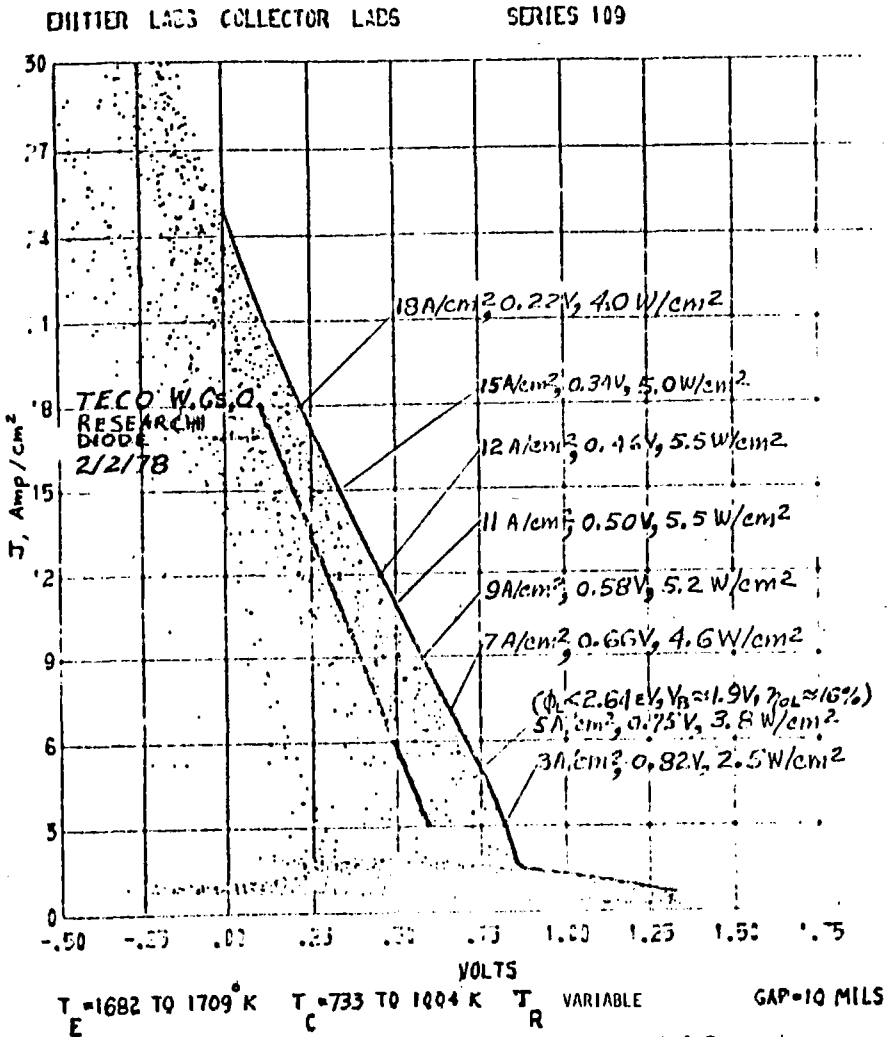

Figure 6. Preliminary Relationship between Generated Current and Voltage in a Cesium Diode using LaB_6 Electrodes. (Private Communication from Jim Morris, NASA Lewis)

X. SESSION VI: INDUSTRIAL CHEMICAL PROCESSES

PRODUCTION OF USEFUL CHEMICAL MATERIALS USING SOLAR ENERGY DEVICES

Dr. John Margrave

Rice University
Houston, Texas

Abstract

Although it has been known for many years that one can attain elevated temperatures by means of solar mirrors and focusing devices, there is still no commercial process for chemicals making use of solar energy. Several chemical reaction systems are adaptable to a batch approach and the effective temperature range limits and special requirements are sufficiently broad so that solar thermal devices of the sort available in Albuquerque or the various other Solar Research Laboratories could be adequate for small scale commercial processes.

Among the chemical reactions which appear most attractive are: (1) The production of cement, sand, clay, calcium carbonate; (2) The production of calcium carbide; and (3) Extraction of boric acid from natural borates.

These three suggested processes are only examples. There must be other chemical reactions and synthesis which could be profitably adapted to solar technology. The main criteria for consideration are: (1) A batch process is feasible; (2) Exact temperature control and exact exposures to temperatures for very precise periods of time are not required; (3) A reasonably large commercial market is available; and (4) Current technology is essentially based on methods which have been in use for 50 years or more.

NOTE: This paper was not available for inclusion in the Proceedings; therefore, we are reprinting the abstract.

LA-UR 78-852

TITLE: Treatment of Molybdenite Ore Using a 2 kW Solar Furnace.*

AUTHOR(S): S. R. Skaggs,** J. P. Coutures,† R. Renard†

SUBMITTED TO: To be presented and included in the Proceedings of the Solar Thermal Test Facility (STTF) Users Association Annual Meeting, 11-12 April 1978, Golden, Colorado. (uncl.)

**University of California, Los Alamos Scientific Laboratory
Los Alamos, New Mexico 87545.

†CNRS Laboratoire des Ultra-Refractaires, Odeillo, France 66120

*Work completed under the auspices of the Department of Energy.

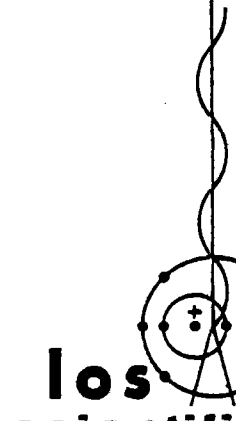

Form No. 836
St. No. 2629
1/75

UNITED STATES
ENERGY RESEARCH AND
DEVELOPMENT ADMINISTRATION
CONTRACT W-7405-ENG. 36

ABSTRACT

In the summer of 1977 several 10 g samples of molybdenite ore containing 5-6% Mo as MoS_2 were heated in one of the 2 kW solar furnaces at the Laboratoire des Ultra-Refractaires, Odeillo, France. The end products showed excellent separation with pure yellow acicular crystals of 99^{+}% MoO_3 and pure white SiO_2 powder being the two major components. Impurity levels in the MoO_3 did not exceed 6000 ppm while only a small fraction of the molybdenite was entrained along with the SiO_2. All treatment was done in a flowing oxygen atmosphere, and other elements condensed out at specific sites in the gas transport system. Analysis of the products was done by x-ray diffraction and x-ray fluorescence, emission spectroscopy, and wet chemical analysis. The ore was donated by Climax Molybdenum Co., Climax Co., and the work is a joint effort of LASL and CNRS Laboratoire des Ultra-Refractaires, Odeillo, France.

Work completed under the auspices of the Department of Energy.

Introduction

This paper describes the use of a 2 kW vertical axis solar furnace to treat small samples of molybdenite ore (MoS_2) concentrate. The original idea arose out of discussions with Coutures, Goldfarb, and Bezerra during a visit to Odeillo in the summer of 1976, and included the treatment of rare-earth containing minerals. A large fraction of the energy required to separate these minerals from their ores comes from fossil fuels. Conventional methods for preparing molybdenite concentrate from the ore utilize hydrometallurgical techniques and require an expenditure of about 25¢/lb of concentrate in electrical energy. Subsequently, the MoS_2 concentrate is roasted in an oxidizing atmosphere to make MoO_3 crystals with a considerable expenditure of fossil fuel energy usually in the form of natural gas. Initial examination of the thermodynamics suggested that a direct extraction process using a solar furnace as a heat source could conserve a considerable fraction of this energy. In the summer of 1977 the authors performed several experiments on small quantities of molybdenite concentrate in a flowing oxygen atmsophere. Subsequent analysis showed that excellent separation was achieved between the molybdenite and the gangue minerals. Results of these experiments are presented below.

Experimental Procedure

The solar furnace used in this experiment was described by Coutures et al (1) and is shown schematically in Fig. 1. The parabolic mirror is 2 m diam. with a focal length of 0.85 m, and it has a focal spot approximately 1 cm diam. The apparatus used was constructed by Goldfarb and Bezerra, (2) and is shown schematically in Fig. 2. It consisted of a

water cooled aluminum hearth surrounded by a 5 liter Pyrex globe with a vacuum tight seal. Sample material was placed on the hearth. The whole unit was evacuated and backfilled with an oxygen atmosphere, and then continuously flushed with gas. Other gases were tried but did not achieve separation of the minerals. The unit was pushed into and removed from the focus of the mirror on a small trolley.

Gas and particulates emitted from the sample during solar heating are carried by an excess flow of oxygen at 5 l/min through the top of the globe into a conductor pipe, thence to a cyclone seprator. Condensate collects on the inside of the globe, in the pipe, and in the cyclone separator. That which does not collect in the cyclone separator by centrifugal action is subsequently filtered by a fine mesh stainless steel screen in the exhaust port. Non-condensable gaseous products, e.g. SO_2, exhaust into the atmosphere.

The sample of molybdenite ore bearing rock furnished by Climax Molybdenum Corp. was ground to pass a 10 mess screen. Without further treatment a 10 g amount was heaped onto the hearth of the furnace. The unit was moved to the focus of the furnace and the pile of powder was heated continuously for 10 min while the evolution of gases and smoke was observed visually. At the end of the heating period the hearth was removed from the focus, and samples were collected from six different locations in the system. The relative temperature of each sample decreases with distance from the hearth; the sample location 1 in Fig. 2 is the hottest and sample location 5 is the coolest.

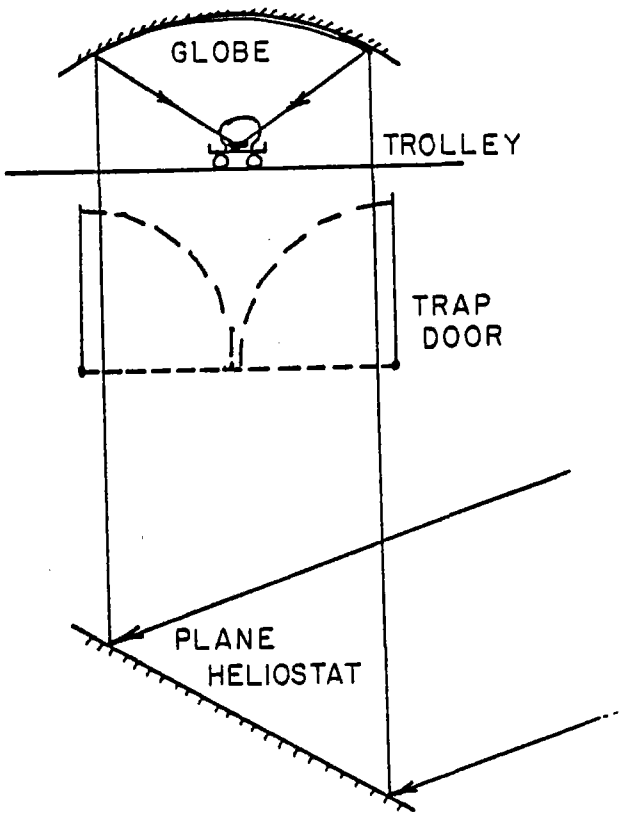

Fig. 1. Schematic of 2 kW vertical axis solar furnace.

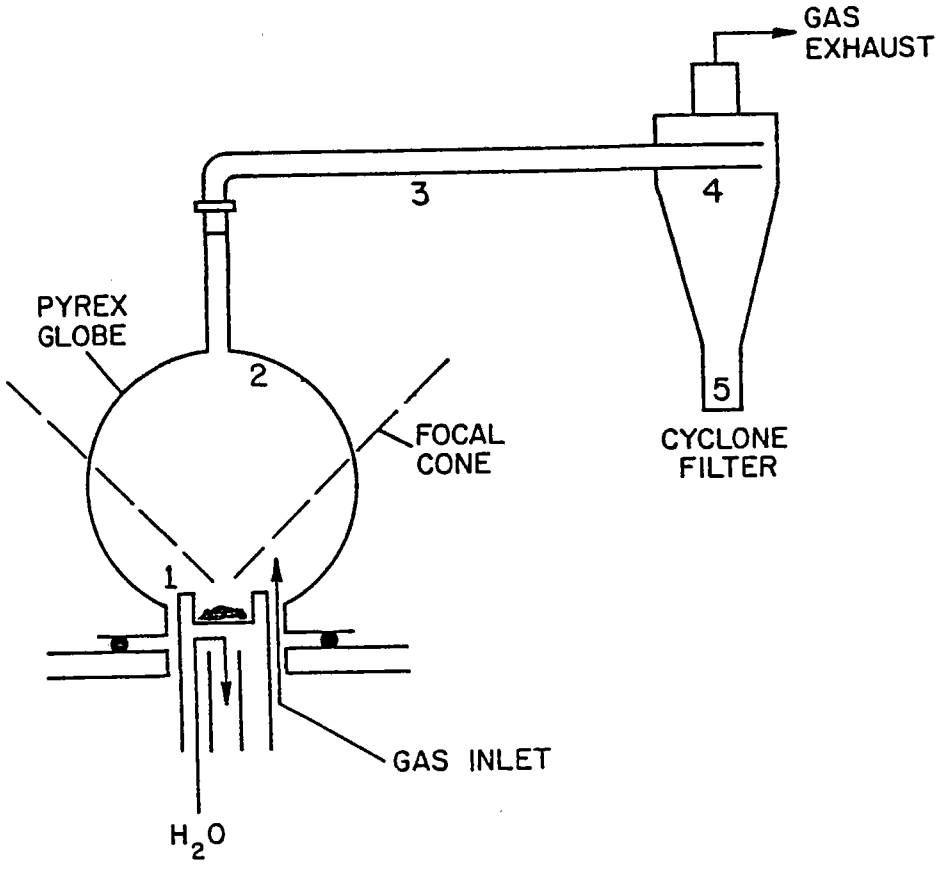

Fig. 2. Schematic of apparatus used to treat molybdenite ore. Numbers are locations where samples were collected.

This experiment was conducted following an International Colloquium at Odeillo and was intended to be a scoping experiment only. A moderate attempt was made to do a mass balance, however because of several trials and the short time available this was not accomplished. Only rough analyses were performed at the time of the experiment; the more careful analyses had to wait for laboratory time. The results presented below are from the more careful analyses.

Results

At location 1 in Fig. 2 yellow crystals of vapor transported MoO_3 were observed to grow at the edge of the pile of powder. These crystals were collected carefully to avoid contamination by other products. The residue left behind after evaporation of the molybdenum oxide was the source of the second sample at the same location. A large fraction of the smoke from the evaporated rock was condensed as a white fluffy powder on the inside of the Pyrex globe. This powder from the surface of the globe formed the third sample, and is shown as location 2 in Fig. 2.

The fourth sample was material condensed as a grayish-white powder on the inside wall of the pipe connecting the globe to the cyclone separator. This is location 3 in Fig. 2. Smoke that condensed by centrifugal action was collected in the bottom of the cyclone separator at location 5 in Fig. 2. The sixth and last sample deposited on the fine mesh stainless steel screen in the exhaust port of the separator shown at location 4.

The samples were divided and a portion of each sample was submitted for the following analyses; x-ray diffraction, x-ray fluorescence, semi-quantitative spectrographic analysis, thermogravimetric analysis, and wet

chemical analysis. Wet chemistry was used to determine the Mo content in each sample except as noted later. Silica content was confirmed by x-ray fluorescence. Impurity content was determined by semi-quantitative spectrographic analysis, and is shown in Table 1. Stoichiometry of the molybdenum oxide was analyzed by thermogravimetric analysis.

The starting ore has a few strong lines in the forward direction which are characteristic of MoO_3, however most of the x-ray diffraction lines are missing as would be expected with a sample as dilute as this ore. Semi-quantitative spectrographic analysis shows relatively high concentrations of Na, Mg, K, CA, Ti, Mn, Fe, Zn, and Pb. The starting material is feldspathic in nature with occassional concentrations of molybdenite which appear as dark lines in the rock, and dark grains in the crushed ore.

Reagent grade molybdenum trioxide was used as the standard for comparison of x-ray diffraction patterns. The vapor grown crystals from sample 1 show an identical pattern with the standard material both for line position and intensity. Wet chemical analysis shows the sample contains 66% Mo which is stoichiometrically correct for MoO_3. Spectrographic analysis shows this sample to be nearly as pure as the reagent grade MoO_3 used as the standard. Only Ca and Si were higher in the sample.

The crystalline material from sample 2, the residue from the rest of the pile, shows a very strong MoO_3 diffraction pattern also; however some of the intensities in the back reflection zone are reduced. This is consistent with the wet chemical analysis which shows 61% Mo present in this sample. Spectrographic analysis shows approximately the same relative distribution of elements in this sample as in the starting ore. It appears that a large fraction of the silica initially in the ore was

evaporated during the heating as it is reduced to 5% in this sample as compared with 30% in the starting ore.

The white powder collected as sample 3 from the inside of the globe yielded an amorphous x-ray diffraction pattern with four diffuse lines in the forward direction and no lines visible in the back reflection zone. X-ray fluorescence measurements on the powder indicated the major constituent was silica. Na, K, and Cr were concentrated in this sample, while Fe and Ti remained about the same concentration as the ore, and all other elements decreased in concentration. Some of this sample was subjected to thermogravimetric analysis. Very little weight was gained, and a large amount of gas was evolved.

The gray powder collected as sample 4 from the transfer pipe, location 3 in Fig. 2, has strong lines in the forward direction characteristic of molybdenum trioxide. Only a small amount of this sample was available for analysis so an exact determination of the amount of Mo was not made. Several of the transition metals concentrated in this region: Cr, Fe, Ni, Cu, Sn, and Bi.

Sample 5 was a gray powder collected from the cyclone cup, however its composition was considerably different than the gray powder in the transfer pipe. Wet chemical analysis on this sample shows 63% Mo present, and this is confirmed by the x-ray diffraction pattern which falls somewhere between sample 1 and sample 2 in intensity. It appears from the spectrographic analysis that this is very finely divided MoO_3 crystals which are relatively pure and are entrained in the gas stream. It is necessary to precipitate them from the gas stream by centrifugal action in the cyclone separator.

Sample 6 was collected from the stainless steel filter screen, and the x-ray diffraction film is similar in pattern and intensity to sample 4 from the transfer pipe. Very little material was collected at this stage as most of it had precipitated out earlier in the system. The spectrographic analysis shows it is still fairly rich in Na, K, Fe, Zn, and Pb. Both Cu and Sn have concentrated at this point in the system.

Thermogravimetric analysis was performed on samples at location 2 and 3 to determine the degree of stoichiometry by oxygen uptake. A large amount of gas was evolved rather than taken up. This coupled with the broad diffraction lines in the x-ray patterns indicate the powder is very finely divided.

Discussion

A mass balance was not performed on this experiment, however the qualitative results show that a very effective method of separating molybdenum as its oxide from the ore containing only a small amount of Mo has been found. Reference to Table I shows that the Mo was concentrated by a factor of 10 from the raw ore to the yellow MoO_3 crystals, and that fractionation of various elements occurred at different stages in the gas train. It also shows that Si was removed from the ore quite effectively by reducing the concentration of Si from 30% to about 4000 ppm in the MoO_3 crystals obtained. Examination of the silica powder from the inside of the Pyrex globe shows it to be relatively pure SiO_2. This suggests that with further treatment in the same process the purity of MoO_3 could be improved, and very pure silica with high surface area could be prepared.

Table I.

Semiquantitative Spectrographic Analysis of Samples by Location.
All Units Are ppm Unless Otherwise Indicated

	Mo	Si	Li	Be	B	Na	Mg	Al	Si	K	Ca	Ti	V	Cr
Standard	66%	10 ppm	< 10	< 1	< 3	40	6	< 30	10	200	5	< 3	< 10	< 3
Starting ore	6.5%	30%	200	4	30	400	2500	1.5%	30%	1%	6000	400	< 10	5
MoO_3 yellow xtals (1)	66%	4000	< 10	< 1	< 3	< 30	8	50	4000	< 200	20	5	< 10	< 3
Residue from pile (1)	61%	5%	15	1	3	300	1000	1%	5%	3000	4000	200	< 10	5
Vapor from globe (2)	N/A	30%	300	1	150	2500	100	300	30%	3%	100	600	10	200
Vapor from transfer pile (3)	N/A	10%	< 10	3	< 6	250	500	800	10%	600	600	100	< 20	1000
Smoke from cyclone (5)	63%	5000	< 10	1	< 3	50	80	400	5000	200	150	15	< 10	3
Smoke from filter (4)	N/A	500	< 10	1	< 3	250	80	100	500	700	80	15	< 10	10

Table I.

Semiquantitative Spectrographic Analysis of Samples by Location.
All Units Are ppm Unless Otherwise Indicated

	Mn	Fe	Co	Ni	Cu	Zn	Ge	Sr	Zr	Nb
Standard	1	< 10	< 100	< 30	40	< 300	< 10	< 1	< 50	< 100
Starting ore	600	5000	< 100	30	250	1500	< 10	25	< 50	< 100
MoO_3 yellow xtals (1)	1	40	< 100	< 30	15	< 30	< 10	< 1	< 50	< 100
Residue from pile (1)	200	600	< 100	30	1500	1000	< 10	30	< 50	< 100
Vapor from globe (2)	60	5000	< 100	200	100	< 300	< 10	1	< 50	< 100
Vapor from transfer pile (3)	600	6000	< 100	400	500	< 600	< 10	< 2	< 100	< 100
Smoke from cyclone (5)	15	250	< 100	< 30	30	< 300	< 10	1	< 50	< 100
Smoke from filter (4)	50	1000	< 100	150	5000	400	< 10	1	< 50	< 100

Table I.

Semiquantitative Spectrographic Analysis of Samples by Location.
All Units Are ppm Unless Otherwise Indicated

	Mo	Ag	Cd	In	Sn	Sb	Ba	Tl	Pb	Bi
Standard	66%	< 3	< 3	< 30	< 30	< 30	< 3	< 50	< 10	< 50
Starting ore	6.5%	6	10	< 30	< 30	< 30	80	< 50	1000	< 50
MoO_3 yellow xtals (1)	66%	< 3	< 3	< 30	30	< 30	< 3	< 50	10	< 50
Residue from pile (1)	61%	30	3	< 30	400	< 30	80	< 50	500	150
Vapor from globe (2)	N/A	3	< 3	< 30	100	< 3	< 50	30	< 50	< 30
Vapor from transfer pile (3)	N/A	6	< 6	< 30	200	< 60	8	< 50	300	200
Smoke from cyclone (5)	63%	< 3	< 3	< 30	100	< 30	< 3	50	80	< 50
Smoke from filter (4)	N/A	8	10	< 30	1500	< 30	< 3	< 50	400	150

The silica may possibly be used in transistor manufacture or for catalysis. Table II shows the degree of separation between some of the important components in the ore and the crystals.

Table II.

Separation of Some Elements Between the Ore and the MoO_3 Crystals

Element	Ore	Crystals	Separation Factor
Mo	6%	66%	11
Si	30%	4000 ppm	75
Al	1.5%	50 ppm	30
K	1%	200 ppm	50

Although Nb and Zr were not present in large concentrations in the raw ore they seemed to follow through the process and remain in the same relative concentrations at each stage. The process may therefore also be useful for the benefication of ores of these two elements. Re was not found in the starting ore; and therefore no analysis was made for it in the products.

Fractions removed at different stages in the system showed widely varying concentrations of elements or groups of elements. For example, the vapor that condensed early in the gas train is high in Si, Ti, Mg, K, Na, and some of the transition elements. Other transition elements condensed later in the train; for example, Fe, Cr, Cu, and Ni are concentrated in the transfer pipe beyond the large surface area in the globe. The selective condensation suggests that it is possible to tap fractions of the

gas stream at various stages downstream, and to obtain enriched concentrations of specific elements.

Comparison of the analysis of MoO_3 yellow crystals made by vapor transport in the solar furnace with the analysis of the MoO_3 reagent grade standard shows that the impurity level for all elements in the crystals prepared by the solar furnace is at least as low as that in the standard except for Ca and Si. This suggets that reagent grade MoO_3 could be prepared rapidly and in quantity using the solar furnace method. It is also possible to reheat the MoO_3 crystals obtained from the initial heating to further refine it. This and subsequent heatings would not significantly increase the cost of the chemical because of the simplicity of the process.

Some elements were concentrated in the residue left behind during the evaporation of molybdenum. These are shown in Table III. The residue thus may be of some economic importance at some later time in the processing.

Table III.

Some Elements in the Ore and the Residue

Element	Ore, ppm	Residue, ppm	Separation Faction
Cu	25 ppm	1500 ppm	60
Fe	5000 ppm	6000	$\sim$ 1
Sn	< 30	400	13
Ag	6	30	5
Bi	< 50	150	3

Examination of Table I shows some interesting results for fractions of the vapor that have condensed in different parts of the apparatus. The following pairs of elements behave quite similarly: Si and Al, Na and K, Mg and Ca, Cu and Sn, and the group Fe-Mn-Cr-Ni. Enrichment of these elements varied from a factor of 2 to about a factor of 5. This may not be of economic importance, however it does suggest that enriched vapor fractions might be removed from the vapor stream at various stages.

Conclusions

It is evident that excellent separation of MoO_3 from SiO_2 is achieved by the treatment of molybdenite ore in an O_2 atmosphere in a solar furnace, and that pure MoO_3 and SiO_2 products may be obtained . Increases or enrichment of many of the elements present in the samples are quite respectable, and this may be of some economic importance.

Niobium and zirconium follow the same path as molybdenum, but the concentration of these elements is low and the data on enrichment are inconclusive. Rhenium, which is almost always present in molybdenum ore, was not found in this material. An experiment should be conducted at some later date with rhemium ore to study its behavior. The vapor pressures of MoO_3 and Re_2O_7 differ widely thus one could expect an effective separation of these two materials in the vapor phase.

This experiment is an example of one that utilizes solar energy for process heat. It does not require a very high solar flux or very high temperatures to obtain results ($\sim$ 1400-1600°C). The oxidation of the MoS to MoO_3 is exothermic, and the kinetics appear to be rapid.

Future Work

The present work on ore refinement appears to yield good sepration of molybdenum from its ore. The authors plan to examine the process using larger quantities in the batch mode. Two experiments are presently planned: 1) to treat kilogram quantities of the raw ore in the 1 MW facility at Odeillo to determine if MoO_3 can effectively be extracted from the raw ore which is very low grade MoS_2 ($\leq$ 1% Mo), and 2) to roast MoS_2 concentrate in large quantities in the batch mode to make MoO_3 crystals of high purity. This latter product is used directly in steelmaking. A mass balance will be performed on both experiments. If the experiments are successful, economic and engineering analysis will be performed to determine if the process is adaptable on a continuous basis. Should this prove feasible, experiments could be prepared for the 5 MW Solar Thermal Test Facility when it is ready to commence operation.

Acknowledgements

The authors would like to acknowledge the pioneering efforts of Goldfarb and Bezerra in this field and their discussions with the authors. The analyses were performed by the CNRS Laboratoire des Ultra-Refractaires at Odeillo and by the Analytical Chemistry Group at the Los Alamos Scientific Laboratory. The ore was donated by the Climax Molybdenum Corp, Climax, Colorado, and its gift was greatly appreciated.

References

1. J. P. Coutures, R. Berjoan, B. Granier, Rev. Int. Htes Temp. et Refract., 1973 - 10- P. 273.

2. J. Goldfarb, A. M. Bezerra, Diplome d'Universite d'Energie Solaire. Available J. P. Coutures, Laboratoire Ultra-Refractaires, BP-5-66120 Odeillo, France.

LA-UR

78-1052

TITLE: Solar-Thermochemical Production of Hydrogen from Water.*

AUTHOR(S): Kenneth E. Cox and Melvin G. Bowman

SUBMITTED TO: To be presented and included in the Proceedings of the Solar Tower Test Facility (STTF) Users Association Annual Meeting, 11-12 April 1978 Golden, Colorado.

*Work completed under the auspices of the Department of Energy.

Division of Basic Energy Science

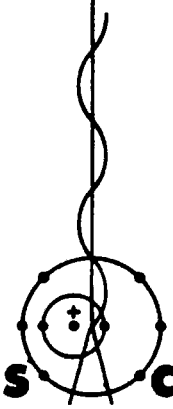

los alamos
scientific laboratory
of the University of California
LOS ALAMOS, NEW MEXICO 87545

Form No. 836
St. No. 2629
1/75

UNITED STATES
ENERGY RESEARCH AND
DEVELOPMENT ADMINISTRATION
CONTRACT W-7405-ENG. 36

Abstract

There is a widespread interest in the development of a "hydrogen economy" as an eventual solution to many of the problems associated with the growing energy crisis. Hydrogen is also valuable as a chemical intermediate. As fossil sources become inadequate, large scale hydrogen production must utilize energy sources such as solar energy for the decomposition of water by thermochemical cycles, electrolysis or perhaps, by a hybrid combination of these methods.

The potential higher efficiency and lower cost for thermochemical methods, versus the overall electrolysis path has been rather widely recognized. This paper details the criteria for the selection of an appropriate thermochemical cycle for matching with a high temperature solar heat source. Advantages of a thermochemical cycle based on a solid sulfate decomposition that makes use of isothermal high temperature energy is detailed and a plan for the implementation of such a cycle on a central tower solar receiver is given.

*Work completed under the auspices of the Department of Energy.

Introduction

The use of solar energy has not yet become widespread due largely to the costs of its collection, conversion and storage. As conventional fuel costs continue to escalate, solar energy has become more cost-effective for a number of applications such as business and residential heating and cooling.

To efficiently use solar energy as a major source of energy, it is highly desirable to convert it and store it in a concentrated form that can easily be transported. This has been the traditional case with fossil fuels, which represent solar energy that has accumulated over a much longer time period, i.e., millenia. Today, faster and more efficient methods of solar energy conversion to a form of chemical (stored) energy are clearly indicated.

A candidate system that appears to offer high potential for solar energy conversion and storage is that of the decomposition of water into its elements, hydrogen and oxygen. Hydrogen is a substance that can be stored in a number of ways, transported with relative ease, and used either in direct combustion to supply thermal energy or converted to electricity via fuel cells. In addition, with water as the only feedstock and the product on combustion, the use of hydrogen would be environmentally acceptable and would help alleviate the world's growing pollution problems (such as the CO_2 problem caused in large measure by our increasing dependence on coal). Additionally, the hydrogen produced would supply the growing demands for hydrogen as a chemical feedstock that has tripled in the last decade.

The use of hydrogen as an energy medium, transferring energy from abundant, clean, massive, renewable energy sources such as the sun to uses in industry, transportation, households and as a basic chemical intermediate has been termed the "hydrogen economy." (1)

It is not the purpose of this paper to engage in the debate regarding the relative merits of hydrogen vs. electricity as media for energy transfer and use, but rather to detail the means by which solar energy can be transfromed into hydrogen.

Hydrogen Production

Most of the hydrogen we use today is derived from fossil fuels. Hydrogen is produced from natural gas by steam reforming and from naphtha by partial oxidation processes. Future production methods for hydrogen will use water as the feedstock. Six possible water-splitting schemes are detailed in Table I below.

TABLE I

Water-Splitting Schemes for Hydrogen Production

1. Electrolysis
2. Direct Thermal Decomposition
3. Thermochemical Decomposition
4. Hybrid, Mixed Electrolytic and Thermochemical Decomposition
5. Hybrid Photochemical-Thermochemical Decomposition
6. Photolysis

With the exception of photolysis, these methods require a high temperature heat source to achieve reasonable conversion efficiencies to hydrogen. Photolysis hinges on the discovery of a chemical system with high quantum yields and broad-band absorption characteristics, which as yet remains undiscovered.

Among the thermal methods, the direct thermal decomposition of water appears to be impractical because of the low partial pressure of hydrogen and

oxygen produced even for temperatures of 3000 K and also because of practical engineering difficulties and low efficiencies for methods conceived for separating the hydrogen, oxygen and water.(2) Direct decomposition of carbon dioxide (rather than water) followed by the shift conversion reaction to produce hydrogen offers the advantage of much larger reaction yields, but formidable separation problems remain.

Electrolytic conversion of water to hydrogen and oxygen is a well-known technology. It however requires a power cycle to convert thermal energy to electricity and is thus inherently limited by thermodynamic constraints. Electricity obtained directly from sunlight via photovoltaic cells suffers from a low conversion efficiency (10-20%) and at today's prices, high capital cost ($10-20 per peak watt). The latter situation could change drastically if a pricing breakthrough is achieved in photovoltaics. (DOE's goal is $0.50 per peak watt by 1985). The efficiencies and relative costs of generating hydrogen by these techniques and thermochemical processing have been surveyed.(3)

A thermochemical step added to a photochemical or a photo-assisted electrolytic step could lead to a "hybrid" type of process for water decomposition which offers greater flexibility in the use of solar energy than either photolytic process on its own. Hybrid cycles of this nature are being studied for future potential as hydrogen producers at LASL.

In the thermochemical process for water-splitting, water is chemically reacted with intermediate chemical species to yield hydrogen or other compounds. These compounds are thermally decomposed at relatively low temperatures ($\sim$ 1000 K) in turn and yield other intermediates or oxygen. All chemical intermediates are recycled internally within the process or "cycle" so that water and thermal energy are the only inputs and hydrogen and oxygen plus a small amount of reject heat are the only outputs.

The prime purpose for pursuing thermochemical cycles as a means of producing hydrogen is the promise of a higher conversion efficiency of heat to hydrogen as contrasted to other methods for this transformation such as water electrolysis. This expected higher efficiency (defined as the ratio of higher heating value of hydrogen, 286 kJ/mol, to all thermal inputs to the cycle) in turn, would yield a lower cost for the hydrogen product. Although no thermochemical cycles are as yet commercialized, there appears to be good reason based on results to date, that thermochemical cycles can be devised within the range of current or near-term technology to yield hydrogen at rates comparable with electrolytic hydrogen at present-day electricity costs. The above is based on laboratory studies that have demonstrated all of the individual steps comprising a single cycle. Promising cycles are being investigated (in the USA) at the Los Alamos Scientific Laboratory, Lawrence Livermore Laboratory, Argonne National Laboratory, the Institute of Gas Technology, the General Atomic Company and the Westinghouse Electric Corporation. Extensive research in this novel area of energy research is also being conducted in Western Europe, primarily by Euratom at Ispra, Italy and also in Japan.

Major technical problems with proposed cycles are those of heat transfer, heat recuperation (internal heat recycle), and chemical species separation. Engineering approaches are being taken to solve these problems so that thermochemical cycle performance may be demonstrated in the near future.

Criteria for Thermochemical Cycle Selection

On a fundamental level, the energy requirements for the thermal decomposition of water can be disscussed in terms of chemical thermodynamics. This approach was first taken by Funk and Reinstrom, who laid the foundation for the concept of thermochemical water splitting.(4) They pointed out that a large ΔS value would be required for the $T\Delta S$ term to equal the ΔH term in

the high temperature reaction of a two-step cycle and concluded that simple two-step cycles would not be possible for temperature around 1000 K available from heat sources such as the high temperature (nuclear) reactor (HTR, or VHTR). We have also repeated the analysis (5) in order to point out that specific values for the sum of the ΔS° terms and the sum of the ΔH° terms are required for the endothermic reactions if maximum heat efficiencies are to be realized. These specific and related values depend on the maximum temperature at which heat is available and the ΔG°_f of water (237 kJ/mol) at the low temperature. Thus for a two-step decomposition cycle,

1. $R + AB = RA + B$ at T_1 (K)
2. $RA = R + A$ at T_2 (K)

"ideal" ΔS° and ΔH° values are given by,

$$\text{ideal } \Delta S^\circ = \frac{-\Delta G^\circ_f (AB)}{(T_2 - T_1)}$$

$$\text{ideal } \Delta H^\circ = \Delta S^\circ \times T_2$$

For the decomposition of water with T_1 at 400 K and T_2 at 1100 K,

3. $R + H_2O = RO + H_2$ 400 K
4. $RO = R + 1/2\ O_2$ 1100 K

ΔS° (reaction 4) = 320 J/K and ΔH° = 350 kJ/mol of H_2.

The striking feature of the above analysis are the large ΔS° values required for the decomposition reactions. Typically, reactions such as 4 exhibit ΔS° changes of about 100 J/K. However by raising the temperature, these thermochemical constraints are no longer so stringent. At temperatures approaching 2500 K, the required ΔS° value drops to 140 J/K approaching the ΔS° values that can be obtained in metal sulfate and metal oxide

decomposition reactions. It should therefore be possible to devise a thermochemical cycle consisting of from two to three steps that provide the necessary ΔS^{o} changes required for maximum efficiency at elevated temperatures.

Suggested Cycles for Hydrogen Production from Solar Energy

A few cycles have already been suggested for matching to a solar energy source. These include the General Atomic (GA) cycle (6); a zinc oxide cycle, (Bilgen, 7); an iron oxide cycle, (Nakamura, 2); and a hybrid (involving electrolysis) bismuth sulfate cycle being developed at the Los Alamos Scientific Laboratory (LASL, 8). Brief descriptions of these cycles follow with details on the General Atomic and LASL concepts.

The GA cycle has been described by Schuster (6), and is characterized by three reactions:

5.	$2H_2O + SO_2 + x\ I_2 = H_2SO_4 + 2\ HI_x$	Aqueous	300 K
6.	$2HI_x = x\ I_2 + H_2$		500 - 600 K
7.	$H_2SO_4 = H_2O + SO_2 + 1/2\ O_2$		1150 K

GA discovered in the laboratory that if excess iodine is added to the first reaction, a separation of the liquid phases into a HI_x-rich layer and a sulfuric acid layer occurs. These acids are readily separated and can be thermally decomposed to yield the desired hydrogen and oxygen as well as iodine and SO_2 for recycle.

The basic problem in coupling a solar energy source to a thermochemical cycle is one of effectively using the time-variant solar thermal input to "drive" the individual cycle reactions. In the GA scheme, the process works due to the availability of intermediate compound storage. In the GA conceptual scheme, the low temperature solution reaction is conducted 24 h/day,

producing H_2SO_4 and HI_x. During daylight hours, the sulfuric acid is decomposed at high temperature (1150 K). An intermediate heat transfer loop, possibly using an eutectic salt, stores thermal energy and supplies heat over the 24 h/day period to perform HI_x decomposition. For the sulfuric acid decomposition reaction, a central receiver solar tower might perform adequately; a fixed mirror solar concentrator (FMSC), invented by John Russell at GA is contemplated for heating the intermediate temperatute eutectic.

The work reported by Bilgen was done in conjunction with Ducarroir, Foex, Sibieude and Trombe at the French (CRNS) solar facility at Odeillo.(7) The cycle chosen is seen below:

8. $2ZnO\ (l) = 2Zn\ (g) + O_2\ (g)$ 2340 K

9. $2Zn\ (g) + 2H_2O\ (g) = 2ZnO\ (s) + 2H_2(g)$ 1500 K

The zinc oxide was diluted in a refractory oxide and a dynamic inert atmosphere was used. A theoretical efficiency of 51% was calculated for this cycle.

Nakamura (2) suggests a conceptual cycle that has the following steps:

10. $3FeO + H_2O = Fe_3O_4 + H_2$ 450 K

11. $Fe_3O_4 = 3FeO + 1/2\ O_2$ 2500 K

Reaction 11 has been studied experimentally by Ducarroir at Odeillo.(8) Fe_3O_4 was heated to 2100 K in the solar furnace at that facility and decomposed partially to give a mixed FeO and Fe_3O_4 material.

Fifty percent efficiency can be obtained if half the heat of the decomposing iron oxide is recoverable. With zero heat recovery, the efficiency would drop to 36 percent which is the upper limit of a thermal-electrolytic alternate process for hydrogen production. Needless to say, a number of engineering problems, particularly heat transfer as well as the kinetics of solid-gas reactions at high temperature need to be solved for this process to function.

The LASL hybrid-bismuth sulfate cycle employs the first step of the corresponding hybrid cycle being developed by Westinghouse,(9) this step is the electrolytic oxidation of SO_2 to give sulfuric acid and hydrogen as seen below:

12. $2H_2O + SO_2 \overset{\text{electrolysis}}{=} H_2SO_4\ (aq.) + H_2$ 300 K

Rather than completing the cycle by the decomposition of sulfuric acid as seen in reaction 7, a reaction in which a solid sulfate is precipitated follows,

13. $H_2SO_4\ (aq.) + 1/3$ Metal Oxide(s)
$= 1/3$ Metal Oxide Sulfate(s)

The metal oxide Bi_2O_3 is being considered, and the metal oxide sulfate is $Bi_2O_3 \cdot 3SO_3$. The next reaction is a high temperature, endothermic decomposition of this metal oxide sulfate and further decomposition of the evolved SO_3.

14. $1/3\ Bi_2O_3 \cdot 3SO_3 \overset{\Delta}{=} 1/3\ Bi_2O_3 + SO_2 + 1/2\ O_2$

The high temperature process heat obtained from the solar furnace will be used to drive this decomposition reaction, part of it being diverted to electricity generation for the electrolysis step, 12. To complete the cycle, O_2 is separated from the SO_2 and O_2 gas mixture and the SO_2 is recycled to the process.

A principal reason for the introduction of a metal oxide species into the thermochemical cycle is to eliminate the large amounts of heat required for the dehydration of sulfuric acid; this requirement is characteristic of the already-mentioned sulfuric acid hybrid and sulfuric acid-iodine cycles. The separation by precipitation of the solid metal oxide sulfate from a relatively low concentration sulfuric acid solution rather than evaporation of

water from a concentrated sulfuric acid solution in principle should reduce the heat requirement. A preliminary estimate of the energy efficiency of the bismuth oxide sulfate cycle relative to the sulfuric acid hybrid cycle (Westinghouse) suggests that the bismuth oxide sulfate cycle offers a potential gain in efficiency of 12%.(8)

The introduction of the metal oxide sulfate has other potential benefits. For example, $Bi_2O_3 \cdot 3SO_3$ decomposes by release of SO_3 at increasing temperatures yielding a series of sulfates terminating in Bi_2O_3 itself at temperatures over 1200 K. Solar energy possesses the feature of being able to deliver to a process essentially isothermal heat at the maximum process temperature.(10) This feature will allow the $Bi_2O_3 \cdot 3SO_3$ to decompose isothermally at temperatures in the 1200-1500 K range. Temperatures in this range should speed reaction kinetics and allow the SO_3 decomposition reaction to equilibrate at $\sim$ 98 percent completion at moderate pressures.

Principal criteria for selection of the particular metal oxide are that the sulfate formed should have a low solubility and should be anhydrous under conditions of interest. A literature survey indicated that both bismuth and antimony (which will also be investigated in the future) form sulfate precipitates which satisfy these criteria. Perhaps the most important unknowns at present are the rates of the bismuth oxide sulfate decomposition reactions. Experiments designed to obtain these data are planned at LASL. Preliminary experiments performed at LASL (11) have shown a value of ΔH^o for equilibria 15 as 148.1 kJ (35.4 kcal) at temperatures from 667 to 828 K.

15. $Bi_2O_3 = Bi_2O_3\ 2SO_3 + SO_3$

The results of these experiments are shown as a plot (log P vs. 1/T) in Figure 1.

Figure 2 depicts a preliminary process flow diagram proposed for $H_2SO_4/Bi_2O_3 \cdot 3SO_3$ thermochemical cycle. The sulfate decomposition rate should be governed by heat transfer to the decomposing particles. If $Bi_2O_3 \cdot 3SO_3$ particles were adequately dispersed, heat transfer might not be a limiting factor, and, assuming the decomposition takes place in less than one minute, a decomposer might operate as a series of countercurrent moving-bed reactors. The bismuth sulfate particles (100-200μm in size) would be circulated through the decomposer system, the $Bi_2O_3 \cdot 3SO_2$ particles would decompose and emerge as Bi_2O_3.

The SO_3, SO_2, and O_2 product gases may have to pass through a catalyst bed to ensure that the SO_3 is decomposed. Equilibrium conversions of the SO_3 to SO_2 and O_2 should be achieved at 1500 K within $\sim$ 98% at moderate pressures. The solar furnace could also supply this energy. Conceptually, the $SO_3/SO_2/O_2$ gas stream may be used as a primary heat-transfer (direct-contact) medium used to drive the decomposition reactions. The bismuth oxide is physically separated from the product gases and is returned to a (chemical) reactor in which occurs contact with H_2SO_4 solution from the electrolyzer to form bismuth sulfate. The gaseous products are separated, the SO_2 is recycled, and O_2 is discarded after purification. As seen in Fig. 2 a conceptual 1513 MWt (equivalent) hydrogen plant requires 1318 MWt of high-temperature process heat, 1190 MWt of electrical energy, 640 MWt of moderate to low temperature heat; this cycle operates with an overall efficiency of $\sim$ 0.48.

This introduction of the metal oxide into the solar thermochemical cycle creates an interesting engineering problem. For an efficient cycle, the significant sensible, latent and transformation heats must be recovered from the

Bi_2O_3 decomposition reaction product; and electricity must be generated, perhaps by using the lower temperature process heat.

Other engineering problems requiring attention that stem from the solar energy aspects of the process are control problems relating to the transient nature of the energy source during daylight hours, as for example, when a cloud shields the sun, and the problems caused by the storage and transfer of intermediate reactants and products during the diurnal solar cycle. Variation in seasonal solar insolation would appear to also present a difficuly unless the solar-thermochemical process was located at Southwestern USA site where seasonal changes are not highly significant.

These engineering and related problems do not appear to be insurmountable. The transport of large masses of solids appears similar to processes used in other heavy-chemical industries and should present no serious difficulty. Indeed, some of the solid processing problems would appear similar to those proposed by other authors at this symposium, i.e., the processing of molybdenite ore (Skaggs) and the pyrolysis of biomass (Antal).

Immediate development of thermochemical means for hydrogen production by water-splitting should be a matter of top priority in solar energy research.

Conclusions

Hydrogen, a versatile element, has a tremendous potential as an energy storage medium. Its production from solar energy using water as the only raw material would open the way to a truly recyclable energy system based on renewable resources.

There are several water-splitting schemes that may be adaptable to use with solar energy, in particular, a concentrated, high temperature heat source

such as the solar tower. Among the thermochemical cycles proposed for water-splitting, the "hybrid" bismuth sulfate cycle being developed at LASL appears to offer potential as a high efficiency solar heat to hydrogen conversion process. This cycle is presently being researched in the laboratory and a concurrent design study (funded by the DOE's Office of Fusion Energy) is being done at LASL to match the cycle's thermal requirements to that of a fusion source for the ultimate production of hydrogen.

Coupling this cycle to a solar energy source would also be an alternate source of clean, non-polluting energy in the form of hydrogen.

References

1. Gregory, D. P., "A Hydrogen-Energy System," Report L. 21173, American Gas Association, August 1972.

2. Nakamura, T., "Hydrogen Production from Water Utilizing Solar Heat at High Temperatures," Solar Energy, 19, 467-475, 1977.

3. Eisenstadt, M. M. and Cox, K. E., "Hydrogen Production from Solar Energy," Solar Energy, 17, 59-65, 1975.

4. Funk, J. E. and Reinstrom, R. M., "Energy Requirements in the Production of Hydrogen from Water," I & EC, Proc. Des. & Dev., 5-3, 1966.

5. Bowman, M. G., "Fundamental Aspects of Systems for the Thermochemical Production of Hydrogen from Water," Proceedings of the First National Topical ANS Meeting on Nuclear Process Heat Applications, Los Alamos, New Mexico, October 1974.

6. Schuster, J. R., "Solar-Thermochemical Hydrogen Production," Report GA-A14308, General Atomic Company, March 1977.

7. Bilgen, E., et al., "Use of Solar Energy for Direct and Two-Step Water Decomposition Cycles," Int. Journ. of Hydrogen Energy, 2, 251-257, 1977.

8. Cox, K. E., "Thermochemical Processes for Hydrogen Production," January 1 - July 31, 1977, Report LA-6970-PR, Los Alamos, New Mexico, October, 1977.

9. Farbman, G. H., "Hydrogen Generation Process Final Report," Report No. FE-2262-15, Westinghouse Electric Corporation, Pittsburgh, PA, June 1977.

10. Pangborn, J. B., "Laboratory Investigation on Thermochemical Hydrogen Production," Proc. First World Hydrogen Energy Conference. Vol. I, 7A-59, Miami Beach, Florida, March 1976.

11. Jones, W. M., Unpublished Data, Los Alamos Scientific Laboratory, Los Alamos, New Mexico, February 1978.

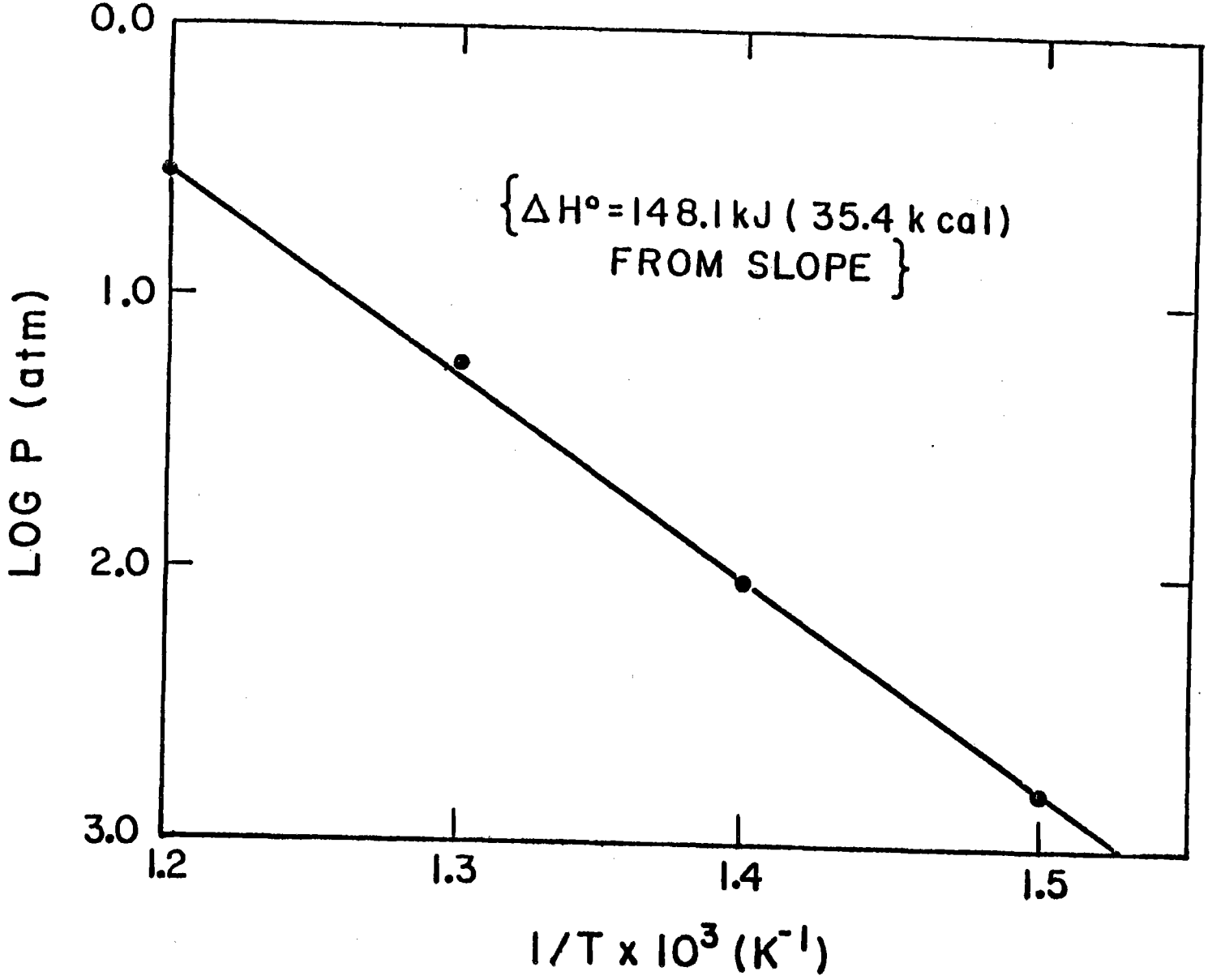

FIGURE 1. RESULTS OF BISMUTH SULFATE DECOMPOSITION

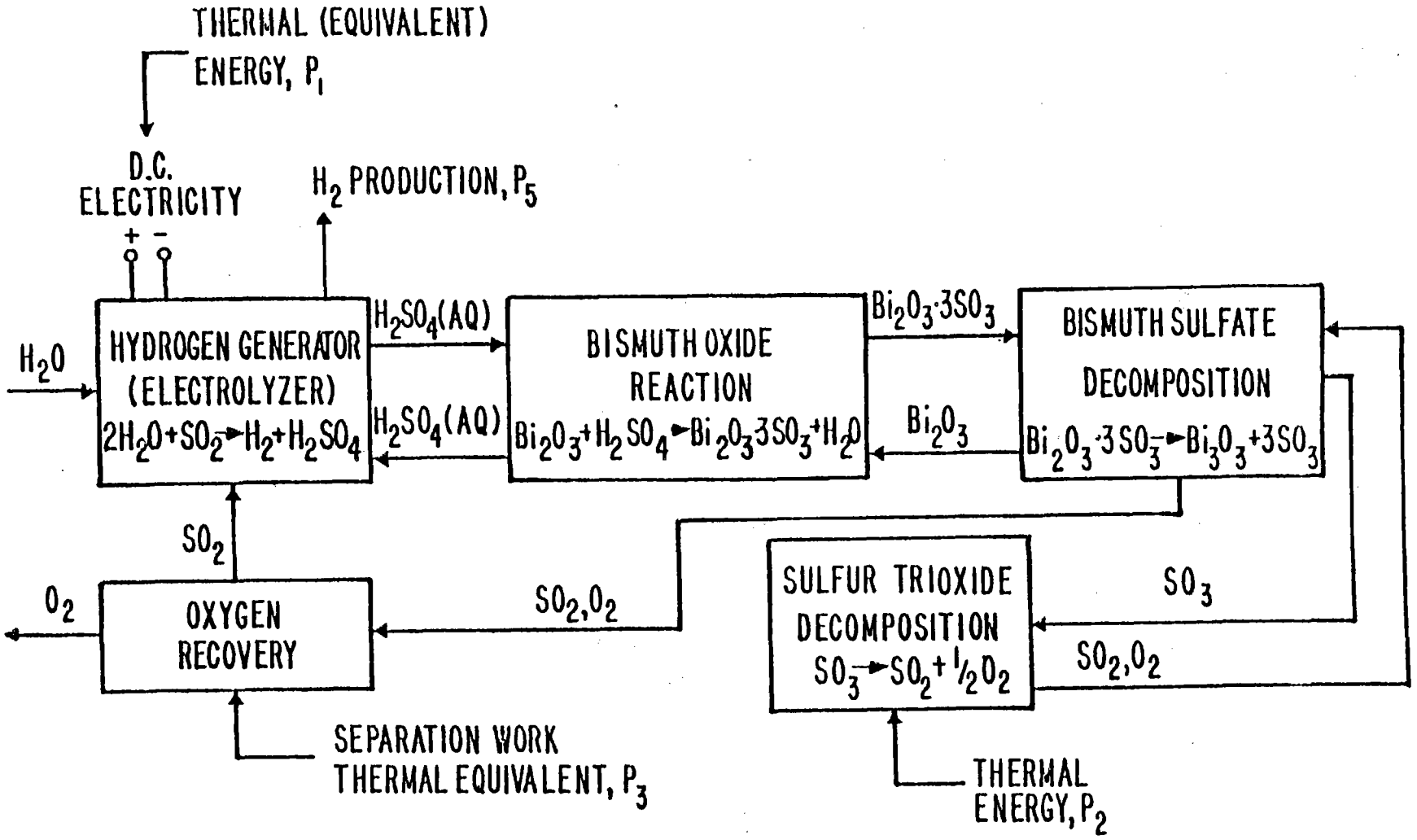

FIGURE 2. BISMUTH SULFATE - HYBRID CYCLE, SCHEMATIC DIAGRAM

RESULTS OF RECENT RESEARCH ON THE USE OF PYROLYSIS/GASIFICATION REACTIONS OF BIOMASS TO CONSUME SOLAR HEAT AND PRODUCE A USABLE GASEOUS FUEL

Michael J. Antal, Jr.
Department of Aerospace and Mechanical Sciences
Princeton University, Princeton, New Jersey 08540

ABSTRACT

Biomass materials can be converted to a medium Btu gaseous fuel (300 to 600 Btu/scf) by pyrolysis/steam gasification chemical reactions. These reactions are endothermic and demand heat over temperatures ranging from 100° to 600° or 700°C. Customarily this heat is supplied by burning a part of the fuel product of the conversion process. Research at Princeton has focused on conserving the fuel product by using solar heat to drive the conversion process. When utilized in this fashion the solar heat is stored in the form of a high quality, easily transportable fuel which could be immediately marketed to consumers, or used to produce methane, methanol, ammonia, or gasoline by commercially available technologies.

INTRODUCTION

Past research on heat consuming chemical reactions suited for use with solar concentrating collectors has emphasized reversible reactions, such as the dissociation of sulfur trioxide or ammonia. Heat stored in the dissociated products is liberated when the products recombine, but only at a significantly lower temperature than was produced initially by the solar concnetrator. This reduction in the *quality* of the heat produced by the concentrator is the penalty which must be paid for storing the solar heat in the form of a chemical fuel using reversible chemical reactions.

The use of irreversible endothermic chemical reactions to store solar heat does not encounter this penalty. In fact, heat liberated by the combustion of gaseous fuels produced by irreversible reactions can be at a higher temperature than the heat initially produced by the solar concentrator (n.b., this is *not* in violation of the second law of thermodynamics). Research going on at Princeton aims at the use of endothermic, irreversible

chemical reactions to consume solar heat. These reactions involve pyrolysis/steam gasification of biomass materials and produce a high quality, gaseous fuel.

Pyrolysis/steam gasification of biomass is a two step process. In an oxygen free atmosphere at moderate temperatures (300° to 500°C) biomass materials pyrolyze, producing volatile matter and char. At somewhat higher temperatures (500° - 700°C) the volatile matter reacts with steam to produce a hydrocarbon rich synthesis gas. The overall gasification process is only mildly endothermic, primarily demanding heat in the temperature range 100° - 400°C. Solar concentrating collectors appear to be an economical source of heat for the gasification reactions.

The following sections briefly describe results from our experimental research program and outline their implications for fuel production from solar heat.

EXPERIMENTAL RESEARCH

Pyrolysis of various representative biomass materials has been studied extensively at Princeton using the Dupont 990 Thermal Analysis System. Curves of weight loss vs sample temperature at five different heating rates have been generated for representative samples of cellulose, newsprint, hard and softwoods, pelletized wood wastes, and cow manure. Figure 1 illustrates the type of data obtained from these experiments. Kinetic rate constants (activation energies, frequency factors and orders) have been derived from these curves for the various heating rates studied. The rate constants can be used in a mathematical model of pyrolysis to simulate the behavior of a particular biomass feedstock undergoing pyrolysis in a chemical reactor.

Steam gasification of volatiles produced by pyrolysis of biomass materials has also been studied extensively at Princeton in a specially designed quartz tubular plug flow reactor. A diagram of the experimental apparatus is given in Figure 2. Volatile matter produced by pyrolysis of small solid samples in the pyrolysis reactor reacts with steam in the gas phase reactor to produce a hydrocarbon rich synthesis gas. By maintaining the gas phase reactor above 600°C tar production is reduced to less than 5% of the initial solid sample weight. Results from a typical experiment are given in Table 1. The overall reaction resulting in the products listed in Table 1 is autothermic within the limits of accuracy of the experiment. The gas produced from this experiment has a heating value above 500 Btu/scf and is relatively rich in ethylene and some higher hydrocarbons. Approximately 80% of the energy of the initial biomass feedstock is carried by the gaseous fuel product of this experiment.

BIOMASS GASIFICATION USING SOLAR HEAT

Pyrolysis/steam reforming of biomass requires a source of moderately high temperature heat. It is only natural to consider solar energy as a

source of heat for the gasification process. Figure 3 provides a comparison of the proposed solar gasification process with alternative conversion technologies. The merits of solar gasification should be obvious from the energy balances given in Figure 3.

The amount of heat required to gasify biomass can be easily estimated using the first law of thermodynamics. Figure 4 and Table 2 summarize the results of this calculation for cellulose, based on both theoretical predictions and experimental results. From the data presented here it is quite clear that the amount of heat required is strongly dependent upon the recovery of sensible heat from the reaction products. If 50% of the sensible heat were recovered, 1.8 million Btu would be required to gasify one metric ton of cellulose. As indicated in Figure 4 and Table 2, this heat is required at temperatures ranging from 100° to 400°C. At the present time it is not clear whether heat will be needed above 400°C.

Solar concentrating collectors are believed to be economical sources of heat in this temperature range; consequently it makes good sense to consider their use for the gasification of biomass. Using the figures given in the paragraph above, a solar furnace producing 1 Mw of usable heat in the indicated temperature range for 6 hours per day could process 11 metric tons of cellulose per day, producing 170 million Btu (50 Mw-hr) of gaseous and solid fuels. If municipal solid wastes were used as the source of biomass feedstock, the 11 metric tons could be supplied by a city with a population of about 11,000 people.

The reader should note that the energy carried by the biomass feedstock is much larger than the solar input. This is because the pyrolysis/steam gasification process is only mildly endothermic, and because the biomass feedstock has a significant heating value. In this scheme the solar heat is being used to *process* the biomass, and is valued for its *quality* (e.g., solar heat is free of chemical contaminants, combustion products, etc.) rather than its *quantity*.

The large ratio of useful energy output per solar energy input (approximately 8:1) results in favorable process economics. Table 3 compares the estimated capital costs of a solar gasification facility located in New Jersey (assuming full recovery of sensible heat) with alternative energy sources. More detailed economic projections will be available shortly in a report to the President's Council on Environmental Quality.

Either linear or point focus concentrating collectors should be well suited for this application. The concept could be tested using the existing 5 Mw_{th} test facility to provide heat to pressurized steam superheaters, whose effluent would fluidize a bed where pyrolysis of the biomass would occur. Gaseous effluent from the bed would be further heated by the solar furnace to about 650°C, and sensible heat from the effluent would ultimately be recovered by raising steam for the superheater (see Figure 5). The construction of a pressurized fluidized bed intended for use with the 5 Mw_{th} test facility will be a costly undertaking. A less ambitious test has been

proposed by Princeton using linear concentrating collectors to gasify 1/2 to 1 ton per day of biomass. To date, this proposal has not received support.

CONCLUSIONS

Biomass can be converted to a medium Btu gas and charcoal by moderate temperature, mildly endothermic pyrolysis/steam reforming reactions. If the heat required for gasification is supplied by solar concentrating collectors, the biomass resource is conserved and the solar concentrators are efficiently and economically employed. During this year ongoing experimental research at Princeton will elucidate the pyrolysis/steam reforming chemistry sufficiently to provide for detailed engineering plans of a process development unit for solar gasification of biomass. Within a decade solar gasification of biomass has the potential of meeting a significant fraction of our nation's energy demand.

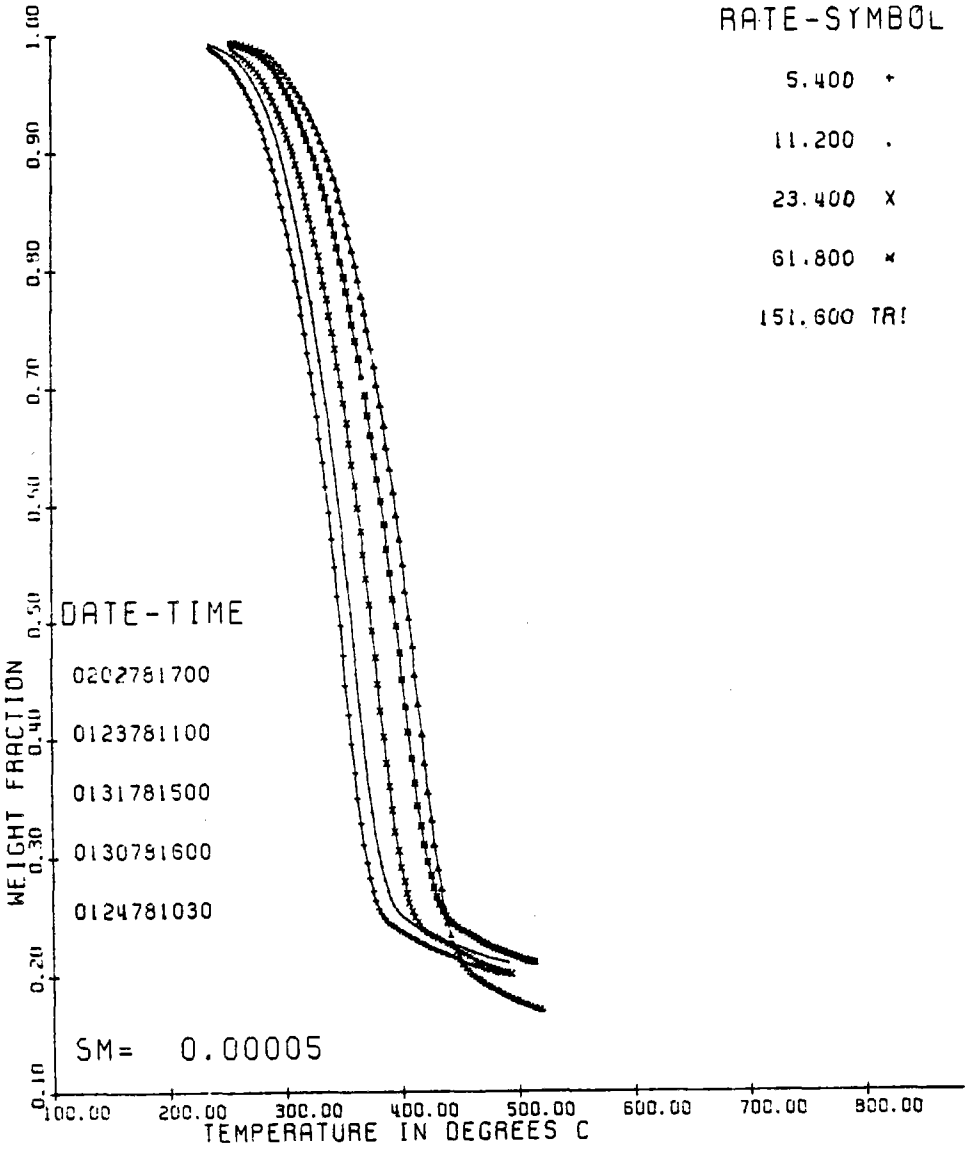

W.S. JOURNAL IN NITROGEN

Figure 1

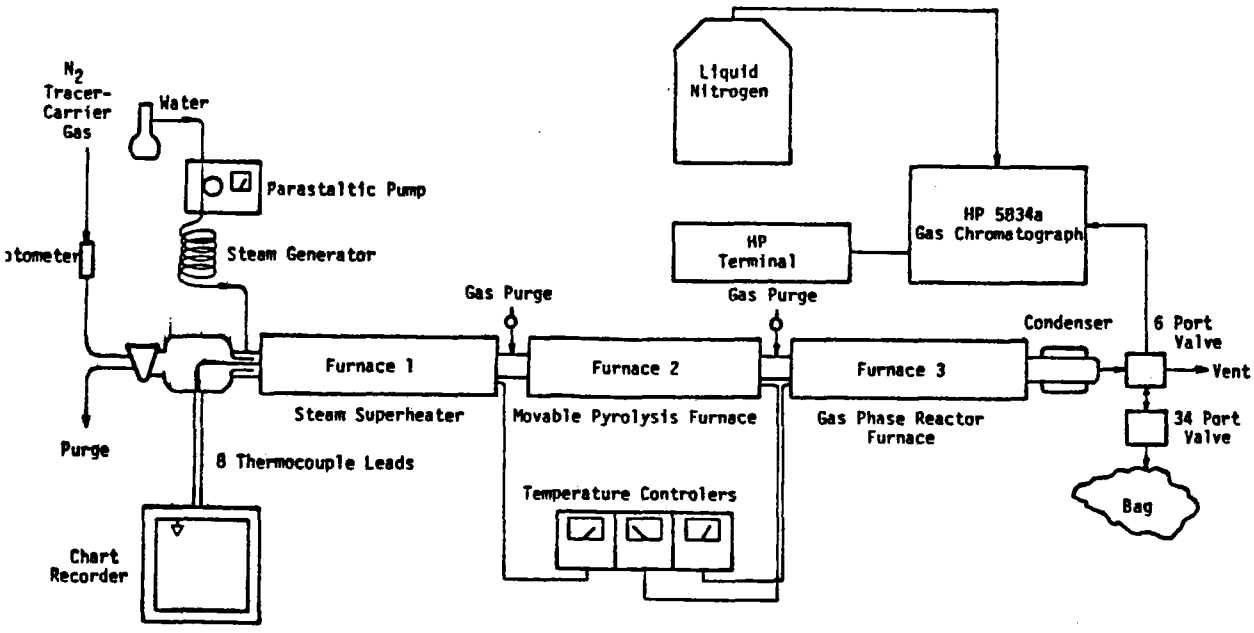

SCHEMATIC OF THE TUBULAR QUARTZ REACTOR EXPERIMENT

Figure 2

A COMPARISON OF THE USEFUL ENERGY DERIVED FROM SELECTED BIOMASS CONVERION TECHNOLOGIES

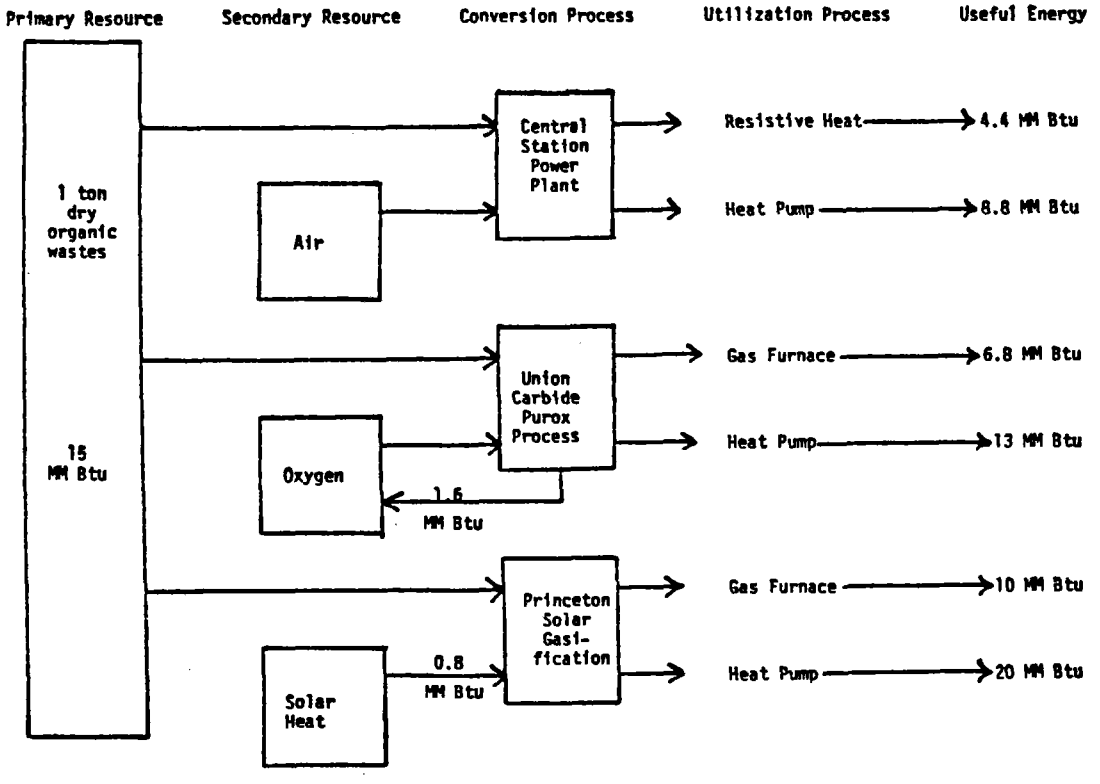

Figure 3

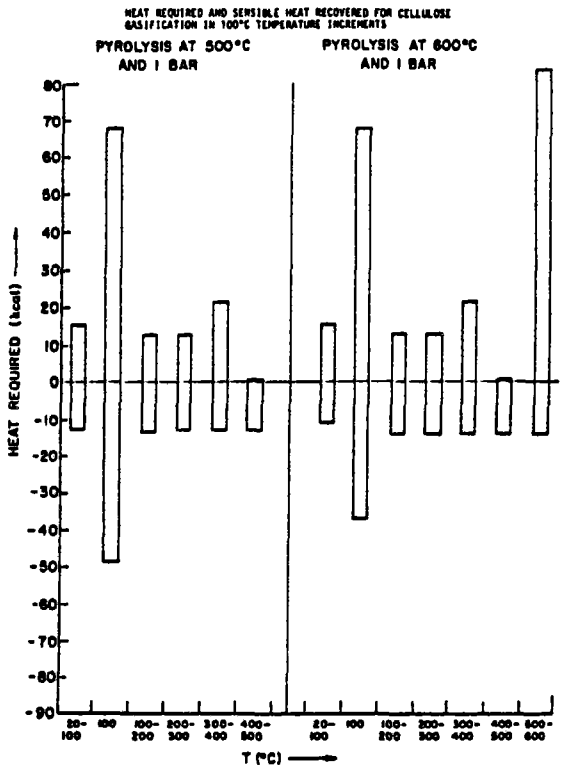

Figure 4

SCHEMATIC OF PROPOSED SOLAR BIOMASS GASIFICATION PROCESS

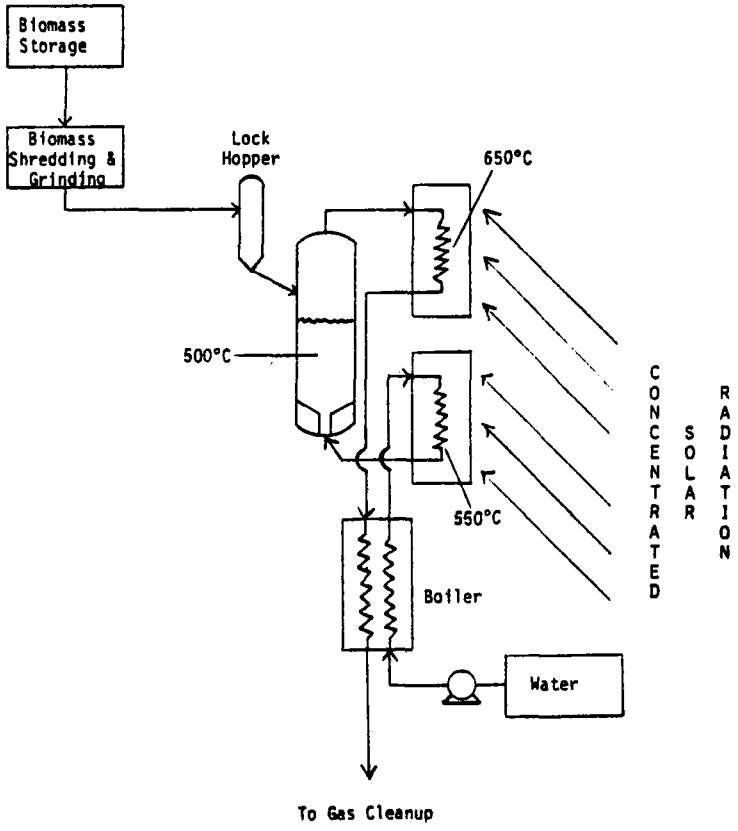

Figure 5

TABLE 1

Steam Superheater Temperature	350°C
Pyrolysis Reactor Temperature	500°C
Gas Phase Reactor Temperature	650°C
Sample Weight	0.0995g
Char Residue Weight	0.0119g
Char Residue Weight Percent	12 %
Tar Residue Weight	0.0046g
Tar Residue Weight Percent	4.7 %
Gas Volume Produced	67.4 cc
Gas Heating Value	531 Btu/scf
Calorific Value of Gases	12.7 MM Btu/mt
Calorific Value of Char	2.4 MM Btu/mt
Calorific Value of Tars	1.1 MM Btu/mt
Mass Balance	0.96
Carbon Balance	1.01
Oxygen Balance	0.96
Hydrogen Balance	0.95
Steam Consumption	0.02g

Gas Analysis

Gas Component	Vol %
CO	54 %
H_2	14
CO_2	12
CH_4	10
C_2H_4	5
C_3H_6	2
C_2H_6	1
other	2

TABLE 2

HEAT REQUIRED TO GASIFY ONE MOLE OF CELLULOSE IN SEVEN MOLES OF WATER AT 500°C AS A FUNCTION OF TEMPERATURE AT A PRESSURE OF ONE BAR*

Temperature Range	Heat Demand by Component			Sensible Heat Recovery at 100% Efficiency	Difference
	H_2O	Cellulose	Sum		
20°-100°C	10 kcal	5 kcal	15 kcal	13 kcal	+ 2 kcal
100°	68	-	68	49	+19
100°-200°	6	7	13	13	0
200°-300°	6	7	13	13	0
300°-400°	6	15	21	13	+ 8
400°-500°	6	-5	1	13	-12
Sum	102 kcal	29 kcal	131 kcal	114 kcal	17 kcal

TABLE 3

CAPITAL COSTS FOR ALTERNATIVE FUEL PRODUCTION TECHNOLOGIES

Source	Capital Cost ($/bbl-day equiv.)
Solar Pyrolysis/Steam Reforming of Biomass	$ 6,000
Persian Gulf Oil	300
North Sea Oil	4,000
Alaskan North Slope Oil	4,000
Imported LNG	10,000
Oil from Shale by Retort	> 20,000
SNG from Coal	28,000
Oil from Alberta Tar Sands	30,000

PROPOSED EXPERIMENT TO UTILIZE A SOLAR FACILITY TO PROVIDE PROCESS HEAT FOR CARBON GASIFICATION

(Talk for STTF Users Association Meeting April 1978)

By

Daniel Cubicciotti

SRI International
Menlo Park, California 94025

ABSTRACT

SRI has proposed to design an experiment for a solar tower facility concerned with metallurgical processing. Preliminary considerations of the reactions that might be conducted in such an experiment are made. Carbon gasification reactions seem to be the most likely because they are the most endothermic steps in the overall reduction of iron ore and also are of interest for production of gaseous fuels in general. Some preliminary ideas of designs for an experiment are presented. The eventual program for designing the experiment will involve optimizing the available parameters which are: the reaction to be studied, the reaction conditions, the physical characteristics of the apparatus, the requirements of the solar tower including safety of operation.

BACKGROUND

The potential application of solar heat to metallurgical operations was suggested many years ago; however there is not enough experience to indicate whether such applications are economically feasible. Farrington Daniels' statements of 15 years ago[1] are still true, namely: "The chief limitations to the use of the sun's energy are economic rather than technological. There has been so little experience with solar devices that reliable cost estimates are not available." At the recent STTF Users' Association workshop on high temperature science,[2] it was recommended that we consider an experiment involving metallurgical processing. Therefore we, at SRI, gave some thought to ore reduction experiments. We considered the carbothermic reduction of Al_2O_3 and Fe_2O_3. Alumina reduction required very high temperatures (above 2000°C) so we concentrated on iron ore. Our deliberations soon indicated that the heat absorbing part of the reactions was really a carbon gasification step. It was also pointed out by M. Gutstein at that workshop[2] that carbon (coal) gasification was important on its own and therefore the thrust of the experiment we proposed became carbon gasification.

Iron Ore Reduction

The reduction of iron ore in the United States entails consumption of large quantities annually of premium coking coal in blast furnaces. More than half of the fossil fuel consumed is used to provide heat for

the process. The rest is needed to react chemically with the oxygen in the ore so the process can operate at manageable temperatures. Use of solar energy to provide the process heat would allow conservation of about 60 percent of the high grade coal consumed. Since the steel industry in the United States currently uses 60 million tons of coal[3] (20 percent of all coal used in the United States), the amount conserved could be significant.

The overall process for the carbothermic reduction of iron ore is the sum of the steps shown in Table 1. The table also shows the amount of heat absorbed[4] by each reaction (ΔH) and the quilibrium constants for 1200 K. At that temperature, each step has a negative free energy change and thus will proceed spontaneously.

It is clear from the values in the table that the heat absorbing step is the reaction of CO_2 with C. The other three steps have small heat effects. A two-step process might be suitable. In one step, CO_2 and C are reacted in a solar heat flux to provide the required heat of reaction and to bring the reactants to temperature. In a second step, the hot CO would be passed over Fe_2O_3, which would then be reduced to Fe in the series of reactions indicated in Table 1.

Processes for reducing iron ore by fuels other than high grade coke are generally called direct-reduction processes.[5] There has already been extensive development of direct reduction processes utilizing CO and H_2

and so a solar furnace experiment need not be concerned with the reduction process except to produce a compatible reducing gas. Figure 1a illustrates the Wiberg-Soderfors process which has been used commercially in Sweden. Reducing gases (H_2 + CO) are generated in an electrically heated gasifier for that process. A solar gasifier could replace that part of the process.

Figure 1b presents a block diagram of a Bethlehem steel process that uses natural gas as a fuel and as a reductant. The fuel is burned with air in an alumina pebble bed reactor which stores heat. When the bed is hot, the air flow is stopped and a stream of CO_2 and H_2O offgas from the reductor is reduced to CO and H_2. The hot reduced gas then is fed to the ore reductor. Solar heat could be applied to that process fairly simply. The pebble bed reactor could be heated by solar concentrators. If the bed were large enough, sufficient heat might be stored to allow overnight operation. The bed could also be equipped with a stand-by system for heating it with natural gas to allow operation during cloudy weather.

Carbon Gasification

The first reaction in Table 1 is essentially a carbon gasification step. A comparable gasification step often considered for coal gasification is the reaction with steam, namely

$$C + H_2O = H_2 + CO$$

The enthalpy and free energy changes at 1200 K for the reaction involving 3/4 mol of C (for comparison with Table 1) are 99 and -22 KJ. That is, the thermodynamics of the steam-carbon reaction are similar to the CO_2 + C reaction, and it could be considered as an alternative gasification step. The product (H_2 + CO) has approximately the same capability thermodynamically, for reducing iron ore.

The carbon gasification steps are the important ones for solar utilization. The remaining iron reduction steps are only secondary and they have been studied extensively enough for our purposes. Coal gasification processes are important for producing fuels for many applications other than iron ore reduction; and so we should direct our attention to solar carbon gasification processes without concern for particular applications. There are other coal gasification processes that yield different products (CH_4, H_2, CH_3OH); however we shall concentrate on the H_2O and CO_2-carbon reactions because they are much more endothermic and so can better utilize solar heat.

The kinetics of the two gasification reactions have been studied in some detail[6] to elucidate the mechanisms, which are complex. For the CO_2 + C reaction the overall rate is given by an expression of the form

$$R(CO_2) = \frac{k\ p(CO_2)}{1 + a\ p(CO) + b\ p(CO_2)}$$

each constant in the rate equation (a, b, k) can be expressed in the Arrhenius form

$$\text{rate const.} = A \exp(-E/RT)$$

It has been found that the rates of the reaction depend markedly on the nature of the carbon studied. Table 2 shows ranges of values and the constants involved.

The rate equation for the carbon-steam reaction has a similar form:

$$R(H_2O) = \frac{k' \, p(H_2O)}{1 + a' \, p(H_2) + b' \, p(H_2O)}$$

and values for the rates and the constants are shown in Table 3. These rates are also very dependent on the carbon studied. One interesting observation made on porous graphite was that the rate constants increased as the carbon was burned off.[7] The variation of the constants with burnoff is illustrated in the first five entries in Table 3.

The reactivity of carbon with CO_2 or H_2O depends on a number of factors including chemical composition and catalysts. A potentially important fact related to solar-assisted gasification is that the temperature history of the carbon effects its reactivity by influencing the extent of annealing, degree of graphitization and crystallite size and structure.[6] The large heat fluxes available in solar towers may be particularly valuable for rapid heating coals which may result in carbons that

are especially ractive in gasification steps. It is also interesting for economic conditions that chars from low rank coals are more reactive than those from high-grade coking coals., partly because chars have higher specific surface areas but also the nature of the carbon is altered in the charring (devolatilization) process.

Devolatilization

Devolatilization of coal by pyrolysis occurs during coal gasification, as well as in the coking process for production of blast furnace coke. Pyrolysis yields fuel gases (primarily H_2, CH_4, and CO) and tars as well as char. The reactivity of the char depends on the temperature and rate of heating. Rapid heating[8,9] to high temperatures produces more volatiles than slow heating. The amounts and compositions of the volatile products also are affected by the heating rate. An example[10] of the effects of heating rates on the gaseous products is shown in Table 4. The rates of heating were greatest by ruby laser and smallest during carbonization. The solid resulting from laser pyrolysis[11] was also significantly different from conventionally heated samples. The density was very low ($\sim$0.02 g/cm^3) and the solubility in organic solvents was greater.

Those results suggest that it may be worthwhile investigating direct heating of coals by a high intensity solar flux. Although that process is not the objective of our proposed experiment, it may be possible to consider including pyrolysis experiments within the context of the program.

SOLAR TOWER EXPERIMENT

The objective of the experiment we propose for a solar tower is to learn how to operate a carbon gasification reactor using solar heat. The experimental reactor must be designed to accommodate the geometry of the solar heat source. Materials of construction must be selected to withstand the temperatures, the chemical conditions involved, and the large energy fluxes. The experiments performed must be planned to obtain information about rates of reaction and energy fluxes to provide a basis for assessing the feasibility and economics of commercial operation. At the same time the experimental system must be flexible so that changes in reaction conditions can be effected.

We have proposed to design an apparatus for a solar tower experiment in carbon gasification[12] by CO_2, H_2O and mixtures of them. We propose to consider various possibilities for reactors for carbon gasification in relation to the available solar tower thermal facilities and to design an apparatus for use in a specific STTF.

We have made some preliminary considerations; however, other possibilities will be investigated before a final design is prepared. An important aspect is the transfer of heat from the solar flux through container walls to the reactants. The solar tower source characteristically provides large heat fluxes that must be controlled to prevent melting or

weakening of container walls and structures. A reasonable system for heat transfer is a fluidized bed of carbon (coke or char), with CO_2 or H_2O as fluidizing gas. Fluidized beds have very high heat transfer coefficients that are essential in transferring heat from the solar absorber wall to the reacting substances. The absorber will be one wall of the container. Because the reaction will occur at temperatures above 1200 K, the outside of the container should be resistant to oxidation or protected by an inert gas (N_2, or possibly CO). Potential container materials are nickel-based alloys, iron-chromium alloys, and silicon carbide, which has a high absorption coefficient and could be used without a protective blanket. The container material should also have high thermal absorbance and high thermal conductivity.

Figure 2 shows a conceptual system for a fluidized bed using a tubular container. An external cyclone would capture carbon particles entrained in the exhaust gas. Although a silicon carbide reactor tube is indicated, other materials and other geometries, including internal ribbing and reentrant cavities, that may provide good overall thermochemical efficiency should also be considered. A water-cooled aperture must also be incorporated to shield parts from the solar flux.

Because solar energy is well suited for direct heating and carbon is an especially good receptor of radiant energy, it seems particularly appropriate to consider design in which the carbon is heated directly by the solar flux. Figure 3 gives a preliminaty sketch of design which

involves having the carbon fall through the solar flux. If the time of fall is not great enough, then more flux would be directed to the static part of the bed. It is important to keep the window clean to prevent damage by heating of dirty spots. The incoming gas flow is used for that purpose in Figure 3. (Another scheme might be to spray the inside with water, especially if the reaction studied is $H_2O + C$). The apparatus in Figure 3 could readily be used to test coal volatilization processes. For that purpose a nonreactive gas such as CO or N_2 would be used instead of CO_2 or H_2O.

Antal[13] has suggested utilizing solar heat for producing synthetic fuels from solid, organic wastes. The system he proposed is shown in Figure 5. In a recent study, Feber and Antal[14] found alkali metal carbonates catalyzed carbon gasification reactions both with CO_2 and steam. They also studied other aspects of carbon gasification in a solar flux. They point out that gaseous H_2O and CO_2 both absorb infrared radiation. That property can probably be invoked to utilize the energy radiated from a hot bed of carbon (Figure 3) to preheat the reacting gas.

The design of an experimental apparatus for a high temperature reactor is a rather complex problem. We feel it will require the combined efforts of high temperature chemists to estimate probable reaction rates and select reactions that would be reasonable, high temperature materials scientists to select suitable materials, metallurgical and chemical

engineers to optimize the design. Close cooperation with the staff of the solar tower selected will be an important part of the design process.

The program we envisage will start with detailed consideration of the various reactions that might be tested in a solar reactor, considering factors such as their potential economic importance in iron ore reduction processes as well as the technical problems involved in promoting them with solar heat. Based on those considerations, a reaction system will be selected and then a solar tower compatible reactor will be designed. The construction and operation of the reactor will be performed in a subsequent phase of the work.

REFERENCES

1. STTF Users Association, High Temperature Sciences Workshop, Albuquerque, New Mexico, November 1977.

2. F. Daniels, "Direct Use of the Sun's Energy," Yale Univ. Press, New Haven, Connecticut, 1964.

3. F. D. Cooper, "Coke and Coal Chemicals" in Bureau of Mines Minerals Yearbook 1974, U.S. Government Printing Office, Washington, D.C. 1976.

4. O. Kubaschewski, E. Evans, and C. B. Alcock, "Metallurgical Thermo-Chemistry," 4th ed, Pergamon Press, Oxford, England, 1967.

5. H. E. McGannon, "The Making, Shaping and Treating of Steel," Chapt. 14, Direct Reduction Processes, U. S. Steel, Co., Pittsburgh, Pa., 9th ed, 1971.

6. C. G. Von Fredersdorff and M. A. Elliott, "Coal Gasification," Chapter 20 in Chemistry of Coal Utilization, Supplementary Volume J. Wiley and Sons, Inc., New York, 1963.

7. H. F. Johnstone, C. Y. Chen and D. S. Scott, Ind. Eng. Chem., 44 1564 (1952).

8. M. Mentser, H. J. O'Donnell, S. Ergun, and R. A. Friedel, "Devolatilization of Coal by Rapid Heating," in Coal Gasification, Adv. in Chem. Series No. 131, Am. Chem. Soc., Washington D.C., 1974.

9. R. L. Coates, C. L. Chen, and B. J. Poper, "Coal Devolatilization in a low Pressure, Low Residence Time Entrained Flow Reactor," Adv. in Chem. Series, No. 131, Am. Chem. Soc., Washington, D.C., 1974.

10. A. G. Sharkey, Jr., S. L. Shultz, and R. A. Friedel, "Comparison of Products from High-Temperature Irradiation and Carbonization of Coal," Report of Investing No. 6868, U. S. Bureau of Mines, Washington, D.C. 1966.

11. F. S. Karn, R. A. Friedel, and A. G. Sharkey, Jr., "Studies of the Solid and Gaseous Products from Laser Pyrolysis of Coal," Fuel, 51, 113 (1972).

12. D. Cubicciotti and R. W. Bartlett, "Design of an Experiment to Test the Utilization of Heat from a Solar Test Facility to Provide Process Heat for the Reaction $C + CO_2 \rightarrow 2CO$." Research Proposal No. PYU 77-344, SRI International, Menlo Park, California, December 16, 1977.

13. M. J. Antal, Jr., "Method for Producing Synthetic Fuels from Solid Waste," U.S. Patent No. 3,993,458, Nov. 23, 1976.

14. R. C. Feber and M. J. Antal, "Synthetic Fuel Production From Solid Wastes," Report EPA-600/2-77-147, U.S. Environmental Protection Agency, Cincinnati, Ohio, September 1977.

Table 1

THERMODYNAMICS OF REACTIONS INVOLVED IN THE CARBOTHERMIC REDUCTION OF IRON ORE
(per mole of Fe)

Reaction	ΔH° KJ	ΔG°(1200 K) KJ	Log K (1200 K)
$3/4\ C + 3/4\ CO_2 = 3/2\ CO$	130	-29	1.3
$1/6\ CO + 1/2\ Fe_2O_3 = 1/6\ CO_2 + 1/3\ Fe_3O_4$	-8.5	-16	0.72
$1/3\ Fe_3O_4 + 1/3\ CO = 1/3\ CO_2 + FeO$	11	- 1.1	0.05
$FeO + CO = CO_2 + Fe$	-17	- 3.8	0.16
$1/2\ Fe_2O_3 + 3/4\ C = 3/4\ CO_2 + Fe$	115.5	-	-

Table 2

ARRHENIUS CONSTANTS FOR THE CARBON-CARBON DIOXIDE REACTION
(From Reference 6)

Carbon Type	Rate* at 1200 K	Constant k A_k g-mole/g-min-atm	Constant k E_k kcal	Constant a A_a 1/atm	Constant a E_a kcal	Constant b A_b 1/atm	Constant b E_b kcal
Coconut-shell charcoal	1×10^{-3}	6.3×10^{8}	58.8	1.26×10^{-6}	-45.5	3.16×10^{6}	30.1
New England coke	1.5×10^{-4}	6.9×10^{5}	47.6	1.4×10^{-2}	-15.0	0.21	-6.3
Electrode carbon	3×10^{-6}	1.0×10^{8}	50.1	3.16×10^{-9}	-60.6	0.16	-6.6
Pitch coke	3×10^{-8}	1.05×10^{7}	40.1	2.0×10^{-9}	-55.1	-	-
Anthracite	3×10^{-4}	2.2×10^{3}	32.5	4.6×10^{-3}	-16.9	1.8×10^{-2}	-16.6

*Rate for pressures of CO and CO_2 of one atmosphere.

Table 3

ARRHENIUS CONSTANTS FOR THE CARBON-STEAM REACTION
(From Reference 6)

Carbon Type and % Burnoff	Rate* at 1200 K	Constant k A_k g-mole/g-min-atm	Constant k E_k, kcal	Constant a A_a 1/atm	Constant a E_a kcal	Constant b A_b 1/atm	Constant b E_b kcal
Graphite tube, 0%	3.4×10^{-6}	29.6	32.7	9.42×10^{-11}	-60.8	7.07×10^{-16}	-79.3
Graphite tube, 1%	3.7×10^{-6}	2.24	26.0	6.48×10^{-11}	-62.0	6.19×10^{-16}	-79.7
Graphite tube, 2%	4.3×10^{-6}	0.357	21.2	4.21×10^{-11}	-63.1	4.80×10^{-16}	-80.2
Graphite tube, 5%	6×10^{-6}	00.0615	16.0	1.00×10^{-11}	-66.7	2.13×10^{-16}	-82.5
Graphite tube, 7.5%	7×10^{-6}	00.0235	13.1	0.377×10^{-11}	-69.2	1.96×10^{-16}	-82.9
Coconut-shell charcoal	2×10^{-3}	1.58×10^{10}	62.3	33	0.0	3.16×10^{4}	20.1
Pitch coke	1.6×10^{-6}	7.75×10^{5}	59.1	1.71×10^{-2}	-20.5	-	-

*Rates for pressures of H_2 and H_2O of one atmosphere.

Table 4

GASEOUS PRODUCTS FROM LASER AND FLASH IRRADIATIONS AND HIGH-TEMPERATURE CARBONIZATION OF COAL*

	Energy Source or Treatment		
	Ruby Laser (~2-joule output)	Xenon Lamp (~4000-joule input)	Carbonization at 900°C
Compound, mole-percent			
Hydrogen	45.4	69.2	55.6
Carbon monoxide	14.4	16.1	7.4
Methane	4.8	4.1	31.5
Acetylene	20.9	7.8	0.05
Ethylene	4.9	0.05	3.4
Ethane	0.6	0.1	1.2
Hydrogen cyanide	1.4	1.7	-
Carbon dioxide	2.0	0.5	0.4
Total hydrocarbons above C_2	5.6	0.4	0.5
Foregoing gases as weight-percent of coal	~ 60	~ 18	15

*Pittsburgh seam, high volatile A, bituminous (hvab) coal.

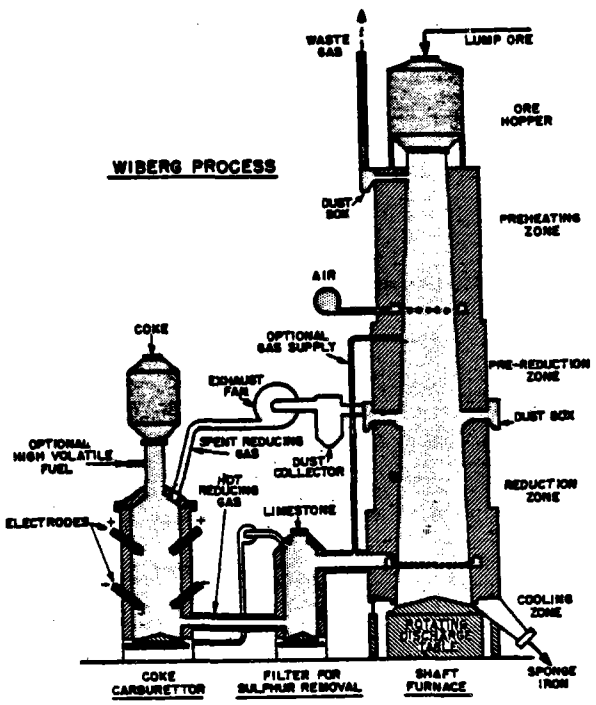

FIG. 1 a Schematic cross-sectional diagram showing the principle of operation of the Wiberg-Soderfors process.

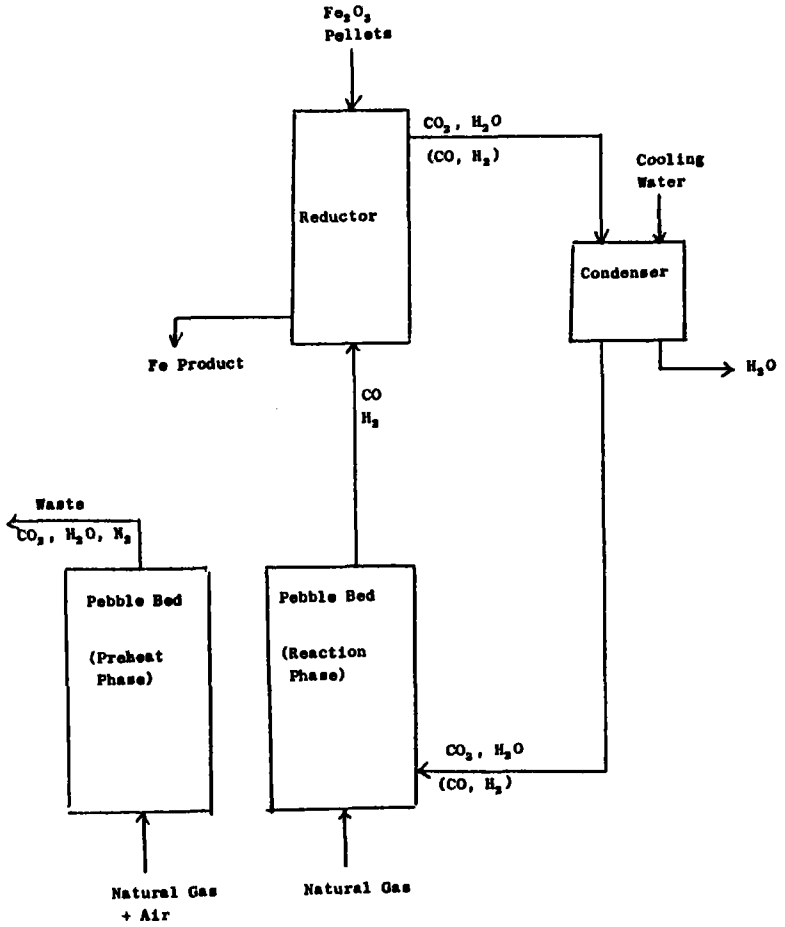

Figure 1b Bethlehem Steel Direct Reduction Process

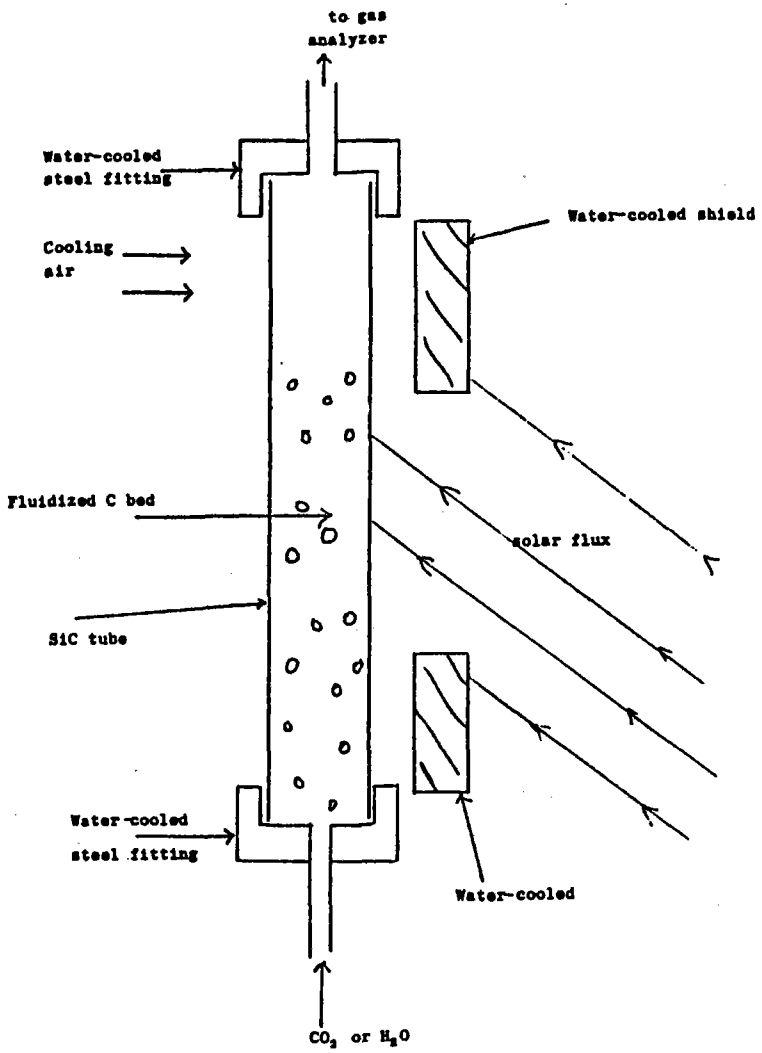

Figure 2 Fluidized Bed Reaction Vessel

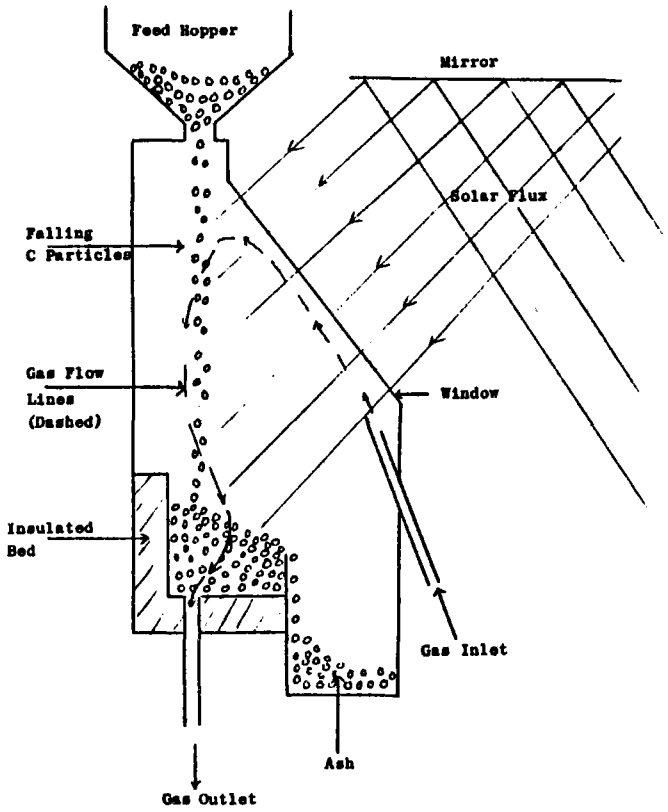

Figure 3 Dropping/Static Bed Reactor

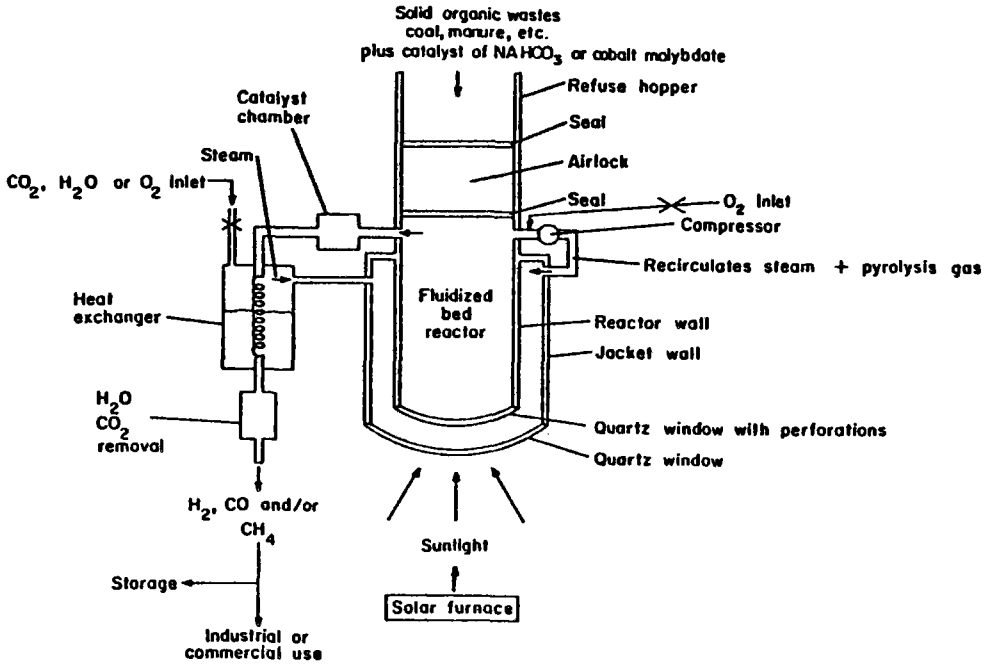

Figure 4 Reactor Suggested by Antal

SOLAR FURNACE MEASUREMENTS OF HIGH TEMPERATURE THERMODYNAMIC PROPERTIES OF OXYGEN ALLOYS OF ELECTROPOSITIVE METALS

Robert I. Sheldon
Dr. Paul W. Gilles

The University of Kansas

Abstract

This investigation is to study high-temperature vaporization phenomena leading to the thermodynamics of liquid and solid oxygen alloys of electropositive metals. A Solar Thermal Test Facility (STTF) will be used as the source of heat so that an alloy can act as its own container and thus avoid contamination. The work will be designed to explore ways of adapting solar furnaces and especially solar thermal test facilities for new roles in high-temperature scientific research.

NOTE: This paper was not available for inclusion in the Proceedings; therefore, we are reprinting the abstract.

XI. SOLAR ENERGY R&D IN JAPAN

Professor Tetsuo Noguchi
Government Industrial Research Institute

Chairman John Russell - Today we have an illustrious visitor from Japan, Dr. Tetsuo Noguchi. He is with the Government Industrial Research Institute in Japan and at that Institute he is chief of the Solar Research Laboratory. He has been there since 1955 involved in solar work, which makes him an old timer, one of the people with foresight instead of hindsight. It is quite a privilege to hear him. It is difficult to match one bureaucratic organization with another, but as best I can tell, Dr. Noguchi is sort of a combination of a Marvin and a Rappaport, if that means anything.

High-temperature solar furnaces and heating and cooling of buildings have been his specialties over the years. His talk today will be "Solar Energy R&D in Japan," and he will do that in two parts: First, a general discussion and then some specific works on the high-temperature solar furnaces and thermal conversion programs in Japan. Dr. Noguchi.

Dr. Noguchi - Thank you, Dr. Russell. Ladies and gentlemen, it is my great pleasure and honor so speak on the recent aspects of research and development of solar energy in Japan and, as Mr. Chairman said, I'd like to divide my talk in two parts: First, I'd like to speak on some recent prospects of solar energy R&D. Perhaps some of you remember my presentation in Las Cruces in 1974 on Project Sunshine, which was inaugurated by the Japanese government under the auspices of the Agency of Industrial Science and Technology, based on the Ministry of International Trade and Industry, in the areas of solar energy, coal gasification, hydrogen extraction, etc.

I'm going to talk about the Solar Energy Division of Project Sunshine which has programs in Photovoltaic Conversion, Solar Thermal Conversion, Solar Heating and Cooling, and Miscellaneous R&D, which are concentrated on high-temperature solar furnace work.

My presentation at Las Cruces included the concept of establishing a new Energy Research and Technology Institute. Unfortunately, this new Institute is not realized yet. It was designated to take care of a large-scale plant as well as testing facilities. However, because of the time limitation of constructing the

1000-kW_e solar convertion plant in 1980, we have the contract to the Electrical Energy Sources Development Company to make subcontracts with the Mitsubishi Heavy Industries Company and the Hitachi Company to construct the 1000-kW_e power plants respectively.

Figure 1 shows the aspect of our Project Sunshine to all solar energy programs included in such a way that the first column shows R&D on solar conversion plants, both on basic studies and receiver systems, etc., and the second column shows the construction of 1-MW electric plants in 1980 and 10-MW_e plants in 1985. We proceed then to further the first demonstration of other solar thermal plants.

The second program is on the R&D of photovoltaic systems. The temporary goal of this program is to achieve the cost reduction of photovoltaic cells to, hopefully, 100ths in both silicon crystal cells and thin films, and also other semiconductor cells. We would then proceed on the system analysis of the photovoltaic systems. This may be expected to proceed up to 1990 but I'm not sure whether we'll proceed further on the photovoltaic system or not at this moment.

The third program is the Solar Heating and Cooling System. It is expected that we will develop heating and cooling and hot water supply systems by the end of 1980 and then will give these new technologies to industries; there is practical market for these industries. The final program is the Miscellaneous R&D, which includes the high-temperature solar furnace work up to the year 2000 in the sense to serve at a high temperature for industrial-chemical processing, etc.

Figure 2 shows the concept of the central receiver system plant to be constructed in the Shikoku Islands. This is now in the design stage and the system itself is a tower receiver type which is very similar to those proposed by Honeywell, Inc., in the US. The central tower will be installed in the center of a mirror field.

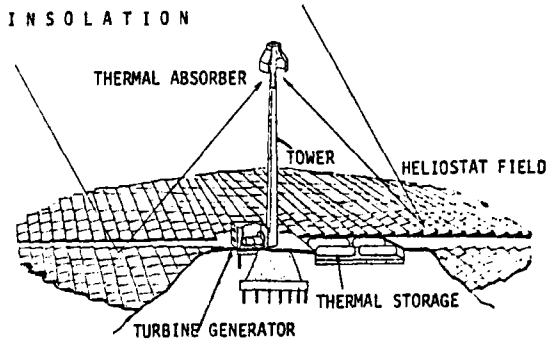

Fig. 2 Central Receiver System

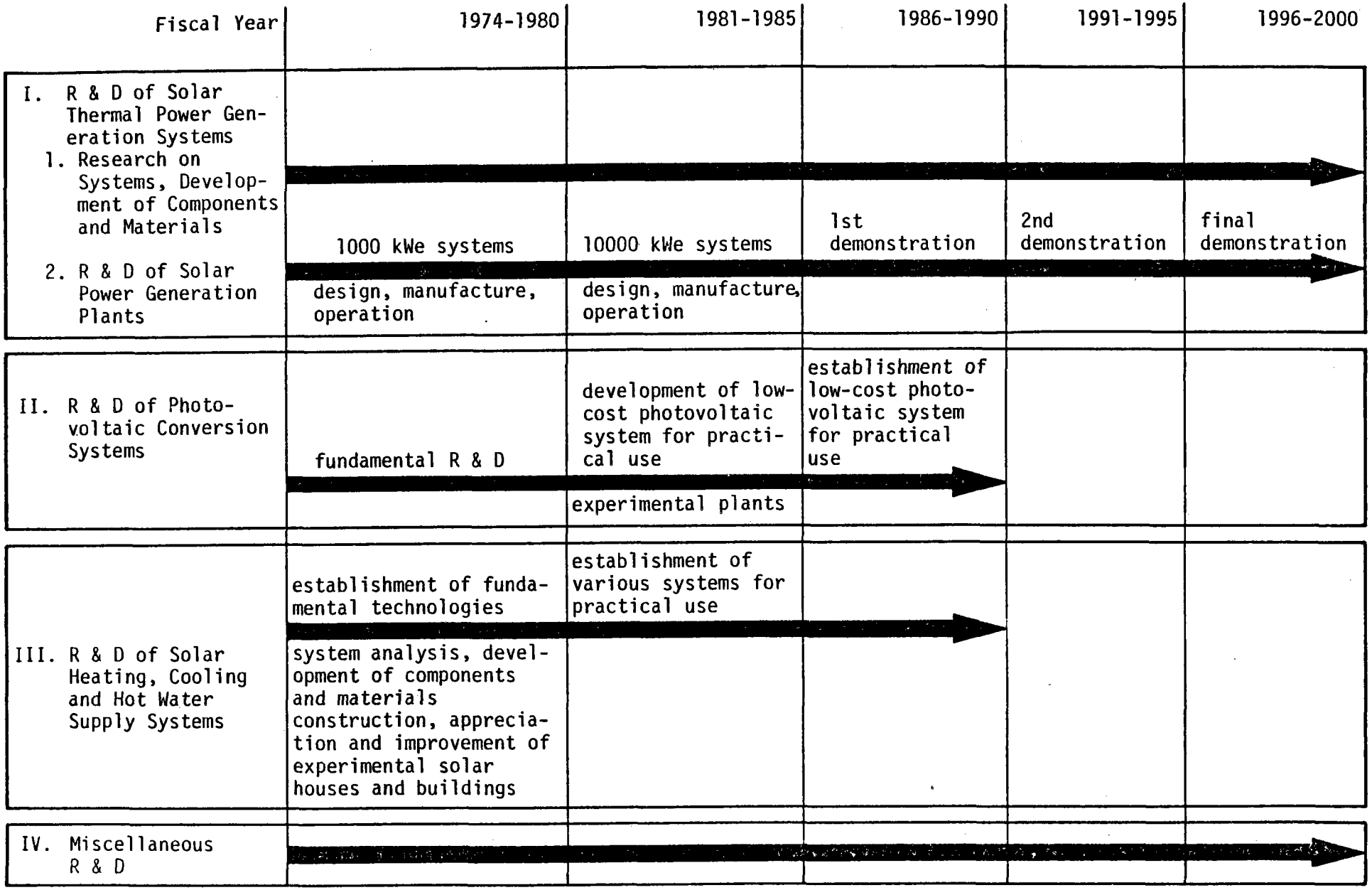

Fig. 1 Solar Energy R & D Program

Figure 3 shows what we call the hybrid system which was developed by the Hitachi Company. This is a combination of a flat-plate mirror and a parabolic trough concentrator and will be established in the 1000-kW plant.

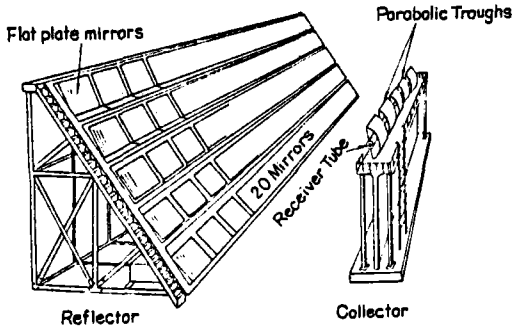

Fig. 3 Basic Unit of Plane-Parabola System

The large-scale hybrid system shown in Figure 4 might be explained in this way, that the first row of parabolic troughs at the right hand faces the plane mirrors which traps the movement of the sun. Behind this plane mirror array, we have parabolic troughs in the same way. Thus, the system will be expanded to the scale of 1000 kW_e, which might be said to be 5 MW thermal.

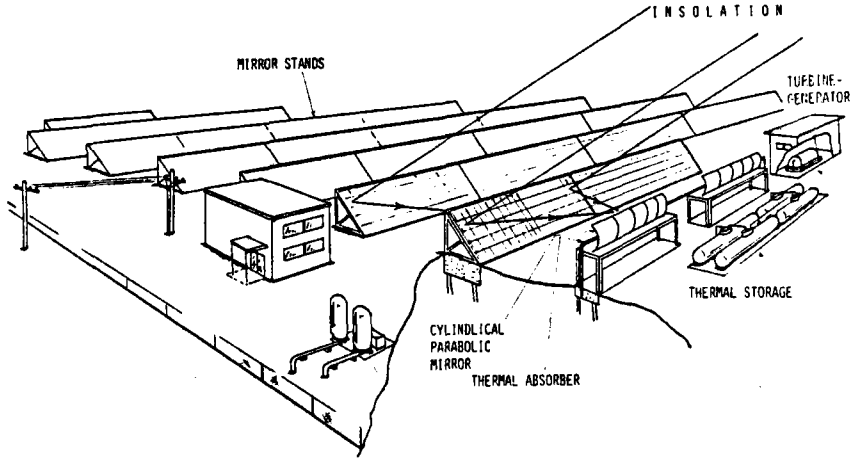

Fig. 4 Plane-Parabola System

Details of these designs will be explained in Table 5 and heat storage capacity of both the hybrid and also the central receiver system counted to three hours. The collector system is designed to match the plane parabolic mirror and other systems, respectively.

Characteristics of plant design:

Item	Plane-parabolic collector system	Central receiver system
1. Output of generators	1,000 kW	1,000 kW
2. Heat storage capacity	3 hours (1,000 kW)	3 hours (1,000 kW)
3. Collector system	Plane-parabolic	Central tower/receiver
4. Heat storage system	Accumulator/molten salt heat storage	Accumulator
5. Heat collector system	Mono-tube type (linear focusing type)	Drum type (capity type)
6. Designed direct solar radiation	0.75 kW/m^2 at 2:00 PM on the vernal equinox day	0.75 kW/m^2 at 2:00 PM on the summer solstice day
7. Pattern of operation	Middle load operation as a standard pattern; no operation at night as a principle	(Same to the left)
8. Area of plane reflectors	11,250 m^2 (Reflector 3m x 1.5m) x 100 pcs./unit x 25 units	12,900 m^2 (Reflector 4m x 4m)/unit x 807 units
9. Type of turbine	Impulse type extraction-condensing turbine	Impulse type condensing turbine
10. Tracking	Computer control	Computer control
11. Area of the site	100,000 m^2 for 2 units	

Fig. 5

As for the heat storage system, molten salt would be used for this hybrid system and for central receiver type. We considered the accumulator.

Another heat collecting system we have is a linear focusing type for the hybrid system. The heat collection system for the tower type plant is a cavity type, one which is similar to the systems the United States has been thinking about, under the expected solar radiation of about 0.75 kW per square meter. Thus, we have mirror fields of about 11,250 m^2 and also 12,900 m^2 for respective systems and this table shows briefly the outline of the design value for these hybrid and concentrating systems.

The location of the expected site is right in the map (Fig. 6) and this area has a high solar insolation. In the old times, the place was very famous for salt production and for salt ponds. We now expect to construct this kind of installation in Nio-Cho by the end of 1980.

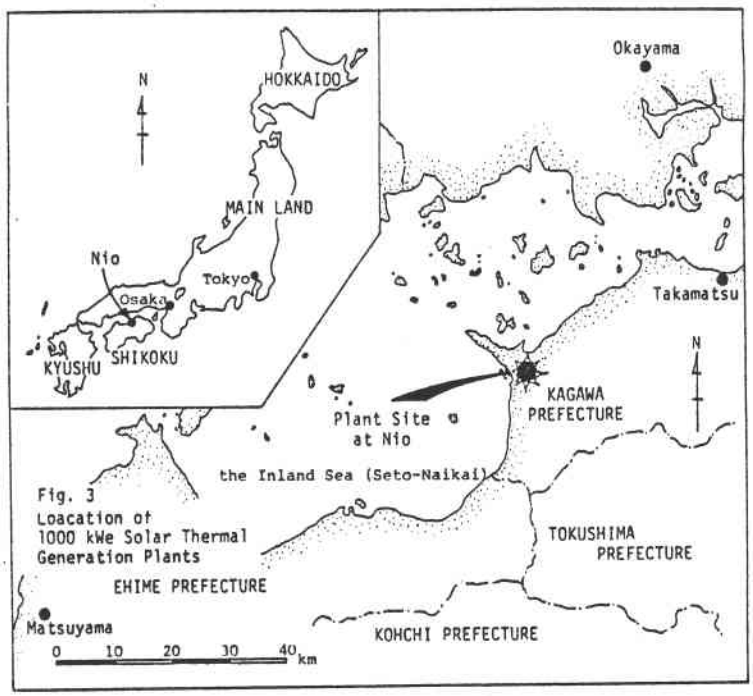

Fig. 6

At this moment, the central receiver type programs are studied by the Mitsubishi Heavy Industries Company. They have already tested a 10-kW solar plant and this 50-kW solar thermal plant was completed two years ago.

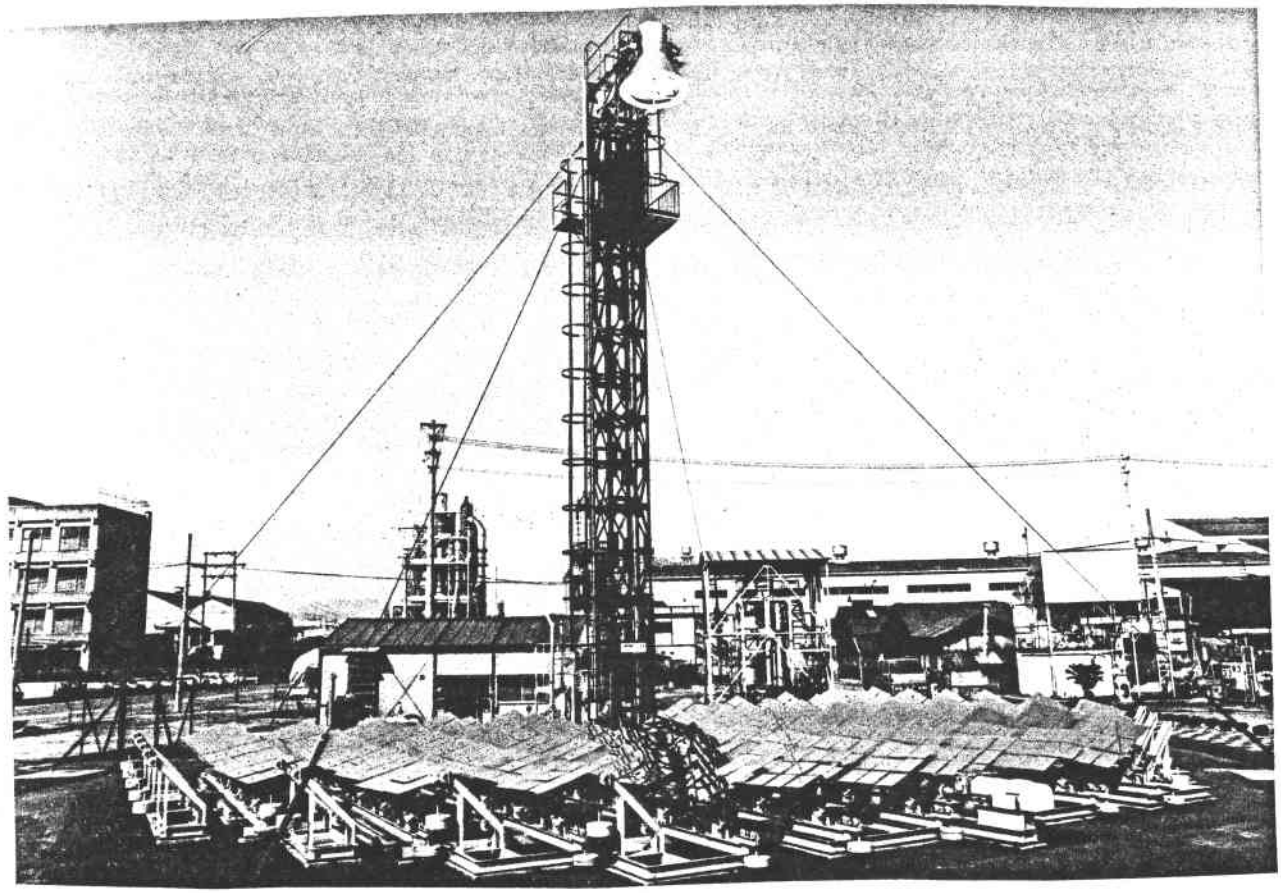

Fig. 7 Central Receiver System (50-kW)

This next slide, Figure 8, shows the 10-kW thermal plants by the Hitachi Company in which we have the plane mirrors on the right side and the parabolic trough on the left upper side. The heat collecting pipe at the focus of this parabolic trough is also equipped with selective surfaces in focusing the solar radiation from the mirror surface.

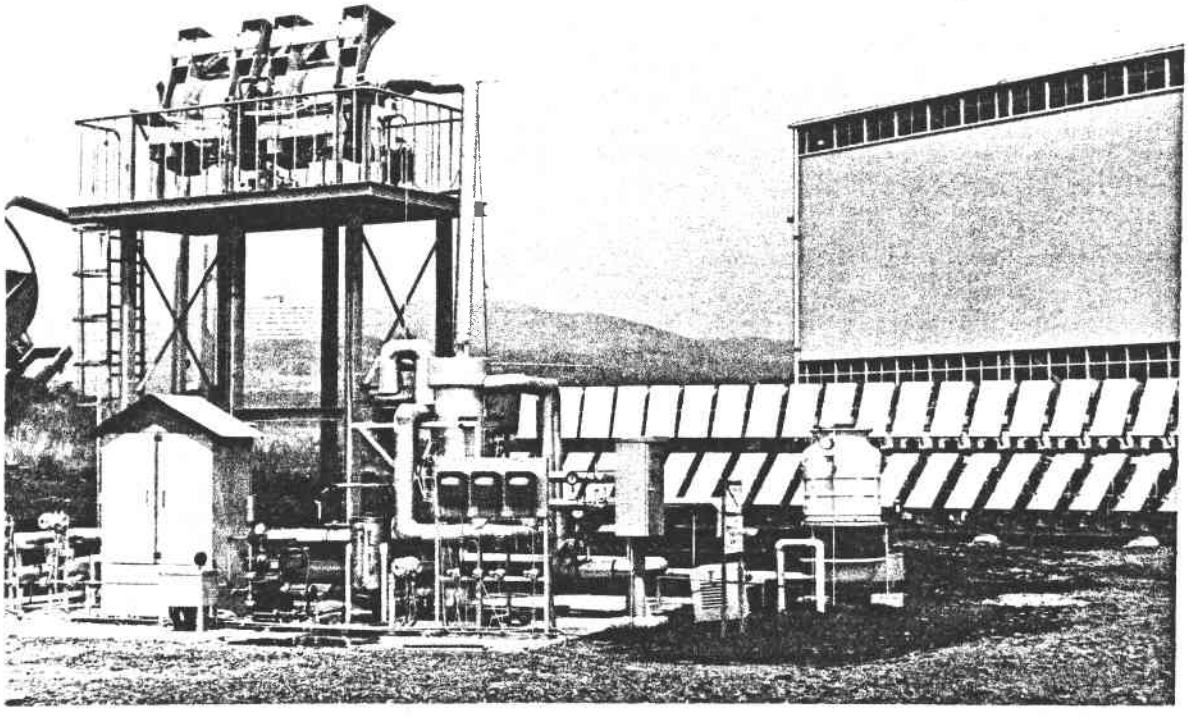

Fig. 8 Hybrid System (10-kW)

These are a brief introduction of solar thermal conversion programs at present in Japan and we are now going to proceed to the second part of my talk on high-temperature solar furnace works. In 1955 we constructed the first solar furnace in Nagoya. It was a direct-type solar furnace like I showed in the slide, 2 meters in diameter and with a 60-cm focal length.

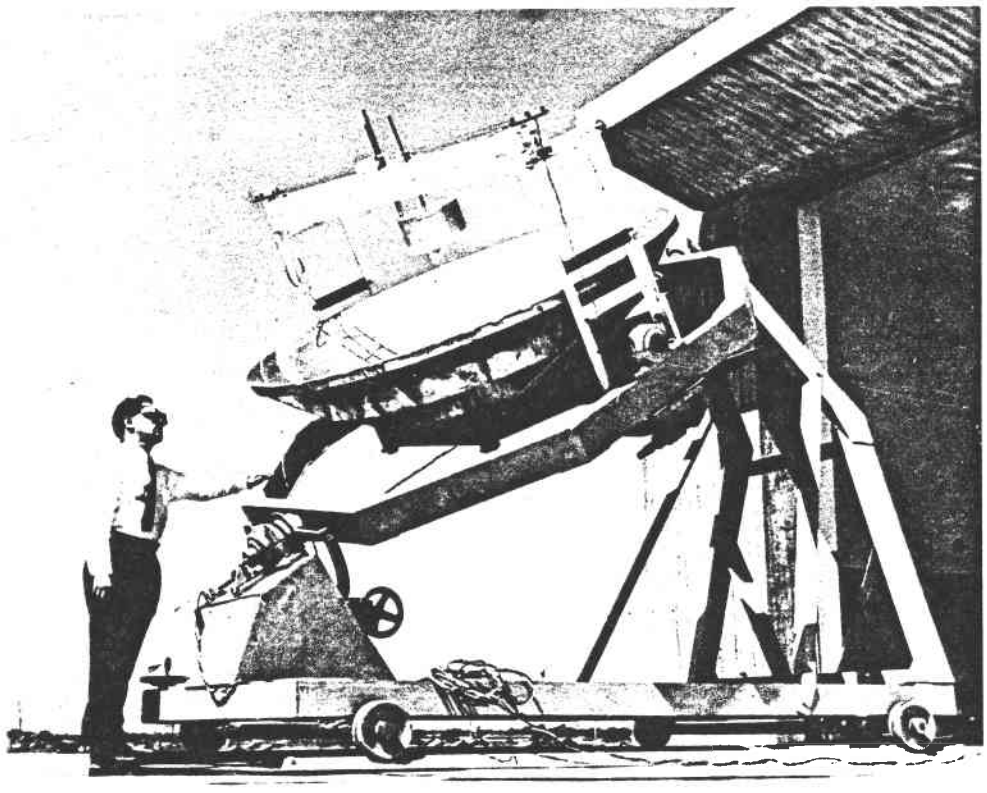

Fig. 9 Solar Furnace Built in 1955

Figure 10-A shows the second solar furnace which we have had for more than 20 years with segmented mirrors to move with the sun and parabolic reflector.

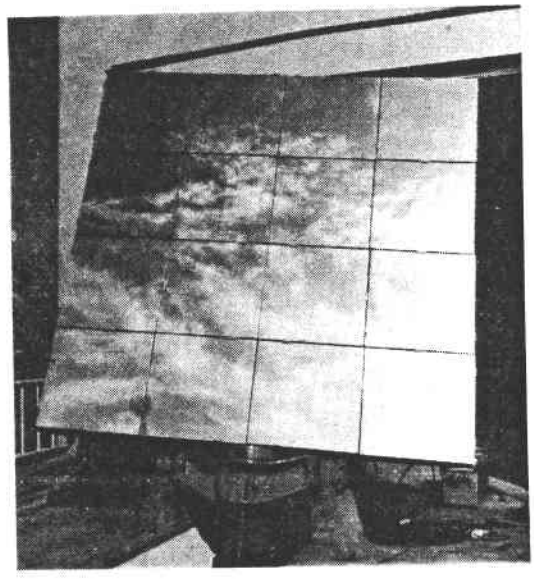

Fig. 10-A Heliostat Plane Mirrors
of the Second Solar Furnace

Figure 10-B shows the X-ray goniometer which was designed for coupling with the solar furnace and to be operated at about 2000-3000°C. Also, on the left side, you have vapor pressure measurement apparatus to face with this parabola and on the right side is the temperature controlling infrared radiometer. We have been using this solar furnace for more than 20 years to estimate the high-temperature phase diagrams relating to metal oxide binary system, as well as high-temperature emissivity and reflectivity data. Also, there are published papers on these highly refractory materials.

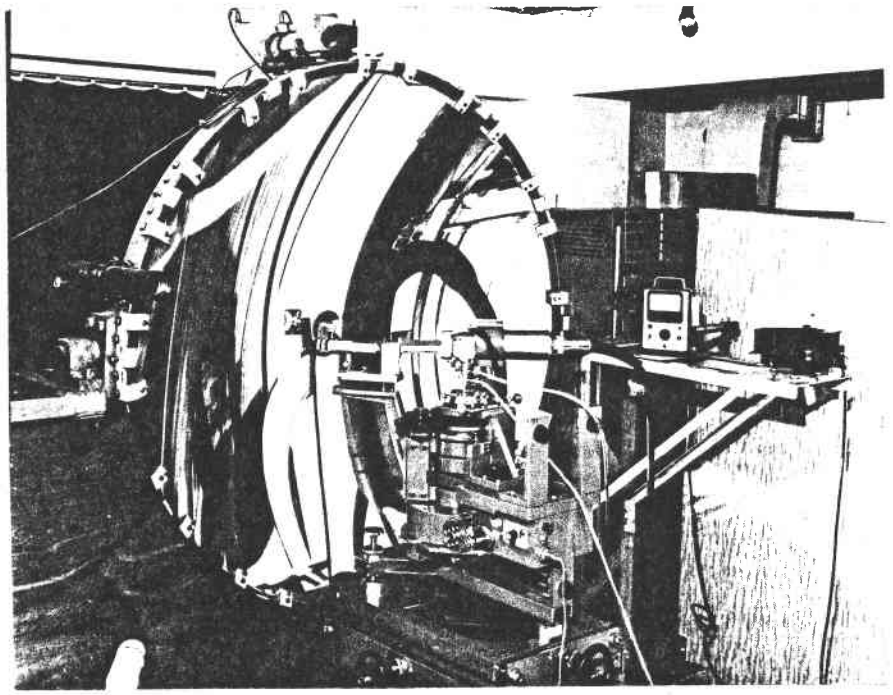

Fig. 10-B X-ray Diffractometer Coupled with the Solar Furnace

In addition to this high-temperature work in the field of basic studies, we have constructed a third solar furnace, which has a vertical optical axis. This program is supported by Project Sunshine and the main purpose was to develop the computer control system in February of this year. We see the heliostat plane mirrors at the lower part and also the image from the sun focuses on the upper part of the buildings.

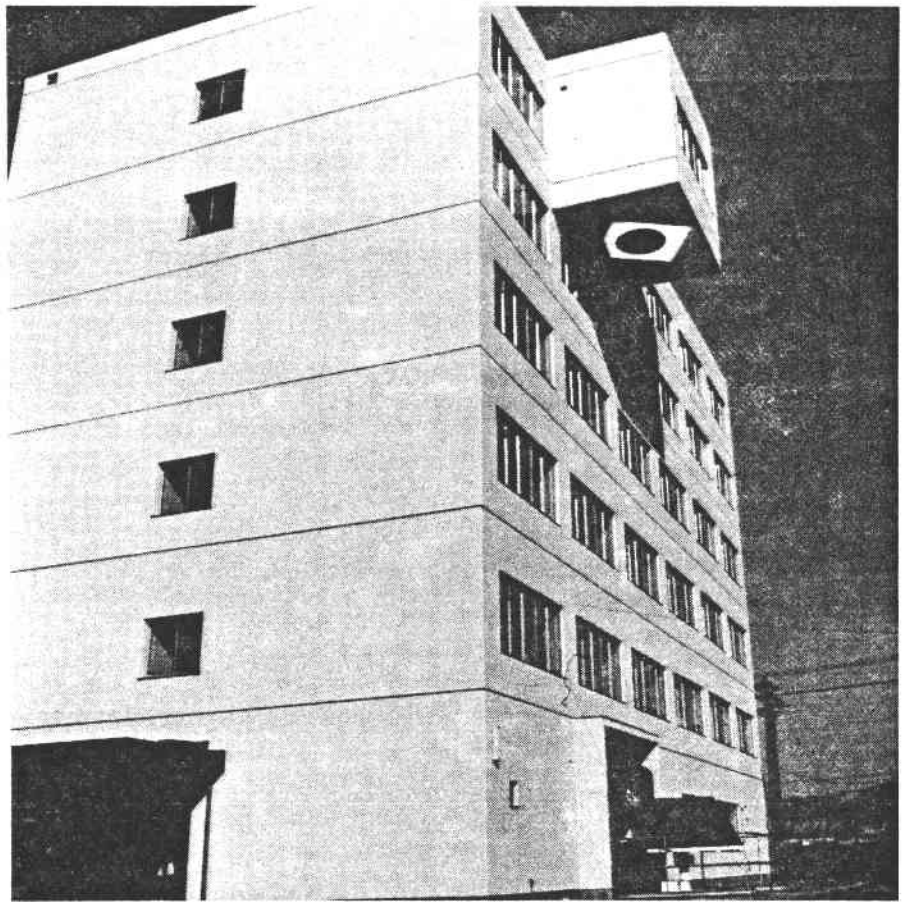

Fig. 11 The Third Solar Furnace with the Vertical Optical Axis

As I mentioned, the movement of this heliostat plane mirror was regulated by a minicomputer installed inside of the building, as shown in Figure 12.

Figure 13 shows a heliostat plane mirror with the azimuth-equatorial mounting.

In Figure 14 you might see some of the damper. This is a temperature controlling attenuator installed inside of the building and the tracking of the sun is performed with an accuracy of 0.5 minutes.

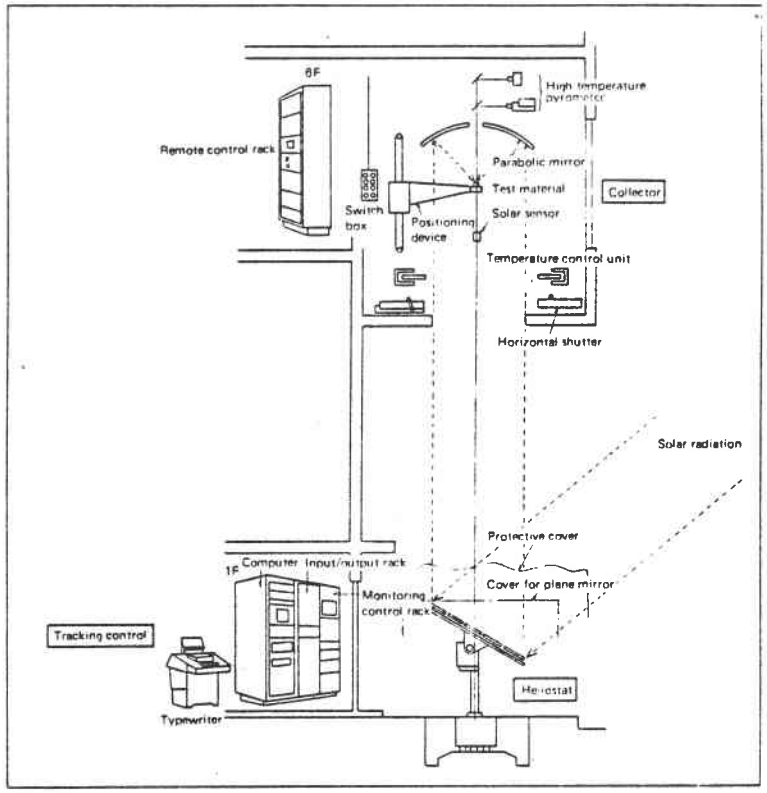

Fig. 12 Illustrative Diagram of Solar Furnace

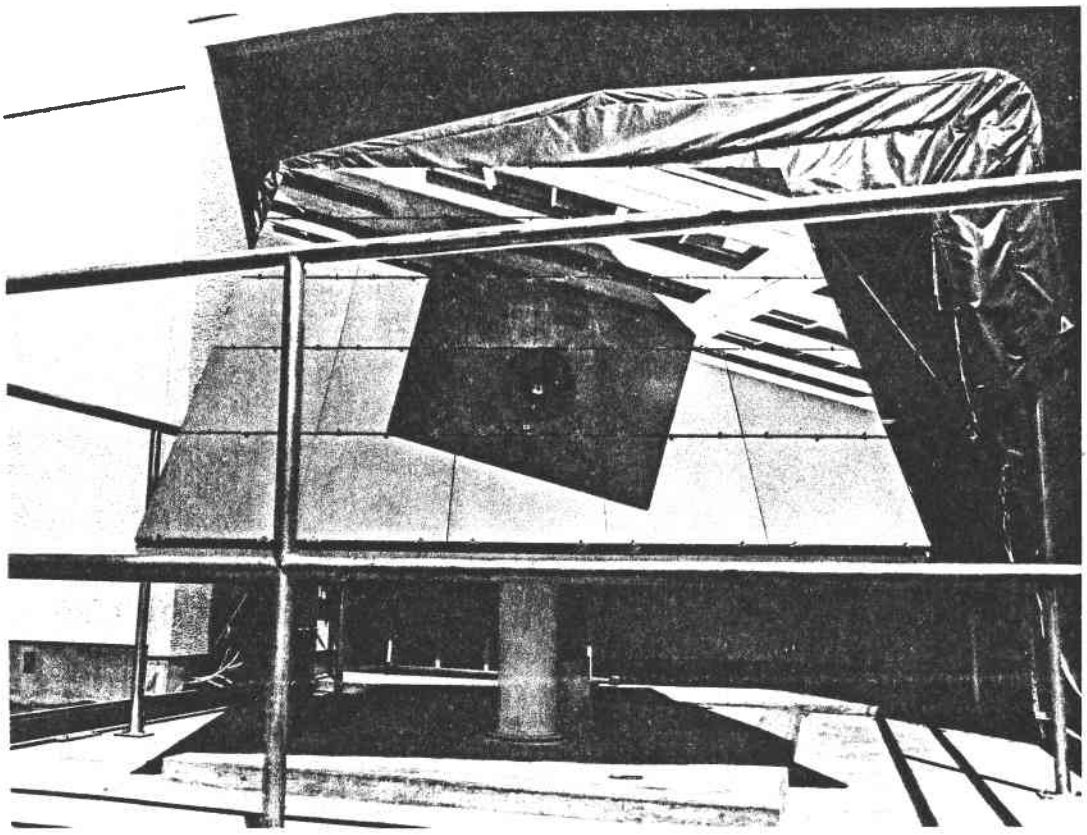

Fig. 13 Heliostat Plane Mirror

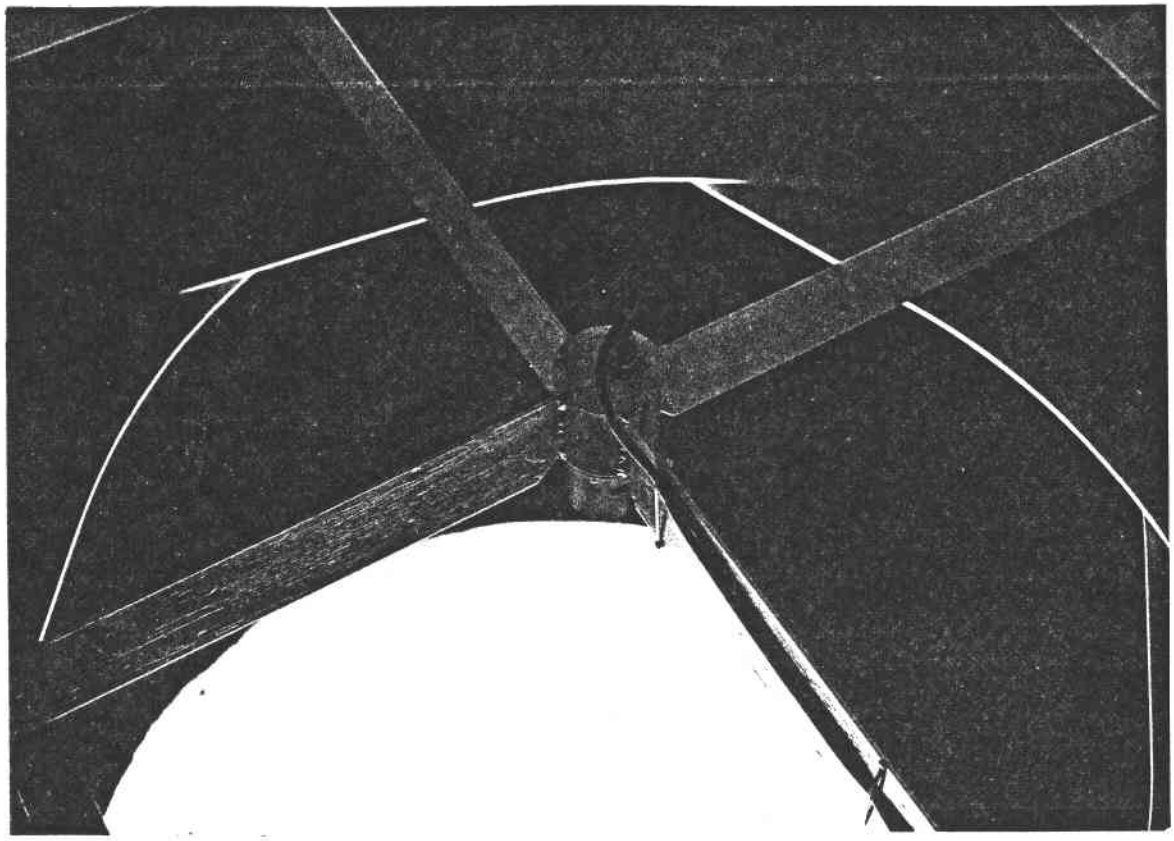

Fig. 14 Temperature Controlling Attenuator
(The photosensor is located at the center)

The computer programs include more than 50 years performance of this system and we will be able to avoid the out-of-control state by the operation of the minicomputer coupled with the photosensors installed in the paraboloidal mirror, see Figures 15-A and 15-B.

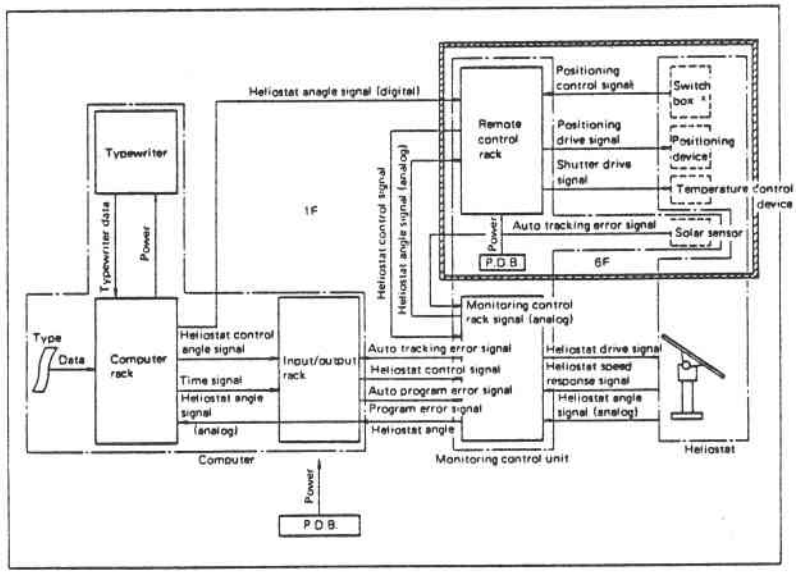

Fig. 15-A Line Diagram of Tracking Control

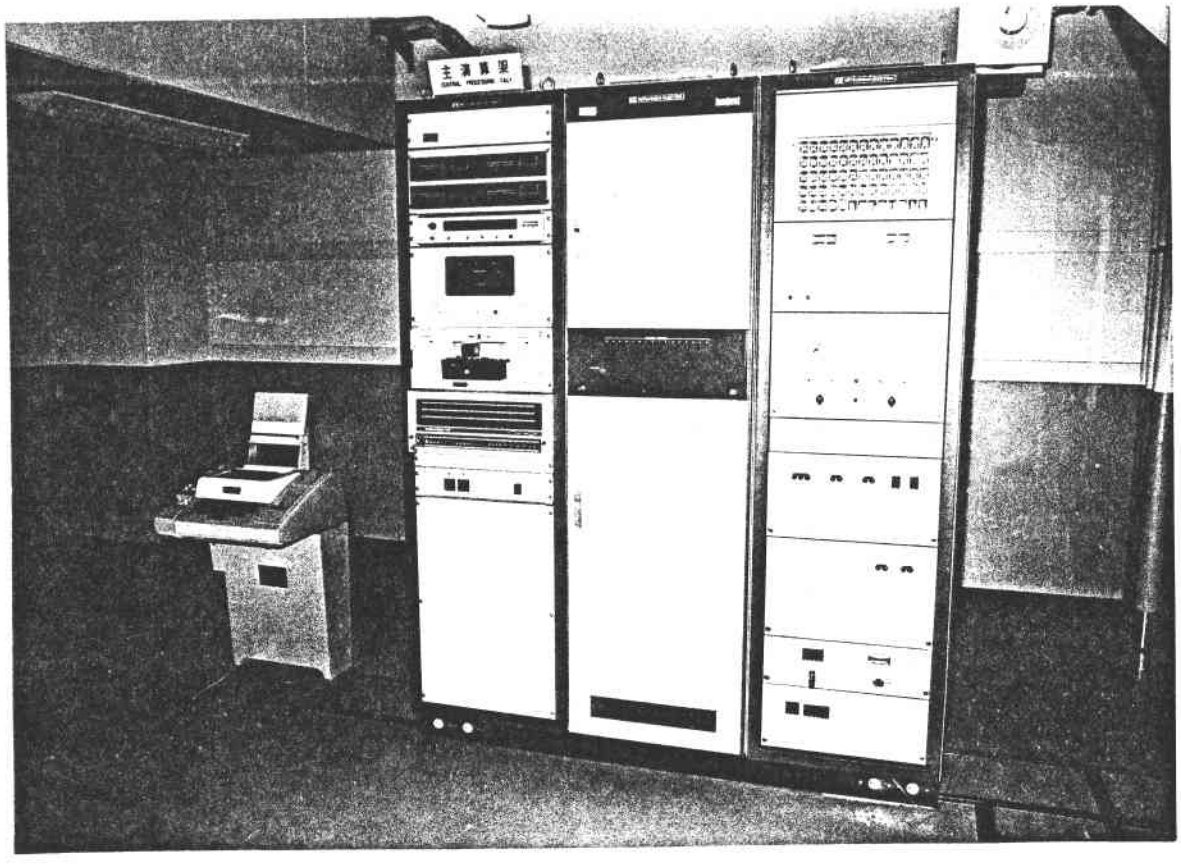

Fig. 15-B Minicomputer for Sun Tracking

In Figure 16 we have a parabaloid mirror on the upper side. Also, some positioning system is located to adjust the angle and position of a sample to be irradiated at the center of the focus. Possibly you might realize that this is a similar system to the one installed in Odeillo, France, and the configuration of the heliostat plane mirror system is about 2.5 x 2.5 m.

The temperature control at this parabolic mirror subsystem is performed in such a way that we have a brightness pyrometer designed by the Solar Research Lab at the wavelength of 0.65 microns to obtain the brightness, temperature and emissivity data of a specimen and also the control of the attenuator performed by infrared radiometer at 1.38 microns, to avoid the effect on the reflection of solar radiation from the molten surface of a specimen, see Figure 17.

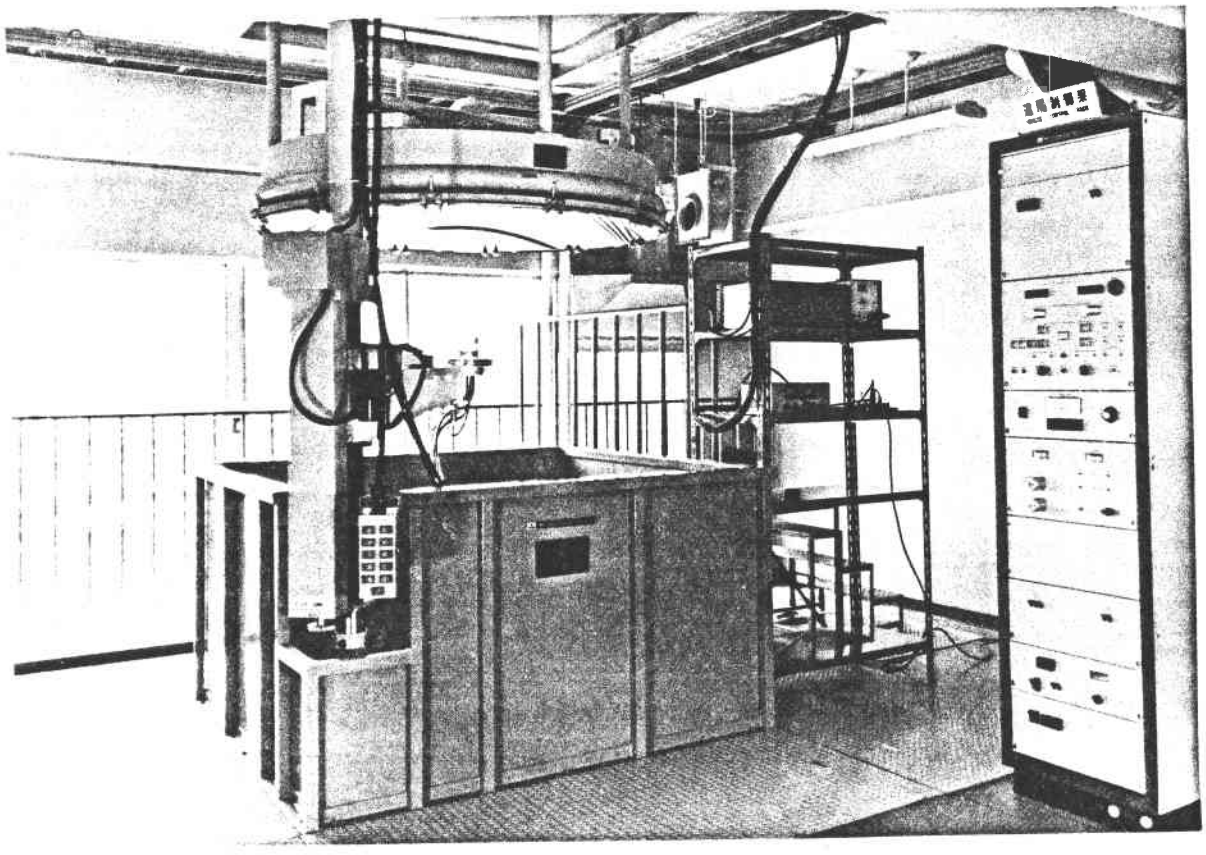

Fig. 16 The Paraboloidal Mirror of the Third Solar Furnace

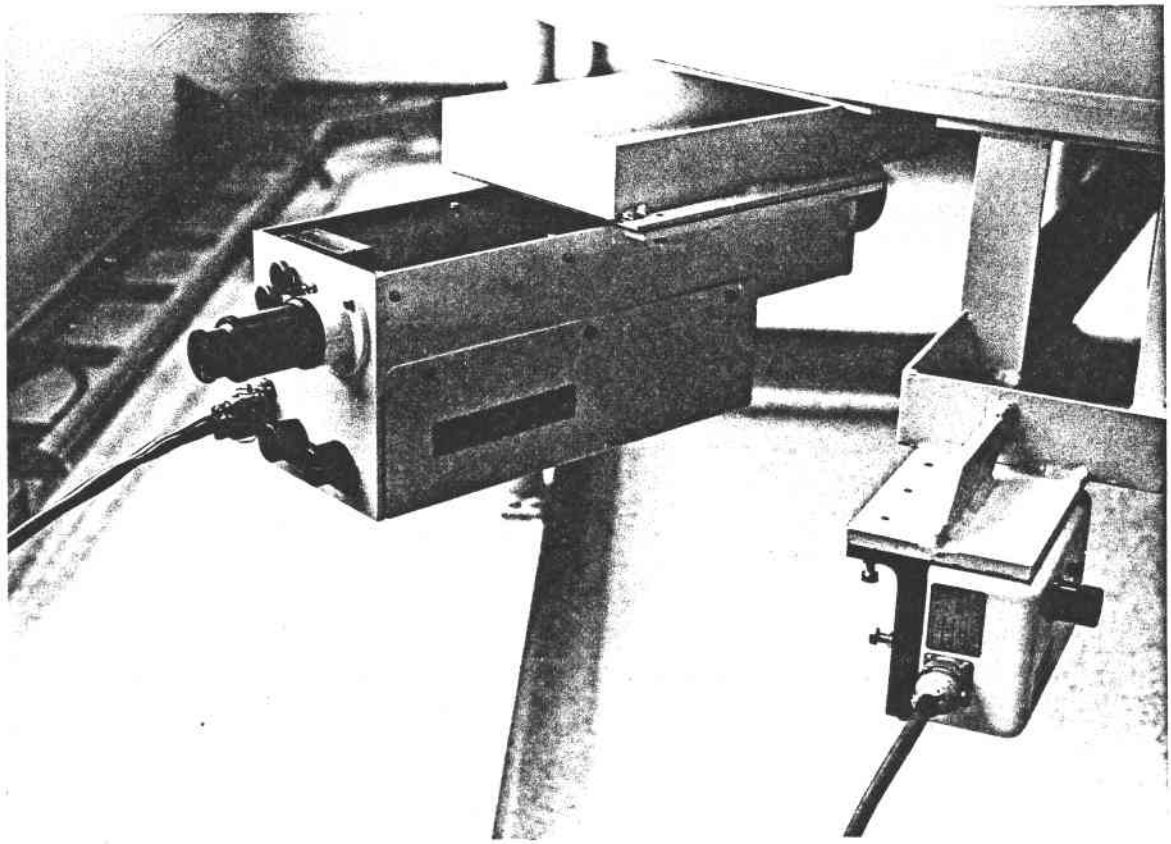

Fig. 17 Brightness Pyrometer (0.65 μm) and Infrared Radiometer (1.38 μm) Both Mounted on the Paraboloidal Mirror

Finally, the Project Sunshine includes the other feasibility studies of several solar systems like photovoltaic conversion, as well as solar thermal conversion, solar furnace, and other total systems. I've chaired the Solar Furnace Committee to do R&D study on the operation of high-temperature solar furnaces for industrial-chemical processings which started in 1974 and continued up to 1976. This three-year program has ended in publication of three volumes of books on studies of high-temperature furnace work, especially in the chemical industrial processing. Unfortunately, these publications are written in Japanese rather than English but if any of you wish to read these documents, contact me and perhaps we might be able to get a translation, including gasification and Si production, etc., as well as decomposition of PCB by the solar furnace and some of the other processes to be expected.

This is a general outline of our high-temperature solar furnace activities as well as solar energy R&D and I'd be very glad to have any comments or questions at this time.

Thank you very much for your kind patience.

Chairman Russell - Are there any questions?

Question - You didn't mention anything about the thermal decomposition of water for hydrogen production. Is that a part of your solar thermal furnace activities?

Dr. Noguchi - It is. Within the feasibility studies we have made the three-year program; we have also included this kind of work on solar decomposition of water by the solar furnace as well as reduction of SiO_2 to produce Si solar cell, but this kind of chemical reaction has to be carefully examined in the case of solar furnace operation because this is a gas reaction and might not be as easy compared with the solid-to-solid reaction to be operated by the solar furnace. We have already examined the possibilities of reduction of SiO_2 and also characteristics and possibilities of decomposition of water into hydrogen but it indicates it would be difficult to separate the hydrogen and the oxygen under the physical conditions in situ. Our new solar furnaces will be tested for doing such work in the future and I also must speak of our earlier program. The program we have had was skipped over in my talk. I was expecting to install six small solar furnaces to operate at the same time for the solar decomposition and X-ray diffraction works, etc., in our earlier program, but we constructed only one at this moment because of the budget limiation.

Mr. Smith - Do you have facilities and arrangements for use of those facilities by researchers from universities or other organizations or is it all handled by the government? Also, do you have anything resembling the Users Association, which we have for those purposes?

Dr. Noguchi - I must say that the facilities we have are open to any professors of universities or persons from the private sector. For the hydrogen work, it is quite a proposal but we'd be glad to work on it at any time.

Chairman Russell - Thank you very much, Dr. Noguchi. Please let us have another hand for Dr. Noguchi.

XII. SESSION VII: TESTING AND SIMULATION

THERMAL RADIATION TESTING FROM A USER'S VIEWPOINT

DR. T. M. KNASEL
MR. R. H. SIEVERS, JR.

A PAPER
PRESENTED AT THE ANNUAL MEETING OF THE
SOLAR THERMAL TEST FACILITIES USERS ASSOCIATION
GOLDEN, COLORADO
APRIL 11 AND 12, 1978

SCIENCE APPLICATIONS, INCORPORATED
8400 WESTPARK DRIVE, MCLEAN, VIRGINIA 22101
(703) 821-4300

OUTLINE

The purpose of this talk is to describe considerations in selecting appropriate sources, control, and instrumentation of high thermal level tests. Coming, as it does, toward the end of the two-day Annual meeting of the Solar Thermal Test Facilities Users Association, this talk tries to summarize what a user must consider in thermal testing. We therefore shall discuss test goals, sources, optics, and test procedures and instruments, roughly paralleling the meeting plan itself.

Science Applications, Incorporated, has been involved with solar furnace operation and testing as well as other means of achieving high thermal flux on test samples since 1973. Research work has involved source selection, new source development, optical system design and fabrication, instrument design and construction, and test and analysis. We will draw from experience gained in these programs in our talk.

OUTLINE

1) THERMAL TEST GOALS

2) CHOICE OF THERMAL SOURCE

3) OPTICAL SYSTEM DESIGNS TO ALTER THERMAL RADIATION

4) MATERIAL TEST PROCEDURES

5) CONCLUSIONS

THERMAL TEST GOALS

Goals of thermal testing include providing accurate controlled exposures and extraction of meaningful data from these tests. State-of-the-art research programs will generally be directed toward high flux, large exposure areas or both. Time control of exposure, test cost and test flexibility are also critical.

---

1) THERMAL TEST GOALS

PROVIDE THERMAL FLUX OVER TEST AREA

- HIGH LEVELS OF FLUX
- LARGE AREAS
- CONTROLLED TIME OF EXPOSURE
- TEST COST REALISM
- TEST FLEXIBILITY

THERMAL TEST REQUIREMENTS FOR AN EXAMPLE SAI PROGRAM

Recently SAI has been asked by the Defense Nuclear Agency to plan for a series of tests of material samples at high fluxes. We shall use this as an example to illustrate how we approach planning for a thermal test series.

In this program, an early decision on the type of thermal energy source to be used is essential as experiment design is dictated by the source selected.

The program involves the exposure of soil samples to intense radiation and the careful analysis of the response of the soil. The soil is expected to react violently, producing a dusty heated air layer above the sample.

THERMAL TEST REQUIREMENTS FOR EXAMPLE SAI PROGRAM

TEST PARAMETERS

FLUX: UP TO 550 CAL/CM^{2}SEC
FLUENCE: UP TO 115 CAL/CM^2
PULSE LENGTH: 11 MILLISECONDS TO 6.5 SECONDS

MEASUREMENT REQUIREMENTS

INCIDENT RADIATION: TO TEST APPARATUS AND ON SAMPLE SURFACE

LOSS OF MASS FROM SAMPLE: TOTAL AND AS FUNCTION OF TIME

AIR TEMPERATURE ABOVE SURFACE: AS FUNCTION OF POSITION AND TIME

PARTICULATE CONCENTRATION ABOVE SURFACE: AS FUNCTION OF POSITION AND TIME

PARTICLE TEMPERATURE AND STATE (SOLID AND LIQUID)

SOUND VELOCITY OF MIXTURE ABOVE SAMPLE SURFACE

OPERATIONAL REQUIREMENTS

SUITABLE FOR AN EXTENDED TEST PROGRAM OF PRECISE PARAMETRIC ANALYSES

CHOICE OF THERMAL SOURCE

The source alternatives considered were (Figure 2):

- Solar Furnace
  3 principal facilities
- Flash Lamps
- Thermochemical Reactions

Characteristics of greatest concern in selecting the nature of the thermal energy source are shown in the viewgraph. Source power, peak flux and sample area are indicated as key parameters. We shall see that in further work, source brightness is often important as well as other factors such as instrumental and computer support.

---

2) CHOICE OF THERMAL SOURCE THERMAL RADIATION SOURCE CHARACTERISTICS

SOURCE	POWER (KW)	NOMINAL PEAK FLUX (CAL/CM^2SEC)	NOMINAL SAMPLE AREA AT PRIME FOCUS (M^2)
SOLAR FURNACES			
ODEILLO-FONT ROMEU	1000	400	0.06
WHITE SANDS MSL RANGE	25	100	0.01
SANDIA	1700 (5000)	60	4.0
FLASH LAMPS	30 EACH	3000-4000	>0.06
THERMOCHEMICAL REACTIONS	10^5	20-200	>10.0

COMPARISON OF ALTERNATIVE SOURCES OF HIGH RADIANT FLUX

Of the variety of sources initially considered, none provides the optimum for all of the desired characteristics. The study is proceeding on the basis of using a solar furnace and concurrently examining alternative sources, especially flash lamps.

As the experiment requires greater flux levels than provided at focus by any of the solar furnaces, beam concentration is necessary. Further, a horizontal sample surface is preferred, requiring an approximately 90^{o} flux diversion. The high flux, small focal area, and adequacy of experimental work area of the Odeillo-Font Romeu facility resulted in its selection as the basis for apparatus development. Special concerns in the development are the need for flux redirection, flux-time variation control, measurement, and laboratory calibration.

COMPARISON OF ALTERNATIVE SOURCES OF HIGH RADIANT FLUX AND FLUENCE ON A PLANE SURFACE SAMPLE

PARAMETERS	SOLAR FURNACES	FLASH LAMPS	THERMO-CHEMICAL	HEAT LAMPS	CONVENTIONAL FURNACES
PEAK FLUX	MODERATE	V. HIGH	MODERATE	LOW	LOW
FLUX CONCENTRATION	FEASIBLE	FEASIBLE	NOT PRACTICAL	FEASIBLE	NONE
PULSE LENGTH	HOURS	$\frac{1}{\text{FLUX}}$	SECS	INDEF.	INDEF.
PULSE CONTROL	FEASIBLE	FEASIBLE	V. LIMITED	FEASIBLE	V. DIFFICULT
REPEATABILITY	GOOD	EXC.	FAIR	EXC.	EXC.
AVAILABILITY	TIME & PLACE RESTRICTED	EXC.	LIMITED	EXC.	SPECIAL RQMT.
TEST COSTS	HIGH	LOW	HIGH	LOW	UNKNOWN
TEST FLEXIBILITY	LIMITED	HIGH	FAIR	HIGH	LOW
LOCATION FLEXIBILITY	NONE	HIGH	FAIR	HIGH	LOW
RELIABILITY	LOW	HIGH	FAIR	HIGH	HIGH
SAMPLE AREA	LOW	MODERATE	HIGH	MODERATE	LOW TO MODERATE
CAPABILITY	PROVED	UNTESTED	PROVED	UNPROVED	UNPROVED

OPTICAL SYSTEMS DESIGN TO ALTER THERMAL RADIATION

The user may be faced with additional requirements for flux manipulation beyond the existing source capabilities. SAI has investigated flux intensity concentration, flux direction changing (diversion) and flux shuttering.

Flux redirection, or beam shaping, is necessary to concentrate and divert thermal energy. The designer has tools from imaging theory and recently developed tools in non-imaging optical theory.

---

3) OPTICAL SYSTEM DESIGN TO ALTER THERMAL RADIATION

DESIGN VARIABLES:

- FLUX CONCENTRATION
- FLUX DIVERSION
- FLUX CONTROL

DESIGN TOOLS:

- FINITE SIZE IMAGING THEORY
- NON-IMAGING THEORY - PHASE SPACE CONSERVATION

OPTICAL SYSTEM DESIGN RESULTS

The results of recent SAI work are referred to in this and the two following slides. We have designed and built and tested apparatus for flux diversion, flux concentration, and flux control--all operable at high flux levels. Ideal Light Collector (ILC) designs have been found useful in this work.

OPTICAL SYSTEM DESIGN RESULTS

- FLUX DIVERSION
  - TWO LENS - ONE MIRROR SYSTEM TO REFOCUS FOCAL PLANE - WSMR
  - IDEAL LIGHT COLLECTOR DESIGN - FOR CNRS
- FLUX CONCENTRATION
  - ILC TESTED AT WSMR
- FLUX CONTROL
  - 10-MSEC FAST RESPONSE SHUTTERS - TESTED
  - USED IN EXPERIMENTAL PROGRAM

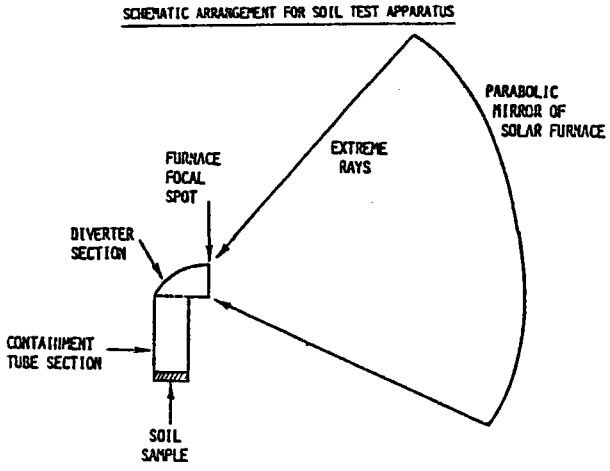

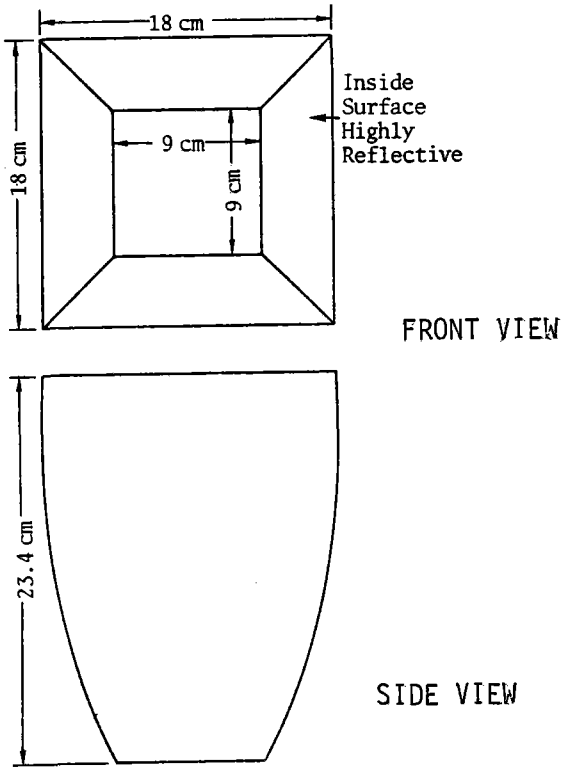

Fig. 4. Basic Design of ILC, Design Angle 30°

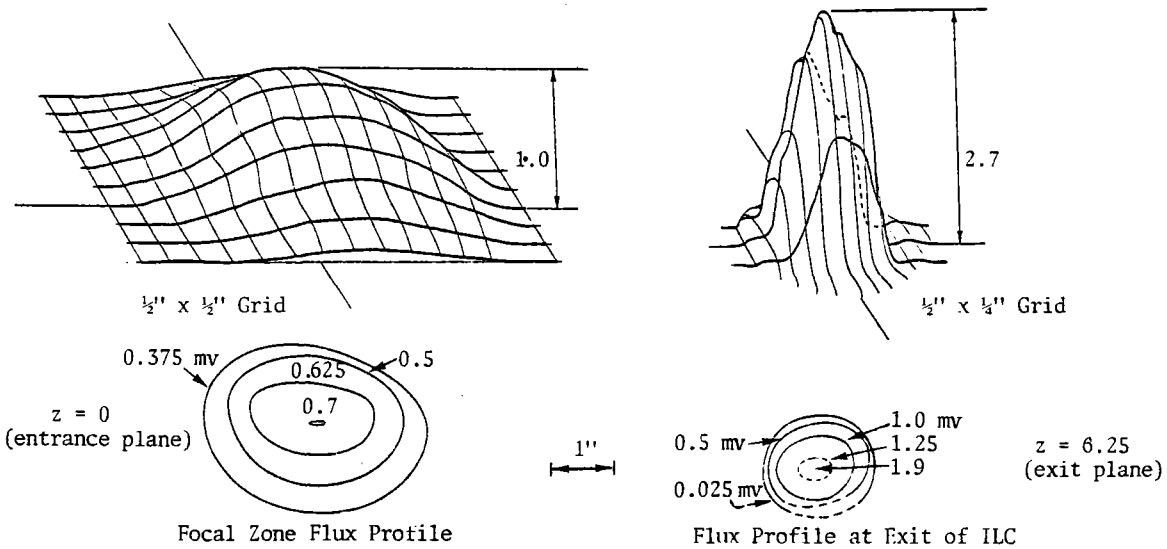

Fig. 5. Flux Profiles from ILC Tests

MATERIAL TEST PROCEDURES

The example SAI program mentioned earlier has evolved a number of specific instrumentation concepts and a system integration scheme. These will be illustrated to show how the experimental design folds in optical, mechanical, electrical and electronic equipment into a working package.

---

4) MATERIAL TEST PROCEDURES

- INSTRUMENTATION
- SYSTEM INTEGRATION

INSTRUMENTATION - IN HIGH FLUX ENVIRONMENT

Although measurement of many of the optical and thermodynamic properties in the flux or temperature regime of these tests is fairly standard, care must always be taken to avoid bias. A case in point involves measurement of the temperature of a semitransparent gas in an optical flux region of 100 cal/cm^2 sec. We have demonstrated total temperature probes, doubly shielded from solar radiation for bias-free recording of gas temperature to about 1800^oC, at 100 cal/cm^2sec incident radiation levels. Some key needs we have are also indicated. When using energy densities obtainable with solar furnaces, the experimenter is apt to find that he needs to design and calibrate his own measurement equipment. The environmental extremes call for protection considerations for available sensors or for special chambers for their use. The soil experiment apparatus requires just such considerations. The lack of test flexibility increases the need for protection of the apparatus in the event of malfunctioning shutters, and of the sensors, to avoid equipment downtime, or the need to take inordinate quantities of spares to the test site.

INSTRUMENTATION - IN HIGH FLUX ENVIRONMENT

STANDARD OR STATE-OF-THE-ART

- THERMOCOUPLES IN SOLIDS, LIQUIDS
- IR THERMOMETERS
- CALORIMETERS - FAST RESPONSE
- CINE PHOTOGRAPHY
- THERMOCOUPLES IN GAS TO 100 CAL/CM^2SEC

NEEDS

- MEASURING EMISSIVITY AT ELEVATED TEMPERATURES

SAI TEST APPARATUS - SCHEMATIC CROSS SECTION

The SAI test apparatus uses a water jacket to protect the beam shaper and test chamber, aspirated thermocouples to test chamber air temperature, remote incident light measurement through use of fiber optics, recessed sound sensors, and separate chambers for temporal and end state particle analyzers. The cost associated with full-scale experimentation necessitates maximum use of laboratory testing to ensure resistance to the environment and for calibration. The test apparatus proof and calibration will be more complex efforts than the eventual soils test program.

Peak flux is adjusted by varying the number of heliostats in use and by partially opening of the test area doors. Pulse shape variation and abrupt termination requirements, however, necessitate shutters developed and controlled as part of the experiment. The test apparatus will have two shutters, a butterfly and a sliding blade. The butterfly is to be driven by a variable speed motor to achieve sinusoidal opening and (different rate) closing of the test chamber. The sliding blade will provide for abrupt termination, and will collect particulate matter for examination. A schematic cross section of the test apparatus is shown in the slide.

SAI TEST APPARATUS - SCHEMATIC CROSS SECTION

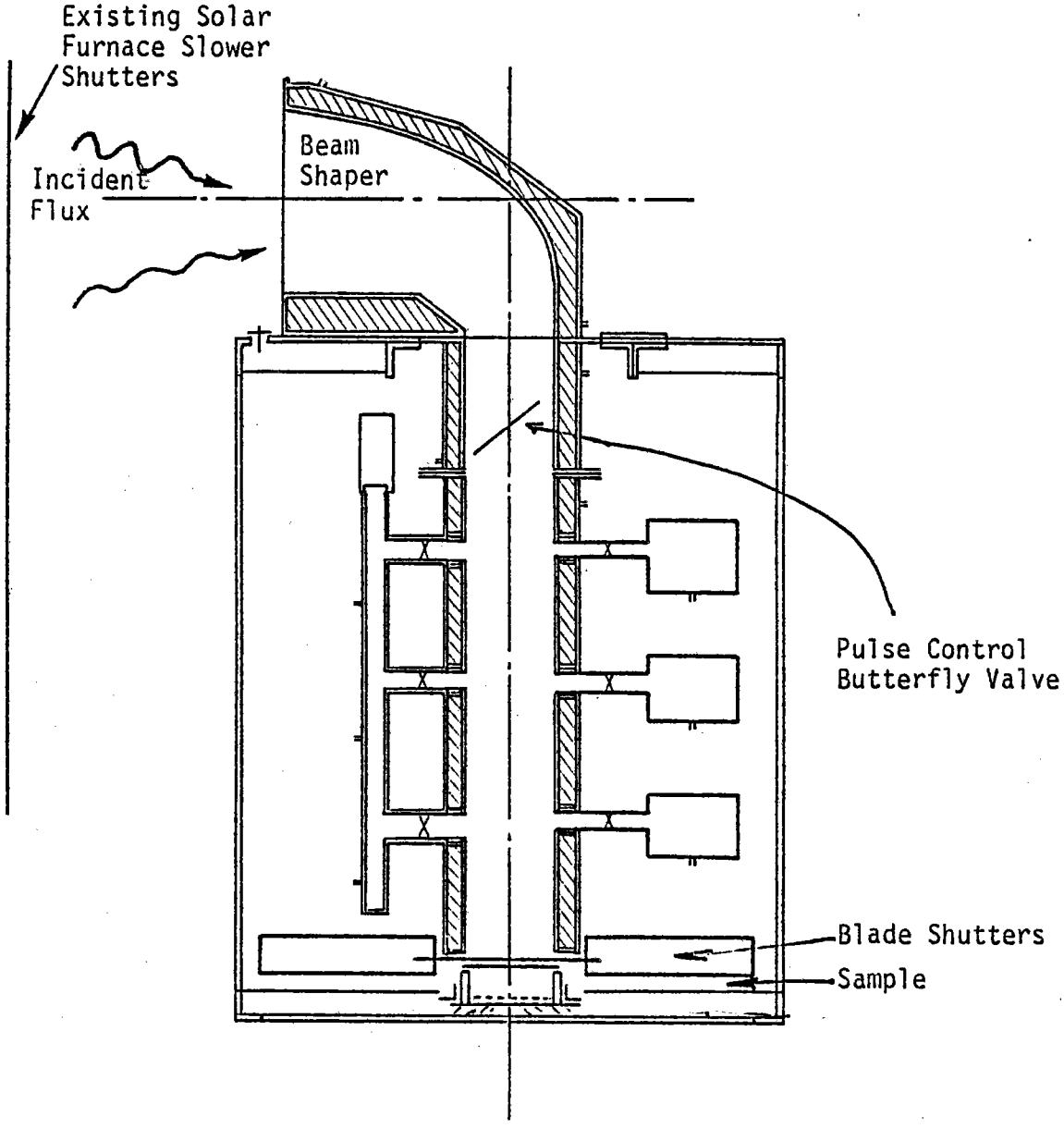

CONCLUSION

The described test apparatus is still in the design and development stage. However, we can foresee applications for elements of the apparatus to problems beyond those of thermal effects on soils. The basic apparatus, for example, would be suitable for fire resistance, and dynamic analysis or collection of combustion products. With alternative beam shaping, the apparatus may be adapted for use with flash lamps.

Regardless of the apparatus or test purpose, there are basic considerations in Solar Furnace experiment development. The successful program must be based on such planning and preparation.

---

5) CONCLUSION BASIC THERMAL RADIATION TEST CONSIDERATIONS

REQUIREMENTS:	FLUX, FLUENCE, PULSE SHAPE, EXPERIMENTAL AREA, TEST FLEXIBILITY
	FACILITY AVAILABILITY, COSTS, SAMPLE AREA, REPEATABILITY, ALTERNATIVES
BEAM SHAPING:	CONCENTRATION, DIVERSION, INTEGRATION WITH EXPERIMENT, PROTECTION
SAMPLE HOLDING MEASUREMENT:	ENVIRONMENT, DURABILITY, PROTECTION, INTEGRATION
PREPARATION:	ENVIRONMENTAL TESTING, CALIBRATION, SPARES, DETAILED COORDINATED PROGRAM

COMPUTER SIMULATION OF THE SOLAR THERMAL TEST FACILITY

C.C. Castellano

Department of Energy
Washington, DC

E.N. Best
J.V. Coggi
R.A. Jamieson
K.L.Zondervan

The Aerospace Corporation
El Segundo, California

ABSTRACT

A transient computer simulation of the Solar Thermal Test Facility (STTF) has been developed to serve as a tool to analyze a variety of experiments proposed for the STTF under differing environmental and test conditions. The STTF is a general solar test facility designed to provide solar thermal energy of up to 5 MWt. The facility consists of a relocatable heliostat field, a tower for mounting experiments, water and electrical resources, a heat rejection system, a computerized control system, and a data acquisition system. In the computer program each of these elements of the facility is modeled by an equivalent computer subroutine. The experiment module is designed with simplified, well-defined interfaces such that the program user may readily insert a new module describing his particular experiment. The experimenter may then design, plan, evaluate and verify safety of his experiment by computer prior to the test at the facility, thereby reducing test costs and improving facility utilization. A simulation of the Martin Subsystem Research Experiment (SRE) 5 MWt receiver at the STTF was performed to verify the capability of the program to simulate the performance of a complex test article and to illustrate program applications.

INTRODUCTION

The STTF provides the opportunity to conduct a variety of experiments at higher solar power levels than previously possible. Optimal utilization of the STTF unique capabilities appears possible only if proposed experiments are carefully analyzed and prioritized prior to hardware implementation.

The STTF computer simulation presented in this paper is an analytical tool designed to be used by the STTF experimenter in the design, test planning, test support, and data evaluation phases of his experiment (Reference 1). Table 1 lists examples of some of the potential uses. The program is best used to predict overall system level interactions, performance, and control; rather than predicting detailed component information, such as temperature distributions, which are better handled by specialized programming.

TABLE 1

STTF COMPUTER SIMULATION APPLICATIONS

Experiment Design/Analysis	Experiment Support
Predict Performance Under STTF Conditions	Test Program Development and Schedule
Parameter Sensitivity Analysis	Test Objective Quantification
Control System Design	Measurement Instrumentation Definition
Safety Verification	Test Operation/Procedure Checkout
	Extend Test Profile
	Operator Training

The simulation is designed with a highly modular structure to provide the maximum flexibility with the minimum programming effort to meet the requirements of a particular experiment. The STTF is divided into distinct subsystems that have well-defined interfaces. Each subsystem is implemented in a separate computer module. Reconfiguring the system is accomplished by redrawing interface connections with no changes required to the module. A user supplied module, describing the experiment, is connected to the STTF through these interfaces.

The simulation is implemented on a CDC 7600 using the FORTRAN language. A computer core memory of 40,000 words is required.

STTF SYSTEM DESCRIPTION

The parts of STTF that are important to a dynamic simulation include the collector field, the heat rejection system, the control systems, and the experimental

hardware. Figure 1 illustrates the subsystem boundaries and their interconnecting interfaces arranged to test a receiver for a solar central receiver power plant. For each subsystem the interface quantities consist of some subset of energy flow, fluid flow, or information transfers. Each of the subsystem modules is described below.

Insolation

Insolation is not a physical part of STTF but is, nevertheless, an essential part of the overall system. Its characteristics and transients largely determine the capability and dynamic behavior of the system at any given time. Lack of control over behavior of the basic energy source places unusual demands on the designers and operators of the experiments. Insolation data for the simulation were extracted from the Albuquerque data tapes (Reference 2).

Collector

Extra foundations are provided in the field to permit moving of heliostats to reconfigure the collector field to support a wide variety of tests as illustrated in Figure 2. A total of 222 heliostats are available. A north field (as is required for the Martin SRE receiver) is set up by mounting the heliostats on the 222 foundations of zones A and B. An annular field is set up by mounting the heliostats on the 222 foundations of zones A, C, D, and E.

Each heliostat consists of a 5 x 5 array of facets. Each facet is 4 ft x 4 ft for a total heliostat area of 400 ft^2. Solar tracking is accomplished by means of an azimuth-elevation gimbal drive system operating open loop on a calculated sun position. Resolvers sense and feed back gimbal angles to the controller.

Heat Rejection System (HRS)

The HRS consists of the feedwater, depressurization/desuperheat, and cooling subsystems as shown in Figure 1. These subsystems are lumped together in the present discussion since they operate essentially as a unit. However, special test requirements may require regrouping them in a different configuration.

The HRS provides preconditioned feedwater to the experiment and receives high temperature, high pressure steam from the experiment. Excess energy is rejected by the cooling loop. Boiler quality feedwater can be supplied at a maximum rate of 25,000 lb/hr, at a pressure of 2250 psi, and at a maximum temperature of 400°F.

Steam from the receiver experiment returns down the tower in a high pressure steam line, passes through a pressure reducing valve, and into the deaerator/desuperheater vessel where it is condensed in the feedwater spray water loop. Part of the drain flow from the vessel is split and returned as condensate to the experiment, thus completing the experiment steam cycle. The remaining flow is directed to a heat exchanger where waste heat is rejected to a cooling tower system. The cooling tower loop uses a 33% ethylene glycol-water solution for coolant and passes the coolant through the cold side of the heat exchanger in the feedwater spray water loop.

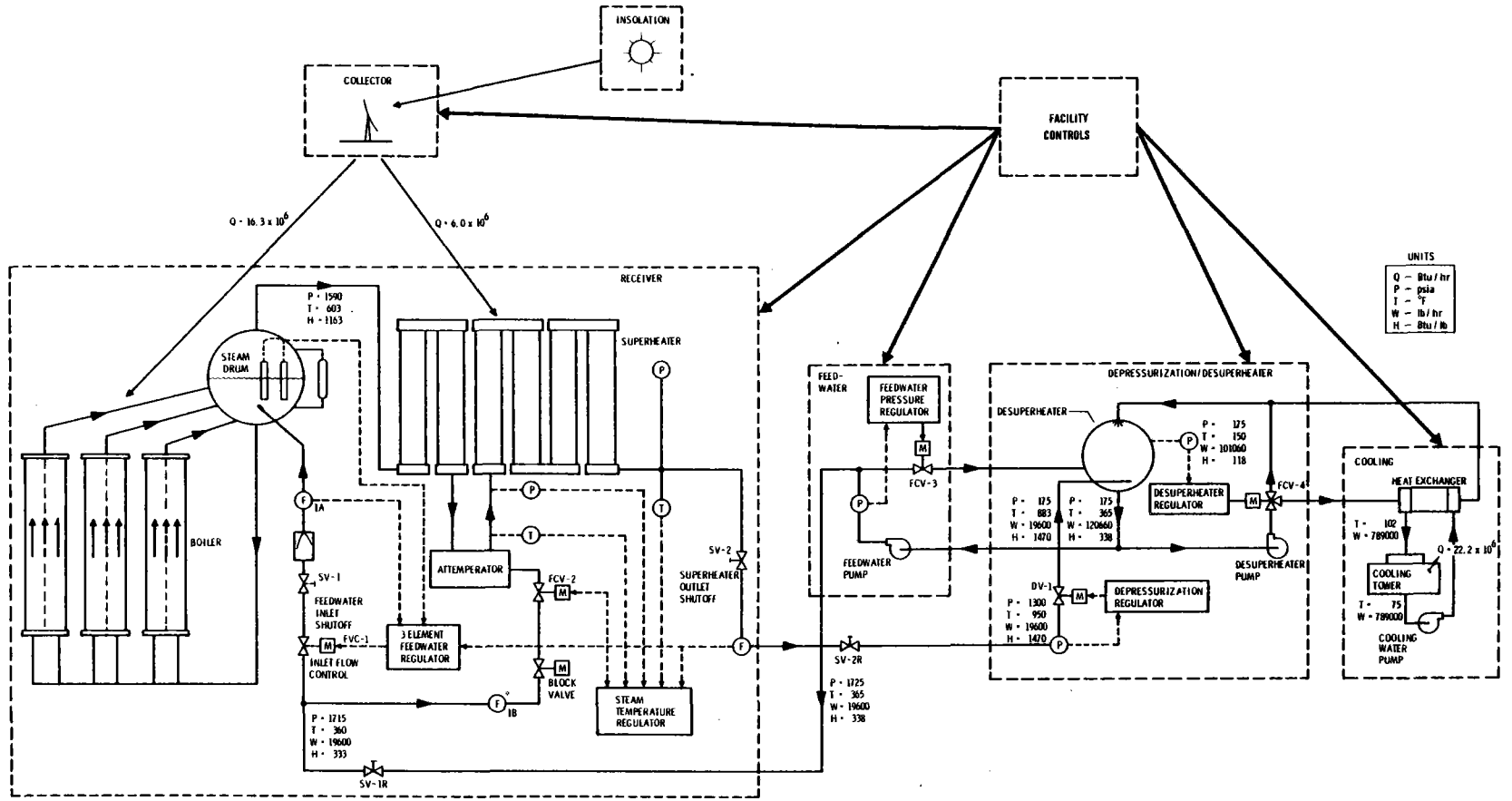

Figure 1. Schematic of Major Components/Subsystems of the STTF

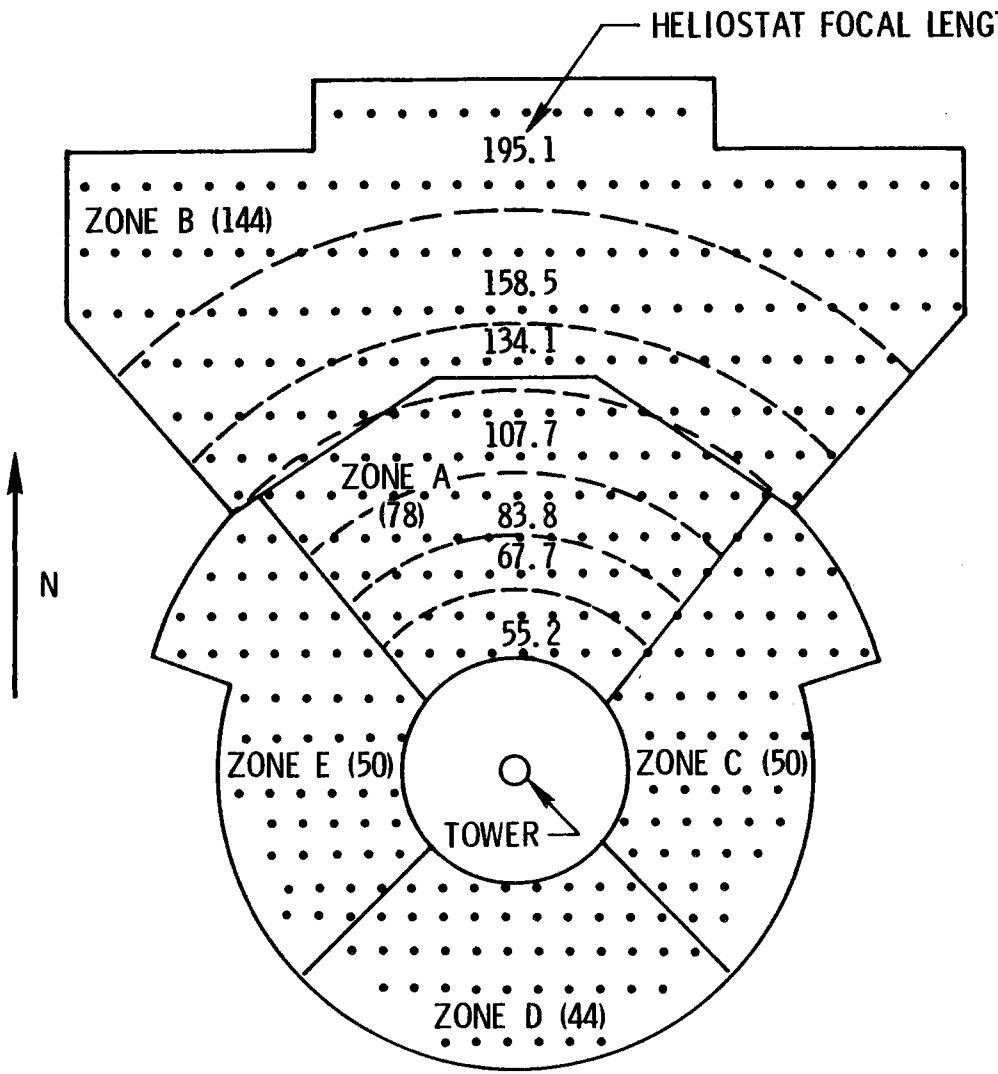

- NORTH FIELD
  ZONES A&B
  222 HELIOSTATS

- ANNULAR FIELD
  ZONES A, C, D, & E
  222 HELIOSTATS

Figure 2. STTF Collector Field Layout

Control System

The control system has three primary functions: mode control, subsystem interaction control, and subsystem control. The STTF uses a multiple-computer distributed control system to control the heliostats, heat rejection, subsystem, experiment, and supporting functions.

The basic operating mode is selected by the operator or by automatic features of the control system. After a mode is selected, the control system configures the plant to support that mode by operating valves and switching equipment on/off.

Subsystem interaction control adjusts the operation of each subsystem to maintain plant efficiency during normal operation and to prevent damage during emergency conditions. For example, loss of feedwater requires emergency defocus of the heliostats to prevent damage to the receiver. All of the numerous interactions between subsystems are handled by this function.

The collector, receiver, depressurization/desuperheat, and feedwater subsystems of Figure 1 have subsystem control loops. Table 2 lists the function, input, and output of each of the controllers. Each regulator is assumed to be of the form of proportional plus integral plus derivative feedback compensations.

Experiment

The Martin Marietta 5 MWt SRE receiver was used to illustrate program experiment application. The receiver is a natural circulation drum boiler which uses solar energy to convert the input feedwater to superheated steam (Reference 3). Design operation conditions for the receiver are shown in Figure 1.

COMPUTER PROGRAM DESCRIPTION

The simulation is implemented as a computer program designed with a highly modular structure as illustrated in Figure 3. The modules are grouped into four different categories: program executive, STTF subsystems, experiment, and general service subroutines. A one-to-one correspondence between program modules and physical subsystems is maintained to provide versatility and adaptability for the user. All communication among physical subsystem modules occurs through the COMMON block dictionary. It is structured to correspond to all input/output interfaces of each of the physical subsystems.

The program executive controls the overall operation of the simulation during analysis of a particular experiment. All variables are initialized in an initialization subroutine at the start of the run. Another subroutine reads in all required input. An output subroutine reads variable values from the COMMON block dictionary and produces plots or listings as desired. Integration of the differential equations and iterative solution of algebraic equations are controlled by the executive and control subroutine.

The computer simulation includes all of the modules required to totally describe the STTF system except the experiment. The modules implement analytical models

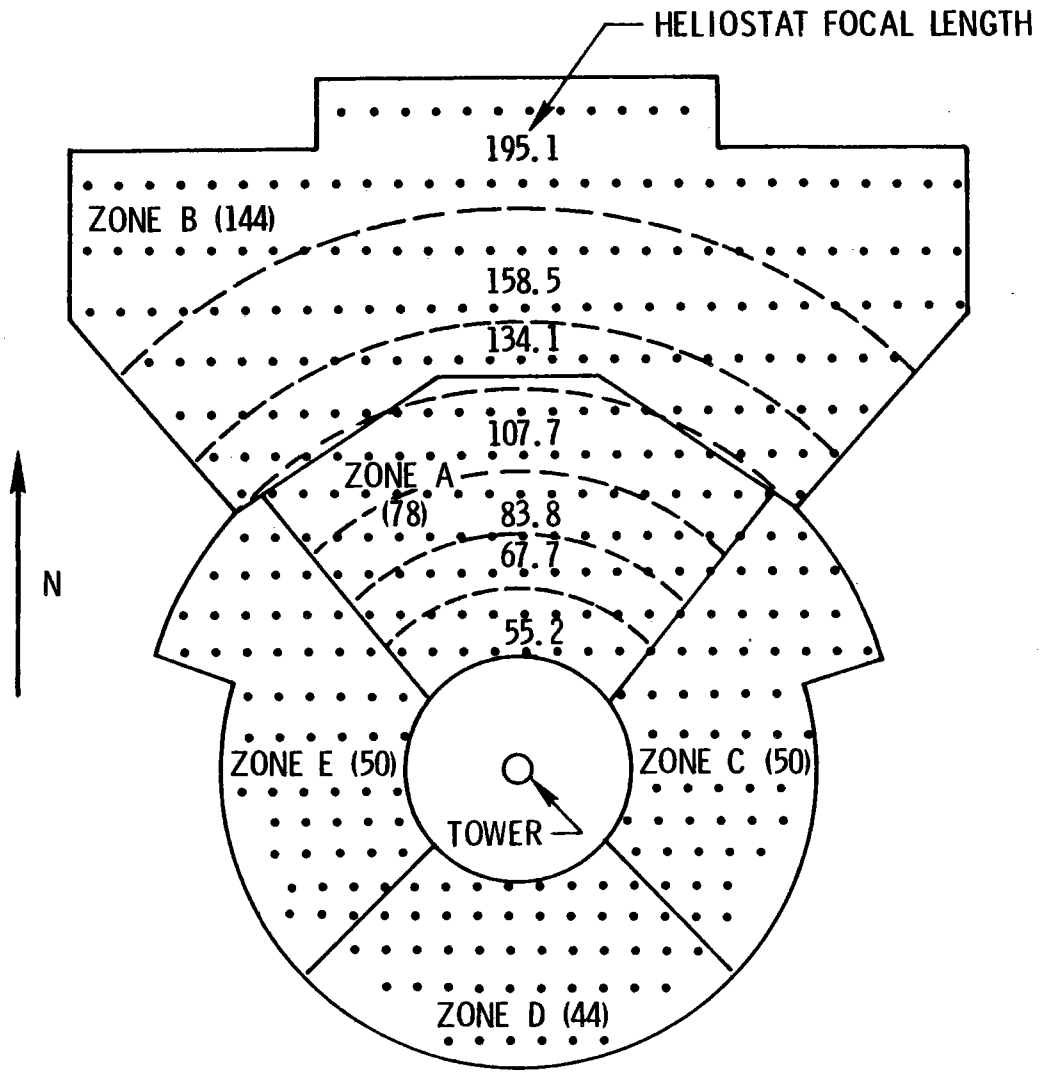

- NORTH FIELD
  ZONES A&B
  222 HELIOSTATS

- ANNULAR FIELD
  ZONES A, C, D, & E
  222 HELIOSTATS

Figure 2. STTF Collector Field Layout

Control System

The control system has three primary functions: mode control, subsystem interaction control, and subsystem control. The STTF uses a multiple-computer distributed control system to control the heliostats, heat rejection, subsystem, experiment, and supporting functions.

The basic operating mode is selected by the operator or by automatic features of the control system. After a mode is selected, the control system configures the plant to support that mode by operating valves and switching equipment on/off.

Subsystem interaction control adjusts the operation of each subsystem to maintain plant efficiency during normal operation and to prevent damage during emergency conditions. For example, loss of feedwater requires emergency defocus of the heliostats to prevent damage to the receiver. All of the numerous interactions between subsystems are handled by this function.

The collector, receiver, depressurization/desuperheat, and feedwater subsystems of Figure 1 have subsystem control loops. Table 2 lists the function, input, and output of each of the controllers. Each regulator is assumed to be of the form of proportional plus integral plus derivative feedback compensations.

Experiment

The Martin Marietta 5 MWt SRE receiver was used to illustrate program experiment application. The receiver is a natural circulation drum boiler which uses solar energy to convert the input feedwater to superheated steam (Reference 3). Design operation conditions for the receiver are shown in Figure 1.

COMPUTER PROGRAM DESCRIPTION

The simulation is implemented as a computer program designed with a highly modular structure as illustrated in Figure 3. The modules are grouped into four different categories: program executive, STTF subsystems, experiment, and general service subroutines. A one-to-one correspondence between program modules and physical subsystems is maintained to provide versatility and adaptability for the user. All communication among physical subsystem modules occurs through the COMMON block dictionary. It is structured to correspond to all input/output interfaces of each of the physical subsystems.

The program executive controls the overall operation of the simulation during analysis of a particular experiment. All variables are initialized in an initialization subroutine at the start of the run. Another subroutine reads in all required input. An output subroutine reads variable values from the COMMON block dictionary and produces plots or listings as desired. Integration of the differential equations and iterative solution of algebraic equations are controlled by the executive and control subroutine.

The computer simulation includes all of the modules required to totally describe the STTF system except the experiment. The modules implement analytical models

TABLE 2

SUBSYSTEM CONTROLLER CHARACTERISTICS

SUBSYSTEM	FUNCTION	INPUT	OUTPUT
Collector	Heliostat Tracking	Gimbal Angle	Gimbal Angle
Receiver	Feedwater Flow Regulator	Feedwater Flow	Feedwater Valve Position
		Steam Flow	
		Steam Drum Level	
	Steam Temperature Regulator	Attemperator Temperature	Attemperator Feedwater Valve
		Attemperator Pressure	
		Superheater Temperature	
		Steam Flow	
Depressurization/ Desuperheater	Depressurization Regulator	Receiver Pressure	Depressurization Valve Position
	Desuperheater Regulator	Desuperheater Pressure	Heater Exchanger By-Pass Valve Position
Feedwater	Feedwater Pressure Regulator	Feedwater Pressure	Feedwater By-Pass Valve Position

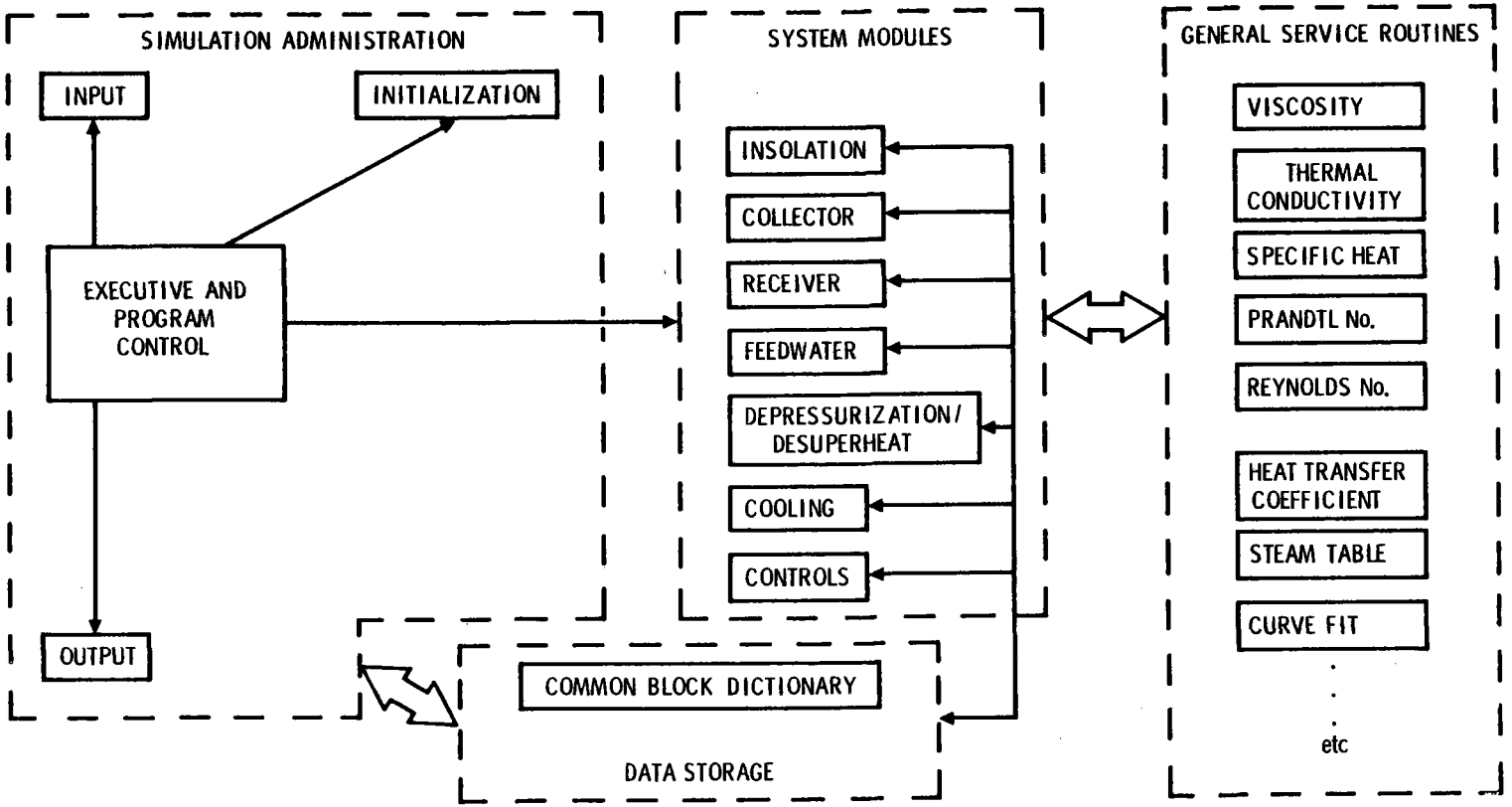

Figure 3. Simulation Program Structure

describing important characteristics of the subsystem. All modules are derived from first principals where possible or commonly accepted empirical formulations. Dynamic models in the form of linear and nonlinear differential equations model transient characteristics important to system operation. Details of the model for the collector field module are given in Appendix A. Model details of the thermal and control subsystems are given in Appendix B.

The experiment module, consisting of one or more subroutines is supplied by the user. Its interfaces must be compatible with the interfaces of facility subsystems to which it will be connected. For the work reported herein, the Martin-Marietta 5 MW SRE receiver is the experiment. Receiver model details are provided in Appendix C.

The general service subroutines consist of a set of subroutines that provide specific products required of a number of different subsystems. Many of them provide fluid heat transfer properties for specified conditions. All data transfers to and from them occur through argument lists rather than COMMON blocks. All of these are available to a user preparing an experiment module.

The highly modular approach to the simulation was selected to provide a wide range of users with a tool that is easily tailored to their particular requirements. By simply reconnecting interfaces between modules logically defined by facility subsystems, the simulation is easily converted to the actual facility configuration used. Various experiments operating under a wide range of conditions can be rapidly analyzed for their system level performance and facility interactions.

RESULTS WITH MARTIN MARIETTA 5 MW RECEIVER

To verify the SRE Receiver Simulation, as well as the basic modeling approach used for the other STTF Subsystems, the results of a computer simulation run were compared with actual test data on the Martin receiver obtained at the Sandia Laboratories - Albuquerque Radiant Heat Facility (Reference 3). The design nominal heat-flux profile of the IR system simulates the profile predicted for the pilot-plant receiver operating at 1400 hrs on the winter solstice under an insolation of 0.8 kW/m^2.

A cold-start test was selected for verification since it subjects the receiver to the greatest anticipated thermal-hydraulic extremes and, therefore, produces maximum transient response. A cold-start test brings the receiver to full power, pressure, and temperature conditions from an ambient start point in a prescribed amount of time. For the cold-start test selected, the design superheater outlet temperature of 789K (960°F) was reached in five hours, and the design outlet pressure of 9136K P_a (1325 psig) was achieved approximately 1.7 hours later. The maximum electrical power input was 4000 kW, resulting in a final steam flow of 3180 kg/hr (7000 lbm/hr). Figure 4 compares actual test data to the computer simulation results. For simulation purposes, the power input and outlet flow were controlled inputs, while steam drum pressure, superheater outlet temperature, and superheater tube temperature were system responses.

During the actual test, the boiler drum pressure and steam flow were controlled by manual operation of an outlet pressure control valve until the drum pressure reached

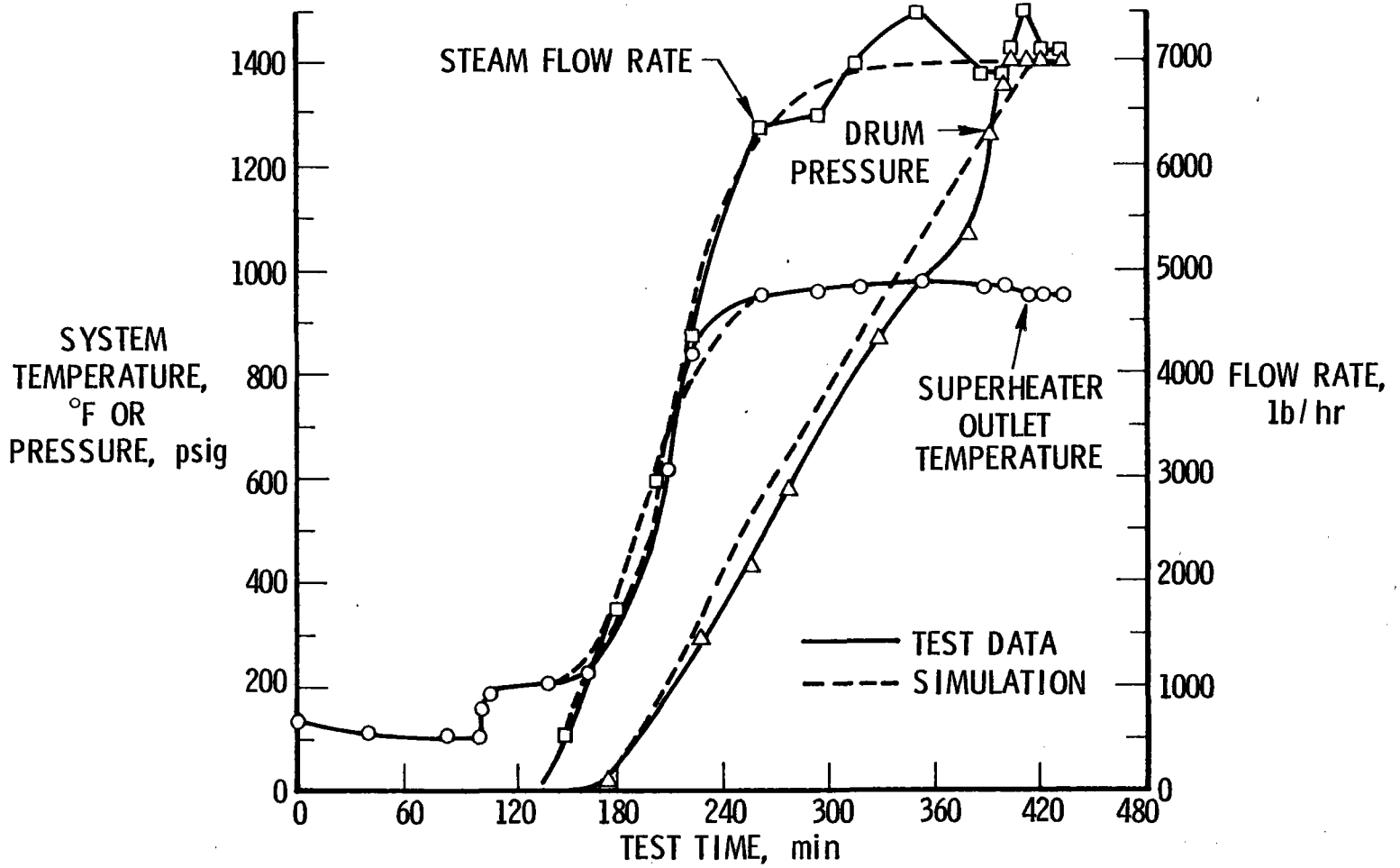

Figure 4. Comparison of Analytical Results with Cold Start Test #2

its design valve of 9136K P_a (1325 psig). Subsequently, automatic control of the valve maintained the boiler drum pressure at the set point. Because superheater outlet pressure data was not available for the cold-start test, the simulation was run with the outlet conditions controlled via the steam flow rate, i.e., the outlet control valve was modeled as a flow control valve rather than a pressure control valve.

The superheater outlet temperature was automatically maintained at its design value of 789K (960°F) by the attemperator flow control valve during the actual test and also during the simulation. The steam drum inlet flow control valve was also modeled for the simulation and maintained the drum water level at its normal operating point.

As seen in Figure 4, predicted temperature and pressure profiles closely match actual measured values. The modeling used in the various subsystems adequately represents transient and equilibrium characteristics of the system and experiment. The simulation appears suitable for its primary use of estimating the transient response of principal performance parameters.

CONCLUSIONS

A computer program has been developed which simulates the key subsystems of the STTF facility. Analytical results from the program are in close agreement with available test data. Copies of the program are available to STTF users through the Department of Energy.

APPENDIX A

COLLECTOR MODELING

The three-step process illustrated in Figure A.1 implements the collector field modeling. This particular approach was selected to provide maximum flexibility and versatility to the simulation while minimizing computing cost by moving expensive and repetitive calculations off-line. The field analysis step generates a set of flux maps (distributions) that completely characterize the field in a single-pass off-line calculation. The projector step, also off-line, projects the flux maps onto the receiver of particular geometry to give input power profiles for the receiver. The simulation step, implemented on-line, uses the power profiles generated by the projector step to calculate receiver power as required in the simulation. Details of each of these steps is given in subsequent paragraphs.

Field Analysis

To minimize total computational effort and resulting data the field is divided into regions or cells, $\pm 5^{o}$ to $\pm 10^{o}$ in azimuth and elevation. The tighter limits apply to distant cells and the looser limits to near cells relative to the tower. Figure A.2 illustrates the resulting 28 cells for the north field. All the heliostats in a cell are characterized by a single heliostat, located at the centroid of the actual heliostats in the cell. Flux distributions are calculated using the methods of McFee (Reference 4). The uniform solar disc illumination of McFee is replaced with a limb darkening model given by

$$I(r) = \frac{1.23 A I_D}{\pi R^2}\left[.44 + .56\sqrt{1 - \left(\frac{r}{R}\right)^2}\right], \quad r \leq R \qquad (1)$$

$$I(r) = 0, \quad r > R$$

where I_D is the average direct insolation, r is the distance from the center of the distribution, A is the area of the refector, and R is the solar disc radius given by

$$R = 4.65 * 10^{-3} S \qquad (2)$$

and S is the slant range from the receiver.

The heliostat is divided into 450 segments each of which reflects a solar image given by equations (1) and (2) onto a screen normal to the reflected beam. Each image is displaced from its nominal position by focusing, segment canting, random waviness errors, and random tracking errors. The composite beam from the 450 images makes up the total flux map given as flux at each of 441 screen grid points.

Compression, smoothing, and interpolation of the tabular data is accomplished by least squares fitting of polynominals to the tabular data. Examination of a number

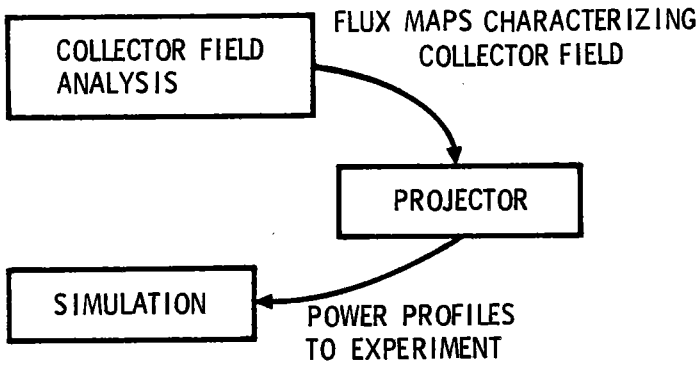

Figure A1. Three Step Process of Analyzing Collector Field for Simulation Use

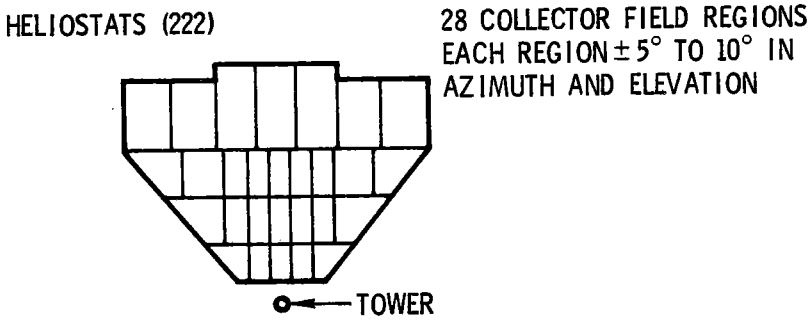

Figure A2. Definition of Field Cells Used in Collector Field Analysis

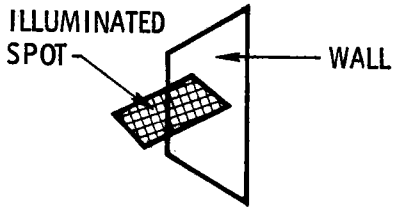

Figure A3. Typical Situation for Projection of Heliostat Illumination Through Rectangular Aperture onto Finite Wall

of flux maps revealed that most of them are nearly axi-symmetric. A fifth degree polynominal of the radial distance from the center of the distribution adequately approximate these maps. During early morning and late afternoon the reflected flux distribution exhibited distinct two-axis characteristics, particularly when incidence angles are large. For these cases, a two-dimensional, fifth-degree curve fit is required for adequate approximation.

All of these flux maps are normalized to the case of 100% reflectivity, no atmospheric attenuation, area of one heliostat, and insolation of one watt/square meter.

Projector

In the simulation the receiver is divided into several thermal nodes. The projector program projects the flux from each cell onto the receiver and integrates it over each of the thermal nodes. Cavity type receivers with a rectangular aperature and one to three flat, four-corner walls can be analyzed. Each wall may have as many as 10 nodes. The Martin-Marietta receiver is of this type.

Three sets of coordinate systems are used. Each wall has a "wall" coordinate system with X and Y axes in plane and Z axis out of plane. Fluxes are integrated in wall coordinates to get power into the receiver nodes. An "aperture" coordinate system is centered in the aperture plane with X axis horizontal and in plane, Y axis in plane, and the Z axis out of plane. The aperture is assumed to be north facing but may be tilted. Wall geometry is given in aperature coordinates by specifying the (X, Y, Z) coordinates of each of the four corners. Flux maps are given in "heliostat" coordinates for each cell with X axis horizontal, Z axis along the beam direction, and Y axis forming right-hand set.

For each cell and each wall the illuminated region is found by projecting the aperature corners (and hence sides) into the plane of the wall. Corners are projected by

$$\underline{X}_P^W = C_A^W \left(\underline{X}_C^A - \underline{X}_i^A \right) + q C_A^W \, \underline{i}_H^A \tag{3}$$

where $\underline{X}_P^W$ is the location of the projected point in wall coordinates, C_A^W is the aperature to wall rotation matrix, $\underline{X}_C^A$ is the corner location in aperature coordinates, $\underline{X}_i^A$ is the offset vector between the i'th wall and the aperture in aperature coordinates, q is the scalar distance from the corner, and $\underline{i}_H^A$ is a unit vector along the beam direction in aperature coordinates. The projection direction in aperature coordinates is

$$\underline{i}_H^A = \begin{bmatrix} -\sin\alpha\cos\epsilon \\ -\sin\epsilon\cos\beta - \cos\alpha\cos\epsilon\sin\beta \\ \sin\epsilon\sin\beta - \cos\alpha\cos\epsilon\cos\beta \end{bmatrix} \tag{4}$$

where α is the azimuth of the heliostat from the tower measured from south, ϵ is the elevation of the receiver, and β is the tilt of the aperture from vertical. The intercept with the wall plane is found by setting the Z component of $\underline{X}_p^W$ to zero, solving the q, substituting back into equation (3), and solving for the (X, Y) coordinates on the wall. Figure A.3 illustrates a typical situation. The various sides and intercepts are searched to find the actual boundaries of the illuminated region on the wall.

The aim point is projected onto the wall with equations (3) and (4) to locate the center of the flux distribution, $\underline{X}_C^W$ in wall coordinates. The coordinates of a point on the wall are converted into heliostat coordinates by

$$\underline{X}_p^H = C_W^H \left(\underline{X}_p^W - \underline{X}_C^W \right) \tag{5}$$

Flux at the point is calculated from the flux map for the field cell scaled by the number of heliostats in the cell and cosine of the incidence angle.

The projector program steps through each cell and wall integrating flux into each receiver node at each time for a given day. Multiple aim point strategies are analyzed by specifying the number of heliostats in each cell associated with each aim point. Total power to each node is found by summing over all of the aim points. The resulting power profiles are written out as FORTRAN data statements directly usable in the on-line collector module.

Simulation Implementation

The on-line collector module used in the simulation is a simple table lookup and interpolation procedure using the data from the projector program. Flux at the correct time is estimated by fitting a quadratic curve to three adjacent table values for each of three days. Flux on the correct day is estimated by fitting a quadratic curve to these values and interpolating for the correct day.

APPENDIX B

MODELING OF HEAT REJECTION/FEEDWATER SYSTEM

Assumptions

The fundamental assumption used in the development of the thermal hydraulic system models was that a distributed parameter process could be represented by a lumped parameter model using the concept of control volumes. Additional modeling assumptions applicable to the entire Heat Rejection/Feedwater (HR/F) System were the following:

(a) Uniform fluid properties at any cross section

(b) Insignificant temporal acceleration and momentum transport contributions

(c) Insignificant kinetic energy contributions

(d) Insignificant energy losses to the environment

(e) Insignificant heat transfer by conduction and radiation

(f) Uniform metal properties

(g) Uniform heat flux over any surface

(h) Uniform flow distributions in multitube devices

(i) Fully-developed, turbulent, single-phase fluid flow

Development of Model Equations

The hardware composing the HR/F system falls essentially into the following four categories:

(a) Heat exchangers

(b) Drums or tanks

(c) Piping, with and without control valves

(d) Pumps

Model equations were developed by (1) sectioning each of these system elements into control volumes; (2) applying to each control volume the laws of heat transfer and of conservation of mass, energy, and momentum as expressed in the General Equations section below; (3) simplifying the result by making additional assumptions about the processes occurring in each control volume.

General Equations

As a result of the nine assumptions presented above, the most general expressions of the four laws are the following:

(a) The rate of heat transfer by convection between a surface and a fluid is expressed by

$$Q_c = U_c S (T_m - T_f) \tag{1}$$

(b) The conservation of mass within a control volume is expressed by

$$\frac{d}{dt} v_{cv} = -\left(\frac{v^2}{V}\right)_{cv} \left(\sum w_i - \sum W_e\right)^* \tag{2}$$

(c) The conservation of energy within a control volume is expressed by

$$\frac{d}{dt} \int \left(\frac{u}{v}\right) dV = Q_{cv} + \sum [w(h + gZ)]_i - \sum [w(h + gZ)]_e + W_{cv}^* \tag{3a}$$

For a closed system such as a tube wall, the statement of conservation of energy is expressed by

$$\left(mC \frac{d}{dt} T\right)_{cv} = Q_{cv} \tag{3b}$$

(d) The conservation of momentum in one dimension within a control volume is expressed by

$$\left(P + \frac{gZ}{v}\right)_i = \left(P + \frac{gZ}{v}\right)_e + \left(Fvw^2\right)_{cv}^* \tag{4}$$

Equations (1) and (4) contain parameters that are calculated from either empirical equations or definitions. These parameters are U_c, the convective heat transfer coefficient, and F, the flow coefficient. The convective heat transfer coefficient was calculated from applicable empirical equations (Reference 5). These equations were slightly modified forms of the Dittus Boelter correlation, depending on whether fluid was flowing inside or over a bank of tubes. The flow coefficient was assumed to be a constant and calculated from its definition evaluated at the steady-state rated conditions of the HR/F system.

---

* The summation signs are included to account for the possibility of several inlet and outlet flow streams.

** In the strict sense, this equation is a definition of F rather than a statement of the momentum conservation law.

All fluid properties not obtained from the solution of the physical laws were evaluated from either the thermodynamic state equations in the form of table lookup procedures or from spatial averaging and extrapolation techniques.

Application of the basis equations to specific HRS components is illustrated in Figure B-1.

HEAT EXCHANGERS

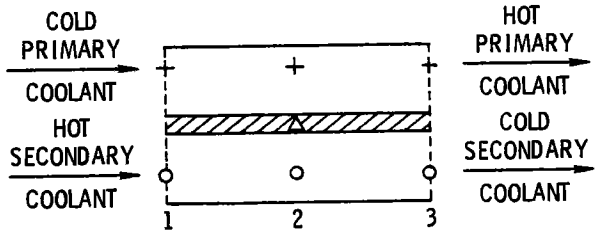

$$Q_2 = U_c S (T_{m2} - T_{f2})$$

$$w_{f3} = w_{f2} = w_{f1}$$

$$\frac{d}{dt} u_{f2} = \frac{v_{f2}}{V}\left[Q_2 + w_{f2}(h_{f1} - h_{f3})\right]$$

$$\frac{d}{dt} T_{m2} = \frac{Q_2}{(mC)_{m2}}$$

$$P_{f3} = P_{f1} - Fv_{f2} w^2_{f2}$$

DRUMS OR TANKS

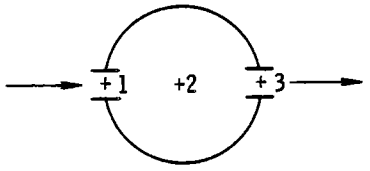

$$\frac{d}{dt} v_{f2} = -\frac{v^2_{f2}}{V}(w_{f1} - w_{f3})$$

$$\frac{d}{dt} u_{f2} = \frac{v_{f2}}{V}\left[w_{f1}(h_{f1} - u_{f2}) - w_{f3}(h_{f3} - u_{f2})\right]$$

PIPING

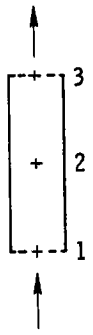

$$w_{f3} = w_{f2} = w_{f1}$$

$$\frac{d}{dt} u_{f3} = 2\frac{v_{f2}}{V} w_{fw}\left[h_{f1} - h_{f3} + g(Z_1 - Z_3)\right]$$

$$P_{f3} = P_{f1} - \frac{g}{v_{f2}}(Z_3 - Z_1) - Fv_{f2} w^2_{f2}$$

PUMPS

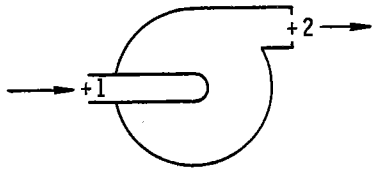

$$w_{f2} = w_{f1}$$

$$h_{f2} = h_{f1} + v_{f1}(P_{f2} - P_{f1})$$

FOR CENTRIFUGAL PUMPS:

$$P_{f2} = P_{f1} + H - Fv_{f1} w^2_{f1}$$

LEGEND

+, 0 - DENOTES FLUID NODES

Δ - DENOTES METAL NODES

f - DENOTES FLUID PROPERTIES

m - DENOTES METAL PROPERTIES

Figure B1. Control Volumes and Modeling Equations for Hardware Components

APPENDIX C

MODELING OF MARTIN MARIETTA RECEIVER

The Receiver (see Figure 1) is in essence a heat exchanger. Consequently, all of the assumptions and equations applicable to the heat exchanger model presented in Appendix B are applicable to the receiver model with the following exceptions:

(a) Energy losses to the environment are significant

(b) Heat transfer by radiation is significant

(c) Mass storage effects are significant

These exceptions produced the following set of general modeling equations for the Martin Marietta Receiver:

Heat Transfer:

$$Q_c = U_c S (T_m - T_f) \tag{1}$$

$$Q_r = \sigma \epsilon S (T_m^4 - T_f^4) \tag{2}$$

Mass Conservation:

$$\frac{d}{dt} v_{cv} = - \left(\frac{v^2}{V}\right)_{cv} (w_i - w_e) \tag{3}$$

Energy Conservation:

$$\frac{d}{dt} u_{cv} = \left(\frac{v}{V}\right)_{cv} \left[Q_{cv} + w_i (h_i - u_{cv}) - w_e (h_e - u_{cv})\right] \tag{4a}$$

$$\left(mC\frac{d}{dt}T\right)_{cv} = Q_{cv} \tag{4b}$$

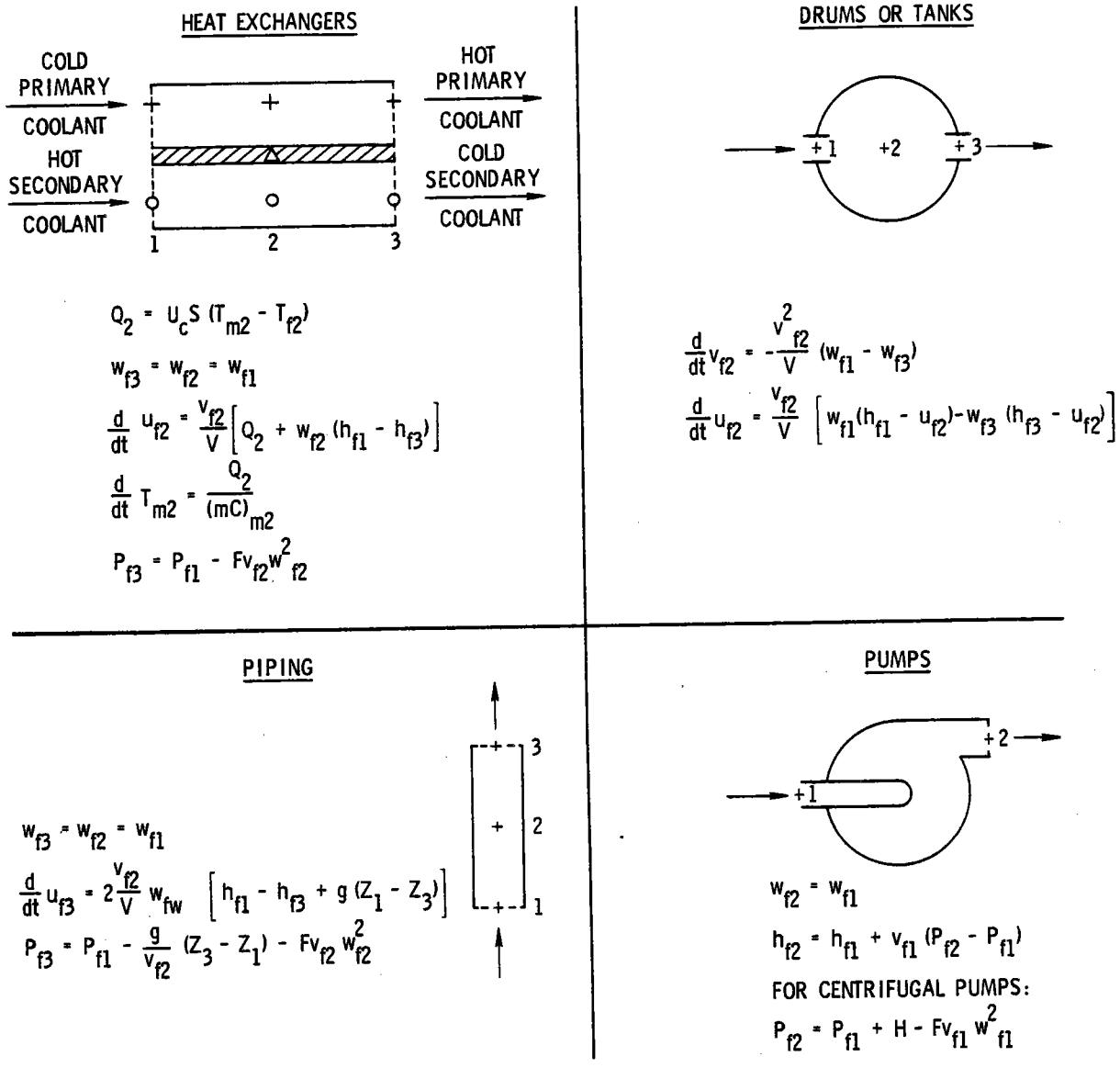

Figure B1. Control Volumes and Modeling Equations for Hardware Components

APPENDIX C

MODELING OF MARTIN MARIETTA RECEIVER

The Receiver (see Figure 1) is in essence a heat exchanger. Consequently, all of the assumptions and equations applicable to the heat exchanger model presented in Appendix B are applicable to the receiver model with the following exceptions:

(a) Energy losses to the environment are significant

(b) Heat transfer by radiation is significant

(c) Mass storage effects are significant

These exceptions produced the following set of general modeling equations for the Martin Marietta Receiver:

Heat Transfer:

$$Q_c = U_c S \, (T_m - T_f) \tag{1}$$

$$Q_r = \acute{\sigma} \epsilon S \, (T_m^{\,4} - T_f^{\,4}) \tag{2}$$

Mass Conservation:

$$\frac{d}{dt} v_{cv} = - \left(\frac{v^2}{V} \right)_{cv} (w_i - w_e) \tag{3}$$

Energy Conservation:

$$\frac{d}{dt} u_{cv} = \left(\frac{v}{V} \right)_{cv} \left[Q_{cv} + w_i \, (h_i - u_{cv}) - w_e \, (h_e - u_{cv}) \right] \tag{4a}$$

$$\left(mC \frac{d}{dt} T \right)_{cv} = Q_{cv} \tag{4b}$$

Momentum Conservation:

$$P_i = P_e + (Fvw^2)_{cv} \quad (5a)$$

$$P_i = P_e + (F_m vw^2)_{cv} \quad (5b)$$

(control volumes with valves only)

The calculation of U_c and F, the use of thermodynamic equations of state, and the averaging and extrapolation of fluid properties supplemented the modeling equations for the Martin Marietta Receiver as was explained in Appendix B for the HR/F system.

The heat transfer in the boiler tubes is primarily due to nucleate boiling of a fluid undergoing natural circulation. A correlation proposed by Thom et al (Reference 6) was considered adequate for this phenomenon and did not require any knowledge of the flow rate through the tubes. Consequently, two-phase flow computations were not required.

Nomenclature

- Parameters

A = cross-sectional area

C = heat capacity

C_A^B = rotation matrix from coordinate system A to coordinate system B

F = steady-state flow coefficient

F_m = modified steady-state flow coefficient

g = local acceleration due to gravity

h = specific enthalpy

H = pump total pressure constant

$\underline{i}_A^B$ = unit vector along A direction in B coordinates

I_D = average direct insolation

$I(r)$ = solar flux at a distance r from center of distribution

m = mass

P = pressure

q = scalar distance

Q = rate of heat transfer

r, R = radius

S = surface area

T = temperature

u = specific internal energy

U = heat transfer coefficient

v = specific volume

w = mass flow rate

W = rate of work

$\underline{X}_A^B$ = position vector of point a in coordinate system B

α = azimuth

β = tilt

σ = Stefan-Boltzman constant

ϵ = emittance

γ = elevation

- Subscripts

c = convective

cv = control volume

f = fluid

m = metal

i = inlet

e = exit

r = radiative

REFERENCES

1. Best, E.N., J.V. Coggi, R.A. Jamieson, K.L. Zondervan, Dynamic Simulation Model of the Solar Thermal Test Facility (STTF), Aerospace Report No. ATR-78(7695-02)-1, March 1978.

2. Insolation Data Base Available from The Aerospace Corporation, Report No. ATR-76(7523-11)-9, The Aerospace Corporation, December 1976.

3. Central Receiver Solar Thermal Power System, Phase 1, Volume IV, Receiver Subsystem, Preliminary Design Report (Draft), Section V, SAN-1110-77-2, Martin-Marietta, April 1977.

4. McFee, R.H., "Power Collection Reduction by Minor Surface Nonflatness and Tracking Error for a Central Receiver Solar Power System," Applied Optics, Vol. 14, pg. 1493, July 1975.

5. Steam, Its Generation and Use, 38th ed., The Babcock and Wilcox Company, 1972.

6. Thom, J.R.S., W.M. Walker, T.A. Fallon, and G.F.S. Reising, "Boiling in Subcooled Water During Flow Up Heated Tubes or Annuli," Proc. Institution of Mechanical Engineers, 3C180, (1965-66).

Agenda

ANNUAL USERS ASSOCIATION MEETING
Golden, Colorado
April 11 & 12, 1978

Monday, April 10

7:00- 9:00 Preregistration, Holiday Inn--West, Lobby

Tuesday, April 11

SESSION I - OPENING REMARKS

Chairman - Dr. A. F. Hildebrandt, University of Houston

8:30- 8:45 Welcome - Dr. A. F. Hildebrandt

8:45- 9:10 Users Association Plans and Activities - F. B. Smith

9:10- 9:35 Proposal Evaluation and Funding Procedures - Dr. G. P. Mulholland, New Mexico State University

9:35-10:15 Major Solar Power Projects - G. W. Braun, DOE

10:15-10:30 Coffee Break

SESSION II-A - SOLAR FACILITIES
Chairman - Dr. John L. Margrave, Rice University

10:30-11:15 CNRS 1000-kW_t Solar Furnace, Odeillo, France - Claude Royere

11:15-12:00 Sandia 5-MW_t STTF, Albuquerque, NM - John T. Holmes

12:00- 1:15 Lunch, Holiday Inn--West
Speaker: Dr. Michel Rodot, CNRS, France, Initial Applications of Highly Concentrated Solar Energy: Another Look at This Topic

1:15- 1:30 SERI Update - Paul Rappaport, SERI

SESSION II-B - SOLAR FACILITIES
Chairman - Dr. John L. Margrave, Rice University

1:30- 2:15 White Sands 30-kW_t Solar Furnace, White Sands, NM - Richard Hays

2:15- 3:00 Georgia Tech 400-kW_t STTF, Atlanta, GA - Dr. C. Thomas Brown

SESSION III - OPTICS AND SYSTEMS
Chairman - Dr. Terry Cole, Ford Motor Company

3:00- 3:20 A Single Heliostat Flux Reconcentrator for Materials Sample Testing, Dr. Marjorie Meinel, The University of Arizona

3:20- 3:35 Coffee Break

3:35- 3:55 Secondary Reconcentrator Design for the Sandia STTF, Dr. G. P. Mulholland, NMSU, and L. K. Matthews, Sandia Labs

3:55- 4:15 White Sands 4-kW Solar Furnace, W. C. Hull, NMSU

Tuesday, April 11

SESSION III - OPTICS AND SYSTEMS (Continued)

4:15- 4:35 Tracking Concentrators, Omnium-G Company

4:35- 5:00 Discussion

5:30- 6:30 Happy Hour, Holiday Inn--West

6:30- 8:00 Dinner, Holiday Inn--West
Speaker: H. H. Marvin, Director, Division of Solar Technology, DOE

EVENING SESSION IV - MATERIALS
Chairman - Dr. Tom H. Springer, Atomics International

8:00- 8:20 Maximal Operating Temperature for Metallic Films Subject to Deterioration by Agglomeration: A First Principles Calculation, Dr. Richard Zito, The University of Arizona

8:20- 8:40 Selective Coatings for High-Temperature Solar Receivers, Dr. Pat Call, SERI

8:40- 9:00 High Temperature/High Heat Flux Material Testing for Large Solar Flux Applications, L. K. Matthews, Sandia Labs, and Dr. G. P. Mulholland, NMSU

9:00- 9:15 Degradation of Concrete Caused by Concentrated Solar Radiation, Dr. G. P. Mulholland, NMSU

9:15- 9:30 Use of STTFs in the Development of Stable High-Temperature Solar Absorbing Coatings, Dr. J. M. Schreyer, Union Carbide

9:30-10:00 Discussion

Wednesday, April 12

There will be concurrent sessions from 9:00 to 12:00 a.m. on Energy Conversion and Industrial Chemical Processes

SESSION V - ENERGY CONVERSION AND STORAGE
Chairman - Dr. R. L. San Martin, New Mexico State University

9:00- 9:20 Engineering Design Study of Conversion of Solar Energy to Chemical Energy through Ammonia Dissociation, Dr. G. G. Lenz, Colorado State University

9:20- 9:40 Experimental Findings on Testing of Honeywell Receiver, W. Oberjohn, Babcock & Wilcox Company

9:40-10:00 Night Storage and Backup Generation with Electrochemical Engines, Dr. G. R. B. Elliott, Los Alamos Scientific Lab

10:00-10:15 Break

10:15-10:35 Sodium Heat Engine, Dr. Terry Cole, Ford Motor Company

Wednesday, April 12

SESSION V - ENERGY CONVERSION AND STORAGE (Continued)

10:35-10:55 Thermionic Energy Conversion in Solar Applications, Dr. G. O. Fitzpatrick, Rasor Associates

10:55-11:15 Thermionic Topping of a Solar Power Plant Using Converters Containing LaB_6 Electrodes, Dr. E. K. Storms, Los Alamos Scientific Lab

11:15-11:45 Discussion

SESSION VI - INDUSTRIAL CHEMICAL PROCESSES
Chairman - Dr. John L. Russell, General Atomic Company

9:00- 9:20 Chemical Processes Applicable to a Solar Thermal Test Facility, Dr. John L. Margrave, Rice University

9:20- 9:40 Treatment of Molybdenite Ore Using 2-kW Solar Furnace, Dr. S. R. Skaggs, Los Alamos Scientific Lab

9:40-10:00 Solar-Thermochemical Production of Hydrogen from Water, Dr. K. E. Cox, Los Alamos Scientific Lab

10:00-10:15 Break

10:15-10:35 Results of Recent Research on the Use of Pyrolysis/Gasification Reactions of Biomass to Consume Solar Heat and Produce a Usable Gaseous Fuel, Dr. M. J. Antal, Princeton University

10:35-10:55 Proposed Experiment to Utilize a Solar Facility to Provide Process Heat for the Reaction $C + CO_2 \rightarrow 2CO$, Dr. D. C. Cubicciotti, SRI International

10:55-11:15 Solar Furnace Measurements of High-Temperature Thermodynamic Properties of Oxygen Alloys of Electropositive Metals, Dr. Robert I. Sheldon, University of Kansas

11:15-11:45 Discussion

11:45- 1:15 Lunch, Holiday Inn--West
Speaker: Prof. Tetsuo Noguchi, Government Industrial Research Institute, Japan, Solar Energy in Japan

SESSION VII - TESTING AND SIMULATION
Chairman - Dr. Fred Manasse, University of New Hampshire

1:15- 1:45 Thermal Radiation Testing from a Users Viewpoint, Dr. T. M. Knasel, Science Applications, Inc.

1:45- 2:15 A Systems Computer Simulation Model of the Solar Thermal Test Facility, J. F. Coggi, The Aerospace Company

Chairman - Dr. A. F. Hildebrandt

2:30- 4:30 Association Business Meeting

4:30 Adjourn

Attendees

SOLAR THERMAL TEST FACILITIES USERS ASSOCIATION

ANNUAL MEETING

Golden, Colorado

April 11-12, 1978

Marylee Adams
STTF Users Association
Suite 1507
First National Bank Bldg. East
Albuquerque, NM 87108
(505) 268-3994

Lee Alhorn
BDM Corporation
2600 Yale, SE
Albuquerque, NM 87105
(505) 843-7870

Michael Antal
D-215 Engineering Quadrangle
Princeton University
Princeton, NJ 08540
(609) 452-5136

D. H. Avery
Division of Engineering
Brown University
Providence, RI 02912
(401) 863-2677

Renato G. Bautista
Dept. of Chemical Engineering
Iowa State University
Ames, IA 50011
(515) 294-1982 or 6763
FTS: 865-1982 or 6763

Charles J. Bishop
SERI
1536 Cole Blvd.
Golden, CO 80401
(303) 234-7121
FTS: 327-7121

Steve Bomar
Engineering Experiment Station
Hinman Research Bldg.
Georgia Institute of Technology
Atlanta, GA 30332
(404) 894-3656

Melvin G. Bowman
Mail Stop 756
Los Alamos Scientific Laboratory
Los Alamos, NM 87545
(505) 667-6014
FTS: 843-6014

Glen E. Brandvold
Solar Energy Projects Department
Sandia Laboratories
Albuquerque, NM 87185
(505) 264-6866
FTS: 475-6866

G. W. Braun
DOE/Division of Solar Technology
600 E Street, NW
Washington, DC 20545
(202) 376-1934

Edward J. Britt
Rasor Associates, Inc.
253 Humboldt Court
Sunnyvale, CA 94086
(408) 734-1622

C. T. Brown
Engineering Experiment Station
Georgia Institute of Technology
Atlanta, GA 30332
(404) 894-3654

Herbert Budd
CNRS New York Office
972 Fifth Avenue
New York, NY 10021
(212) 737-9725

Aaron Burke
Monsanto Research Corporation
Mound Laboratories
Miamisburg, OH 45342
(513) 866-7444

Talbot A. Chubb
Code 7120
Naval Research Laboratory
Washington, DC 20375
(202) 767-3580

John Coggi
Aerospace Corporation
PO Box 92957
El Segundo, CA 90009
(213) 648-5333

Terry Cole
Mail Stop S-2015
Research & Engineering Staff
Ford Motor Company
PO Box 2053
Dearborn, MI 48121
(313) 323-2968

Robert J. Copeland
SERI
1536 Cole Blvd.
Golden, CO 80401
(303) 234-7120
FTS: 327-7120

Kenneth E. Cox
Mail Stop 348
Los Alamos Scientific Laboratory
Los Alamos, NM 87545
(505) 667-7059 or 6074
FTS: 843-7059 or 6074

D. Cubicciotti
SRI International
333 Ravenswood Avenue
Menlo Park, CA 94025
(415) 326-6200, Ext. 3940

John Cummings
EPRI
10412 Hillview Avenue
Palo Alto, CA 95070
(415) 855-2166

Darian N. Diachok
SERI
1536 Cole Blvd.
Golden, CO 80401
(303) 234-7234
FTS: 327-7234

Robert V. Dumke
Engelhard Industries
70 Wood Avenue South
Metro Park Plaza
Iselin, NJ 08830
(201) 321-5988

Guy R. B. Elliott
G-7, Mail Stop 738
Los Alamos Scientific Laboratory
Los Alamos, NM 87545
(505) 667-6651
FTS: 843-6651

E. R. Elzinga
Exxon Research & Engineering Company
PO Box 45
Linden, NJ 07036
(201) 474-2802

Joseph Farber
Solar Research Systems
3001 Redhill Avenue, I-105
Costa Mesa, CA 92626
(714) 545-4941

Gary O. Fitzpatrick
Rasor Associates, Inc.
253 Humboldt Court
Sunnyvale, CA 94086
(408) 734-1622

M. W. Frank
Entropy, Ltd.
5735 Arapahoe Avenue
Boulder, CO 80303
(303) 443-5103

Richard Grau
Air Force Weapons Laboratory
Kirtland Air Force Base
Albuquerque, NM 87115

Charles Grosskreutz
SERI
1536 Cole Blvd.
Golden, CO 80401
(303) 234-7314
FTS: 327-7314

Martin Gutstein
DOE/Division of Solar Technology
600 E Street, NW
Washington, DC 20545
(201) 376-1937

Richard A. Hays
White Sands Solar Facility
STEWS-TE-AN
White Sands, NM 88002
(915) 678-1161
FTS: 898-1161

A. Hertzberg
Director, Aerospace & Energetics
120 Aero. & Engr. Bldg., FL-10
University of Washington
Seattle, WA 98195
(206) 543-6321

A. F. Hildebrandt
Solar Energy Lab
University of Houston
Houston, TX 77004
(713) 749-3184

John T. Holmes
Division 5713
Sandia Laboratories
Albuquerque, NM 87185
(505) 264-6871
FTS: 475-6871

Wendell C. Hull
New Mexico State University
Box 3450
Las Cruces, NM 88001
(505) 646-3501

Robert Jamieson
Aerospace Corporation
2350 E. El Segundo Blvd.
El Segundo, CA 90245
(213) 684-6317

Philip Jarvinen
MIT, Lincoln Laboratory
Box 73, I-215
Lexington, MA 02173
(617) 862-5500, Ext. 7591

Stan Jaskolski
Marquette University
1515 West Wisconsin Avenue
Milwaukee, WI 53233
(414) 224-6820

T. S. Jayadev
SERI
1536 Cole Blvd.
Golden, CO 80401
(303) 234-7210
FTS: 327-7210

Thomas M. Knasel
Science Applications, Inc.
8400 Westpark Drive
McLean, VA 22101
(703) 821-4499

Allen Kuhl
R&D Associates
Marina Del Rey
Los Angeles, CA 90291
(213) 822-1715

Samuel Lazzara
Omnium-G
1815-1/2 Orangethorpe Park
Anaheim, CA 92801
(714) 879-8421

Terry Lenz
Agricultural & Chemical Engr. Dept.
117 Engineering Bldg.
Colorado State University
Fort Collins, CO 80523
(303) 491-5535

Fred K. Manasse
University of New Hampshire
117 Silver Street
Dover, NH 03824
(603) 862-1779

John Margrave
Advanced Studies and Research
Rice University
Houston, TX 77001
(713) 527-4820

B. W. Marshall
Division 5713
Sandia Laboratories
Albuquerque, NM 87185
(505) 264-2280
FTS: 475-2280

H. H. Marvin
DOE/Division of Solar Technology
600 E Street, NW
Washington, DC 20545
(202) 376-4424

Keith Masterson
SERI
1536 Cole Blvd.
Golden, CO 80401
(303) 234-7111
FTS: 327-7111

Edward McBride
Black & Veatch
PO Box 8405
Kansas City, MO 64114
(913) 967-2000

David McDaniels
Physics Department
University of Oregon
Eugene, OR 97403
(503) 686-4765

Richard C. Rozycki
Martin Marietta Corporation
PO Box 179
Denver, CO 80201
(303) 973-3149 or 3669

John L. Russell, Jr.
General Atomic Company
PO Box 81608
San Diego, CA 92138
(714) 455-2090

J. M. Schreyer
Union Carbide Corporation
Nuclear Division
Oak Ridge Y-12 Plant
Oak Ridge, TN 37830
(615) 483-8611
FTS: 850-8611

Robert I. Sheldon
Department of Chemistry
University of Kansas
Lawrence, KS 66045
(913) 864-3829

Ralph H. Sievers
Science Applications, Inc.
8400 Westpark Drive
McLean, VA 22101
(703) 821-4504

S. R. Skaggs
Mail Stop 348
Los Alamos Scientific Laboratory
Los Alamos, NM 87545
(505) 667-6921 or 6074
FTS: 843-6921 or 6074

Frank B. Smith
STTF Users Association
Suite 1507
First National Bank Bldg. East
Albuquerque, NM 87108
(505) 268-3994

Otto J. M. Smith
EECS Department
University of California
Berkeley, CA 94720
(415) 525-9126

Ned B. Spake
Florida Power Corporation
3201 34th Street South
St. Petersburg, FL 33733
(813) 866-4763

Thomas H. Springer
Atomics International
8900 De Soto Avenue
Canoga Park, CA 91304
(213) 341-1000, Ext. 1325

Edmund Storms
MS 348
Los Alamos Scientific Laboratory
Los Alamos, NM 87545
(505) 667-5818

Robert T. Taussig
Math Sciences N.W.
PO Box 1887
Bellevue, WA 98009
(206) 827-0460

Charles C. Thacker
Prototype Development Associates
1740 Garry Avenue, Suite 201
Santa Ana, CA 92705

Lorin L. Vant-Hull
Solar Energy Laboratory
University of Houston
Houston, TX 77004
(713) 749-4861

Wayne Wasson
Air Force Weapons Laboratory
Kirtland Air Force Base
Albuquerque, NM 87115

Layton J. Wittenberg
Monsanto Research Corporation
PO Box 32
Miamisburg, OH 45342
(513) 866-7444

Neil Woodley
SERI
1536 Cole Blvd.
Golden, CO 80401
(303) 234-7107
FTS: 327-7107

John Wright
Dept. of Agricultural & Chemical Engr.
117 Engineering Bldg.
Colorado State University
Fort Collins, CO 80523
(303) 491-5535

Aden B. Meinel
Optical Sciences Center
University of Arizona
Tucson, AZ 85721
(602) 884-3138

Marjorie P. Meinel
Optical Sciences Center
University of Arizona
Tucson, AZ 85721
(602) 884-3138

Savino F. Mercurio
Sperry Rand Corporation
Marcus Avenue
Great Neck, NY 11020
(516) 574-2976

Thomas A. Milne
SERI
1536 Cole Blvd.
Golden, CO 80401
(303) 234-7101
FTS: 327-7101

Adolf Muenker
Exxon Research & Engineering Co.
PO Box 45
Linden, NJ 07036
(201)474-2314

George P. Mulholland
New Mexico State University
PO Box 3450
Las Cruces, NM 88003
(505) 646-3501

Tetsuo Noguchi
Government Industrial Research Inst.
1. Hirate Machi, Kita-Ku
Nagoya, Japan 511
052-911-2111, Ext. 475

William J. Oberjohn
Babcock and Wilcox
Box 835
Alliance, OH 44601
(216) 821-9110

J. Steve O'Kelley
Carter & Burgess, Inc.
1100 Macon Street
Fort Worth, TX 76102
(817) 335-2611

John A. Owen
Solar North Energy Systems, Ltd.
610 G-70th Avenue, SE
Calgary, Alberta, T2H 2J6, Canada
(403) 253-0486

Ted Prythero
Solar Planning Office--West
Suite 2500
3333 Quebec
Denver, CO 80207
(303) 837-5386

Mke Rafferty
Headquarters, Defense Nuclear Agency
Attention: SPAS
Washington, DC 20305
(202) 325-7024

Paul Rappaport
SERI
1536 Cole Blvd.
Golden, CO 80401
(303) 234-7300
FTS: 327-7300

Michel Rodot
Director of PIRDES
CNRS
15 Quai Anatole, 75700
Paris, France
555-9225

Darrell L. Ross
MS 198-220
Jet Propulsion Laboratory
4800 Oak Grove Drive
Pasadena, CA 91103
(213) 354-4049

Don H. Ross
MS MER 12-1124
Sanders Associates, Inc.
95 Canal Street
Nashua, NH 03060
(603) 885-5069

Claude Royere
CNRS, Solar Energy Laboratory
Odeillo, Font-Romeu
France 66120
33-68-301024

Stan Zelinger
Omnium-G
1815-1/2 Orangethorpe Park
Anaheim, CA 92801
(714) 879-8421

Richard Zito
University of Arizona
1345 East Helen Street
Tucson, AZ 85719

Solomon Zwerdling
Northeast Solar Energy Center
70 Memorial Drive
Cambridge, MA 02142
(617) 661-3500